

**Appendix A**  
**Background**  
**Water Quality Study**



## Table of Contents

<b>Section</b>	<b>Page</b>
Appendix A. Background Water Quality.....	1
A.1 Introduction.....	1
A.1.1 Background .....	1
A.1.2 Overview of Mine Facilities.....	2
A.1.3 History of Operations.....	3
A.2 Overview of Geology, Mineralogy and Geochemistry .....	5
A.2.1 Geologic Setting .....	6
A.2.2 Mineralogy.....	8
A.2.3 Geochemistry .....	11
A.3 Geochemistry of Tyrone Background Water Quality .....	13
A.3.1 Calcium to Magnesium Ratios.....	14
A.3.2 Water Composition by Rock Type.....	15
A.3.3 Mineralogical Controls on Groundwater Composition .....	16
A.3.4 Saturation Indices.....	19
A.4 Statistical Evaluation of Background Dataset to Determine Alternative Standards.....	20
A.4.1 Compiling Background Concentration Dataset.....	21
A.4.2 Background Dataset.....	27
A.4.3 Calculation of Maximum Concentrations and Upper Prediction Limits.....	33
A.5 Summary and Conclusions.....	38
References.....	38

## List of Tables

<b>Table</b>	<b>Page</b>
A-1 Dominant Water Facies by Rock Unit Tyrone Mining District .....	15
A-2 Saturation Indices by Rock Type .....	20
A-3 Summary of Wells Selected for Background Water Quality Analysis .....	25
A-4 Maximum Concentrations and 95 Percent Upper Prediction Limits of Fluoride and Manganese in Background Wells .....	33





## List of Figures

<b>Figure</b>	<b>Page</b>
A-1 Site Location Map	
A-2 Wells Selected for Use in Background Dataset	
A-3 Cross Plot for Calcium to Magnesium Ratio	
A-4 Piper Diagram for All Rock Types	
A-5 Piper Diagram for Precambrian Granite	
A-6 Piper Diagram for Tertiary Quartz Monzonite	
A-7 Piper Diagram for Quaternary-Tertiary Gila Conglomerate	
A-8 Piper Diagram for Quaternary Alluvium	
A-9 Halite Dissolution Reaction	
A-10 Calcite Dissolution Reaction	
A-11 Gypsum Dissolution Reaction	
A-12 Ion Exchange Reactions	
A-13 Feldspar Hydrolysis (anorthite)	
A-14 Pyrite Dissolution Reaction	
A-15 Sphalerite Dissolution Reaction	
A-16 Fluoride Concentrations in Groundwater Over Time, Well 2-11	
A-17 Fluoride Concentrations in Groundwater Over Time, Well LRW-5	
A-18 Fluoride Concentrations in Groundwater Over Time, Well TWS-7	
A-19 Manganese Concentrations in Groundwater Over Time, Well TWS-33	
A-20 Histogram of Field pH in All Background Wells Screened in Quartz Monzonite	
A-21 Histograms of Manganese in All Background Wells Grouped by Geologic Unit	
A-22 Histogram of Fluoride in All Background Wells Screened in Quartz Monzonite	



## List of Figures (Continued)

<b>Figure</b>	<b>Page</b>
A-23 Histograms of Fluoride in Individual Background Wells Screened in Quartz Monzonite	
A-24 Box Plots of Field pH in Individual Background Wells Screened in Quartz Monzonite	
A-25 Box Plots of Fluoride in Individual Background Wells Screened in Quartz Monzonite	
A-26 Normal Q-Q Plot of Fluoride in All Background Wells Screened in Granite	
A-27 Normal Q-Q Plots of Fluoride in Individual Background Wells Screened in Granite	
A-28 Histograms of Fluoride in Individual Background Wells Screened in Granite	
A-29 Box Plots of Manganese in Individual Background Wells Screened in Granite	
A-30 Box Plots of Manganese in Individual Background Wells Screened in Quartz Monzonite	
A-31 Box Plots of Manganese in Individual Background Wells Screened in Quaternary Alluvium	
A-32 Box Plots of Manganese in Individual Background Wells Screened in Gila Conglomerate	
A-33 Manganese Concentrations in Groundwater and Groundwater Elevations Over Time, Well TWS-8	

## List of Attachments

### Attachment

- A-1 Temporal Trends in Background Dataset



## **Appendix A. Background Water Quality**

### **A.1 Introduction**

Daniel B. Stephens & Associates, Inc. (DBS&A) conducted an analysis of site-specific background concentrations of inorganic chemicals to be monitored and evaluated under the Stage 1 and Stage 2 Abatement Plan Proposals (APPs). The objective of the study was to calculate naturally occurring background concentrations for constituents that exceed New Mexico Water Quality Control Commission (NMWQCC) NMAC 20.6.2.3103 standards. In order to define the extent and magnitude of groundwater contamination, it is necessary to estimate what the pre-mine background water quality was at the site. It is also necessary to estimate background water quality in order to establish realistic abatement goals for constituents that may be naturally elevated in groundwater.

Initial review of the water quality information and DBS&A's experience with the analysis and evaluation of water quality issues at Tyrone suggested that exceedances at some locations of NMWQCC standards for fluoride (F), manganese (Mn), and perhaps several other constituents could be due to natural causes. Statistical analysis and geochemical evaluation of data from background monitoring wells confirmed and quantified the natural exceedances for F and Mn, leading to recommendations for background standards of 2.9 milligrams per liter (mg/L) and 3.1 mg/L, respectively. Additional analytes in the background water quality dataset exhibited infrequent exceedances that do not support establishing other background standards at this time, although the observations do have implications for the interpretation of one-time or sporadic exceedances.

#### **A.1.1 Background**

The mining process generates pregnant leach solution (PLS), which is characterized by low pH and elevated concentrations of sulfate, total dissolved solids (TDS), and metals. Recovery systems intercept the vast majority of PLS at leach stockpiles, but some PLS has escaped capture at some locations and has impacted groundwater beneath and adjacent to stockpiles. At some locations groundwater has also been impacted by seepage through waste rock piles



and tailing impoundments. Groundwater impacted by mining operations would be expected to have roughly similar characteristics to the leachate except with lower concentrations due to mixing with non-impacted groundwater and other attenuation mechanisms.

The following constituents are routinely monitored for compliance with NMWQCC groundwater standards at Tyrone as part of various operational discharge permits (DPs): aluminum, arsenic, cadmium, chloride, chromium, cobalt, copper, fluoride, iron, lead, manganese, nickel, pH, sulfate, TDS, and zinc. Existing and historical groundwater conditions at the Tyrone Mine are presented in numerous reports and are most recently summarized in DBS&A (2011).

Although pre-mining water quality data in the Tyrone area are limited, the observation that multiple wells exhibit elevated levels of one or two constituents without concurrently elevated TDS or sulfate suggests that some constituents may naturally exceed NMWQCC standards. In particular, elevated fluoride concentrations may occur in the Tyrone area in groundwater downgradient from rocks containing the mineral fluorite (Trauger, 1972), and elevated manganese may occur periodically as geochemical conditions fluctuate near rocks containing manganese minerals in veins or as coatings (Hewitt, 1959). The analysis herein quantifies such occurrences in order to determine appropriate standards for compliance for those constituents that appear to naturally exceed NMWQCC standards.

### ***A.1.2 Overview of Mine Facilities***

Figure A-1 provides a current (2011) aerial photograph of the mine facilities. The northern portion of the mine area along Mangas Creek contains six inactive tailing impoundments that cover approximately 2,300 acres and contain approximately 304 million tons of processed mill tailings. All of the tailing impoundments have been reclaimed as of 2009 in accordance with the DP-27 Settlement Agreement and Stipulated Final Order (DP-27 Settlement Agreement) signed by Tyrone Mine and the New Mexico Environment Department (NMED) in 2003.

South of the tailing impoundments are the primary mining operations. This area encompasses several open pits, leach ore stockpiles, waste rock piles, the solution extraction/electrowinning (SX/EW) plant, PLS collection impoundments, seepage interception systems, stormwater detention impoundments, a maintenance and lubrication area, process solution pumping



stations, process solution conveyance systems, former mill and concentrator facilities, the former precipitation plant area and acid unloading facility, and the Burro Mountain tailing impoundment.

The open pits at the Tyrone Mine Facility cover approximately 2,000 acres and include the Main, West Main, Valencia, Gettysburg, Copper Mountain, South Rim, Savanna, and San Salvador pits. The various leach ore stockpiles and waste rock piles at the Tyrone Mine Facility encompass approximately 2,800 acres and contain approximately 1.7 billion tons of rock deposited near and adjacent to the open pits. The current designation of mine facilities is provided in Figure A-1.

The SX/EW plant area encompasses approximately 51 acres. This plant removes copper from PLS and reacidifies recycled and make-up water with sulfuric acid to produce raffinate for leaching. Raffinate is applied to the tops of the leach ore stockpiles, and it percolates through the stockpiles, leaching copper and other minerals, and becomes PLS. PLS is captured at stockpile toes by collection systems and then pumped to the SX/EW plant for extraction of copper.

### ***A.1.3 History of Operations***

Freeport McMoRan and its predecessor Phelps Dodge Corporation have mined copper in the Tyrone area since the early 1900s. Early mining was conducted underground, with ore shipped off-site for smelting or concentrated in a mill located just east of the No. 1 leach stockpile and tailing material deposited at the Burro Mountain tailing impoundment. In 1921, a drop in copper prices and lack of high-grade ore caused the underground mines to shut down. Limited leaching and precipitation operations occurred between 1921 and 1929 and intermittently between 1941 and 1950.

In 1967, Phelps Dodge began open-pit mining operations, installing a mill and concentrator along with other mine support facilities. The mill and concentrator operated between 1969 and 1992. Its operations consisted of the crushing and froth-flotation of ore to generate copper concentrate that was transported to the Phelps Dodge Hidalgo Smelter for final metallurgical processing. Tailing slurry was thickened, and tailing material subsequently deposited to six



tailing impoundments located in the Mangas Valley. Based on a review of readily available historical aerial photographs and the operational timeline provided in DBS&A (1997), the Nos. 1, 2, and 3 tailing impoundments were constructed shortly after open-pit mining began. Nos. 1X and 3X were added between 1979 and 1982, along with diversion structures to reroute stormwater descending from the canyons upslope from the No. 1X tailing impoundment. The No. 1A tailing impoundment was added in 1985. The footprints of all six tailing impoundments expanded gradually over time as they were filled, just as the stockpiles and pits expanded gradually. The area of undisturbed land between the tailing impoundments and other mine operations to the south, therefore, was significantly larger in the early 1980s than it is today.

A previous operator, United States Natural Resource, Inc (USNR), conducted mining and leach operations in the Deadman Canyon area from about 1970 to 1976. The former USNR leach ore stockpile was removed from this area and placed on the No. 2A leach stockpile in 2000. Mining activities in this portion of the Deadman Canyon area appear to have been conducted by previous operators even before the 1970s.

In 1972, Phelps Dodge began limited stockpile leaching at the No. 1 stockpile, concurrent with the opening of a precipitation plant. The precipitation plant was closed in 1997. Copper matte from the precipitation plant was transported to either the Hurley or Hidalgo smelter for final metallurgical processing.

In 1984, Phelps Dodge expanded stockpile leaching operations and opened the SX/EW plant located southwest of the No. 3A leach stockpile (Figure A-1). Current mine operations consist of open-pit mining, stockpile leaching, and SX/EW processing.

As noted above, Tyrone has reclaimed some mine facilities:

- The Mangas Valley tailing impoundments, reclaimed between 2005 and 2009
- The Burro Mountain tailing impoundment, reclaimed in 2004
- The No. 1 leach stockpile, reclaimed in 2009
- The former concentrator area, reclaimed in 2007



- Significant portions of the Nos. 1C and 7A waste rock piles, reclaimed starting in 2010, to be completed in 2012

## **A.2 Overview of Geology, Mineralogy and Geochemistry**

Very few studies of the Tyrone Mine have focused on the issue of background water quality. Only the *Preliminary Site Wide Groundwater Study* (PSWGS) (DBS&A, 1997a) and Trauger (1972) address this issue. The following discussion is summarized from the PSWGS.

Due to its location along the Continental Divide, the Tyrone Mine is in a groundwater recharge area. As the groundwater flows from recharge areas to discharge areas, it entrains dissolved constituents as it flows through the various rock types. As a consequence, groundwater quality decreases as it gains dissolved constituents. The evolution of groundwater quality occurs in areas both unaffected and affected by mining activities. As the groundwater migrates through the host soil and rocks, it interacts with the associated minerals and gases, undergoing a variety of inorganic reactions. These reactions are a function of the initial groundwater chemistry, the kind of soil and minerals present, and the rate of groundwater flow, and they generally result in a net increase in the concentrations of dissolved constituents. The minerals present in this area include primary igneous minerals, unoxidized sulfide deposits, zones of oxidation, alteration minerals, and vein deposits. Of particular importance to water quality in the Tyrone Mine area is the presence of fluorite deposits in the quartz veins. These deposits result in naturally elevated concentrations of fluoride in the surrounding area groundwater (Trauger, 1972).

Mining and mineral processing activities occurring primarily since the 1960s, including blasting, excavating, and dumping, have increased the surface area of mineralized and reactive rocks and exposed them to oxygen, water, and leach solutions that have greatly accelerated their rates of chemical and physical weathering. The weathering of these materials has increased the concentrations of dissolved constituents in groundwater in the vicinity of mining and mineral processing areas. The mining and mineral processing operations appear to have also increased dissolved constituent concentrations, principally of sulfate and TDS, in shallow groundwater.

Sections 2.1 through 2.3 discuss the complex geology and mineralogy of the Tyrone mine area.



### **A.2.1 Geologic Setting**

The Tyrone Mine copper deposit is classified as a porphyry copper deposit. The geology of the deposit and surrounding area has been summarized by DuHamel et al. (1993), Kolessar (1982), and Paige (1922), and detailed geologic maps of the quadrangles that encompass the mine area have been published by Hedlund (1978). The Tyrone Mine copper deposit is generally confined to a polygonal area several miles in diameter at the northeast end of the Big Burro Mountains and is bounded by the Burro Chief Fault on the northwest, the Sprouse-Copeland Fault on the southeast, and multiple smaller unnamed faults on the south (Figure A-2).

The rocks that crop out in the Big Burro Mountains, the Mangas Valley, and the Little Burro Mountains range in age from Precambrian to Quaternary. The Big Burro Mountains are predominantly composed of the Precambrian Burro Mountain granite (pCg), and this batholith was subsequently intruded by the Tertiary quartz monzonite (Tqm) nearly 56 million years ago (Kolessar, 1982). The Tqm dominates the southern half of the orebody, while the orebody is hosted by Precambrian granites in the northern half of the Tyrone deposit. The Tyrone laccolith is composed of four stages of porphyry intrusions (DuHamel et al., 1993). Each porphyry type differs in composition, texture, and timing of intrusion. For the purpose of the background water quality evaluation, all four types are presented as a single unit referred to as the Tertiary quartz monzonite of Tyrone (Tqm).

Exposures of Cretaceous rocks are limited to the Little Burro Mountains. The Cretaceous units are predominantly sedimentary rocks, which include the Beartooth quartzite and the Colorado Formation. The Beartooth quartzite is a thin-bedded to massive, fine-grained sandstone that unconformably overlies Precambrian granite. The Colorado Formation is a sandy shale that conformably overlies the Beartooth quartzite (Kolessar, 1982). Cretaceous and Tertiary volcanic rocks—primarily andesites and rhyolites—overlie the Cretaceous sedimentary units.

The youngest rocks in the area are of late Tertiary and Quaternary age, and they consist mostly of sands, gravels, and conglomerates. The Gila Conglomerate (QTg), the oldest of the recent sedimentary rocks, was deposited as bolson fill and as fan deposits derived from late Tertiary and older uplifts. The youngest sedimentary units (Qal) were deposited unconformably on Gila Conglomerate and as valley fill along present-day drainages.





The geology of the Mangas Valley area is dominated by the Gila Conglomerate and older fan deposits described by Hedlund (1978). The Gila Conglomerate consists of semiconsolidated sediments eroded from the Little and Big Burro Mountains that were deposited during the late Tertiary and Quaternary ages. The youngest, unconsolidated sedimentary units were deposited unconformably during the Quaternary age as valley alluvial fill (Qal) along present-day drainages. Both the Cretaceous sediments and the Gila Conglomerate lie unconformably on the Precambrian Burro Mountain granite (pCg).

The main geologic structures in the Big Burro Mountains, the Mangas Valley, and the Little Burro Mountains are northeast- and northwest-trending faults. The traces of two regional faults, the Mangas Fault and the Sprouse-Copeland Fault, are shown in Figure A-1. The Mangas Fault strikes northwest-southeast with a dip of about 60 degrees southwest, and it forms a prominent scarp on the Little Burro Mountains. The Mangas Fault has juxtaposed Gila Conglomerate and bolson fill against the older rocks of the little Burro Mountains (Kolesar, 1982).

Fractures and joints typically lack the displacement associated with faults and are of a much smaller scale, ranging from inches to tens of feet. Within the area of the mine, numerous intrusions or vein swarms have developed a complex jointing and fracture network. DuHamel et al. (1993) point out that the vein swarms probably established the pattern of groundwater flow during supergene enrichment.

Another structural feature is roof pendants that are remnants of country rock found within an igneous intrusive body. Several Precambrian granite pendants are evident within the Tertiary quartz monzonite laccolith.

The Mangas Fault appears to be a half-graben that separates the Little Burro Mountains from the Big Burro Mountains. Rotation of the down-dropped block has tilted the Tyrone orebody about 8 degrees toward the plane of the fault (DuHamel et al., 1993). This rotation has also preserved a wedge of the Gila Conglomerate and possibly Cretaceous rocks in the down-dropped block. The Gila Conglomerate section in the down-dropped block is thickest on the northeastern side of the Mangas Valley and thins to a feather edge on the southwest side.



### **A.2.2 Mineralogy**

The mineralized rocks in and around the mine have been highly fractured and extensively intruded and mineralized. The weathering of these rocks over geologic time periods has contributed dissolved constituents to groundwater. Following the hydrothermal mineralization event that occurred about 56 million years ago, the rocks were uplifted, and the subsequent leaching and enrichment (supergene) processes were initiated in the late Eocene (Duhamel et al., 1993). The supergene process mobilizes sulfur and metals from the oxidized zone above the regional water table and transports them to the water table. At the water table they may be redeposited as sulfides or may be transported some distance in the groundwater. This process has occurred sporadically in the area to the present time. The areal extent of the supergene mineralization and alteration in the Gila Conglomerate and pre-Gila Conglomerate rocks is not delineated and extends beyond the limits of the mine site.

The Precambrian granite, quartz monzonite, and andesites are dominantly composed of silicate minerals, with feldspars and quartz being the most common. Primary minerals include:

- Plagioclase feldspar, typically oligoclase composition
- Potassium feldspar (K-feldspar)
- Quartz
- Amphiboles-hornblende
- Biotite
- Muscovite
- Pyrite

The rocks at Tyrone have undergone at least four alteration phases (DBS&A, 1997a) which have led to the formation of alteration minerals generally associated with copper enrichment, including:

- Quartz-sericite-pyrite (QSP), typical alteration of porphyry deposits



- Propylitic alteration, mafic minerals (hornblende, biotite) altered to chlorite and rutile
- Plagioclase feldspar alteration, feldspar altered to chlorite and sericite
- Argillic alteration, potassium feldspars altered to clay (kaolinite)

#### *A.2.2.1 Fluorite Occurrence in the Tyrone Mining District*

Fluorite is a commonly occurring ore mineral in the vicinity of Tyrone that has been extracted at several historical mines (Hedlund, 1985; Williams, 1966; McNulty, 1978). In Grant County, and in particular in the Tyrone Mining District, more than 144,500 tons of fluorite have been produced from numerous mines and deposits, including the Burro Chief Mine (Williams, 1966) which is now encompassed by the Tyrone Mine (the historical Burro Chief Mine was located due west of the Main Pit and south of the SX/EW Plant). Significant quantities of fluorite are most likely still present within the aquifer systems at Tyrone and influence the calcium ( $\text{Ca}^{2+}$ ) and fluoride ( $\text{F}^-$ ) concentrations observed in the background water quality.

The Burro Chief Mine was an underground mine extracting fluorite within fault breccia of the Burro Chief Fault from veins ranging from 10 to 100 feet wide (Williams, 1966). The workings included a shaft to 700 feet below ground surface (ft bgs) and multiple drifts developed as far as 1,000 feet south and 300 feet north of the shaft that extracted more than 70,000 tons of fluorite (Williams, 1966).

Deposits consisting of fluorite veins are also documented in California Gulch and Oak Grove (Williams, 1966). The California Gulch Prospect is located just west of Deadman Canyon and consists of fault breccia cemented by fluorite in granite associated with chalcedony, chrysocolla, specularite, and limonite. Several veins are traceable for more than 1,000 feet and are up to 8 inches wide (Williams, 1966). The Oak Grove deposit is reported as a vein exposed at the surface in an exploratory pit developed in granite, and the vein had a strike of 70 degrees east and a dip of 60 degrees north (Williams, 1966). The Oak Grove deposit most likely formed along a fault or within a fracture system.

Fluoride minerals are widely distributed throughout the Tyrone Mining District and occur as veins and cement fracture-fill within some deposits. The widespread distribution and often extensive deposits often extending to depth along faults are important considerations for this



background water quality study. The fluoride may be present across the entire site, and deposits are present at and below the water table, allowing for dissolution in the regional groundwater system.

#### *A.2.2.2 Manganese-Oxide Occurrence at Tyrone*

Manganese is a common oxide (Mn-oxide) noted throughout the Tyrone Mining District that often forms a coating on fractures and mineral grains. Psilomelane and lesser amounts of pyrolusite “occur in narrow veins, as small pockets in veins, and as thin fracture coatings in the Burro Mountains granite,” and multiple deposits of manganese oxides are recorded on the west side of the Burro Mountains (Hewitt, 1959). The Black Eagle Mine produced “a few truckloads” of manganese ore from one of these deposits in which the hypogene manganese oxides found in association with calcite and fluorite are related to late stages of fluorite mineralization during the Tertiary age (Hewitt, 1959). Hewitt (1959) also referred more generally to epithermal fluorite deposits in the region being associated with manganese oxides. Other deposits on the west side of the Burro Mountains are related to supergene concentration of manganese oxides by weathering processes (Hewitt, 1959).

Gillerman (1964) reported that within the Tyrone deposits, chrysocolla is the most abundant copper mineral in the oxidized zone and that locally the chrysocolla is stained dark brown to black by manganese. In the nearby Little Burro Mountains within 1 mile of the Tyrone district, manganese was mined at the Contact Mine, and more than 140 tons were produced in the 1930s and 1940s (Gillerman, 1964). The Contact vein is a well-defined quartz fissure vein in the Precambrian granite following a well-defined fault plane along which manganese is “conspicuously abundant” as a mixture of oxides (Paige, 1911).

In summary, the Tyrone deposits contain many manganese oxides related to multiple geologic processes that are relevant to the background water quality of these geologic units, including both manganese oxides related to the occurrence of fluoride minerals and those occurring independently of fluoride mineralization.



### **A.2.3 Geochemistry**

Understanding the geochemistry and mineralogy of manganese and fluoride provides insight into the behavior of these elements in groundwater. Both elements are widely distributed throughout the site and likely associated with several episodes of mineralization and alteration. The relative solubility and widespread distribution have allowed these elements to dissolve into groundwater, affecting the background water quality at the site. The following sections provide a brief overview of the sources of manganese and fluoride at Tyrone and the geochemical processes that affect the concentrations of these constituents and the overall quality of the groundwater.

#### *A.2.3.1 Sources of Manganese and Fluoride at Tyrone*

Naturally occurring groundwater concentrations of manganese and fluoride at the Tyrone Mine are controlled predominantly by the solubility of the minerals that are composed of these elements. As a mineral is weathered, the elements that make up the mineral are released and dissolve into the groundwater. The elements may remain dissolved as ions, neutral species, or complexes, or they may react to form the same minerals (congruent reaction) or new minerals (incongruent reactions).

Manganese is a common constituent in mafic minerals that typically occur in igneous rocks such as the granite and monzonite at the Tyrone Mine. Mafic minerals include olivine, pyroxene, amphiboles, and biotite. Hornblende, an amphibole, and biotite are common minerals in the igneous rocks at Tyrone. Based on petrographic studies, the quartz monzonite at Tyrone contains up to 5 percent biotite and about 1 percent hornblende (Hedlund, 1985).

Biotite composition is variable, and during crystallization, both manganese and fluoride may substitute for other elements within a biotite mineral phase (Bisdorn et al., 1982). Biotite is susceptible to weathering and will likely decompose more readily than other silicate minerals such as feldspars, muscovite, and quartz. Several cations will readily substitute interchangeably, including iron, titanium, magnesium, and manganese. In biotite, the hydroxide (OH<sup>-</sup>) anion may be replaced by fluoride (F<sup>-</sup>) during crystallization.



#### *A.2.3.2 Fluoride Geochemistry*

Fluorine occurs as fluoride in water and has the greatest electronegative nature of all the elements, which results in a negatively charged ion in solution ( $F^-$ ). Fluoride is the typical dissolved form of fluorine in groundwater. Fluoride has a similar charge and ionic radius to hydroxide ( $OH^-$ ) that allows fluoride to readily substitute in many minerals including apatite, biotite, and hornblende (Hem, 1985). Fluorite ( $CaF_2$ ) is one of the most common fluoride minerals.

Under equilibrium conditions, fluorite solubility may control fluoride concentrations in groundwater. The solubility will be dependent on calcium ( $Ca^{2+}$ ) activities, and as the calcium activity increases, fluorite may precipitate, resulting in lower calcium and fluoride concentrations in groundwater. In general, groundwater with elevated calcium will have relatively low fluoride concentrations due to the water reaching a saturation point for fluoride, thereby allowing the mineral to precipitate from solution and remove the calcium and fluoride ions from solution during mineral formation. The equilibrium is sensitive to temperature such that fluoride concentrations may be somewhat elevated at temperatures warmer than 20 degrees Celsius ( $^{\circ}C$ ), other factors being equal. Most monitoring wells at Tyrone have temperatures close to this value, but some deeper wells have temperatures of  $25^{\circ}C$  or warmer, which may measurably increase fluoride concentrations.

The presence of gypsum within an aquifer will influence fluoride behavior in groundwater (Appelo and Postma, 2005). As discussed above, when calcium reaches sufficient concentration ( $\approx$  activity), fluorite may form. When gypsum dissolves into groundwater, calcium and sulfate ( $SO_4^{2-}$ ) are released into solution, and the additional calcium may react with fluoride, forming fluorite. Due to the removal of calcium, this reaction leaves elevated sulfate in solution relative to calcium, based on the assumed  $1Ca^{2+}$  to  $1SO_4^{2-}$  stoichiometry for gypsum dissolution.

#### *A.2.3.3 Manganese Geochemistry*

Manganese is a common metallic element and, like iron, participates in redox reactions (Hem, 1985). The manganese ion ( $Mn^{2+}$ ) is the most likely form to be mobile in groundwater. Manganese is a common constituent in mafic minerals including biotite and hornblende, and the



manganese will substitute for magnesium, iron, or calcium in silicate minerals (Hem, 1985). Under acidic reducing conditions, the manganese ion is mobile following dissolution of these mafic minerals (Rose et al., 1979). Generally, manganese concentrations in groundwater will tend to decrease as pH increases. Manganese commonly forms oxide coatings on fractures and mineral grains, indicating that it is mobile in the geochemical environment at Tyrone.

### **A.3 Geochemistry of Tyrone Background Water Quality**

To gain conceptual insights to support interpretation of the background dataset and its statistics, DBS&A performed a geochemical assessment to determine water-rock interactions that are most likely controlling the water quality in the area. This assessment comprised analysis of chemical time series and inter-element correlation plots, and saturation indices were prepared to compare observed data to the solubilities of naturally occurring minerals that influence groundwater quality near Tyrone.

Groundwater geochemistry was evaluated to help determine if the water quality data selected for this study is representative of background quality without impacts from mining activities. Background water quality represents the pre-mining conditions, when the natural hydrogeological and geochemical environment controlled groundwater chemistry. This dataset generally represents water quality upgradient of the mine site.

The data were used to assess compositional trends based on major ion chemistry; specifically, the data were plotted on Piper diagrams and elemental cross-plots to discern apparent trends in the data. The trends were used to determine if certain mineralogical controls were affecting the chemical data and what minerals control the water quality. As the trends were analyzed, any data indicative of mining impacts were considered for removal from the dataset.

Saturation index calculations help identify minerals that may dissolve into or precipitate out of solution in the groundwater near Tyrone. Common minerals such as gypsum, calcite, and fluorite were evaluated using the geochemical analysis software AquaChem. Pyrite and other sulfide minerals were also considered. The AquaChem calculations identified water types for background water quality in each rock type.



The following sections present data for more than 700 samples collected over time in the vicinity of the Tyrone Mine, representing aquifers from four different rock types:

- Precambrian granite (pCg)
- Tertiary quartz monzonite (Tqm)
- Quaternary-Tertiary Gila Conglomerate (QTg)
- Quaternary alluvium (Qal)

Section A.3.1 provides information on calcium to magnesium ratios. Section A.3.2 presents chemical data based on water types and plots of piper diagrams. A series of elemental cross-plots were compiled in Section A.3.3.1 in order to understand mineralogical controls on the background dataset. Section A.3.3.2 discusses results of saturation index calculations for several minerals that appear to exert control on water quality based on data presented in Sections A.3.1 and A.3.2.

### ***A.3.1 Calcium to Magnesium Ratios***

The ratio of calcium to magnesium (Ca/Mg) has been used in the past to help determine if impacts from PLS had occurred at a monitor well (DBS&A, 1997c). Groundwater that has not been impacted will typically have a Ca/Mg molar ratio greater than 2 (mass ratio greater than 3), and groundwater with known impacts may have a lower ratio near 0.15 (or 0.25 by mass). Due to PLS impacts, the magnesium concentrations have been observed to increase dramatically, resulting in a low Ca/Mg ratio (DBS&A, 1997c). The magnesium may be related to the dissolution of chlorite, a common magnesium-bearing alteration mineral at the site. When the background data for calcium and magnesium are plotted in units of milligrams per liter (mg/L), the majority of the data plot between a Ca/Mg ratio of about 4 to 5 (Figure A-3). For reference, the Ca/Mg ratio of 0.25 is shown on Figure A-3 to show the potential Ca/Mg ratio related to PLS impacts. This reference point helps demonstrate that the groundwater samples selected for this study represent background quality.





### A.3.2 Water Composition by Rock Type

Water facies were determined for samples that included analyses for major ions from the same sampling event totaling over 700 samples. Major ions include the cations calcium, magnesium, sodium, and potassium, and the anions sulfate, bicarbonate, and chloride.

The water facies represent the major cation and anion composition of the water samples. Calcium bicarbonate ( $\text{Ca-HCO}_3$ ) is the dominant water type for the background dataset (Table A-1). The  $\text{Ca-HCO}_3$  type represents dissolution of calcium carbonate minerals such as calcite or caliche. Calcium sulfate ( $\text{Ca-SO}_4$ ) is also important but occurs much less frequently, and it generally represents dissolution of gypsum ( $\text{CaSO}_4 \cdot 2\text{H}_2\text{O}$ ).

**Table A-1. Dominant Water Facies by Rock Unit  
Tyrone Mining District**

Rock Type	Water Facies
Precambrian granite	$\text{Ca-HCO}_3$
Quaternary alluvium	$\text{Ca-HCO}_3 \gg \text{Ca-SO}_4$
Quaternary-Tertiary Gila Conglomerate	$\text{Ca-HCO}_3 \gg \text{Ca-SO}_4$
Tertiary quartz monzonite	$\text{Ca-HCO}_3 \gg \text{Ca-SO}_4$

To help illustrate the water composition graphically, Piper diagrams were created using samples that included analyses for major ions. Data for the major ions are plotted as relative compositions in terms of percentage. Five Piper diagrams were developed: one for all samples and one for each of the four rock types (pCg, Tqm, QTg, and Qal) (Figures A-4 through A-8). As the water facies indicated and as evident on each of the Piper diagrams, the major ions controlling water chemistry are calcium and bicarbonate. The data generally plot near the calcium apex of the cation triangle and the bicarbonate apex of the anion triangle. When the entire dataset is plotted (Figure A-4), cations appear to be 50 percent or greater calcium with sodium varying between 5 and 55 percent and magnesium always below 40 percent; anions plot along a trend between bicarbonate and sulfate, with low concentrations of chloride. As the Piper diagrams by rock type show, these compositional trends are evident for each aquifer



(Figures A-5 through A-8), supporting the treatment of the background dataset as a single dataset regardless of aquifer rock type.

### **A.3.3 Mineralogical Controls on Groundwater Composition**

Background water quality represents the mixture of groundwater and recharge components that are influenced by reactions occurring between groundwater and the aquifer matrix. The composition and mineralogy of the aquifer matrix will likely exert control on the overall composition of groundwater, with the solubility of these aquifer minerals controlling the dissolved concentration of ions in solution. When an equilibrium state is achieved, minerals will dissolve into and precipitate out of solution, maintaining an equilibrium concentration. Throughout this discussion, it is assumed that concentration approximately equals activity, which is reasonable given the low TDS of the background water quality.

#### *A.3.3.1 Elemental Cross Plots*

Minerals may dissolve congruently or incongruently. Congruent dissolution may be considered a reversible reaction and describes a mineral that may dissolve and precipitate into the same mineral such as calcite. Incongruent dissolution occurs when a mineral dissolves but will not re-precipitate from solution such as when pyrite oxidizes releasing iron and sulfate into solution.

The following equations (A-1 through A-7) represent the governing equations for mineral dissolution and precipitation reactions that occur in aqueous systems and are usually the dominant controls on water quality:

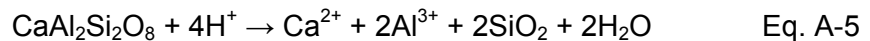
#### *Congruent reactions*

- Halite dissolution:  $\text{NaCl} + \text{H}_2\text{O} \leftrightarrow \text{Na}^+ + \text{Cl}^- + \text{H}_2\text{O}$  Eq. A-1
- Calcite dissolution:  $\text{CaCO}_3 + \text{CO}_2 + \text{H}_2\text{O} \leftrightarrow \text{Ca}^{2+} + 2\text{HCO}_3^-$  Eq. A-2
- Gypsum dissolution:  $\text{CaSO}_4 \cdot 2\text{H}_2\text{O} + \text{H}_2\text{O} \leftrightarrow \text{Ca}^{2+} + \text{SO}_4^{2-} + 3\text{H}_2\text{O}$  Eq. A-3
- Ion exchange:  $2\text{Na}(\text{clay}) + \text{Ca}^{2+} \leftrightarrow \text{Ca}(\text{clay}) + 2\text{Na}^+$  Eq. A-4



### Incongruent reactions

- Plagioclase feldspar hydrolysis (anorthite):



- Pyrite oxidation:  $\text{FeS}_2 + 7/2 \text{O}_2 + \text{H}_2\text{O} \rightarrow \text{Fe}^{2+} + 2\text{SO}_4^{2-} + 2\text{H}^+$  Eq. A-6

- Sphalerite oxidation:  $\text{ZnS} + 8\text{Fe}^{3+} + 4\text{H}_2\text{O} \rightarrow 8\text{H}^+ + \text{SO}_4^{2-} + \text{Zn}^{2+} + 8\text{Fe}^{2+}$  Eq. A-7

Elemental cross-plots and Piper diagrams developed to evaluate the chemical reactions occurring in samples representing background water quality at Tyrone indicate that typical water-rock interactions are occurring, and impacts from pyrite oxidation and mining activities are not a major influence on the water quality in this background dataset.

In Figure A-9, the sodium and chloride do not have a trend close to the 1:1 trend based on the halite dissolution reaction (Equation A-1), indicating that halite dissolution is probably not contributing to the observed water quality. The majority of the data for the rock types indicate that excess sodium is dissolved in the water beyond what may be derived from halite dissolution. Given the hydrothermal history of the vicinity, the absence of halite is not surprising.

In Figure A-4, the relationship between calcium versus alkalinity (bicarbonate) is shown. Based on the stoichiometry of calcite dissolution (Equation A-2), if all of the calcium were derived from limestone/calcite dissolution, the data should follow a 2:1 trend. The calcium and bicarbonate at Tyrone appear to have a limestone/calcite source (Figure A-10). Calcite is known to occur as an alteration mineral in the Tertiary quartz monzonite (Hedlund, 1985), and the Gila Conglomerate has calcareous cement (Paige, 1922). Each rock type appears to correlate with the calcite dissolution trend and also agrees with the calcium-bicarbonate water facies analyses previously discussed.

Gypsum dissolution following Equation A-3 should result in a 1:1 relationship for calcium and sulfate (Figure A-11). This relationship is roughly observed for the Quaternary alluvium rock type, which has a linear relationship parallel to the 1:1 trend with a correlation coefficient ( $r^2$ ) of 0.66 but with excess calcium unaccounted for by gypsum dissolution. This reaction appears to



be a partial control on the observed water quality in the Quaternary alluvium but not in the other rock types.

Ion exchange may be an important control on cations in solution, when calcium and magnesium substitute for exchangeable sodium found on clay minerals (Equation A-4). To evaluate the potential for ion exchange reactions to be occurring, the concentration of sodium minus chloride ( $\text{Na} - \text{Cl}$ ) was plotted against the calculation  $\text{Ca} + \text{Mg} - \text{SO}_4 - \frac{1}{2}\text{HCO}_3$ . The quantity of sodium minus chloride represents excess sodium that may originate from sources other than halite dissolution and assumes that all chloride is from halite. The calculation  $\text{Ca} + \text{Mg} - \text{SO}_4 - \frac{1}{2}\text{HCO}_3$  represents the calcium and/or magnesium coming from sources other than gypsum and carbonate dissolution, likely feldspar dissolution. These two quantities represent the maximum amount of sodium and calcium plus magnesium available for ion-exchange processes or potentially derived from other sources. The potential for cation exchange exists and would follow the trend shown in Figure A-12; this is a likely control on calcium and sodium concentrations when clay minerals are present in the aquifer.

Clay minerals generally have the greatest cation-exchange capacity, and several have been identified at Tyrone. Kaolinite, chlorite, and sericite (fine-grained muscovite mica) are common clay minerals at Tyrone (DBS&A, 1997b) related to argillic and quartz-sericite-pyrite alteration, all of which have limited cation-exchange capacity. Smectite and mixed layer illite-smectite are also reported from clay mineral analyses at Tyrone as significant components (DBS&A, 1997b). Smectite in particular has a very high cation-exchange capacity and readily exchanges inter-layer cations, usually sodium, for those in solution, typically calcium. The exchange of sodium for calcium is a natural water softening reaction.

Other reactions that may influence sodium and calcium concentrations are the hydrolysis of feldspars. Both plagioclase and potassium feldspars are important constituents in the rocks at Tyrone (DBS&A, 1997b; Hedlund, 1985).

Feldspar dissolution by hydrolysis reactions is most likely occurring within the rocks at Tyrone. As the feldspar anorthite (calcium plagioclase) dissolves incongruently, calcium and aluminum ions are released into solution (Equation A-5). As shown in Figure A-13, there is no correlation between the calcium and aluminum ions, but this is not surprising given that this is an



incongruent reaction. The identification of kaolinite (DBS&A, 1997b) is a good indicator that feldspar has dissolved, with subsequent formation of clays that sequester aluminum (and silica) reactants. Aluminum ions that do not form clay minerals will also tend to precipitate out of solution as gibbsite or alunite at the given circumneutral pH range of approximately 6 to 8 for samples in this background dataset.

The oxidation of sulfide minerals, such as pyrite and sphalerite, has the potential to release metals and sulfate into solution (Equations A-6 and A-7). These reactions, often catalyzed by dissolved oxygen and ferric iron in groundwater, will lead to acid rock drainage. Based on the cross-plots in Figures A-14 and A-15, these oxidation reactions do not appear to be a significant source of metals or sulfate for this dataset because the data do not match the oxidation trends.

#### A.3.4 Saturation Indices

A saturation index is calculated using the law of mass action and is expressed on a logarithmic scale. Gypsum dissolution (Equation A-3) is used here as an example:

*Law of Mass Action-stability constant (Appelo and Postma, 2005):*

$$K = \frac{[\text{CaSO}_4]}{[\text{Ca}^{2+}] \cdot [\text{SO}_4^{2-}]} = 10^{2.5} \quad \text{Eq. A-8}$$

- Ion activity product (IAP):  $\text{IAP}_{\text{gypsum}} = [\text{Ca}^{2+}] [\text{SO}_4^{2-}]$  Eq. A-9

- Saturation index (SI):  $\text{SI} = \log(\text{IAP}/K)$  Eq. A-10

The IAP represents the concentration (activity) in a given water sample, and K represents the concentration (activity) at equilibrium. The ratio will provide information on the state of equilibrium in the water. Saturation indices help to predict how minerals may behave in groundwater as follows:

- SI > 0: Saturation (mineral phase may precipitate from solution)
- SI = 0: Equilibrium



- $SI < 0$ : Undersaturated (mineral phase may dissolve into solution)

Saturation indices for each rock type were calculated using the geochemical program PHREEQ (Table A-2). Calcite, gypsum, and fluorite are minerals of interest for this study, and values indicate that many of the samples are undersaturated with respect to these minerals, particularly gypsum. So these minerals would tend to dissolve into solution and contribute ions to the dissolved concentrations observed in the monitoring data. The highest saturation indices for fluorite in the dataset indicate saturated conditions at which equilibrium processes constrain the concentration of fluoride ions dissolved in the groundwater; in other words, there is an abundance of fluoride-bearing aquifer minerals with respect to the solubility of fluoride in the background water quality.

**Table A-2. Saturation Indices by Rock Type**

Rock Type	Calcite		Fluorite		Gypsum	
	Min	Max	Min	Max	Min	Max
Precambrian granite	-2.2	0.26	-2.5	-0.087	-3.3	-1.2
Quaternary alluvium	-1.9	-0.09	-2.5	0.41	-2.8	-1.2
Quaternary-Tertiary Gila Conglomerate	-3.1	1.3	-3.0	0.33	-2.9	-0.36
Tertiary quartz monzonite	-2.4	0.67	-3.0	1.4	-3.5	-1.2

#### **A.4 Statistical Evaluation of Background Dataset to Determine Alternative Standards**

Criteria were developed to identify background monitoring wells suitable for statistical purposes, and water quality data from these background wells were compiled and analyzed using ProUCL Version 4.1 statistical analysis software (Singh et al., 2011; Singh and Singh, 2011) and other methods. This section details the procedures used, the factors considered, and the results of the statistical evaluation. The same dataset was independently evaluated with respect to geochemical processes, as described in Section A.3, to gain further insight into background water quality in order to validate the findings of the statistical evaluation.



When comparing a single data value such as a future sample analysis to a background distribution for environmental compliance, an appropriate statistic should reflect the upper range of the background distribution such that, to the extent possible, data values that exceed the statistic will have a low probability of having occurred naturally. Statistics useful in this context include maximum background concentrations and 95 percent upper prediction limits (UPL95s). A UPL gives an estimate for a threshold value in the upper tail of the data distribution, and as the statistical sample size increases, the UPL95 approaches the 95th percentile (Singh and Singh, 2011).

The U.S. Environmental Protection Agency (EPA) publishes the ProUCL software package, which calculates UPLs and related statistics together with graphics and functions that are useful in background constituent concentration evaluations (Singh et al., 2011; Singh and Singh, 2011). In addition to ease of use, a major reason for selection of ProUCL was that it supports statistically rigorous treatment of datasets that include non-detections for background water quality calculations. Rigorous support for non-detections is critical when interpreting background datasets for minor constituents, because background distributions frequently include both a low tail below typical reporting limits and a high tail above reporting limits. The effects of improper treatment methods for rigorous evaluation of non-detections are discussed at length by Helsel (2005) and Singh and Singh (2011).

Both maximum concentrations and UPL95s were determined for the background dataset for constituents exceeding NMWQCC standards, and the maximum concentrations observed at the wells were determined to reflect background conditions. Selected wells believed to be indicative of background conditions are proposed for determining background concentrations as discussed in Section A.4.1.

#### ***A.4.1 Compiling Background Concentration Dataset***

DBS&A maintains a database of historical water quality for the Tyrone Mine. At the time this background water quality study was initiated, the database was complete through 2010. Groundwater data are provided directly by the mine or obtained from other sources, such as USGS historical data files. Supplemental water quality data from Trauger (1972) were separately compiled for the immediate vicinity of the mine. While the Trauger (1972) data are



useful in that they provide examples of regional water quality at times that pre-date most of the major surface mining operations, they are sparse in spatial and temporal coverage. Data from the Trauger (1972) report for the few local wells that were subsequently resampled were included in background statistics. Generally, wells sampled only once were not included in the statistical analysis because they lacked the degree of characterization and resulting weight of the long-term monitor wells in the DBS&A database. Some single samples from recently installed wells in the database were included in the analysis because they provide relevant information concerning background water quality, but these wells do not exhibit the highest concentrations and carry little weight relative to the monitor wells with a long-term record of water quality.

Datasets for calculation of background water quality were compiled for major geologic and hydrostratigraphic units in which wells are screened at the mine: Precambrian granite (pCg), Tertiary quartz monzonite (Tqm), Tertiary to Quaternary Gila Conglomerate (TQg), and Quaternary alluvium (Qal). Combinations of units were evaluated for statistical purposes, and single standards are proposed herein without regard to geologic units. However, background water quality for each of the units is discussed individually in order to present attributes of their statistical distributions. Since a separate characterization was prepared for each major geologic unit, wells believed to obtain significant quantities of water from more than one unit were not used in the analysis of background concentrations.

Previous review of available boring logs identified fewer than 100 wells screened in either the granite or the quartz monzonite that also had available water quality analyses in the database. A targeted supplemental review of the water quality database and boring logs identified a handful of additional wells that meet these criteria. Given the manageable total number of wells with water samples from the igneous rock formations, geographic information system (GIS) software was used to roughly determine whether each of these wells could be readily identified as potentially part of a background population. The rough determination was based on the well location relative to surface mining and related operations, observed direction of groundwater flow, and mapped faults.

Vertical as well as horizontal components of hydraulic gradients were considered. For example, an upward gradient between a deep well and nearby shallower wells at a location laterally





upgradient of but close to the mine gives additional confidence that the deep well's water quality reflects background conditions, whereas a downward gradient would have been interpreted as a reason for increased caution. The sample dates for each well were considered so that early data reflecting background conditions could be identified in localized areas where operations began at later times. Time frames of localized operations were verified where possible by reviewing historical aerial photographs for the years 1973, 1977, 1982, 1986, 1996, 2004, and 2009.

Due to the much larger number of wells screened in Gila Conglomerate or alluvium compared to igneous rocks, the same criteria were applied in a stepwise fashion to identify potential background wells in the sedimentary units. First, known regions of impacted water and regions bordering mining operations were eliminated from consideration; the remaining wells were evaluated more closely to determine if they could be considered representative of background concentrations. Monitor wells downgradient of current or historical operations were not necessarily excluded from analysis if the wells were sufficiently distant to not be impacted by mining activities during part or all of the period of record, as confirmed by key water quality constituents that generally exhibit strong responses to impacts from mining operations (e.g., pH was neutral and TDS and sulfate were low and not trending upward). Wells more than 1 mile downgradient of any operation were excluded to avoid the complication of undefined influences from adjacent watersheds on the alluvial water quality distribution.

The approach described above is conservative with respect to selection of background water quality data in that it assumes that water quality was potentially impacted anywhere that operations were occurring, even though measured water quality may not have indicated impacts due to operations. In particular, wells screened in Gila Conglomerate or alluvium were only included from areas peripheral to historical operations; thus some background wells located relatively near operations may have been excluded from the analysis. For the igneous rocks, it was more undesirable to exclude background data collected near operations, as the same mineralized zones that provide opportunities for economic mining could also give rise to elevated background concentrations of some solutes. However, as a practical limitation, no data are available from the most highly mineralized areas that predate mining operations.



Additional factors considered in the selection of background data are detailed in the following subsections, and the wells selected for each geologic unit are listed in Table A-3 and shown on Figure A-2.

#### *A.4.1.1 Choices with Respect to Consistent Sample Handling*

Precautions were taken to select data generated from samples collected and analyzed under similar conditions. Nearly all samples considered included a filtered sample for cation analyses and an unfiltered sample for anion analyses. Unfiltered samples for cations occurred so infrequently that meaningful statistical evaluation was not possible. Such samples, therefore, were excluded and only filtered samples were evaluated. Several samples had both field- and laboratory-measured pH results; only the field analyses were used. In instances in which the location of the pH determination was not specified for historical data, the data were retained unless other data from the same time frame implied laboratory measurement. There is a possibility that additional, more specific differences in data quality exist that arose from use of different sampling techniques, field staff, or laboratories over time. The effects of such factors on sample results were assumed to be negligible.

#### *A.4.1.2 Identification of Temporal Trends*

Time series plots of analytical data for each constituent were prepared for all wells considered for potential inclusion in the background dataset (Attachment A-1). Time series plots graphically display the data over the entire period of record so that trends may be considered in addition to current and maximum concentrations. Some natural variation in constituent concentrations is expected, but that natural variation is generally not expected to display a sustained upward or downward trend. Therefore, wells that may have been initially considered as potential background wells based on the above criteria were eliminated from further consideration if the sampling data exhibited trends over several sampling events, regardless of whether constituent concentrations exceeded standards. An impact could be observed as a rising trend beginning partway through a time series in response to a change in local site conditions. In such a case the early, flat part of the time series would still be acceptable for application to determine the background statistics. One such example is well 4-1. Other wells, such as well 5, were located in areas that would not have been considered under present conditions, but were retained because the historical record indicated and the time series plots confirmed that no impacts occurred during the time the well was monitored.



**Table A-3. Summary of Wells Selected for Background Water Quality Analysis**  
**Page 1 of 2**

Geologic Unit	Well Number <sup>a</sup>	Rationale
Precambrian granite (pCg)	27-2005-03	Reasonable distance (relative to well depth) upgradient from tailing pond, which lies mostly across the Mangas Fault. Low TDS and sulfate indicate lack of impact.
	435-2005-01	Cross-gradient from mining operations. Low TDS and sulfate indicate lack of impact. Originally logged as Tqm but location and composition are consistent with granite. The producing interval coincides with stratum logged as andesite.
	435-2005-03	Location far downgradient or cross-gradient from stockpile. Low TDS and sulfate indicate lack of impact.
	MB-31	Low TDS and sulfate indicate lack of impact. East side of Sprouse-Copeland Fault.
Tertiary quartz monzonite (Tqm)	2-11	Upgradient location.
	2-15	Upgradient location.
	166-2008-02	Deep test well in San Salvador Pit near upgradient side of mine in zone of upward vertical gradient. Low TDS and sulfate indicate lack of impact from mining.
	363-2005-01	Low TDS and sulfate indicate lack of impact. East side of Sprouse-Copeland Fault.
	4-1	TDS and sulfate trend upward starting sometime after 1985; data before 1985 have no trend. Aerial photography from 1986 shows that location was outside mine footprint.
	6-1	Upgradient location.
	LRW-5	Upgradient location.
	MB-44	Upgradient location.
TWS-8	Upgradient location. Water quality influenced by recharge as evidenced by water level fluctuations.	
Quaternary-Tertiary Gila Conglomerate (QTg)	2	Upgradient location. Water supply well for Tyrone.
	5	Last sampled in 1981; predates any nearby operations.
	9	Last sampled in 1982; predates any nearby tailing ponds expansions or stormwater rerouting operations that may have affected hydrograph later.
	26	Location far downgradient or cross-gradient from stockpile. Uplift on north side of Southern Star Fault prevents communication from south side. Low TDS indicates lack of impact.
	27	Location far downgradient or cross-gradient from stockpile. Uplift on north side of Southern Star Fault prevents communication from south side. Low TDS indicates lack of impact.
	286-2007-09	Upgradient from tailing pond and cross-gradient or downgradient from stockpile. Low TDS and sulfate indicate lack of impact from mining operations. Single data point carries little weight in pooled dataset.

<sup>a</sup> All wells are regional aquifer wells unless noted otherwise.

TDS = Total dissolved solids



**Table A-3. Summary of Wells Selected for Background Water Quality Analysis**  
**Page 2 of 2**

Geologic Unit	Well Number <sup>a</sup>	Rationale
Quaternary-Tertiary Gila Conglomerate (cont.)	286-2007-10	Upgradient from tailing pond and cross-gradient or downgradient from stockpile. Low TDS and sulfate indicate lack of impact. Single data point carries little weight in pooled dataset.
	286-2007-11	Upgradient from tailing pond and cross-gradient or downgradient from stockpile. Low TDS and sulfate indicate lack of impact. Single data point carries little weight in pooled dataset.
	LRW-6	Distant from mining operations except for a downgradient stormwater diversion that should not affect water quality at the well. Located outside watershed of Little Rock Mine or Deadman Canyon.
	MB-41	Low TDS and sulfate indicate lack of impact. East side of Sprouse-Copeland Fault.
	P-3	Location far downgradient or cross-gradient from stockpile. Low TDS and sulfate indicate lack of impact.
Quaternary alluvium (Qal)	166-2006-01	Upgradient location; perched groundwater in Deadman Canyon.
	TWS-33	Perched groundwater in Deadman Canyon. Footprint of mine did not approach this location until after 2004, and water quality has remained similar to upgradient well TWS-35; upgradient of impacts in Deadman Canyon.
	TWS-35	Upgradient location; perched groundwater in Deadman Canyon.
	TWS-40	Upgradient location in an unnamed tributary to Deadman Canyon. Perched groundwater.

<sup>a</sup> All wells are regional aquifer wells unless noted otherwise.

TDS = Total dissolved solids



Time series plots also allow the identification of outlier analytical results that may arise from errors in sample collection, handling, or analysis, or in data reporting or transcription. Individual data points that caused an abrupt leap upward or downward in the time series beyond the apparent range of natural variations were removed from the background dataset, especially if statistical measures indicated a low probability that the data point was valid. In contrast, high or low values from fluctuations that recurred with similar magnitudes throughout the time series and/or values that were preceded or followed by additional data points supporting a discrete fluctuation rather than an instantaneous jump were retained in the background dataset. The use of time series plots to interpret apparent outliers is discussed further in Section A.4.2.3.

Because the observed groundwater quality impacts of different operations around the mine are most easily and consistently defined in terms of elevated levels of TDS and sulfate, these analytes were used to screen for potential impacts before proceeding with evaluations of other constituents. Another strong indicator of impacts was pH. Background water quality in the Tyrone region appears to have TDS and sulfate concentrations well below standards, so wells exhibiting elevated concentrations of these constituents and/or increasing trends over time are likely or potentially impacted and were therefore excluded. Many impacted wells have exhibited stable concentrations of TDS and sulfate despite large changes in hydrologic conditions, so these were eliminated because the concentrations have always been elevated rather than because of any measurable trend. Conversely, wells that showed TDS and sulfate fluctuations at consistently low levels without any appearance of a trend were generally included in the background dataset. This approach often proved less ambiguous than considering the time series of other constituents in the same wells, because other constituents often had fewer historical data points and more complicated responses to variable geochemical conditions.

#### **A.4.2 Background Dataset**

Table A-3 lists the wells selected as background locations for statistical analysis (see also Figure A-2) and briefly summarizes the rationale by which each well satisfies the criteria described in Section A.4.1. Additional tests of data quality and representativeness were conducted prior to including observations in background datasets for statistical analysis. Plots of water quality time series, described in detail in Section A.4.1, were prepared for each analyte



and evaluated for occurrence of temporal trends or obvious outliers. Other considerations are described Sections A.4.2.1 through A.4.2.4.

#### *A.4.2.1 Analytical Data Quality*

Analytical quality assurance data is monitored by Tyrone and was not independently evaluated under this scope of work. Data imported from the March 2006 NMOps Database included results with qualifiers of R and K, apparently indicating previously rejected outliers and samples with poor charge balance, respectively. Data with R and K qualifiers were excluded from the background evaluation, but data with other qualifiers for estimated laboratory values or out-of-hold analyses were not excluded.

#### *A.4.2.2 Statistical Independence of Data Points*

The statistical independence between observations was considered qualitatively to avoid introducing the bias of including multiple dependent data observations in calculations. To better characterize background distributions using the relatively small number of background wells identified, the entire time series of samples was included for each well, despite the different time periods and unequal numbers of samples available from well to well. (For well 4-1, only early data were included due to apparent impacts later in the time series). This inequality could potentially introduce bias toward relatively well-characterized wells or areas; however, the test of the statistical validity of this approach is the independence of the observations in both time and space.

All of the wells selected in the background dataset for each geologic unit were at least 250 feet from any other well in the same geologic unit dataset, so it is reasonable to assume that their observations of background water quality are statistically independent. Similarly, the monitoring schedule for most wells is quarterly, such that seasonal fluctuations can be characterized but consecutive observations can likewise be assumed statistically independent. In some instances when water quality in a well appeared unusual relative to past data, the well could have been resampled for confirmation. However, such occurrences did not appear with noticeable frequency in the selected background datasets, and samples were not excluded based on occurrence of confirmation sampling. The only instance in which data were excluded based on potential statistical dependence was a set of nine samples from well 9 collected within a two-



month period in 1974; after verifying that all the measurements appeared to be similar, all but the first of these nine samples were excluded from background analysis.

#### *A.4.2.3 Apparent Outliers*

The ProUCL 4.1 Technical Guide (Singh and Singh, 2011) contains numerous warnings concerning the distorting effect of outliers and multiple populations on UPLs. Two procedures are available in ProUCL to test for possible outliers: the Dixon test for small statistical sample sizes and the Rosner test for larger sample sizes. Both tests identify possible outliers based on the distance to an extreme value from the remainder of the sample population relative to test statistics for assumed normal distributions. The Dixon test identifies a single potential outlier by comparing either the maximum or the minimum value to the rest of a small dataset. The Rosner test can identify up to 10 potential outliers that are farthest from the mean of a large dataset.

ProUCL offers two options for handling non-detections in outlier tests. One option is to identify the outliers among only the detections while ignoring the non-detections. The second method is to substitute values for the non-detections at one-half the reporting limits. Neither method is a fully rigorous way to describe the dataset, but the substitution method is preferred (in the context of outliers only) for two reasons. First, in a dataset with a large proportion of non-detections, if the non-detections are ignored, it may appear that the highest detection is similar to the remaining data (the other detections), when in fact it could be a high outlier that is extremely dissimilar from the mean of the dataset (a rigorous estimate of the mean would account for the non-detections). Using the substitution method, the estimate of the mean itself is incorrect, but the estimate at least accounts for the non-detections so that the potential high outliers are more likely to be identified for further evaluation. Second, a non-detection at a low reporting limit may be extremely dissimilar from a dataset that consists primarily of detections, but discarding the non-detection from the outlier test and including it in later statistics fails to examine the value, whereas substitution would identify it as a low outlier.

The assumption of normality for the background datasets is often not valid, in which case outlier identifications may frequently turn out to be correct but the reported significance levels for outlier identifications are generally not valid. Nevertheless, the Dixon and Rosner tests were applied to datasets for each analyte from each individual background well as a convenient way to flag the most extreme values for additional interpretation regarding whether they were actual outliers.



The additional interpretation was accomplished by reference to time series plots and graphical plots of the statistical distributions for the entire sample population and for the individual wells. Characterization of statistical distributions is discussed more generally in Section A.4.2.4.

Some examples of outliers discarded from the datasets used in the final statistics are circled in Figures A-16 through A-19:

- The circled fluoride detection in well LRW-5 (Figure A-16) is not as drastically different from the rest of the time series, but it was still rejected as an outlier because there are neither any similarly high values nor any data from a similar time frame indicating that it could be part of a fluctuation with multiple, supporting measurements. The two non-detections were also rejected as outliers because they are much lower than the other values and they disrupt an otherwise relatively smooth trend with limited fluctuations in the data.
- The circled fluoride concentration in the time series for well 2-11 (Figure A-17) is obviously unique among the observed concentrations measured in the well, which otherwise vary across a much smaller range.
- The fluoride time series for TWS-7 (Figure A-18) is more variable and thus harder to interpret in terms of outliers. The three circled values were determined to be outliers because they depart from the time series more sharply than the other fluctuations. In contrast, the Rosner test identifies the top five manganese concentrations in the well TWS-33 time series (Figure A-19) as outliers even at the relatively permissive 1 percent significance level (note that the dataset exhibits a log-normal rather than a normal distribution). However, none of the five values were rejected because there is nothing unusual about them when considered in the context of the entire period of record for the well.

#### *A.4.2.4 Characterization of Statistical Distributions*

Characterization of statistical distributions is necessary because many statistical methods used to calculate background concentration thresholds require assumptions about the nature of the distribution. If those assumptions are not supported by at least approximate adherence of the





site data to the assumed theoretical distribution, then only a smaller set of methods can be rigorously applied. These methods, called non-parametric methods, are not based on the assumption that the sample dataset conforms to any particular statistical distribution. When UPLs are calculated, ProUCL provides results of statistical tests for goodness-of-fit to normal, log-normal, and gamma distributions along with recommendations based on those tests to either use one of the distributions as a model or to use a non-parametric method. With outliers removed from a dataset, the goodness-of-fit tests are fairly sound, but it is much easier to assess the distribution using graphical methods, and it is beneficial to consider both types of characterization. Graphical methods include histograms, box plots, and Q-Q plots.

Histograms show the frequency with which sub-ranges of values or percentiles of the distribution are encountered within the statistical sample. ProUCL includes a model normal distribution with the familiar bell shape fit to the observed data on the histograms it generates, and although lognormal distributions are common for minor constituents (Helsel, 2005), it is convenient to have a visual guideline for at least one type of distribution. For example, Figure A-20 shows that the field pH of background wells screened in quartz monzonite fits a single, continuous normal distribution quite well. In fact, a normal distribution for pH means the hydrogen ion activity is lognormally distributed.

A histogram may also reveal a different type of distribution or indicate that pooled data have more than one underlying distribution. Figure A-21 shows side-by-side histograms for manganese in the pooled background wells in each geologic unit. The different units' distributions are similar in their medians, ranges, and their overall shapes. Most manganese concentrations are low, skewing the medians to the left, but the distributions have long high tails, suggesting that lognormal distributions would provide a better statistical model of manganese concentrations than normal distributions.

Figure A-22 shows the histogram for fluoride data pooled from background wells screened in quartz monzonite. The multiple peaks suggest multiple underlying statistical distributions, that is, multiple distinct populations of fluoride concentrations. Multiple populations could theoretically result from combining impacted and un-impacted wells from a site dataset, so the graphical analysis is useful as a screening tool. However, in this case, multiple populations result from different wells within the set of background locations, a result that recurred



throughout the background evaluation, as discussed in Section A.4.3. Although the pooled dataset could be roughly modeled as a single lognormal distribution, the side-by-side histograms for the individual wells (Figure A-23) show approximately normal distributions for each well that fall into multiple distinct groups. One alternative is to treat the pooled data using non-parametric statistics, but as illustrated by the histograms, such statistics can describe only the particular pool of available data that fails to capture the tendency of fluoride concentrations toward higher or lower values in certain locations.

Box plots similarly summarize the range and major percentiles of sample datasets and are most useful for comparing multiple datasets side by side. Normality of each distribution may also be gauged using the symmetry of the box plot or lack thereof. Box plots do not show as detailed a view of the sample distribution as histograms, so using the key features of the distributions, the multiple datasets may be quickly assessed as broadly similar (as in the field pH distributions for different wells screened in the quartz monzonite shown in Figure A-24) or dissimilar (as in the fluoride distributions for the same dataset shown in Figure A-25).

Q-Q plots depict the goodness-of-fit of sample data to model distributions as an array of the ordered observations that will form a linear trend when the model is accurate. A smooth but nonlinear trend may suggest a different model distribution. ProUCL also displays the linear fit of the model to the data for easy reference. Outliers will fall far off the line. Multiple populations can become evident as breaks in the slope of the linear trend of sample data, as seen in pooled fluoride data for the background wells screened in granite (Figure A-26). Shown as separate Q-Q plots for each well (Figure A-27), the fluoride data again exhibit approximately normal distributions for each well, with two wells showing somewhat similar distributions, one well showing a distribution at somewhat higher values, and one well showing a distinct distribution at lower values. For other background datasets that contain non-detections, Q-Q plots allow more explicit depiction of the individual non-detections than the other plots by using various models to simulate the types of values that may have led to the observed non-detections.

Only selected plots are shown and discussed in the preceding text, but generally all of the types of plots discussed were consulted while analyzing the datasets for each analyte in each geologic unit.



### A.4.3 Calculation of Potential Alternative Standards

Once the outliers were removed from the dataset as described above, potential background standards for each constituent were determined for wells screened in each geologic unit using both the maximum observed values and the calculated UPL95s for the background well dataset. This analysis indicated that for the selected background wells only two constituents, fluoride and manganese, exhibited regular exceedances of NMWQCC groundwater quality standards. This result is consistent with observations of groundwater quality at Tyrone, where some wells exceed standards for fluoride and/or manganese, but do not appear to be impacted by mining operations as indicated by TDS, sulfate, pH, and metal concentrations. As more wells are drilled and additional data are collected in the future, additional naturally elevated background constituents could be identified. The maximum observed values and the calculated UPL95s for fluoride and manganese are provided in Table A-4.

**Table A-4. Maximum Concentrations and 95 Percent Upper Prediction Limits of Fluoride and Manganese in Background Wells**

Analyte	Geologic Unit	Concentration (mg/L)		
		NMWQCC Standard	UPL95 <sup>a</sup>	Maximum <sup>b</sup>
Fluoride	Precambrian granite	1.6	2.6	<b>2.9</b>
	Tertiary quartz monzonite	1.6	1.6	2.5
	Quaternary alluvium	1.6	1.1	1.4
	Quaternary-Tertiary Gila Conglomerate	1.6	1.3	2.5
Manganese	Precambrian granite	0.2	0.65	1.1
	Tertiary quartz monzonite	0.2	0.60	2.1
	Quaternary alluvium	0.2	0.99	<b>3.1</b>
	Quaternary-Tertiary Gila Conglomerate	0.2	0.18	0.79

<sup>a</sup> 95 percent upper prediction limits (UPL95s) calculated by Kaplan-Meier method.

<sup>b</sup> Bold values proposed as background standards.

#### A.4.3.1 Upper Prediction Limits and Maximum Concentrations as Background Standards

UPL95s were considered in this analysis because they are commonly applied by regulatory bodies as site-specific background conditions. Due to their predictive nature using various



distribution models, UPL95s are particularly applicable for analysis of smaller datasets. Smaller datasets may include a number of samples that is sufficient to estimate the shape of the background statistical distribution but not sufficient to effectively determine that the distribution will not likely lead to future samples that will exceed the maximum observed value to date. In other words, a small dataset may not contain sufficient data to fully represent the natural variability of the groundwater quality. In these cases, the UPL95s may be viewed as a more robust approach to setting a background standard than using maximum observed values because UPL95s can be used to objectively estimate how much higher background concentrations might get relative to the maximum observed concentration to date.

Evaluation of the background dataset compiled for this study led to the conclusion that in this case there are valid reasons to use maximum observed values rather than UPL95s. As described in Sections 4.1 and 4.2.2, the selected background dataset pools data from multiple wells over the entire period of record, yielding an adequate number of independent observations to describe the shape of the statistical distribution. The number of observations is also large enough that the UPL95s approach the 95th percentile values. However, a key feature of the dataset is that large numbers of water samples are pooled from a relatively small number of wells. Whereas data from individual wells may appear to match one or more statistical distribution models, the pooled data tend to fall into multiple, distinct distributions from different wells or groups of wells. This is true even within a larger set of background wells screened in the same geologic formation. In order to calculate a UPL95 for the pooled data, the resulting choice is to either (1) treat the pooled data as approximately matching one distribution model and use a corresponding parametric method or (2) use a nonparametric method.

The calculated UPL95s for the Tyrone data were similar using parametric or non-parametric methods, but unless the distribution model is nearly perfect, ProUCL tends to favor the non-parametric methods. Where non-parametric methods are used, the UPL95 is calculated by estimating the 95th percentile of the dataset by linear interpolation (Singh and Singh, 2011). This approach has two drawbacks. First and most important, in the relatively large pooled datasets, approximately 5 percent of the observed background data (not including possible outliers) exceed the calculated threshold value intended for use as a background concentration standard. This approach is similar to proposing a background standard with the expectation that one in every 20 future samples of unimpacted groundwater would exceed that standard.



Second, the UPL95 is sensitive to the available data, even more so than the maximum in the following sense. Consider the case where one additional background water sample or one additional background well is added to the calculation, and the analytical results contain a value higher than the previously determined maximum. In this case, a more accurate estimate of the true (unknown) background maximum would be obtained. In the case that the results contain anything else, then the previously determined maximum would be unchanged. Stated another way, additional data may only improve a threshold value estimate based on the maximum observed value. On the other hand, if additional background samples or wells are included in a UPL95 calculation that in any way fails to represent the true (unknown) background distribution in accurate proportion, then the previously determined UPL95 may increase or decrease depending on whether the pooled data are now biased toward the high tail or the low tail of the true distribution.

#### *A.4.3.2 Discussion of Fluoride*

Figures A-23 and A-28 are histograms of fluoride in individual wells in the quartz monzonite and the granite, respectively. It is readily apparent that different background wells in a given geologic unit have distinct fluoride distributions in terms of both medians and variances, with some subsets of similar wells and some apparently unique wells. Similarities of fluoride distributions within subsets do not appear to be attributable to spatial relationships between the wells or recorded differences in mineralization or lithology.

Well 435-2005-01 has the highest fluoride of the selected background wells, potentially attributable to a 6-foot-thick interval of andesite logged within a screened interval that is otherwise granite. Every sample from 435-2005-01 exceeded the fluoride standard of 1.6 mg/L, in contrast to distributions entirely below the standard for well MB-31 or most of the quartz monzonite wells selected, and also in contrast to the distributions from wells 27-2005-03, 435-2005-03, and 2-15, which are mostly above the standard but have few values in common with the distribution of 435-2005-01. The andesite interval within the screened interval of 435-2005-01 does not make it unrepresentative of the igneous water quality; on the contrary, the granite and quartz monzonite at Tyrone are characterized by irregularly distributed younger intrusions of various rock types. If local intrusive rocks are associated with natural exceedances, it is appropriate that they be represented in the background dataset.



Even if 435-2005-01 were removed from the background water quality dataset for separate statistical treatment, the remaining wells screened in granite would still exhibit at least two distinct types of fluoride distributions, one almost completely exceeding the standard and one entirely below. Similarly, the background wells screened in quartz monzonite exhibit multiple types of fluoride distributions, including at least one above and at least two below the standard. Making distinctions between distributions from one well to another quickly leads to an unworkably high number of statistics from which to determine alternative standards, yet it is clear that when the data are pooled, even relatively robust nonparametric statistics will be dependent on the proportions of available data drawn from each type of distribution. The statistics, including UPL95s, can easily change from not exceeding the NMWQCC standard to exceeding the standard based on the decision to include or exclude observed data from one additional well. Given the facts that exceedances of the fluoride standard routinely occur in multiple background wells and that the natural exceedances are relatively small (within about a factor of 2 or less), the approach of using the maximum observed background well fluoride concentration as a background standard appears reasonable.

#### *A.4.3.3 Discussion of Manganese*

Figures A-29 through A-32 are box plots of manganese in individual background wells for each geologic unit. Similar to fluoride, manganese exhibits distributions with different medians and variances from well to well and even within each geologic unit. The pattern of the wells that have distributions above or below the NMWQCC standard of 0.2 mg/L is different from that of fluoride, which is not surprising since there are differences between the processes controlling the occurrence of fluoride and manganese minerals.

The same remarks regarding the sensitivity of statistics to the available fluoride data apply to manganese, but the especially high variance in the manganese dataset deserves specific mention because of its implications for compliance monitoring. Manganese solubility will generally depend on the redox condition of the aquifer, and the redox condition may be expected to exhibit natural variation. The fact that manganese concentrations may range across three orders of magnitude within a single background well is visible on a box plot or histogram, but is more clearly illustrated on a time series plot such as Figure A-33. Though not representative of the conditions at every well in the background dataset, this figure shows the potential sensitivity of manganese concentration to environmental factors. Significant temporal



variation of observed manganese concentration to environmental factors (e.g. recharge) is evident in the record of multiple background wells.

Figure A-33 shows the manganese time series in well TWS-8, which is screened in the Tertiary quartz monzonite in the Deadman Canyon area upgradient from the mine. The manganese concentration is below the standard of 0.2 mg/L for the vast majority of the dataset, but it regularly spikes above the standard for one or two sampling rounds before declining again. Note that the maximum manganese concentration for TWS-8 in the database, a value of 33.5 mg/L was rejected as an outlier because there is no similar temporary increase of such magnitude in the rest of the record. In contrast, although the other spikes are identified as potential outliers by the Rosner test using an incorrect assumption of normal distribution, their regularity suggests they are a natural feature of the groundwater system, an interpretation supported by independent observations. TWS-8 has a hydrograph with large oscillations of many tens of feet, suggesting regular, episodic recharge through permeable pathways; the manganese concentration appears to exhibit an inverse response to the hydrograph. The same inverse response to the hydrograph is apparent in TDS concentrations (Attachment A-1), suggesting that recharge events flush fresh water into the aquifer that subsequently disperses to mix with resident water and leaches soluble salts from the fracture walls and aquifer matrix. The behavior of manganese may be governed by concurrent fluctuations in the net redox condition as opposed to being a direct function of TDS. In any case, it is evident that the manganese concentration in background groundwater is not naturally stable, an observation confirmed by observed data at other Tyrone monitor wells.

Comparison of observed manganese concentrations to standards should therefore recognize that a low probability calculated for excursions above a standard does not mean that such excursions are unexpected, but rather that they are expected with low frequency. Therefore, it is appropriate that the alternative background standard be selected as a higher value, such as the maximum observed background concentration, to reflect a higher tolerance for natural variability.

#### *A.4.3.4 Proposed Alternative Standards*

Because (1) the occurrence of fluoride and manganese minerals does not depend solely on rock type, (2) the statistical values ultimately determined are broadly similar between geologic



units, (3) water within different rocks types may interact at many locations, and (4) it would be difficult to consider multiple standards for the same constituents in different monitoring wells, it is proposed that the highest statistical values from any data subset be applied as the background standards throughout the site regardless of the geologic unit(s) within which a well is completed. Using the maximum concentrations observed in background wells (barring outliers), alternative standards of 2.9 milligrams per liter (mg/L) for fluoride and 3.1 mg/L for manganese are proposed (Table A-4).

## **A.5 Summary and Conclusions**

Statistical analysis and geochemical evaluation of data from background monitoring wells confirmed that fluoride and manganese occur naturally in site groundwater at concentrations that exceed NMWQCC NMAC 20.6.2.3103 standards. Based on the maximum concentrations observed in background wells (excluding outliers) in the statistical evaluation, alternative standards of 2.9 mg/L for fluoride and 3.1 mg/L for manganese are recommended. Additional analytes in the background water quality dataset exhibited only infrequent exceedances such that the data do not support establishing other alternative background standards at this time. It is possible that additional data or analyses could reveal elevated background concentrations of other constituents at some time in the future.

## **References**

- Appelo, C.A.J. and D. Postma. 2005. *Geochemistry, groundwater and pollution*, 2nd ed. A.A. Balkema Publishers, Amsterdam, The Netherlands. 649p.
- Bisdorf, E.B.A., G. Stoops, J. Delvigne, P. Curmi, H.J. Altemüller. 1982. Micromorphology of weathering biotite and its secondary products. *Pedologie* XXXII 2:225-252.
- Daniel B. Stephens & Associates, Inc. (DBS&A). 1997a. *Preliminary site-wide groundwater study, Tyrone closure/closeout*. Prepared for Phelps Dodge Tyrone, Inc., Tyrone, New Mexico. May 31, 1997.





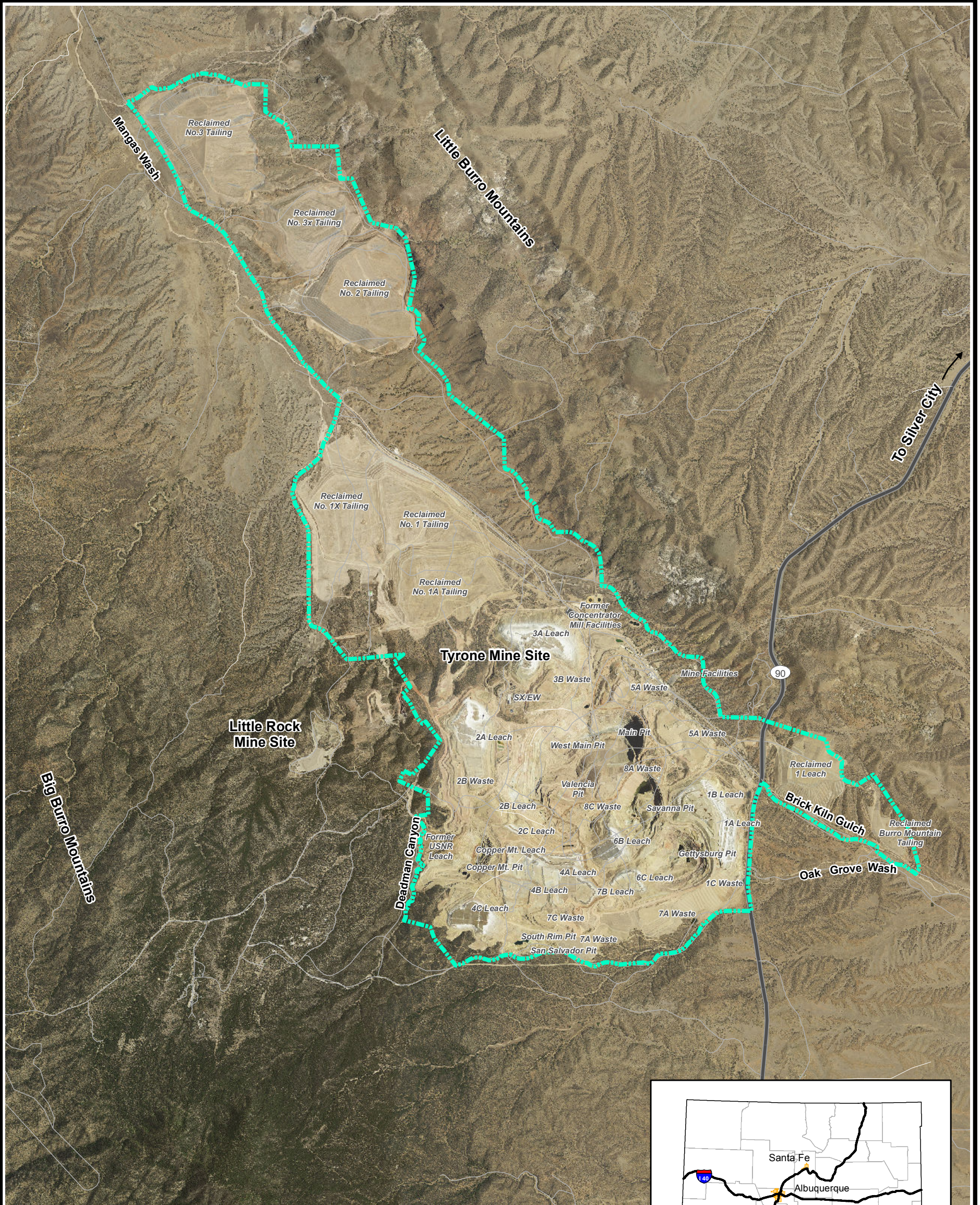
- DBS&A. 1997b. *Supplemental materials characterization, Tyrone Mine closure/closeout*. Prepared for Phelps Dodge Tyrone, Inc., Tyrone, New Mexico. October 31, 1997.
- DBS&A. 1997c. *Supplemental Groundwater Study, Tyrone closure/closeout*. Prepared for Phelps Dodge Tyrone, Inc., Tyrone, New Mexico. November 14, 1997.
- DBS&A. 2011. *Tyrone Mine Facility, Stage 1 abatement plan: Final report*. Prepared for Freeport McMoRan Tyrone, Inc., Tyrone, New Mexico. June 30, 2011.
- Duhamel, J.E., S.S. Cook., and J. Kolessar. 1993. *Draft report, Geology of the Tyrone porphyry copper deposit, New Mexico*.
- Gillerman, E. 1964. *Mineral deposits of western Grant County, New Mexico*. Bulletin 83, New Mexico Bureau of Mines & Mineral Resources. 213p.
- Hedlund, D.C., 1978. *Geologic map of the Tyrone quadrangle, Grant County, New Mexico*. Miscellaneous field studies. U.S. Geological Survey Map MF-1037. Denver, Colorado. Scale 1:24,000.
- Hedlund, D.C. 1985. *Geology, mines, and prospects of the Tyrone stock and vicinity, Grant County, New Mexico*. Open-file report 85-0232, U.S. Geological Survey. 31p.
- Helsel, D.R. 2005. *Nondetects and data analysis: Statistics for censored environmental data*. John Wiley & Sons, Inc. Hoboken, New Jersey.
- Hem, J.D. 1985. *Study and interpretation of the chemical characteristics of natural water*, 3rd ed. Water Supply Paper 2254, U.S. Geological Survey. 263p.
- Hewitt, C.H. 1959. *Geology and mineral deposits of the northern Big Burro Mountains-Redrock area, Grant County, New Mexico*. Bulletin 60, State Bureau of Mines and Mineral Resources, Socorro, New Mexico. 151p.



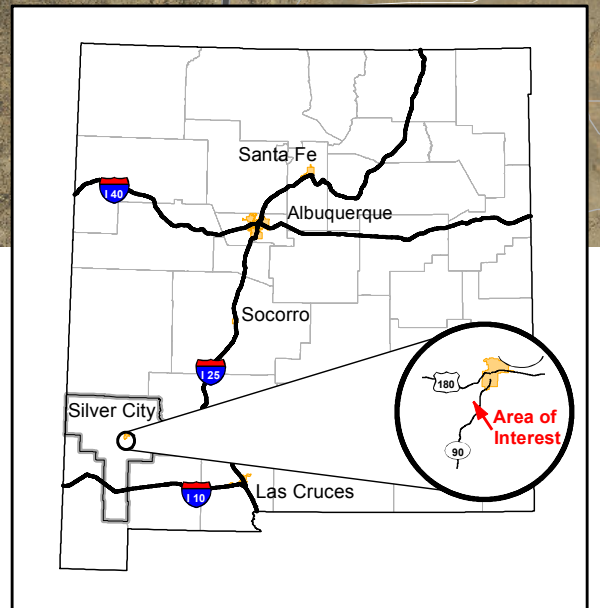
- Kolessar, J. 1982. The Tyrone copper deposit. *Advances in geology of the porphyry copper deposits southwestern North America*. University of Arizona Press. Tucson, Arizona in Titley, S. R. (ed.) pp327-333.
- McAnulty, W.N. 1978. *Fluorspar in New Mexico*. Memoir 34, New Mexico Bureau of Mines and Minerals Resources. 64p.
- Paige, S. 1911. Copper. Advance chapter from *Contributions to economic geology (short papers and preliminary reports), 1910: Part I.—Metals and nonmetals except fuels*. Bulletin 470-C, U.S. Geological Survey. 47p.
- Paige, S. 1922. *Copper deposits of the Tyrone district, New Mexico*. U.S. Geological Survey Professional Paper 122. U.S. Government Printing Office, Washington, D.C., 53p.
- Rose, A.W, H.E. Hawkes, and J.S. Webb. 1979. *Geochemistry in mineral exploration*. 2nd edition. Academic Press. 657p.
- Singh, A. and A.K. Singh. 2011. *ProUCL Version 4.1.00 technical guide (Draft): Statistical software for environmental applications for data sets with and without nondetect observations*. EPA/600/R-07/041, U.S. Environmental Protection Agency. Updated March 2011. Available at <[http://www.epa.gov/osp/hstl/tsc/ProUCL\\_v4.1\\_tech.pdf](http://www.epa.gov/osp/hstl/tsc/ProUCL_v4.1_tech.pdf)>.
- Singh, A., R. Maichle, and N. Armbya. 2011. *ProUCL Version 4.1 user guide (Draft): Statistical software for environmental applications for data sets with and without nondetect observations*. EPA/600/R-07/041, U.S. Environmental Protection Agency. Updated March 2011. Available at <[http://www.epa.gov/osp/hstl/tsc/ProUCL\\_v4.1\\_user.pdf](http://www.epa.gov/osp/hstl/tsc/ProUCL_v4.1_user.pdf)>.
- Trauger, F.D., 1972. *Water resources and general geology of Grant County, New Mexico*. New Mexico State Bureau of Mines and Mineral Resources, Socorro, New Mexico. p211.
- Williams, F.E. 1966. *Fluorspar deposits of New Mexico*. Circular 8307, U.S. Bureau of Mines Information. 143p.

## Figures





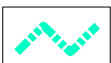
Base Map Source: National Agriculture Imagery Program (NAIP)  
Orthoimagery for Grant County (2011)



0 2,500 5,000 Feet



**Explanation**



Tyrone mine permit boundary



Grant County

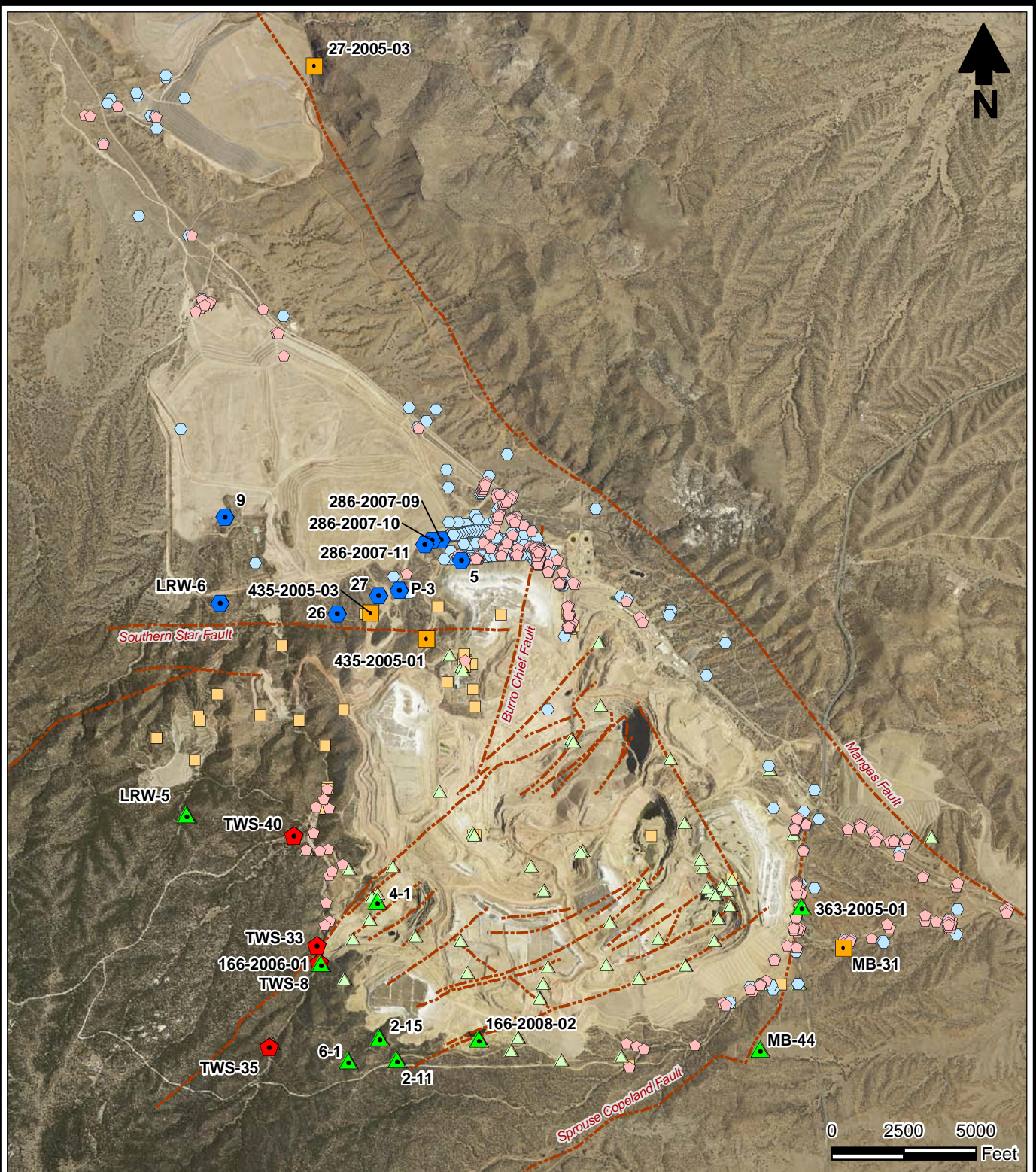


**Daniel B. Stephens & Associates, Inc.**  
11/19/2011 JN ES11.0090



**TYRONE BACKGROUND WATER QUALITY  
Site Location Map**





2011 aerial photography

**Explanation**

- |  |  |  |
|--|--|--|
| <ul style="list-style-type: none"> <li> Qal</li> <li> QTg</li> <li> Tqm</li> <li> pCg</li> </ul> | <ul style="list-style-type: none"> <li> Qal</li> <li> QTg</li> <li> Tqm</li> <li> pCg</li> </ul> | <ul style="list-style-type: none"> <li> Fault</li> </ul> |
|--|--|--|



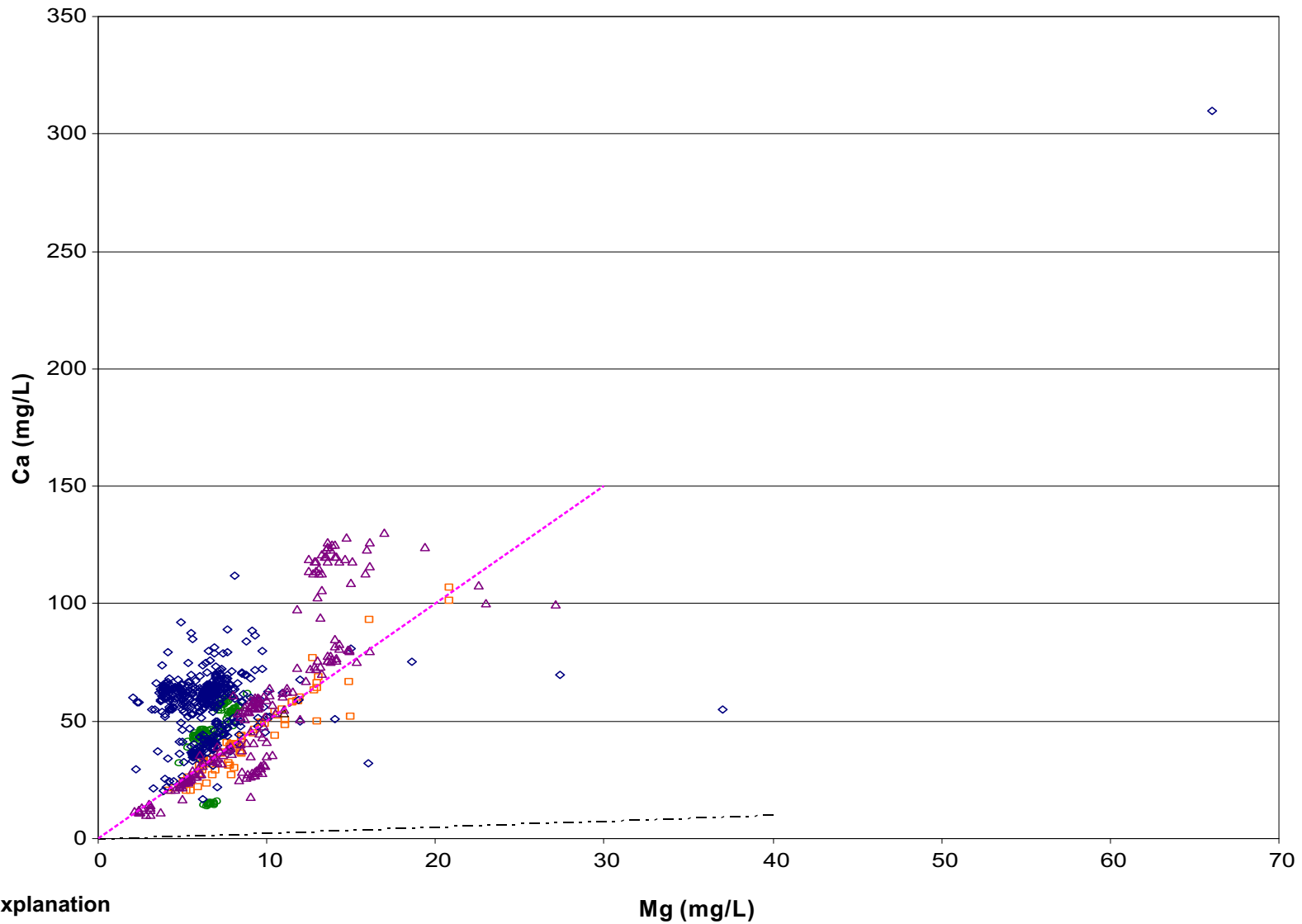
**TYRONE BACKGROUND WATER QUALITY  
Wells Selected for Use in  
Background Dataset**

S:\PROJECTS\MINE\_TYRONE\GIS\MXDSIES11.0090\FIGA2\_BACKGROUND\_DATASET\_WELLS.MXD 121301



**Daniel B. Stephens & Associates, Inc.**  
01/13/2012 JN ES11.0090

Figure A-2



Explanation

- |     |     |              |
|-----|-----|--------------|
| pCg | QTg | Ca/Mg = 0.25 |
| Qal | Tqm | Ca/Mg = 5    |

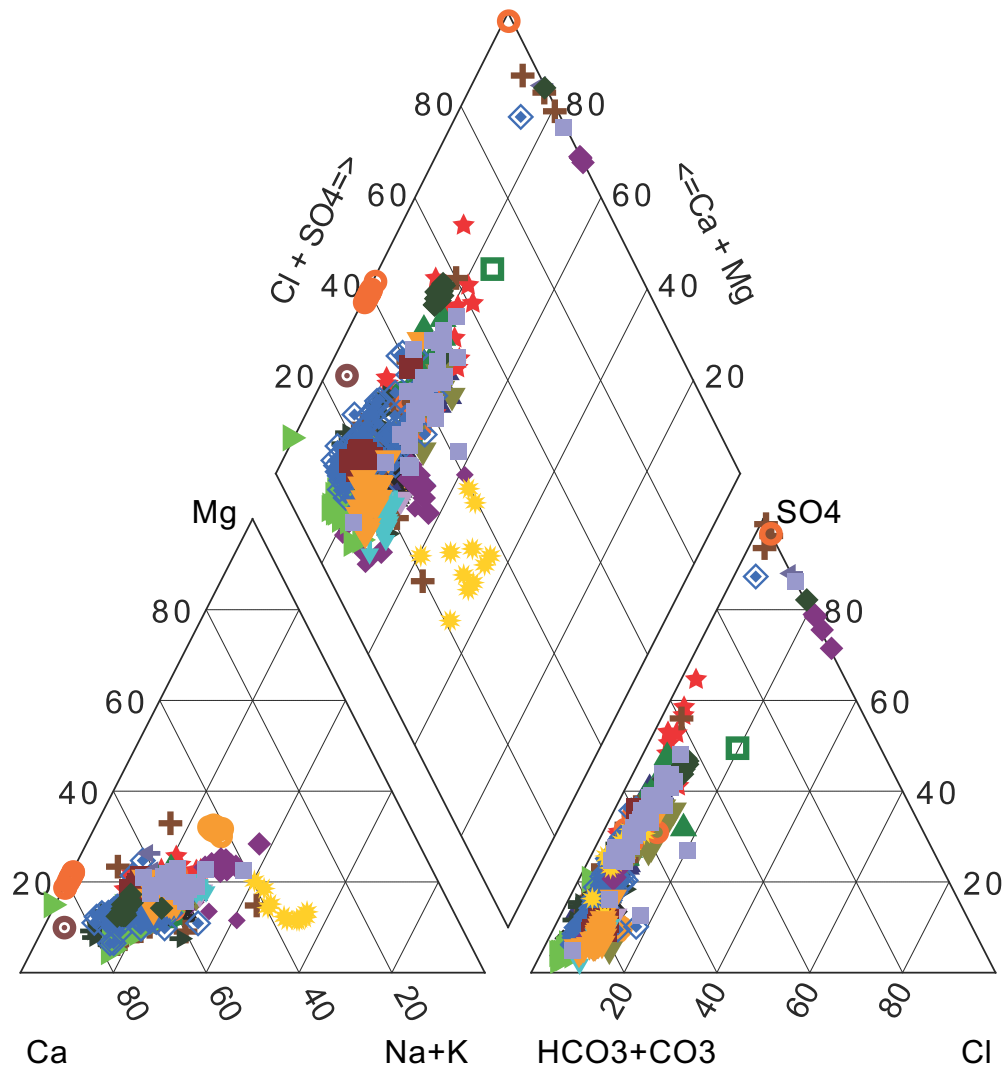


TYRONE BACKGROUND WATER QUALITY  
**Cross Plot for Calcium to Magnesium Ratio**

Figure A-3







**Explanation**

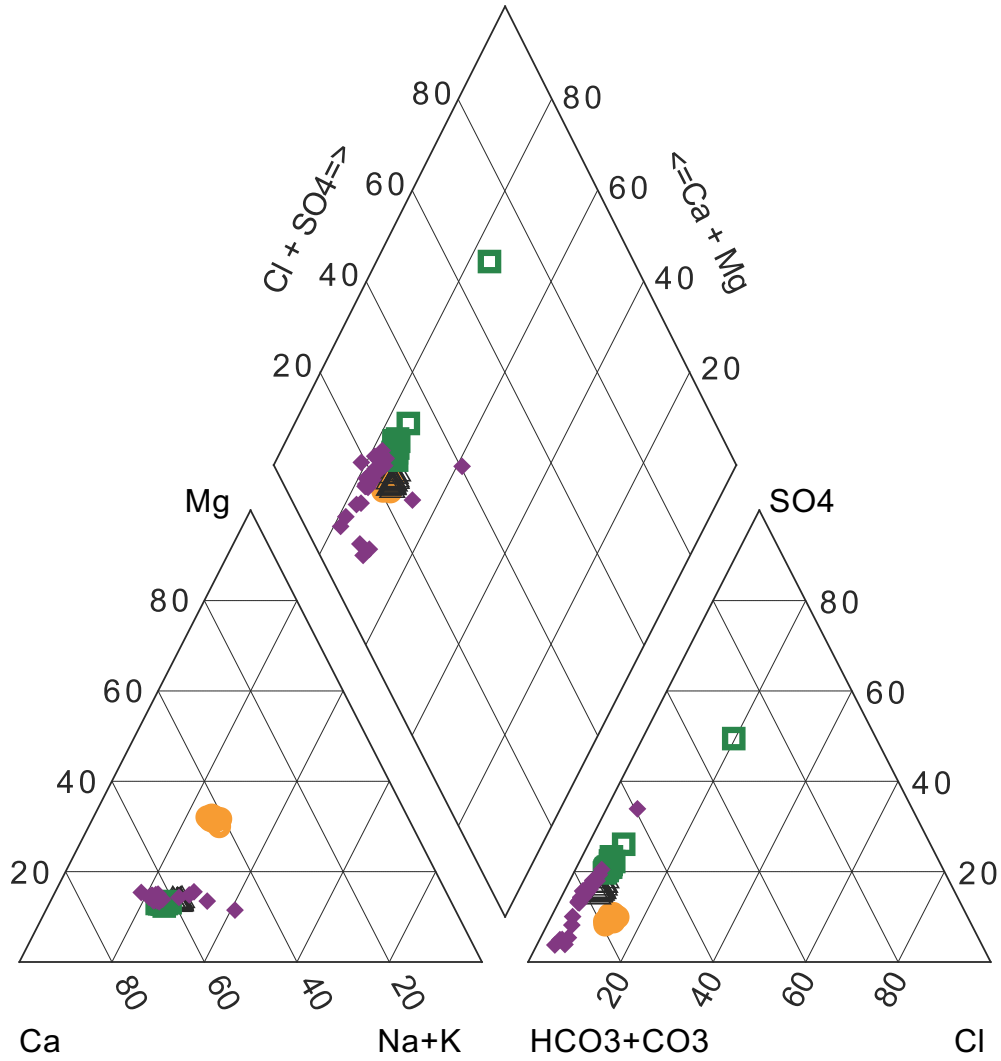
- |               |          |
|---------------|----------|
| ■ 435-2005-03 | ■ TWS-8  |
| ▲ 166-2006-01 | ▼ TWS-40 |
| ▼ 166-2008-02 | ▲ TWS-35 |
| ■ 2-11        | ★ TWS-33 |
| ◆ 2-15        | ◇ P-3    |
| ⊕ 26          | ⊙ 4-1    |
| ➤ 27          | ⊙ LRW-6  |
| ⊙ 27-2005-03  | ▼ LRW-5  |
| ▼ 363-2005-01 | 9        |
| △ 435-2005-01 | 6-1      |
| ◆ MB-31       | ○ 5      |
|               | ◆ MB-44  |



**TYRONE BACKGROUND WATER QUALITY  
Piper Diagram for All Rock Types**



S:\PROJECTS\MINE\_TYRONE\DWGS\_ES05\_THRU\_ES11\ES11\_0090\FIGS\_A-4\_TO\_A-8\_PIPER\_DIAGRAMS.CDR



**Explanation**

- 435-2005-03
- 27-2005-03
- △ 435-2005-01
- ◆ MB-31



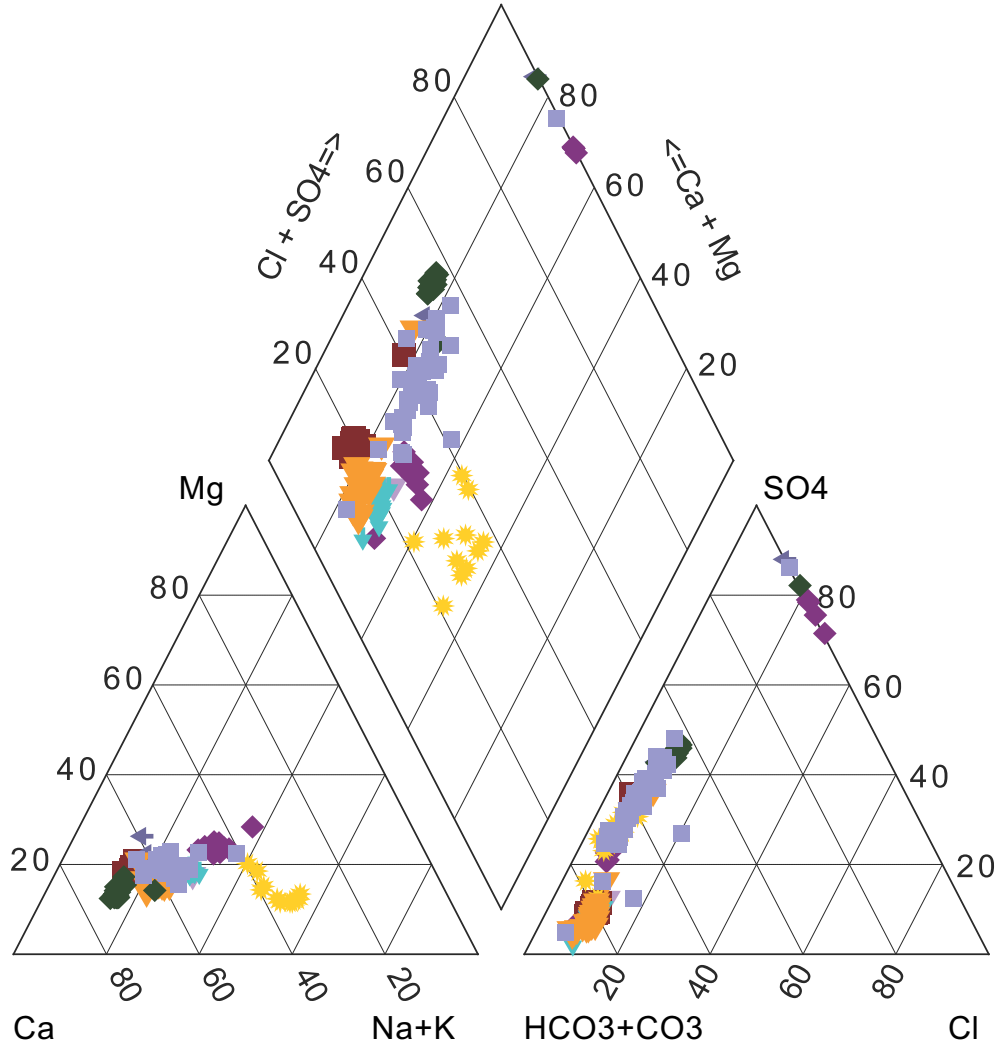
**TYRONE BACKGROUND WATER QUALITY  
Piper Diagram for Precambrian Granite**



**Daniel B. Stephens & Associates, Inc.**  
11-18-11 JN ES11.0090

Figure A-5





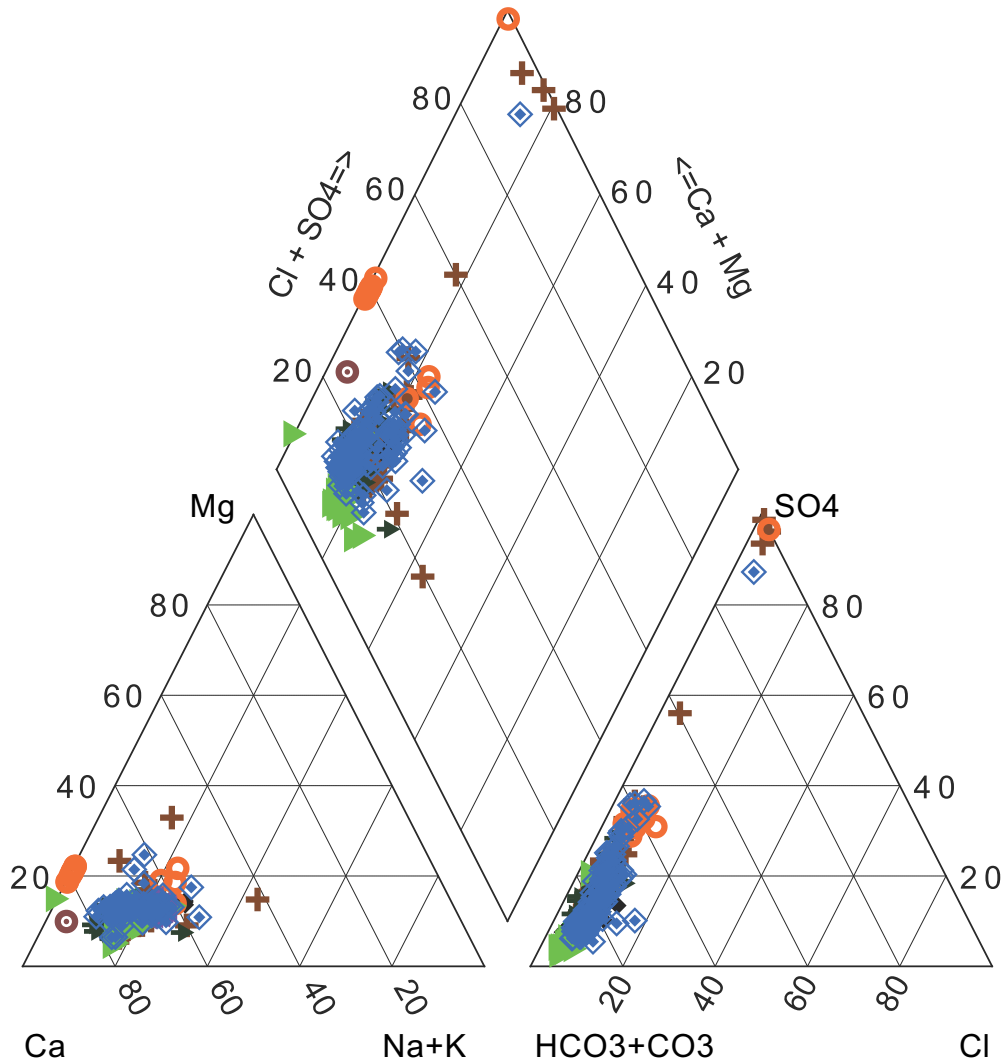
**Explanation**

- ▼ 166-2008-02
- 2-11
- ◆ 2-15
- ▼ 363-2005-01
- TWS-8
- ☀ 4-1
- ▼ LRW-5
- ▲ 6-1
- ◆ MB-44



**TYRONE BACKGROUND WATER QUALITY  
Piper Diagram for Tertiary Quartz Monzonite**





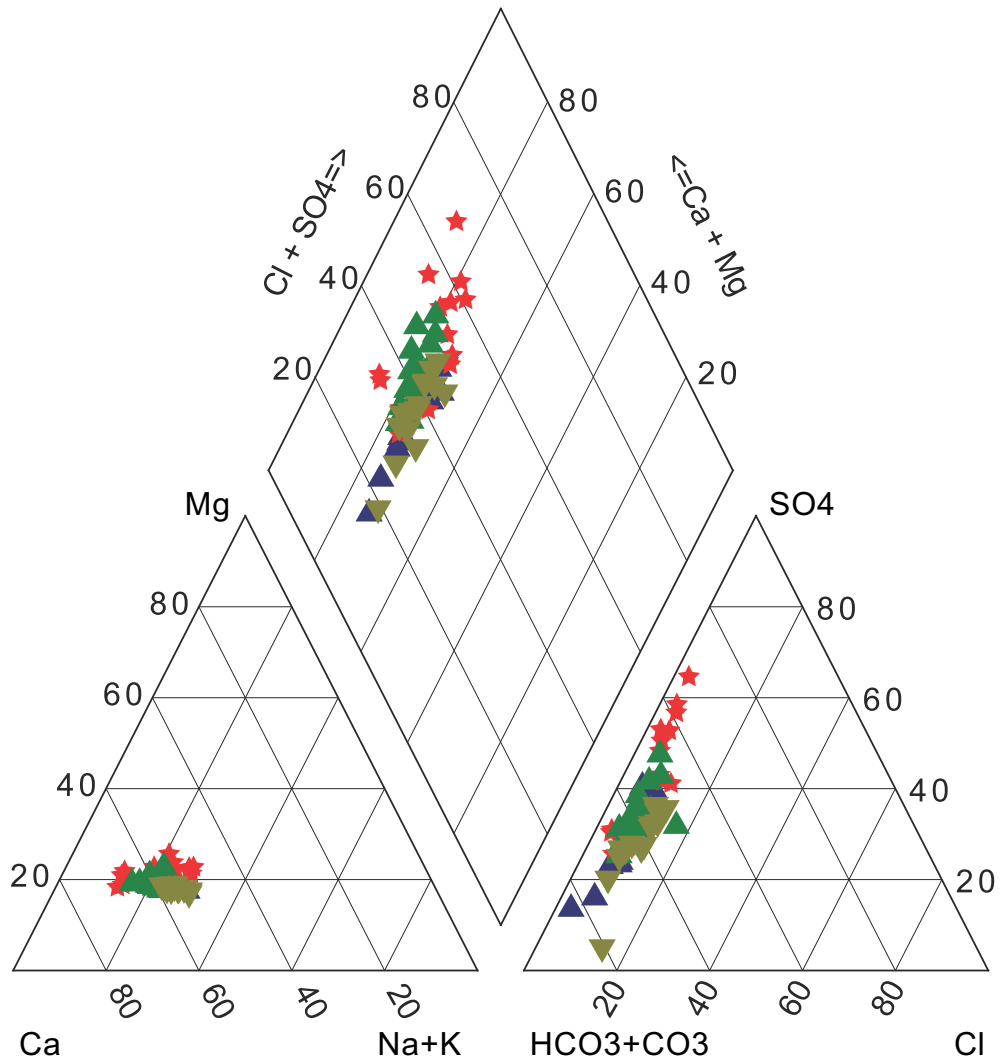
**Explanation**

- + 26
- ▲ 27
- ◊ P-3
- ⊙ LRW-6
- ▲ 9
- 5



TYRONE BACKGROUND WATER QUALITY

**Piper Diagram for Quaternary-Tertiary Gila Conglomerate**



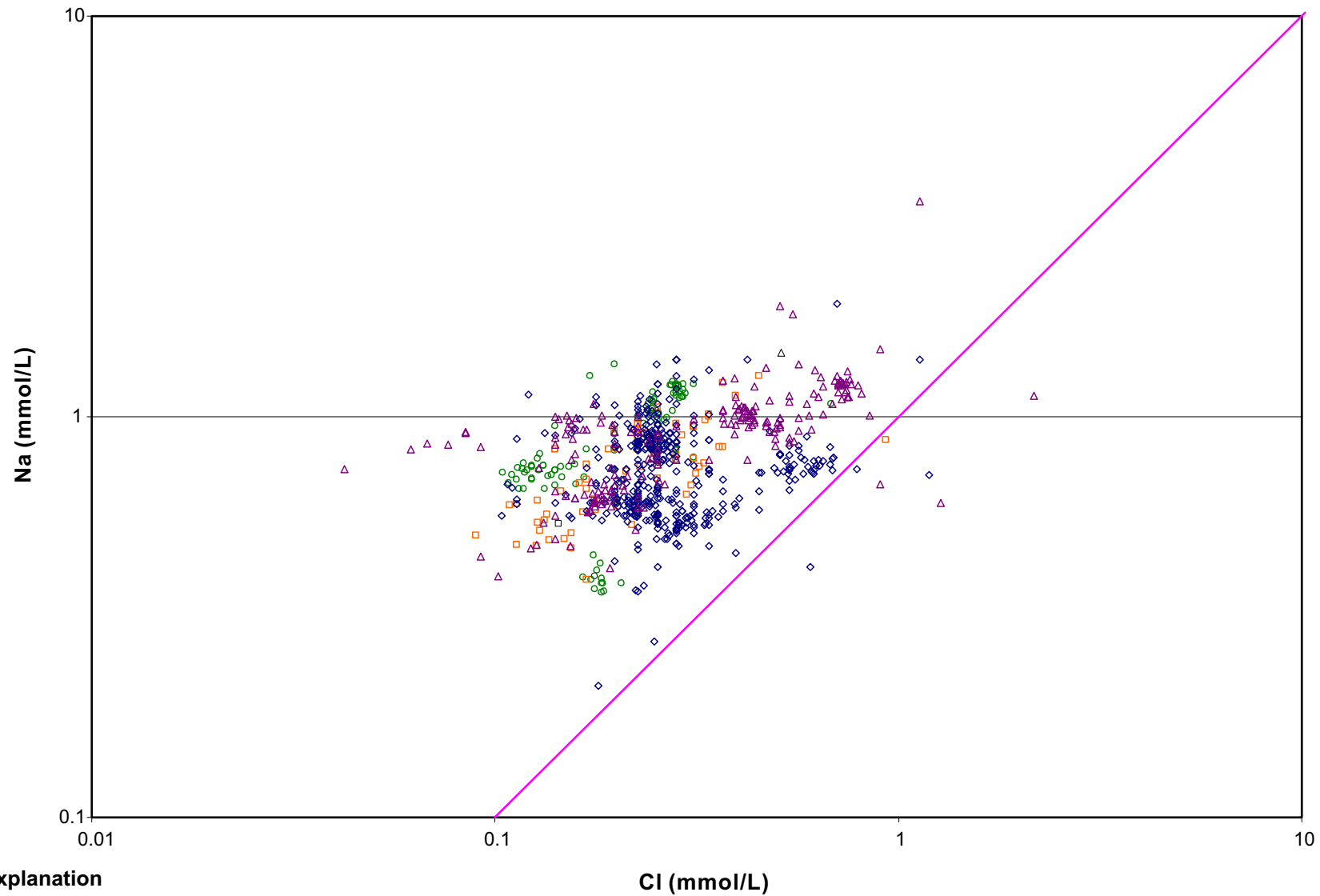
**Explanation**

- ▲ 166-2006-01
- ▼ TWS-40
- ▲ TWS-35
- ★ TWS-33



**TYRONE BACKGROUND WATER QUALITY  
Piper Diagram for Quaternary Alluvium**





Explanation

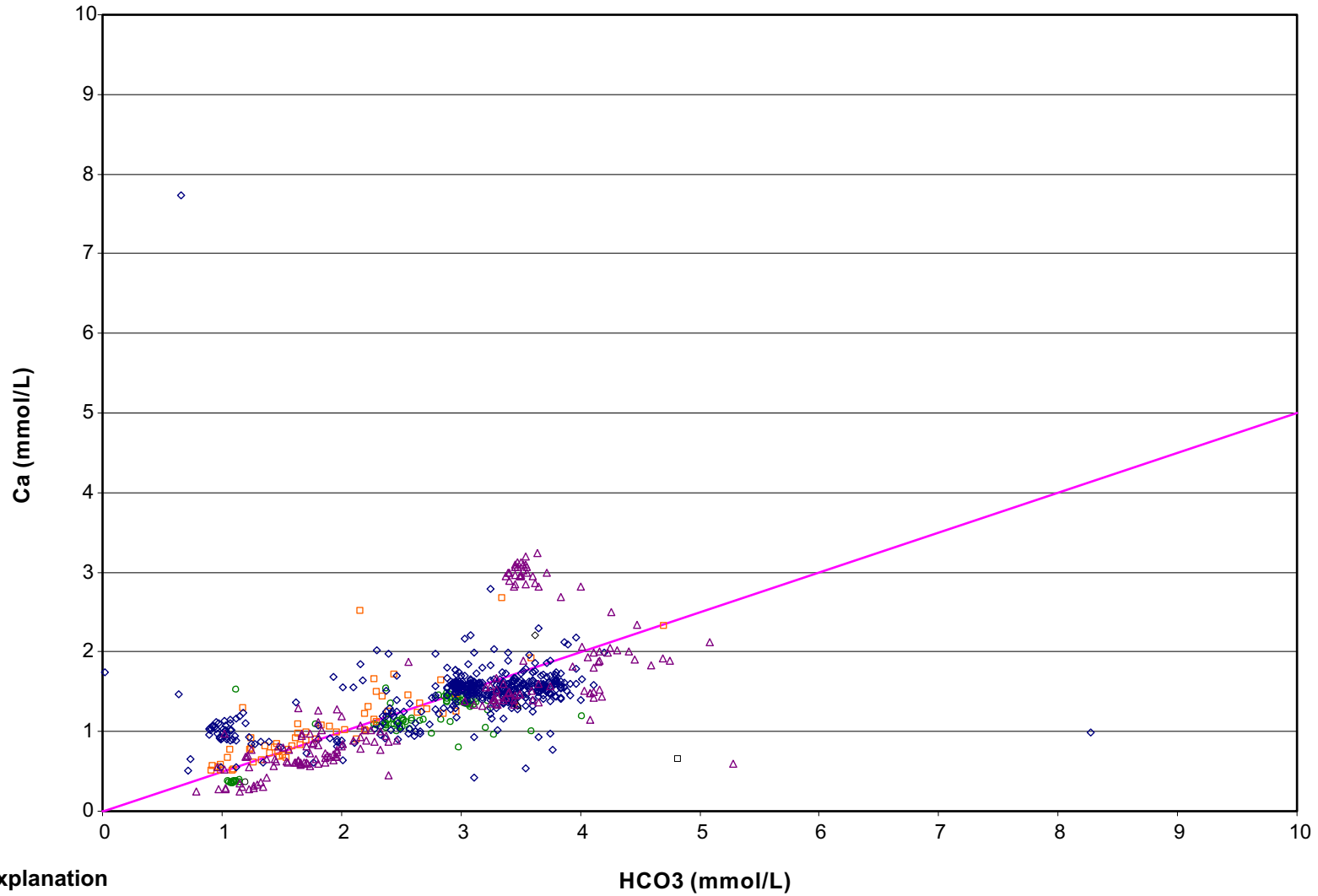
- |     |     |           |
|-----|-----|-----------|
| pCg | QTg | Trend 1:1 |
| Qal | Tqm |           |



TYRONE BACKGROUND WATER QUALITY  
**Halite Dissolution Reaction**

Figure A-9





Explanation

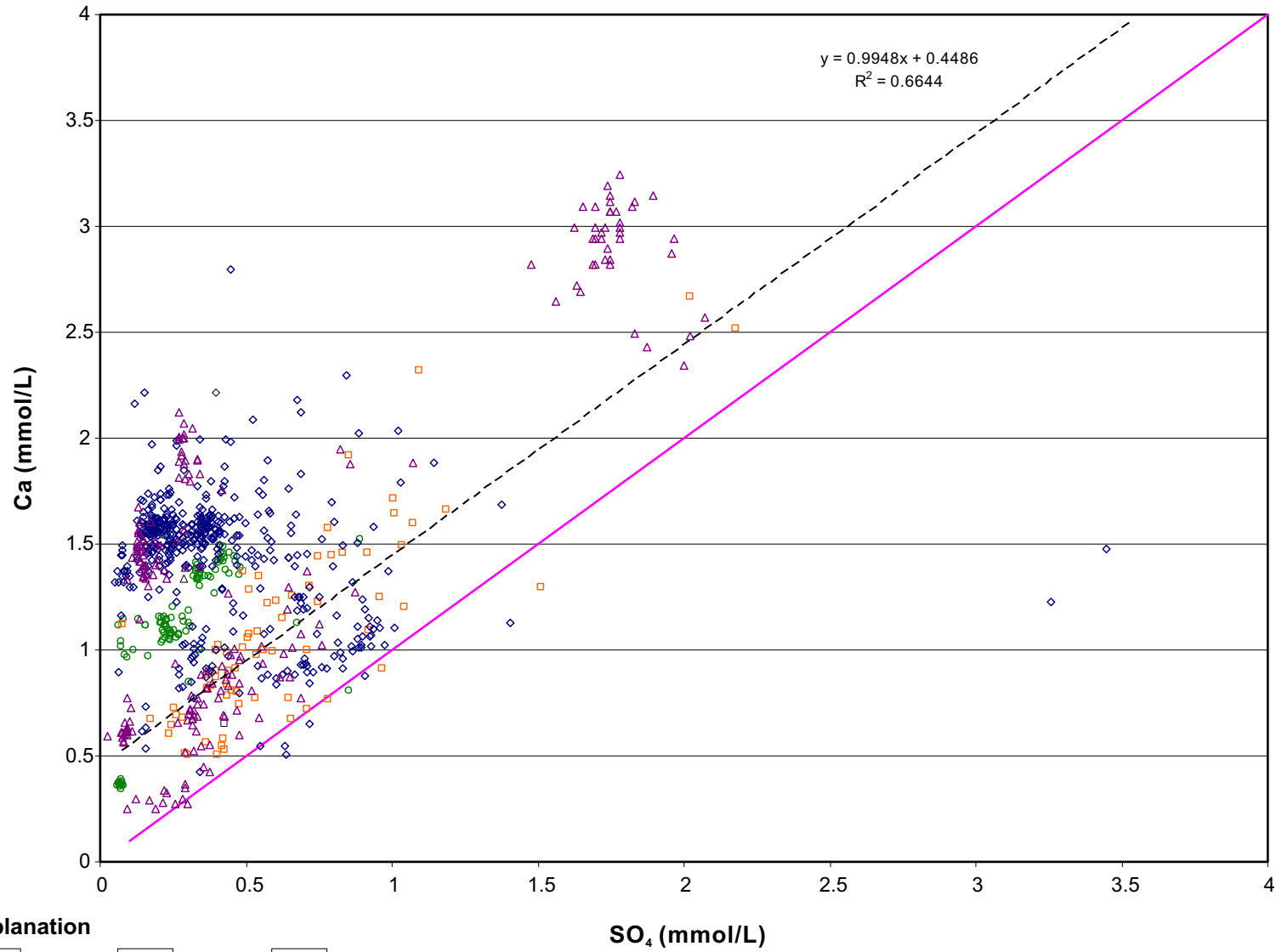
- |     |     |                   |
|-----|-----|-------------------|
| pCg | QTg | Calcite trend 2:1 |
| Qal | Tqm |                   |



TYRONE BACKGROUND WATER QUALITY  
**Calcite Dissolution Reaction**

Figure A-10





**Explanation**

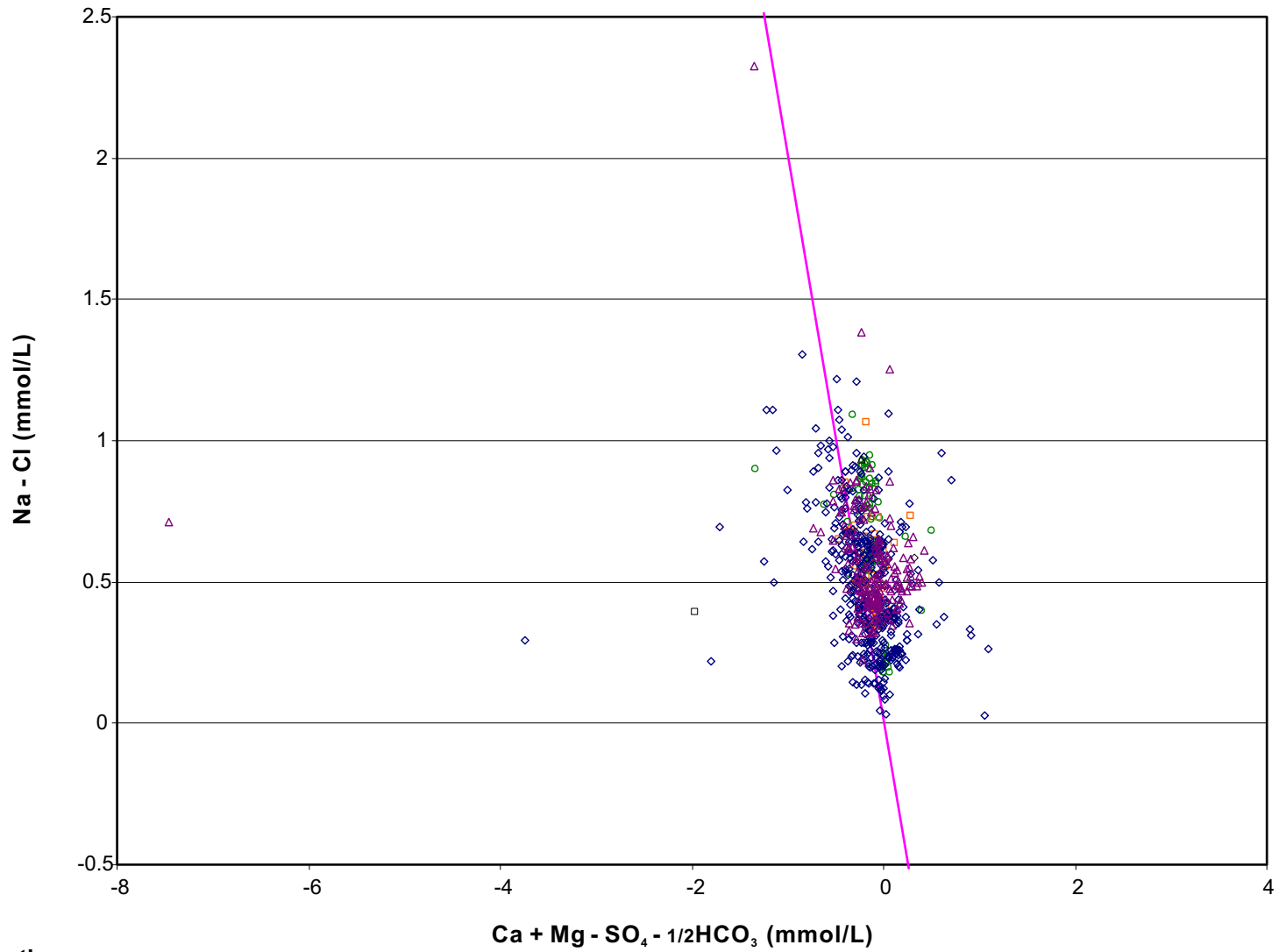
- |     |     |                  |
|-----|-----|------------------|
| pCg | QTg | Gypsum trend 1:1 |
| Qal | Tqm | Linear (Qal)     |



TYRONE BACKGROUND WATER QUALITY  
**Gypsum Dissolution Reaction**

Figure A-11





**Explanation**

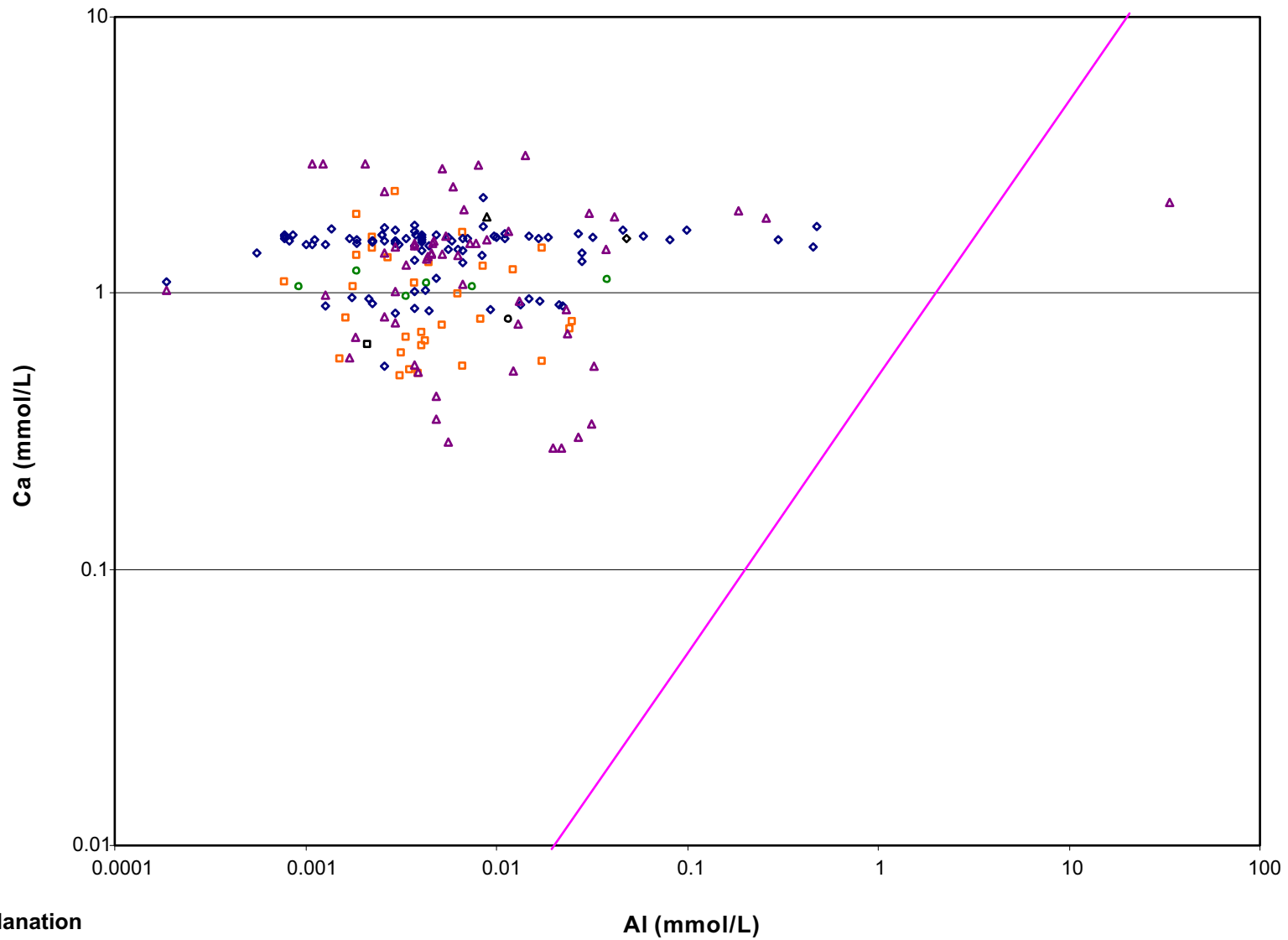
- pCg
- ◇ QTg
- Cation exchange trend
- Qal
- △ Tqm



TYRONE BACKGROUND WATER QUALITY  
**Ion Exchange Reactions**

Figure A-12





Explanation

- pCg
- QTg
- Feldspar trend 2:1
- Qal
- Tqm

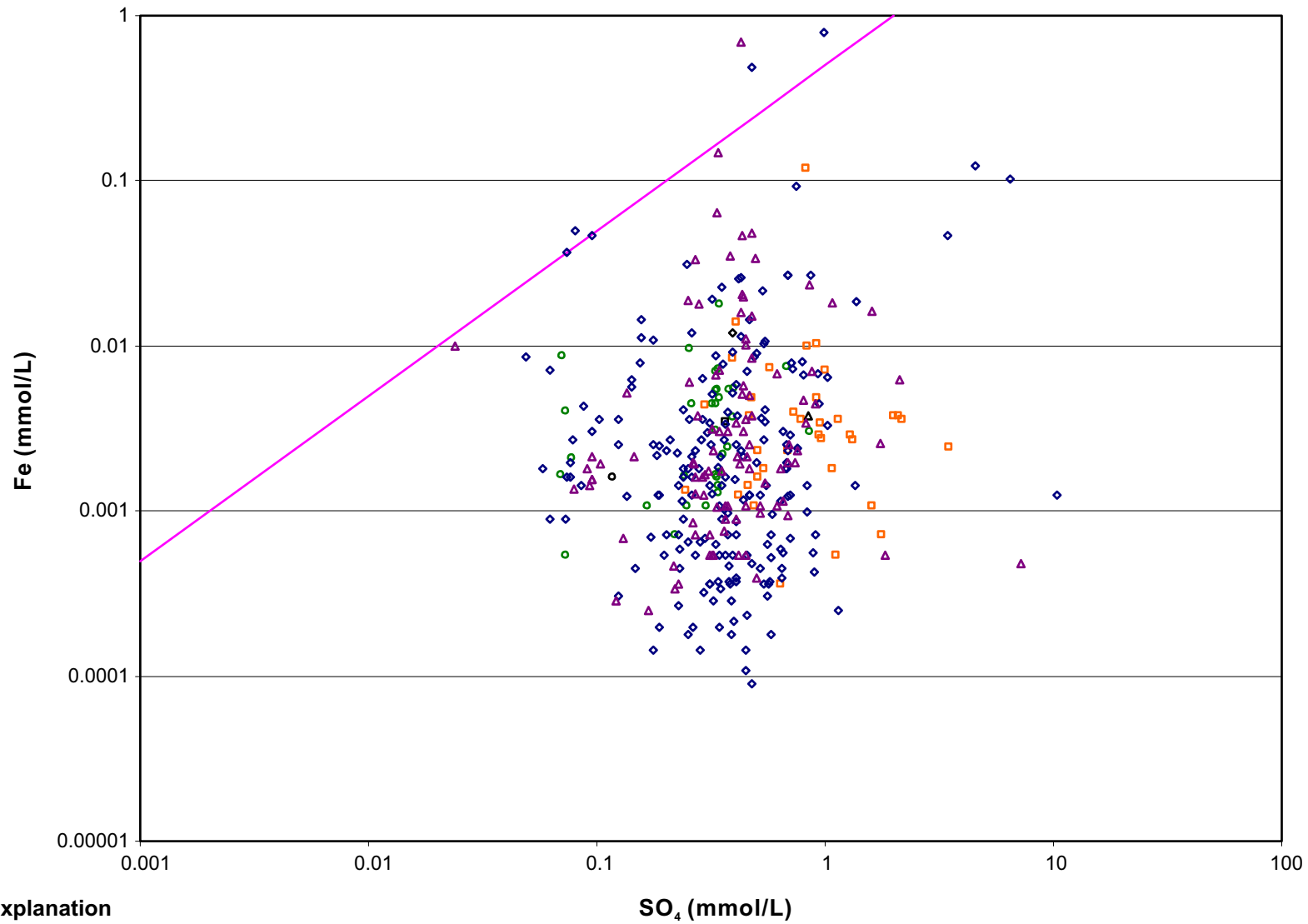


TYRONE BACKGROUND WATER QUALITY  
**Feldspar Hydrolysis (anorthite)**

Figure A-13







Explanation

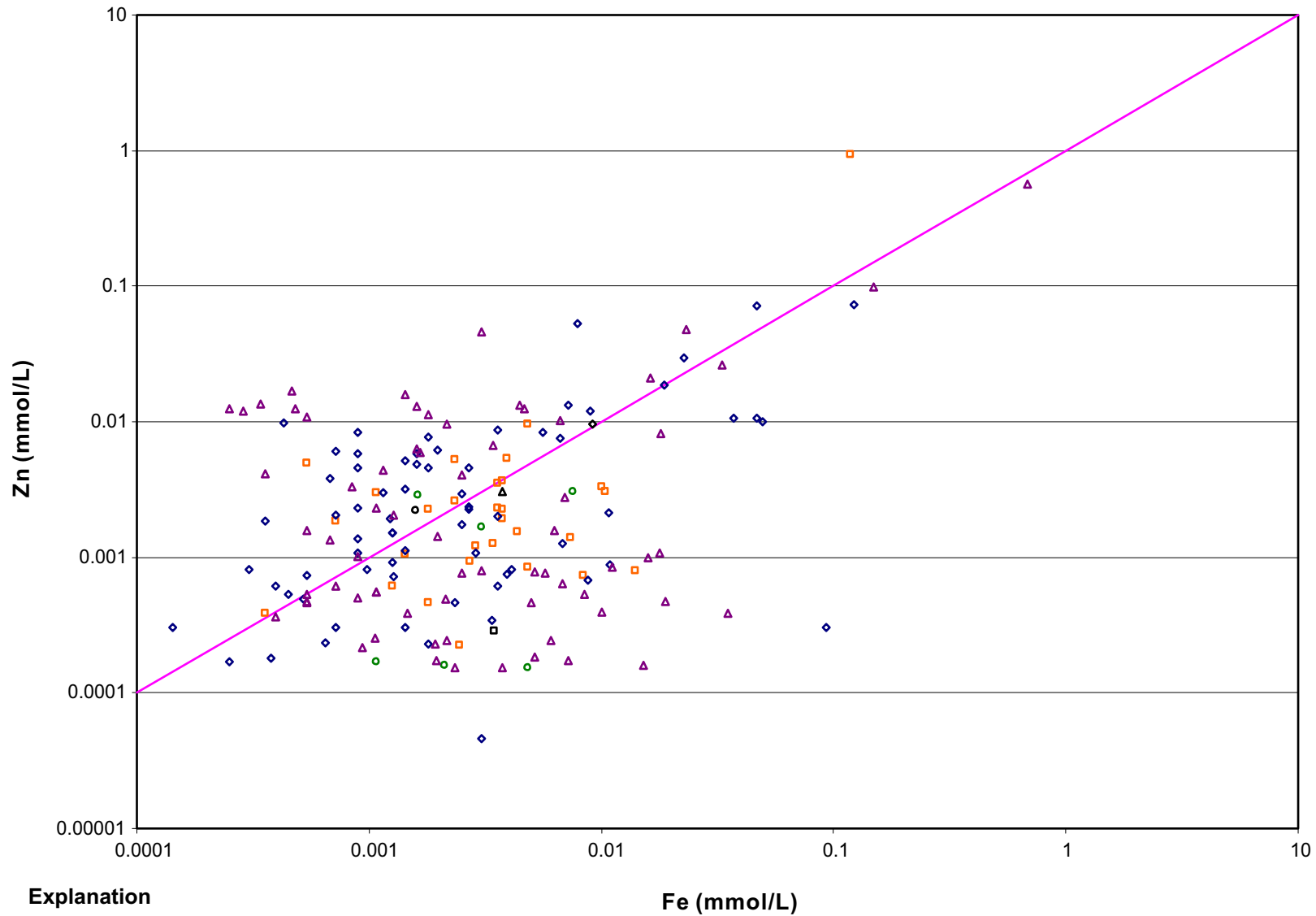
- |     |     |                  |
|-----|-----|------------------|
| pCg | QTg | Pyrite oxidation |
| Qal | Tqm |                  |



TYRONE BACKGROUND WATER QUALITY  
**Pyrite Dissolution Reaction**

Figure A-14





Explanation

- pCg
- QTg
- 1:1 trend
- Qal
- Tqm

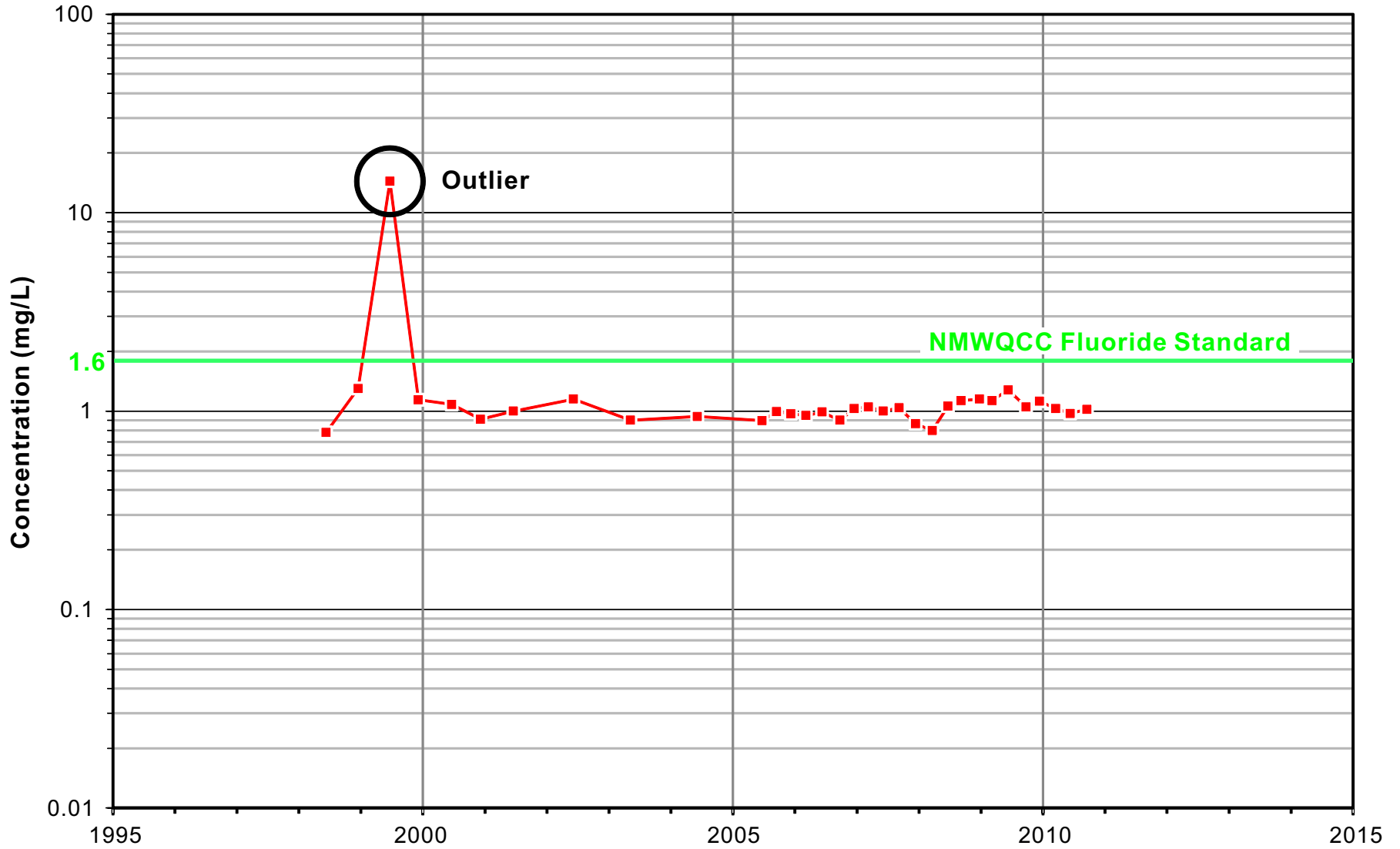


TYRONE BACKGROUND WATER QUALITY  
**Sphalerite Dissolution Reaction**

Figure A-15



Daniel B. Stephens & Associates, Inc.  
1/16/2012 JN ES11.0090



**Explanation**

■ Fluoride concentration (mg/L)



TYRONE BACKGROUND WATER QUALITY  
**Fluoride Concentrations in Groundwater Over Time**  
**Well 2-11**

Figure A-16



Daniel B. Stephens & Associates, Inc.  
11/21/2011 JN ES11.0090

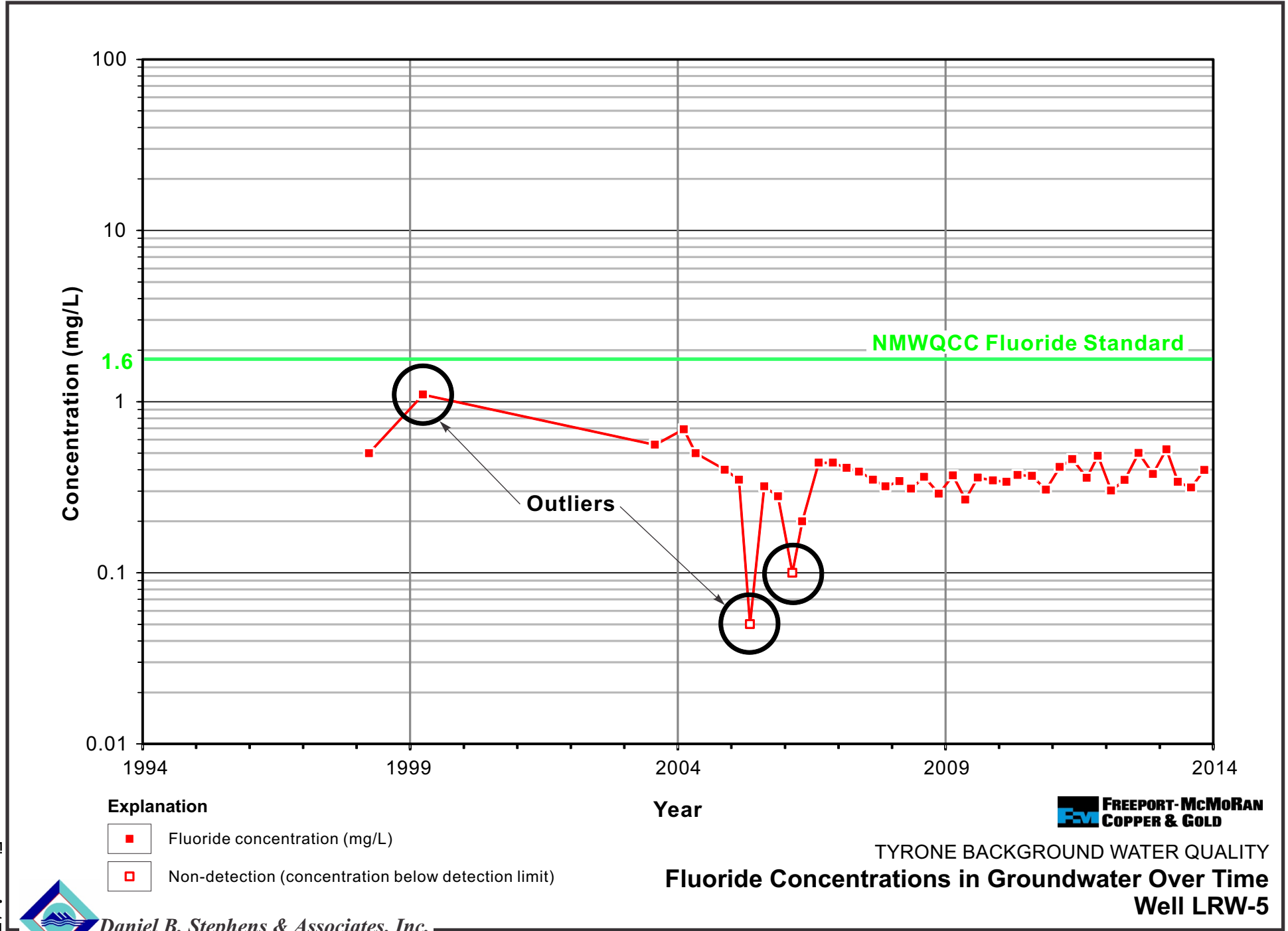
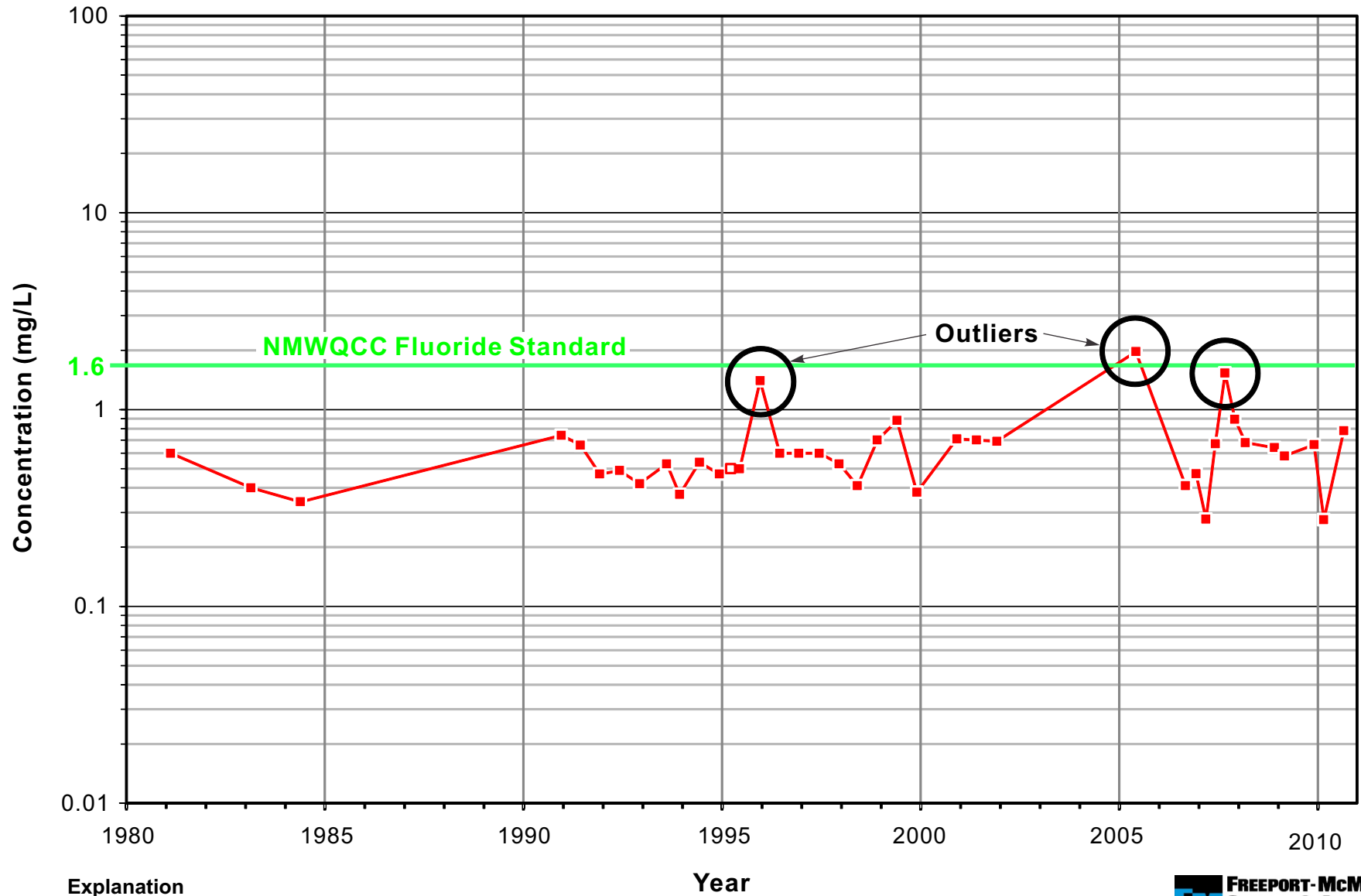


Figure A-17





**Explanation**

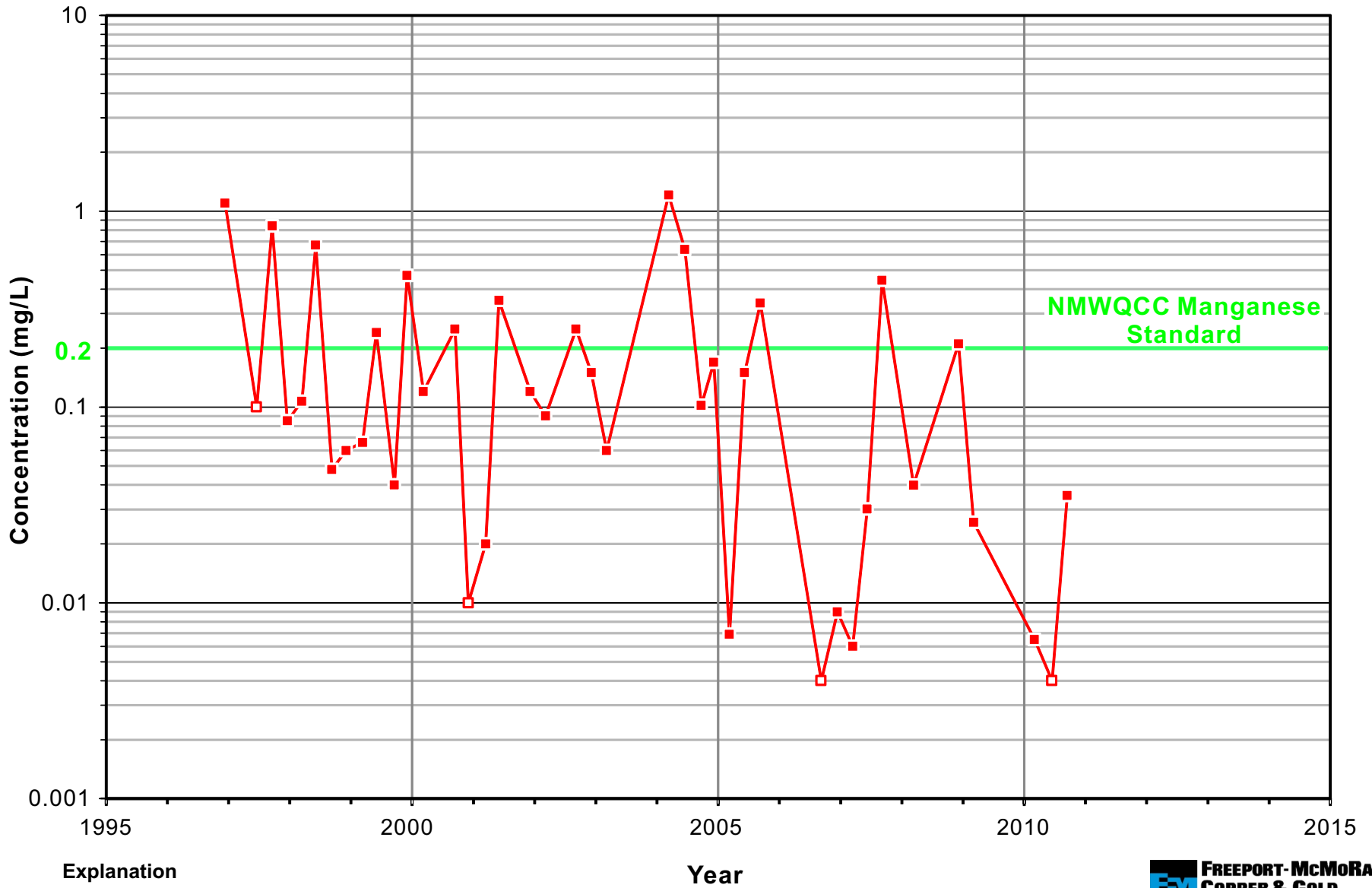
- Fluoride concentration (mg/L)
- Non-detection (concentration below detection limit)



TYRONE BACKGROUND WATER QUALITY  
**Fluoride Concentrations in Groundwater Over Time**  
Well TWS-7

Figure A-18





**Explanation**

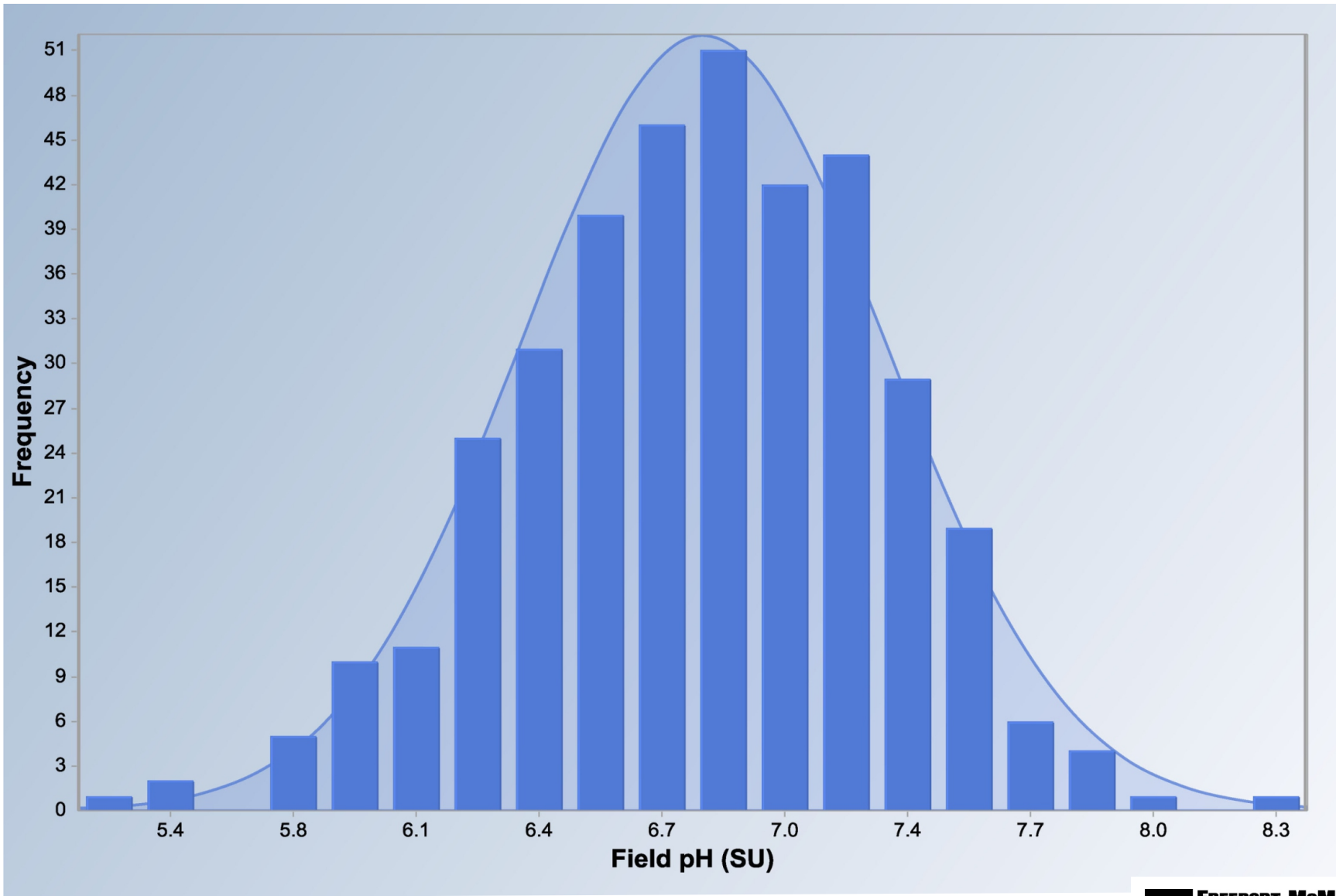
- Manganese concentration (mg/L)
- Non-detection (concentration below detection limit)



TYRONE BACKGROUND WATER QUALITY  
**Manganese Concentrations in Groundwater Over Time**  
Well TWS-33

Figure A-19

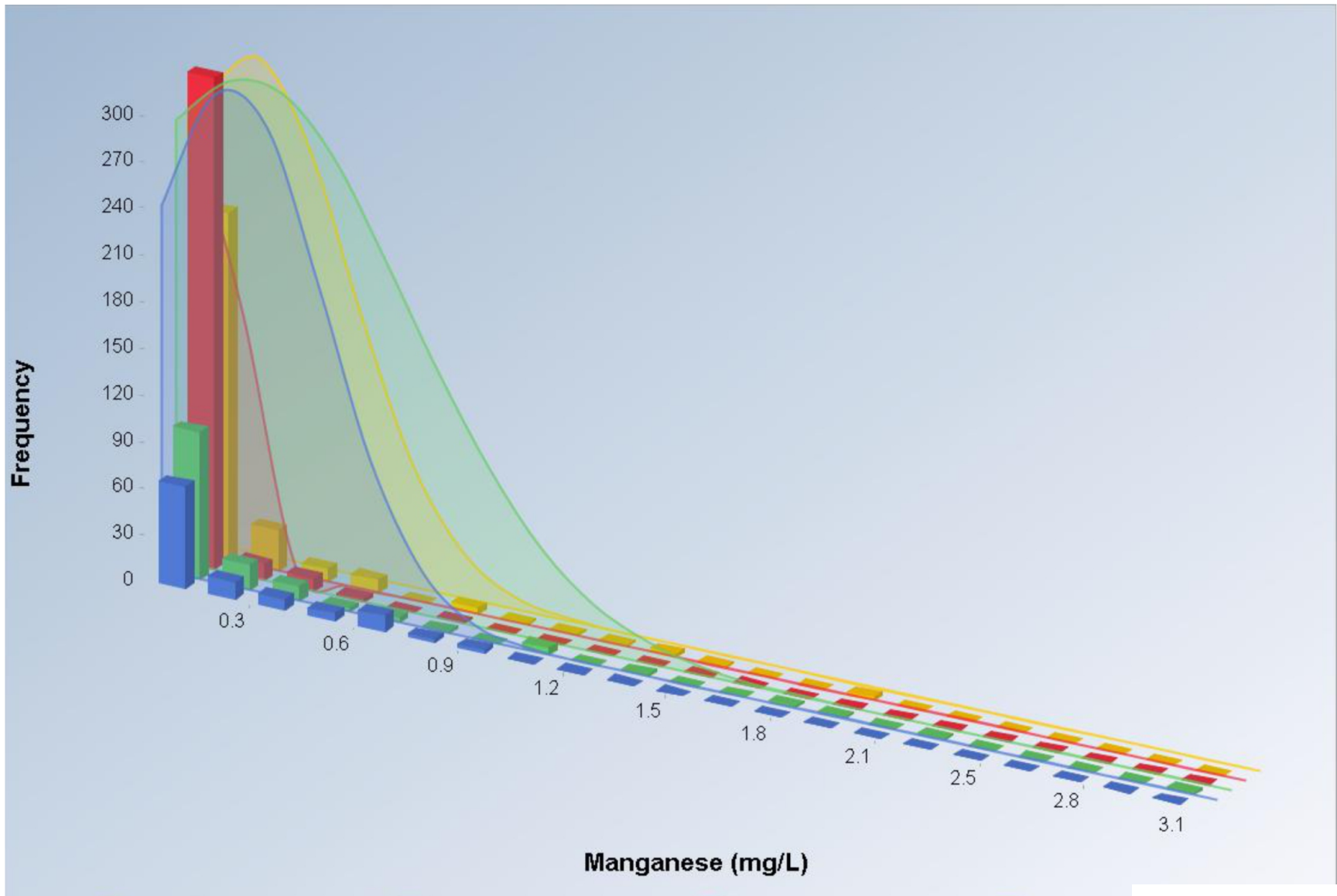




TYRONE BACKGROUND WATER QUALITY  
**Histogram of Field pH in All Background  
Wells Screened in Quartz Monzonite**

Figure A-20





Explanation	
<span style="color: blue;">■</span> pCg	<span style="color: red;">■</span> QTg
<span style="color: green;">■</span> Qal	<span style="color: yellow;">■</span> Tqm

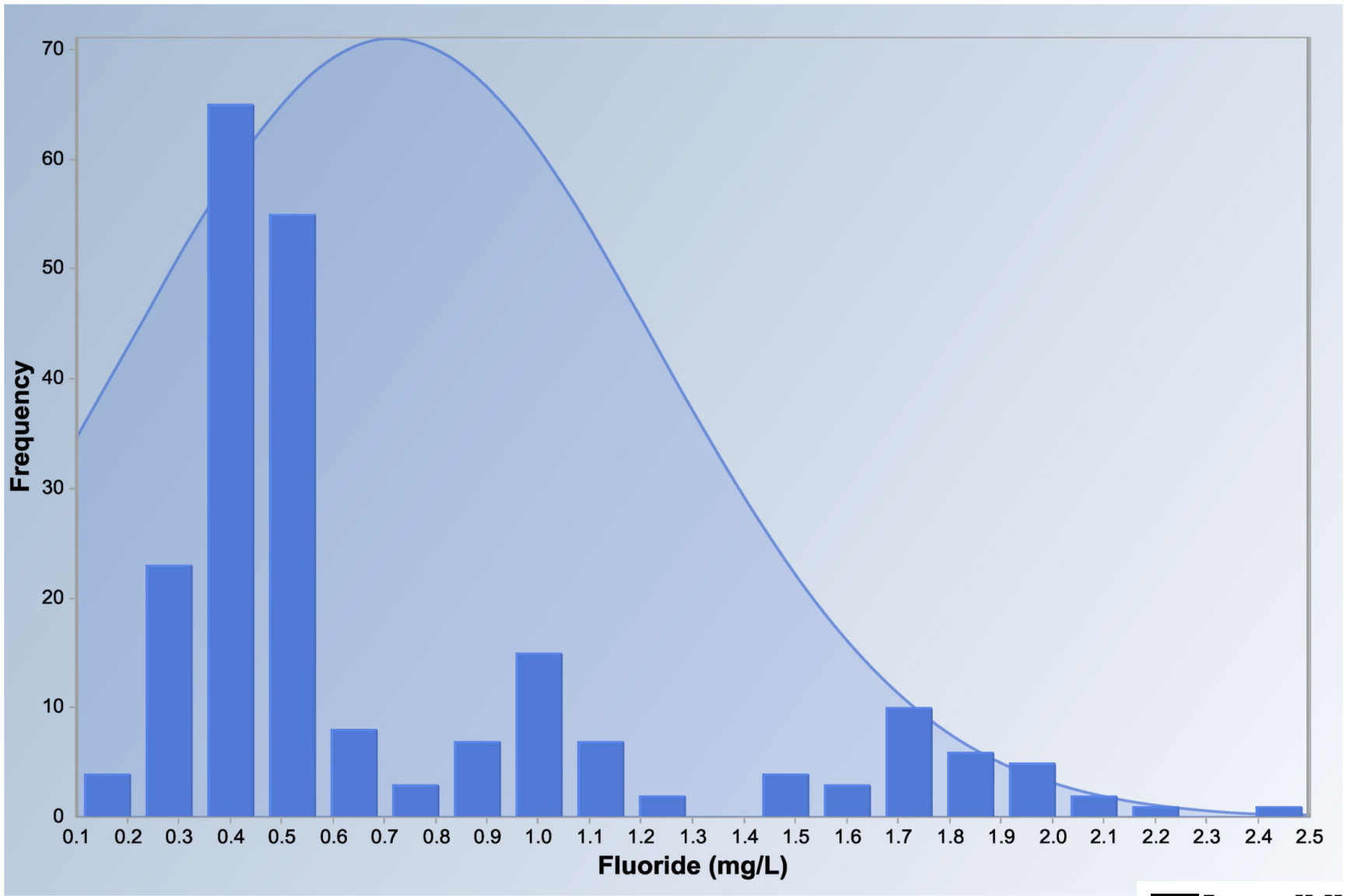


TYRONE BACKGROUND WATER QUALITY  
**Histograms of Manganese in All Background Wells Grouped by Geologic Unit**

Figure A-21



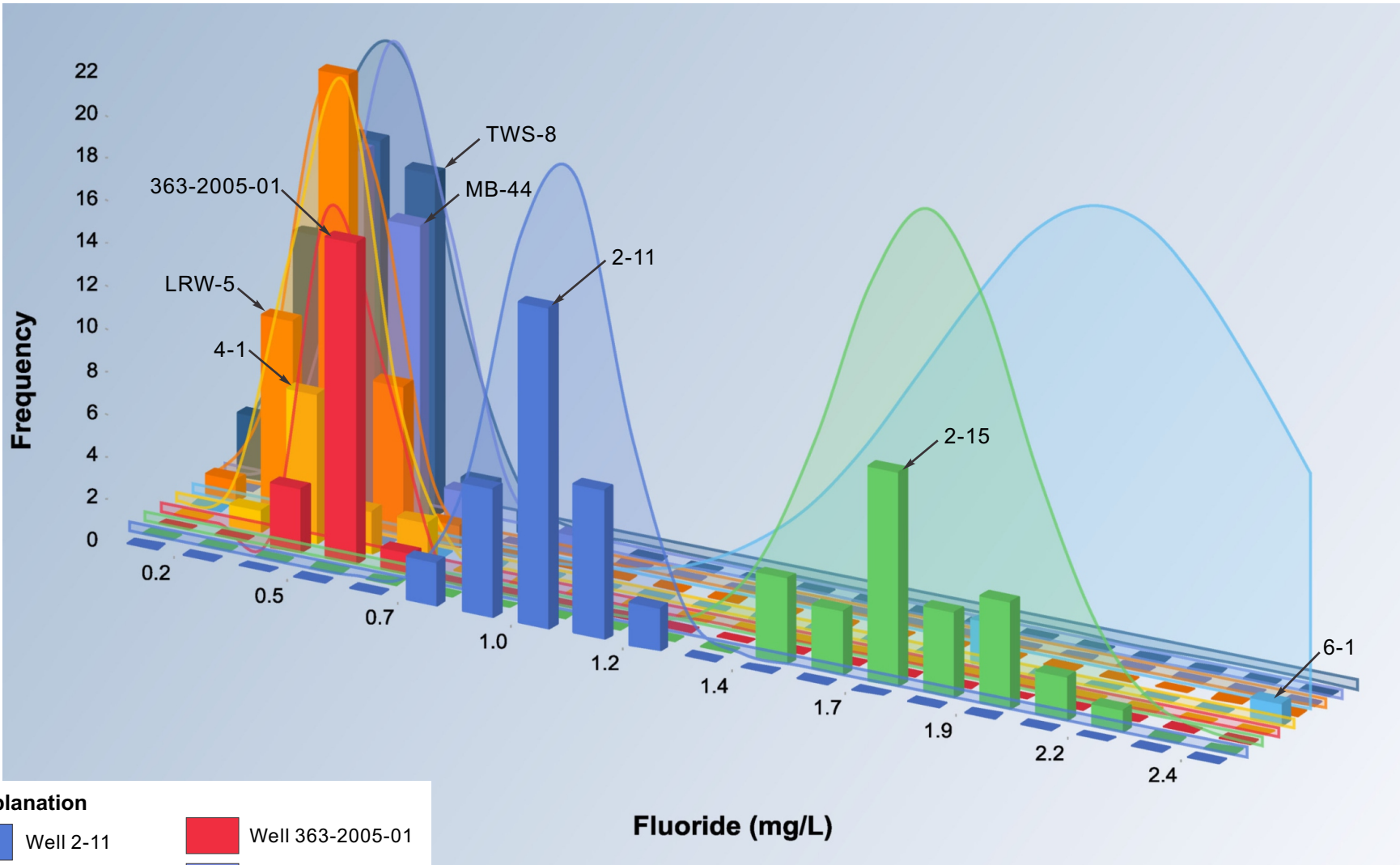












TYRONE BACKGROUND WATER QUALITY  
**Histogram of Fluoride in All Background  
Wells Screened in Quartz Monzonite**

Figure A-22





**Explanation**

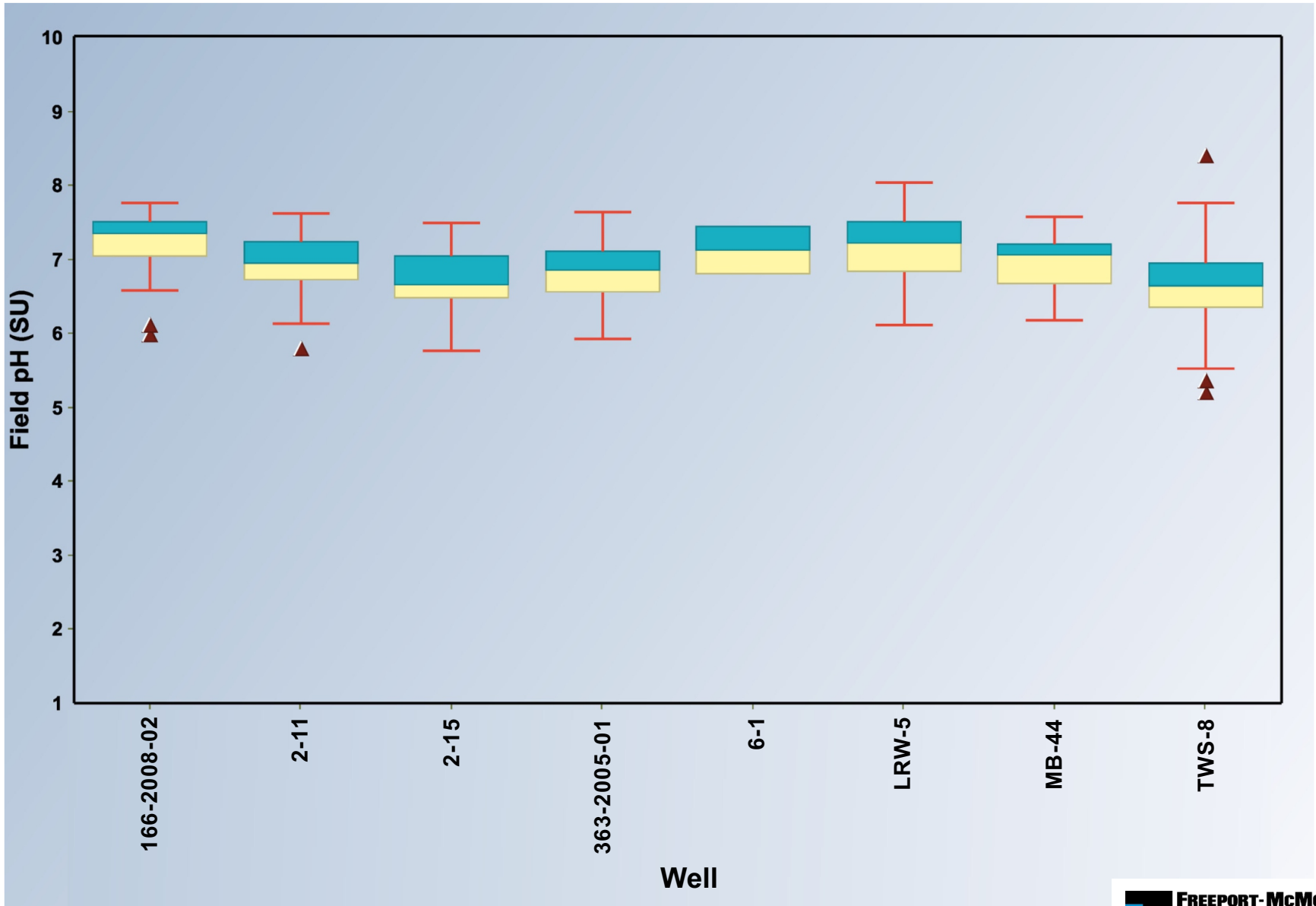
- |   |            |   |                  |
|---|------------|---|------------------|
|  | Well 2-11  |  | Well 363-2005-01 |
|  | Well 6-1   |  | Well MB-44       |
|  | Well 2-15  |  | Well 4-1         |
|  | Well LRW-5 |  | Well TWS-8       |



TYRONE BACKGROUND WATER QUALITY  
**Histograms of Fluoride in Individual  
 Background Wells Screened in Quartz Monzonite**

Figure A-23

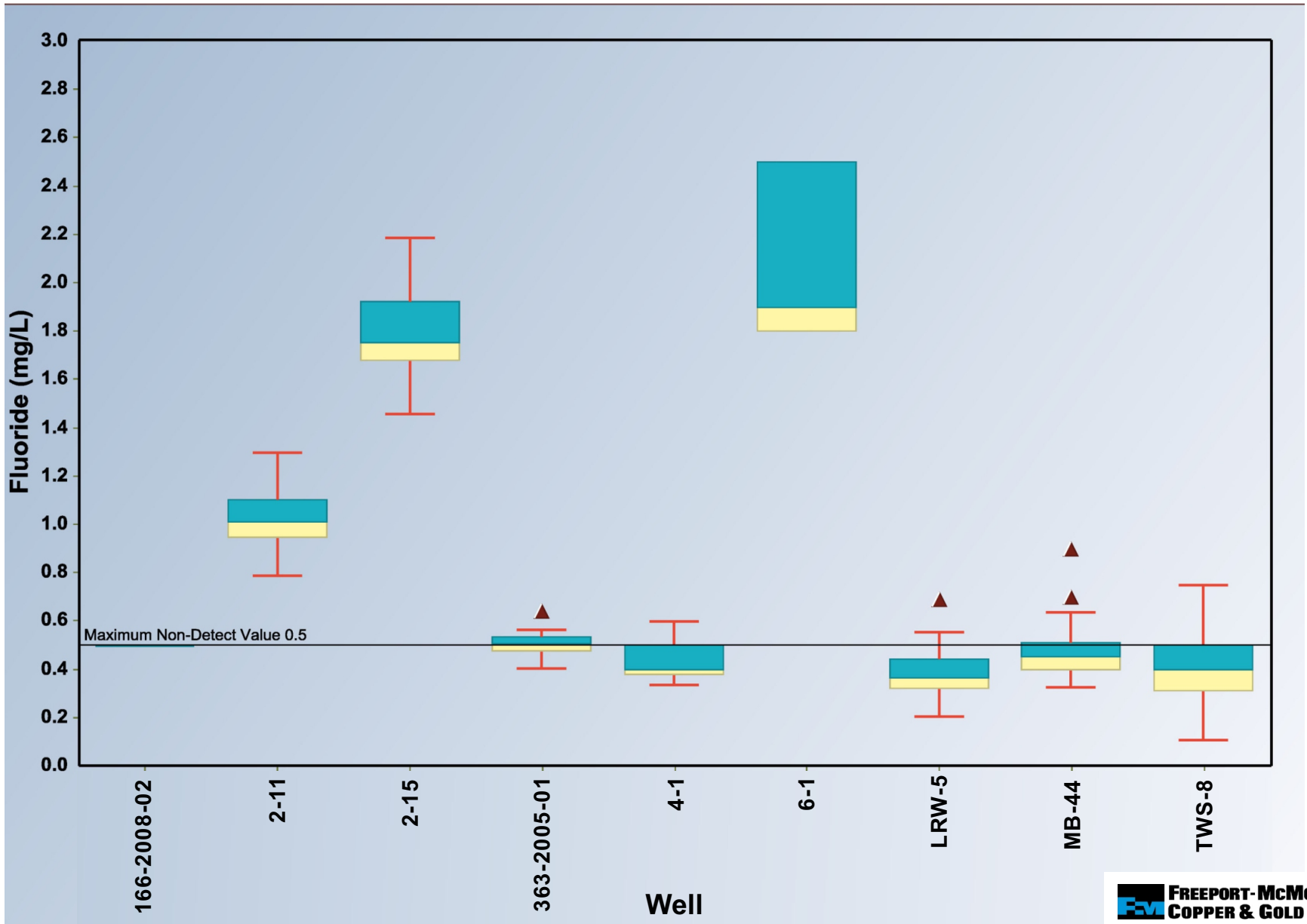




TYRONE BACKGROUND WATER QUALITY  
**Box Plots of Field pH in Individual  
Background Wells Screened in Quartz Monzonite**

Figure A-24

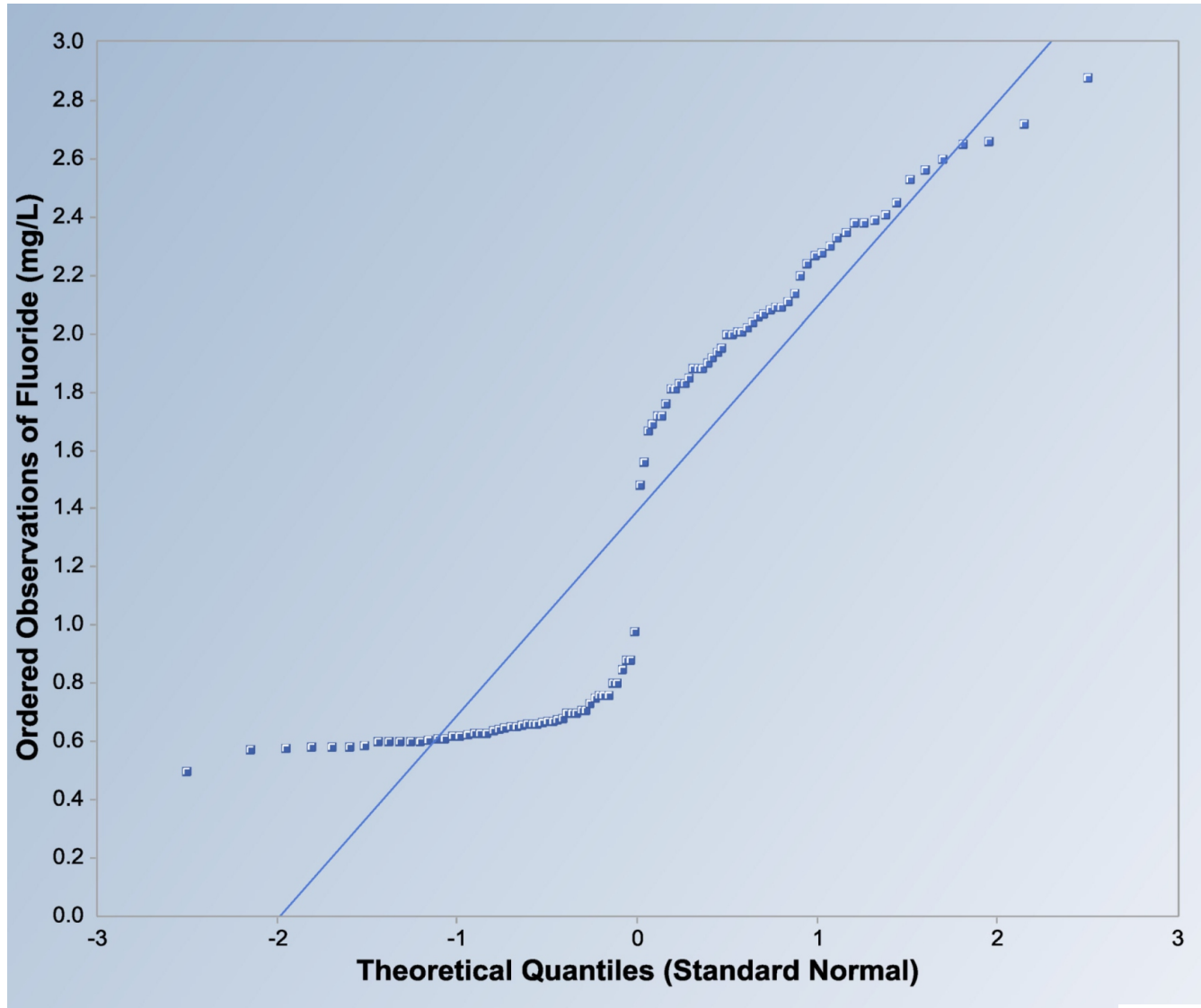




TYRONE BACKGROUND WATER QUALITY  
**Box Plots of Fluoride in Individual  
Background Wells Screened in Quartz Monzonite**

Figure A-25





**Notes:**

n = 102  
Mean = 1.389  
Sd = 0.757  
Slope = 0.702  
Intercept = 1.389  
Correlation, R = 0.917  
Lilliefors test  
Test value = 0.242  
Critical value (0.05) = 0.088  
Data not normal



TYRONE BACKGROUND WATER QUALITY  
**Normal Q-Q Plot of Fluoride in All  
Background Wells Screened in Granite**

Figure A-26



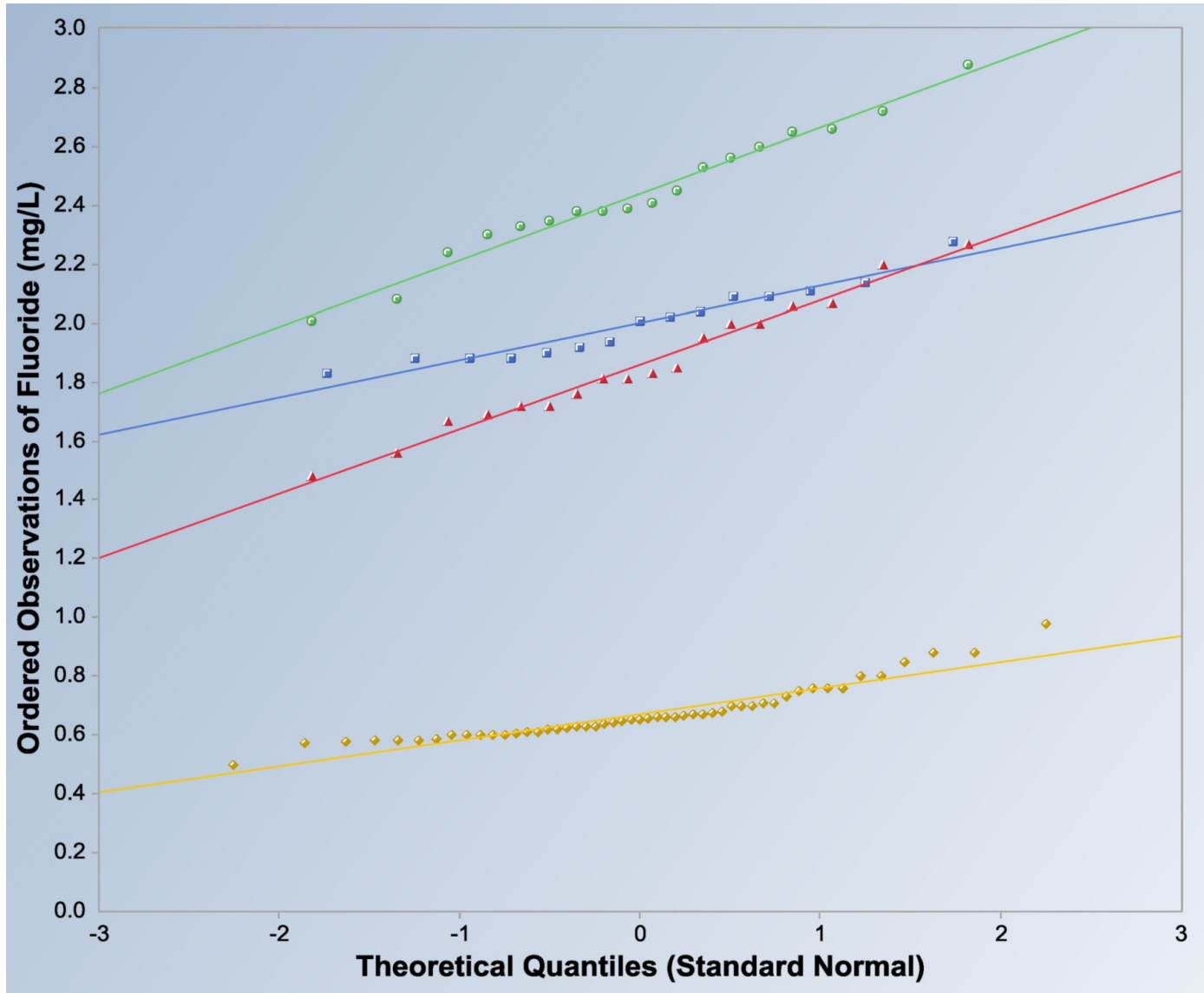
**Explanation**

**Well 435-2005-01**  
 n = 18  
 Mean = 2.44  
 Sd = 0.219  
 Slope = 0.226  
 Intercept = 2.44  
 Correlation, R = 0.989  
 Lilliefors Test  
 Test value = 0.110  
 Critical val(0.05) = 0.209  
 Data appear normal

**Well 27-2005-03**  
 n = 15  
 Mean = 2.001  
 Sd = 0.125  
 Slope = 0.127  
 Intercept = 2.001  
 Correlation, R = 0.969  
 Lilliefors Test  
 Test value = 0.152  
 Critical val(0.05) = 0.229  
 Data appear normal

**Well 435-2005-03**  
 n = 18  
 Mean = 1.858  
 Sd = 0.213  
 Slope = 0.219  
 Intercept = 1.858  
 Correlation, R = 0.991  
 Lilliefors Test  
 Test value = 0.127  
 Critical val(0.05) = 0.209  
 Data appear normal

**Well MB-31**  
 n = 51  
 Mean = 0.672  
 Sd = 0.0916  
 Slope = 0.0882  
 Intercept = 0.672  
 Correlation, R = 0.945  
 Lilliefors Test  
 Test value = 0.154  
 Critical val(0.05) = 0.124  
 Data not normal

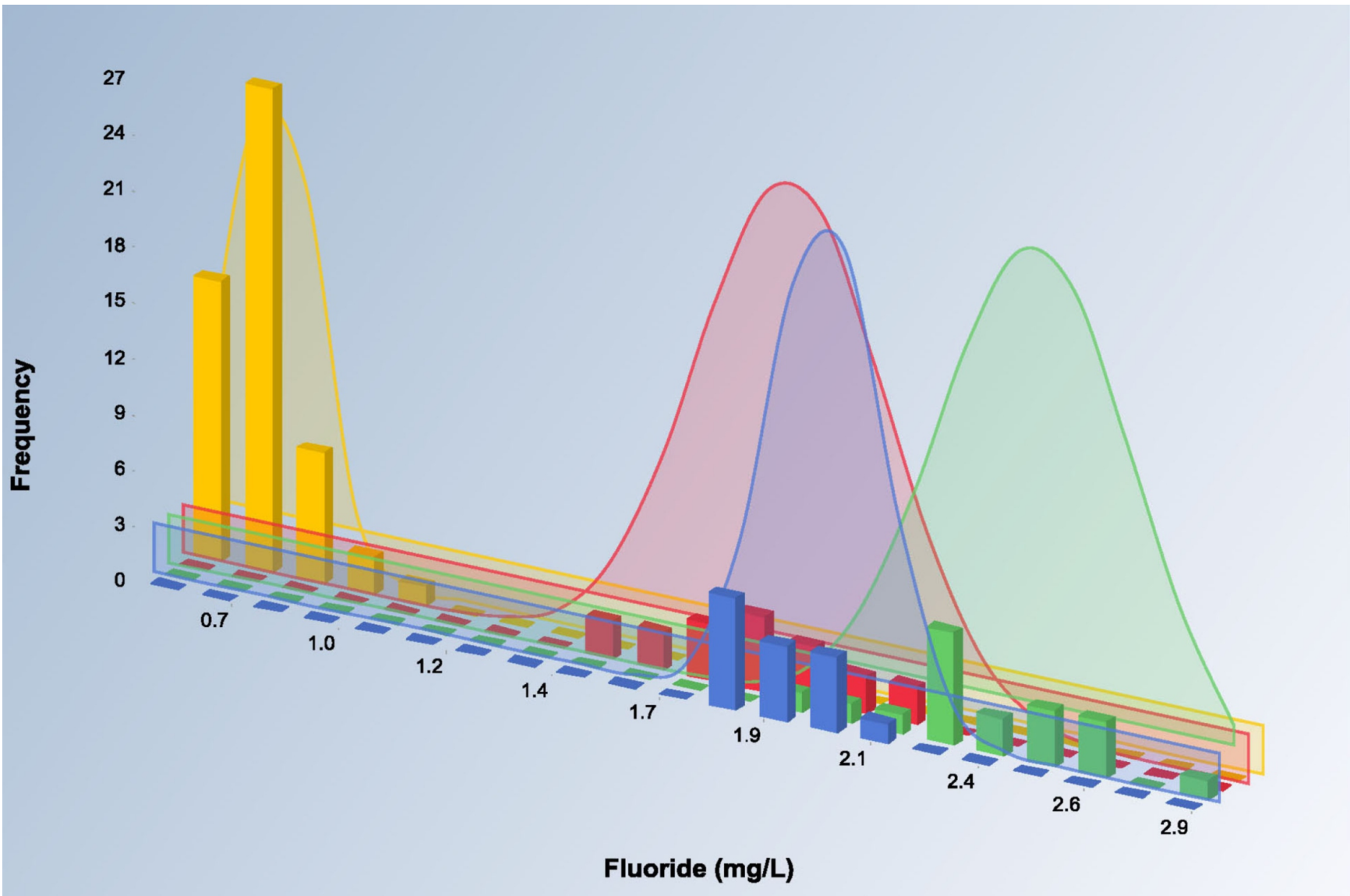


TYRONE BACKGROUND WATER QUALITY  
**Normal Q-Q Plots of Fluoride in Individual  
 Background Wells Screened in Granite**

Figure A-27







**Explanation**

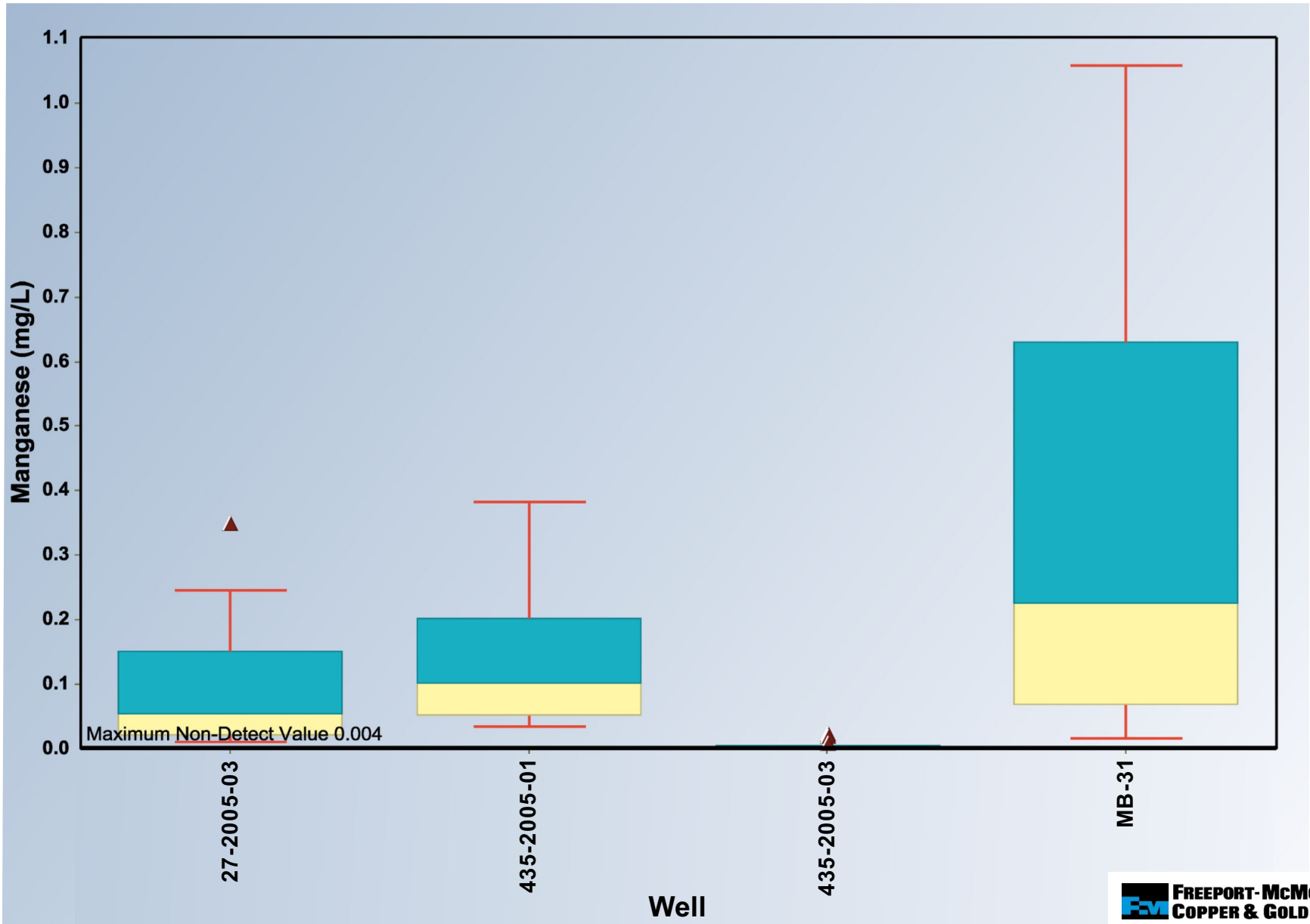
<span style="color: blue;">■</span> Well 27-2005-03	<span style="color: red;">■</span> Well 435-2005-03
<span style="color: green;">■</span> Well 435-2005-01	<span style="color: yellow;">■</span> Well MB-31



TYRONE BACKGROUND WATER QUALITY  
**Histograms of Fluoride in Individual  
 Background Wells Screened in Granite**

Figure A-28



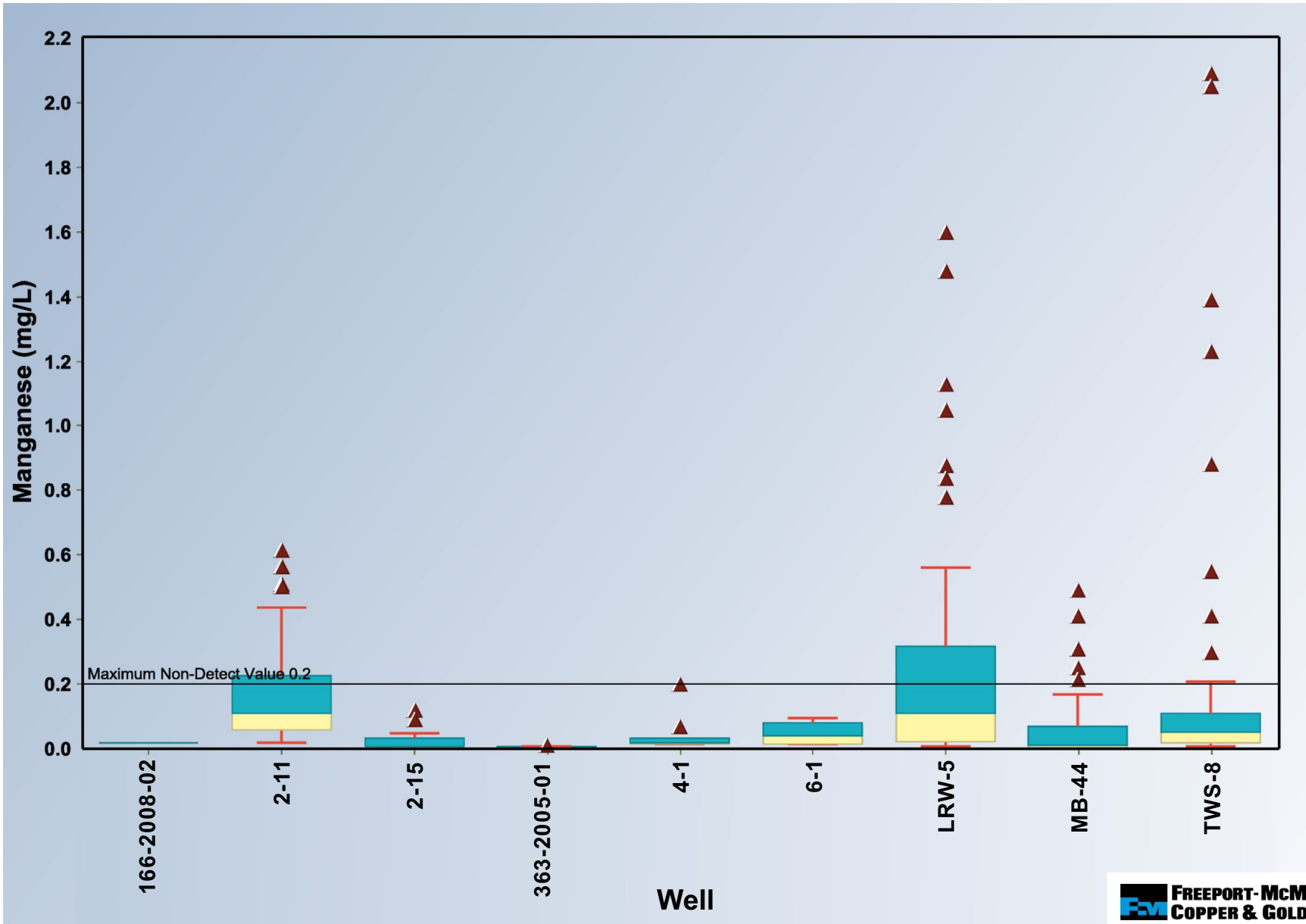


TYRONE BACKGROUND WATER QUALITY  
**Box Plots of Manganese in Individual  
Background Wells Screened in Granite**

Figure A-29







TYRONE BACKGROUND WATER QUALITY  
**Box Plots of Manganese in Individual  
Background Wells Screened in Quartz Monzonite**

Figure A-30



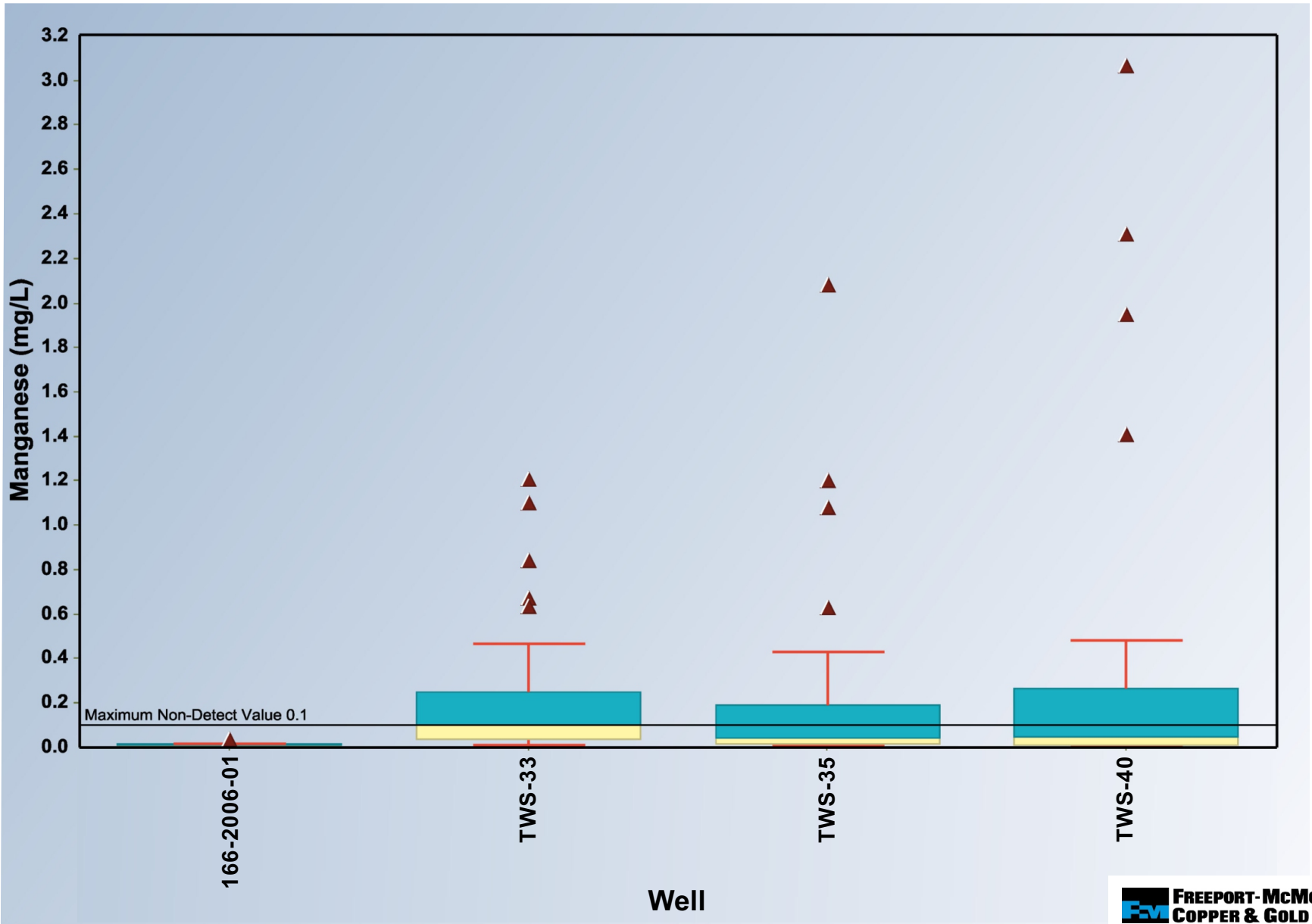
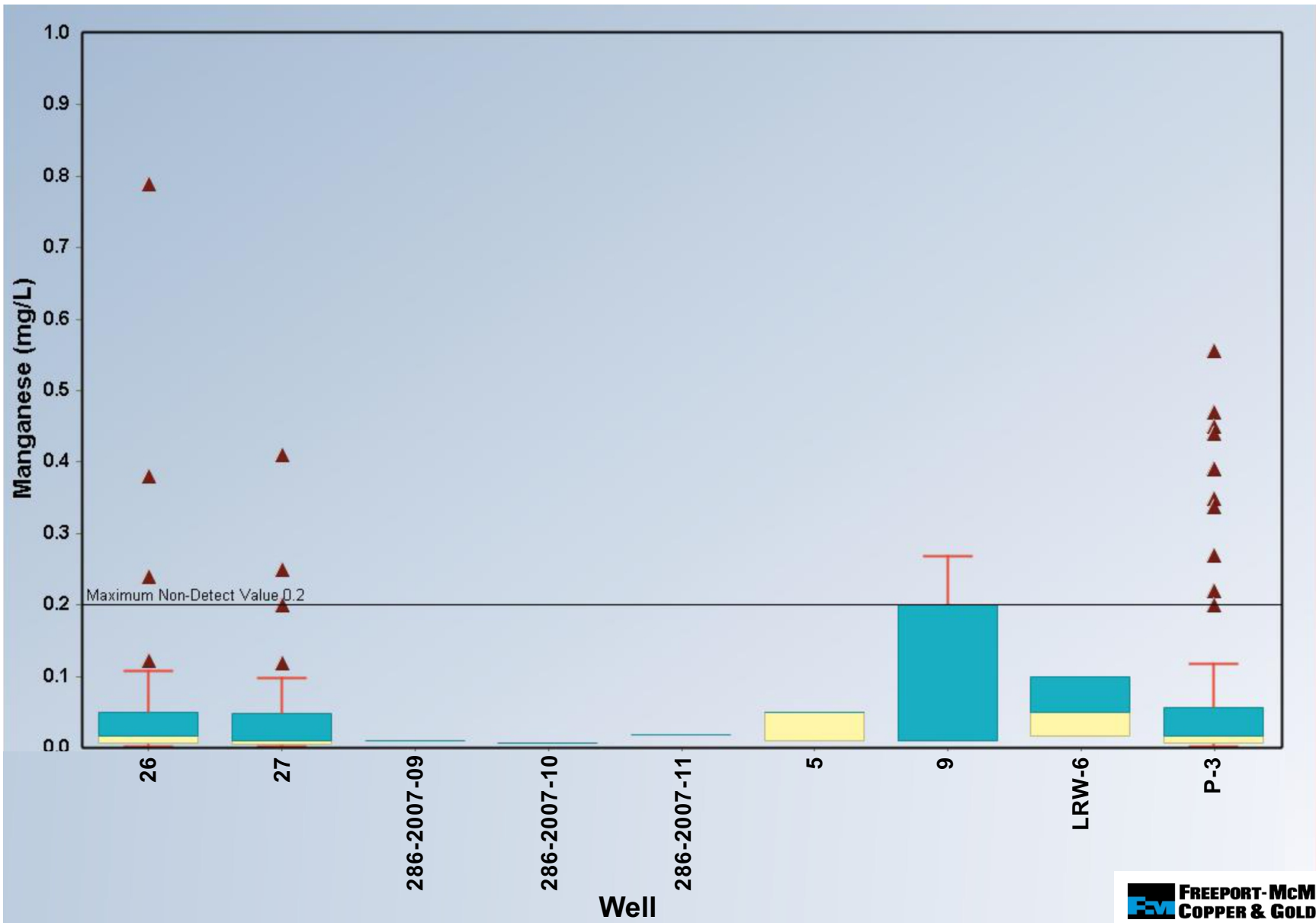


Figure A-31

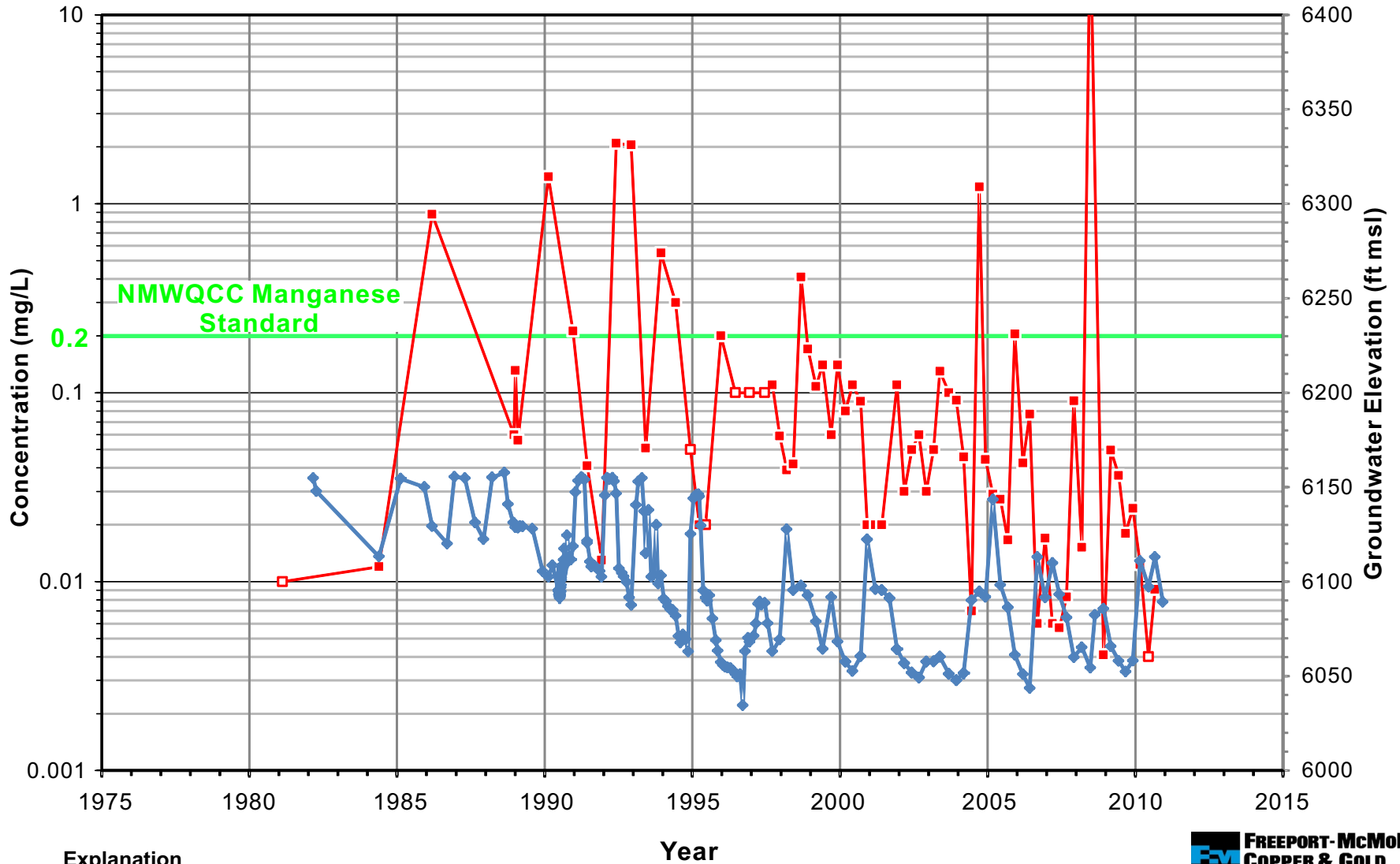




TYRONE BACKGROUND WATER QUALITY  
**Box Plots of Manganese in Individual  
Background Wells Screened in Gila Conglomerate**

Figure A-32





**Explanation**

- Manganese concentration (mg/L)
- Non-detection (concentration below detection limit)
- ◆ Groundwater elevation (ft msl)



TYRONE BACKGROUND WATER QUALITY

**Manganese Concentrations in Groundwater and Groundwater Elevations Over Time Well TWS-8**

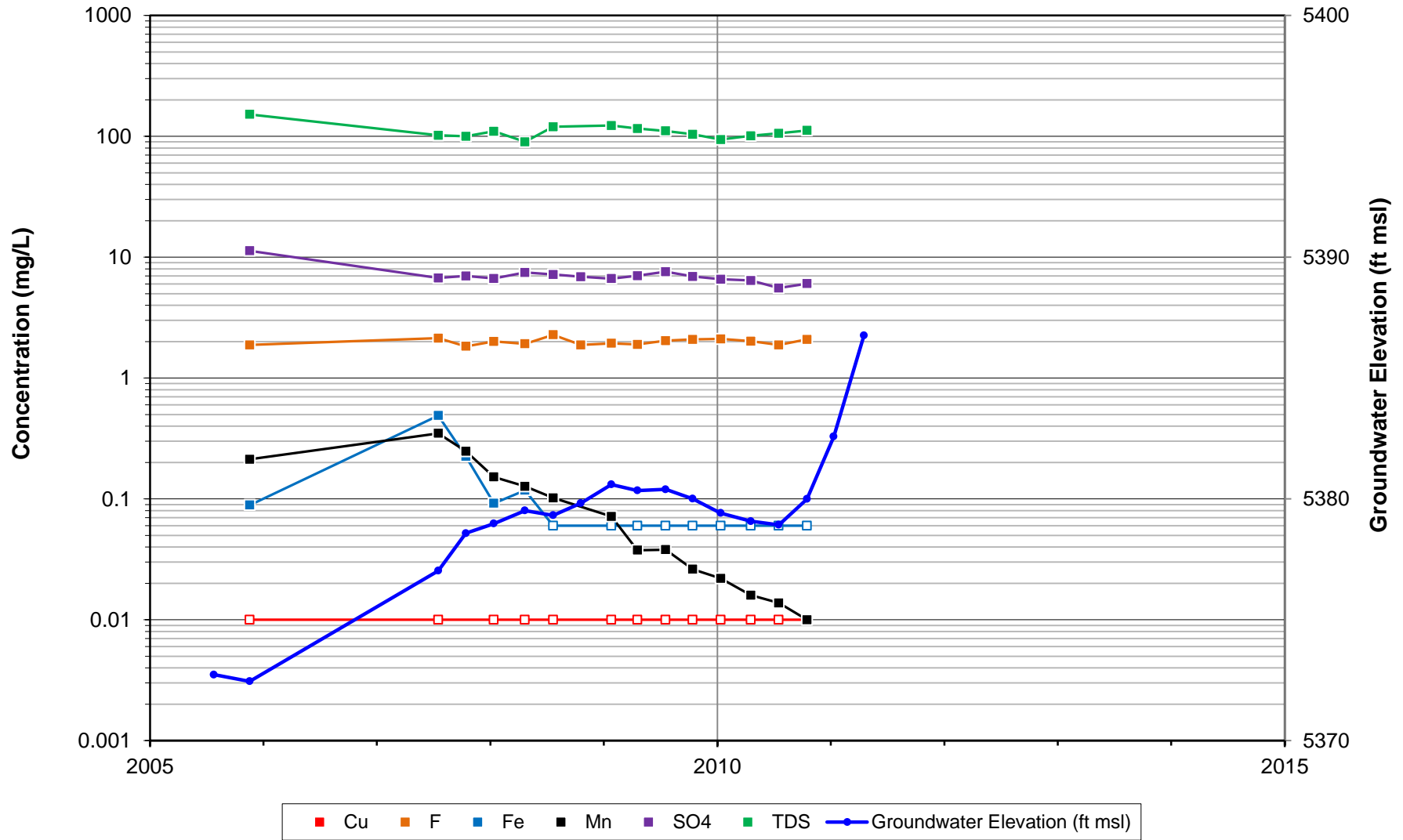
Figure A-33



## **Attachment A-1**

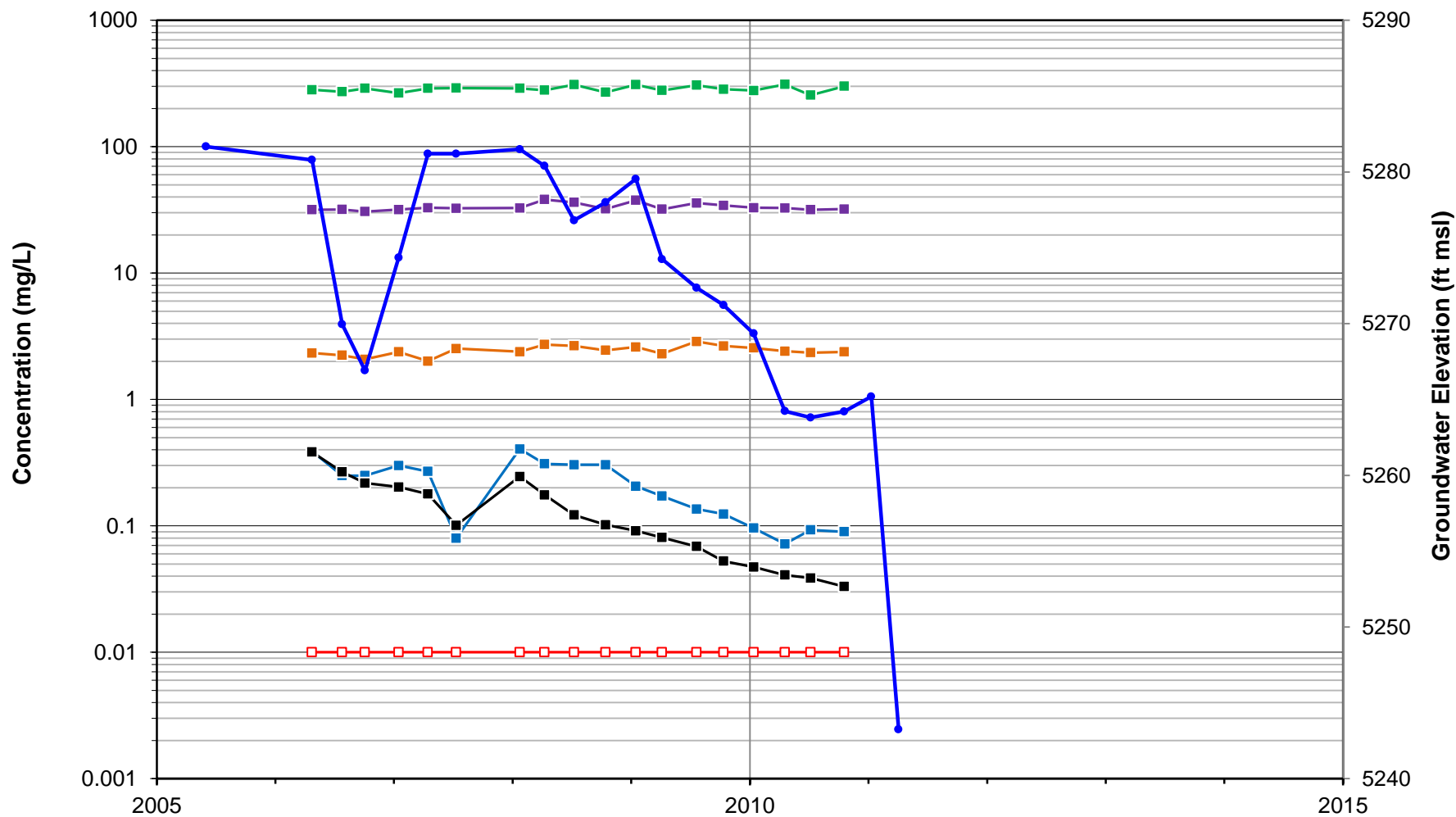
### **Temporal Trends in Background Dataset**

**Chemical Timeseries and Well Hydrograph  
27-2005-03 (pCg)**



**Note: Open symbols indicate nondetections posted at relevant reporting limits.  
Some unknown historical reporting limits assumed from common values.  
All concentration and groundwater elevation data plotted (outliers included).**

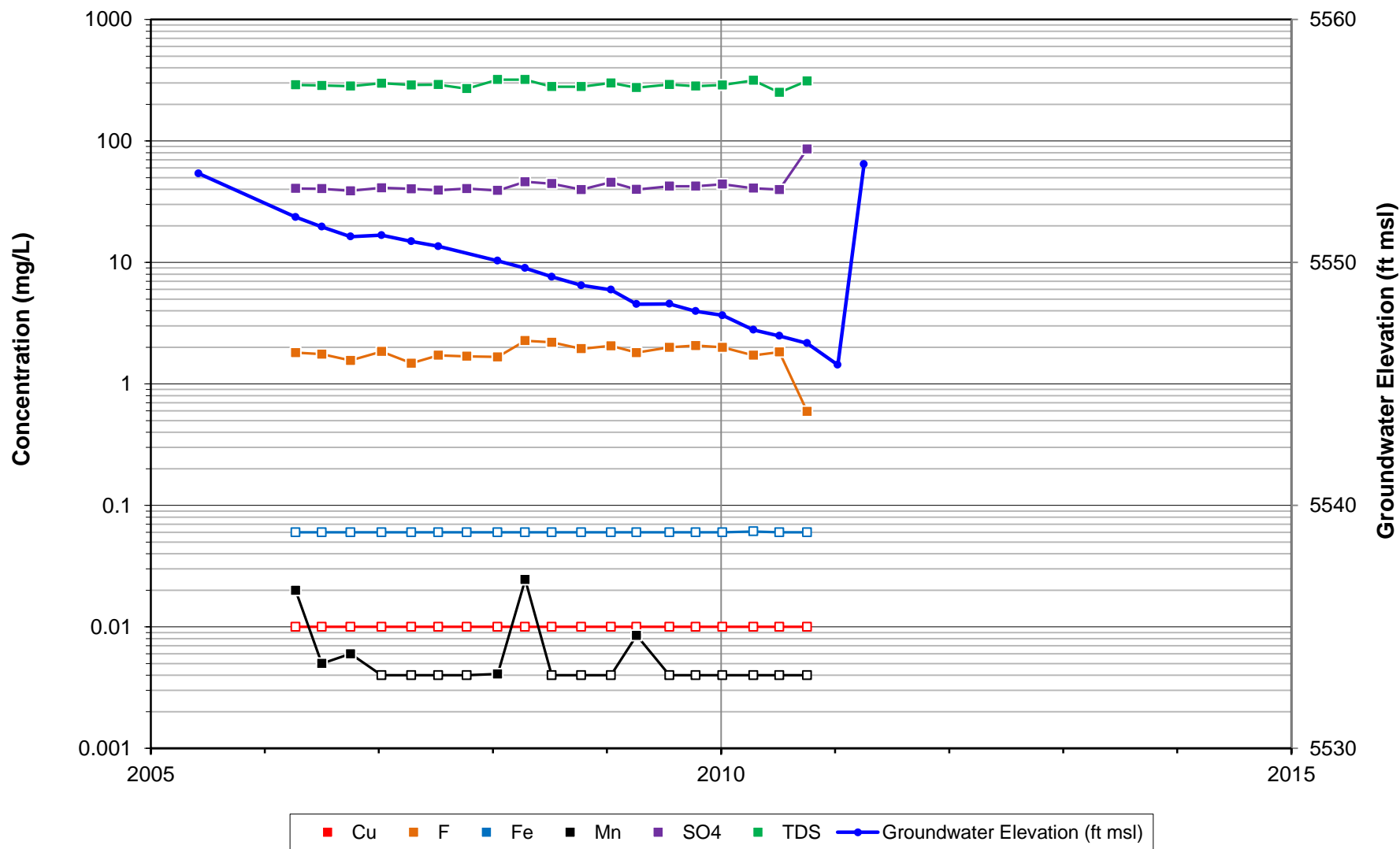
### Chemical Timeseries and Well Hydrograph 435-2005-01 (pCg)



■ Cu   
 ■ F   
 ■ Fe   
 ■ Mn   
 ■ SO4   
 ■ TDS   
 —●— Groundwater Elevation (ft msl)

**Note: Open symbols indicate nondetections posted at relevant reporting limits.  
 Some unknown historical reporting limits assumed from common values.  
 All concentration and groundwater elevation data plotted (outliers included).**

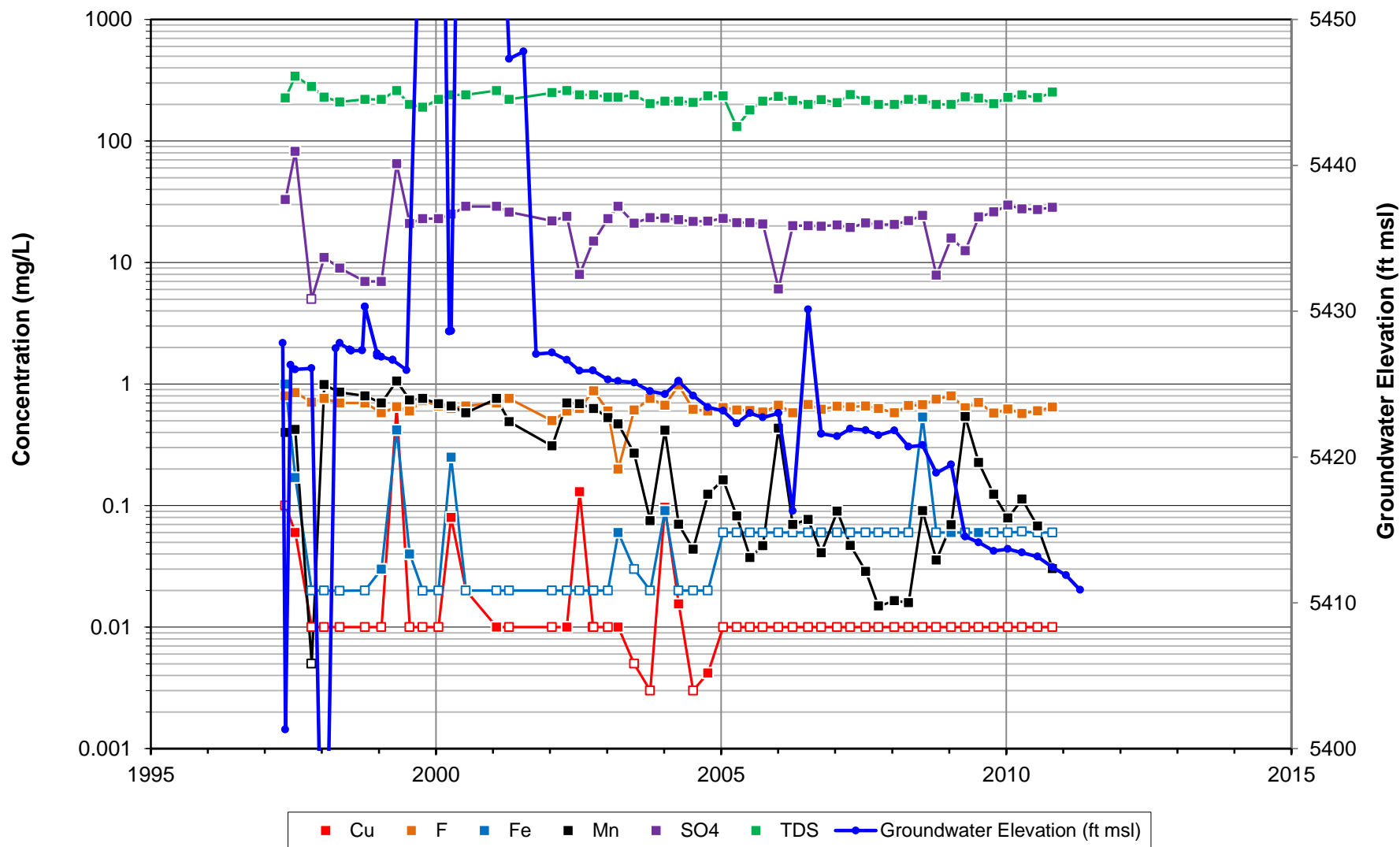
### Chemical Timeseries and Well Hydrograph 435-2005-03 (pCg)



**Note: Open symbols indicate nondetections posted at relevant reporting limits.  
Some unknown historical reporting limits assumed from common values.  
All concentration and groundwater elevation data plotted (outliers included).**

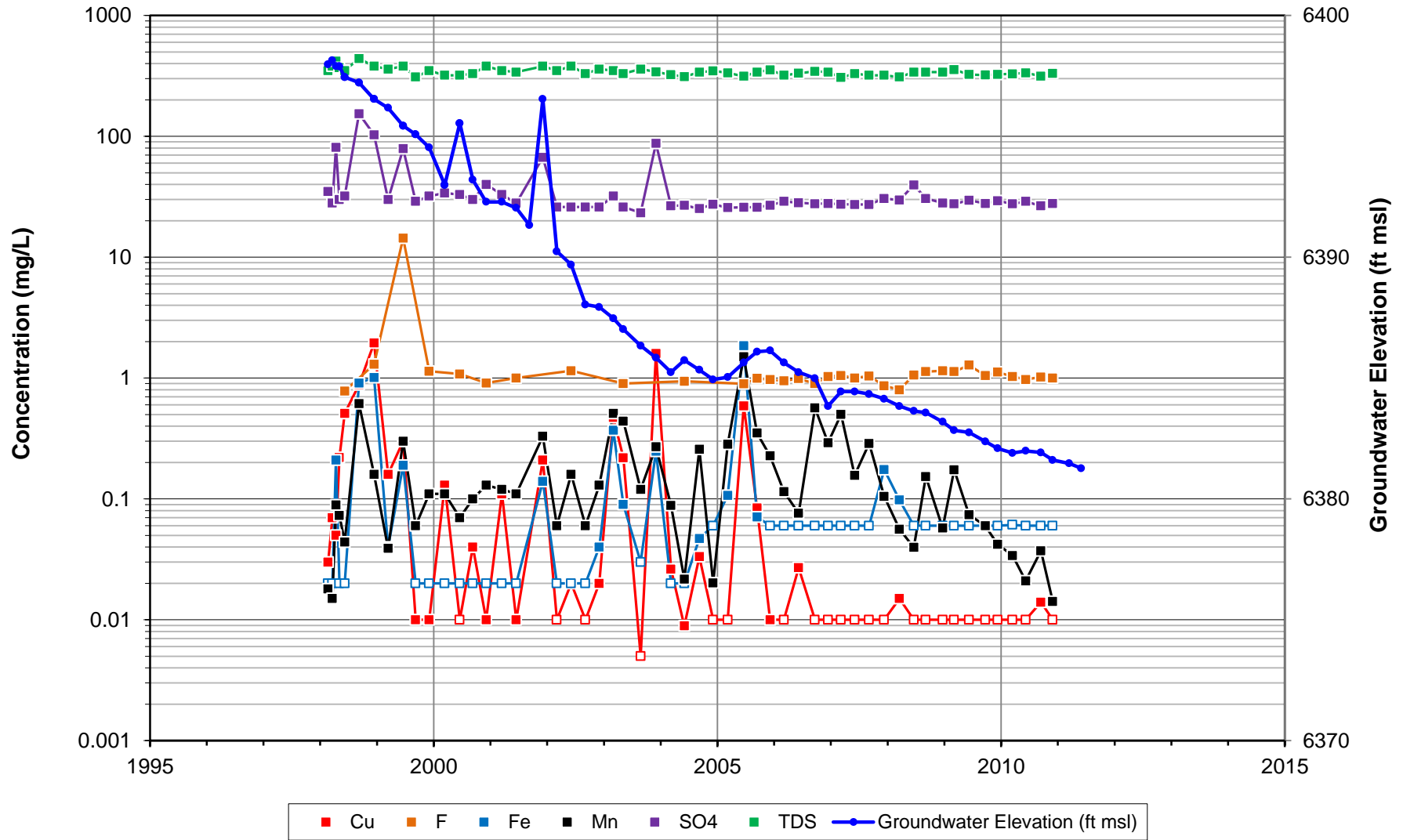


### Chemical Timeseries and Well Hydrograph MB-31 (pCg)



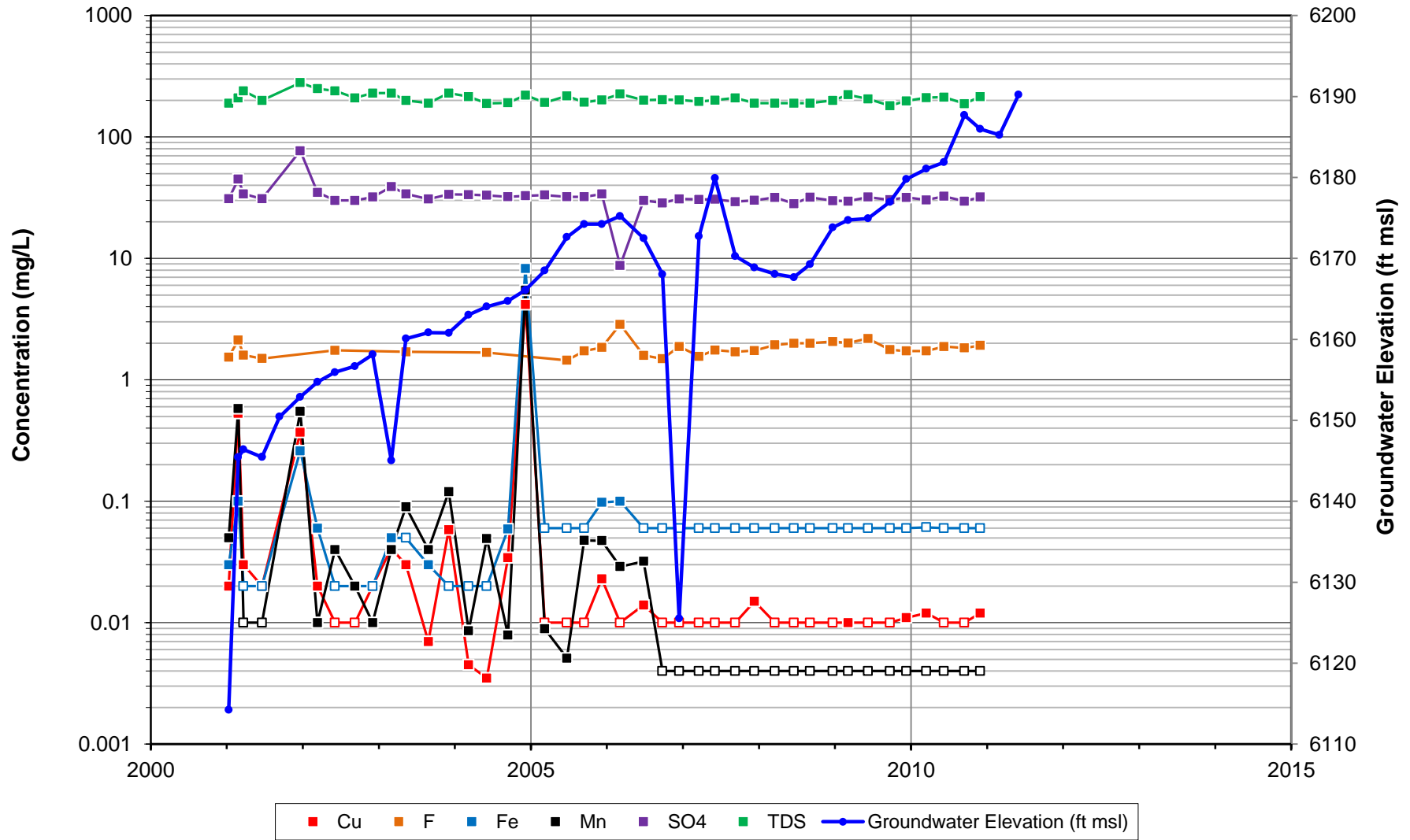
**Note: Open symbols indicate nondetections posted at relevant reporting limits.  
Some unknown historical reporting limits assumed from common values.  
All concentration and groundwater elevation data plotted (outliers included).**

### Chemical Timeseries and Well Hydrograph 2-11 (Tqm)



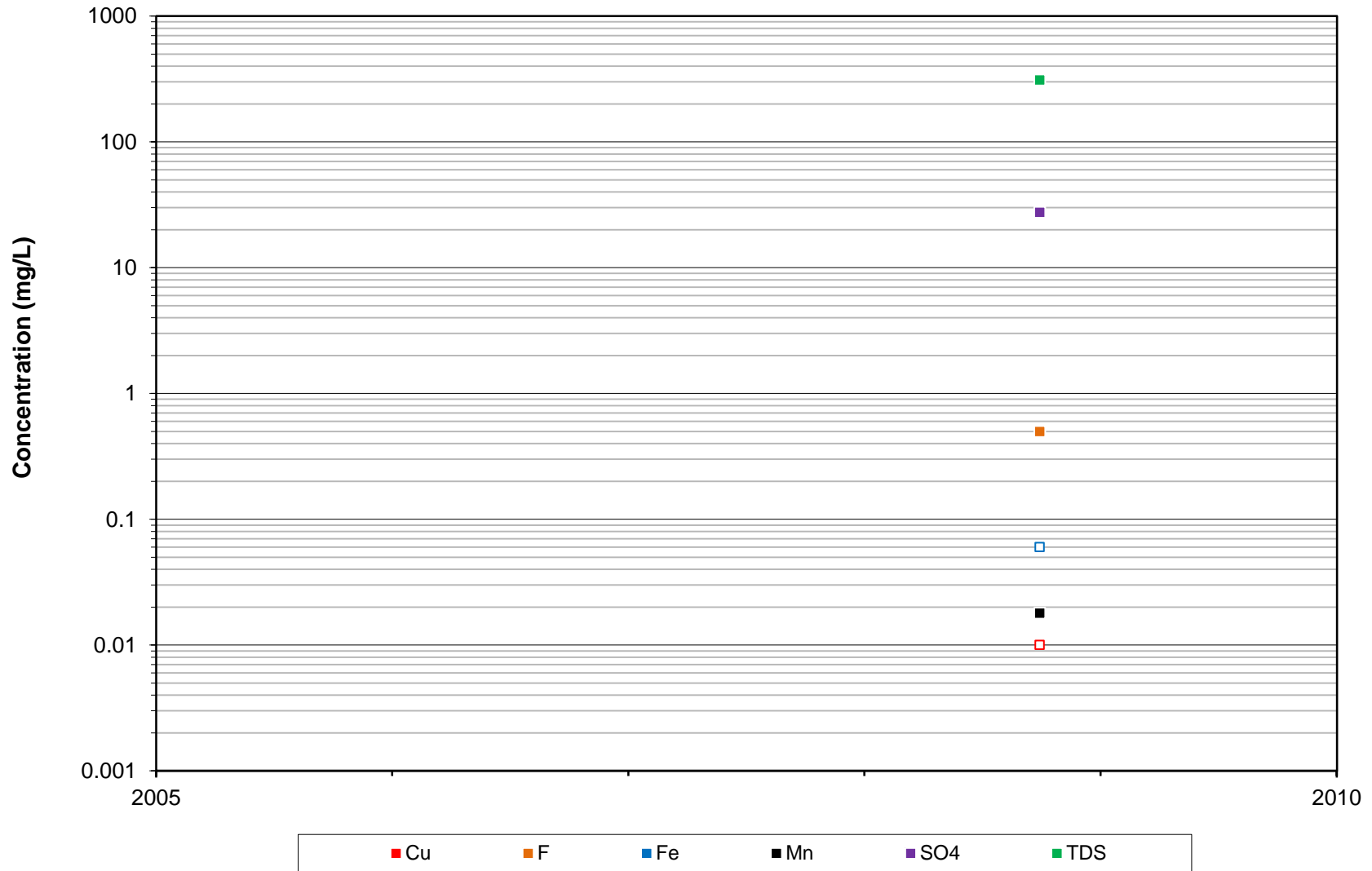
**Note: Open symbols indicate nondetections posted at relevant reporting limits.  
Some unknown historical reporting limits assumed from common values.  
All concentration and groundwater elevation data plotted (outliers included).**

### Chemical Timeseries and Well Hydrograph 2-15 (Tqm)



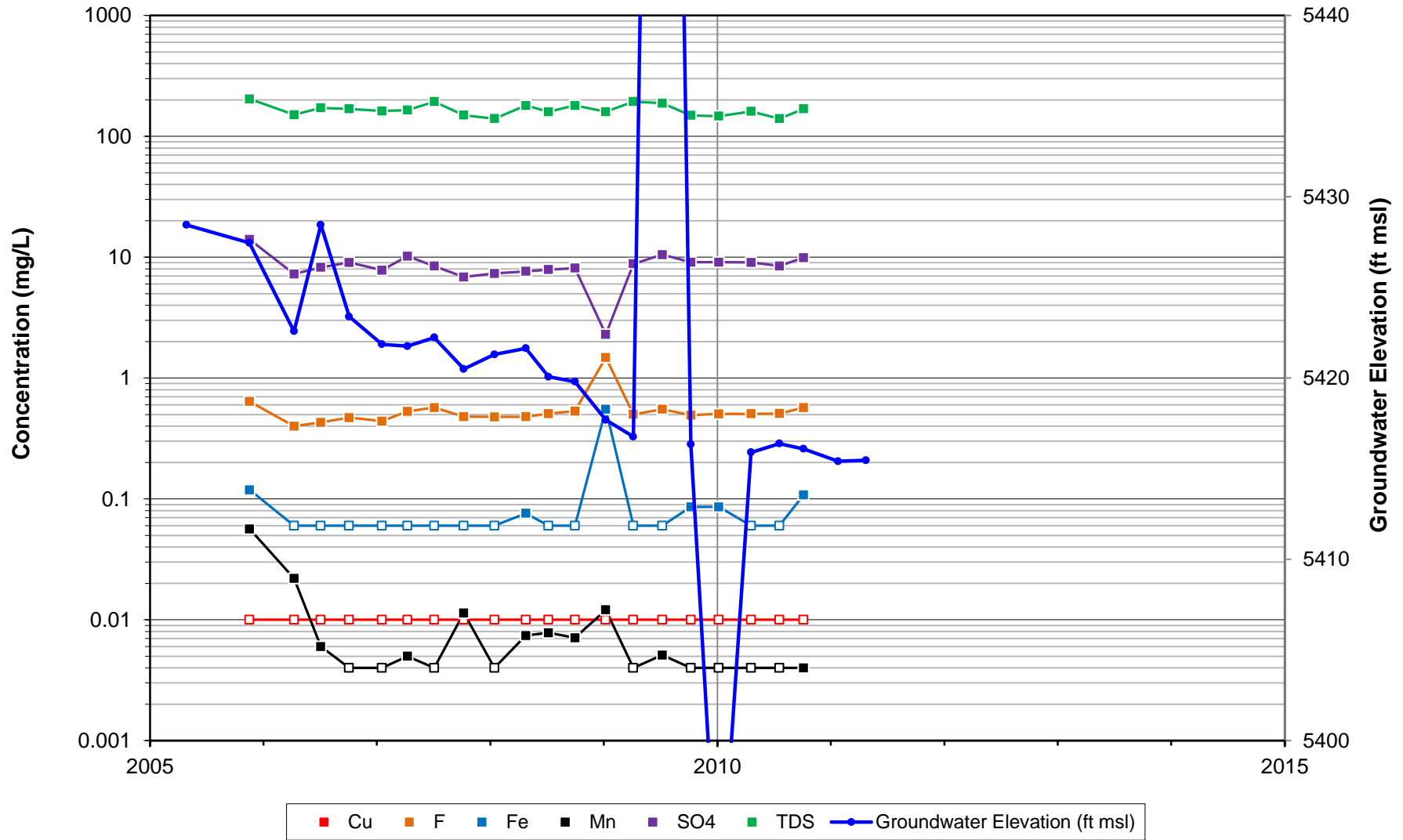
**Note: Open symbols indicate nondetections posted at relevant reporting limits.  
Some unknown historical reporting limits assumed from common values.  
All concentration and groundwater elevation data plotted (outliers included).**

### Chemical Timeseries and Well Hydrograph 166-2008-02 (Tqm)



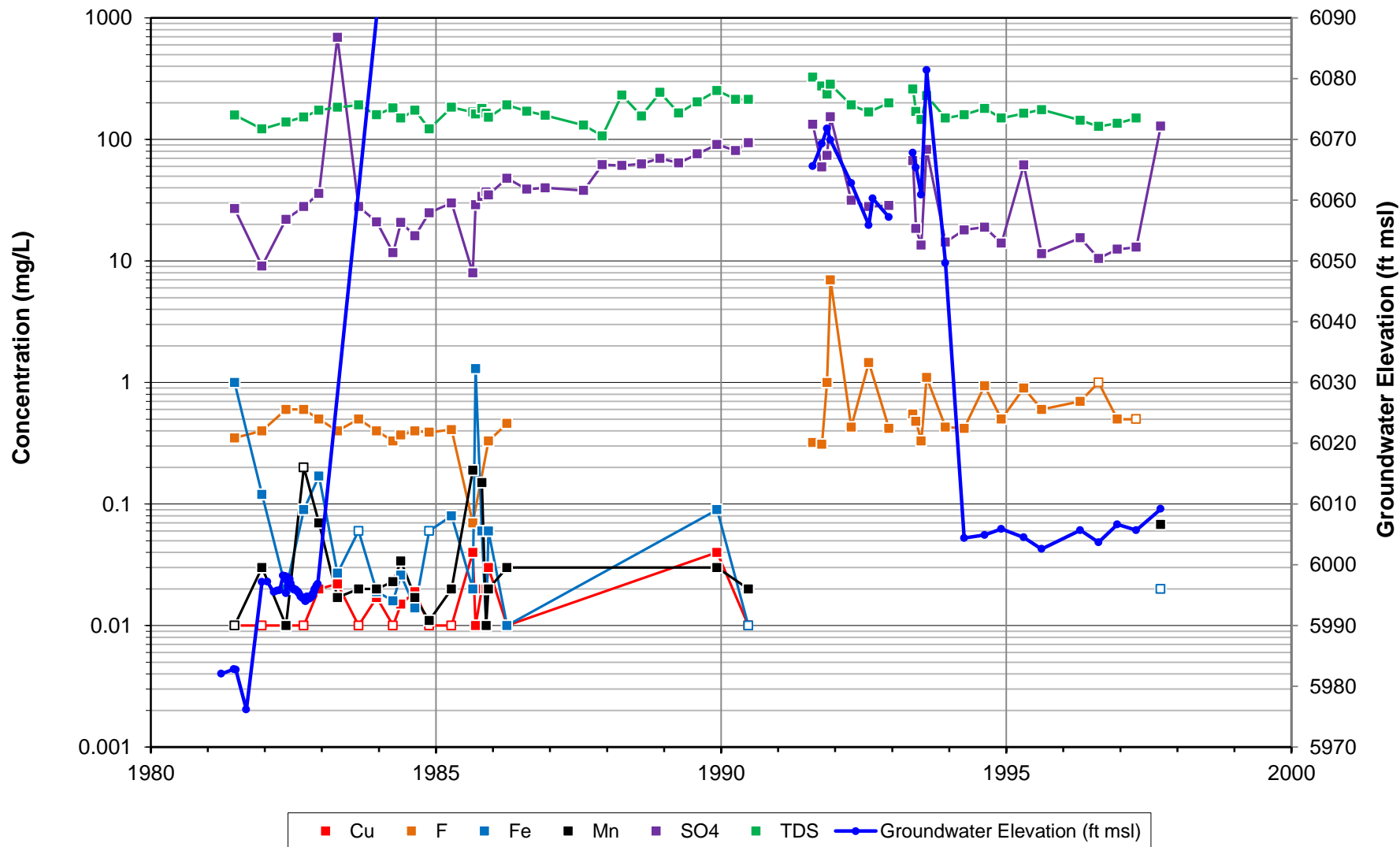
**Note: Open symbols indicate nondetections posted at relevant reporting limits.  
Some unknown historical reporting limits assumed from common values.  
All concentration and groundwater elevation data plotted (outliers included).**

### Chemical Timeseries and Well Hydrograph 363-2005-01 (Tqm)



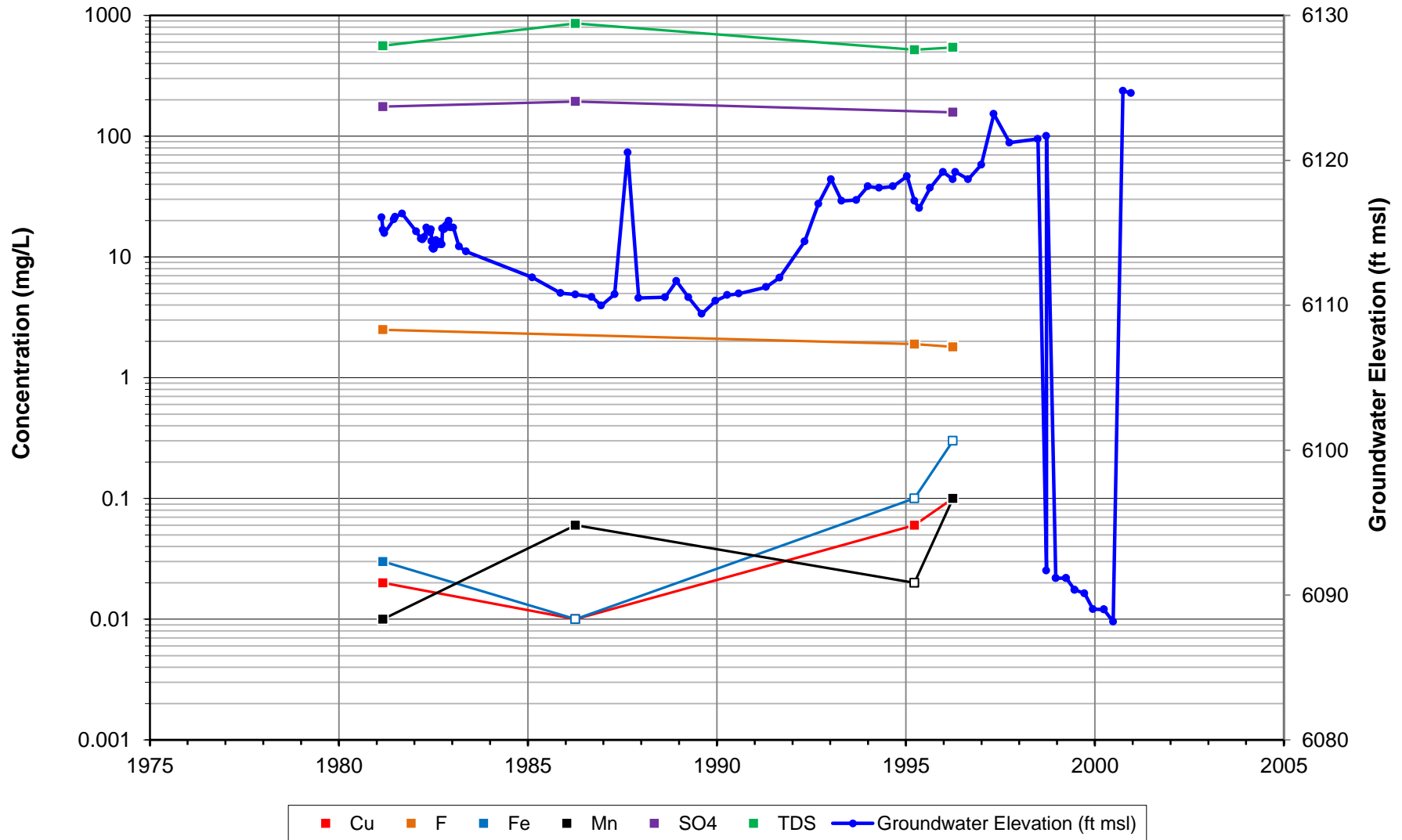
**Note: Open symbols indicate nondetections posted at relevant reporting limits.  
Some unknown historical reporting limits assumed from common values.  
All concentration and groundwater elevation data plotted (outliers included).**

### Chemical Timeseries and Well Hydrographs 4-1, 4-1R, 4-1A (Tqm)



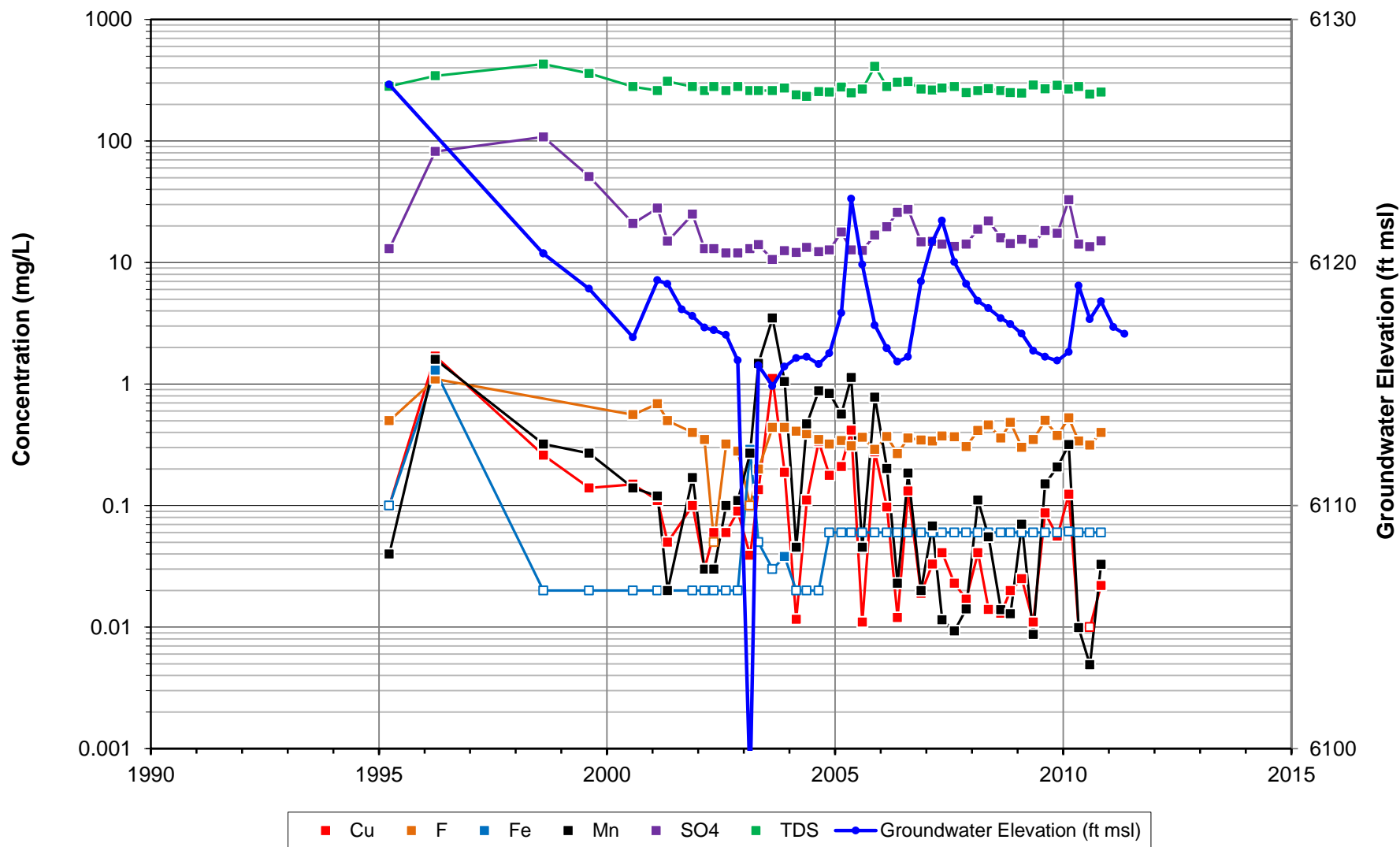
**Note: Open symbols indicate nondetections posted at relevant reporting limits.  
Some unknown historical reporting limits assumed from common values.  
All concentration and groundwater elevation data plotted (outliers included).**

### Chemical Timeseries and Well Hydrograph 6-1 (Tqm)



**Note: Open symbols indicate nondetections posted at relevant reporting limits.  
Some unknown historical reporting limits assumed from common values.  
All concentration and groundwater elevation data plotted (outliers included).**

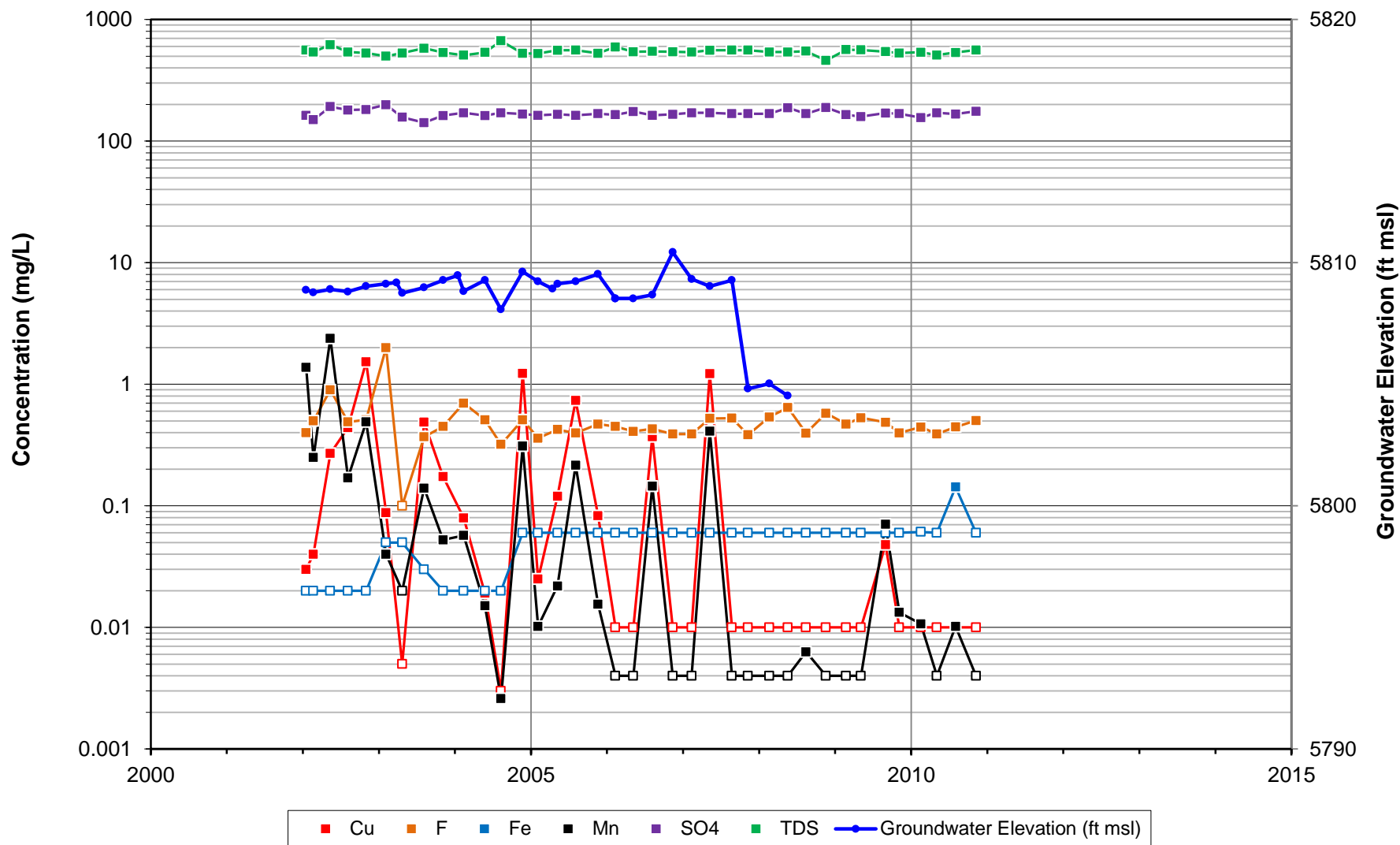
### Chemical Timeseries and Well Hydrograph LRW-5 (Tqm)



**Note: Open symbols indicate nondetections posted at relevant reporting limits.  
Some unknown historical reporting limits assumed from common values.  
All concentration and groundwater elevation data plotted (outliers included).**

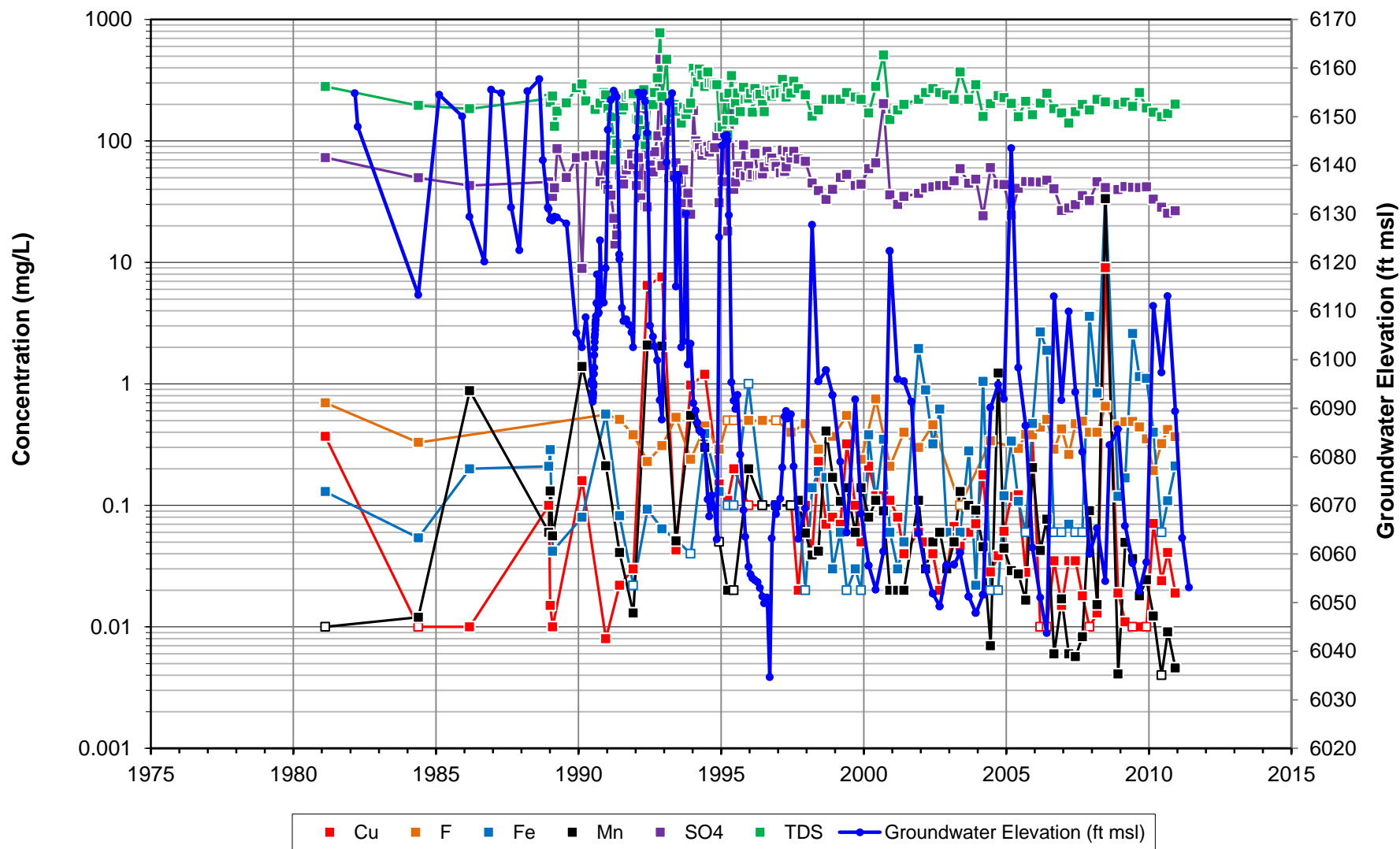


### Chemical Timeseries and Well Hydrograph MB-44 (Tqm)



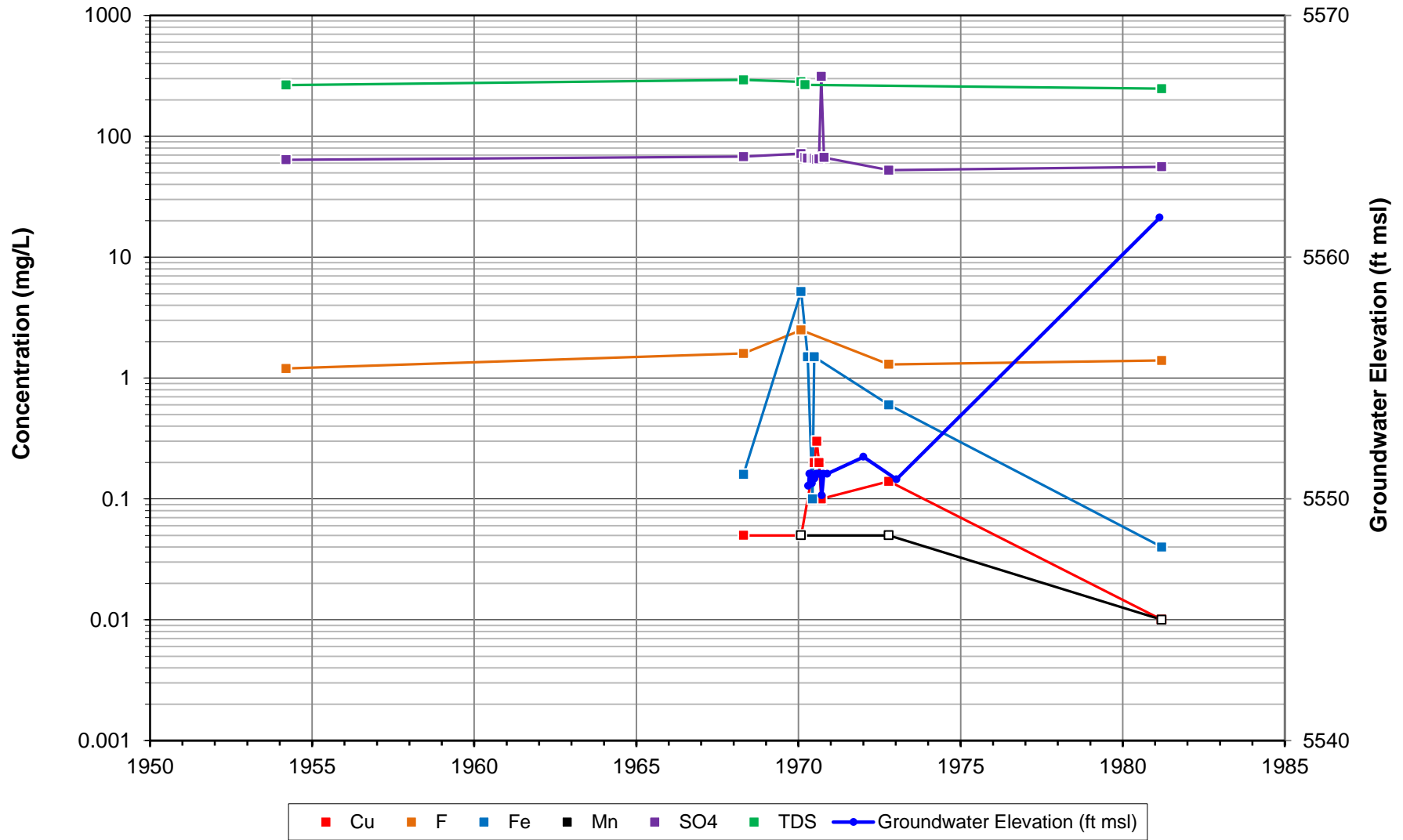
**Note: Open symbols indicate nondetections posted at relevant reporting limits.  
Some unknown historical reporting limits assumed from common values.  
All concentration and groundwater elevation data plotted (outliers included).**

### Chemical Timeseries and Well Hydrograph TWS-8 (Tqm)



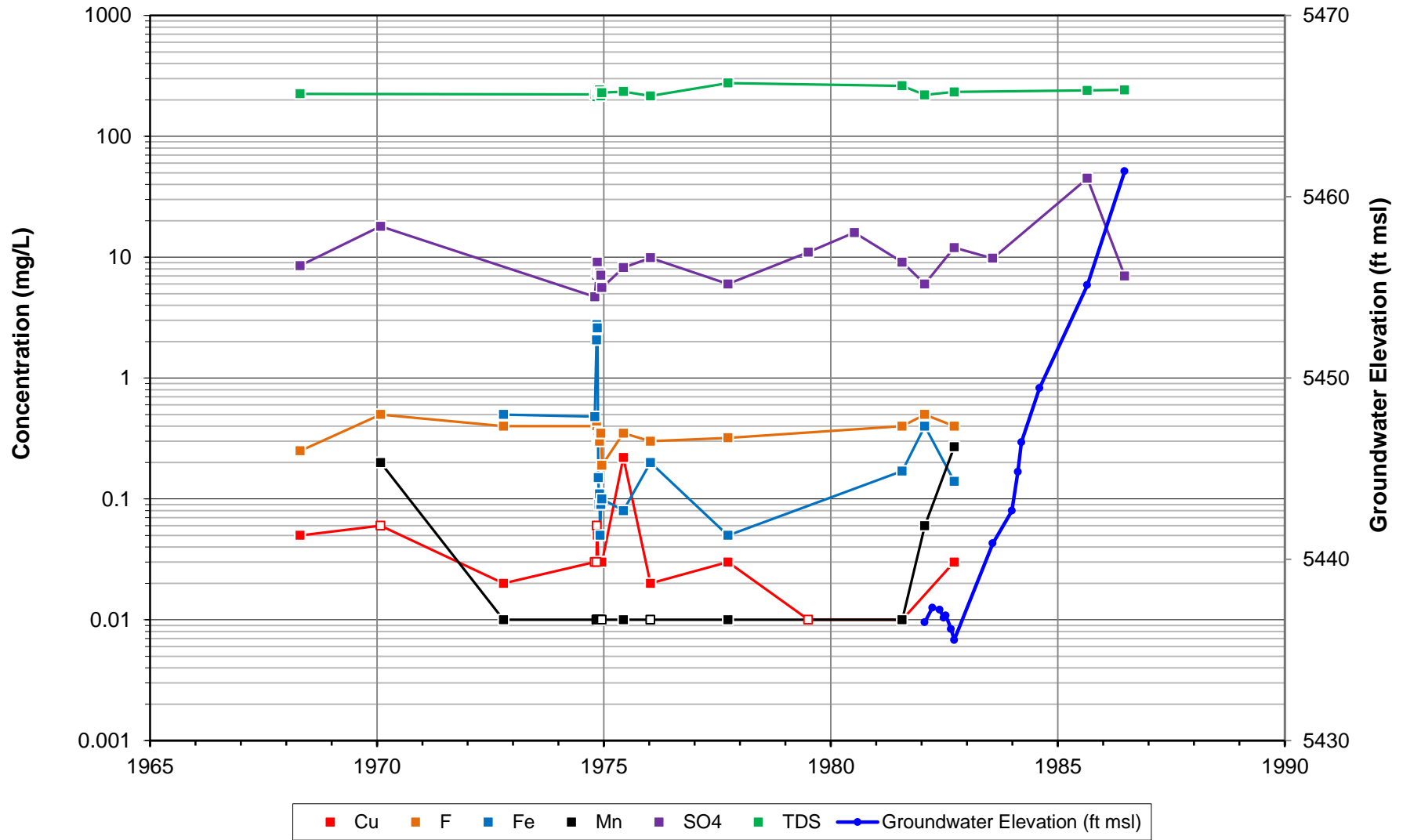
**Note: Open symbols indicate nondetections posted at relevant reporting limits.  
Some unknown historical reporting limits assumed from common values.  
All concentration and groundwater elevation data plotted (outliers included).**

### Chemical Timeseries and Well Hydrograph 5 (QTg)



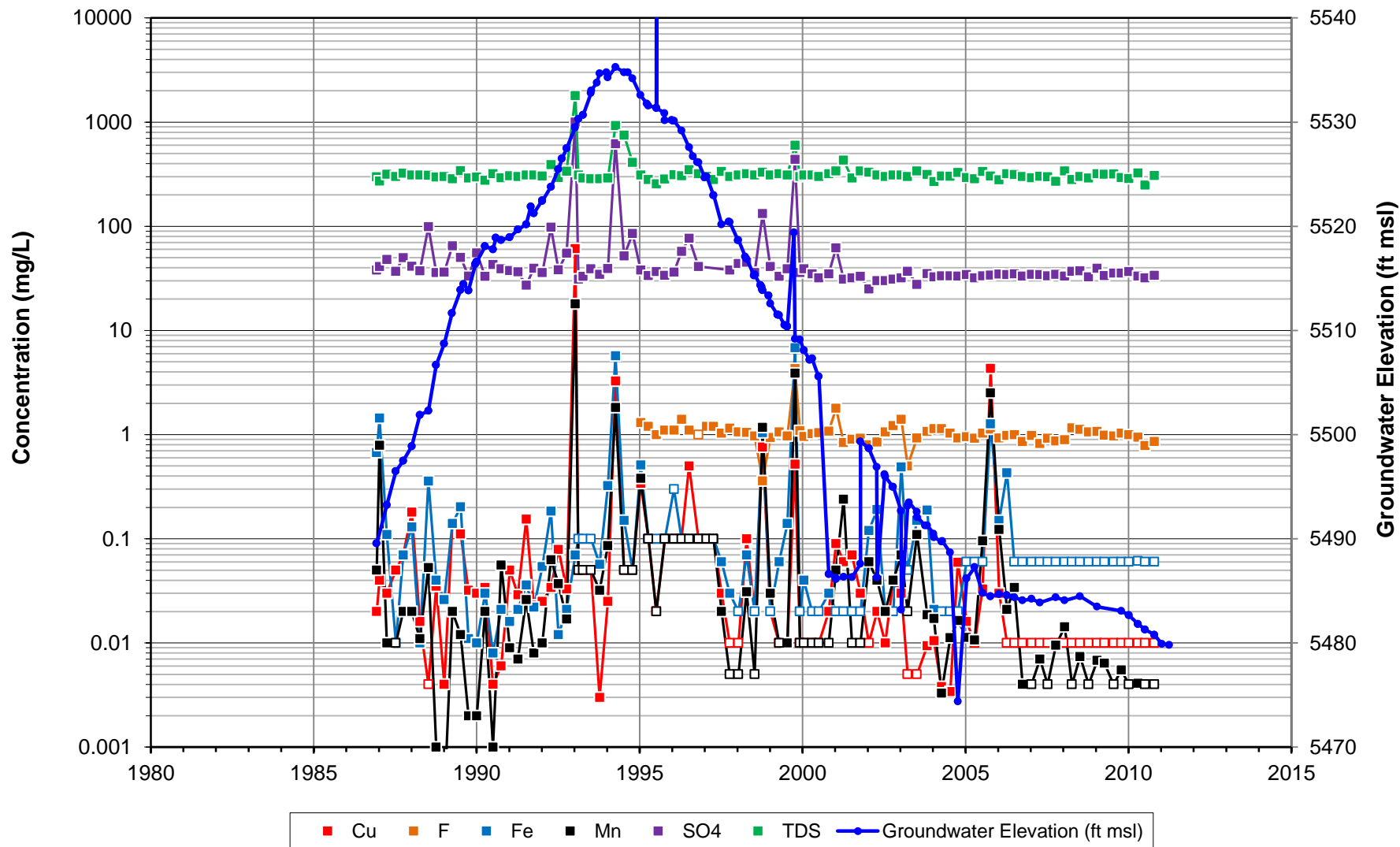
**Note: Open symbols indicate nondetections posted at relevant reporting limits.  
Some unknown historical reporting limits assumed from common values.  
All concentration and groundwater elevation data plotted (outliers included).**

### Chemical Timeseries and Well Hydrograph 9 (QTg)



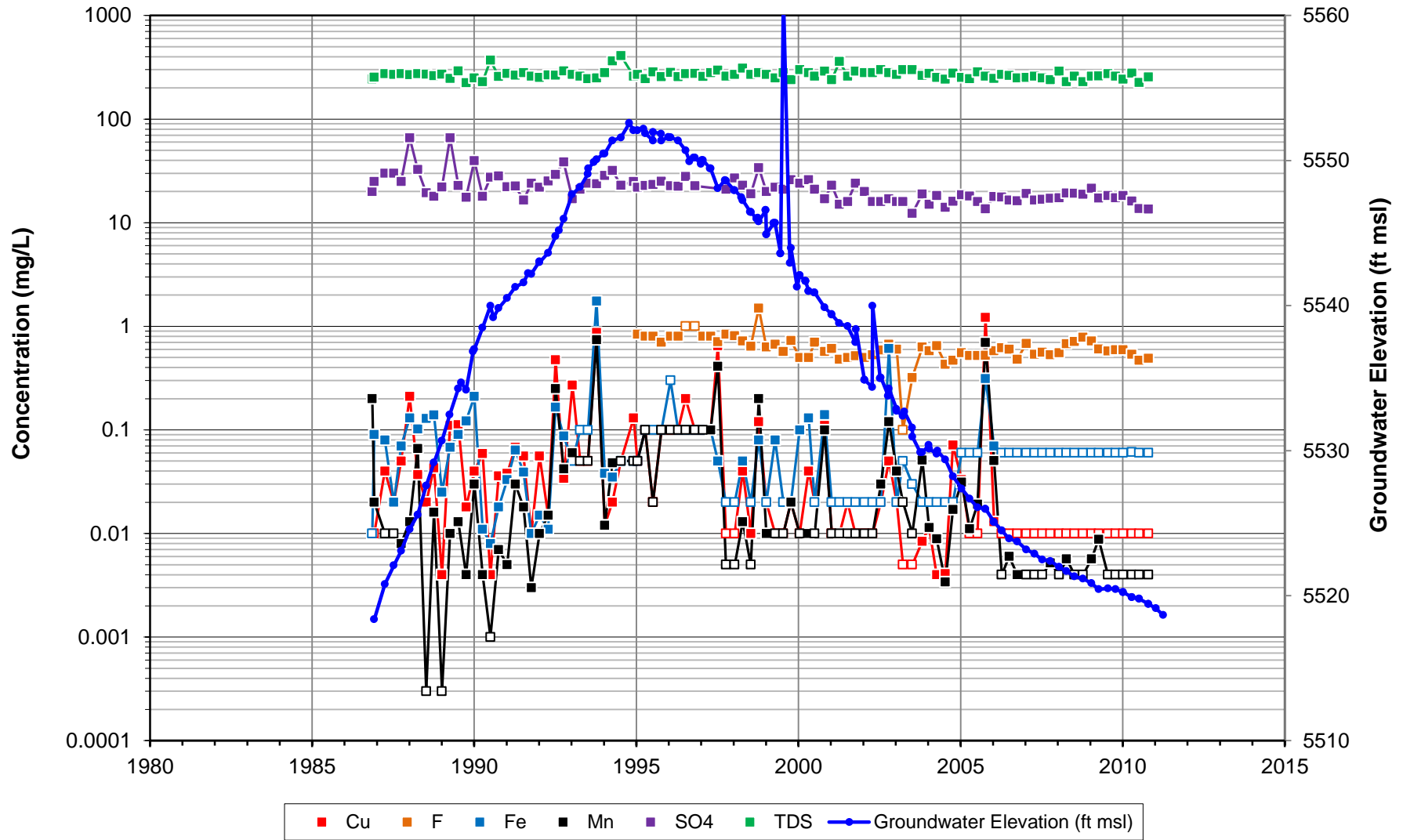
**Note: Open symbols indicate nondetections posted at relevant reporting limits.  
Some unknown historical reporting limits assumed from common values.  
All concentration and groundwater elevation data plotted (outliers included).**

### Chemical Timeseries and Well Hydrograph 26 (QTg)



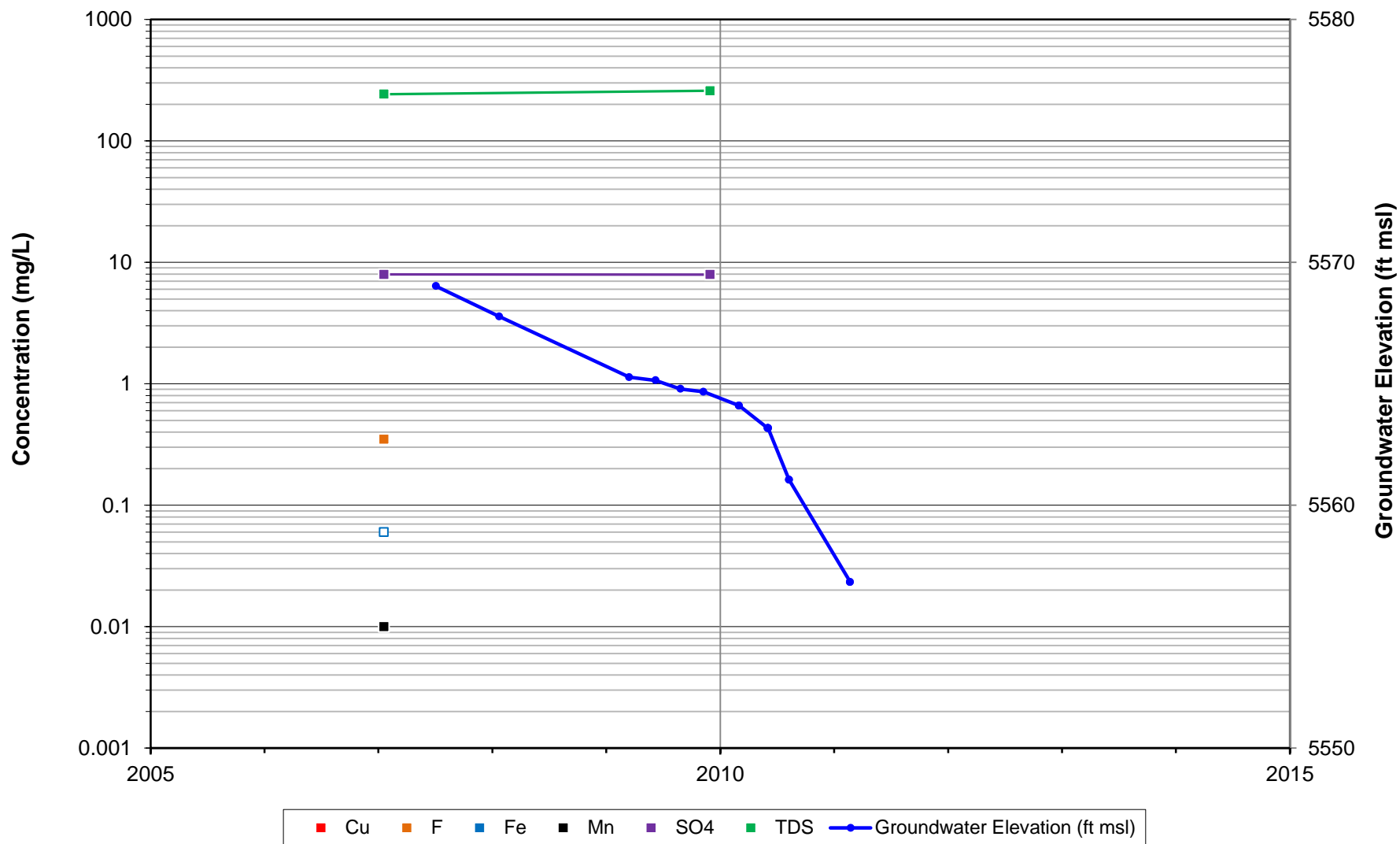
**Note: Open symbols indicate nondetections posted at relevant reporting limits.  
Some unknown historical reporting limits assumed from common values.  
All concentration and groundwater elevation data plotted (outliers included).**

### Chemical Timeseries and Well Hydrograph 27 (QTg)



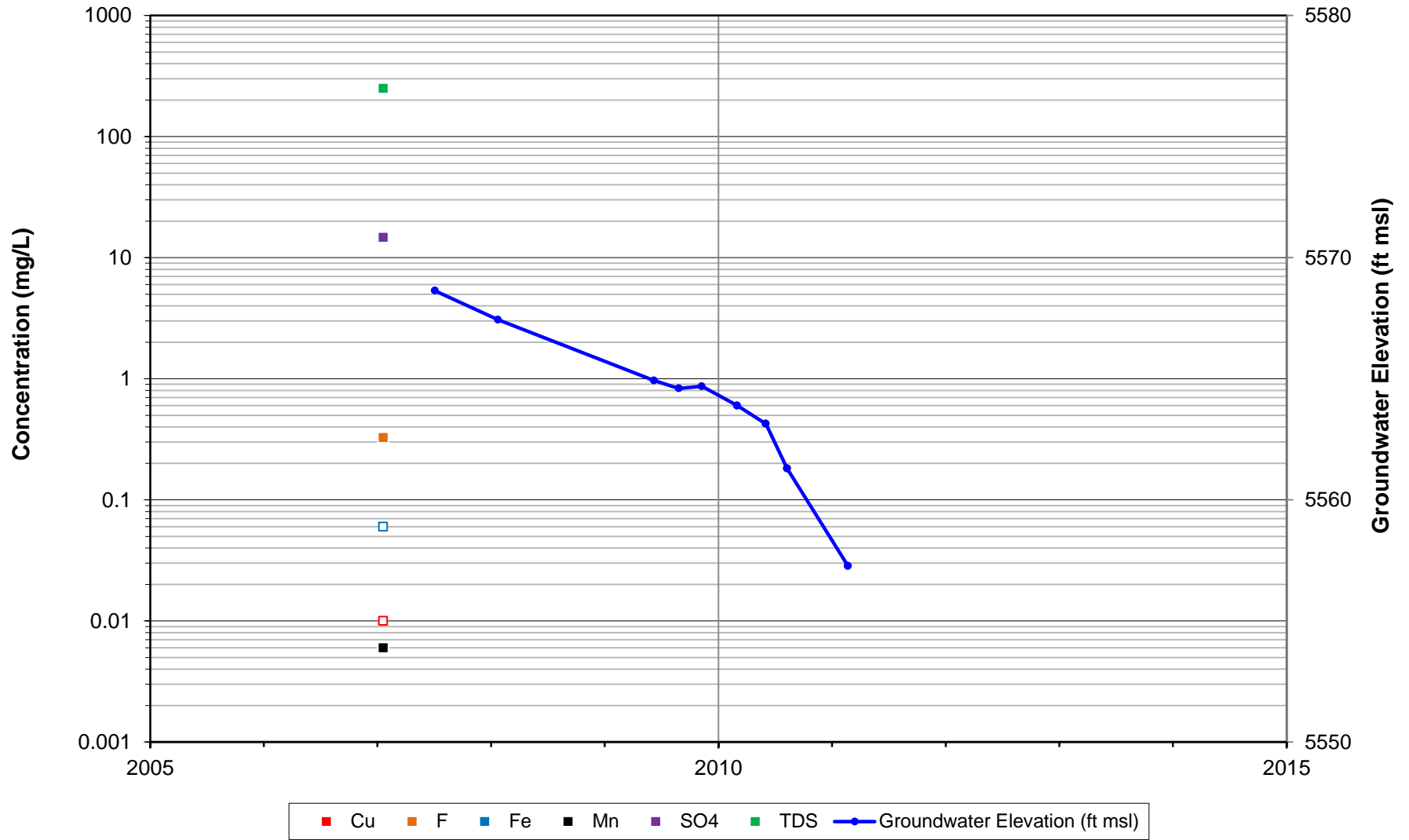
**Note: Open symbols indicate nondetections posted at relevant reporting limits.  
Some unknown historical reporting limits assumed from common values.  
All concentration and groundwater elevation data plotted (outliers included).**

### Chemical Timeseries and Well Hydrograph 286-2007-09 (QTg)



**Note: Open symbols indicate nondetections posted at relevant reporting limits.  
Some unknown historical reporting limits assumed from common values.  
All concentration and groundwater elevation data plotted (outliers included).**

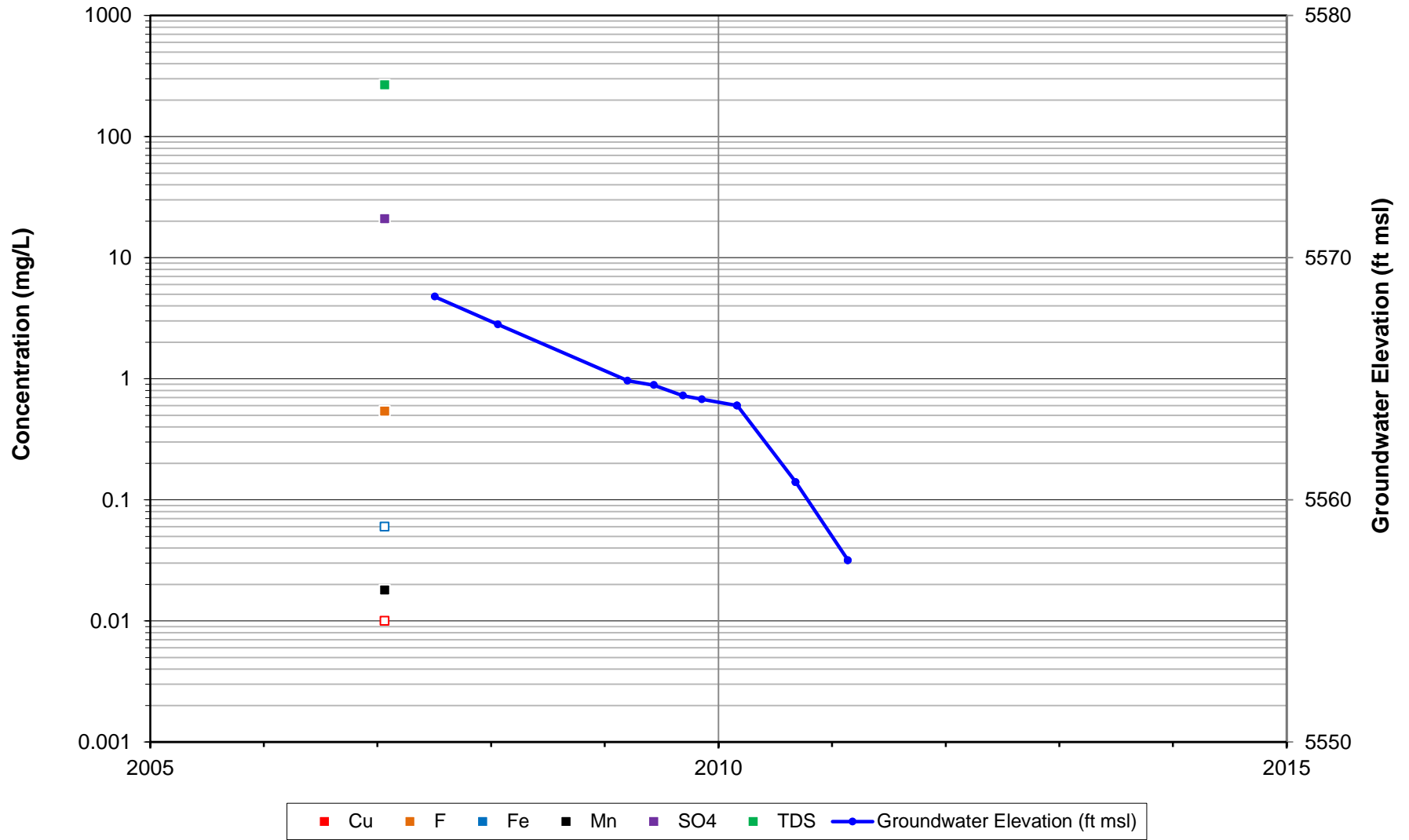
### Chemical Timeseries and Well Hydrograph 286-2007-10 (QTg)



**Note: Open symbols indicate nondetections posted at relevant reporting limits.  
Some unknown historical reporting limits assumed from common values.  
All concentration and groundwater elevation data plotted (outliers included).**

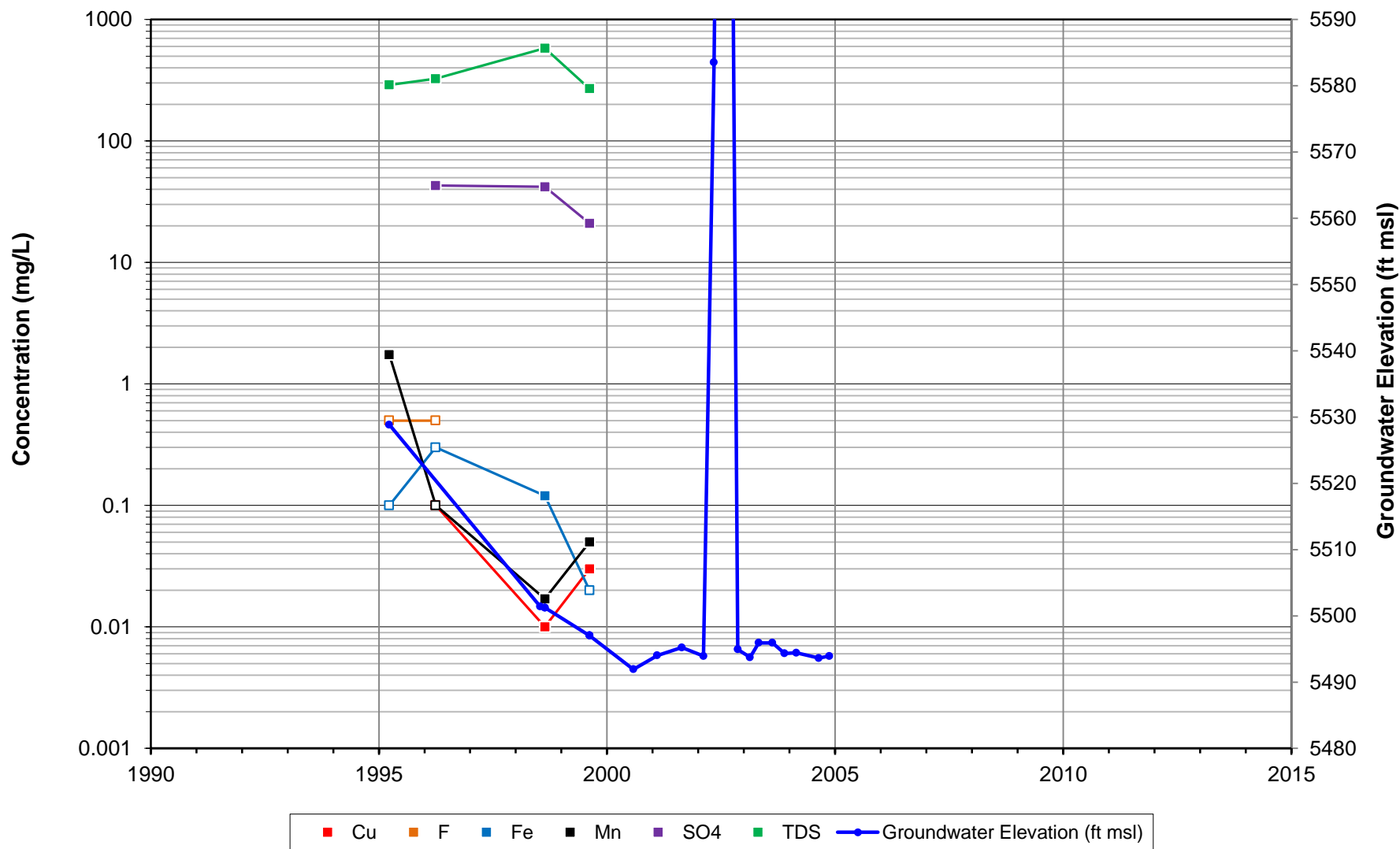


### Chemical Timeseries and Well Hydrograph 286-2007-11 (QTg)



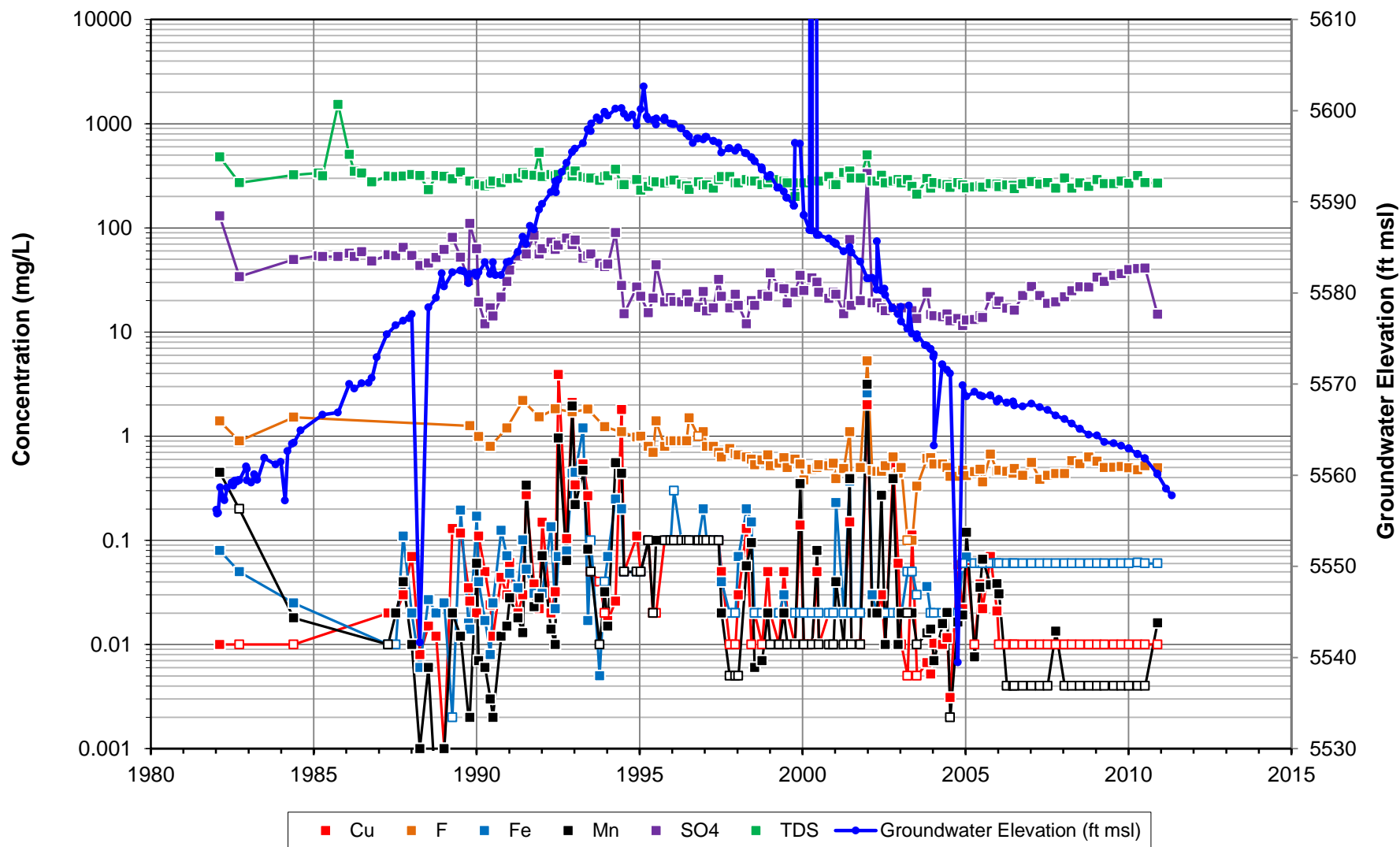
**Note: Open symbols indicate nondetections posted at relevant reporting limits.  
Some unknown historical reporting limits assumed from common values.  
All concentration and groundwater elevation data plotted (outliers included).**

### Chemical Timeseries and Well Hydrograph LRW-6 (QTg)



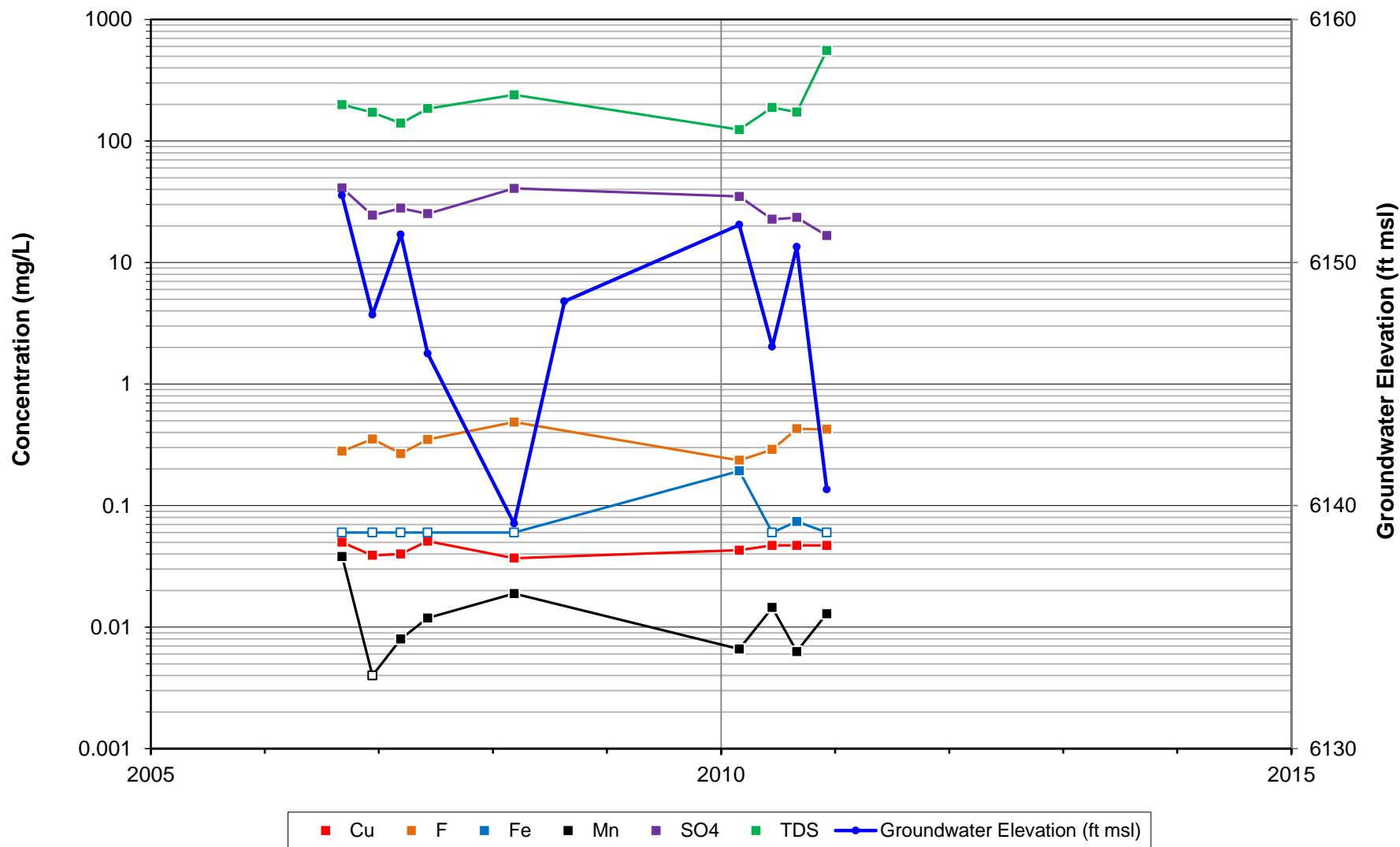
**Note: Open symbols indicate nondetections posted at relevant reporting limits.  
Some unknown historical reporting limits assumed from common values.  
All concentration and groundwater elevation data plotted (outliers included).**

### Chemical Timeseries and Well Hydrograph P-3 (QTg)



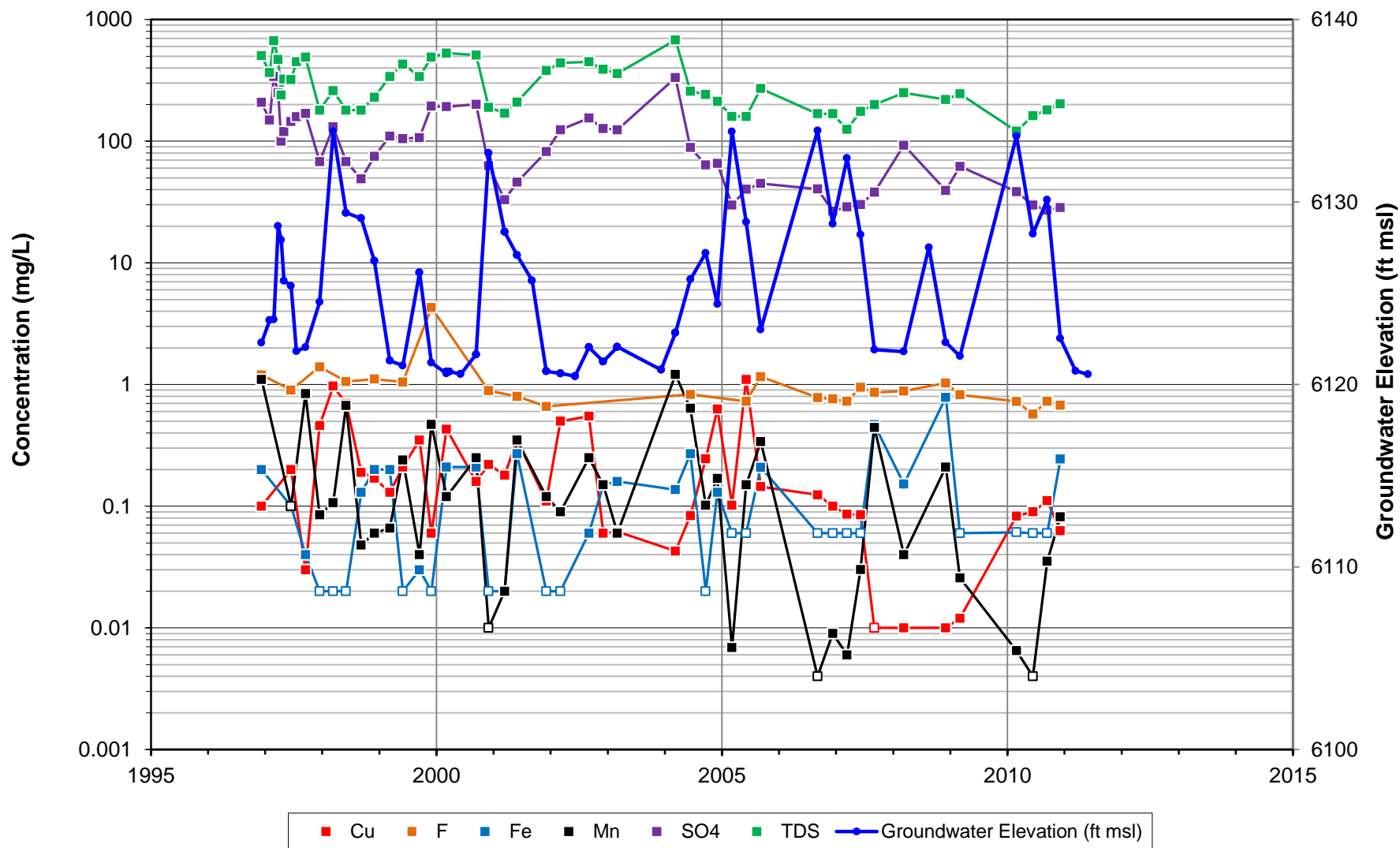
**Note: Open symbols indicate nondetections posted at relevant reporting limits.  
Some unknown historical reporting limits assumed from common values.  
All concentration and groundwater elevation data plotted (outliers included).**

### Chemical Timeseries and Well Hydrograph 166-2006-01 (Qa1)



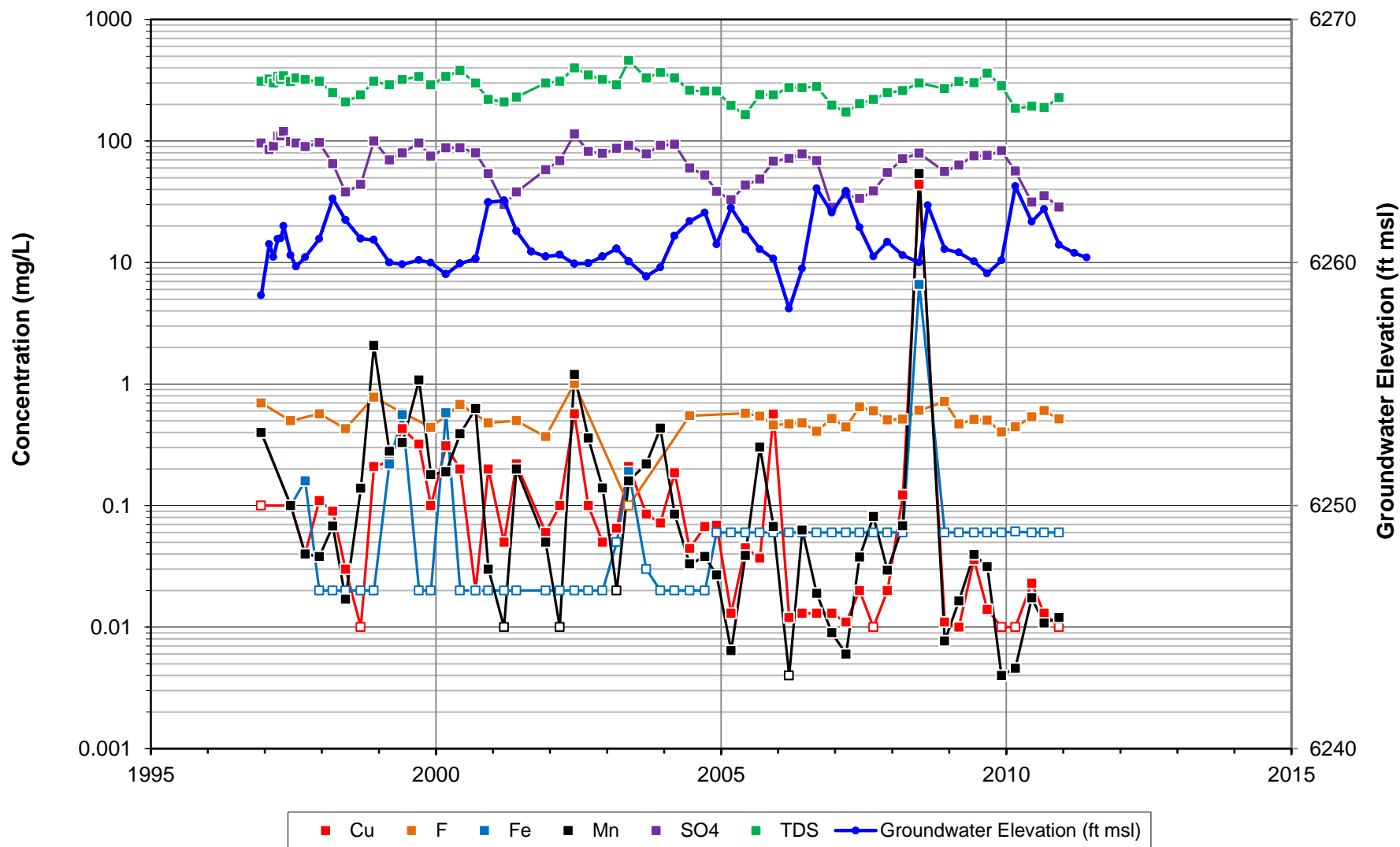
**Note: Open symbols indicate nondetections posted at relevant reporting limits.  
Some unknown historical reporting limits assumed from common values.  
All concentration and groundwater elevation data plotted (outliers included).**

### Chemical Timeseries and Well Hydrograph TWS-33 (Qa1)



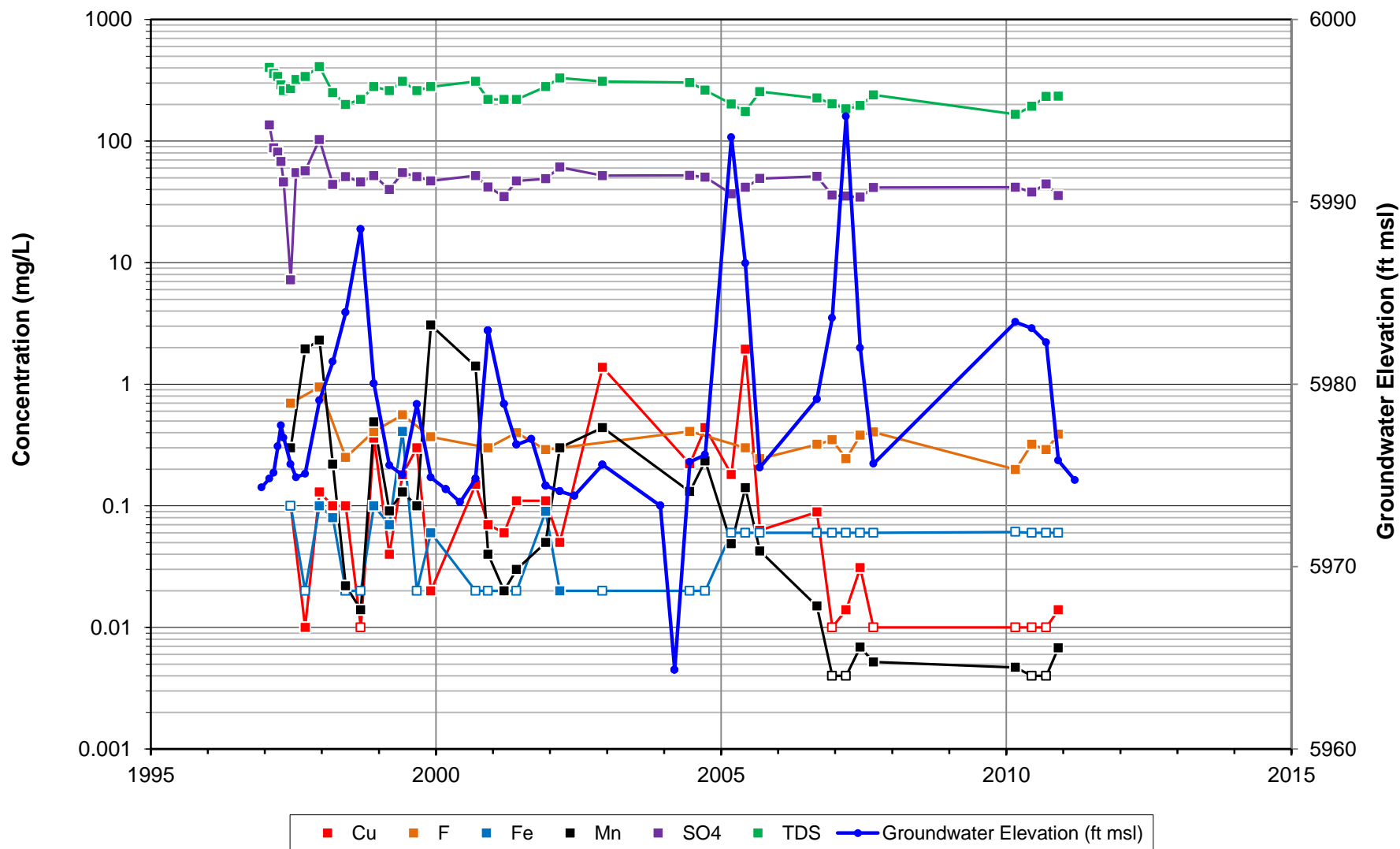
**Note: Open symbols indicate nondetections posted at relevant reporting limits.  
Some unknown historical reporting limits assumed from common values.  
All concentration and groundwater elevation data plotted (outliers included).**

### Chemical Timeseries and Well Hydrograph TWS-35 (Qa1)



**Note: Open symbols indicate nondetections posted at relevant reporting limits.  
Some unknown historical reporting limits assumed from common values.  
All concentration and groundwater elevation data plotted (outliers included).**

### Chemical Timeseries and Well Hydrograph TWS-40 (Qa1)



**Appendix B**  
**Infiltration Analysis**



**Date:** 21 February 2012

**Project No.:** 113-80013

**To:** Neil Blandford

**Company:** DBS&A

**From:** Lewis Munk, Ph.D.  
Todd Stein

**cc:**

**RE: UNSAT-H Simulations for the Stage 2 Abatement Plan Proposal  
Groundwater Modeling – Tyrone Mine**

## 1.0 INTRODUCTION

Freeport-McMoRan Tyrone Inc. (Tyrone) and the New Mexico Environment Department (NMED) entered into a Settlement Agreement and Stipulated Final Order (Settlement Agreement) in December 2010. The Settlement Agreement was entered into in response to the Decision and Order on Remand issued by the New Mexico Water Quality Control Commission (NMWQCC) on February 4, 2009 and Tyrone's appeal thereof.

In June 2011, Tyrone submitted the proposed modeling approach for the prediction of groundwater quality after implementation of closure measures. The modeling and analysis will be submitted with the Tyrone Stage 2 Abatement Plan as required by Item 31 of the Settlement Agreement. The simulation results from this effort will be used to assist with the determination of alternative abatement standards (AAS) for groundwater at Tyrone.

Drainage rates from the covered and uncovered leach and waste rock stockpiles are required as a component in the Stage 2 Abatement Plan Proposal groundwater modeling. Drainage rates from the leach stockpiles and waste rock piles will be based on a site-specific water balance using the UNSAT-H model (Fayer, 2000). The water balance model will update drainage estimates made as part of the Condition 98 (Feasibility Study) by incorporating information collected from the Tyrone test plots.

### 1.1 Objective

This memorandum presents revised soil water balance estimates for the stockpile facilities at Tyrone developed using the UNSAT-H model. The primary objective is to provide long-term estimates of drainage from covered and uncovered stockpiles. These data will be incorporated into the Stage 2 Abatement Plan Proposal groundwater model. The secondary objective is to provide preliminary UNSAT-H calibration results using data from the Tyrone No. 1 Stockpile test plots.



## 2.0 GENERAL ENVIRONMENTAL CONDITIONS

The design and configuration of the No. 1 Stockpile test plots is described in detailed in the test plot As-built reports (Golder, 2006 and 2007). The focus of this evaluation is on the three top surface test plots with covers composed of Gila Conglomerate that are 2-, 3-, and 4-ft thick. The plots are nearly level and occupy about 1.2 acres each. This section is intended to provide details relevant to modeling (Section 2.1) and updates the current conditions with respect to precipitation (Section 2.2) and vegetation (Section 2.3).

### 2.1 Cover and Waste Physical and Hydraulic Characteristics

The cover materials are composed of Gila Conglomerate and are moderately-coarse textured. They are represented mainly by sandy loams and sandy clay loams (9 to 29 % clay) with moderate amounts of rock fragments. The rock fragments are mostly gravel with lesser amounts of cobbles and occasional stones. The volumetric rock fragment content ranges from 25 to 65%, with most of the soils containing about 50 % by volume (Golder, 2006).

The physical characteristics of the waste rock are fairly consistent across the site (Golder, 2006). The samples are mainly classified as sandy clay loams and loams with 20 to 27 % clay. The rock fragment content of the waste rock is similar to the cover materials and ranges from about 35 to 65 % by volume.

The general consistency in physical characteristic of the cover and waste rock is reflected in the hydraulic properties. The relatively limited distribution of the soil water characteristics curves (SWCC) for the cover (Figure 2) and waste rock (Figure 3) demonstrate the similarities for the materials. The laboratory SWCC's were corrected to account for rock fragments. The range in the fine-earth fraction saturated hydraulic conductivity is fairly limited for both the cover ( $5.0 \times 10^{-3}$  to  $1.1 \times 10^{-2}$  cm/s) and waste rock ( $1.9 \times 10^{-4}$  to  $1.3 \times 10^{-3}$  cm/s). The hydraulic characterization data for the cover and waste rock are detailed in Golder 2005a, 2005b, and 2006.

### 2.2 Precipitation

The long-term average annual precipitation at Ft. Bayard is about 16 inches (40 cm). A summary of the monthly precipitation for the period of record at the No. 1 Stockpile is included in Table 1. The No. 1 Stockpile test plots have experienced 3 years of near average annual precipitation (2006, 2007, and 2008), 2 years of below average precipitation (2009 and 2011) and 1 year of above average precipitation (2010). The prevailing precipitation during the test plot period so far can be categorized as near normal to wet from a regional perspective. This conclusion is predicated on the occurrence of extreme monthly and seasonal precipitation, more so than total annual precipitation. Consecutive months of above average precipitation fell in July and August 2008 with 5.5 inches per month and nearly 6.5 inches fell in July 2010. Monthly precipitation totals exceeding 6.5 inches are rare and were only recorded on about seven occasions between 1897 and 2010 at Ft. Bayard. Similarly, two consecutive months with precipitation

that total 11 inches are uncommon. In addition to the extreme July precipitation, the winter of 2010 was wet with the January and February precipitation nearly 2.5 times the long-term regional average for those months. In contrast to the above average 2010 precipitation, 2009 is considered dry and ranks in the bottom 15 percent of years based on the Ft. Bayard record. For the No. 1 Stockpile, 2011 is on track for being one of the driest years on record with only about 6.5 inches measured through October.

## 2.3 Vegetation

The test plots were seeded in the late summer of 2005. Favorable growing season precipitation in 2005 and 2006 resulted in early establishment and the vegetation has subsequently progressed well. Past evaluations of the vegetation were semi-quantitative and based on unconstrained ocular estimates of canopy cover and plant occurrence. Like most semi-arid regions, the vegetation cover is patchy and varies substantially over short distances.

Overall, the test plots progressed from preliminary establishment of vegetation in 2005 to about 20 percent cover in 2008. Because of the subdued summer precipitation in 2009, there was little change in the overall vegetation canopy cover compared to 2008. In 2010, quantitative vegetation data were collected at the No. 1 Stockpile test plots. Mean total canopy cover on the top surface plots ranged from 30.7 to 36.7% (Golder, 2011). Total canopy cover was 36.7% on the 2-ft treatment, 32.5% on the 3-ft treatment, 30.7% on the 4-ft treatment. Although there was a trend of decreasing vegetation cover with increasing cover thickness, the canopy cover estimates were not considered statistically different. In response to the drought conditions in 2011, canopy cover was slightly lower than 2010 mainly because of less vigorous growth of yellow sweet clover.

## 3.0 METHODS

This section is intended to provide a summary of the pertinent vadose zone monitoring techniques (Section 3.1); water balance modeling (Section 3.2); and the approach used to calibrate the model (Section 3.3).

### 3.1 Vadose Zone Monitoring

Heat dissipation sensors (HDS) are the primary sensors used in the UNSAT-H model calibration process. Stacked nests of HDS were installed using a downhole emplacement and profile reconstruction method. Monitoring of the vadose zone network began in December 2005. The locations of the vadose zone monitoring nests are shown on Figure 3. The configuration of the test plots and instrumentation was detailed in previous reports (Golder, 2006 and 2007).

Campbell Scientific 229-L Heat Dissipation Sensors were installed at varying depths to indirectly measure matric potential (Golder, 2006). The 229-L sensor is designed to estimate matric potentials in the 100 to 25,000 cm (10 to 2,500 kPa) range with a resolution of about 10 cm (1 kPa) at matric potentials greater

than 1,000 cm (100 kPa) (Campbell Scientific, 2006). Campbell and Gee (1986) indicated that the precision of similar instruments is about 100 cm (10 kPa) in the < 1,000 cm (100 kPa) range, and that the sensitivity decreases at lower water potentials. Each sensor was calibrated in the laboratory prior to installation. The sensor calibration coefficients were refined to correct for field and laboratory variances. The HDS data include the initial soil temperature [ $T_0$ ] and change in temperature [ $\Delta T$ ] following heating of the porous ceramic body of the HDS. The  $T_0$  and  $\Delta T$  data are averaged on a daily basis and then corrected for ambient temperature variations according to the methods developed by Flint et al., (2002). Following the temperature correction, the HDS data are converted to matric potentials ( $\psi$ ) using the calibration coefficients listed in Table 2.

Data from the individual sensors were originally collected on an hourly basis until the first half of 2008 and then reduced to every six hours in June 2008 (Golder 2008). Data from the vadose zone instrumentation were manually downloaded from the data loggers on an approximate weekly basis until the telemetry system was integrated in September 2008 to remotely download the data to servers maintained by Tyrone. Comprehensive database files developed for each vadose zone monitoring nest are routinely updated as new data are acquired. The quality of the raw data are assessed prior to integration into the database.

### 3.2 Water Balance Model

Developed by Battelle Pacific Northwest Laboratory, UNSAT-H is a one-dimensional soil water and heat flux model that simulates the dynamic processes of infiltration, redistribution, evaporation, transpiration, and drainage (Fayer et al., 2000). Key input parameters used in the simulations are summarized in Table 3. The soil hydrologic properties of the cover and stockpile materials used in the simulations are summarized in Table 4. The UNSAT-H Input files are included in Attachment 1.

The simulated soil covers are conceptualized as nearly level, vegetated, homogenous layers of earthen materials of varying thickness overlying homogenous waste materials. Vegetation is represented by a relatively low leaf area index (0 to 0.29 maximum) that is assumed to vary systematically throughout the year in response to temperature and water availability (Golder, 2005a). Roots are distributed throughout the cover profile according to a function developed from site-specific data (Golder, 2005a; Golder, 2006a). The root function was arbitrarily terminated at the cover-waste contact with the same distribution used for the 2-, 3-, and 4-ft cover thickness scenarios.

The long-term simulations were conducted using a 110 year precipitation and temperature record from a local weather station (Ft. Bayard; NOAA Station # 293265). The calibration simulations were conducted using both hourly and daily data from the No. 1 Stockpile station. Precipitation is assumed to be rain that falls at a maximum rate of 1.2 cm/hour when daily data are used. Runoff occurs whenever the precipitation rate exceeds the infiltration capacity of the soil surface, which varies as a function of

wetness. Water that is allocated to runoff is removed from the model domain and no longer considered in the storage, redistribution, or evapotranspiration components of the model. The model domains contain 87 nodes with the bottom boundary at 4 m below the top of the cover. The distribution of nodes varies depending on the cover thickness. The lower boundary is specified as a unit gradient (i.e., free-draining) boundary.

The saturated and unsaturated soil hydraulic properties used in the model include saturated water content ( $\theta_s$ ), residual water content ( $\theta_r$ ), van Genuchten alpha ( $\alpha$ ) and N parameters, and hydraulic conductivity. The soil properties were originally estimated using the RETC code (van Genuchten et al., 1991) following correction of the fine-earth fraction data for rock fragments. The properties were varied within the approximate range of measured properties during the calibration process as discussed below.

### 3.3 Soil Water Balance Model Calibration Approach

The soil water balance model was calibrated to data from the test plots by attempting to match model-generated and field matric potentials ( $\Psi$ ). Time series of simulated matric potentials were compared to field matric potential data from corresponding depths. A trial and error approach was used whereby the material properties ( $K_{sat}$ ,  $\theta_s$ ,  $\theta_r$ ,  $\alpha$ , and N) and LAI were varied to achieve close correspondence of the simulated and measured matric potentials. The calibration process was aimed at optimizing the fit among the simulated and measured matric potentials at depth intervals corresponding to the HDS placements.

An iterative, top down approach was used in the calibration process, whereby we focused on achieving approximate concurrence of the simulated and measured matric potentials in the upper layers first and then lower layers. The process was iterative because changes in the lower layers affect simulated matric potentials in the upper layers, which would require changes to the lower layers, and so on. The calibrations were developed using data from the 2-, 3-, and 4-ft cover thickness plots. We emphasized the use of data from nests 1B, 3B, and 2A because they are least affected by external factors, such as the lysimeter rehabilitation (nests 1A and 3A) and the formation of depressions (nests 1C and 3C). Recognizing that field soil hydraulic properties vary substantially, our goal was to find a single set of material properties that resulted in a reasonable fit among the simulated and measured data with respect to the trend, magnitude, and gradient for all sites.

Initial conditions for the calibration simulations were obtained from the field matric potential data. Because some of the sensors were not definitively equilibrated to the cover and waste until after the July and August rains, the model simulations were started in August 2006. Thus, drainage results from 2006 simulation reflect partial year data.

The calibration simulations were initially performed using hourly precipitation data with no constraints on rainfall intensity. Additional simulations were then performed using daily rainfall data and the rainfall intensity factor (HPR) was adjusted until approximately similar annual drainage and runoff results were

obtained along with maintaining the fit among the simulated and measured matric potentials. Simulations that yielded excessively high (> 25% of annual precipitation) or low (< 5% of annual precipitation) runoff results were rejected. During the model calibration process we accepted simulation results that generated matric potentials less than 100 cm, recognizing the limitations of the HDS in the low matric potential region.

## 4.0 RESULTS

This section provides the results of the field data (Section 4.1), preliminary calibration of the simulated matric potentials (Section 4.2), short-term drainage estimates based on the simulations (Section 4.3), alternative drainage estimates made using a unit gradient approach (Section 4.4), and long-term drainage estimates based on the preliminary model calibrations (Section 4.5).

### 4.1 Matric Potential Trends

Monitoring of the HDS began in December 2005. Based on the analysis of the HDS data, many, but not all, of the sensors appeared to have reached equilibrium with the cover materials and waste rock by about March 2006. All the sensors demonstrated a definitive response to the extremely wet conditions that prevailed in August 2006.

Plots of the matric potentials from the top surface HDS nests for the calibration period (August 2006 to October 2011) are shown in Figure 4 (2-Ft Cover Treatment), Figure 5 (3-Ft Cover Treatment), and Figure 6 (4-Ft Cover Treatment). The graphs are arranged so that data from equivalent sensor depth intervals are displayed together for each cover treatment. It should be noted that the depth of the instruments within the cover are not the same across cover treatments. In most cases, the sensors responded to wetting and drying in unison over time, although the magnitude of the response varied.

As expected, the shallower sensors tended to display a greater range in matric potentials than the deeper sensors. The time-series plots of matric potentials for the 200-cm sensors reveal that all the sensors attained matric potentials near the lower limits of their functional range of measurement (e.g.,  $\approx 100$  cm) in association with the August 2006 rains. The matric potentials generally decreased following the episodic 2006 wetting event until the spring of 2007. Since then, the matric potentials generally increased with evidence of seasonal reductions associated with the summer rains at most sites. The extreme monthly precipitation in the winter 2010 resulted in universal reductions in matric potential followed by general increases in matric potential near the end of 2010. The general trend of increasing matric potentials extended into the fall of 2011.

### 4.2 Simulated and Measured Matric Potentials

The calibration was complicated somewhat by the relatively high degree of wetness of the soils and waste rock for most of the period of record and the lack of sensitivity of the HDS near  $\Psi \leq 100$  cm. The cover

and waste profiles were brought to near saturation during the July and August 2006 rains. Because of incomplete development of the vegetation and the above normal precipitation in July and August 2008, increases in matric potential (drying) in the cover layers were limited in magnitude until the summer of 2009 or 2010. Increases in matric potential in the waste rock were generally limited until the summer of 2011. The subdued changes in matric potential provided limited opportunities to assess the model calibration to higher matric potential (drier) conditions.

The simulated and measured matric potentials are compared in Figure 4 for the 2-ft cover thickness, Figure 5 for the 3-ft cover thickness, and Figure 6 for the 4-ft cover thickness plots. The model calibration was intended to approximate the entire range of measured matric potential values, recognizing that an exact fit to any particular case was probably not realistic. With the exceptions of layer thicknesses and root distributions, the simulated material properties and vegetation conditions are the same for all the model scenarios.

For the simulation period, the degree of fit for the simulated and measured matric potentials is poor when the plant function is turned off in all years (Figure 7). Comparison of Figures 5 and 7 show that the fit among the simulated and measured matric potentials improves when the LAI function is incrementally increased starting in 2008. The LAI functions used in the simulations are shown in Figure 8. We believe that a reasonably good fit was achieved by turning off the plant function in 2006 and 2007, and then applying a maximum LAI of 0.03625 in 2008 and 2009 and 0.145 in 2010 and 2011. For reference, the maximum LAI of 0.145 used in the model was about half of the LAI measured at Tyrone on the South Main Repository (Golder, 2005a). The vegetation functions applied in the model approximate the trend in vegetation progression observed at the No. 1 Stockpile test plots (see Section 2.3). Application of a higher LAI (0.29) in 2010 and 2011 did not materially improve or diminish the observed fit among the simulated and measured matric potentials in the model calibration process. Thus, we believe that the LAI of 0.145 is probably a reasonable surrogate for the existing vegetation conditions.

The root function in the model was not modified over time, even though root growth probably progressed in a manner similar to the above ground biomass.

### 4.3 Simulated Drainage Estimates

Annual drainage estimates for three cover thickness scenarios for the test plot period of record are listed in Table 5. The results reflect the liquid water flow output from UNSAT-H at a depth of 222.5 cm. The somewhat higher annual drainage estimates for 2006 and 2007 partially reflect the lack of transpiration in the simulations. The no plants scenario (Run 40) provides a baseline to compare the relative effects of transpiration on the simulated drainage estimates in the later years.

Precipitation intensity strongly influences soil water relations in nature and in the simulation realm. Preliminary calibration work at the Tyrone tailing test plots revealed poor correspondence of simulated



and measured matric potential when rainfall intensity was not adequately accounted for in the simulation process. When only daily precipitation data are available, the amount of precipitation entering the model domain can be controlled by changing the surface hydraulic properties and/or the hourly precipitation rate (HPR). When hourly precipitation data are available, the model can be structured to allow the precipitation to be introduced at the measured hourly rate. Precipitation intensity data on an hourly and shorter duration basis is available from the test plot precipitation record but not the long-term simulation record, which contains only daily data. Thus, we attempted to reconcile the results obtained from the hourly simulations with results obtained using total daily precipitation and varying the rainfall intensity factor (HPR).

Comparison of the results from the daily and hourly simulations indicates that the daily precipitation simulations predicted lower drainage in most years (Table 5). In 2007, the No. 1 Stockpile received several high intensity storms, which probably explains why daily precipitation simulations result in higher drainage than the hourly simulations. The highest magnitude hourly event was in July 2007 with an intensity equivalent to a 25-year recurrence interval. The representativeness of the rainfall intensity for the period of record has not been fully evaluated with respect to long-term conditions.

The general trend of reduced drainage with increasing cover thickness in the simulated data is partially a function of the imposed root distribution, whereby the roots are arbitrarily extended to and terminated at the base of the cover. The extraction of water deep in the profile is an important process for limiting drainage, but the simulated affects have not been verified by empirical data as discussed in the next section.

#### 4.4 Unit Gradient Drainage Estimates

Alternative drainage estimates were made using the measured matric potential data to allow comparison to the simulated drainage estimates. Previous attempts to calculate flux using a Darcian method were unsuccessful across the full range of wetness conditions and in many cases yielded results suggesting net negative drainage during periods with documented drainage. Otherwise relatively minor precision limitations among the sensors and sensor spacing probably explain the inconsistent drainage estimate results. The deepest sensors are typically spaced about 50 cm apart (i.e., 150 and 200 cm). Sensor spacing is mainly a problem during the drainage process because as the wetting front moves down the matric potential of the upper sensor increases relative to the lower sensor resulting in an apparent negative head gradient. Using the Darcian method results in negative rather than positive drainage estimates in these situations.

The precision limitations result from the inherent variability among sensors and because the sensor calibration process is imperfect. The inherent variations in the sensors are probably on the order +/- 50 to 100 cm, which are relatively minor given the range of conditions that can occur, but are important when



assessing localized potential gradients. Thus, under low matric potential conditions apparent head gradients may be more related to sensor variation than real variations in wetness.

The imperfect calibration process is important because some sensors appear to have higher or lower baselines and different responsiveness to wetting and drying. Data from Nest 3B (Figure 6) illustrates the differential baseline concept whereby, the two lower sensors on this nest never achieve matric potentials as low as the sensors in the companion nests. Field calibration corrections are commonly applied to adjust the response of the sensors to provide equivalent baseline responses. The process of field calibrating the sensors introduces additional uncertainty in the analysis, but may be warranted by the improvement in comparisons among sites.

In consideration of the operational constraints of the HDS, a unit gradient approach was adopted to make drainage estimates. This approach eliminates concerns associated with the spacing issue, but is still affected by imperfect calibration process (accuracy). A unit gradient approach was applied whereby the head gradient was assumed to be positive (1) and the flux equal to the time integrated unsaturated hydraulic conductivity as a function of matric potential. For the sake of consistency, the same material properties used in the calibrated model were used in the unit gradient flux calculations. Of the material properties ( $K_{sat}$ ,  $\theta_s$ ,  $\theta_r$ ,  $\alpha$ , and  $N$ ) used in this analysis, the drainage estimates are most strongly influenced by the saturated hydraulic conductivity. The flux was integrated over the period of record on a daily basis using data from the deepest sensors (200 cm).

Data from this analysis reveals the degree of variation in drainage estimates that exists among the instrument sites. For the 2- and 3-ft cover treatments, matric potential data are missing for parts of 2008 and 2009. Because the second half of 2008 received substantial rainfall ( $\approx 14$  inches) we expect that the 2- and 3-ft cover treatments would have had higher drainage than reported in Table 6. In contrast, because of the relatively dry conditions in the first half of 2009 ( $\approx 0.6$  inches) we expect the drainage estimates for the 2- and 3-ft treatments are only marginally lower than reported. Localized subsidence of the waste rock above some of the sensor nests has resulted in the formation of small depressions with the potential to pond water. Depressions associated with nests 3C (4-ft cover) and 1C (2-ft cover) are most pronounced and appear to have been accentuated by the 2010 rains. Nest 1C was rehabilitated in 2009, but has subsequently continued to settle. The somewhat higher relative drainage estimated for nests 1C and 3C may be explained by accentuated recharge associated with ponding.

The variations in drainage estimates among the sites are problematic with respect to the comparison to the modeled drainage estimates (Section 4.3) and from the perspective of relative performance evaluations. The drainage estimated by the unit gradient method (Table 6) is generally lower than the simulated drainage estimates (Table 5), especially in the years with periods of higher effective precipitation (e.g., 2010). Because the sensors are somewhat unresponsive to matric potentials in the  $< 100$  cm range, the unit gradient approach results in under prediction of drainage associated with

periods of significant rainfall. Thus, we believe that the modeled data provides a better estimate of drainage than the unit gradient approach using the measured data for times with significant rainfall events.

The conclusion that the modeled data provide better drainage estimates is tempered by recognition of the bias introduced by the root functions when the performance of the various cover thicknesses is compared. In nearly all instances, increasing the depth of root distribution to match the cover thickness will result in decreases in drainage. The issues of sensor variation notwithstanding, the empirical data do not support the systematic decrease in drainage with increasing cover thickness predicted by the model simulations.

#### 4.5 Long-Term Drainage Estimates

Southern New Mexico climate is characterized by a high degree of variability, particularly with respect to precipitation. Because of this climatic variation, the water balance simulations were performed using a natural precipitation and temperature record from a local weather station with more than 100 years of daily data. Use of this climate simulation record allows the evaluation of drainage in relation to precipitation variability on a number of scales ranging from short term (daily and weekly) to long term (seasonal, annual, and decadal).

Long-term drainage estimates were developed by using the material properties, maximum LAI and RLD functions from the 3-ft calibration simulation and applying the long-term climate record. The average drainage of the 3-ft cover assuming a LAI of 0.145 are shown in Figure 9. The predicted drainage is episodic, varies in magnitude, and occurs about half of the time on an annual basis (58 out of 110 years). The model results are sensible in that they reflect the prolonged droughts that occurred in 1930's and 1950's and the pronounced wet period that occurred in the late-1970's through the early 1990's. cursory examination of the Ft Bayard precipitation record indicates that the largest magnitude drainage events are associated with above normal winter precipitation, such as the 16.6 inches received December 1904 through April 1905. Somewhat lower magnitude drainage events occur in association with above normal summer precipitation events (e.g., late-1920's and 1996).

Long-term drainage and runoff were estimated for the uncovered stockpile (no plants) and 3-ft cover treatment (0.145 and 0.29 LAI scenarios). Table 7 lists the long-term estimated drainage and runoff for these cases. Attachment 2 contains summaries of the data on an annual basis for the period of record. The estimated drainage from the 0.29 LAI scenario is about a third of the drainage predicted for the 0.145 LAI case. Drainage from the uncovered stockpile is about an order of magnitude higher than the covered treatments.

The long term average drainage rate determined for an uncovered stockpile surface is 4.6 cm/yr (1.81 in/yr) compared to 6.8 cm/yr predicted for the Condition 89 Feasibility Study (Golder, 2007). From a conservative perspective, we propose using the 0.145 LAI scenario (Run 18) for estimating long-term

drainage from the covered stockpiles (0.55 cm/y) (0.22 in/yr), which is higher than the rates (0.15 and 0.20 cm/y) estimated for the 3-ft cover in the Feasibility Study.

## 5.0 LITERATURE

Campbell G. S. and G. W. Gee. 1986. Water potential: Miscellaneous methods. In: Methods of soil analysis. Part 1. Physical and Mineralogical Methods. 2<sup>nd</sup> Edition. Agronomy 9 (Part 1). Soil Science Society of America. Madison, WI.

Dunn, A.J., and G.R. Mehuys, 1984. *Relationship between Gravel Content of Soils and Saturated Hydraulic Conductivity in Laboratory Tests*. In: D.M. Kral (ed). Erosion and Productivity of Soils Containing Rock Fragments. SSSA Special Publication No. 13. Soil Science Society of America, Madison, WI.

Fayer, M.S., 2000. *UNSAT-H Version 3.0: Unsaturated Soil Water and Heat Flow Model*. PNL-13249, U.S. Department of Energy, Pacific Northwest Laboratory, Richland, Washington.

Golder Associates Inc. (Golder), 2005a. *Comprehensive Cover Performance Evaluation: Stockpiles and Tailing Impoundments*. Prepared for Phelps Dodge Tyrone, Inc., Tyrone, NM. January 2005.

Golder, 2005b. Preliminary Borrow Source Materials Investigation - Leach Ore and Waste Rock Stockpiles. DP-1341, Condition 79. Prepared for Phelps Dodge Tyrone, Inc.

Golder, 2006b. *As-built Report: Cover, Erosion, and Revegetation Test Plot Study*, Tyrone Mine Stockpiles, Report No. 1. Prepared for Phelps Dodge Tyrone, Inc. Tyrone, NM. September 2006.

Golder. 2011. No. 1 Stockpile test plots annual report- Report No. 5. Prepared for Freeport-McMoRan Tyrone, Inc. February 28, 2011.

U.S. Department of Agriculture-Agriculture Research Service, 2006. Solar Calc Software.

van Genuchten, M.Th., F.J. Leji, and S.R. Yates, 1991. *The RETC Code for Quantifying Hydraulic Functions of Unsaturated Soils*. U.S. Environmental Protection Agency. EPA/600/2-9/065.

Enclosures: Tables  
Figures  
Attachment 1: UNSAT-H Input Files  
Attachment 2: Summary Data

## **TABLES**

Table 1: Precipitation Summary for the No. 1a Stockpile Test Plots

Year	January	February	March	April	May	June	July	August	September	October	November	December	Annual
	Precipitation (inches)												
<b>2006</b>	0.00	0.06	0.23	0.15	0.08	0.27	4.80	3.45	2.80	2.11	0.20	0.39	14.54
<b>2007</b>	1.50	0.61	0.38	0.66	0.69	1.30	3.80	1.45	0.94	0.16	1.03	1.66	14.18
<b>2008</b>	0.81	0.20	0.01	0.00	0.55	0.14	5.63	5.51	0.55	0.18	0.90	1.08	15.56
<b>2009</b>	0.06	0.11	0.26	0.01	0.73	1.51	0.94	1.95	1.54	0.64	1.12	0.72	9.59
<b>2010</b>	2.18	2.02	0.53	0.24	0.22	0.56	6.45	2.73	1.57	0.36	0.02	0.38	17.26
<b>2011</b>	0.04	0.11	0.01	0.03	0.00	0.09	2.67	2.56	0.83	0.22	--	--	6.56

**Table 2: HDS Calibration Coefficients - Top Surface Test Plots**

Treatment	Nest	Instrument Depth	alpha	N	delta T <sub>dry</sub>	delta T <sub>wet</sub>
2-ft Cover	Nest 1A	50cm	0.0074	1.668	3.23	0.16
		100cm	0.0063	1.605	2.84	0.14
		150cm	0.0042	1.708	2.69	0.46
		200cm	0.0036	1.821	2.93	0.42
	Nest 1B	50cm	0.0043	1.633	2.96	0.39
		100cm	0.0069	1.536	2.57	0.16
		150cm	0.0050	1.601	2.68	0.32
		200cm	0.0068	1.566	2.85	0.11
	Nest 1C	50cm	0.0076	1.548	2.91	0.23
		100cm	0.0042	1.863	2.98	0.18
		150cm	0.0055	1.507	2.55	0.39
		200cm	0.0064	1.669	2.80	0.16
3-ft Cover	Nest 2A	75cm	0.0073	1.494	2.85	0.39
		100cm	0.0064	1.618	2.76	0.22
		150cm	0.0083	1.544	2.69	0.18
		200cm	0.0069	1.644	2.60	0.17
4-ft Cover	Nest 3A	100cm	0.0039	1.861	3.12	0.39
		150cm	0.0060	1.504	2.62	0.38
		180cm	0.0064	1.584	2.64	0.40
		200cm	0.0075	1.580	2.83	0.19
	Nest 3B	100cm	0.0055	1.677	2.86	0.45
		150cm	0.0054	1.628	2.86	0.39
		180cm	0.0037	1.863	2.92	0.39
		200cm	0.0058	1.766	2.75	0.28
	Nest 3C	100cm	0.0061	1.501	2.64	0.42
		150cm	0.0064	1.591	2.84	0.43
		180cm	0.0085	1.549	2.81	0.15
		200cm	0.0067	1.529	2.78	0.41

**Table 3: Cover Modeling Input Parameters**

Input Parameter	Model Variable	Values	Units	Comments
Precipitation	--	110 years of daily data	in/day	Ft. Bayard (1987-2006); first 2 years set initial soil-water conditions
Temperature	--	110 years of daily data	°F	Ft. Bayard (1987-2006); same as above
Dewpoint	--	9.8-22.7	°F	Monthly average calculated from average temperature and relative humidity.
Solar radiation	--	270-777	langleys	Calculated from Solar Calc software (USDA-ARS, 2006)
Wind speed	--	8.3-12.7	mi/hr	Monthly average for Deming, NM.
Cloud cover	--	3.4-5.1	tenths	Monthly average for Albuquerque, NM
Leaf area index	NDLAI, IDLAI, VLAI	0.0 to 0.29	none	Functional relationship (Golder, 2005a)
Root density	AA, B1, B2	7.0E-01, 6.0E-02, 1.6E-02	none	Functional relationship $RLD = a \exp(-bz) + c$ (Golder, 2005a and 2006a)
Day roots are at model node	NTROOT	1 - cover 366 -stockpile	NA	Assumes roots are present only in cover: 1 - roots always at node, 366 - no roots at node
Water uptake	NUPTAK	See Head values below		Sink term
PET partitioning	NFPET	calculated		Program partitions based on LAI
PET partitioning coefficients	PETPC	0.0, 0.52, 0.5, 0.0, 3.7		Coefficients of Ritchie equation ( $= a + bLAIc$ )
Head				
Wilting pint	HW	2.0E+04	cm	Head below which plant wilt and stop transpiring
Dry conditions	HD	3.0E+03	cm	Head below which plant decrease transpiration rate
Anaeroic	HN	1.0E+00	cm	Head above which transpiration stops due to anaerobic conditions
$K_{sat}$	SK	See Table 4	cm/hr	
Saturated water content	THET	See Table 4	$cm^3/cm^3$	
Residual water content	THTR	See Table 4	$cm^3/cm^3$	
$\alpha$	VGA	See Table 4	$cm^{-1}$	
n	VGN	See Table 4	none	
Conductivity model	RKMOD			Mualem ( $m = 1-1/n$ )
Lower boundary domain	--	variable	cm	4 m below surface
Surface boundary condition	ITOPBC	Flux	NA	
Upper boundary- heat flow	UPPERH	Calculated	NA	based on weather and soil parameters
Surface evaporation	IEVOPT	Allow	NA	
PET distribution	NFHOUR	Hourly	NA	sine wave function from 6am to 6pm
Lower boundary condition	LOWER	unit gradient	NA	

**Table 3: Cover Modeling Input Parameters**

Input Parameter	Model Variable	Values	Units	Comments
Lower boundary- heat flow	LOWERH	None	NA	
Minimum head -wet	HIRRI	0	cm	
Maximum head - dry	HDRY	1.0E+06	cm	
Constant head at surface	HTOP	0	cm	
Vapor flow	IVAPOR	Allowed	NA	
Tortuosity	TORT	0.66		
Vapor diffusion coefficient	VAPDIF	0.24	cm <sup>2</sup> /s	
PET	ALBEDO	0.35	cm/day	
Altitude	ALT	1872.1	m	
Height of wind measure	ZU	6.1	m	
Average atmospheric pressure	PMB	838.4	mb	

**Notes:**cm<sup>3</sup>/cm<sup>3</sup> = cubic centimeters per cubic centimeter

m = meters

in/day = inches per day

cm<sup>2</sup>/s = square centimeters per second

mb = millibars

mi/hr = miles per hour

cm/day = centimeters per day

cm = centimeters

cm/hr = centimeters per hour



**Table 4: Material Properties and Thickness for Calibrated Simulations**

Simulation Scenarios	Ksat (cm/s)	$\alpha$	N	$\theta_s$	$\theta_r$
<b>Uncovered Stockpile</b>					
Waste Rock layer (400 cm thick)	2.78E-04	0.0400	1.20	0.25	0.05
<b>Gila Conglomerate Cover (3-ft Thick)</b>					
Cover Surface Layer (9.5 cm thick)	2.78E-04	0.0500	1.25	0.25	0.05
Cover subsurface layer (81.9 cm thick)	8.33E-03	0.0605	1.25	0.25	0.05
Waste Rock layer (308.6 cm thick)	2.78E-04	0.0400	1.20	0.25	0.05
<b>Gila Conglomerate Cover (2-ft Thick)</b>					
Cover Surface Layer (9.5 cm thick)	2.78E-04	0.0500	1.25	0.25	0.05
Cover subsurface layer (51.5 cm thick)	8.33E-03	0.0605	1.25	0.25	0.05
Waste Rock layer (339 cm thick)	2.78E-04	0.0400	1.20	0.25	0.05
<b>Gila Conglomerate Cover (4-ft Thick)</b>					
Cover Surface Layer (9.5 cm thick)	2.78E-04	0.0500	1.25	0.25	0.05
Cover subsurface layer (112.4 cm thick)	8.33E-03	0.0605	1.25	0.25	0.05
Waste Rock layer (278.1 cm thick)	2.78E-04	0.0400	1.20	0.25	0.05
<b>Range of Laboratory Measured Values (Golder 2006)</b>					
Stockpile	8.5E-05 - 1.4E-03	0.0455 - 0.1731	1.1564 - 1.1877	0.1683 - 0.3008	0.0 - 0.0
Cover	1.0E-03 - 1.4E-02	0.0119 - 0.1465	1.2114 - 1.2783	0.1453 - 0.2454	0.0 - 0.0

**Table 5: Simulated Drainage for the No.1 Stockpile Test Plots**

Cover Thickness	Annual Precip. (cm)	Estimated Annual Drainage (cm)						
		Hourly Precip Simulations			Daily Precip Simulations			No Plants
		2-ft	3-ft	4-ft	2-ft	3-ft	4-ft	3-ft
<b>2006</b>	22.7	7.6	10.2	10.9	6	8.6	9.3	10.2
<b>2007</b>	36	6.6	8.1	9.5	8.9	10.5	11.9	8.1
<b>2008</b>	39.5	8.9	9.8	10.1	7.6	9.2	9.6	15.4
<b>2009</b>	24.4	1.9	1.5	1.4	1.7	1.3	1.2	3.7
<b>2010</b>	43.8	4.9	5.2	5.4	4.5	4.6	4.9	18.3
<b>2011</b>	16.1	0.9	0.7	0.4	0.9	0.6	0.3	1.4
<b>Run #</b>	--	179	37	295	178	39	294	40

**Notes:**

2006 - Partial year: August through end of year

2011 - Partial year: Through October 4<sup>th</sup>

**Table 6: Flux Estimates for the No.1 Stockpile Test Plots**

Cover Thickness	Estimated Annual Drainage (cm)						
	2-ft Top Surface			3-ft TS	4-ft Top Surface		
Site/Year	Nest 1A	Nest 1B	Nest 1C	Nest 2A	Nest 3A	Nest 3B	Nest 3C
<b>2006</b>	0.6	1.0	1.3	1.3	3.2	0.7	3.1
<b>2007</b>	1.4	3.0	2.7	3.2	4.6	1.6	7.1
<b>2008</b>	1.2	2.0	1.7	1.7	4.2	1.7	6.9
<b>2009</b>	0.8	1.6	1.2	1.2	2.7	0.4	6.5
<b>2010</b>	2.2	2.6	3.2	3.2	4.9	1.1	6.9
<b>2011</b>	0.4	0.1	0.8	0.4	1.1	0.0	3.6

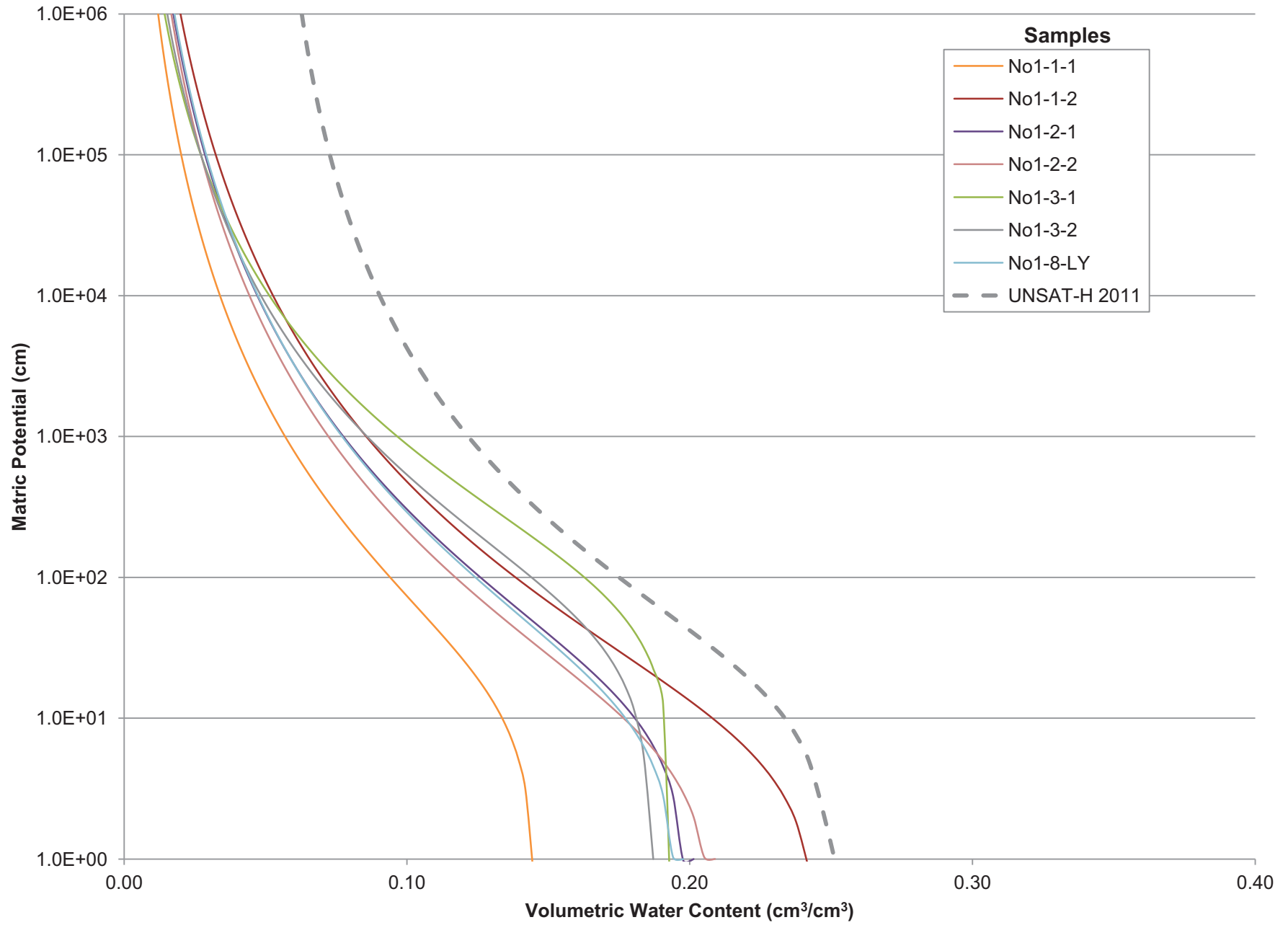
**Notes:**

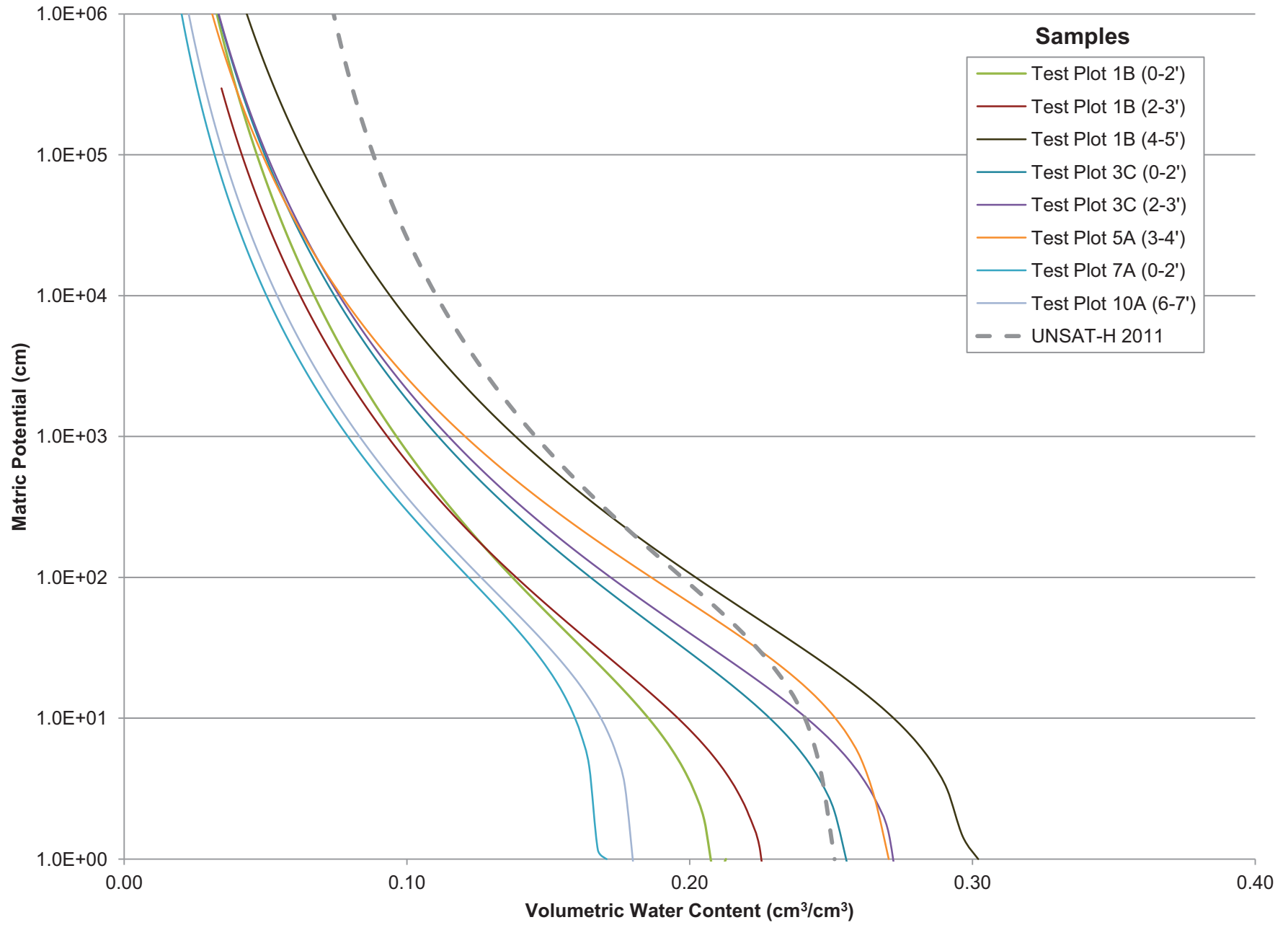
2008 and 2009 - Missing data for 2- and 3-ft test plots

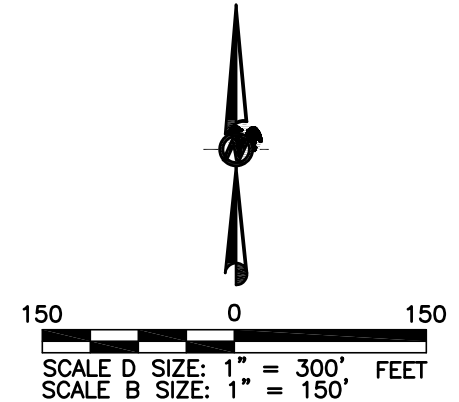
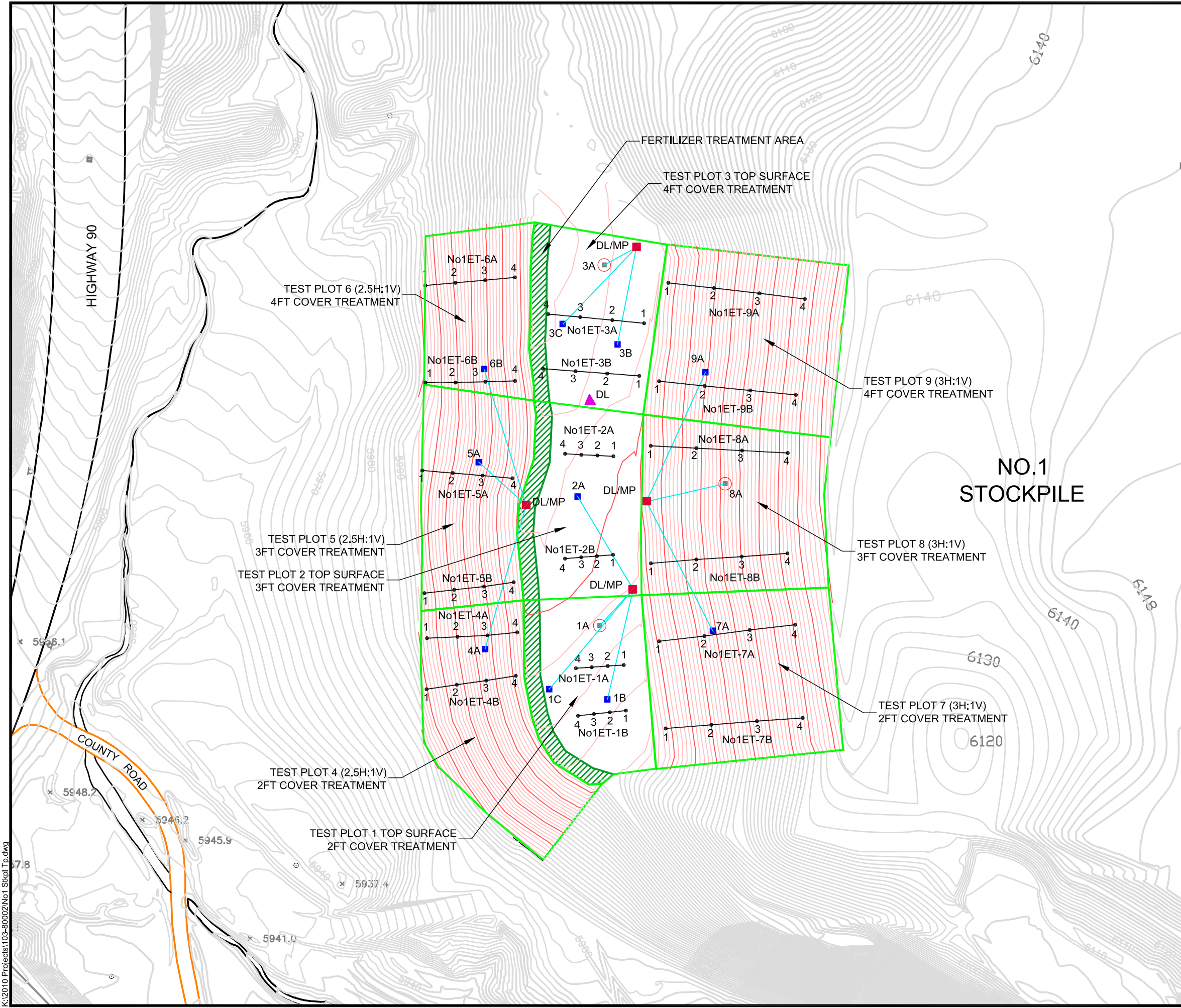
**Table 7: Long-term Average Drainage and Runoff for Covered and Uncovered Stockpiles**

110 Year Runs	Average Drainage (cm)	% Mean Annual Precipitation	Runoff (cm)	% Mean Annual Runoff
<b>Covered</b>				
3ft-Run 18 LAI 0.0145	0.55	1.4	6.5	16.3
3ft-Run 19 LAI 0.29	0.19	0.5	7.1	17.7
<b>Uncovered</b>				
4ft-Run 38 LAI 0	4.58	11.4	7.1	17.8

## FIGURES







**LEGEND**

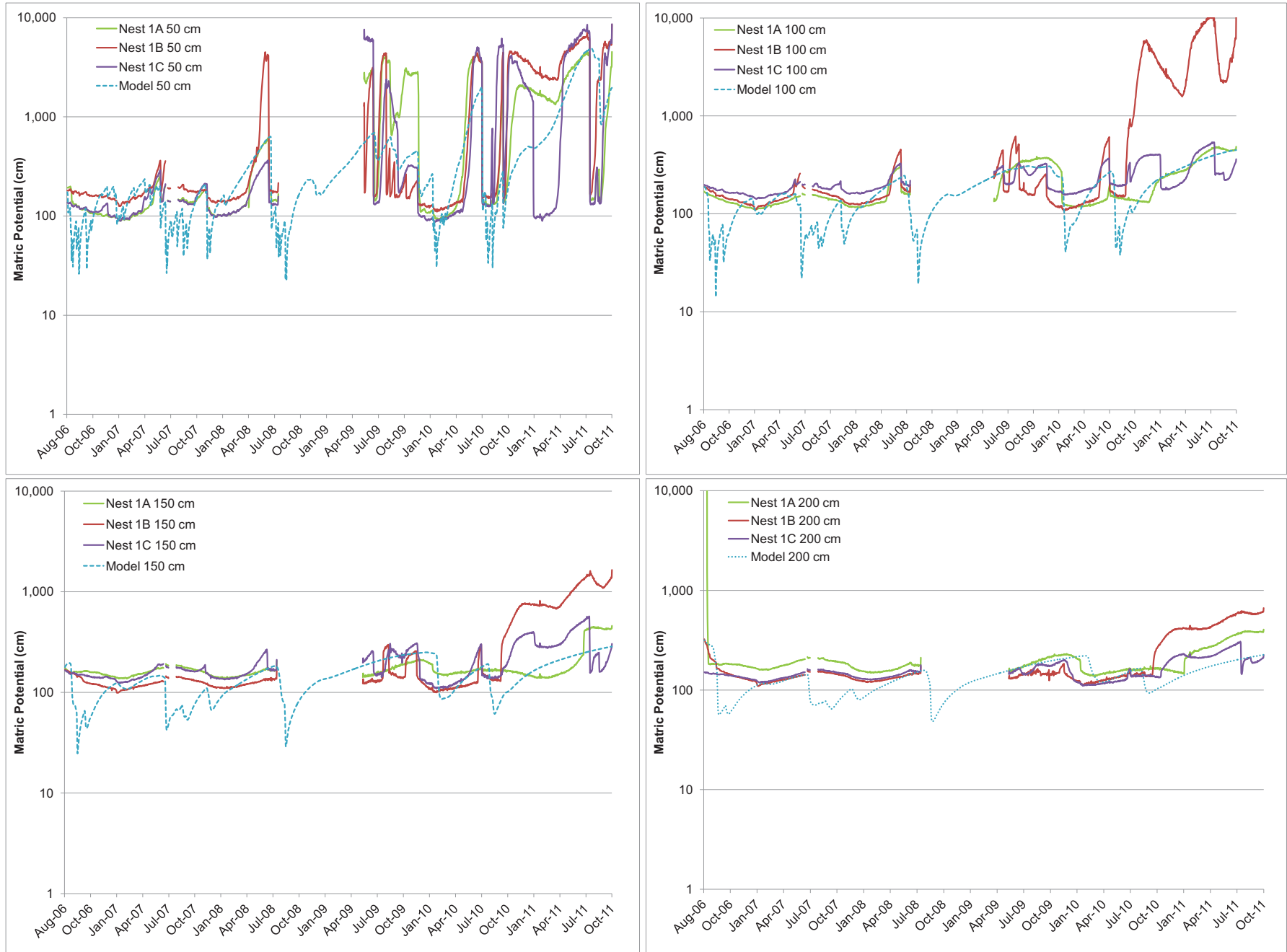
- TEST PLOT BOUNDARY
- SURVEY BOUNDARY
- ▲ AUTOMATED WEATHER STATION
- 1B INSTRUMENTATION NEST
- 8A VOLUMETRIC LYSIMETER INSTRUMENTATION NEST
- DL/MP DATA LOGGER/MULTIPLEXER
- PRE-RECLAMATION TOPOGRAPHY
- AS-BUILT TOPOGRAPHY (BY M3 ENGINEERING, AUGUST 2006)
- EROSION TRANSECT AND STATIONS

PROJECT		FREEPORT-McMoRan TYRONE INC. NO.1 STOCKPILE TEST PLOTS GRANT COUNTY, NEW MEXICO			
TITLE		<b>TREATMENT AND INSTRUMENTATION LAYOUT</b>			
 <b>Golder Associates</b> Albuquerque, New Mexico	PROJECT No.	103-80002	FILE No.	No1 Stkpl Tp	
	DESIGN	DR	01/23/08	SCALE	AS SHOWN REV. 0
	CADD	CM	02/25/11		
	CHECK	EC	02/25/11		
	REVIEW	LM	02/25/11		
<b>FIGURE 3</b>					

K:\2010 Projects\103-80002\No1 Stkpl Tp.dwg



Figure 4: Simulated and Measured Matrix Potentials  
Top Surface 2-ft Cover Treatments



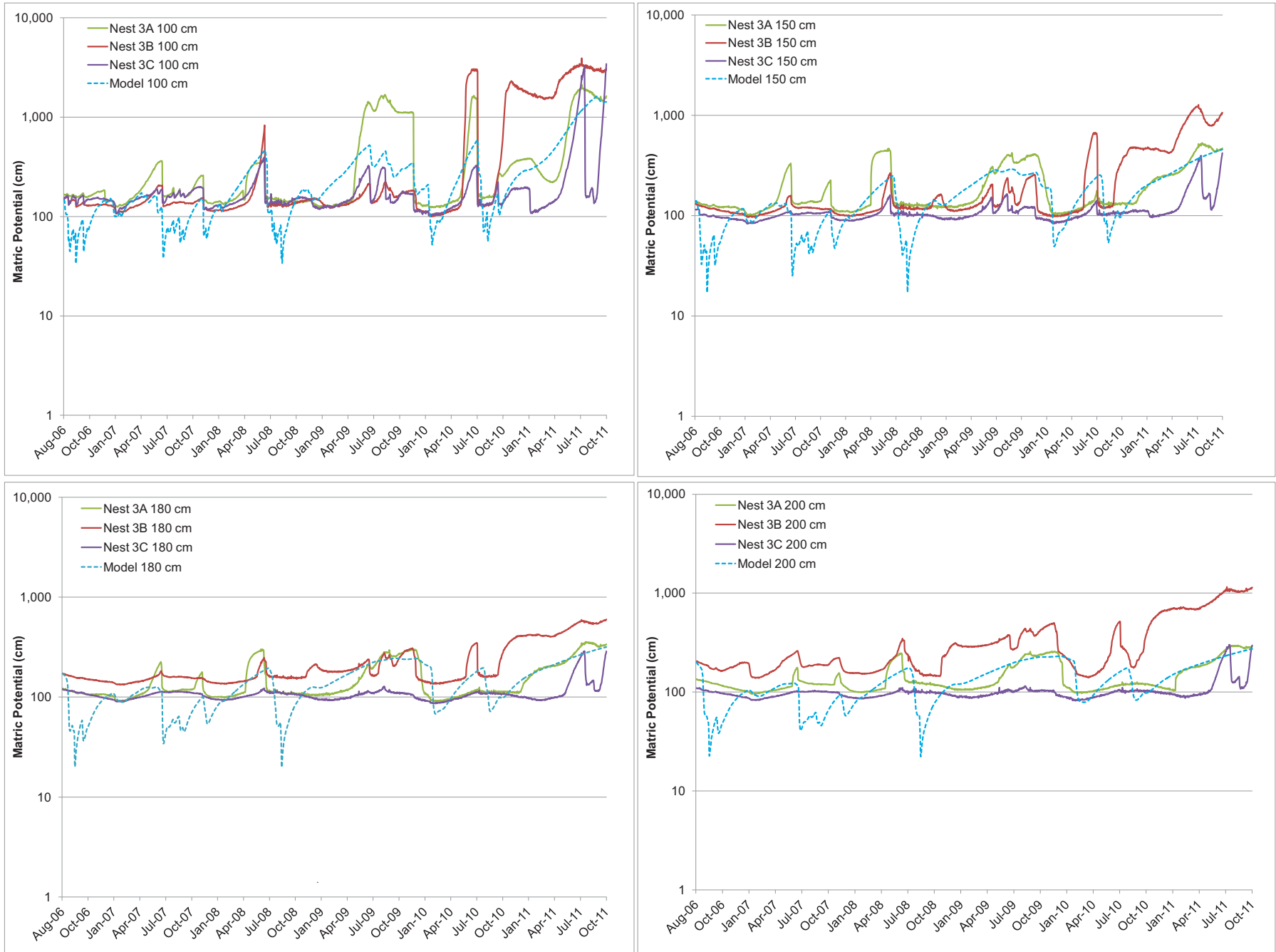
Simulation Scenario – 2006-2007 No Plants: 2008-2009 Max Leaf Area Index: 0.03625: 2010-2011 Max Leaf Area Index: 0.145: Daily Precipitation. HPR=1.2

Figure 5: Simulated and Measured Matrix Potentials  
Top Surface 3-ft Cover Treatment



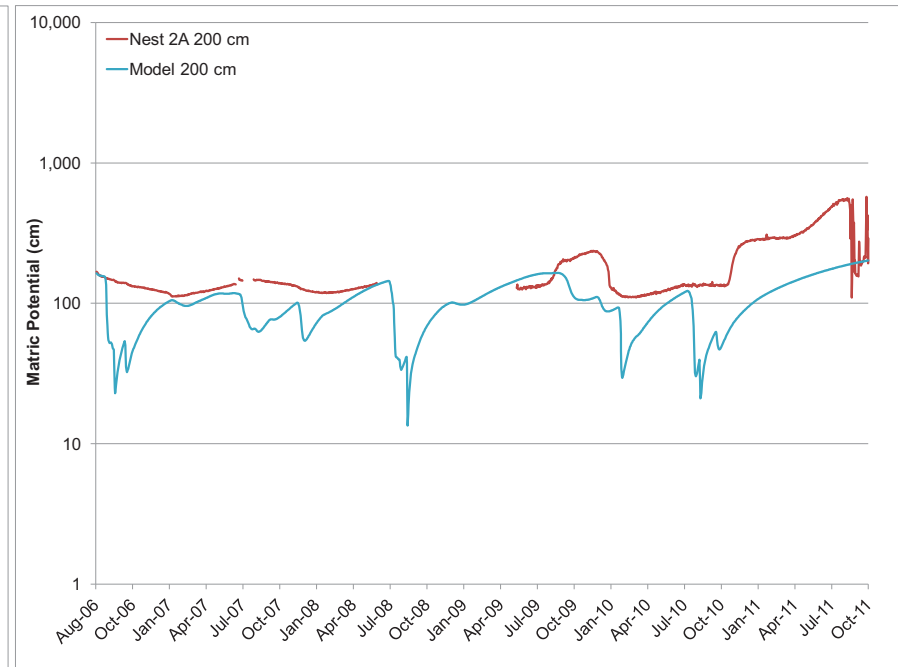
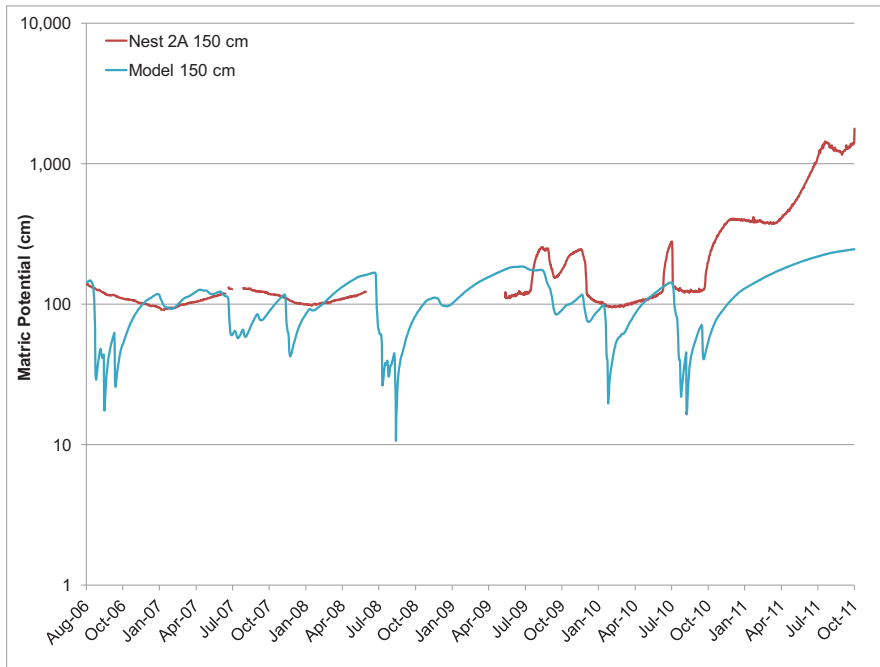
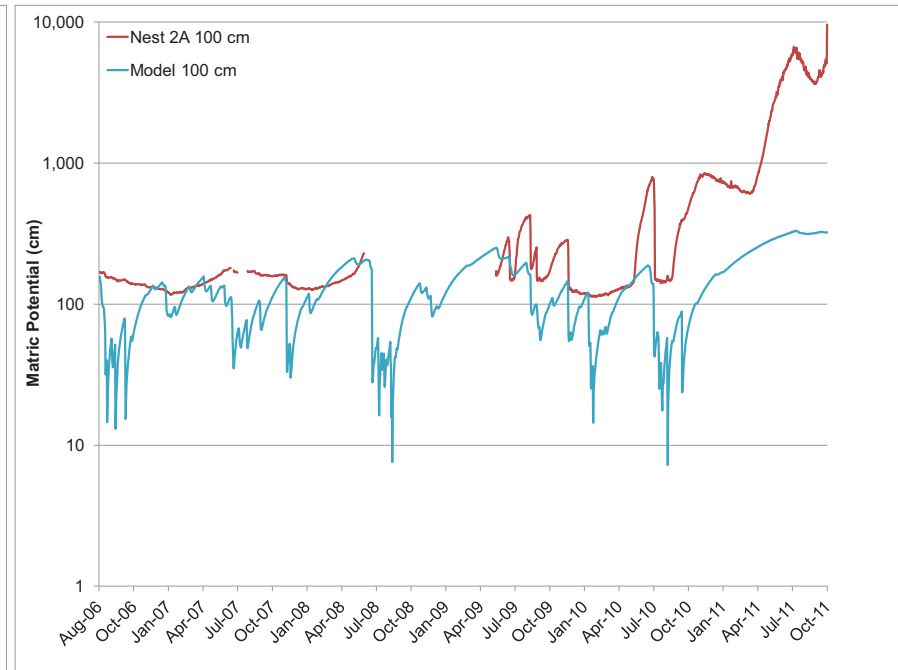
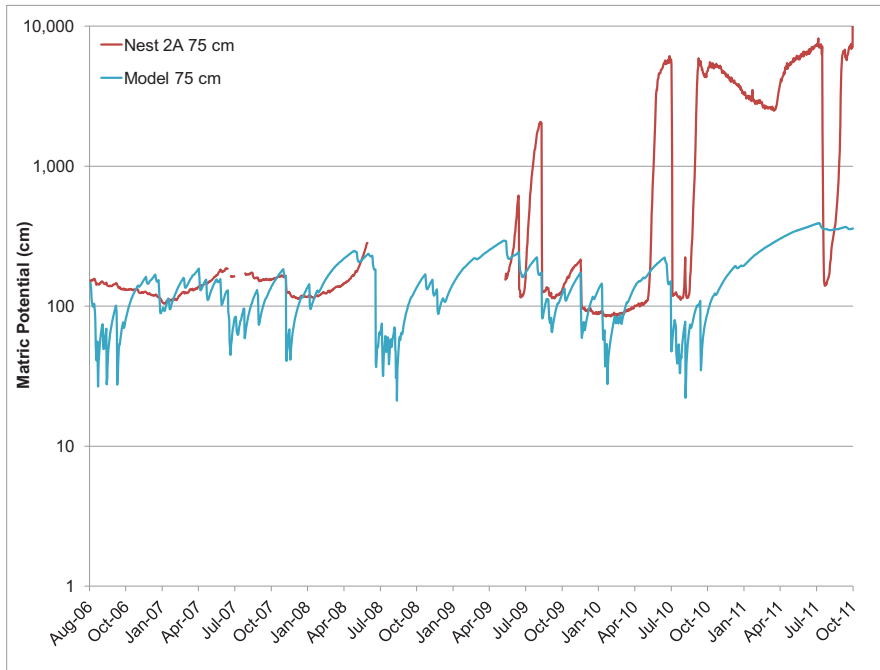
Simulation Scenario -- 2006-2007: No Plants: 2008-2009 Max Leaf Area Index: 0.03625 cm: 2010-2011 Max Leaf Area Index: 0.145 cm: Daily Precipitation. HPR=1.2

Figure 6: Simulated and Measured Matrix Potentials  
Top Surface 4-ft Cover Treatment



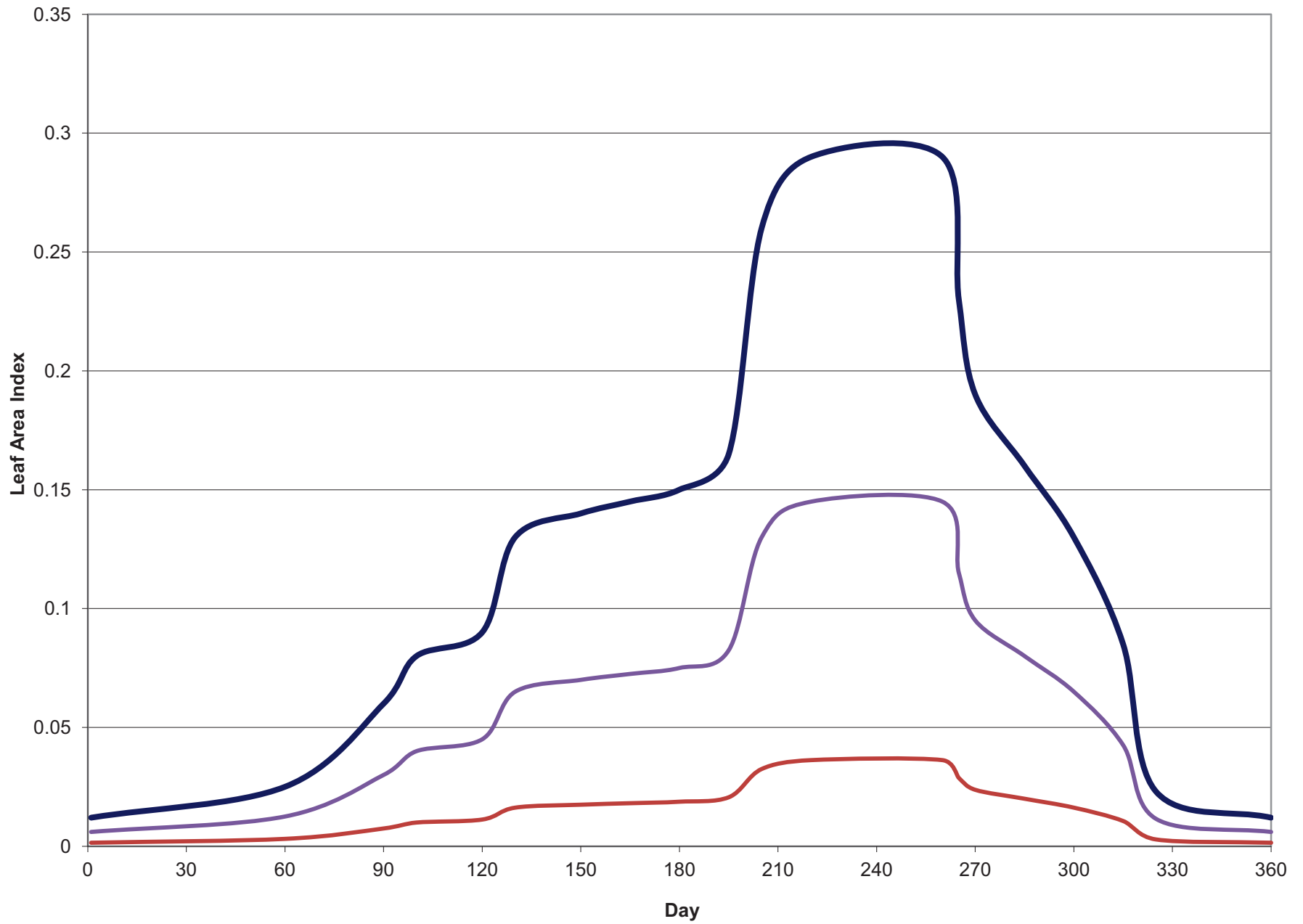
Simulation Scenario – 2006-2007 No Plants: 2008-2009 Max Leaf Area Index: 0.03625: 2010-2011 Max Leaf Area Index: 0.145: Daily Precipitation. HPR=1.2

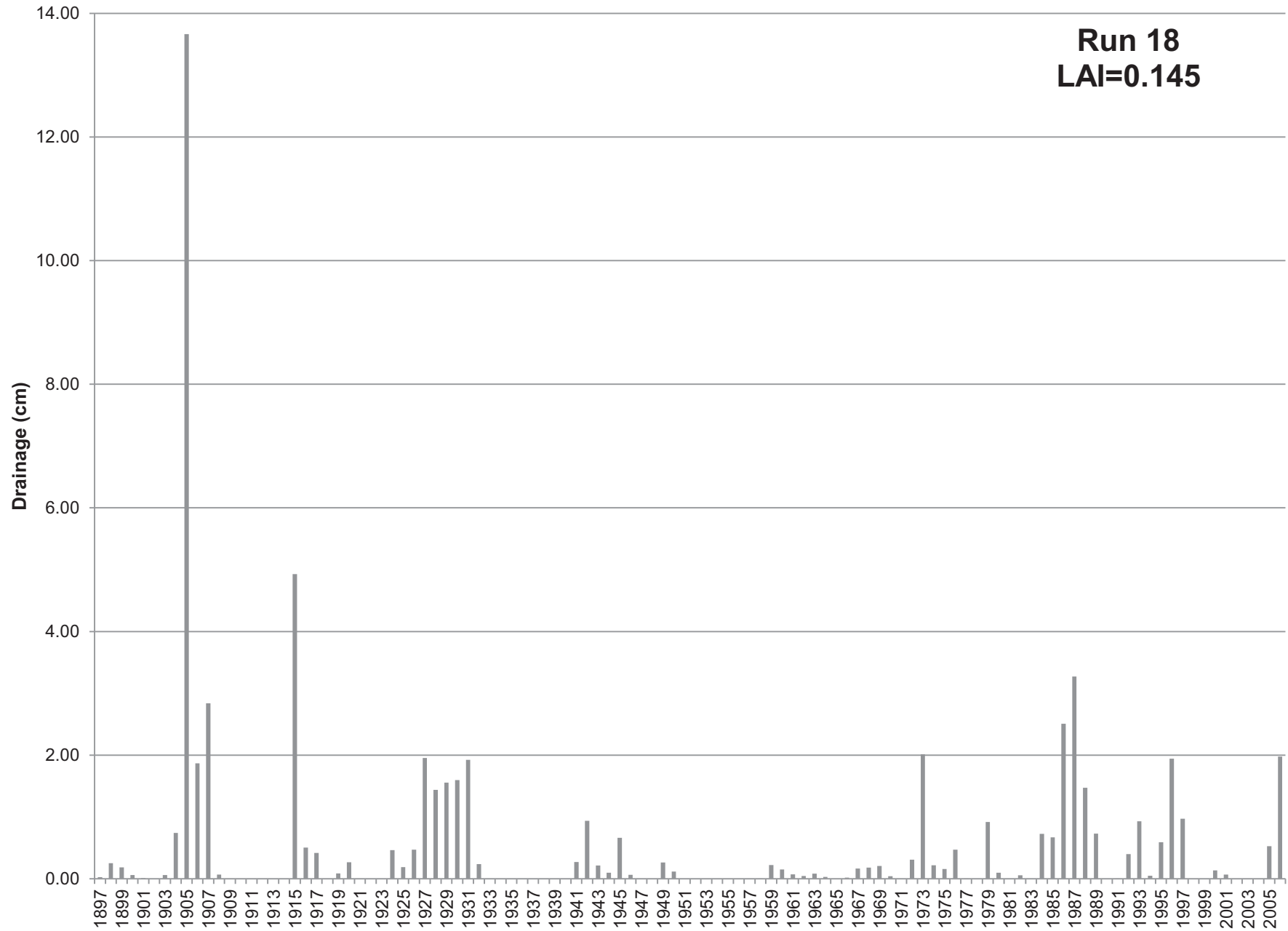
Figure 7: Simulated and Measured Matrix Potentials  
Top Surface 3-ft Cover Treatment -- No Plants Scenario



Simulation Scenario: 2006-2011: No Plants: Hourly Precipitation







**ATTACHMENT 1  
UNSAT-H INPUT FILES**

Run 178.1-2ft, No Plants

0,1,  
151,1,151,  
2006,1,0,2,1,  
0,0.0,  
0,4,1,1.0E-04,  
1.0,8.0E-10,0,  
1.02,1.0E-05,0,0,0,  
4,3,0.5,  
0,1,2,1,  
0.0,1.0E+06,0.0,0.99,  
1,1,1,  
1,1.2,  
0,0,0,0,0,  
0,0,0,  
0,2.880E+02,1.0E+01,0,  
0,0.0,0,  
1,0.66,288.46,0.24,  
3,87,  
1,0.0, 1,0.1, 1,0.2, 1,0.5,  
1,1.0, 1,2.0, 1,4.0, 1,7.0,  
2,12.0, 2,18.0, 2,24.0, 2,30.0,  
2,36.0, 2,42.0, 2,47.0, 2,48.0,  
2,49.0, 2,49.5, 2,50.0, 2,50.5,  
2,51.0, 2,52.0, 2,53.0, 2,56.0,  
2,58.0, 2,59.0, 2,60.0, 2,60.5,  
3,61.5, 3,64.0, 3,70.0, 3,77.0,  
3,83.0, 3,89.0, 3,95.0, 3,96.0,  
3,97.0, 3,98.0, 3,99.0, 3,99.5,  
3,100.0, 3,100.5, 3,101.0, 3,102.0,  
3,103.0, 3,104.0, 3,107.0, 3,112.0,  
3,118.0, 3,124.0, 3,130.0, 3,136.0,  
3,142.0, 3,148.0, 3,149.0, 3,149.5,  
3,150.0, 3,150.5, 3,151.0, 3,152.0,  
3,153.0, 3,155.0, 3,158.0, 3,163.0,  
3,169.0, 3,175.0, 3,181.0, 3,187.0,  
3,193.0, 3,196.0, 3,197.0, 3,198.0,  
3,199.0, 3,199.5, 3,200.0, 3,200.5,  
3,201.0, 3,202.0, 3,203.0, 3,205.0,  
3,210.0, 2,215.0, 3,230.0, 3,260.0,  
3,300.0, 3,390.0, 3,400.0,  
MAT#1: -WATER RETENTION DATA  
0.25,0.05,0.05,1.25, THET, THTR, VGA, VGN  
MAT#1: - CONDUCTIVITY DATA  
2.0,1.0,0.05,1.25,0.5, RKMOD, SK, VGA, VGN, EPIT  
MAT#2: - WATER RETENTION DATA  
0.25,0.05,0.0605,1.25, THET, THTR, VGA, VGN  
MAT#2: - CONDUCTIVITY DATA  
2.0,30.0,0.0605,1.25,0.5, RKMOD, SK, VGA, VGN, EPIT  
MAT#3: - WATER RETENTION DATA  
0.25,0.05,0.04,1.2, THET, THTR, VGA, VGN  
MAT#3: - CONDUCTIVITY DATA  
2.0,1.0,0.04,1.2,0.5, RKMOD, SK, VGA, VGN, EPIT  
0, NDAY  
1.81E+02,1.81E+02,1.81E+02,1.81E+02, H(1....NPT)  
1.81E+02,1.81E+02,1.81E+02,1.81E+02,  
1.81E+02,1.81E+02,1.81E+02,1.81E+02,  
1.81E+02,1.81E+02,1.81E+02,1.81E+02,  
1.81E+02,1.81E+02,1.81E+02,1.81E+02,  
1.81E+02,1.81E+02,1.82E+02,1.82E+02,  
1.83E+02,1.83E+02,1.83E+02,1.83E+02,  
1.83E+02,1.84E+02,1.85E+02,1.86E+02,  
1.87E+02,1.88E+02,1.89E+02,1.90E+02,  
1.90E+02,1.90E+02,1.90E+02,1.90E+02,  
1.90E+02,1.90E+02,1.90E+02,1.89E+02,  
1.89E+02,1.89E+02,1.87E+02,1.85E+02,  
1.82E+02,1.80E+02,1.77E+02,1.74E+02,

IPLANT, NGRAV  
IFDEND, IDTBEG, IDTEND  
IYS, NYEARS, ISTEAD, IFLIST, NFLIST  
NPRINT, STOPHR  
ISMETH, INMAX, ISWDIF, DMAXBA  
DELMAX, DELMIN, OUTTIM  
RFACT, RAINIF, DHTOL, DHMAX, DHFACT  
KOPT, KEST, WTF  
ITOPBC, IEVOPT, NFHOUR, LOWER  
HIRRI, HDRIY, HTOP, RHA  
IETOPT, ICLOUD, ISHOPT  
IRAIN, HPR  
IHYS, AIRTOL, HYSTOL, HYSMXH, HYFILE  
IHEAT, ICONVH, DMAXHE  
UPPERH, TSMEAN, TSAMP, QHCTOP  
LOWERH, QHLEAK, TGRAD  
IVAPOR, TORT, TSOIL, VAPDIF  
MATN, NPT  
MAT, Z



1.72E+02,1.69E+02,1.69E+02,1.68E+02,  
1.68E+02,1.70E+02,1.71E+02,1.74E+02,  
1.77E+02,1.84E+02,1.93E+02,2.09E+02,  
2.27E+02,2.46E+02,2.64E+02,2.83E+02,  
3.02E+02,3.11E+02,3.14E+02,3.17E+02,  
3.20E+02,3.22E+02,3.23E+02,3.23E+02,  
3.23E+02,3.23E+02,3.23E+02,3.23E+02,  
3.23E+02,3.23E+02,3.23E+02,3.23E+02,  
3.23E+02,3.23E+02,3.23E+02,  
0.35,1872.1,6.1,838.4,  
SP2006.dat

ALBEDO, ALT, ZU, PMB

Run 178.2-2ft, No Plants

0,1,  
365,1,365,  
2007,1,0,2,1,  
0,0.0,  
0,4,1,1.0E-04,  
1.0,8.0E-10,0,  
1.02,1.0E-05,0,0,0,  
4,3,0.5,  
0,1,2,1,  
0.0,1.0E+06,0.0,0.99,  
1,1,1,  
1,1.2,  
0,0,0,0,0,  
0,0,0,  
0,2.880E+02,1.0E+01,0,  
0,0.0,0,  
1,0.66,288.46,0.24,  
3,87,  
1,0.0, 1,0.1, 1,0.2, 1,0.5,  
1,1.0, 1,2.0, 1,4.0, 1,7.0,  
2,12.0, 2,18.0, 2,24.0, 2,30.0,  
2,36.0, 2,42.0, 2,47.0, 2,48.0,  
2,49.0, 2,49.5, 2,50.0, 2,50.5,  
2,51.0, 2,52.0, 2,53.0, 2,56.0,  
2,58.0, 2,59.0, 2,60.0, 2,60.5,  
3,61.5, 3,64.0, 3,70.0, 3,77.0,  
3,83.0, 3,89.0, 3,95.0, 3,96.0,  
3,97.0, 3,98.0, 3,99.0, 3,99.5,  
3,100.0, 3,100.5, 3,101.0, 3,102.0,  
3,103.0, 3,104.0, 3,107.0, 3,112.0,  
3,118.0, 3,124.0, 3,130.0, 3,136.0,  
3,142.0, 3,148.0, 3,149.0, 3,149.5,  
3,150.0, 3,150.5, 3,151.0, 3,152.0,  
3,153.0, 3,155.0, 3,158.0, 3,163.0,  
3,169.0, 3,175.0, 3,181.0, 3,187.0,  
3,193.0, 3,196.0, 3,197.0, 3,198.0,  
3,199.0, 3,199.5, 3,200.0, 3,200.5,  
3,201.0, 3,202.0, 3,203.0, 3,205.0,  
3,210.0, 2,215.0, 3,230.0, 3,260.0,  
3,300.0, 3,390.0, 3,400.0,  
MAT#1: -WATER RETENTION DATA  
0.25,0.05,0.05,1.25, THET, THTR, VGA, VGN  
MAT#1: - CONDUCTIVITY DATA  
2.0,1.0,0.05,1.25,0.5, RKMOD, SK, VGA, VGN, EPIT  
MAT#2: - WATER RETENTION DATA  
0.25,0.05,0.0605,1.25, THET, THTR, VGA, VGN  
MAT#2: - CONDUCTIVITY DATA  
2.0,30.0,0.0605,1.25,0.5, RKMOD, SK, VGA, VGN, EPIT  
MAT#3: - WATER RETENTION DATA  
0.25,0.05,0.04,1.2, THET, THTR, VGA, VGN  
MAT#3: - CONDUCTIVITY DATA  
2.0,1.0,0.04,1.2,0.5, RKMOD, SK, VGA, VGN, EPIT  
0, NDAY  
5.78E+05,3.97E+05,2.37E+05,1.18E+03, H(1....NPT)  
7.78E+02,5.13E+02,3.42E+02,2.51E+02,  
2.28E+02,2.18E+02,2.09E+02,2.01E+02,  
1.93E+02,1.86E+02,1.81E+02,1.79E+02,  
1.78E+02,1.78E+02,1.77E+02,1.77E+02,  
1.76E+02,1.75E+02,1.74E+02,1.71E+02,  
1.69E+02,1.68E+02,1.67E+02,1.66E+02,  
1.65E+02,1.62E+02,1.55E+02,1.49E+02,  
1.44E+02,1.40E+02,1.36E+02,1.36E+02,  
1.35E+02,1.35E+02,1.34E+02,1.34E+02,  
1.33E+02,1.33E+02,1.33E+02,1.32E+02,  
1.32E+02,1.31E+02,1.29E+02,1.27E+02,  
1.24E+02,1.21E+02,1.18E+02,1.15E+02,

IPLANT, NGRAV  
IFDEND, IDTBEG, IDTEND  
IYS, NYEARS, ISTEAD, IFLIST, NFLIST  
NPRINT, STOPHR  
ISMETH, INMAX, ISWDIF, DMAXBA  
DELMAX, DELMIN, OUTTIM  
RFACT, RAINIF, DHTOL, DHMAX, DHFACT  
KOPT, KEST, WTF  
ITOPBC, IEVOPT, NFHOUR, LOWER  
HIRRI, HDRI, HTOP, RHA  
IETOPT, ICLOUD, ISHOPT  
IRAIN, HPR  
IHYS, AIRTOL, HYSTOL, HYSMXH, HYFILE  
IHEAT, ICONVH, DMAXHE  
UPPERH, TSMEAN, TSAMP, QHCTOP  
LOWERH, QHLEAK, TGRAD  
IVAPOR, TORT, TSOIL, VAPDIF  
MATN, NPT  
MAT, Z

1.13E+02,1.11E+02,1.10E+02,1.10E+02,  
1.10E+02,1.10E+02,1.10E+02,1.09E+02,  
1.09E+02,1.08E+02,1.07E+02,1.06E+02,  
1.04E+02,1.03E+02,1.02E+02,1.01E+02,  
9.98E+01,9.95E+01,9.94E+01,9.93E+01,  
9.92E+01,9.92E+01,9.92E+01,9.91E+01,  
9.91E+01,9.90E+01,9.89E+01,9.88E+01,  
9.87E+01,9.50E+01,8.35E+01,7.74E+01,  
6.78E+01,1.21E+02,1.23E+02,  
0.35,1872.1,6.1,838.4,  
SP2007.dat

ALBEDO, ALT, ZU, PMB

Run 178.3-2ft, 1/8 LAI

1,1,  
365,1,365,  
2008,2,0,2,2,  
0,0,0,  
0,4,1,1.0E-04,  
1.0,8.0E-10,0,  
1.02,1.0E-05,0,0,0,  
4,3,0.5,  
0,1,2,1,  
0.0,1.0E+06,0.0,0.99,  
1,1,1,  
1,1.2,  
0,0,0,0,0,  
0,0,0,  
0,2.880E+02,1.0E+01,0,  
0,0,0,0,  
1,0.66,288.46,0.24,  
3,87,  
1,0.0, 1,0.1, 1,0.2, 1,0.5,  
1,1.0, 1,2.0, 1,4.0, 1,7.0,  
2,12.0, 2,18.0, 2,24.0, 2,30.0,  
2,36.0, 2,42.0, 2,47.0, 2,48.0,  
2,49.0, 2,49.5, 2,50.0, 2,50.5,  
2,51.0, 2,52.0, 2,53.0, 2,56.0,  
2,58.0, 2,59.0, 2,60.0, 2,60.5,  
3,61.5, 3,64.0, 3,70.0, 3,77.0,  
3,83.0, 3,89.0, 3,95.0, 3,96.0,  
3,97.0, 3,98.0, 3,99.0, 3,99.5,  
3,100.0, 3,100.5, 3,101.0, 3,102.0,  
3,103.0, 3,104.0, 3,107.0, 3,112.0,  
3,118.0, 3,124.0, 3,130.0, 3,136.0,  
3,142.0, 3,148.0, 3,149.0, 3,149.5,  
3,150.0, 3,150.5, 3,151.0, 3,152.0,  
3,153.0, 3,155.0, 3,158.0, 3,163.0,  
3,169.0, 3,175.0, 3,181.0, 3,187.0,  
3,193.0, 3,196.0, 3,197.0, 3,198.0,  
3,199.0, 3,199.5, 3,200.0, 3,200.5,  
3,201.0, 3,202.0, 3,203.0, 3,205.0,  
3,210.0, 2,215.0, 3,230.0, 3,260.0,  
3,300.0, 3,390.0, 3,400.0,  
MAT#1: -WATER RETENTION DATA  
0.25,0.05,0.05,1.25, THET, THTR, VGA, VGN  
MAT#1: - CONDUCTIVITY DATA  
2.0,1.0,0.05,1.25,0.5, RKMOD, SK, VGA, VGN, EPIT  
MAT#2: - WATER RETENTION DATA  
0.25,0.05,0.0605,1.25, THET, THTR, VGA, VGN  
MAT#2: - CONDUCTIVITY DATA  
2.0,5.0,0.0605,1.25,0.5, RKMOD, SK, VGA, VGN, EPIT  
MAT#3: - WATER RETENTION DATA  
0.25,0.05,0.04,1.2, THET, THTR, VGA, VGN  
MAT#3: - CONDUCTIVITY DATA  
2.0,1.0,0.04,1.2,0.5, RKMOD, SK, VGA, VGN, EPIT  
0, NDAY  
1.05E+06,7.24E+05,4.60E+05,1.02E+03, H(1....NPT)  
6.55E+02,4.24E+02,2.76E+02,1.94E+02,  
1.74E+02,1.64E+02,1.56E+02,1.48E+02,  
1.40E+02,1.33E+02,1.27E+02,1.26E+02,  
1.25E+02,1.24E+02,1.24E+02,1.23E+02,  
1.23E+02,1.22E+02,1.20E+02,1.17E+02,  
1.15E+02,1.14E+02,1.13E+02,1.12E+02,  
1.11E+02,1.08E+02,1.01E+02,9.43E+01,  
8.98E+01,8.60E+01,8.28E+01,8.23E+01,  
8.19E+01,8.14E+01,8.10E+01,8.08E+01,  
8.05E+01,8.03E+01,8.01E+01,7.97E+01,  
7.93E+01,7.89E+01,7.79E+01,7.63E+01,  
7.47E+01,7.33E+01,7.23E+01,7.16E+01,

IPLANT, NGRAV  
IFDEND, IDTBEG, IDTEND  
IYS, NYEARS, ISTEAD, IFLIST, NFLIST  
NPRINT, STOPHR  
ISMETH, INMAX, ISWDIF, DMAXBA  
DELMAX, DELMIN, OUTTIM  
RFACT, RAINIF, DHTOL, DHMAX, DHFACT  
KOPT, KEST, WTF  
ITOPBC, IEVOPT, NFHOUR, LOWER  
HIRRI, HDRI, HTOP, RHA  
IETOPT, ICLOUD, ISHOPT  
IRAIN, HPR  
IHYS, AIRTOL, HYSTOL, HYSMXH, HYFILE  
IHEAT, ICONVH, DMAXHE  
UPPERH, TSMEAN, TSAMP, QHCTOP  
LOWERH, QHLEAK, TGRAD  
IVAPOR, TORT, TSOIL, VAPDIF  
MATN, NPT  
MAT, Z

```

7.11E+01,7.09E+01,7.09E+01,7.09E+01,
7.09E+01,7.09E+01,7.09E+01,7.09E+01,
7.09E+01,7.10E+01,7.12E+01,7.16E+01,
7.25E+01,7.37E+01,7.53E+01,7.73E+01,
7.99E+01,8.14E+01,8.19E+01,8.25E+01,
8.31E+01,8.34E+01,8.37E+01,8.40E+01,
8.43E+01,8.49E+01,8.56E+01,8.70E+01,
9.09E+01,8.83E+01,7.91E+01,8.24E+01,
8.04E+01,7.42E+01,7.41E+01,
1,1,1,1,01,365,
LEAF,NFROOT,NUPTAK,NFPET,NSOW,NHRVST
0.10,
20,
1,0.0015, 60,0.003125, 90,0.0075, 100,0.01,
120,0.01125, 130,0.01625, 150,0.0175, 165,0.018125,
180,0.01875, 195,0.0205, 205,0.0325, 220,0.03625,
260,0.03625, 265,0.02875, 270,0.02375, 285,0.02,
300,0.01625, 315,0.010625, 325,0.002875, 360,0.0015,
7.0E-01,6.0E-02,1.6E-02,
1,1,1,1,1,1,1,1,1,1,
1,1,1,1,1,1,1,1,1,1,
1,1,1,1,366,366,366,366,366,366,
366,366,366,366,366,366,366,366,366,366,
366,366,366,366,366,366,366,366,366,366,
366,366,366,366,366,366,366,366,366,366,
366,366,366,366,366,366,366,366,366,366,
366,366,366,
2.0E+04,3.0E+03,1.0E+0,
2.0E+04,3.0E+03,1.0E+0,
2.0E+04,3.0E+03,1.0E+0,
0.0,0.52,0.5,0.0,2.7,
0.35,1872.1,6.1,838.4,
SP2008.dat
SP2009.dat

```

BARE  
NDLAI  
IDLAI,VLAI  
AA,B1,B2  
NTROOT  
HW,HD,HN  
HW,HD,HN  
HW,HD,HN  
PETPC  
ALBEDO,ALT,ZU,PMB

Run 178.4-2ft, 1/2 LAI

```

1,1,
365,1,365,
2010,1,0,2,1,
0,0.0,
0,4,1,1.0E-04,
1.0,8.0E-10,0,
1.02,1.0E-05,0,0,0,
4,3,0.5,
0,1,2,1,
0.0,1.0E+06,0.0,0.99,
1,1,1,
1,1.2,
0,0,0,0,0,
0,0,0,
0,2.880E+02,1.0E+01,0,
0,0.0,0,
1,0.66,288.46,0.24,
3,87,
1,0.0, 1,0.1, 1,0.2, 1,0.5,
1,1.0, 1,2.0, 1,4.0, 1,7.0,
2,12.0, 2,18.0, 2,24.0, 2,30.0,
2,36.0, 2,42.0, 2,47.0, 2,48.0,
2,49.0, 2,49.5, 2,50.0, 2,50.5,
2,51.0, 2,52.0, 2,53.0, 2,56.0,
2,58.0, 2,59.0, 2,60.0, 2,60.5,
3,61.5, 3,64.0, 3,70.0, 3,77.0,
3,83.0, 3,89.0, 3,95.0, 3,96.0,
3,97.0, 3,98.0, 3,99.0, 3,99.5,
3,100.0, 3,100.5, 3,101.0, 3,102.0,
3,103.0, 3,104.0, 3,107.0, 3,112.0,
3,118.0, 3,124.0, 3,130.0, 3,136.0,
3,142.0, 3,148.0, 3,149.0, 3,149.5,
3,150.0, 3,150.5, 3,151.0, 3,152.0,
3,153.0, 3,155.0, 3,158.0, 3,163.0,
3,169.0, 3,175.0, 3,181.0, 3,187.0,
3,193.0, 3,196.0, 3,197.0, 3,198.0,
3,199.0, 3,199.5, 3,200.0, 3,200.5,
3,201.0, 3,202.0, 3,203.0, 3,205.0,
3,210.0, 2,215.0, 3,230.0, 3,260.0,
3,300.0, 3,390.0, 3,400.0,
MAT#1: -WATER RETENTION DATA
0.25,0.05,0.05,1.25, THET, THTR, VGA, VGN
MAT#1: - CONDUCTIVITY DATA
2.0,1.0,0.05,1.25,0.5, RKMOD, SK, VGA, VGN, EPIT
MAT#2: - WATER RETENTION DATA
0.25,0.05,0.0605,1.25, THET, THTR, VGA, VGN
MAT#2: - CONDUCTIVITY DATA
2.0,30.0,0.0605,1.25,0.5, RKMOD, SK, VGA, VGN, EPIT
MAT#3: - WATER RETENTION DATA
0.25,0.05,0.04,1.2, THET, THTR, VGA, VGN
MAT#3: - CONDUCTIVITY DATA
2.0,1.0,0.04,1.2,0.5, RKMOD, SK, VGA, VGN, EPIT
0, NDAY
6.54E+05,2.70E+05,3.87E+03,9.91E+02, H(1....NPT)
5.96E+02,3.87E+02,2.69E+02,2.16E+02,
2.01E+02,2.01E+02,2.06E+02,2.11E+02,
2.13E+02,2.12E+02,2.09E+02,2.09E+02,
2.08E+02,2.08E+02,2.07E+02,2.07E+02,
2.07E+02,2.06E+02,2.06E+02,2.04E+02,
2.03E+02,2.03E+02,2.03E+02,2.02E+02,
2.02E+02,2.03E+02,2.08E+02,2.16E+02,
2.24E+02,2.34E+02,2.45E+02,2.46E+02,
2.48E+02,2.50E+02,2.51E+02,2.52E+02,
2.53E+02,2.53E+02,2.54E+02,2.55E+02,
2.57E+02,2.58E+02,2.61E+02,2.65E+02,
2.67E+02,2.67E+02,2.64E+02,2.61E+02,
IPLANT, NGRAV
IFDEND, IDTBEG, IDTEND
IYS, NYEARS, ISTEAD, IFLIST, NFLIST
NPRINT, STOPHR
ISMETH, INMAX, ISWDIF, DMAXBA
DELMAX, DELMIN, OUTTIM
RFACT, RAINIF, DHTOL, DHMAX, DHFACT
KOPT, KEST, WTF
ITOPBC, IEVOPT, NFHOUR, LOWER
HIRRI, HDRI, HTOP, RHA
IETOPT, ICLOUD, ISHOPT
IRAIN, HPR
IHYS, AIRTOL, HYSTOL, HYSMXH, HYFILE
IHEAT, ICONVH, DMAXHE
UPPERH, TSMEAN, TSAMP, QHCTOP
LOWERH, QHLEAK, TGRAD
IVAPOR, TORT, TSOIL, VAPDIF
MATN, NPT
MAT, Z

```

```

2.56E+02,2.51E+02,2.50E+02,2.50E+02,
2.50E+02,2.49E+02,2.49E+02,2.48E+02,
2.47E+02,2.45E+02,2.43E+02,2.39E+02,
2.34E+02,2.30E+02,2.25E+02,2.21E+02,
2.17E+02,2.16E+02,2.15E+02,2.14E+02,
2.14E+02,2.13E+02,2.13E+02,2.13E+02,
2.12E+02,2.12E+02,2.11E+02,2.10E+02,
2.07E+02,2.04E+02,1.94E+02,1.81E+02,
1.68E+02,1.54E+02,1.54E+02,
1,1,1,1,01,365,
LEAF,NFROOT,NUPTAK,NFPET,NSOW,NHRVST
0.10,
20,
1,0.006, 60,0.0125, 90,0.03, 100,0.04,
120,0.045, 130,0.065, 150,0.07, 165,0.0725,
180,0.075, 195,0.082, 205,0.13, 220,0.145,
260,0.145, 265,0.115, 270,0.095, 285,0.08,
300,0.065, 315,0.0425, 325,0.0115, 360,0.006,
7.0E-01,6.0E-02,1.6E-02,
1,1,1,1,1,1,1,1,1,1,
1,1,1,1,1,1,1,1,1,1,
1,1,1,1,366,366,366,366,366,366,
366,366,366,366,366,366,366,366,366,366,
366,366,366,366,366,366,366,366,366,366,
366,366,366,366,366,366,366,366,366,366,
366,366,366,366,366,366,366,366,366,366,
366,366,366,
2.0E+04,3.0E+03,1.0E+0,
2.0E+04,3.0E+03,1.0E+0,
2.0E+04,3.0E+03,1.0E+0,
0.0,0.52,0.5,0.0,2.7,
0.35,1872.1,6.1,838.4,
SP2010.dat
BARE
NDLAI
IDLAI,VLAI
AA,B1,B2
NTROOT
HW,HD,HN
HW,HD,HN
HW,HD,HN
PETPC
ALBEDO,ALT,ZU,PMB

```

Run 178.5-2ft, 1/2 LAI

```

1,1,
298,1,298,
2011,1,0,2,1,
0,0.0,
0,4,1,1.0E-04,
1.0,8.0E-10,0,
1.02,1.0E-05,0,0,0,
4,3,0.5,
0,1,2,1,
0.0,1.0E+06,0.0,0.99,
1,1,1,
1,1.2,
0,0,0,0,0,
0,0,0,
0,2.880E+02,1.0E+01,0,
0,0.0,0,
1,0.66,288.46,0.24,
3,87,
1,0.0, 1,0.1, 1,0.2, 1,0.5,
1,1.0, 1,2.0, 1,4.0, 1,7.0,
2,12.0, 2,18.0, 2,24.0, 2,30.0,
2,36.0, 2,42.0, 2,47.0, 2,48.0,
2,49.0, 2,49.5, 2,50.0, 2,50.5,
2,51.0, 2,52.0, 2,53.0, 2,56.0,
2,58.0, 2,59.0, 2,60.0, 2,60.5,
3,61.5, 3,64.0, 3,70.0, 3,77.0,
3,83.0, 3,89.0, 3,95.0, 3,96.0,
3,97.0, 3,98.0, 3,99.0, 3,99.5,
3,100.0, 3,100.5, 3,101.0, 3,102.0,
3,103.0, 3,104.0, 3,107.0, 3,112.0,
3,118.0, 3,124.0, 3,130.0, 3,136.0,
3,142.0, 3,148.0, 3,149.0, 3,149.5,
3,150.0, 3,150.5, 3,151.0, 3,152.0,
3,153.0, 3,155.0, 3,158.0, 3,163.0,
3,169.0, 3,175.0, 3,181.0, 3,187.0,
3,193.0, 3,196.0, 3,197.0, 3,198.0,
3,199.0, 3,199.5, 3,200.0, 3,200.5,
3,201.0, 3,202.0, 3,203.0, 3,205.0,
3,210.0, 2,215.0, 3,230.0, 3,260.0,
3,300.0, 3,390.0, 3,400.0,
MAT#1: -WATER RETENTION DATA
0.25,0.05,0.05,1.25, THET, THTR, VGA, VGN
MAT#1: - CONDUCTIVITY DATA
2.0,1.0,0.05,1.25,0.5, RKMOD, SK, VGA, VGN, EPIT
MAT#2: - WATER RETENTION DATA
0.25,0.05,0.0605,1.25, THET, THTR, VGA, VGN
MAT#2: - CONDUCTIVITY DATA
2.0,30.0,0.0605,1.25,0.5, RKMOD, SK, VGA, VGN, EPIT
MAT#3: - WATER RETENTION DATA
0.25,0.05,0.04,1.2, THET, THTR, VGA, VGN
MAT#3: - CONDUCTIVITY DATA
2.0,1.0,0.04,1.2,0.5, RKMOD, SK, VGA, VGN, EPIT
0, NDAY
1.90E+04,2.50E+03,1.76E+03,1.03E+03, H(1....NPT)
6.87E+02,4.86E+02,4.06E+02,5.06E+02,
5.60E+02,5.63E+02,5.56E+02,5.43E+02,
5.28E+02,5.13E+02,5.00E+02,4.97E+02,
4.94E+02,4.93E+02,4.92E+02,4.91E+02,
4.89E+02,4.87E+02,4.84E+02,4.77E+02,
4.72E+02,4.69E+02,4.67E+02,4.66E+02,
4.60E+02,4.25E+02,3.62E+02,3.12E+02,
2.81E+02,2.57E+02,2.38E+02,2.35E+02,
2.33E+02,2.30E+02,2.27E+02,2.26E+02,
2.25E+02,2.24E+02,2.23E+02,2.20E+02,
2.18E+02,2.16E+02,2.10E+02,2.01E+02,
1.92E+02,1.84E+02,1.77E+02,1.71E+02,
IPLANT,NGRAV
IFDEND, IDTBEG, IDTEND
IYS,NYEARS, ISTEAD, IFLIST,NFLIST
NPRINT, STOPHR
ISMETH, INMAX, ISWDIF, DMAXBA
DELMAX, DELMIN, OUTTIM
RFACT, RAINIF, DHTOL, DHMAX, DHFACT
KOPT, KEST, WTF
ITOPBC, IEVOPT, NFHOUR, LOWER
HIRRI, HDRI, HTOP, RHA
IETOPT, ICLOUD, ISHOPT
IRAIN, HPR
IHYS, AIRTOL, HYSTOL, HYSMXH, HYFILE
IHEAT, ICONVH, DMAXHE
UPPERH, TSMEAN, TSAMP, QHCTOP
LOWERH, QHLEAK, TGRAD
IVAPOR, TORT, TSOIL, VAPDIF
MATN,NPT
MAT,Z

```



```

1.65E+02,1.61E+02,1.60E+02,1.60E+02,
1.59E+02,1.59E+02,1.59E+02,1.58E+02,
1.57E+02,1.56E+02,1.54E+02,1.51E+02,
1.48E+02,1.45E+02,1.43E+02,1.41E+02,
1.39E+02,1.38E+02,1.38E+02,1.37E+02,
1.37E+02,1.37E+02,1.37E+02,1.37E+02,
1.36E+02,1.36E+02,1.36E+02,1.35E+02,
1.34E+02,1.31E+02,1.19E+02,1.12E+02,
1.07E+02,1.10E+02,1.10E+02,
1,1,1,1,01,365,
LEAF,NFROOT,NUPTAK,NFPET,NSOW,NHRVST
0.10,
20,
1,0.006, 60,0.0125, 90,0.03, 100,0.04,
120,0.045, 130,0.065, 150,0.07, 165,0.0725,
180,0.075, 195,0.082, 205,0.13, 220,0.145,
260,0.145, 265,0.115, 270,0.095, 285,0.08,
300,0.065, 315,0.0425, 325,0.0115, 360,0.006,
7.0E-01,6.0E-02,1.6E-02,
1,1,1,1,1,1,1,1,1,1,
1,1,1,1,1,1,1,1,1,1,
1,1,1,1,366,366,366,366,366,366,
366,366,366,366,366,366,366,366,366,366,
366,366,366,366,366,366,366,366,366,366,
366,366,366,366,366,366,366,366,366,366,
366,366,366,366,366,366,366,366,366,366,
366,366,366,
2.0E+04,3.0E+03,1.0E+0,
2.0E+04,3.0E+03,1.0E+0,
2.0E+04,3.0E+03,1.0E+0,
0.0,0.52,0.5,0.0,2.7,
0.35,1872.1,6.1,838.4,
SP2011.dat
BARE
NDLAI
IDLAI,VLAI
AA,B1,B2
NTROOT
HW,HD,HN
HW,HD,HN
HW,HD,HN
PETPC
ALBEDO,ALT,ZU,PMB

```

Run 37.1-3ft, No Plants

```

0,1,
151,1,151,
2006,1,0,2,1,
0,24,
0,4,1,1.0E-04,
1.0,8.0E-10,0,
1.02,1.0E-05,0,0,0,
4,3,0.5,
0,1,2,1,
0.0,1.0E+06,0.0,0.99,
1,1,1,
0,0,
0,0,0,0,0,
0,0,0,
0,2.880E+02,1.0E+01,0,
0,0,0,0,
1,0.66,288.46,0.24,
3,87,
1,0.0, 1,0.1, 1,0.2, 1,0.5,
1,1.0, 1,2.0, 1,4.0, 1,7.0,
2,12.0, 2,18.0, 2,24.0, 2,30.0,
2,36.0, 2,42.0, 2,48.0, 2,54.0,
2,60.0, 2,66.0, 2,72.0, 2,73.0,
2,74.0, 2,74.5, 2,75.0, 2,75.5,
2,76.0, 2,77.0, 2,80.0, 2,83.0,
2,86.0, 2,90.0, 2,90.5, 2,91.0,
2,91.2, 3,91.6, 3,93.0, 3,96.0,
3,98.0, 3,99.0, 3,99.5, 3,100.0,
3,100.5, 3,101.0, 3,102.0, 3,105.0,
3,108.0, 3,113.0, 3,119.0, 3,125.0,
3,131.0, 3,137.0, 3,143.0, 3,145.0,
3,147.0, 3,148.0, 3,149.0, 3,150.0,
3,150.5, 3,151.0, 3,152.0, 3,153.0,
3,155.0, 3,158.0, 3,163.0, 3,169.0,
3,175.0, 3,182.0, 3,188.0, 3,194.0,
3,196.0, 3,197.0, 3,198.0, 3,199.0,
3,199.5, 3,200.0, 3,200.5, 3,201.0,
3,202.0, 3,203.0, 3,205.0, 3,210.0,
3,215.0, 3,230.0, 3,260.0, 3,300.0,
3,340.0, 3,390.0, 3, 400.0,
MAT#1: -WATER RETENTION DATA
0.25,0.05,0.05,1.25, THET, THTR, VGA, VGN
MAT#1: - CONDUCTIVITY DATA
2.0,1.0,0.05,1.25,0.5, RKMOD, SK, VGA, VGN, EPIT
MAT#2: - WATER RETENTION DATA
0.25,0.05,0.0605,1.25, THET, THTR, VGA, VGN
MAT#2: - CONDUCTIVITY DATA
2.0,30.0,0.0605,1.25,0.5, RKMOD, SK, VGA, VGN, EPIT
MAT#3: - WATER RETENTION DATA
0.25,0.05,0.04,1.2, THET, THTR, VGA, VGN
MAT#3: - CONDUCTIVITY DATA
2.0,1.0,0.04,1.2,0.5, RKMOD, SK, VGA, VGN, EPIT
0, NDAY
1.52E+02,1.52E+02,1.52E+02,1.52E+02, H(1....NPT)
1.52E+02,1.52E+02,1.52E+02,1.52E+02,
1.52E+02,1.52E+02,1.52E+02,1.52E+02,
1.52E+02,1.52E+02,1.52E+02,1.52E+02,
1.52E+02,1.52E+02,1.52E+02,1.52E+02,
1.52E+02,1.52E+02,1.52E+02,1.52E+02,
1.52E+02,1.53E+02,1.55E+02,1.57E+02,
1.59E+02,1.61E+02,1.62E+02,1.62E+02,
1.62E+02,1.62E+02,1.63E+02,1.65E+02,
1.66E+02,1.67E+02,1.67E+02,1.68E+02,
1.67E+02,1.67E+02,1.67E+02,1.65E+02,
1.63E+02,1.60E+02,1.57E+02,1.54E+02,
1.50E+02,1.47E+02,1.44E+02,1.43E+02,
IPLANT, NGRAV
IFDEND, IDTBEG, IDTEND
IYS, NYEARS, ISTEAD, IFLIST, NFLIST
NPRINT, STOPHR
ISMETH, INMAX, ISWDIF, DMAXBA
DELMAX, DELMIN, OUTTIM
RFACT, RAINIF, DHTOL, DHMAX, DHFACT
KOPT, KEST, WTF
ITOPBC, IEVOPT, NFHOUR, LOWER
HIRRI, HDRI, HTOP, RHA
IETOPT, ICLOUD, ISHOPT
IRAIN, HPR
IHYS, AIRTOL, HYSTOL, HYSMXH, HYFILE
IHEAT, ICONVH, DMAXHE
UPPERH, TSMEAN, TSAMP, QHCTOP
LOWERH, QHLEAK, TGRAD
IVAPOR, TORT, TSOIL, VAPDIF
MATN, NPT
MAT, Z

```

1.41E+02,1.41E+02,1.40E+02,1.40E+02,  
1.39E+02,1.40E+02,1.40E+02,1.40E+02,  
1.41E+02,1.41E+02,1.43E+02,1.44E+02,  
1.47E+02,1.51E+02,1.54E+02,1.58E+02,  
1.62E+02,1.65E+02,1.66E+02,1.67E+02,  
1.67E+02,1.68E+02,1.68E+02,1.68E+02,  
1.68E+02,1.68E+02,1.68E+02,1.68E+02,  
1.68E+02,1.68E+02,1.68E+02,1.68E+02,  
1.68E+02,1.68E+02,1.68E+02,  
0.35,1872.1,6.1,838.4,  
SP2006.dat  
2006 SP.dat

ALBEDO, ALT, ZU, PMB

Run 37.2-3ft, No Plants

```

0,1,
365,1,365,
2007,1,0,2,1,
0,24,
0,4,1,1.0E-04,
1.0,8.0E-10,0,
1.02,1.0E-05,0,0,0,
4,3,0.5,
0,1,2,1,
0.0,1.0E+06,0.0,0.99,
1,1,1,
0,0,
0,0,0,0,0,
0,0,0,
0,2.880E+02,1.0E+01,0,
0,0,0,0,
1,0.66,288.46,0.24,
3,87,
1,0.0, 1,0.1, 1,0.2, 1,0.5,
1,1.0, 1,2.0, 1,4.0, 1,7.0,
2,12.0, 2,18.0, 2,24.0, 2,30.0,
2,36.0, 2,42.0, 2,48.0, 2,54.0,
2,60.0, 2,66.0, 2,72.0, 2,73.0,
2,74.0, 2,74.5, 2,75.0, 2,75.5,
2,76.0, 2,77.0, 2,80.0, 2,83.0,
2,86.0, 2,90.0, 2,90.5, 2,91.0,
2,91.2, 3,91.6, 3,93.0, 3,96.0,
3,98.0, 3,99.0, 3,99.5, 3,100.0,
3,100.5, 3,101.0, 3,102.0, 3,105.0,
3,108.0, 3,113.0, 3,119.0, 3,125.0,
3,131.0, 3,137.0, 3,143.0, 3,145.0,
3,147.0, 3,148.0, 3,149.0, 3,150.0,
3,150.5, 3,151.0, 3,152.0, 3,153.0,
3,155.0, 3,158.0, 3,163.0, 3,169.0,
3,175.0, 3,182.0, 3,188.0, 3,194.0,
3,196.0, 3,197.0, 3,198.0, 3,199.0,
3,199.5, 3,200.0, 3,200.5, 3,201.0,
3,202.0, 3,203.0, 3,205.0, 3,210.0,
3,215.0, 3,230.0, 3,260.0, 3,300.0,
3,340.0, 3,390.0, 3, 400.0,
MAT#1: -WATER RETENTION DATA
0.25,0.05,0.05,1.25, THET, THTR, VGA, VGN
MAT#1: - CONDUCTIVITY DATA
2.0,1.0,0.05,1.25,0.5, RKMOD, SK, VGA, VGN, EPIT
MAT#2: - WATER RETENTION DATA
0.25,0.05,0.0605,1.25, THET, THTR, VGA, VGN
MAT#2: - CONDUCTIVITY DATA
2.0,30.0,0.0605,1.25,0.5, RKMOD, SK, VGA, VGN, EPIT
MAT#3: - WATER RETENTION DATA
0.25,0.05,0.04,1.2, THET, THTR, VGA, VGN
MAT#3: - CONDUCTIVITY DATA
2.0,1.0,0.04,1.2,0.5, RKMOD, SK, VGA, VGN, EPIT
0, NDAY
5.35E+05,2.50E+05,1.75E+04,1.18E+03, H(1....NPT)
7.27E+02,4.71E+02,3.22E+02,2.46E+02,
2.26E+02,2.17E+02,2.09E+02,2.02E+02,
1.95E+02,1.88E+02,1.81E+02,1.75E+02,
1.69E+02,1.63E+02,1.56E+02,1.55E+02,
1.54E+02,1.54E+02,1.53E+02,1.53E+02,
1.52E+02,1.51E+02,1.48E+02,1.45E+02,
1.43E+02,1.39E+02,1.38E+02,1.38E+02,
1.37E+02,1.37E+02,1.36E+02,1.34E+02,
1.33E+02,1.32E+02,1.32E+02,1.31E+02,
1.31E+02,1.31E+02,1.30E+02,1.28E+02,
1.27E+02,1.24E+02,1.21E+02,1.19E+02,
1.16E+02,1.13E+02,1.11E+02,1.10E+02,

```

1.09E+02,1.09E+02,1.08E+02,1.08E+02,  
1.08E+02,1.08E+02,1.07E+02,1.07E+02,  
1.06E+02,1.05E+02,1.03E+02,1.01E+02,  
9.87E+01,9.64E+01,9.45E+01,9.27E+01,  
9.21E+01,9.18E+01,9.16E+01,9.13E+01,  
9.11E+01,9.10E+01,9.09E+01,9.07E+01,  
9.05E+01,9.02E+01,8.96E+01,8.83E+01,  
8.71E+01,8.36E+01,7.78E+01,7.17E+01,  
6.70E+01,6.38E+01,6.36E+01,  
0.35,1872.1,6.1,838.4,  
SP2007.dat  
2007 SP.dat

ALBEDO, ALT, ZU, PMB

Run 37.3-3ft,1/8 LAI

```

1,1, IPLANT, NGRAV
365,1,365, IFDEND, IDTBEG, IDTEND
2008,2,0,2,2, IYS, NYEARS, ISTEAD, IFLIST, NFLIST
0,24, NPRINT, STOPHR
0,4,1,1.0E-04, ISMETH, INMAX, ISWDIF, DMAXBA
1.0,8.0E-10,0, DELMAX, DELMIN, OUTTIM
1.02,1.0E-05,0,0,0, RFACT, RAINIF, DHTOL, DHMAX, DHFACT
4,3,0.5, KOPT, KEST, WTF
0,1,2,1, ITOPBC, IEVOPT, NFHOUR, LOWER
0.0,1.0E+06,0.0,0.99, HIRRI, HDRI, HTOP, RHA
1,1,1, IETOPT, ICLOUD, ISHOPT
0,0, IRAIN, HPR
0,0,0,0,0, IHYS, AIRTOL, HYSTOL, HYSMXH, HYFILE
0,0,0, IHEAT, ICONVH, DMAXHE
0,2.880E+02,1.0E+01,0, UPPERH, TSMEAN, TSAMP, QHCTOP
0,0,0,0, LOWERH, QHLEAK, TGRAD
1,0.66,288.46,0.24, IVAPOR, TORT, TSOIL, VAPDIF
3,87, MATN, NPT
1,0.0, 1,0.1, 1,0.2, 1,0.5, MAT, Z
1,1.0, 1,2.0, 1,4.0, 1,7.0,
2,12.0, 2,18.0, 2,24.0, 2,30.0,
2,36.0, 2,42.0, 2,48.0, 2,54.0,
2,60.0, 2,66.0, 2,72.0, 2,73.0,
2,74.0, 2,74.5, 2,75.0, 2,75.5,
2,76.0, 2,77.0, 2,80.0, 2,83.0,
2,86.0, 2,90.0, 2,90.5, 2,91.0,
2,91.2, 3,91.6, 3,93.0, 3,96.0,
3,98.0, 3,99.0, 3,99.5, 3,100.0,
3,100.5, 3,101.0, 3,102.0, 3,105.0,
3,108.0, 3,113.0, 3,119.0, 3,125.0,
3,131.0, 3,137.0, 3,143.0, 3,145.0,
3,147.0, 3,148.0, 3,149.0, 3,150.0,
3,150.5, 3,151.0, 3,152.0, 3,153.0,
3,155.0, 3,158.0, 3,163.0, 3,169.0,
3,175.0, 3,182.0, 3,188.0, 3,194.0,
3,196.0, 3,197.0, 3,198.0, 3,199.0,
3,199.5, 3,200.0, 3,200.5, 3,201.0,
3,202.0, 3,203.0, 3,205.0, 3,210.0,
3,215.0, 3,230.0, 3,260.0, 3,300.0,
3,340.0, 3,390.0, 3, 400.0,
MAT#1: -WATER RETENTION DATA
0.25,0.05,0.05,1.25, THET, THTR, VGA, VGN
MAT#1: - CONDUCTIVITY DATA
2.0,1.0,0.05,1.25,0.5, RKMOD, SK, VGA, VGN, EPIT
MAT#2: - WATER RETENTION DATA
0.25,0.05,0.0605,1.25, THET, THTR, VGA, VGN
MAT#2: - CONDUCTIVITY DATA
2.0,30.0,0.0605,1.25,0.5, RKMOD, SK, VGA, VGN, EPIT
MAT#3: - WATER RETENTION DATA
0.25,0.05,0.04,1.2, THET, THTR, VGA, VGN
MAT#3: - CONDUCTIVITY DATA
2.0,1.0,0.04,1.2,0.5, RKMOD, SK, VGA, VGN, EPIT
0, NDAY
1.05E+06,7.38E+05,4.82E+05,1.21E+03, H(1....NPT)
7.16E+02,4.49E+02,2.87E+02,2.01E+02,
1.79E+02,1.69E+02,1.60E+02,1.52E+02,
1.44E+02,1.37E+02,1.30E+02,1.23E+02,
1.16E+02,1.10E+02,1.04E+02,1.03E+02,
1.02E+02,1.01E+02,1.01E+02,1.00E+02,
9.96E+01,9.86E+01,9.55E+01,9.25E+01,
8.95E+01,8.56E+01,8.51E+01,8.46E+01,
8.44E+01,8.41E+01,8.31E+01,8.11E+01,
7.98E+01,7.92E+01,7.89E+01,7.86E+01,
7.83E+01,7.80E+01,7.75E+01,7.59E+01,
7.44E+01,7.21E+01,6.97E+01,6.75E+01,
6.56E+01,6.40E+01,6.25E+01,6.20E+01,

```

```

6.16E+01,6.14E+01,6.12E+01,6.10E+01,
6.09E+01,6.08E+01,6.06E+01,6.04E+01,
6.00E+01,5.95E+01,5.88E+01,5.80E+01,
5.73E+01,5.68E+01,5.64E+01,5.63E+01,
5.62E+01,5.62E+01,5.62E+01,5.62E+01,
5.62E+01,5.62E+01,5.62E+01,5.62E+01,
5.63E+01,5.63E+01,5.63E+01,5.65E+01,
5.69E+01,5.88E+01,6.88E+01,8.09E+01,
8.40E+01,8.29E+01,8.28E+01,
1,1,1,1,01,365,
LEAF,NFROOT,NUPTAK,NFPET,NSOW,NHRVST
0.10,
20,
1,0.0015, 60,0.003125, 90,0.0075, 100,0.01,
120,0.01125, 130,0.01625, 150,0.0175, 165,0.018125,
180,0.01875, 195,0.0205, 205,0.0325, 220,0.03625,
260,0.03625, 265,0.02875, 270,0.02375, 285,0.02,
300,0.01625, 315,0.010625, 325,0.002875, 360,0.0015,
7.0E-01,6.0E-02,1.6E-02,
1,1,1,1,1,1,1,1,1,1,
1,1,1,1,1,1,1,1,1,1,
1,1,1,1,1,1,1,1,1,1,
1,1,1,366,366,366,366,366,366,366,
366,366,366,366,366,366,366,366,366,366,
366,366,366,366,366,366,366,366,366,366,
366,366,366,366,366,366,366,366,366,366,
366,366,366,
2.0E+04,3.0E+03,1.0E+0,
2.0E+04,3.0E+03,1.0E+0,
2.0E+04,3.0E+03,1.0E+0,
0.0,0.52,0.5,0.0,2.7,
0.35,1872.1,6.1,838.4,
SP2008.dat
SP2009.dat
2008 SP.dat
2009 SP.dat

```

BARE  
NDLAI  
IDLAI,VLAI  
AA,B1,B2  
NTROOT  
HW,HD,HN  
HW,HD,HN  
HW,HD,HN  
PETPC  
ALBEDO,ALT,ZU,PMB

Run 37.4-3FT, 1/2 LAI

```

1,1,
365,1,365,
2010,1,0,2,1,
0,24,
0,4,1,1.0E-04,
1.0,8.0E-10,0,
1.02,1.0E-05,0,0,0,
4,3,0.5,
0,1,2,1,
0.0,1.0E+06,0.0,0.99,
1,1,1,
0,0,
0,0,0,0,0,
0,0,0,
0,2.880E+02,1.0E+01,0,
0,0,0,0,
1,0.66,288.46,0.24,
3,87,
1,0.0, 1,0.1, 1,0.2, 1,0.5,
1,1.0, 1,2.0, 1,4.0, 1,7.0,
2,12.0, 2,18.0, 2,24.0, 2,30.0,
2,36.0, 2,42.0, 2,48.0, 2,54.0,
2,60.0, 2,66.0, 2,72.0, 2,73.0,
2,74.0, 2,74.5, 2,75.0, 2,75.5,
2,76.0, 2,77.0, 2,80.0, 2,83.0,
2,86.0, 2,90.0, 2,90.5, 2,91.0,
2,91.2, 3,91.6, 3,93.0, 3,96.0,
3,98.0, 3,99.0, 3,99.5, 3,100.0,
3,100.5, 3,101.0, 3,102.0, 3,105.0,
3,108.0, 3,113.0, 3,119.0, 3,125.0,
3,131.0, 3,137.0, 3,143.0, 3,145.0,
3,147.0, 3,148.0, 3,149.0, 3,150.0,
3,150.5, 3,151.0, 3,152.0, 3,153.0,
3,155.0, 3,158.0, 3,163.0, 3,169.0,
3,175.0, 3,182.0, 3,188.0, 3,194.0,
3,196.0, 3,197.0, 3,198.0, 3,199.0,
3,199.5, 3,200.0, 3,200.5, 3,201.0,
3,202.0, 3,203.0, 3,205.0, 3,210.0,
3,215.0, 3,230.0, 3,260.0, 3,300.0,
3,340.0, 3,390.0, 3, 400.0,
MAT#1: -WATER RETENTION DATA
0.25,0.05,0.05,1.25, THET, THTR, VGA, VGN
MAT#1: - CONDUCTIVITY DATA
2.0,1.0,0.05,1.25,0.5, RKMOD, SK, VGA, VGN, EPIT
MAT#2: - WATER RETENTION DATA
0.25,0.05,0.0605,1.25, THET, THTR, VGA, VGN
MAT#2: - CONDUCTIVITY DATA
2.0,30.0,0.0605,1.25,0.5, RKMOD, SK, VGA, VGN, EPIT
MAT#3: - WATER RETENTION DATA
0.25,0.05,0.04,1.2, THET, THTR, VGA, VGN
MAT#3: - CONDUCTIVITY DATA
2.0,1.0,0.04,1.2,0.5, RKMOD, SK, VGA, VGN, EPIT
0, NDAY
6.28E+05,2.48E+05,3.02E+03,9.69E+02, H(1....NPT)
5.89E+02,3.86E+02,2.72E+02,2.21E+02,
2.11E+02,2.06E+02,2.01E+02,1.98E+02,
1.96E+02,1.93E+02,1.91E+02,1.88E+02,
1.85E+02,1.81E+02,1.77E+02,1.77E+02,
1.76E+02,1.75E+02,1.75E+02,1.75E+02,
1.74E+02,1.74E+02,1.71E+02,1.69E+02,
1.66E+02,1.63E+02,1.63E+02,1.62E+02,
1.62E+02,1.62E+02,1.62E+02,1.63E+02,
1.64E+02,1.64E+02,1.65E+02,1.65E+02,
1.65E+02,1.65E+02,1.66E+02,1.67E+02,
1.69E+02,1.74E+02,1.80E+02,1.89E+02,
1.99E+02,2.10E+02,2.21E+02,2.25E+02,
IPLANT, NGRAV
IFDEND, IDTBEG, IDTEND
IYS, NYEARS, ISTEAD, IFLIST, NFLIST
NPRINT, STOPHR
ISMETH, INMAX, ISWDIF, DMAXBA
DELMAX, DELMIN, OUTTIM
RFACT, RAINIF, DHTOL, DHMAX, DHFACT
KOPT, KEST, WTF
ITOPBC, IEVOPT, NFHOUR, LOWER
HIRRI, HDRI, HTOP, RHA
IETOPT, ICLOUD, ISHOPT
IRAIN, HPR
IHYS, AIRTOL, HYSTOL, HYSMXH, HYFILE
IHEAT, ICONVH, DMAXHE
UPPERH, TSMEAN, TSAMP, QHCTOP
LOWERH, QHLEAK, TGRAD
IVAPOR, TORT, TSOIL, VAPDIF
MATN, NPT
MAT, Z

```



```

2.28E+02,2.30E+02,2.31E+02,2.33E+02,
2.34E+02,2.34E+02,2.36E+02,2.37E+02,
2.39E+02,2.42E+02,2.46E+02,2.47E+02,
2.46E+02,2.43E+02,2.39E+02,2.35E+02,
2.34E+02,2.33E+02,2.32E+02,2.31E+02,
2.31E+02,2.31E+02,2.30E+02,2.30E+02,
2.29E+02,2.28E+02,2.27E+02,2.23E+02,
2.20E+02,2.10E+02,1.93E+02,1.76E+02,
1.65E+02,1.58E+02,1.58E+02,
1,1,1,1,01,365,
LEAF,NFROOT,NUPTAK,NFPET,NSOW,NHRVST
0.10,
20,
1,0.006, 60,0.0125, 90,0.03, 100,0.04,
120,0.045, 130,0.065, 150,0.07, 165,0.0725,
180,0.075, 195,0.082, 205,0.13, 220,0.145,
260,0.145, 265,0.115, 270,0.095, 285,0.08,
300,0.065, 315,0.0425, 325,0.0115, 360,0.006,
7.0E-01,6.0E-02,1.6E-02,
1,1,1,1,1,1,1,1,1,1,
1,1,1,1,1,1,1,1,1,1,
1,1,1,1,1,1,1,1,1,1,
1,1,1,366,366,366,366,366,366,366,
366,366,366,366,366,366,366,366,366,366,
366,366,366,366,366,366,366,366,366,366,
366,366,366,366,366,366,366,366,366,366,
366,366,366,
2.0E+04,3.0E+03,1.0E+0,
2.0E+04,3.0E+03,1.0E+0,
2.0E+04,3.0E+03,1.0E+0,
0.0,0.52,0.5,0.0,2.7,
0.35,1872.1,6.1,838.4,
SP2010.dat
2010 SP.dat

```

```

BARE
NDLAI
IDLAI,VLAI

```

```

AA,B1,B2
NTROOT

```

```

HW,HD,HN
HW,HD,HN
HW,HD,HN
PETPC
ALBEDO,ALT,ZU,PMB

```

Run 33.5-3FT, 1/2 LAI

```

1,1,
298,1,298,
2011,1,0,2,1,
0,24,
0,4,1,1.0E-04,
1.0,8.0E-10,0,
1.02,1.0E-05,0,0,0,
4,3,0.5,
0,1,2,1,
0.0,1.0E+06,0.0,0.99,
1,1,1,
0,0,
0,0,0,0,0,
0,0,0,
0,2.880E+02,1.0E+01,0,
0,0,0,0,
1,0.66,288.46,0.24,
3,87,
1,0.0, 1,0.1, 1,0.2, 1,0.5,
1,1.0, 1,2.0, 1,4.0, 1,7.0,
2,12.0, 2,18.0, 2,24.0, 2,30.0,
2,36.0, 2,42.0, 2,48.0, 2,54.0,
2,60.0, 2,66.0, 2,72.0, 2,73.0,
2,74.0, 2,74.5, 2,75.0, 2,75.5,
2,76.0, 2,77.0, 2,80.0, 2,83.0,
2,86.0, 2,90.0, 2,90.5, 2,91.0,
2,91.2, 3,91.6, 3,93.0, 3,96.0,
3,98.0, 3,99.0, 3,99.5, 3,100.0,
3,100.5, 3,101.0, 3,102.0, 3,105.0,
3,108.0, 3,113.0, 3,119.0, 3,125.0,
3,131.0, 3,137.0, 3,143.0, 3,145.0,
3,147.0, 3,148.0, 3,149.0, 3,150.0,
3,150.5, 3,151.0, 3,152.0, 3,153.0,
3,155.0, 3,158.0, 3,163.0, 3,169.0,
3,175.0, 3,182.0, 3,188.0, 3,194.0,
3,196.0, 3,197.0, 3,198.0, 3,199.0,
3,199.5, 3,200.0, 3,200.5, 3,201.0,
3,202.0, 3,203.0, 3,205.0, 3,210.0,
3,215.0, 3,230.0, 3,260.0, 3,300.0,
3,340.0, 3,390.0, 3, 400.0,
MAT#1: -WATER RETENTION DATA
0.25,0.05,0.05,1.25, THET, THTR, VGA, VGN
MAT#1: - CONDUCTIVITY DATA
2.0,1.0,0.05,1.25,0.5, RKMOD, SK, VGA, VGN, EPIT
MAT#2: - WATER RETENTION DATA
0.25,0.05,0.0605,1.25, THET, THTR, VGA, VGN
MAT#2: - CONDUCTIVITY DATA
2.0,30.0,0.0605,1.25,0.5, RKMOD, SK, VGA, VGN, EPIT
MAT#3: - WATER RETENTION DATA
0.25,0.05,0.04,1.2, THET, THTR, VGA, VGN
MAT#3: - CONDUCTIVITY DATA
2.0,1.0,0.04,1.2,0.5, RKMOD, SK, VGA, VGN, EPIT
0, NDAY
5.24E+02,5.08E+02,4.94E+02,4.59E+02, H(1....NPT)
4.15E+02,3.61E+02,3.22E+02,3.59E+02,
3.96E+02,4.02E+02,4.03E+02,3.99E+02,
3.93E+02,3.84E+02,3.74E+02,3.64E+02,
3.54E+02,3.44E+02,3.35E+02,3.33E+02,
3.32E+02,3.31E+02,3.30E+02,3.29E+02,
3.28E+02,3.27E+02,3.23E+02,3.18E+02,
3.14E+02,3.08E+02,3.07E+02,3.07E+02,
3.07E+02,3.06E+02,2.99E+02,2.85E+02,
2.76E+02,2.72E+02,2.70E+02,2.68E+02,
2.66E+02,2.64E+02,2.61E+02,2.50E+02,
2.41E+02,2.28E+02,2.14E+02,2.02E+02,
1.92E+02,1.84E+02,1.76E+02,1.74E+02,
IPLANT, NGRAV
IFDEND, IDTBEG, IDTEND
IYS, NYEARS, ISTEAD, IFLIST, NFLIST
NPRINT, STOPHR
ISMETH, INMAX, ISWDIF, DMAXBA
DELMAX, DELMIN, OUTTIM
RFACT, RAINIF, DHTOL, DHMAX, DHFACT
KOPT, KEST, WTF
ITOPBC, IEVOPT, NFHOUR, LOWER
HIRRI, HDRI, HTOP, RHA
IETOPT, ICLOUD, ISHOPT
IRAIN, HPR
IHYS, AIRTOL, HYSTOL, HYSMXH, HYFILE
IHEAT, ICONVH, DMAXHE
UPPERH, TSMEAN, TSAMP, QHCTOP
LOWERH, QHLEAK, TGRAD
IVAPOR, TORT, TSOIL, VAPDIF
MATN, NPT
MAT, Z

```

```

1.72E+02,1.71E+02,1.70E+02,1.69E+02,
1.68E+02,1.68E+02,1.67E+02,1.66E+02,
1.64E+02,1.62E+02,1.58E+02,1.53E+02,
1.49E+02,1.45E+02,1.42E+02,1.39E+02,
1.38E+02,1.38E+02,1.38E+02,1.37E+02,
1.37E+02,1.37E+02,1.37E+02,1.36E+02,
1.36E+02,1.36E+02,1.35E+02,1.33E+02,
1.31E+02,1.27E+02,1.22E+02,1.19E+02,
1.19E+02,1.20E+02,1.20E+02,
1,1,1,1,01,365,
LEAF,NFROOT,NUPTAK,NFPET,NSOW,NHRVST
0.10,
20,
1,0.006, 60,0.0125, 90,0.03, 100,0.04,
120,0.045, 130,0.065, 150,0.07, 165,0.0725,
180,0.075, 195,0.082, 205,0.13, 220,0.145,
260,0.145, 265,0.115, 270,0.095, 285,0.08,
300,0.065, 315,0.0425, 325,0.0115, 360,0.006,
7.0E-01,6.0E-02,1.6E-02,
1,1,1,1,1,1,1,1,1,1,
1,1,1,1,1,1,1,1,1,1,
1,1,1,1,1,1,1,1,1,1,
1,1,1,366,366,366,366,366,366,366,
366,366,366,366,366,366,366,366,366,366,
366,366,366,366,366,366,366,366,366,366,
366,366,366,366,366,366,366,366,366,366,
366,366,366,
2.0E+04,3.0E+03,1.0E+0,
2.0E+04,3.0E+03,1.0E+0,
2.0E+04,3.0E+03,1.0E+0,
0.0,0.52,0.5,0.0,2.7,
0.35,1872.1,6.1,838.4,
SP2011.dat
2011 SP.dat

```

BARE  
NDLAI  
IDLAI,VLAI  
AA,B1,B2  
NTROOT  
HW,HD,HN  
HW,HD,HN  
HW,HD,HN  
PETPC  
ALBEDO,ALT,ZU,PMB

Run 39.1-3ft, No Plants

```

0,1,
151,1,151,
2006,1,0,2,1,
0,24,
0,4,1,1.0E-04,
1.0,8.0E-10,0,
1.02,1.0E-05,0,0,0,
4,3,0.5,
0,1,2,1,
0.0,1.0E+06,0.0,0.99,
1,1,1,
1,1.2,
0,0,0,0,0,
0,0,0,
0,2.880E+02,1.0E+01,0,
0,0,0,0,
1,0.66,288.46,0.24,
3,87,
1,0.0, 1,0.1, 1,0.2, 1,0.5,
1,1.0, 1,2.0, 1,4.0, 1,7.0,
2,12.0, 2,18.0, 2,24.0, 2,30.0,
2,36.0, 2,42.0, 2,48.0, 2,54.0,
2,60.0, 2,66.0, 2,72.0, 2,73.0,
2,74.0, 2,74.5, 2,75.0, 2,75.5,
2,76.0, 2,77.0, 2,80.0, 2,83.0,
2,86.0, 2,90.0, 2,90.5, 2,91.0,
2,91.2, 3,91.6, 3,93.0, 3,96.0,
3,98.0, 3,99.0, 3,99.5, 3,100.0,
3,100.5, 3,101.0, 3,102.0, 3,105.0,
3,108.0, 3,113.0, 3,119.0, 3,125.0,
3,131.0, 3,137.0, 3,143.0, 3,145.0,
3,147.0, 3,148.0, 3,149.0, 3,150.0,
3,150.5, 3,151.0, 3,152.0, 3,153.0,
3,155.0, 3,158.0, 3,163.0, 3,169.0,
3,175.0, 3,182.0, 3,188.0, 3,194.0,
3,196.0, 3,197.0, 3,198.0, 3,199.0,
3,199.5, 3,200.0, 3,200.5, 3,201.0,
3,202.0, 3,203.0, 3,205.0, 3,210.0,
3,215.0, 3,230.0, 3,260.0, 3,300.0,
3,340.0, 3,390.0, 3, 400.0,
MAT#1: -WATER RETENTION DATA
0.25,0.05,0.05,1.25, THET, THTR, VGA, VGN
MAT#1: - CONDUCTIVITY DATA
2.0,1.0,0.05,1.25,0.5, RKMOD, SK, VGA, VGN, EPIT
MAT#2: - WATER RETENTION DATA
0.25,0.05,0.0605,1.25, THET, THTR, VGA, VGN
MAT#2: - CONDUCTIVITY DATA
2.0,30.0,0.0605,1.25,0.5, RKMOD, SK, VGA, VGN, EPIT
MAT#3: - WATER RETENTION DATA
0.25,0.05,0.04,1.2, THET, THTR, VGA, VGN
MAT#3: - CONDUCTIVITY DATA
2.0,1.0,0.04,1.2,0.5, RKMOD, SK, VGA, VGN, EPIT
0, NDAY
1.52E+02,1.52E+02,1.52E+02,1.52E+02, H(1....NPT)
1.52E+02,1.52E+02,1.52E+02,1.52E+02,
1.52E+02,1.52E+02,1.52E+02,1.52E+02,
1.52E+02,1.52E+02,1.52E+02,1.52E+02,
1.52E+02,1.52E+02,1.52E+02,1.52E+02,
1.52E+02,1.52E+02,1.52E+02,1.52E+02,
1.52E+02,1.53E+02,1.55E+02,1.57E+02,
1.59E+02,1.61E+02,1.62E+02,1.62E+02,
1.62E+02,1.62E+02,1.63E+02,1.65E+02,
1.66E+02,1.67E+02,1.67E+02,1.68E+02,
1.67E+02,1.67E+02,1.67E+02,1.65E+02,
1.63E+02,1.60E+02,1.57E+02,1.54E+02,
1.50E+02,1.47E+02,1.44E+02,1.43E+02,
IPLANT, NGRAV
IFDEND, IDTBEG, IDTEND
IYS, NYEARS, ISTEAD, IFLIST, NFLIST
NPRINT, STOPHR
ISMETH, INMAX, ISWDIF, DMAXBA
DELMAX, DELMIN, OUTTIM
RFACT, RAINIF, DHTOL, DHMAX, DHFACT
KOPT, KEST, WTF
ITOPBC, IEVOPT, NFHOUR, LOWER
HIRRI, HDRI, HTOP, RHA
IETOPT, ICLOUD, ISHOPT
IRAIN, HPR
IHYS, AIRTOL, HYSTOL, HYSMXH, HYFILE
IHEAT, ICONVH, DMAXHE
UPPERH, TSMEAN, TSAMP, QHCTOP
LOWERH, QHLEAK, TGRAD
IVAPOR, TORT, TSOIL, VAPDIF
MATN, NPT
MAT, Z

```

1.41E+02,1.41E+02,1.40E+02,1.40E+02,  
1.39E+02,1.40E+02,1.40E+02,1.40E+02,  
1.41E+02,1.41E+02,1.43E+02,1.44E+02,  
1.47E+02,1.51E+02,1.54E+02,1.58E+02,  
1.62E+02,1.65E+02,1.66E+02,1.67E+02,  
1.67E+02,1.68E+02,1.68E+02,1.68E+02,  
1.68E+02,1.68E+02,1.68E+02,1.68E+02,  
1.68E+02,1.68E+02,1.68E+02,1.68E+02,  
1.68E+02,1.68E+02,1.68E+02,  
0.35,1872.1,6.1,838.4,  
SP2006.dat

ALBEDO,ALT,ZU,PMB

Run 39.2-3FT, No Plants

```

0,1,
365,1,365,
2007,1,0,2,1,
0,24,
0,4,1,1.0E-04,
1.0,8.0E-10,0,
1.02,1.0E-05,0,0,0,
4,3,0.5,
0,1,2,1,
0.0,1.0E+06,0.0,0.99,
1,1,1,
1,1.2,
0,0,0,0,0,
0,0,0,
0,2.880E+02,1.0E+01,0,
0,0,0,0,
1,0.66,288.46,0.24,
3,87,
1,0.0, 1,0.1, 1,0.2, 1,0.5,
1,1.0, 1,2.0, 1,4.0, 1,7.0,
2,12.0, 2,18.0, 2,24.0, 2,30.0,
2,36.0, 2,42.0, 2,48.0, 2,54.0,
2,60.0, 2,66.0, 2,72.0, 2,73.0,
2,74.0, 2,74.5, 2,75.0, 2,75.5,
2,76.0, 2,77.0, 2,80.0, 2,83.0,
2,86.0, 2,90.0, 2,90.5, 2,91.0,
2,91.2, 3,91.6, 3,93.0, 3,96.0,
3,98.0, 3,99.0, 3,99.5, 3,100.0,
3,100.5, 3,101.0, 3,102.0, 3,105.0,
3,108.0, 3,113.0, 3,119.0, 3,125.0,
3,131.0, 3,137.0, 3,143.0, 3,145.0,
3,147.0, 3,148.0, 3,149.0, 3,150.0,
3,150.5, 3,151.0, 3,152.0, 3,153.0,
3,155.0, 3,158.0, 3,163.0, 3,169.0,
3,175.0, 3,182.0, 3,188.0, 3,194.0,
3,196.0, 3,197.0, 3,198.0, 3,199.0,
3,199.5, 3,200.0, 3,200.5, 3,201.0,
3,202.0, 3,203.0, 3,205.0, 3,210.0,
3,215.0, 3,230.0, 3,260.0, 3,300.0,
3,340.0, 3,390.0, 3, 400.0,
MAT#1: -WATER RETENTION DATA
0.25,0.05,0.05,1.25, THET, THTR, VGA, VGN
MAT#1: - CONDUCTIVITY DATA
2.0,1.0,0.05,1.25,0.5, RKMOD, SK, VGA, VGN, EPIT
MAT#2: - WATER RETENTION DATA
0.25,0.05,0.0605,1.25, THET, THTR, VGA, VGN
MAT#2: - CONDUCTIVITY DATA
2.0,30.0,0.0605,1.25,0.5, RKMOD, SK, VGA, VGN, EPIT
MAT#3: - WATER RETENTION DATA
0.25,0.05,0.04,1.2, THET, THTR, VGA, VGN
MAT#3: - CONDUCTIVITY DATA
2.0,1.0,0.04,1.2,0.5, RKMOD, SK, VGA, VGN, EPIT
0, NDAY
5.78E+05,3.99E+05,2.40E+05,1.21E+03, H(1....NPT)
7.91E+02,5.21E+02,3.48E+02,2.55E+02,
2.31E+02,2.21E+02,2.12E+02,2.04E+02,
1.96E+02,1.89E+02,1.82E+02,1.75E+02,
1.68E+02,1.62E+02,1.56E+02,1.55E+02,
1.54E+02,1.53E+02,1.53E+02,1.52E+02,
1.52E+02,1.51E+02,1.48E+02,1.45E+02,
1.42E+02,1.38E+02,1.37E+02,1.37E+02,
1.37E+02,1.36E+02,1.35E+02,1.33E+02,
1.32E+02,1.31E+02,1.31E+02,1.31E+02,
1.30E+02,1.30E+02,1.30E+02,1.28E+02,
1.26E+02,1.24E+02,1.21E+02,1.19E+02,
1.16E+02,1.14E+02,1.11E+02,1.10E+02,

```

1.10E+02,1.09E+02,1.09E+02,1.08E+02,  
1.08E+02,1.08E+02,1.08E+02,1.07E+02,  
1.06E+02,1.05E+02,1.03E+02,1.01E+02,  
9.92E+01,9.69E+01,9.50E+01,9.32E+01,  
9.27E+01,9.24E+01,9.21E+01,9.18E+01,  
9.17E+01,9.15E+01,9.14E+01,9.13E+01,  
9.10E+01,9.07E+01,9.02E+01,8.89E+01,  
8.76E+01,8.42E+01,7.84E+01,7.23E+01,  
6.76E+01,6.44E+01,6.43E+01,  
0.35,1872.1,6.1,838.4,  
SP2007.dat

ALBEDO, ALT, ZU, PMB

Run 39.3-3FT, 1/8 LAI

```

1,1,
365,1,365,
2008,2,0,2,2,
0,24,
0,4,1,1.0E-04,
1.0,8.0E-10,0,
1.02,1.0E-05,0,0,0,
4,3,0.5,
0,1,2,1,
0.0,1.0E+06,0.0,0.99,
1,1,1,
1,1.2,
0,0,0,0,0,
0,0,0,
0,2.880E+02,1.0E+01,0,
0,0,0,0,
1,0.66,288.46,0.24,
3,87,
1,0.0, 1,0.1, 1,0.2, 1,0.5,
1,1.0, 1,2.0, 1,4.0, 1,7.0,
2,12.0, 2,18.0, 2,24.0, 2,30.0,
2,36.0, 2,42.0, 2,48.0, 2,54.0,
2,60.0, 2,66.0, 2,72.0, 2,73.0,
2,74.0, 2,74.5, 2,75.0, 2,75.5,
2,76.0, 2,77.0, 2,80.0, 2,83.0,
2,86.0, 2,90.0, 2,90.5, 2,91.0,
2,91.2, 3,91.6, 3,93.0, 3,96.0,
3,98.0, 3,99.0, 3,99.5, 3,100.0,
3,100.5, 3,101.0, 3,102.0, 3,105.0,
3,108.0, 3,113.0, 3,119.0, 3,125.0,
3,131.0, 3,137.0, 3,143.0, 3,145.0,
3,147.0, 3,148.0, 3,149.0, 3,150.0,
3,150.5, 3,151.0, 3,152.0, 3,153.0,
3,155.0, 3,158.0, 3,163.0, 3,169.0,
3,175.0, 3,182.0, 3,188.0, 3,194.0,
3,196.0, 3,197.0, 3,198.0, 3,199.0,
3,199.5, 3,200.0, 3,200.5, 3,201.0,
3,202.0, 3,203.0, 3,205.0, 3,210.0,
3,215.0, 3,230.0, 3,260.0, 3,300.0,
3,340.0, 3,390.0, 3, 400.0,
MAT#1: -WATER RETENTION DATA
0.25,0.05,0.05,1.25, THET, THTR, VGA, VGN
MAT#1: - CONDUCTIVITY DATA
2.0,1.0,0.05,1.25,0.5, RKMOD, SK, VGA, VGN, EPIT
MAT#2: - WATER RETENTION DATA
0.25,0.05,0.0605,1.25, THET, THTR, VGA, VGN
MAT#2: - CONDUCTIVITY DATA
2.0,30.0,0.0605,1.25,0.5, RKMOD, SK, VGA, VGN, EPIT
MAT#3: - WATER RETENTION DATA
0.25,0.05,0.04,1.2, THET, THTR, VGA, VGN
MAT#3: - CONDUCTIVITY DATA
2.0,1.0,0.04,1.2,0.5, RKMOD, SK, VGA, VGN, EPIT
0, NDAY
1.05E+06,7.50E+05,5.03E+05,1.49E+03, H(1....NPT)
7.89E+02,4.76E+02,3.00E+02,2.08E+02,
1.86E+02,1.76E+02,1.67E+02,1.58E+02,
1.50E+02,1.43E+02,1.36E+02,1.29E+02,
1.22E+02,1.15E+02,1.09E+02,1.08E+02,
1.07E+02,1.07E+02,1.06E+02,1.06E+02,
1.05E+02,1.04E+02,1.01E+02,9.80E+01,
9.50E+01,9.11E+01,9.06E+01,9.01E+01,
8.99E+01,8.95E+01,8.85E+01,8.64E+01,
8.51E+01,8.44E+01,8.41E+01,8.38E+01,
8.35E+01,8.32E+01,8.27E+01,8.10E+01,
7.95E+01,7.72E+01,7.48E+01,7.27E+01,
7.09E+01,6.93E+01,6.80E+01,6.76E+01,
IPLANT, NGRAV
IFDEND, IDTBEG, IDTEND
IYS, NYEARS, ISTEAD, IFLIST, NFLIST
NPRINT, STOPHR
ISMETH, INMAX, ISWDIF, DMAXBA
DELMAX, DELMIN, OUTTIM
RFACT, RAINIF, DHTOL, DHMAX, DHFACT
KOPT, KEST, WTF
ITOPBC, IEVOPT, NFHOUR, LOWER
HIRRI, HDRI, HTOP, RHA
IETOPT, ICLLOUD, ISHOPT
IRAIN, HPR
IHYS, AIRTOL, HYSTOL, HYSMXH, HYFILE
IHEAT, ICONVH, DMAXHE
UPPERH, TSMEAN, TSAMP, QHCTOP
LOWERH, QHLEAK, TGRAD
IVAPOR, TORT, TSOIL, VAPDIF
MATN, NPT
MAT, Z

```



```

6.72E+01,6.70E+01,6.69E+01,6.67E+01,
6.66E+01,6.65E+01,6.64E+01,6.62E+01,
6.59E+01,6.55E+01,6.50E+01,6.45E+01,
6.41E+01,6.40E+01,6.40E+01,6.42E+01,
6.43E+01,6.44E+01,6.44E+01,6.45E+01,
6.45E+01,6.46E+01,6.46E+01,6.47E+01,
6.47E+01,6.48E+01,6.50E+01,6.56E+01,
6.62E+01,6.88E+01,7.56E+01,7.84E+01,
7.65E+01,7.39E+01,7.37E+01,
1,1,1,1,01,365,
LEAF,NFROOT,NUPTAK,NFPET,NSOW,NHRVST
0.10,
20,
1,0.0015, 60,0.003125, 90,0.0075, 100,0.01,
120,0.01125, 130,0.01625, 150,0.0175, 165,0.018125,
180,0.01875, 195,0.0205, 205,0.0325, 220,0.03625,
260,0.03625, 265,0.02875, 270,0.02375, 285,0.02,
300,0.01625, 315,0.010625, 325,0.002875, 360,0.0015,
7.0E-01,6.0E-02,1.6E-02,
1,1,1,1,1,1,1,1,1,1,
1,1,1,1,1,1,1,1,1,1,
1,1,1,1,1,1,1,1,1,1,
1,1,1,366,366,366,366,366,366,366,
366,366,366,366,366,366,366,366,366,366,
366,366,366,366,366,366,366,366,366,366,
366,366,366,366,366,366,366,366,366,366,
366,366,366,
2.0E+04,3.0E+03,1.0E+0,
2.0E+04,3.0E+03,1.0E+0,
2.0E+04,3.0E+03,1.0E+0,
0.0,0.52,0.5,0.0,2.7,
0.35,1872.1,6.1,838.4,
SP2008.dat
SP2009.dat

```

BARE  
NDLAI  
IDLAI,VLAI  
AA,B1,B2  
NTROOT  
HW,HD,HN  
HW,HD,HN  
HW,HD,HN  
PETPC  
ALBEDO,ALT,ZU,PMB

Run 39.4-3FT, 1/2 LAI,

1,1,  
 365,1,365,  
 2010,1,0,2,1,  
 0,24,  
 0,4,1,1.0E-04,  
 1.0,8.0E-10,0,  
 1.02,1.0E-05,0,0,0,  
 4,3,0.5,  
 0,1,2,1,  
 0.0,1.0E+06,0.0,0.99,  
 1,1,1,  
 1,1.2,  
 0,0,0,0,0,  
 0,0,0,  
 0,2.880E+02,1.0E+01,0,  
 0,0,0,0,  
 1,0.66,288.46,0.24,  
 3,87,  
 1,0.0, 1,0.1, 1,0.2, 1,0.5,  
 1,1.0, 1,2.0, 1,4.0, 1,7.0,  
 2,12.0, 2,18.0, 2,24.0, 2,30.0,  
 2,36.0, 2,42.0, 2,48.0, 2,54.0,  
 2,60.0, 2,66.0, 2,72.0, 2,73.0,  
 2,74.0, 2,74.5, 2,75.0, 2,75.5,  
 2,76.0, 2,77.0, 2,80.0, 2,83.0,  
 2,86.0, 2,90.0, 2,90.5, 2,91.0,  
 2,91.2, 3,91.6, 3,93.0, 3,96.0,  
 3,98.0, 3,99.0, 3,99.5, 3,100.0,  
 3,100.5, 3,101.0, 3,102.0, 3,105.0,  
 3,108.0, 3,113.0, 3,119.0, 3,125.0,  
 3,131.0, 3,137.0, 3,143.0, 3,145.0,  
 3,147.0, 3,148.0, 3,149.0, 3,150.0,  
 3,150.5, 3,151.0, 3,152.0, 3,153.0,  
 3,155.0, 3,158.0, 3,163.0, 3,169.0,  
 3,175.0, 3,182.0, 3,188.0, 3,194.0,  
 3,196.0, 3,197.0, 3,198.0, 3,199.0,  
 3,199.5, 3,200.0, 3,200.5, 3,201.0,  
 3,202.0, 3,203.0, 3,205.0, 3,210.0,  
 3,215.0, 3,230.0, 3,260.0, 3,300.0,  
 3,340.0, 3,390.0, 3, 400.0,  
 MAT#1: -WATER RETENTION DATA  
 0.25,0.05,0.05,1.25, THET, THTR, VGA, VGN  
 MAT#1: - CONDUCTIVITY DATA  
 2.0,1.0,0.05,1.25,0.5, RKMOD, SK, VGA, VGN, EPIT  
 MAT#2: - WATER RETENTION DATA  
 0.25,0.05,0.0605,1.25, THET, THTR, VGA, VGN  
 MAT#2: - CONDUCTIVITY DATA  
 2.0,30.0,0.0605,1.25,0.5, RKMOD, SK, VGA, VGN, EPIT  
 MAT#3: - WATER RETENTION DATA  
 0.25,0.05,0.04,1.2, THET, THTR, VGA, VGN  
 MAT#3: - CONDUCTIVITY DATA  
 2.0,1.0,0.04,1.2,0.5, RKMOD, SK, VGA, VGN, EPIT  
 0, NDAY  
 7.30E+05,3.33E+05,3.32E+04,1.00E+03, H(1....NPT)  
 6.42E+02,4.22E+02,2.94E+02,2.35E+02,  
 2.22E+02,2.16E+02,2.11E+02,2.08E+02,  
 2.05E+02,2.02E+02,1.99E+02,1.96E+02,  
 1.93E+02,1.90E+02,1.86E+02,1.86E+02,  
 1.85E+02,1.85E+02,1.84E+02,1.84E+02,  
 1.84E+02,1.83E+02,1.81E+02,1.78E+02,  
 1.76E+02,1.73E+02,1.72E+02,1.72E+02,  
 1.72E+02,1.71E+02,1.72E+02,1.74E+02,  
 1.75E+02,1.75E+02,1.75E+02,1.76E+02,  
 1.76E+02,1.76E+02,1.76E+02,1.78E+02,  
 1.80E+02,1.83E+02,1.89E+02,1.96E+02,  
 2.04E+02,2.12E+02,2.20E+02,2.22E+02,

IPLANT, NGRAV  
 IFDEND, IDTBEG, IDTEND  
 IYS, NYEARS, ISTEAD, IFLIST, NFLIST  
 NPRINT, STOPHR  
 ISMETH, INMAX, ISWDIF, DMAXBA  
 DELMAX, DELMIN, OUTTIM  
 RFACT, RAINIF, DHTOL, DHMAX, DHFACT  
 KOPT, KEST, WTF  
 ITOPBC, IEVOPT, NFHOUR, LOWER  
 HIRRI, HDRI, HTOP, RHA  
 IETOPT, ICLOUD, ISHOPT  
 IRAIN, HPR  
 IHYS, AIRTOL, HYSTOL, HYSMXH, HYFILE  
 IHEAT, ICONVH, DMAXHE  
 UPPERH, TSMEAN, TSAMP, QHCTOP  
 LOWERH, QHLEAK, TGRAD  
 IVAPOR, TORT, TSOIL, VAPDIF  
 MATN, NPT  
 MAT, Z

```

2.24E+02,2.25E+02,2.26E+02,2.27E+02,
2.28E+02,2.28E+02,2.29E+02,2.30E+02,
2.31E+02,2.33E+02,2.35E+02,2.35E+02,
2.35E+02,2.32E+02,2.30E+02,2.27E+02,
2.25E+02,2.25E+02,2.24E+02,2.24E+02,
2.24E+02,2.23E+02,2.23E+02,2.23E+02,
2.22E+02,2.22E+02,2.21E+02,2.18E+02,
2.15E+02,2.07E+02,1.93E+02,1.78E+02,
1.67E+02,1.61E+02,1.60E+02,
1,1,1,1,01,365,
LEAF,NFROOT,NUPTAK,NFPET,NSOW,NHRVST
0.10,
20,
1,0.006, 60,0.0125, 90,0.03, 100,0.04,
120,0.045, 130,0.065, 150,0.07, 165,0.0725,
180,0.075, 195,0.082, 205,0.13, 220,0.145,
260,0.145, 265,0.115, 270,0.095, 285,0.08,
300,0.065, 315,0.0425, 325,0.0115, 360,0.006,
7.0E-01,6.0E-02,1.6E-02,
1,1,1,1,1,1,1,1,1,1,
1,1,1,1,1,1,1,1,1,1,
1,1,1,1,1,1,1,1,1,1,
1,1,1,366,366,366,366,366,366,366,
366,366,366,366,366,366,366,366,366,366,
366,366,366,366,366,366,366,366,366,366,
366,366,366,366,366,366,366,366,366,366,
366,366,366,
2.0E+04,3.0E+03,1.0E+0,
2.0E+04,3.0E+03,1.0E+0,
2.0E+04,3.0E+03,1.0E+0,
0.0,0.52,0.5,0.0,2.7,
0.35,1872.1,6.1,838.4,
SP2010.dat
BARE
NDLAI
IDLAI,VLAI
AA,B1,B2
NTROOT
HW,HD,HN
HW,HD,HN
HW,HD,HN
PETPC
ALBEDO,ALT,ZU,PMB

```

Run 39.5-3FT, 1/2 LAI

```

1,1,
298,1,298,
2011,1,0,2,1,
0,24,
0,4,1,1.0E-04,
1.0,8.0E-10,0,
1.02,1.0E-05,0,0,0,
4,3,0.5,
0,1,2,1,
0.0,1.0E+06,0.0,0.99,
1,1,1,
1,1.2,
0,0,0,0,0,
0,0,0,
0,2.880E+02,1.0E+01,0,
0,0,0,0,
1,0.66,288.46,0.24,
3,87,
1,0.0, 1,0.1, 1,0.2, 1,0.5,
1,1.0, 1,2.0, 1,4.0, 1,7.0,
2,12.0, 2,18.0, 2,24.0, 2,30.0,
2,36.0, 2,42.0, 2,48.0, 2,54.0,
2,60.0, 2,66.0, 2,72.0, 2,73.0,
2,74.0, 2,74.5, 2,75.0, 2,75.5,
2,76.0, 2,77.0, 2,80.0, 2,83.0,
2,86.0, 2,90.0, 2,90.5, 2,91.0,
2,91.2, 3,91.6, 3,93.0, 3,96.0,
3,98.0, 3,99.0, 3,99.5, 3,100.0,
3,100.5, 3,101.0, 3,102.0, 3,105.0,
3,108.0, 3,113.0, 3,119.0, 3,125.0,
3,131.0, 3,137.0, 3,143.0, 3,145.0,
3,147.0, 3,148.0, 3,149.0, 3,150.0,
3,150.5, 3,151.0, 3,152.0, 3,153.0,
3,155.0, 3,158.0, 3,163.0, 3,169.0,
3,175.0, 3,182.0, 3,188.0, 3,194.0,
3,196.0, 3,197.0, 3,198.0, 3,199.0,
3,199.5, 3,200.0, 3,200.5, 3,201.0,
3,202.0, 3,203.0, 3,205.0, 3,210.0,
3,215.0, 3,230.0, 3,260.0, 3,300.0,
3,340.0, 3,390.0, 3, 400.0,
MAT#1: -WATER RETENTION DATA
0.25,0.05,0.05,1.25, THET, THTR, VGA, VGN
MAT#1: - CONDUCTIVITY DATA
2.0,1.0,0.05,1.25,0.5, RKMOD, SK, VGA, VGN, EPIT
MAT#2: - WATER RETENTION DATA
0.25,0.05,0.0605,1.25, THET, THTR, VGA, VGN
MAT#2: - CONDUCTIVITY DATA
2.0,30.0,0.0605,1.25,0.5, RKMOD, SK, VGA, VGN, EPIT
MAT#3: - WATER RETENTION DATA
0.25,0.05,0.04,1.2, THET, THTR, VGA, VGN
MAT#3: - CONDUCTIVITY DATA
2.0,1.0,0.04,1.2,0.5, RKMOD, SK, VGA, VGN, EPIT
0, NDAY
2.50E+03,1.81E+03,1.45E+03,9.29E+02, H(1....NPT)
6.38E+02,4.51E+02,3.66E+02,4.15E+02,
4.50E+02,4.52E+02,4.48E+02,4.40E+02,
4.29E+02,4.18E+02,4.06E+02,3.95E+02,
3.83E+02,3.73E+02,3.62E+02,3.61E+02,
3.59E+02,3.58E+02,3.57E+02,3.56E+02,
3.55E+02,3.54E+02,3.49E+02,3.44E+02,
3.39E+02,3.33E+02,3.32E+02,3.32E+02,
3.31E+02,3.30E+02,3.22E+02,3.04E+02,
2.94E+02,2.89E+02,2.87E+02,2.85E+02,
2.82E+02,2.80E+02,2.76E+02,2.64E+02,
2.53E+02,2.38E+02,2.22E+02,2.09E+02,
1.98E+02,1.89E+02,1.81E+02,1.78E+02,
IPLANT, NGRAV
IFDEND, IDTBEG, IDTEND
IYS, NYEARS, ISTEAD, IFLIST, NFLIST
NPRINT, STOPHR
ISMETH, INMAX, ISWDIF, DMAXBA
DELMAX, DELMIN, OUTTIM
RFACT, RAINIF, DHTOL, DHMAX, DHFACT
KOPT, KEST, WTF
ITOPBC, IEVOPT, NFHOUR, LOWER
HIRRI, HDRI, HTOP, RHA
IETOPT, ICLLOUD, ISHOPT
IRAIN, HPR
IHYS, AIRTOL, HYSTOL, HYSMXH, HYFILE
IHEAT, ICONVH, DMAXHE
UPPERH, TSMEAN, TSAMP, QHCTOP
LOWERH, QHLEAK, TGRAD
IVAPOR, TORT, TSOIL, VAPDIF
MATN, NPT
MAT, Z

```

```

1.76E+02,1.75E+02,1.73E+02,1.72E+02,
1.72E+02,1.71E+02,1.70E+02,1.69E+02,
1.67E+02,1.64E+02,1.60E+02,1.55E+02,
1.51E+02,1.46E+02,1.43E+02,1.40E+02,
1.39E+02,1.38E+02,1.38E+02,1.37E+02,
1.37E+02,1.37E+02,1.37E+02,1.36E+02,
1.36E+02,1.36E+02,1.35E+02,1.33E+02,
1.31E+02,1.26E+02,1.19E+02,1.14E+02,
1.13E+02,1.14E+02,1.14E+02,
1,1,1,1,01,365,
LEAF,NFROOT,NUPTAK,NFPET,NSOW,NHRVST
0.10,
20,
1,0.006, 60,0.0125, 90,0.03, 100,0.04,
120,0.045, 130,0.065, 150,0.07, 165,0.0725,
180,0.075, 195,0.082, 205,0.13, 220,0.145,
260,0.145, 265,0.115, 270,0.095, 285,0.08,
300,0.065, 315,0.0425, 325,0.0115, 360,0.006,
7.0E-01,6.0E-02,1.6E-02,
1,1,1,1,1,1,1,1,1,1,
1,1,1,1,1,1,1,1,1,1,
1,1,1,1,1,1,1,1,1,1,
1,1,1,366,366,366,366,366,366,366,
366,366,366,366,366,366,366,366,366,366,
366,366,366,366,366,366,366,366,366,366,
366,366,366,366,366,366,366,366,366,366,
366,366,366,
2.0E+04,3.0E+03,1.0E+0,
2.0E+04,3.0E+03,1.0E+0,
2.0E+04,3.0E+03,1.0E+0,
0.0,0.52,0.5,0.0,2.7,
0.35,1872.1,6.1,838.4,
SP2011.dat
BARE
NDLAI
IDLAI,VLAI
AA,B1,B2
NTROOT
HW,HD,HN
HW,HD,HN
HW,HD,HN
PETPC
ALBEDO,ALT,ZU,PMB

```

Run 40.1-3ft, No Plants

0,1,  
151,1,151,  
2006,1,0,2,1,  
0,24,  
0,4,1,1.0E-04,  
1.0,8.0E-10,0,  
1.02,1.0E-05,0,0,0,  
4,3,0.5,  
0,1,2,1,  
0.0,1.0E+06,0.0,0.99,  
1,1,1,  
0,0,  
0,0,0,0,0,  
0,0,0,  
0,2.880E+02,1.0E+01,0,  
0,0,0,0,  
1,0.66,288.46,0.24,  
3,87,  
1,0.0, 1,0.1, 1,0.2, 1,0.5,  
1,1.0, 1,2.0, 1,4.0, 1,7.0,  
2,12.0, 2,18.0, 2,24.0, 2,30.0,  
2,36.0, 2,42.0, 2,48.0, 2,54.0,  
2,60.0, 2,66.0, 2,72.0, 2,73.0,  
2,74.0, 2,74.5, 2,75.0, 2,75.5,  
2,76.0, 2,77.0, 2,80.0, 2,83.0,  
2,86.0, 2,90.0, 2,90.5, 2,91.0,  
2,91.2, 3,91.6, 3,93.0, 3,96.0,  
3,98.0, 3,99.0, 3,99.5, 3,100.0,  
3,100.5, 3,101.0, 3,102.0, 3,105.0,  
3,108.0, 3,113.0, 3,119.0, 3,125.0,  
3,131.0, 3,137.0, 3,143.0, 3,145.0,  
3,147.0, 3,148.0, 3,149.0, 3,150.0,  
3,150.5, 3,151.0, 3,152.0, 3,153.0,  
3,155.0, 3,158.0, 3,163.0, 3,169.0,  
3,175.0, 3,182.0, 3,188.0, 3,194.0,  
3,196.0, 3,197.0, 3,198.0, 3,199.0,  
3,199.5, 3,200.0, 3,200.5, 3,201.0,  
3,202.0, 3,203.0, 3,205.0, 3,210.0,  
3,215.0, 3,230.0, 3,260.0, 3,300.0,  
3,340.0, 3,390.0, 3, 400.0,  
MAT#1: -WATER RETENTION DATA  
0.25,0.05,0.05,1.25, THET, THTR, VGA, VGN  
MAT#1: - CONDUCTIVITY DATA  
2.0,1.0,0.05,1.25,0.5, RKMOD, SK, VGA, VGN, EPIT  
MAT#2: - WATER RETENTION DATA  
0.25,0.05,0.0605,1.25, THET, THTR, VGA, VGN  
MAT#2: - CONDUCTIVITY DATA  
2.0,30.0,0.0605,1.25,0.5, RKMOD, SK, VGA, VGN, EPIT  
MAT#3: - WATER RETENTION DATA  
0.25,0.05,0.04,1.2, THET, THTR, VGA, VGN  
MAT#3: - CONDUCTIVITY DATA  
2.0,1.0,0.04,1.2,0.5, RKMOD, SK, VGA, VGN, EPIT  
0, NDAY  
1.52E+02,1.52E+02,1.52E+02,1.52E+02, H(1....NPT)  
1.52E+02,1.52E+02,1.52E+02,1.52E+02,  
1.52E+02,1.52E+02,1.52E+02,1.52E+02,  
1.52E+02,1.52E+02,1.52E+02,1.52E+02,  
1.52E+02,1.52E+02,1.52E+02,1.52E+02,  
1.52E+02,1.52E+02,1.52E+02,1.52E+02,  
1.52E+02,1.53E+02,1.55E+02,1.57E+02,  
1.59E+02,1.61E+02,1.62E+02,1.62E+02,  
1.62E+02,1.62E+02,1.63E+02,1.65E+02,  
1.66E+02,1.67E+02,1.67E+02,1.68E+02,  
1.67E+02,1.67E+02,1.67E+02,1.65E+02,  
1.63E+02,1.60E+02,1.57E+02,1.54E+02,  
1.50E+02,1.47E+02,1.44E+02,1.43E+02,

IPLANT, NGRAV  
IFDEND, IDTBEG, IDTEND  
IYS, NYEARS, ISTEAD, IFLIST, NFLIST  
NPRINT, STOPHR  
ISMETH, INMAX, ISWDIF, DMAXBA  
DELMAX, DELMIN, OUTTIM  
RFACT, RAINIF, DHTOL, DHMAX, DHFACT  
KOPT, KEST, WTF  
ITOPBC, IEVOPT, NFHOUR, LOWER  
HIRRI, HDRI, HTOP, RHA  
IETOPT, ICLOUD, ISHOPT  
IRAIN, HPR  
IHYS, AIRTOL, HYSTOL, HYSMXH, HYFILE  
IHEAT, ICONVH, DMAXHE  
UPPERH, TSMEAN, TSAMP, QHCTOP  
LOWERH, QHLEAK, TGRAD  
IVAPOR, TORT, TSOIL, VAPDIF  
MATN, NPT  
MAT, Z

1.41E+02,1.41E+02,1.40E+02,1.40E+02,  
1.39E+02,1.40E+02,1.40E+02,1.40E+02,  
1.41E+02,1.41E+02,1.43E+02,1.44E+02,  
1.47E+02,1.51E+02,1.54E+02,1.58E+02,  
1.62E+02,1.65E+02,1.66E+02,1.67E+02,  
1.67E+02,1.68E+02,1.68E+02,1.68E+02,  
1.68E+02,1.68E+02,1.68E+02,1.68E+02,  
1.68E+02,1.68E+02,1.68E+02,1.68E+02,  
1.68E+02,1.68E+02,1.68E+02,  
0.35,1872.1,6.1,838.4,  
SP2006.dat  
2006 SP.dat

ALBEDO, ALT, ZU, PMB

Run 40.2-3FT, NO Plants

```

0,1,
365,1,365,
2007,4,0,2,4,
0,24,
0,4,1,1.0E-04,
1.0,8.0E-10,0,
1.02,1.0E-05,0,0,0,
4,3,0.5,
0,1,2,1,
0.0,1.0E+06,0.0,0.99,
1,1,1,
0,0,
0,0,0,0,0,
0,0,0,
0,2.880E+02,1.0E+01,0,
0,0,0,0,
1,0.66,288.46,0.24,
3,87,
1,0.0, 1,0.1, 1,0.2, 1,0.5,
1,1.0, 1,2.0, 1,4.0, 1,7.0,
2,12.0, 2,18.0, 2,24.0, 2,30.0,
2,36.0, 2,42.0, 2,48.0, 2,54.0,
2,60.0, 2,66.0, 2,72.0, 2,73.0,
2,74.0, 2,74.5, 2,75.0, 2,75.5,
2,76.0, 2,77.0, 2,80.0, 2,83.0,
2,86.0, 2,90.0, 2,90.5, 2,91.0,
2,91.2, 3,91.6, 3,93.0, 3,96.0,
3,98.0, 3,99.0, 3,99.5, 3,100.0,
3,100.5, 3,101.0, 3,102.0, 3,105.0,
3,108.0, 3,113.0, 3,119.0, 3,125.0,
3,131.0, 3,137.0, 3,143.0, 3,145.0,
3,147.0, 3,148.0, 3,149.0, 3,150.0,
3,150.5, 3,151.0, 3,152.0, 3,153.0,
3,155.0, 3,158.0, 3,163.0, 3,169.0,
3,175.0, 3,182.0, 3,188.0, 3,194.0,
3,196.0, 3,197.0, 3,198.0, 3,199.0,
3,199.5, 3,200.0, 3,200.5, 3,201.0,
3,202.0, 3,203.0, 3,205.0, 3,210.0,
3,215.0, 3,230.0, 3,260.0, 3,300.0,
3,340.0, 3,390.0, 3, 400.0,
MAT#1: -WATER RETENTION DATA
0.25,0.05,0.05,1.25, THET, THTR, VGA, VGN
MAT#1: - CONDUCTIVITY DATA
2.0,1.0,0.05,1.25,0.5, RKMOD, SK, VGA, VGN, EPIT
MAT#2: - WATER RETENTION DATA
0.25,0.05,0.0605,1.25, THET, THTR, VGA, VGN
MAT#2: - CONDUCTIVITY DATA
2.0,30.0,0.0605,1.25,0.5, RKMOD, SK, VGA, VGN, EPIT
MAT#3: - WATER RETENTION DATA
0.25,0.05,0.04,1.2, THET, THTR, VGA, VGN
MAT#3: - CONDUCTIVITY DATA
2.0,1.0,0.04,1.2,0.5, RKMOD, SK, VGA, VGN, EPIT
0, NDAY
5.35E+05,2.50E+05,1.75E+04,1.18E+03, H(1....NPT)
7.27E+02,4.71E+02,3.22E+02,2.46E+02,
2.26E+02,2.17E+02,2.09E+02,2.02E+02,
1.95E+02,1.88E+02,1.81E+02,1.75E+02,
1.69E+02,1.63E+02,1.56E+02,1.55E+02,
1.54E+02,1.54E+02,1.53E+02,1.53E+02,
1.52E+02,1.51E+02,1.48E+02,1.45E+02,
1.43E+02,1.39E+02,1.38E+02,1.38E+02,
1.37E+02,1.37E+02,1.36E+02,1.34E+02,
1.33E+02,1.32E+02,1.32E+02,1.31E+02,
1.31E+02,1.31E+02,1.30E+02,1.28E+02,
1.27E+02,1.24E+02,1.21E+02,1.19E+02,
1.16E+02,1.13E+02,1.11E+02,1.10E+02,

```



1.09E+02,1.09E+02,1.08E+02,1.08E+02,  
1.08E+02,1.08E+02,1.07E+02,1.07E+02,  
1.06E+02,1.05E+02,1.03E+02,1.01E+02,  
9.87E+01,9.64E+01,9.45E+01,9.27E+01,  
9.21E+01,9.18E+01,9.16E+01,9.13E+01,  
9.11E+01,9.10E+01,9.09E+01,9.07E+01,  
9.05E+01,9.02E+01,8.96E+01,8.83E+01,  
8.71E+01,8.36E+01,7.78E+01,7.17E+01,  
6.70E+01,6.38E+01,6.36E+01,  
0.35,1872.1,6.1,838.4,  
SP2007.dat  
SP2008.dat  
SP2009.dat  
SP2010.dat  
2007 SP.dat  
2008 SP.dat  
2009 SP.dat  
2010 SP.dat

ALBEDO, ALT, ZU, PMB

Run 40.3-3FT, No Plants

```

0,1,
298,1,298,
2011,1,0,2,1,
0,24,
0,4,1,1.0E-04,
1.0,8.0E-10,0,
1.02,1.0E-05,0,0,0,
4,3,0.5,
0,1,2,1,
0.0,1.0E+06,0.0,0.99,
1,1,1,
0,0,
0,0,0,0,0,
0,0,0,
0,2.880E+02,1.0E+01,0,
0,0,0,0,
1,0.66,288.46,0.24,
3,87,
1,0.0, 1,0.1, 1,0.2, 1,0.5,
1,1.0, 1,2.0, 1,4.0, 1,7.0,
2,12.0, 2,18.0, 2,24.0, 2,30.0,
2,36.0, 2,42.0, 2,48.0, 2,54.0,
2,60.0, 2,66.0, 2,72.0, 2,73.0,
2,74.0, 2,74.5, 2,75.0, 2,75.5,
2,76.0, 2,77.0, 2,80.0, 2,83.0,
2,86.0, 2,90.0, 2,90.5, 2,91.0,
2,91.2, 3,91.6, 3,93.0, 3,96.0,
3,98.0, 3,99.0, 3,99.5, 3,100.0,
3,100.5, 3,101.0, 3,102.0, 3,105.0,
3,108.0, 3,113.0, 3,119.0, 3,125.0,
3,131.0, 3,137.0, 3,143.0, 3,145.0,
3,147.0, 3,148.0, 3,149.0, 3,150.0,
3,150.5, 3,151.0, 3,152.0, 3,153.0,
3,155.0, 3,158.0, 3,163.0, 3,169.0,
3,175.0, 3,182.0, 3,188.0, 3,194.0,
3,196.0, 3,197.0, 3,198.0, 3,199.0,
3,199.5, 3,200.0, 3,200.5, 3,201.0,
3,202.0, 3,203.0, 3,205.0, 3,210.0,
3,215.0, 3,230.0, 3,260.0, 3,300.0,
3,340.0, 3,390.0, 3, 400.0,
MAT#1: -WATER RETENTION DATA
0.25,0.05,0.05,1.25, THET, THTR, VGA, VGN
MAT#1: - CONDUCTIVITY DATA
2.0,1.0,0.05,1.25,0.5, RKMOD, SK, VGA, VGN, EPIT
MAT#2: - WATER RETENTION DATA
0.25,0.05,0.0605,1.25, THET, THTR, VGA, VGN
MAT#2: - CONDUCTIVITY DATA
2.0,30.0,0.0605,1.25,0.5, RKMOD, SK, VGA, VGN, EPIT
MAT#3: - WATER RETENTION DATA
0.25,0.05,0.04,1.2, THET, THTR, VGA, VGN
MAT#3: - CONDUCTIVITY DATA
2.0,1.0,0.04,1.2,0.5, RKMOD, SK, VGA, VGN, EPIT
0, NDAY
3.66E+02,3.60E+02,3.54E+02,3.38E+02, H(1....NPT)
3.15E+02,2.82E+02,2.48E+02,2.42E+02,
2.46E+02,2.44E+02,2.41E+02,2.38E+02,
2.34E+02,2.29E+02,2.24E+02,2.18E+02,
2.11E+02,2.05E+02,1.98E+02,1.97E+02,
1.96E+02,1.95E+02,1.95E+02,1.94E+02,
1.94E+02,1.93E+02,1.90E+02,1.86E+02,
1.83E+02,1.79E+02,1.78E+02,1.78E+02,
1.78E+02,1.77E+02,1.75E+02,1.71E+02,
1.69E+02,1.67E+02,1.67E+02,1.66E+02,
1.66E+02,1.65E+02,1.64E+02,1.61E+02,
1.57E+02,1.53E+02,1.47E+02,1.42E+02,
1.38E+02,1.34E+02,1.30E+02,1.28E+02,
IPLANT, NGRAV
IFDEND, IDTBEG, IDTEND
IYS, NYEARS, ISTEAD, IFLIST, NFLIST
NPRINT, STOPHR
ISMETH, INMAX, ISWDIF, DMAXBA
DELMAX, DELMIN, OUTTIM
RFACT, RAINIF, DHTOL, DHMAX, DHFACT
KOPT, KEST, WTF
ITOPBC, IEVOPT, NFHOUR, LOWER
HIRRI, HDRIY, HTOP, RHA
IETOPT, ICLOUD, ISHOPT
IRAIN, HPR
IHYS, AIRTOL, HYSTOL, HYSMXH, HYFILE
IHEAT, ICONVH, DMAXHE
UPPERH, TSMEAN, TSAMP, QHCTOP
LOWERH, QHLEAK, TGRAD
IVAPOR, TORT, TSOIL, VAPDIF
MATN, NPT
MAT, Z

```

1.27E+02,1.27E+02,1.26E+02,1.26E+02,  
1.25E+02,1.25E+02,1.24E+02,1.24E+02,  
1.23E+02,1.21E+02,1.19E+02,1.16E+02,  
1.13E+02,1.10E+02,1.08E+02,1.06E+02,  
1.05E+02,1.05E+02,1.04E+02,1.04E+02,  
1.04E+02,1.04E+02,1.03E+02,1.03E+02,  
1.03E+02,1.03E+02,1.02E+02,1.01E+02,  
9.90E+01,9.50E+01,8.84E+01,8.15E+01,  
7.63E+01,7.29E+01,7.27E+01,  
0.35,1872.1,6.1,838.4,  
SP2011.dat  
2011 SP.dat

ALBEDO, ALT, ZU, PMB



```

1.0E+03,1.0E+03,1.0E+03,1.0E+03,
1.0E+03,1.0E+03,1.0E+03,1.0E+03,
1.0E+03,1.0E+03,1.0E+03,1.0E+03,
1.0E+03,1.0E+03,1.0E+03,1.0E+03,
1.0E+03,1.0E+03,1.0E+03,1.0E+03,
1.0E+03,1.0E+03,1.0E+03,1.0E+03,
1.0E+03,1.0E+03,1.0E+03,1.0E+03,
1.0E+03,1.0E+03,1.0E+03,1.0E+03,
1.0E+03,1.0E+03,1.0E+03,
1,1,1,1,01,365,
LEAF,NFROOT,NUPTAK,NFPET,NSOW,NHRVST
0.10,
20,
1,0.006,60,0.0125,90,0.03,100,0.04,
120,0.045,130,0.065,150,0.07,165,0.0725,
180,0.075,195,0.082,205,0.13,220,0.145,
260,0.145,265,0.115,270,0.095,285,0.08,
300,0.065,315,0.0425,325,0.0115,360,0.006,
7.0E-01,6.0E-02,1.6E-02,
1,1,1,1,1,1,1,1,1,1,
1,1,1,1,1,1,1,1,1,1,
1,1,1,1,1,1,1,1,1,1,
1,1,1,366,366,366,366,366,366,366,
366,366,366,366,366,366,366,366,366,366,
366,366,366,366,366,366,366,366,366,366,
366,366,366,366,366,366,366,366,366,366,
366,366,366,366,366,366,366,366,366,366,
366,366,366,
2.0E+04,3.0E+03,1.0E+0,
2.0E+04,3.0E+03,1.0E+0,
2.0E+04,3.0E+03,1.0E+0,
0.0,0.52,0.5,0.0,2.7,
0.35,1872.1,6.1,838.4,
met1897.dat
met1898.dat
met1899.dat
met1900.dat
met1901.dat
met1902.dat
met1903.dat
met1904.dat
met1905.dat
met1906.dat
met1907.dat
met1908.dat
met1909.dat
met1910.dat
met1911.dat
met1912.dat
met1913.dat
met1914.dat
met1915.dat
met1916.dat
met1917.dat
met1918.dat
met1919.dat
met1920.dat
met1921.dat
met1922.dat
met1923.dat
met1924.dat
met1925.dat
met1926.dat
met1927.dat
met1928.dat
met1929.dat

```

```

BARE
NDLAI
IDLAI,VLAI

```

```

AA,B1,B2
NTROOT

```

```

HW,HD,HN
HW,HD,HN
HW,HD,HN
PETPC
ALBEDO,ALT,ZU,PMB

```

met1930.dat  
met1931.dat  
met1932.dat  
met1933.dat  
met1934.dat  
met1935.dat  
met1936.dat  
met1937.dat  
met1938.dat  
met1939.dat  
met1940.dat  
met1941.dat  
met1942.dat  
met1943.dat  
met1944.dat  
met1945.dat  
met1946.dat  
met1947.dat  
met1948.dat  
met1949.dat  
met1950.dat  
met1951.dat  
met1952.dat  
met1953.dat  
met1954.dat  
met1955.dat  
met1956.dat  
met1957.dat  
met1958.dat  
met1959.dat  
met1960.dat  
met1961.dat  
met1962.dat  
met1963.dat  
met1964.dat  
met1965.dat  
met1966.dat  
met1967.dat  
met1968.dat  
met1969.dat  
met1970.dat  
met1971.dat  
met1972.dat  
met1973.dat  
met1974.dat  
met1975.dat  
met1976.dat  
met1977.dat  
met1978.dat  
met1979.dat  
met1980.dat  
met1981.dat  
met1982.dat  
met1983.dat  
met1984.dat  
met1985.dat  
met1986.dat  
met1987.dat  
met1988.dat  
met1989.dat  
met1990.dat  
met1991.dat  
met1992.dat  
met1993.dat  
met1994.dat  
met1995.dat  
met1996.dat

met1997.dat  
met1998.dat  
met1999.dat  
met2000.dat  
met2001.dat  
met2002.dat  
met2003.dat  
met2004.dat  
met2005.dat  
met2006.dat





```

1.0E+03,1.0E+03,1.0E+03,1.0E+03,
1.0E+03,1.0E+03,1.0E+03,1.0E+03,
1.0E+03,1.0E+03,1.0E+03,1.0E+03,
1.0E+03,1.0E+03,1.0E+03,1.0E+03,
1.0E+03,1.0E+03,1.0E+03,1.0E+03,
1.0E+03,1.0E+03,1.0E+03,1.0E+03,
1.0E+03,1.0E+03,1.0E+03,1.0E+03,
1.0E+03,1.0E+03,1.0E+03,1.0E+03,
1.0E+03,1.0E+03,1.0E+03,
1,1,1,1,01,365,
LEAF,NFROOT,NUPTAK,NFPET,NSOW,NHRVST
0.10,
20,
1,0.012, 60,0.025, 90,0.06, 100,0.08,
120,0.09, 130,0.13, 150,0.14, 165,0.145,
180,0.15, 195,0.165, 205,0.26, 220,0.29,
260,0.29, 265,0.23, 270,0.19, 285,0.16,
300,0.13, 315,0.085, 325,0.023,360,0.012,
7.0E-01,6.0E-02,1.6E-02,
1,1,1,1,1,1,1,1,1,1,
1,1,1,1,1,1,1,1,1,1,
1,1,1,1,1,1,1,1,1,1,
1,1,1,366,366,366,366,366,366,366,
366,366,366,366,366,366,366,366,366,366,
366,366,366,366,366,366,366,366,366,366,
366,366,366,366,366,366,366,366,366,366,
366,366,366,366,366,366,366,366,366,366,
366,366,366,
2.0E+04,3.0E+03,1.0E+0,
2.0E+04,3.0E+03,1.0E+0,
2.0E+04,3.0E+03,1.0E+0,
0.0,0.52,0.5,0.0,2.7,
0.35,1872.1,6.1,838.4,
met1897.dat
met1898.dat
met1899.dat
met1900.dat
met1901.dat
met1902.dat
met1903.dat
met1904.dat
met1905.dat
met1906.dat
met1907.dat
met1908.dat
met1909.dat
met1910.dat
met1911.dat
met1912.dat
met1913.dat
met1914.dat
met1915.dat
met1916.dat
met1917.dat
met1918.dat
met1919.dat
met1920.dat
met1921.dat
met1922.dat
met1923.dat
met1924.dat
met1925.dat
met1926.dat
met1927.dat
met1928.dat
met1929.dat

```

```

BARE
NDLAI
IDLAI,VLAI

```

```

AA,B1,B2
NTROOT

```

```

HW,HD,HN
HW,HD,HN
HW,HD,HN
PETPC
ALBEDO,ALT,ZU,PMB

```

met1930.dat  
met1931.dat  
met1932.dat  
met1933.dat  
met1934.dat  
met1935.dat  
met1936.dat  
met1937.dat  
met1938.dat  
met1939.dat  
met1940.dat  
met1941.dat  
met1942.dat  
met1943.dat  
met1944.dat  
met1945.dat  
met1946.dat  
met1947.dat  
met1948.dat  
met1949.dat  
met1950.dat  
met1951.dat  
met1952.dat  
met1953.dat  
met1954.dat  
met1955.dat  
met1956.dat  
met1957.dat  
met1958.dat  
met1959.dat  
met1960.dat  
met1961.dat  
met1962.dat  
met1963.dat  
met1964.dat  
met1965.dat  
met1966.dat  
met1967.dat  
met1968.dat  
met1969.dat  
met1970.dat  
met1971.dat  
met1972.dat  
met1973.dat  
met1974.dat  
met1975.dat  
met1976.dat  
met1977.dat  
met1978.dat  
met1979.dat  
met1980.dat  
met1981.dat  
met1982.dat  
met1983.dat  
met1984.dat  
met1985.dat  
met1986.dat  
met1987.dat  
met1988.dat  
met1989.dat  
met1990.dat  
met1991.dat  
met1992.dat  
met1993.dat  
met1994.dat  
met1995.dat  
met1996.dat

met1997.dat  
met1998.dat  
met1999.dat  
met2000.dat  
met2001.dat  
met2002.dat  
met2003.dat  
met2004.dat  
met2005.dat  
met2006.dat



1.0E+03,1.0E+03,1.0E+03,1.0E+03,  
1.0E+03,1.0E+03,1.0E+03,1.0E+03,  
1.0E+03,1.0E+03,1.0E+03,1.0E+03,  
1.0E+03,1.0E+03,1.0E+03,1.0E+03,  
1.0E+03,1.0E+03,1.0E+03,1.0E+03,  
1.0E+03,1.0E+03,1.0E+03,1.0E+03,  
1.0E+03,1.0E+03,1.0E+03,1.0E+03,  
1.0E+03,1.0E+03,1.0E+03,1.0E+03,  
1.0E+03,1.0E+03,1.0E+03,1.0E+03,  
1.0E+03,1.0E+03,1.0E+03,1.0E+03,  
1.0E+03,1.0E+03,1.0E+03,  
0.35,1872.1,6.1,838.4,

ALBEDO, ALT, ZU, PMB

met1897.dat  
met1898.dat  
met1899.dat  
met1900.dat  
met1901.dat  
met1902.dat  
met1903.dat  
met1904.dat  
met1905.dat  
met1906.dat  
met1907.dat  
met1908.dat  
met1909.dat  
met1910.dat  
met1911.dat  
met1912.dat  
met1913.dat  
met1914.dat  
met1915.dat  
met1916.dat  
met1917.dat  
met1918.dat  
met1919.dat  
met1920.dat  
met1921.dat  
met1922.dat  
met1923.dat  
met1924.dat  
met1925.dat  
met1926.dat  
met1927.dat  
met1928.dat  
met1929.dat  
met1930.dat  
met1931.dat  
met1932.dat  
met1933.dat  
met1934.dat  
met1935.dat  
met1936.dat  
met1937.dat  
met1938.dat  
met1939.dat  
met1940.dat  
met1941.dat  
met1942.dat  
met1943.dat  
met1944.dat  
met1945.dat  
met1946.dat  
met1947.dat  
met1948.dat  
met1949.dat  
met1950.dat

met1951.dat  
met1952.dat  
met1953.dat  
met1954.dat  
met1955.dat  
met1956.dat  
met1957.dat  
met1958.dat  
met1959.dat  
met1960.dat  
met1961.dat  
met1962.dat  
met1963.dat  
met1964.dat  
met1965.dat  
met1966.dat  
met1967.dat  
met1968.dat  
met1969.dat  
met1970.dat  
met1971.dat  
met1972.dat  
met1973.dat  
met1974.dat  
met1975.dat  
met1976.dat  
met1977.dat  
met1978.dat  
met1979.dat  
met1980.dat  
met1981.dat  
met1982.dat  
met1983.dat  
met1984.dat  
met1985.dat  
met1986.dat  
met1987.dat  
met1988.dat  
met1989.dat  
met1990.dat  
met1991.dat  
met1992.dat  
met1993.dat  
met1994.dat  
met1995.dat  
met1996.dat  
met1997.dat  
met1998.dat  
met1999.dat  
met2000.dat  
met2001.dat  
met2002.dat  
met2003.dat  
met2004.dat  
met2005.dat  
met2006.dat

Run 294.1-4', No Plants

```

0,1,
151,1,151,
2006,1,0,2,1,
0,24,
0,4,1,1.0E-04,
1.0,8.0E-10,0,
1.02,1.0E-05,0,0,0,
4,3,0.5,
0,1,2,1,
0.0,1.0E+06,0.0,0.99,
1,1,1,
1,1.2,
0,0,0,0,0,
0,0,0,
0,2.880E+02,1.0E+01,0,
0,0,0,0,
1,0.66,288.46,0.24,
3,87,
1,0.0, 1,0.1, 1,0.2, 1,0.5,
1,1.0, 1,2.0, 1,4.0, 1,7.0,
2,12.0, 2,18.0, 2,24.0, 2,30.0,
2,36.0, 2,42.0, 2,48.0, 2,54.0,
2,60.0, 2,66.0, 2,72.0, 2,78.0,
2,84.0, 2,90.0, 2,96.0, 2,97.0,
2,98.0, 2,99.0, 2,99.5, 2,100.0,
2,100.5, 2,101.0, 2,102.0, 2,105.0,
2,108.0, 2,113.0, 2,119.0, 2,120.0,
2,121.0, 2,121.6, 3,122.2, 3,125.0,
3,131.0, 3,137.0, 3,143.0, 3,145.0,
3,147.0, 3,148.0, 3,149.0, 3,149.5,
3,150.0, 3,150.5, 3,151.0, 3,152.0,
3,153.0, 3,155.0, 3,158.0, 3,163.0,
3,169.0, 3,175.0, 3,178.0, 3,179.0,
3,179.5, 3,180.0, 3,180.5, 3,181.0,
3,182.0, 3,183.0, 3,185.0, 3,188.0,
3,194.0, 3,196.0, 3,197.0, 3,198.0,
3,199.0, 3,199.5, 3,200.0, 3,200.5,
3,201.0, 3,202.0, 3,203.0, 3,205.0,
3,210.0, 3,215.0, 3,230.0, 3,260.0,
3,300.0, 3,390.0, 3, 400.0,
MAT#1: -WATER RETENTION DATA
0.25,0.05,0.05,1.25, THET, THTR, VGA, VGN
MAT#1: - CONDUCTIVITY DATA
2.0,1.0,0.05,1.25,0.5, RKMOD, SK, VGA, VGN, EPIT
MAT#2: - WATER RETENTION DATA
0.25,0.05,0.0605,1.25, THET, THTR, VGA, VGN
MAT#2: - CONDUCTIVITY DATA
2.0,30.0,0.0605,1.25,0.5, RKMOD, SK, VGA, VGN, EPIT
MAT#3: - WATER RETENTION DATA
0.25,0.05,0.04,1.2, THET, THTR, VGA, VGN
MAT#3: - CONDUCTIVITY DATA
2.0,1.0,0.04,1.2,0.5, RKMOD, SK, VGA, VGN, EPIT
0, NDAY
1.54E+02,1.54E+02,1.54E+02,1.54E+02, H(1....NPT)
1.54E+02,1.54E+02,1.54E+02,1.54E+02,
1.54E+02,1.54E+02,1.54E+02,1.54E+02,
1.54E+02,1.54E+02,1.54E+02,1.54E+02,
1.54E+02,1.54E+02,1.54E+02,1.54E+02,
1.54E+02,1.54E+02,1.54E+02,1.54E+02,
1.54E+02,1.54E+02,1.54E+02,1.54E+02,
1.54E+02,1.54E+02,1.54E+02,1.54E+02,
1.54E+02,1.54E+02,1.53E+02,1.52E+02,
1.51E+02,1.48E+02,1.46E+02,1.45E+02,
1.45E+02,1.44E+02,1.44E+02,1.43E+02,
1.40E+02,1.37E+02,1.35E+02,1.34E+02,
1.33E+02,1.32E+02,1.32E+02,1.32E+02,
1.32E+02,1.32E+02,1.33E+02,1.34E+02,

```

1.36E+02,1.38E+02,1.43E+02,1.49E+02,  
1.58E+02,1.66E+02,1.70E+02,1.71E+02,  
1.72E+02,1.73E+02,1.74E+02,1.74E+02,  
1.76E+02,1.78E+02,1.81E+02,1.86E+02,  
1.96E+02,1.99E+02,2.01E+02,2.02E+02,  
2.04E+02,2.06E+02,2.06E+02,2.06E+02,  
2.06E+02,2.06E+02,2.06E+02,2.06E+02,  
2.06E+02,2.06E+02,2.06E+02,2.06E+02,  
2.06E+02,2.06E+02,2.06E+02,  
0.35,1872.1,6.1,838.4,  
SP2006.dat

ALBEDO,ALT,ZU,PMB



Run 294.2-4', No Plants

```

0,1,
365,1,365,
2007,1,0,2,1,
0,24,
0,4,1,1.0E-04,
1.0,8.0E-10,0,
1.02,1.0E-05,0,0,0,
4,3,0.5,
0,1,2,1,
0.0,1.0E+06,0.0,0.99,
1,1,1,
1,1.2,
0,0,0,0,0,
0,0,0,
0,2.880E+02,1.0E+01,0,
0,0,0,0,
1,0.66,288.46,0.24,
3,87,
1,0.0, 1,0.1, 1,0.2, 1,0.5,
1,1.0, 1,2.0, 1,4.0, 1,7.0,
2,12.0, 2,18.0, 2,24.0, 2,30.0,
2,36.0, 2,42.0, 2,48.0, 2,54.0,
2,60.0, 2,66.0, 2,72.0, 2,78.0,
2,84.0, 2,90.0, 2,96.0, 2,97.0,
2,98.0, 2,99.0, 2,99.5, 2,100.0,
2,100.5, 2,101.0, 2,102.0, 2,105.0,
2,108.0, 2,113.0, 2,119.0, 2,120.0,
2,121.0, 2,121.6, 3,122.2, 3,125.0,
3,131.0, 3,137.0, 3,143.0, 3,145.0,
3,147.0, 3,148.0, 3,149.0, 3,149.5,
3,150.0, 3,150.5, 3,151.0, 3,152.0,
3,153.0, 3,155.0, 3,158.0, 3,163.0,
3,169.0, 3,175.0, 3,178.0, 3,179.0,
3,179.5, 3,180.0, 3,180.5, 3,181.0,
3,182.0, 3,183.0, 3,185.0, 3,188.0,
3,194.0, 3,196.0, 3,197.0, 3,198.0,
3,199.0, 3,199.5, 3,200.0, 3,200.5,
3,201.0, 3,202.0, 3,203.0, 3,205.0,
3,210.0, 3,215.0, 3,230.0, 3,260.0,
3,300.0, 3,390.0, 3, 400.0,
MAT#1: -WATER RETENTION DATA
0.25,0.05,0.05,1.25, THET, THTR, VGA, VGN
MAT#1: - CONDUCTIVITY DATA
2.0,1.0,0.05,1.25,0.5, RKMOD, SK, VGA, VGN, EPIT
MAT#2: - WATER RETENTION DATA
0.25,0.05,0.0605,1.25, THET, THTR, VGA, VGN
MAT#2: - CONDUCTIVITY DATA
2.0,30.0,0.0605,1.25,0.5, RKMOD, SK, VGA, VGN, EPIT
MAT#3: - WATER RETENTION DATA
0.25,0.05,0.04,1.2, THET, THTR, VGA, VGN
MAT#3: - CONDUCTIVITY DATA
2.0,1.0,0.04,1.2,0.5, RKMOD, SK, VGA, VGN, EPIT
0, NDAY
5.78E+05,4.04E+05,2.49E+05,1.30E+03, H(1....NPT)
8.29E+02,5.44E+02,3.64E+02,2.68E+02,
2.44E+02,2.34E+02,2.25E+02,2.17E+02,
2.09E+02,2.01E+02,1.94E+02,1.88E+02,
1.81E+02,1.75E+02,1.68E+02,1.62E+02,
1.56E+02,1.50E+02,1.44E+02,1.43E+02,
1.42E+02,1.41E+02,1.41E+02,1.40E+02,
1.40E+02,1.39E+02,1.38E+02,1.36E+02,
1.33E+02,1.28E+02,1.22E+02,1.21E+02,
1.20E+02,1.20E+02,1.19E+02,1.18E+02,
1.16E+02,1.13E+02,1.11E+02,1.11E+02,
1.10E+02,1.10E+02,1.10E+02,1.09E+02,
1.09E+02,1.09E+02,1.09E+02,1.09E+02,
IPLANT, NGRAV
IFDEND, IDTBEG, IDTEND
IYS, NYEARS, ISTEAD, IFLIST, NFLIST
NPRINT, STOPHR
ISMETH, INMAX, ISWDIF, DMAXBA
DELMAX, DELMIN, OUTTIM
RFACT, RAINIF, DHTOL, DHMAX, DHFACT
KOPT, KEST, WTF
ITOPBC, IEVOPT, NFHOUR, LOWER
HIRRI, HDRIY, HTOP, RHA
IETOPT, ICLOUD, ISHOPT
IRAIN, HPR
IHYS, AIRTOL, HYSTOL, HYSMXH, HYFILE
IHEAT, ICONVH, DMAXHE
UPPERH, TSMEAN, TSAMP, QHCTOP
LOWERH, QHLEAK, TGRAD
IVAPOR, TORT, TSOIL, VAPDIF
MATN, NPT
MAT, Z

```

1.08E+02,1.08E+02,1.07E+02,1.05E+02,  
1.03E+02,1.01E+02,1.00E+02,1.00E+02,  
9.98E+01,9.97E+01,9.95E+01,9.94E+01,  
9.90E+01,9.87E+01,9.81E+01,9.72E+01,  
9.54E+01,9.48E+01,9.45E+01,9.42E+01,  
9.39E+01,9.38E+01,9.37E+01,9.35E+01,  
9.34E+01,9.31E+01,9.28E+01,9.23E+01,  
9.09E+01,8.96E+01,8.58E+01,7.95E+01,  
7.24E+01,6.48E+01,6.46E+01,  
0.35,1872.1,6.1,838.4,  
SP2007.dat

ALBEDO, ALT, ZU, PMB

Run 294.3-4', 1/8 LAI

```

1,1,
365,1,365,
2008,2,0,2,2,
0,24,
0,4,1,1.0E-04,
1.0,8.0E-10,0,
1.02,1.0E-05,0,0,0,
4,3,0.5,
0,1,2,1,
0.0,1.0E+06,0.0,0.99,
1,1,1,
1,1.2,
0,0,0,0,0,
0,0,0,
0,2.880E+02,1.0E+01,0,
0,0,0,0,
1,0.66,288.46,0.24,
3,87,
1,0.0, 1,0.1, 1,0.2, 1,0.5,
1,1.0, 1,2.0, 1,4.0, 1,7.0,
2,12.0, 2,18.0, 2,24.0, 2,30.0,
2,36.0, 2,42.0, 2,48.0, 2,54.0,
2,60.0, 2,66.0, 2,72.0, 2,78.0,
2,84.0, 2,90.0, 2,96.0, 2,97.0,
2,98.0, 2,99.0, 2,99.5, 2,100.0,
2,100.5, 2,101.0, 2,102.0, 2,105.0,
2,108.0, 2,113.0, 2,119.0, 2,120.0,
2,121.0, 2,121.6, 3,122.2, 3,125.0,
3,131.0, 3,137.0, 3,143.0, 3,145.0,
3,147.0, 3,148.0, 3,149.0, 3,149.5,
3,150.0, 3,150.5, 3,151.0, 3,152.0,
3,153.0, 3,155.0, 3,158.0, 3,163.0,
3,169.0, 3,175.0, 3,178.0, 3,179.0,
3,179.5, 3,180.0, 3,180.5, 3,181.0,
3,182.0, 3,183.0, 3,185.0, 3,188.0,
3,194.0, 3,196.0, 3,197.0, 3,198.0,
3,199.0, 3,199.5, 3,200.0, 3,200.5,
3,201.0, 3,202.0, 3,203.0, 3,205.0,
3,210.0, 3,215.0, 3,230.0, 3,260.0,
3,300.0, 3,390.0, 3, 400.0,
MAT#1: -WATER RETENTION DATA
0.25,0.05,0.05,1.25, THET, THTR, VGA, VGN
MAT#1: - CONDUCTIVITY DATA
2.0,1.0,0.05,1.25,0.5, RKMOD, SK, VGA, VGN, EPIT
MAT#2: - WATER RETENTION DATA
0.25,0.05,0.0605,1.25, THET, THTR, VGA, VGN
MAT#2: - CONDUCTIVITY DATA
2.0,30.0,0.0605,1.25,0.5, RKMOD, SK, VGA, VGN, EPIT
MAT#3: - WATER RETENTION DATA
0.25,0.05,0.04,1.2, THET, THTR, VGA, VGN
MAT#3: - CONDUCTIVITY DATA
2.0,1.0,0.04,1.2,0.5, RKMOD, SK, VGA, VGN, EPIT
0, NDAY
1.05E+06,8.05E+05,5.96E+05,1.01E+05, H(1....NPT)
6.94E+02,4.81E+02,3.22E+02,2.30E+02,
2.06E+02,1.96E+02,1.87E+02,1.78E+02,
1.70E+02,1.62E+02,1.54E+02,1.47E+02,
1.40E+02,1.34E+02,1.27E+02,1.21E+02,
1.15E+02,1.09E+02,1.03E+02,1.02E+02,
1.01E+02,9.96E+01,9.91E+01,9.86E+01,
9.82E+01,9.77E+01,9.67E+01,9.37E+01,
9.08E+01,8.60E+01,8.02E+01,7.92E+01,
7.82E+01,7.77E+01,7.72E+01,7.59E+01,
7.34E+01,7.13E+01,6.94E+01,6.88E+01,
6.82E+01,6.80E+01,6.77E+01,6.76E+01,
6.75E+01,6.73E+01,6.72E+01,6.70E+01,
IPLANT, NGRAV
IFDEND, IDTBEG, IDTEND
IYS, NYEARS, ISTEAD, IFLIST, NFLIST
NPRINT, STOPHR
ISMETH, INMAX, ISWDIF, DMAXBA
DELMAX, DELMIN, OUTTIM
RFACT, RAINIF, DHTOL, DHMAX, DHFACT
KOPT, KEST, WTF
ITOPBC, IEVOPT, NFHOUR, LOWER
HIRRI, HDRI, HTOP, RHA
IETOPT, ICLOUD, ISHOPT
IRAIN, HPR
IHYS, AIRTOL, HYSTOL, HYSMXH, HYFILE
IHEAT, ICONVH, DMAXHE
UPPERH, TSMEAN, TSAMP, QHCTOP
LOWERH, QHLEAK, TGRAD
IVAPOR, TORT, TSOIL, VAPDIF
MATN, NPT
MAT, Z

```

```

6.67E+01,6.62E+01,6.56E+01,6.46E+01,
6.35E+01,6.27E+01,6.23E+01,6.21E+01,
6.21E+01,6.20E+01,6.20E+01,6.19E+01,
6.18E+01,6.17E+01,6.15E+01,6.12E+01,
6.08E+01,6.07E+01,6.07E+01,6.06E+01,
6.06E+01,6.06E+01,6.05E+01,6.05E+01,
6.05E+01,6.05E+01,6.04E+01,6.04E+01,
6.04E+01,6.04E+01,6.13E+01,6.67E+01,
7.53E+01,7.34E+01,7.33E+01,
1,1,1,1,01,365,
0.10,
20,
1,0.0015, 60,0.003125, 90,0.0075, 100,0.01,
120,0.01125, 130,0.01625, 150,0.0175, 165,0.018125,
180,0.01875, 195,0.0205, 205,0.0325, 220,0.03625,
260,0.03625, 265,0.02875, 270,0.02375, 285,0.02,
300,0.01625, 315,0.010625, 325,0.002875, 360,0.0015,
7.0E-01,6.0E-02,1.6E-02,
1,1,1,1,1,1,1,1,1,1,
1,1,1,1,1,1,1,1,1,1,
1,1,1,1,1,1,1,1,1,1,
1,1,1,1,1,1,1,1,366,366,
366,366,366,366,366,366,366,366,366,366,
366,366,366,366,366,366,366,366,366,366,
366,366,366,366,366,366,366,366,366,366,
366,366,366,
2.0E+04,3.0E+03,1.0E+0,
2.0E+04,3.0E+03,1.0E+0,
2.0E+04,3.0E+03,1.0E+0,
0.0,0.52,0.5,0.0,2.7,
0.35,1872.1,6.1,838.4,
SP2008.dat
SP2009.dat

```

LEAF, NFROOT, NUPTAK, NFPET, NSOW, NHRVST  
BARE

NDLAI

IDLAI, VLAI

AA, B1, B2  
NTROOT

HW, HD, HN  
HW, HD, HN  
HW, HD, HN  
PETPC

ALBEDO, ALT, ZU, PMB

Run 294.4-4', 1/2 LAI

```

1,1,
365,1,365,
2010,1,0,2,1,
0,24,
0,4,1,1.0E-04,
1.0,8.0E-10,0,
1.02,1.0E-05,0,0,0,
4,3,0.5,
0,1,2,1,
0.0,1.0E+06,0.0,0.99,
1,1,1,
1,1.2,
0,0,0,0,0,
0,0,0,
0,2.880E+02,1.0E+01,0,
0,0,0,0,
1,0.66,288.46,0.24,
3,87,
1,0.0, 1,0.1, 1,0.2, 1,0.5,
1,1.0, 1,2.0, 1,4.0, 1,7.0,
2,12.0, 2,18.0, 2,24.0, 2,30.0,
2,36.0, 2,42.0, 2,48.0, 2,54.0,
2,60.0, 2,66.0, 2,72.0, 2,78.0,
2,84.0, 2,90.0, 2,96.0, 2,97.0,
2,98.0, 2,99.0, 2,99.5, 2,100.0,
2,100.5, 2,101.0, 2,102.0, 2,105.0,
2,108.0, 2,113.0, 2,119.0, 2,120.0,
2,121.0, 2,121.6, 3,122.2, 3,125.0,
3,131.0, 3,137.0, 3,143.0, 3,145.0,
3,147.0, 3,148.0, 3,149.0, 3,149.5,
3,150.0, 3,150.5, 3,151.0, 3,152.0,
3,153.0, 3,155.0, 3,158.0, 3,163.0,
3,169.0, 3,175.0, 3,178.0, 3,179.0,
3,179.5, 3,180.0, 3,180.5, 3,181.0,
3,182.0, 3,183.0, 3,185.0, 3,188.0,
3,194.0, 3,196.0, 3,197.0, 3,198.0,
3,199.0, 3,199.5, 3,200.0, 3,200.5,
3,201.0, 3,202.0, 3,203.0, 3,205.0,
3,210.0, 3,215.0, 3,230.0, 3,260.0,
3,300.0, 3,390.0, 3, 400.0,
MAT#1: -WATER RETENTION DATA
0.25,0.05,0.05,1.25, THET, THTR, VGA, VGN
MAT#1: - CONDUCTIVITY DATA
2.0,1.0,0.05,1.25,0.5, RKMOD, SK, VGA, VGN, EPIT
MAT#2: - WATER RETENTION DATA
0.25,0.05,0.0605,1.25, THET, THTR, VGA, VGN
MAT#2: - CONDUCTIVITY DATA
2.0,30.0,0.0605,1.25,0.5, RKMOD, SK, VGA, VGN, EPIT
MAT#3: - WATER RETENTION DATA
0.25,0.05,0.04,1.2, THET, THTR, VGA, VGN
MAT#3: - CONDUCTIVITY DATA
2.0,1.0,0.04,1.2,0.5, RKMOD, SK, VGA, VGN, EPIT
0, NDAY
7.92E+05,4.49E+05,1.82E+05,9.60E+02, H(1....NPT)
6.55E+02,4.39E+02,3.09E+02,2.51E+02,
2.40E+02,2.35E+02,2.31E+02,2.28E+02,
2.26E+02,2.24E+02,2.22E+02,2.20E+02,
2.17E+02,2.14E+02,2.11E+02,2.06E+02,
2.02E+02,1.97E+02,1.92E+02,1.91E+02,
1.90E+02,1.89E+02,1.89E+02,1.88E+02,
1.88E+02,1.87E+02,1.87E+02,1.84E+02,
1.81E+02,1.77E+02,1.72E+02,1.71E+02,
1.70E+02,1.69E+02,1.69E+02,1.70E+02,
1.74E+02,1.79E+02,1.85E+02,1.87E+02,
1.90E+02,1.91E+02,1.92E+02,1.93E+02,
1.93E+02,1.94E+02,1.95E+02,1.96E+02,
IPLANT, NGRAV
IFDEND, IDTBEG, IDTEND
IYS, NYEARS, ISTEAD, IFLIST, NFLIST
NPRINT, STOPHR
ISMETH, INMAX, ISWDIF, DMAXBA
DELMAX, DELMIN, OUTTIM
RFACT, RAINIF, DHTOL, DHMAX, DHFACT
KOPT, KEST, WTF
ITOPBC, IEVOPT, NFHOUR, LOWER
HIRRI, HDRI, HTOP, RHA
IETOPT, ICLOUD, ISHOPT
IRAIN, HPR
IHYS, AIRTOL, HYSTOL, HYSMXH, HYFILE
IHEAT, ICONVH, DMAXHE
UPPERH, TSMEAN, TSAMP, QHCTOP
LOWERH, QHLEAK, TGRAD
IVAPOR, TORT, TSOIL, VAPDIF
MATN, NPT
MAT, Z

```

```

1.97E+02,2.00E+02,2.04E+02,2.10E+02,
2.17E+02,2.23E+02,2.25E+02,2.25E+02,
2.26E+02,2.26E+02,2.26E+02,2.26E+02,
2.27E+02,2.27E+02,2.28E+02,2.28E+02,
2.29E+02,2.28E+02,2.28E+02,2.28E+02,
2.28E+02,2.28E+02,2.27E+02,2.27E+02,
2.27E+02,2.27E+02,2.27E+02,2.26E+02,
2.24E+02,2.22E+02,2.14E+02,1.99E+02,
1.82E+02,1.65E+02,1.64E+02,
1,1,1,1,01,365,
0.10,
20,
1,0.006, 60,0.0125, 90,0.03, 100,0.04,
120,0.045, 130,0.065, 150,0.07, 165,0.0725,
180,0.075, 195,0.082, 205,0.13, 220,0.145,
260,0.145, 265,0.115, 270,0.095, 285,0.08,
300,0.065, 315,0.0425, 325,0.0115, 360,0.006,
7.0E-01,6.0E-02,1.6E-02,
1,1,1,1,1,1,1,1,1,1,
1,1,1,1,1,1,1,1,1,1,
1,1,1,1,1,1,1,1,1,1,
1,1,1,1,1,1,1,1,366,366,
366,366,366,366,366,366,366,366,366,366,
366,366,366,366,366,366,366,366,366,366,
366,366,366,366,366,366,366,366,366,366,
366,366,366,366,366,366,366,366,366,366,
366,366,366,
2.0E+04,3.0E+03,1.0E+0,
2.0E+04,3.0E+03,1.0E+0,
2.0E+04,3.0E+03,1.0E+0,
0.0,0.52,0.5,0.0,2.7,
0.35,1872.1,6.1,838.4,
SP2010.dat
LEAF,NFROOT,NUPTAK,NFPET,NSOW,NHRVST
BARE
NDLAI
IDLAI,VLAI
AA,B1,B2
NTROOT
HW,HD,HN
HW,HD,HN
HW,HD,HN
PETPC
ALBEDO,ALT,ZU,PMB

```

Run 294.5-4', 1/2 LAI

```

1,1,
298,1,298,
2011,1,0,2,1,
0,24,
0,4,1,1.0E-04,
1.0,8.0E-10,0,
1.02,1.0E-05,0,0,0,
4,3,0.5,
0,1,2,1,
0.0,1.0E+06,0.0,0.99,
1,1,1,
1,1.2,
0,0,0,0,0,
0,0,0,
0,2.880E+02,1.0E+01,0,
0,0,0,0,
1,0.66,288.46,0.24,
3,87,
1,0.0, 1,0.1, 1,0.2, 1,0.5,
1,1.0, 1,2.0, 1,4.0, 1,7.0,
2,12.0, 2,18.0, 2,24.0, 2,30.0,
2,36.0, 2,42.0, 2,48.0, 2,54.0,
2,60.0, 2,66.0, 2,72.0, 2,78.0,
2,84.0, 2,90.0, 2,96.0, 2,97.0,
2,98.0, 2,99.0, 2,99.5, 2,100.0,
2,100.5, 2,101.0, 2,102.0, 2,105.0,
2,108.0, 2,113.0, 2,119.0, 2,120.0,
2,121.0, 2,121.6, 3,122.2, 3,125.0,
3,131.0, 3,137.0, 3,143.0, 3,145.0,
3,147.0, 3,148.0, 3,149.0, 3,149.5,
3,150.0, 3,150.5, 3,151.0, 3,152.0,
3,153.0, 3,155.0, 3,158.0, 3,163.0,
3,169.0, 3,175.0, 3,178.0, 3,179.0,
3,179.5, 3,180.0, 3,180.5, 3,181.0,
3,182.0, 3,183.0, 3,185.0, 3,188.0,
3,194.0, 3,196.0, 3,197.0, 3,198.0,
3,199.0, 3,199.5, 3,200.0, 3,200.5,
3,201.0, 3,202.0, 3,203.0, 3,205.0,
3,210.0, 3,215.0, 3,230.0, 3,260.0,
3,300.0, 3,390.0, 3, 400.0,
MAT#1: -WATER RETENTION DATA
0.25,0.05,0.05,1.25, THET, THTR, VGA, VGN
MAT#1: - CONDUCTIVITY DATA
2.0,1.0,0.05,1.25,0.5, RKMOD, SK, VGA, VGN, EPIT
MAT#2: - WATER RETENTION DATA
0.25,0.05,0.0605,1.25, THET, THTR, VGA, VGN
MAT#2: - CONDUCTIVITY DATA
2.0,30.0,0.0605,1.25,0.5, RKMOD, SK, VGA, VGN, EPIT
MAT#3: - WATER RETENTION DATA
0.25,0.05,0.04,1.2, THET, THTR, VGA, VGN
MAT#3: - CONDUCTIVITY DATA
2.0,1.0,0.04,1.2,0.5, RKMOD, SK, VGA, VGN, EPIT
0, NDAY
1.92E+03,1.54E+03,1.29E+03,8.81E+02, H(1....NPT)
6.17E+02,4.37E+02,3.51E+02,3.86E+02,
4.15E+02,4.16E+02,4.12E+02,4.05E+02,
3.96E+02,3.85E+02,3.74E+02,3.64E+02,
3.53E+02,3.43E+02,3.33E+02,3.24E+02,
3.15E+02,3.06E+02,2.98E+02,2.96E+02,
2.95E+02,2.94E+02,2.93E+02,2.92E+02,
2.92E+02,2.91E+02,2.90E+02,2.86E+02,
2.82E+02,2.75E+02,2.68E+02,2.66E+02,
2.65E+02,2.64E+02,2.63E+02,2.54E+02,
2.36E+02,2.21E+02,2.08E+02,2.04E+02,
2.01E+02,1.99E+02,1.97E+02,1.96E+02,
1.96E+02,1.95E+02,1.94E+02,1.92E+02,

```

```

1.91E+02,1.88E+02,1.84E+02,1.77E+02,
1.71E+02,1.64E+02,1.62E+02,1.61E+02,
1.60E+02,1.60E+02,1.60E+02,1.59E+02,
1.58E+02,1.57E+02,1.56E+02,1.54E+02,
1.49E+02,1.48E+02,1.47E+02,1.47E+02,
1.46E+02,1.46E+02,1.45E+02,1.45E+02,
1.45E+02,1.44E+02,1.44E+02,1.43E+02,
1.40E+02,1.37E+02,1.31E+02,1.21E+02,
1.13E+02,1.13E+02,1.13E+02,
1,1,1,1,01,365,
0.10,
20,
1,0.006, 60,0.0125, 90,0.03, 100,0.04,
120,0.045, 130,0.065, 150,0.07, 165,0.0725,
180,0.075, 195,0.082, 205,0.13, 220,0.145,
260,0.145, 265,0.115, 270,0.095, 285,0.08,
300,0.065, 315,0.0425, 325,0.0115, 360,0.006,
7.0E-01,6.0E-02,1.6E-02,
1,1,1,1,1,1,1,1,1,1,
1,1,1,1,1,1,1,1,1,1,
1,1,1,1,1,1,1,1,1,1,
1,1,1,1,1,1,1,1,366,366,
366,366,366,366,366,366,366,366,366,366,
366,366,366,366,366,366,366,366,366,366,
366,366,366,366,366,366,366,366,366,366,
366,366,366,366,366,366,366,366,366,366,
366,366,366,
2.0E+04,3.0E+03,1.0E+0,
2.0E+04,3.0E+03,1.0E+0,
2.0E+04,3.0E+03,1.0E+0,
0.0,0.52,0.5,0.0,2.7,
0.35,1872.1,6.1,838.4,
SP2011.dat
LEAF,NFROOT,NUPTAK,NFPET,NSOW,NHRVST
BARE
NDLAI
IDLAI,VLAI
AA,B1,B2
NTROOT
HW,HD,HN
HW,HD,HN
HW,HD,HN
PETPC
ALBEDO,ALT,ZU,PMB

```



**ATTACHMENT 2  
SUMMARY DATA**

Table A-1  
3-ft Cover, LAI = 0.145, Run 18

Year	Transpiration (cm)		Evaporation (cm)		Total Runoff (cm)	Total Infiltration (cm)	Total Basal Liq Flux (cm)	Actual Rainfall (cm)	Mass Balance Error (cm)	Liquid Water Flow @ 222.5 cm (cm)	Reported Liquid Water Flow (cm)	Mass Balance Error (%)
	Potential	Actual	Potential	Actual								
1897	30.22	19.68	227.35	16.96	7.88	39.65	0.02	47.52	-0.35	0.02	0.02	0.01
1898	30.71	20.94	230.25	15.14	6.06	32.19	0.02	38.25	-0.31	0.25	0.25	0.01
1899	30.47	13.26	230.43	11.70	4.83	22.56	0.02	27.38	-0.18	0.18	0.18	0.01
1900	31.23	12.53	237.56	12.16	6.42	25.61	0.03	32.03	-0.54	0.06	0.06	0.02
1901	30.91	9.23	233.73	10.91	3.75	18.96	0.03	22.71	-0.11	0.01	0.01	0.00
1902	30.71	13.02	234.17	12.79	7.78	32.02	0.03	39.80	-0.12	-0.01	0.00	0.00
1903	30.77	18.71	231.97	13.24	4.89	26.43	0.03	31.32	-0.83	0.06	0.06	0.03
1904	30.94	12.84	235.87	15.63	9.48	40.33	0.03	49.81	-0.34	0.74	0.74	0.01
1905	30.28	26.12	226.73	29.36	11.29	67.66	7.03	78.94	-0.98	13.66	13.66	0.01
1906	30.86	20.82	233.97	19.42	6.69	40.25	2.84	46.94	-0.68	1.87	1.87	0.01
1907	30.98	21.24	237.58	18.23	6.27	34.37	2.73	40.64	-0.87	2.84	2.84	0.02
1908	30.25	15.12	230.81	14.21	5.00	26.80	1.53	31.80	-0.31	0.07	0.07	0.01
1909	30.74	12.91	232.59	12.60	4.77	24.37	0.79	29.13	-0.32	-0.10	0.00	0.01
1910	32.12	7.95	246.59	9.33	4.91	16.14	0.50	21.06	-0.09	-0.14	0.00	0.00
1911	30.92	20.96	234.68	18.18	9.63	42.80	0.36	52.43	-0.38	-0.14	0.00	0.01
1912	29.68	20.24	224.54	15.05	7.24	32.54	0.27	39.78	-0.44	-0.05	0.00	0.01
1913	29.85	14.67	224.08	16.31	7.39	32.41	0.22	39.80	-0.55	-0.02	0.00	0.01
1914	30.19	22.01	229.85	21.30	10.94	51.04	0.18	61.98	-0.96	-0.05	0.00	0.02
1915	29.79	23.34	223.43	20.85	8.21	43.53	0.68	51.74	-0.61	4.93	4.93	0.01
1916	30.35	22.19	230.80	16.76	7.76	38.26	1.55	46.03	-0.22	0.50	0.50	0.00
1917	30.66	12.30	232.68	11.76	1.57	18.86	0.98	20.42	-0.14	0.42	0.42	0.01
1918	30.16	16.62	226.48	17.29	9.11	38.47	0.71	47.57	-0.69	-0.05	0.00	0.01
1919	29.90	25.08	224.29	19.12	7.70	41.62	0.49	49.33	-0.83	0.09	0.09	0.02
1920	30.15	20.97	228.09	19.10	7.08	38.25	0.38	45.34	-0.21	0.27	0.27	0.00
1921	30.53	9.08	232.93	11.19	4.87	18.83	0.34	23.70	-0.14	0.00	0.00	0.01
1922	30.92	13.69	234.59	15.35	6.41	31.13	0.29	37.54	-0.50	-0.09	0.00	0.01
1923	29.57	22.32	223.54	20.30	8.34	46.50	0.24	54.84	-1.02	-0.08	0.00	0.02
1924	31.28	15.27	234.88	13.47	2.83	21.18	0.20	24.00	-0.17	0.46	0.46	0.01
1925	31.04	17.90	237.26	15.57	8.91	38.36	0.20	47.27	-0.59	0.19	0.19	0.01
1926	30.46	23.22	229.73	21.02	8.13	47.17	0.20	55.30	-0.55	0.47	0.47	0.01
1927	30.86	24.74	236.46	20.61	7.29	46.87	0.24	54.15	-0.76	1.95	1.95	0.01
1928	30.40	24.51	231.49	20.13	9.66	45.05	0.65	54.71	-0.77	1.44	1.44	0.01
1929	30.43	23.00	230.06	18.81	6.36	41.42	1.13	47.78	-0.93	1.55	1.55	0.02
1930	30.47	24.04	229.92	18.90	8.16	44.24	1.30	52.40	-0.74	1.60	1.60	0.01
1931	30.75	27.90	232.42	22.07	8.31	49.02	1.72	57.33	-0.34	1.92	1.92	0.01
1932	30.66	17.78	231.46	15.06	4.97	29.50	1.54	34.47	-0.38	0.23	0.23	0.01
1933	30.86	18.80	234.23	16.70	5.47	33.52	0.85	38.99	-0.32	-0.09	0.00	0.01
1934	32.03	14.26	245.82	13.07	7.83	27.99	0.53	35.81	-0.12	-0.13	0.00	0.00
1935	30.93	18.37	235.59	16.74	8.32	34.91	0.37	43.23	-0.83	-0.10	0.00	0.02
1936	31.38	15.04	238.73	13.93	4.98	26.57	0.28	31.55	-0.22	-0.07	0.00	0.01
1937	31.26	18.30	235.00	14.96	7.35	32.68	0.23	40.03	-0.50	-0.08	0.00	0.01
1938	30.78	17.54	235.17	13.26	8.30	32.65	0.19	40.95	-0.98	-0.09	0.00	0.02
1939	31.01	17.66	234.80	15.15	6.45	30.07	0.16	36.53	-0.19	-0.03	0.00	0.01
1940	30.62	19.32	233.60	18.91	8.96	42.40	0.14	51.36	-0.92	-0.02	0.00	0.02
1941	29.72	25.11	226.10	24.98	7.49	51.21	0.12	58.70	-1.36	0.27	0.27	0.02
1942	30.12	21.71	228.60	16.64	5.93	34.64	0.12	40.56	-0.72	0.94	0.94	0.02
1943	30.87	18.68	234.68	13.74	5.63	29.40	0.16	35.03	-0.73	0.21	0.21	0.02
1944	29.82	18.30	223.75	16.36	7.89	40.65	0.20	48.54	-0.27	0.10	0.10	0.01
1945	30.23	15.74	226.64	12.40	4.80	22.18	0.21	26.98	-0.15	0.66	0.66	0.01
1946	30.70	13.42	231.41	15.69	3.90	27.65	0.24	31.55	-0.13	0.06	0.06	0.00
1947	30.64	7.57	228.85	11.50	2.46	18.06	0.24	20.52	-0.13	-0.06	0.00	0.01
1948	30.95	11.56	230.78	13.26	6.02	28.45	0.22	34.47	-0.30	-0.10	0.00	0.01
1949	29.76	19.60	222.23	16.78	6.24	34.07	0.18	40.31	-1.45	0.26	0.26	0.04
1950	30.76	8.98	235.11	9.48	2.95	15.08	0.17	18.03	-0.11	0.12	0.12	0.01
1951	31.32	5.68	234.58	12.27	2.87	19.66	0.17	22.53	-0.07	-0.03	0.00	0.00
1952	30.35	14.04	227.29	13.41	6.40	26.49	0.16	32.89	-0.13	-0.07	0.00	0.00
1953	30.45	11.83	230.04	10.71	4.31	20.20	0.14	24.51	-0.18	-0.09	0.00	0.01
1954	31.01	15.37	235.68	12.81	7.84	30.56	0.12	38.41	-0.61	-0.09	0.00	0.02
1955	30.20	14.48	228.23	12.24	3.32	24.14	0.11	27.46	-0.13	-0.07	0.00	0.00
1956	30.81	8.30	232.19	9.73	3.23	17.15	0.10	20.37	-0.13	-0.05	0.00	0.01
1957	29.79	16.71	228.29	17.65	5.94	37.52	0.09	43.46	-0.96	-0.06	0.00	0.02
1958	30.27	22.07	227.27	21.03	7.43	45.22	0.08	52.65	-0.99	0.00	0.00	0.02
1959	30.51	17.82	230.89	14.11	4.20	29.73	0.07	33.93	-0.20	0.22	0.22	0.01
1960	30.55	18.16	228.20	14.91	6.55	31.78	0.07	38.33	-0.27	0.15	0.15	0.01
1961	29.52	14.51	224.86	15.49	6.50	31.65	0.07	38.15	-1.06	0.07	0.07	0.03
1962	30.25	19.29	228.90	16.05	5.47	34.01	0.07	39.47	-0.39	0.04	0.04	0.01
1963	30.67	18.84	230.93	14.95	4.90	29.26	0.07	34.16	-0.65	0.08	0.08	0.02
1964	29.68	12.49	219.98	11.94	5.49	25.27	0.07	30.76	-0.15	0.03	0.03	0.00
1965	29.67	18.26	222.88	18.17	5.54	40.63	0.07	46.18	-0.52	-0.02	0.00	0.01
1966	30.02	21.90	224.96	14.87	8.18	35.35	0.07	43.54	-0.40	0.02	0.02	0.01
1967	30.32	16.71	230.35	12.58	8.47	29.86	0.07	38.33	-0.56	0.16	0.16	0.01
1968	29.94	20.09	226.41	15.84	7.50	34.03	0.07	41.53	-0.52	0.18	0.18	0.01
1969	30.75	17.32	230.74	15.15	6.39	30.69	0.07	37.08	-0.36	0.21	0.21	0.01
1970	30.31	14.67	229.62	12.90	4.98	24.67	0.07	29.64	-0.31	0.04	0.04	0.01
1971	30.31	10.18	229.18	13.05	5.65	25.77	0.08	31.42	-0.13	-0.02	0.00	0.00
1972	30.44	20.16	232.26	19.43	9.91	46.91	0.08	56.82	-1.05	0.31	0.31	0.02
1973	30.13	20.82	224.43	15.34	5.34	29.78	0.09	35.13	-0.81	2.01	2.01	0.02
1974	30.84	15.77	233.67	14.08	4.74	29.17	0.21	33.91	-0.38	0.22	0.22	0.01
1975	29.99	19.45	225.22	15.79	8.45	39.18	0.29	47.63	-1.05	0.16	0.16	0.02
1976	30.33	18.09	230.14	14.00	5.37	26.31	0.29	31.67	-0.34	0.47	0.47	0.01
1977	31.08	12.19	234.23	13.11	5.92	24.13	0.30	30.05	-0.18	0.00	0.00	0.01
1978	31.25	14.51	236.10	17.75	7.02	39.89	0.28	46.91	-1.52	-0.09	0.00	0.03
1979	30.75	20.24	232.07	15.09	6.57	28.08	0.24	34.65	-0.71	0.92	0.92	0.02
1980	30.77	9.25	233.41	9.71	4.71	16.60	0.28	21.31	-0.13	0.10	0.10	0.01
1981	30.75	17.14	234.09	14.31	8.51	34.16	0.29	42.67	-0.76	-0.04	0.00	0.02
1982	30.77	13.86	231.78	14.98	4.86	28.32	0.25	33.17	-0.14	0.05	0.05	0.00
1983	30.69	15.40	230.29	19.00	6.65	39.85	0.22	46.51	-0.90	-0.02	0.00	0.02
1984	30.77	20.22	233.17	18.96	6.75	38.36	0.20	45.11	-0.78	0.72	0.72	0.02
1985	30.93	21.52	233.72	19.35	7.39	40.14	0.22	47.52	-0.71	0.67	0.67	0.01
1986	30.91	24.27	236.77	22.46	11.08	54.58	0.29	65.66	-1.48	2.51	2.51	0.02
1987	30.64	21.77	231.32	17.54	5.10	33.03	2.53	38.13	-0.74	3.27	3.27	0.02
1988	30.04	23.28	232.64	20.38	8.70	47.15	1.53	55.86	-0.95	1.47	1.47	0.02
1989	31.23	18.96	240.06	12.28	5.78	25.71	1.56	31.50	-0.63	0.73	0.73	0.02

Table A-2  
3-ft Cover, LAI = 0.29, Run 19

Year	Transpiration (cm)		Evaporation (cm)		Total Runoff (cm)	Total Infiltration (cm)	Total Basal Liq Flux (cm)	Actual Rainfall (cm)	Mass Balance Error (cm)	Liquid Water Flow @ 222.5 cm (cm)	Reported Liquid Water Flow (cm)	Mass Balance Error (%)
	Potential	Actual	Potential	Actual								
1897	42.74	23.94	214.83	15.38	9.29	38.23	0.02	47.52	-0.41	0.02	0.02	0.86%
1898	43.44	20.18	217.52	13.86	6.77	31.48	0.02	38.25	-0.26	0.02	0.02	0.69%
1899	43.10	12.75	217.80	11.13	4.95	22.43	0.02	27.38	-0.19	0.02	0.02	0.68%
1900	44.17	13.00	224.62	11.68	6.64	25.39	0.02	32.03	-0.47	0.00	0.00	1.46%
1901	43.72	9.21	220.92	10.46	3.92	18.79	0.02	22.71	-0.09	-0.02	0.00	0.40%
1902	43.44	14.78	221.44	11.90	8.57	31.24	0.02	39.80	-0.15	-0.03	0.00	0.39%
1903	43.52	18.57	219.22	12.10	5.25	26.07	0.02	31.32	-0.34	-0.03	0.00	1.09%
1904	43.76	13.77	223.05	14.61	9.98	39.83	0.02	49.81	-0.27	-0.01	0.00	0.55%
1905	42.83	31.03	214.18	27.45	12.36	66.58	2.50	78.94	-0.95	10.26	10.26	1.20%
1906	43.64	22.47	221.18	17.58	7.04	39.90	2.07	46.94	-0.42	0.53	0.53	0.90%
1907	43.82	23.03	224.74	17.08	6.78	33.86	1.31	40.64	-0.83	1.40	1.40	2.05%
1908	42.79	14.75	218.27	13.53	5.32	26.48	1.08	31.80	-0.33	-0.02	0.00	1.02%
1909	43.47	12.50	219.85	12.06	5.33	23.81	0.65	29.13	-0.25	-0.12	0.00	0.85%
1910	45.43	8.04	233.28	8.93	5.07	15.99	0.43	21.06	-0.09	-0.14	0.00	0.42%
1911	43.73	23.29	221.86	17.04	10.50	41.93	0.32	52.43	-0.32	-0.14	0.00	0.61%
1912	41.98	20.28	212.24	14.06	7.80	31.97	0.24	39.78	-0.41	-0.12	0.00	1.04%
1913	42.22	14.24	211.70	15.67	7.68	32.13	0.19	39.80	-0.55	-0.10	0.00	1.39%
1914	42.71	25.78	217.33	19.69	11.91	50.07	0.16	61.98	-0.82	-0.10	0.00	1.33%
1915	42.13	26.86	211.08	19.17	8.70	43.04	0.14	51.74	-0.65	1.43	1.43	1.27%
1916	42.92	23.57	218.23	15.09	9.08	36.94	0.20	46.03	-0.24	0.20	0.20	0.53%
1917	43.36	11.26	219.98	10.74	1.73	18.70	0.25	20.42	-0.18	0.02	0.02	0.86%
1918	42.66	17.42	213.98	16.46	9.88	37.70	0.24	47.57	-0.47	-0.06	0.00	0.98%
1919	42.29	26.44	211.90	17.43	9.39	39.94	0.21	49.33	-0.67	-0.09	0.00	1.35%
1920	42.64	20.72	215.59	17.88	7.50	37.84	0.18	45.34	-0.26	-0.08	0.00	0.57%
1921	43.18	8.66	220.28	10.82	4.97	18.73	0.15	23.70	-0.19	-0.08	0.00	0.81%
1922	43.74	13.93	221.77	14.67	7.03	30.51	0.13	37.54	-0.47	-0.09	0.00	1.25%
1923	41.83	26.31	211.28	18.33	9.29	45.55	0.12	54.84	-0.92	-0.09	0.00	1.67%
1924	44.25	13.94	221.92	12.26	3.21	20.80	0.10	24.00	-0.16	-0.07	0.00	0.68%
1925	43.90	20.08	224.40	14.55	9.85	37.42	0.09	47.27	-0.58	-0.05	0.00	1.23%
1926	43.09	24.82	217.10	19.27	9.32	45.97	0.08	55.30	-0.57	0.04	0.04	1.03%
1927	43.66	28.90	223.67	17.90	8.63	45.52	0.07	54.15	-0.64	0.03	0.03	1.19%
1928	43.00	26.74	218.89	17.36	11.30	43.42	0.07	54.71	-0.65	0.13	0.13	1.18%
1929	43.05	26.54	217.45	16.28	7.48	40.30	0.07	47.78	-0.78	0.09	0.09	1.63%
1930	43.10	25.41	217.29	16.82	9.20	43.20	0.07	52.40	-0.67	0.10	0.10	1.27%
1931	43.50	30.43	219.67	19.72	10.03	47.29	0.07	57.33	-0.36	0.16	0.16	0.63%
1932	43.36	15.38	218.76	14.21	5.56	28.90	0.07	34.47	-0.42	0.09	0.09	1.22%
1933	43.65	18.97	221.44	15.90	5.94	33.05	0.07	38.99	-0.32	-0.01	0.00	0.83%
1934	45.30	14.41	232.54	12.50	8.32	27.49	0.07	35.81	-0.09	-0.04	0.00	0.25%
1935	43.75	18.86	222.77	15.77	9.05	34.18	0.07	43.23	-0.83	-0.06	0.00	1.92%
1936	44.39	14.33	225.72	13.29	5.35	26.20	0.07	31.55	-0.25	-0.06	0.00	0.78%
1937	44.21	19.25	222.04	14.30	7.75	32.28	0.06	40.03	-0.54	-0.06	0.00	1.36%
1938	43.53	18.10	222.41	12.56	8.54	32.40	0.06	40.95	-0.93	-0.06	0.00	2.27%
1939	43.86	17.23	221.95	14.34	7.09	29.43	0.06	36.53	-0.19	-0.06	0.00	0.51%
1940	43.31	19.38	220.91	18.02	9.49	41.86	0.05	51.36	-0.65	-0.05	0.00	1.26%
1941	42.04	29.60	213.78	22.66	8.70	50.00	0.05	58.70	-1.16	-0.02	0.00	1.98%
1942	42.60	22.67	216.11	14.93	6.54	34.02	0.04	40.56	-0.69	0.06	0.06	1.71%
1943	43.67	17.44	221.89	12.87	6.23	28.79	0.04	35.03	-0.67	0.04	0.04	1.90%
1944	42.19	20.99	211.39	14.77	9.29	39.25	0.04	48.54	-0.25	0.00	0.00	0.52%
1945	42.76	15.06	214.11	11.08	5.16	21.81	0.04	26.98	-0.17	0.01	0.01	0.62%
1946	43.42	13.10	218.69	15.11	4.01	27.53	0.04	31.55	-0.17	0.02	0.02	0.54%
1947	43.33	7.37	216.15	11.14	2.53	18.00	0.04	20.52	-0.13	-0.01	0.00	0.62%
1948	43.78	11.90	217.95	12.77	6.42	28.05	0.04	34.47	-0.35	-0.03	0.00	1.01%
1949	42.09	21.09	209.90	15.75	6.63	33.68	0.04	40.31	-1.42	0.03	0.03	3.53%
1950	43.51	8.04	222.36	9.11	3.01	15.03	0.04	18.03	-0.10	0.09	0.09	0.57%
1951	44.30	6.23	221.59	11.83	3.00	19.53	0.03	22.53	-0.06	0.02	0.02	0.24%
1952	42.93	14.11	214.71	12.86	6.64	26.26	0.03	32.89	-0.13	-0.01	0.00	0.39%
1953	43.07	11.75	217.42	10.27	4.49	20.03	0.03	24.51	-0.17	-0.03	0.00	0.69%
1954	43.86	17.28	222.83	12.01	8.41	29.99	0.03	38.41	-0.30	-0.04	0.00	0.77%
1955	42.71	13.53	215.72	11.64	3.61	23.85	0.03	27.46	-0.15	-0.04	0.00	0.53%
1956	43.57	7.79	219.42	9.37	3.32	17.05	0.03	20.37	-0.10	-0.04	0.00	0.48%
1957	42.14	19.50	215.94	16.66	6.46	37.00	0.03	43.46	-0.92	-0.05	0.00	2.11%
1958	42.82	24.14	214.72	19.17	8.55	44.11	0.03	52.65	-0.95	-0.05	0.00	1.80%
1959	43.15	16.97	218.25	13.27	4.46	29.47	0.03	33.93	-0.27	-0.04	0.00	0.80%
1960	43.21	18.51	215.54	14.13	6.96	31.37	0.03	38.33	-0.28	-0.03	0.00	0.74%
1961	41.75	14.78	212.63	14.72	6.90	31.25	0.03	38.15	-0.51	-0.02	0.00	1.34%
1962	42.78	19.81	216.37	15.05	5.84	33.63	0.02	39.47	-0.38	-0.02	0.00	0.97%
1963	43.38	18.62	218.22	14.04	5.36	28.80	0.02	34.16	-0.58	-0.02	0.00	1.71%
1964	41.98	12.71	207.68	11.40	5.97	24.79	0.02	30.76	-0.15	-0.02	0.00	0.48%
1965	41.96	19.43	210.58	17.29	5.94	40.24	0.02	46.18	-0.51	-0.02	0.00	1.10%
1966	42.46	24.20	212.52	13.34	9.36	34.17	0.02	43.54	-0.30	-0.03	0.00	0.69%
1967	42.88	14.93	217.79	11.97	8.86	29.46	0.02	38.33	-0.56	-0.02	0.00	1.46%
1968	42.34	21.62	214.00	14.66	8.13	33.40	0.02	41.53	-0.46	-0.02	0.00	1.10%
1969	43.49	16.67	217.99	14.41	6.86	30.23	0.02	37.08	-0.23	0.00	0.00	0.62%
1970	42.87	14.22	217.06	12.34	5.18	24.46	0.02	29.64	-0.30	0.00	0.00	1.01%
1971	42.87	10.59	216.61	12.46	5.90	25.52	0.02	31.42	-0.15	-0.01	0.00	0.48%
1972	43.06	22.86	219.64	17.82	10.69	46.13	0.02	56.82	-0.96	-0.02	0.00	1.69%
1973	42.62	21.98	211.94	14.19	5.95	29.17	0.02	35.13	-0.79	0.44	0.44	2.25%
1974	43.63	16.40	220.89	13.42	4.88	29.03	0.02	33.91	-0.39	0.24	0.24	1.14%
1975	42.43	21.24	212.79	14.65	9.01	38.62	0.02	47.63	-1.15	0.08	0.08	2.42%
1976	42.90	17.03	217.57	13.16	5.82	25.86	0.02	31.67	-0.28	0.13	0.13	0.90%
1977	43.96	11.50	221.35	12.62	6.27	23.78	0.02	30.05	-0.14	0.06	0.06	0.46%
1978	44.20	15.23	223.15	17.06	7.40	39.52	0.02	46.91	-1.45	0.01	0.01	3.09%
1979	43.49	21.08	219.32	14.14	6.98	27.67	0.03	34.65	-0.71	0.36	0.36	2.05%
1980	43.52	8.84	220.66	9.33	4.80	16.51	0.03	21.31	-0.17	0.18	0.18	0.78%
1981	43.49	19.07	221.35	13.50	9.03	33.65	0.03	42.67	-0.76	0.04	0.04	1.79%
1982	43.52	12.86	219.03	14.40	5.24	27.93	0.04	33.17	-0.15	0.01	0.01	0.44%
1983	43.42	17.31	217.56	17.64	6.94	39.57	0.04	46.51	-0.51	-0.01	0.00	1.09%
1984	43.52	20.71	220.42	17.92	7.17	37.95	0.04	45.11	-0.82	0.15	0.15	1.82%
1985	43.74	23.70	220.90	17.69	8.51	39.01	0.04	47.52	-0.71	0.28	0.28	1.50%
1986	43.72	27.64	223.96	20.17	12.50	53.16	0.04	65.66	-1.39	0.17	0.17	2.12%
1987	43.34	23.10	218.62	16.37	5.64	32.49	0.05	38.13	-0.43	1.25	1.25	1.14%
1988	42.50	28.37	220.19	17.81	9.89	45.96	0.07	55.86	-0.58	0.20	0.20	1.04%
1989	44.17	17.85	227.12	11.28	6.15	25.35	0.11	31.50	-0.61	0.19	0.19	1.9



**Table A-3**  
Uncovered Stockpile, No Plants, Run 38

Year	Transpiration (cm)		Evaporation (cm)		Total Runoff (cm)	Total Infiltration (cm)	Total Basal Liq Flux (cm)	Actual Rainfall (cm)	Mass Balance Error (cm)	Liquid Water Flow @ 222.5 cm (cm)	Reported Liquid Water Flow (cm)	Mass Balance Error (%)
	Potential	Actual	Potential	Actual								
1897	0.00	0.00	257.57	30.14	9.71	37.81	0.02	47.52	-0.80	0.44	0.44	1.68%
1898	0.00	0.00	260.97	28.60	6.58	31.68	0.02	38.25	-0.66	3.56	3.56	1.74%
1899	0.00	0.00	260.91	22.44	4.07	23.31	0.19	27.38	-0.52	2.25	2.25	1.91%
1900	0.00	0.00	268.79	22.82	6.03	26.00	1.15	32.03	-0.49	2.39	2.39	1.54%
1901	0.00	0.00	264.64	20.26	2.38	20.33	2.23	22.71	-0.22	1.80	1.80	0.97%
1902	0.00	0.00	264.88	23.60	8.94	30.86	1.72	39.80	-0.59	3.21	3.21	1.49%
1903	0.00	0.00	262.74	25.19	5.39	25.93	3.98	31.32	-0.51	4.40	4.40	1.64%
1904	0.00	0.00	266.81	25.81	11.93	37.88	7.39	49.81	-0.31	9.61	9.61	0.61%
1905	0.00	0.00	257.01	50.18	16.50	62.44	14.06	78.94	-1.86	13.35	13.35	2.35%
1906	0.00	0.00	264.83	33.28	8.07	38.87	6.93	46.94	-0.93	5.75	5.75	1.97%
1907	0.00	0.00	268.56	32.68	5.87	34.77	7.41	40.64	-0.80	7.13	7.13	1.96%
1908	0.00	0.00	261.06	25.57	4.97	26.83	3.94	31.80	-0.31	2.73	2.73	0.98%
1909	0.00	0.00	263.32	24.17	3.87	25.27	2.30	29.13	-0.62	1.55	1.55	2.14%
1910	0.00	0.00	278.70	18.21	3.02	18.04	1.72	21.06	-0.30	1.33	1.33	1.44%
1911	0.00	0.00	265.59	35.10	10.77	41.65	1.43	52.43	-0.50	3.87	3.87	0.95%
1912	0.00	0.00	254.22	28.64	7.75	32.02	4.65	39.78	-0.56	4.85	4.85	1.41%
1913	0.00	0.00	253.93	29.67	6.85	32.95	4.01	39.80	-0.67	2.50	2.50	1.69%
1914	0.00	0.00	260.04	38.13	12.69	49.28	5.05	61.98	-1.06	7.91	7.91	1.72%
1915	0.00	0.00	253.22	35.64	10.35	41.40	10.71	51.74	-0.48	10.12	10.12	0.93%
1916	0.00	0.00	261.15	31.18	10.24	35.78	5.93	46.03	-0.52	6.15	6.15	1.12%
1917	0.00	0.00	263.34	19.36	1.67	18.75	5.53	20.42	-0.22	2.88	2.88	1.07%
1918	0.00	0.00	256.64	32.61	8.91	38.67	2.06	47.57	-0.69	2.07	2.07	1.44%
1919	0.00	0.00	254.20	36.08	8.95	40.38	4.77	49.33	-0.86	6.90	6.90	1.75%
1920	0.00	0.00	258.23	35.37	7.24	38.10	4.88	45.34	-0.62	3.58	3.58	1.36%
1921	0.00	0.00	263.46	19.95	3.65	20.05	3.18	23.70	-0.23	1.92	1.92	0.98%
1922	0.00	0.00	265.51	28.42	6.21	31.33	1.78	37.54	-0.44	1.24	1.24	1.18%
1923	0.00	0.00	253.11	37.00	10.70	44.14	2.72	54.84	-0.95	6.41	6.41	1.74%
1924	0.00	0.00	266.17	23.08	2.02	21.99	5.80	24.00	-0.49	3.28	3.28	2.03%
1925	0.00	0.00	268.30	28.55	9.77	37.50	5.03	47.27	-0.62	7.41	7.41	1.32%
1926	0.00	0.00	260.19	37.66	10.42	44.88	5.74	55.30	-0.71	6.05	6.05	1.29%
1927	0.00	0.00	267.32	35.98	9.92	44.23	10.93	54.15	-1.17	10.83	10.83	2.17%
1928	0.00	0.00	261.89	35.77	12.14	42.57	7.18	54.71	-0.85	7.78	7.78	1.55%
1929	0.00	0.00	260.49	32.13	8.89	38.89	8.56	47.78	-0.73	7.85	7.85	1.53%
1930	0.00	0.00	260.39	33.58	10.93	41.47	8.67	52.40	-0.75	8.55	8.55	1.43%
1931	0.00	0.00	263.17	39.88	11.11	46.22	7.56	57.33	-1.06	7.46	7.46	1.85%
1932	0.00	0.00	262.12	27.77	4.77	29.70	4.91	34.47	-0.59	2.87	2.87	1.73%
1933	0.00	0.00	265.09	32.10	5.15	33.84	2.79	38.99	-0.73	2.69	2.69	1.88%
1934	0.00	0.00	277.85	24.89	7.36	28.45	2.78	35.81	-0.31	3.35	3.35	0.87%
1935	0.00	0.00	266.52	31.92	7.73	35.50	3.55	43.23	-0.60	3.63	3.63	1.39%
1936	0.00	0.00	270.11	26.33	4.10	27.45	3.81	31.55	-0.56	3.20	3.20	1.76%
1937	0.00	0.00	266.25	29.81	6.98	33.05	2.67	40.03	-0.84	3.38	3.38	2.10%
1938	0.00	0.00	265.95	26.29	8.53	32.42	4.37	40.95	-0.54	5.76	5.76	1.31%
1939	0.00	0.00	265.81	28.30	6.30	30.23	5.09	36.53	-0.55	3.12	3.12	1.49%
1940	0.00	0.00	264.22	36.14	9.44	41.92	3.20	51.36	-0.92	3.94	3.94	1.78%
1941	0.00	0.00	255.83	42.82	9.58	49.12	7.11	58.70	-1.15	8.84	8.84	1.96%
1942	0.00	0.00	258.72	30.12	7.24	33.32	6.26	40.56	-0.73	5.10	5.10	1.80%
1943	0.00	0.00	265.56	26.19	5.58	29.44	4.98	35.03	-0.69	4.83	4.83	1.97%
1944	0.00	0.00	253.57	29.71	10.53	38.01	5.96	48.54	-0.72	7.14	7.14	1.47%
1945	0.00	0.00	256.87	22.16	4.67	22.31	5.67	26.98	-0.33	2.96	2.96	1.24%
1946	0.00	0.00	262.11	27.70	3.05	28.50	2.40	31.55	-0.72	1.79	1.79	2.29%
1947	0.00	0.00	259.49	18.50	2.20	18.32	1.79	20.52	-0.16	1.29	1.29	0.77%
1948	0.00	0.00	261.73	24.35	6.07	28.40	1.37	34.47	-0.53	1.14	1.14	1.52%
1949	0.00	0.00	251.99	30.12	6.93	33.38	2.53	40.31	-0.84	5.49	5.49	2.09%
1950	0.00	0.00	265.87	16.84	2.01	16.02	4.04	18.03	-0.25	1.93	1.93	1.39%
1951	0.00	0.00	265.90	19.29	2.31	20.22	1.76	22.53	-0.28	0.77	0.77	1.24%
1952	0.00	0.00	257.64	25.02	5.94	26.96	1.12	32.89	-0.34	0.93	0.93	1.02%
1953	0.00	0.00	260.49	20.47	3.94	20.57	1.11	24.51	-0.40	1.73	1.73	1.62%
1954	0.00	0.00	266.68	25.29	8.10	30.31	1.46	38.41	-0.68	3.56	3.56	1.77%
1955	0.00	0.00	258.43	22.99	3.43	24.03	3.68	27.46	-0.49	2.82	2.82	1.80%
1956	0.00	0.00	262.99	17.71	2.39	17.98	2.47	20.37	-0.40	1.52	1.52	1.98%
1957	0.00	0.00	258.08	31.10	7.51	35.95	1.67	43.46	-0.62	3.24	3.24	1.43%
1958	0.00	0.00	257.54	37.84	8.99	43.66	4.06	52.65	-0.94	5.93	5.93	1.79%
1959	0.00	0.00	261.40	25.50	4.66	29.28	5.69	33.93	-0.56	4.29	4.29	1.66%
1960	0.00	0.00	258.75	27.48	7.65	30.68	4.24	38.33	-0.54	4.16	4.16	1.41%
1961	0.00	0.00	254.38	28.72	6.19	31.96	3.70	38.15	-0.84	2.75	2.75	2.19%
1962	0.00	0.00	259.15	29.32	6.36	33.11	3.67	39.47	-0.66	4.88	4.88	1.68%
1963	0.00	0.00	261.60	28.26	4.84	29.32	4.36	34.16	-0.72	3.58	3.58	2.11%
1964	0.00	0.00	249.66	22.90	5.47	25.29	3.12	30.76	-0.64	2.94	2.94	2.08%
1965	0.00	0.00	252.54	33.06	7.09	39.09	3.15	46.18	-1.05	3.88	3.88	2.28%
1966	0.00	0.00	254.97	28.52	9.70	33.84	6.89	43.54	-0.75	8.32	8.32	1.73%
1967	0.00	0.00	260.67	24.21	8.11	30.22	5.58	38.33	-0.60	4.53	4.53	1.56%
1968	0.00	0.00	256.35	29.28	8.15	33.38	6.17	41.53	-0.56	6.80	6.80	1.36%
1969	0.00	0.00	261.48	28.75	5.70	31.39	4.72	37.08	-0.60	3.27	3.27	1.62%
1970	0.00	0.00	259.92	24.70	4.11	25.53	3.26	29.64	-0.51	2.53	2.53	1.71%
1971	0.00	0.00	259.48	23.76	5.64	25.78	2.37	31.42	-0.52	1.67	1.67	1.66%
1972	0.00	0.00	262.70	34.14	12.22	44.60	5.87	56.82	-1.02	10.02	10.02	1.80%
1973	0.00	0.00	254.57	26.65	6.36	28.77	7.38	35.13	-0.63	5.51	5.51	1.80%
1974	0.00	0.00	264.52	25.72	5.56	28.35	3.85	33.91	-0.52	2.34	2.34	1.52%
1975	0.00	0.00	255.21	28.88	9.75	37.87	6.08	47.63	-0.74	8.55	8.55	1.55%
1976	0.00	0.00	260.47	26.49	4.68	27.00	5.19	31.67	-0.40	2.67	2.67	1.28%
1977	0.00	0.00	265.31	24.00	4.52	25.53	2.43	30.05	-0.41	1.89	1.89	1.38%
1978	0.00	0.00	267.35	32.69	7.94	38.98	1.95	46.91	-1.17	1.89	1.89	2.50%
1979	0.00	0.00	262.81	27.62	6.38	28.27	4.52	34.65	-0.48	6.36	6.36	1.39%
1980	0.00	0.00	264.18	18.88	3.08	18.24	3.64	21.31	-0.41	1.89	1.89	1.91%
1981	0.00	0.00	264.84	26.85	9.06	33.61	2.36	42.67	-0.57	4.53	4.53	1.34%
1982	0.00	0.00	262.55	26.94	4.54	28.63	4.22	33.17	-0.40	2.29	2.29	1.20%
1983	0.00	0.00	260.98	31.92	8.06	38.44	2.54	46.51	-0.80	5.38	5.38	1.72%
1984	0.00	0.00	263.94	33.72	6.95	38.16	5.83	45.11	-1.00	3.85	3.85	2.22%
1985	0.00	0.00	264.64	34.72	8.96	38.57	5.04	47.52	-1.06	7.07	7.07	2.23%
1986	0.00	0.00	267.69	38.89	14.64	51.02	9.77	65.66	-0.99	11.07	11.07	1.50%
1987	0.00	0.00	261.96	29.30	5.87	32.26	8.48	38.13	-0.58	6.14	6.14	1.53%
1988	0.00	0.00	262.68	36.32	11.92	43.93	7.96	55.86	-0.75	8.90	8.90	1.34%
1989	0.00	0.00	271.28	23.85	5.11	26.38	5.24	31.50	-0.78	3.70	3.70	2.48%
1990	0.00	0.00	263.40	33.90	5.26	37.52	3.46	42.77	-0.71	2.61	2.61	1.67%
1991	0.00											

## Run 37, LAI=0.29

Year	Transpiration (cm)		Evaporation (cm)		Total Runoff (cm)	Total Infiltration (cm)	Total Basal Liq Flux (cm)	Actual Rainfall (cm)	Mass Balance Error (cm)	Liquid Water Flow @ 222.5 cm (cm)	Reported Liquid Water Flow (cm)	Mass Balance Error (%)
	Potential	Actual	Potential	Actual								
2006	0.00	0.00	55.45	10.35	1.95	20.79	6.42	22.73	-0.40	10.16	10.16	1.76%
2007	0.00	0.00	179.31	21.45	4.28	31.89	8.40	36.17	-0.13	8.11	8.11	0.37%
2008	10.54	9.32	178.16	16.59	7.16	32.97	10.51	40.13	-0.26	9.78	9.78	0.65%
2009	10.77	9.23	179.45	11.76	1.76	20.08	4.45	21.84	-0.11	1.53	1.53	0.53%
2010	20.62	16.98	158.24	15.63	4.71	36.49	3.50	41.20	-0.61	5.16	5.16	1.48%
2011	21.69	6.55	162.51	5.01	0.05	5.15	2.48	5.21	-0.01	0.66	0.66	0.27%
<b>Average</b>	<b>10.60</b>	<b>7.01</b>	<b>152.19</b>	<b>13.47</b>	<b>3.32</b>	<b>24.56</b>	<b>5.96</b>	<b>27.88</b>	<b>-0.26</b>	<b>5.90</b>	<b>5.90</b>	<b>0.84%</b>

## Run 39, 0.145 LAI

Year	Transpiration (cm)		Evaporation (cm)		Total Runoff (cm)	Total Infiltration (cm)	Total Basal Liq Flux (cm)	Actual Rainfall (cm)	Mass Balance Error (cm)	Liquid Water Flow @ 222.5 cm (cm)	Reported Liquid Water Flow (cm)	Mass Balance Error (%)
	Potential	Actual	Potential	Actual								
2006	0.00	0.00	55.45	11.87	2.30	20.43	4.92	22.73	-0.71	8.63	8.63	3.11%
2007	0.00	0.00	179.31	24.38	4.23	36.13	10.69	40.36	-0.83	10.50	10.50	2.05%
2008	10.54	9.55	178.16	18.03	6.19	33.34	10.02	39.52	-0.76	9.20	9.20	1.91%
2009	10.77	9.62	179.45	12.90	2.69	21.67	4.26	24.36	-0.40	1.33	1.33	1.65%
2010	20.62	17.24	158.24	17.32	6.22	37.62	2.77	43.84	-0.73	4.63	4.63	1.67%
2011	21.69	11.85	162.51	7.96	2.58	14.08	2.61	16.66	-0.39	0.62	0.62	2.32%
<b>Average</b>	<b>10.60</b>	<b>8.04</b>	<b>152.19</b>	<b>15.41</b>	<b>4.04</b>	<b>27.21</b>	<b>5.88</b>	<b>31.25</b>	<b>-0.63</b>	<b>5.82</b>	<b>5.82</b>	<b>2.12%</b>

## Run 40, No Plants

Year	Transpiration (cm)		Evaporation (cm)		Total Runoff (cm)	Total Infiltration (cm)	Total Basal Liq Flux (cm)	Actual Rainfall (cm)	Mass Balance Error (cm)	Liquid Water Flow @ 222.5 cm (cm)	Reported Liquid Water Flow (cm)	Mass Balance Error (%)
	Potential	Actual	Potential	Actual								
2006	0.00	0.00	55.45	10.35	1.95	20.79	6.42	22.73	-0.40	10.16	10.16	1.76%
2007	0.00	0.00	179.31	21.45	4.28	31.89	8.40	36.17	-0.13	8.11	8.11	0.37%
2008	0.00	0.00	188.70	19.74	7.03	33.10	15.88	40.13	-0.41	15.35	15.35	1.03%
2009	0.00	0.00	190.22	16.57	1.15	20.69	5.13	21.84	-0.07	3.70	3.70	0.31%
2010	0.00	0.00	178.86	21.90	3.86	37.34	16.65	41.20	-0.65	18.33	18.33	1.57%
2011	0.00	0.00	184.20	7.57	0.00	5.21	4.37	5.21	-0.02	1.37	1.37	0.43%
<b>Average</b>	<b>0.00</b>	<b>0.00</b>	<b>162.79</b>	<b>16.26</b>	<b>3.04</b>	<b>24.84</b>	<b>9.47</b>	<b>27.88</b>	<b>-0.28</b>	<b>9.50</b>	<b>9.50</b>	<b>0.91%</b>

**Table A-5  
4-ft Cover**

**Run 294, 0.145 LAI**

Year	Transpiration (cm)		Evaporation (cm)		Total Runoff (cm)	Total Infiltration (cm)	Total Basal Liq Flux (cm)	Actual Rainfall (cm)	Mass Balance Error (cm)	Liquid Water Flow @ 222.5 cm (cm)	Reported Liquid Water Flow (cm)	Mass Balance Error (%)
	Potential	Actual	Potential	Actual								
<b>2006</b>	0.00	0.00	55.45	11.10	2.36	20.37	4.81	22.73	-0.66	9.35	9.35	2.91%
<b>2007</b>	0.00	0.00	179.31	23.12	4.24	36.12	11.75	40.36	-0.81	11.85	11.85	2.01%
<b>2008</b>	10.54	9.65	178.16	17.43	6.05	33.47	10.79	39.52	-0.73	9.62	9.62	1.86%
<b>2009</b>	10.77	9.72	179.45	12.87	2.62	21.74	4.12	24.36	-0.28	1.16	1.16	1.15%
<b>2010</b>	20.62	17.58	158.24	16.80	6.21	37.63	2.95	43.84	-0.74	4.92	4.92	1.69%
<b>2011</b>	21.69	12.80	162.51	8.07	2.52	14.14	2.52	16.66	-0.40	0.33	0.33	2.38%
<b>Average</b>	<b>10.60</b>	<b>8.29</b>	<b>152.19</b>	<b>14.90</b>	<b>4.00</b>	<b>27.25</b>	<b>6.16</b>	<b>31.25</b>	<b>-0.60</b>	<b>6.21</b>	<b>6.21</b>	<b>2.00%</b>

**Table A-6  
2-ft Cover**

**Run 179, 0.145 LAI**

Year	Transpiration (cm)		Evaporation (cm)		Total Runoff (cm)	Total Infiltration (cm)	Total Basal Liq Flux (cm)	Actual Rainfall (cm)	Mass Balance Error (cm)	Liquid Water Flow @ 222.5 cm (cm)	Reported Liquid Water Flow (cm)	Mass Balance Error (%)
	Potential	Actual	Potential	Actual								
<b>2006</b>	0.00	0.00	55.45	11.42	1.96	20.77	1.03	22.73	-0.50	7.64	7.64	2.19%
<b>2007</b>	0.00	0.00	179.31	23.01	4.34	31.83	7.52	36.17	-0.13	6.57	6.57	0.37%
<b>2008</b>	10.54	8.60	178.16	17.93	7.37	32.76	8.88	40.13	-0.34	8.91	8.91	0.84%
<b>2009</b>	10.77	8.20	179.45	12.27	2.18	19.66	4.76	21.84	-0.11	1.86	1.86	0.51%
<b>2010</b>	20.62	16.21	158.24	16.42	4.71	36.49	3.32	41.20	-0.64	4.86	4.86	1.56%
<b>2011</b>	21.69	5.15	162.51	4.90	0.05	5.15	2.66	5.21	-0.01	0.89	0.89	0.28%
<b>Average</b>	<b>10.60</b>	<b>6.36</b>	<b>152.19</b>	<b>14.32</b>	<b>3.44</b>	<b>24.44</b>	<b>4.70</b>	<b>27.88</b>	<b>-0.29</b>	<b>5.12</b>	<b>5.12</b>	<b>0.96%</b>

## **Appendix C**

# **Updated Groundwater Flow Modeling**





## Table of Contents

<b>Section</b>	<b>Page</b>
Appendix C. Tyrone Groundwater Flow Model Update .....	C-1
C.1 Introduction.....	C-1
C.2 Background .....	C-2
C.3 Conceptual Model of Groundwater Flow .....	C-4
C.4 Model Development and Calibration .....	C-6
C.4.1 Overview of Simulation Approach.....	C-7
C.4.2 Model Code Selection.....	C-7
C.4.3 Model Domain and Grid .....	C-8
C.4.4 Boundary Conditions.....	C-9
C.4.5 Model Input Parameters.....	C-13
C.4.6 Model Calibration .....	C-20
C.4.7 Sensitivity Analysis .....	C-24
C.5 Predictive Simulation .....	C-24
C.6 Summary and Conclusions.....	C-25
References.....	C-25

## List of Tables

<b>Table</b>	<b>Page</b>
C-1 Groundwater Recharge .....	C-18
C-2 Historical Groundwater Pumping .....	C-19
C-3 Simulated Mass Balance for Steady-State (Predevelopment) Model.....	C-21
C-4 Simulated 2010 Mass Balance for Historical Transient Model.....	C-23



## List of Figures

### Figure

- C-1 Tyrone Mine Location Map
- C-2 Mine Facilities and Significant Geographic Features
- C-3 Approximate Surface Geologic Contacts Between Major Rock Types at Tyrone
- C-4 Plan View of Active Model Grid
- C-5 Vertical Profile of Model Grid from Southwest to Northeast Along Model Row 50 Through the Main Pit
- C-6 Boundary Conditions in Model Layer 1
- C-7 Boundary Conditions in Model Layer 2
- C-8 Boundary Conditions in Model Layer 3
- C-9 Boundary Conditions in Model Layer 4
- C-10 Observed Water Levels at Well 10 near Northwest Model Boundary
- C-11 Hydraulic Conductivity in Model Layer 1
- C-12 Hydraulic Conductivity in Model Layer 2
- C-13 Hydraulic Conductivity in Model Layer 3
- C-14 Hydraulic Conductivity in Model Layer 4
- C-15 Storage in Model Layer 1
- C-16 Storage in Model Layer 2
- C-17 Storage in Model Layer 3
- C-18 Storage in Model Layer 4
- C-19 Simulated Steady-State Recharge
- C-20 Simulated Post-Development Groundwater Recharge
- C-21 Simulated Steady-State Water Table
- C-22 Simulated vs. Observed Hydraulic Heads for Steady-State Model



## **List of Figures (Continued)**

### **Figure**

- C-23 Simulated 2010 Water Table
- C-24 Simulated vs. Observed 2005 Hydraulic Heads
- C-25 Observation Wells with Hydrographs Used for Model Calibration
- C-26 Simulated Historical Groundwater Discharge to the Gettysburg Pit
- C-27 Simulated Historical Groundwater Discharge to the Main Pit

## **List of Attachments**

### **Attachment**

- C-1 Simulated and Observed Historical Water Levels



## **Appendix C. Tyrone Groundwater Flow Model Update**

### **C.1 Introduction**

The purpose of this appendix is to document the most recent version of the Tyrone groundwater flow model developed as part of the Stage 2 Abatement Plan Proposal (APP) modeling process. The initial version of the Tyrone groundwater flow model was developed in 1999 (DBS&A, 1999a) to:

- Estimate the post-closure recovery period of water levels in the mine pits and surrounding aquifers and project the post-closure steady-state pit lake(s) surface elevation(s).
- Examine the potential for pit lake outflows.
- Evaluate the potential interactions of pit lake(s) with other mine facilities, hydrologic features, and geologic structures.
- Provide supporting groundwater flow information for a pit lake water quality study.

The model focused primarily on the regional groundwater flow system in the Mine/Stockpile APP Study Area, although portions of the Mangas Valley and Oak Grove Wash/Brick Kiln Gulch APP Study Areas are also included within the model boundaries. The original model was based on the 1998 mine configuration and was used to simulate both current and future groundwater conditions. Predictive model simulations are documented in a pit lake formation modeling report (DBS&A, 1999b), and a detailed model sensitivity analysis and verification study was provided in March 2002 (DBS&A, 2002a).

The original groundwater flow model was substantially updated as part of Condition 83 of DP-1341 (DBS&A, 2007b). The purpose of the updated model was to:

- Estimate the post-closure recovery period of water levels in the mine pits and surrounding aquifer, and evaluate the potential for pit lake outflows in the future.



- Serve as a simulation tool to assist with the evaluation of potential closure alternatives, such as interceptor well pumping or partial backfill of certain open pits.

The Tyrone groundwater flow model documented in the DP-1341 Condition 83 report (DBS&A, 2007b) is the model that was updated for the Stage 2 APP. The purpose of the model update was to (1) include additional faults in the model that are believed to affect groundwater flow but were not included in the previous version of the model (e.g., the Townsite and West Main Faults), (2) extend the historical simulation period in the model from 2005 to 2010, and (3) develop a better representation of some other features in the Mine/Stockpile APP Study Area, such as observed water levels on the south side of the mine.

Applicable background reports and previous groundwater modeling efforts are briefly summarized in Section C.2. More detail regarding these issues can be found in the Condition 83 report (DBS&A, 2007b) and other referenced reports. Section C.3 provides an overview of the hydrogeologic conceptual model of groundwater flow at Tyrone, while Section C.4 presents the model development and calibration results for the updated model. Sections C.5 and C.6 summarize the predictive simulation approach and key points and conclusions, respectively.

## **C.2 Background**

The Tyrone Mine is an open-pit copper mine located just off State Highway 90 approximately 10 miles southwest of Silver City in Grant County, New Mexico (Figure C-1). The general layout of the existing mining facilities at Tyrone is shown in Figure C-2. Previous reports that discuss groundwater conditions at Tyrone in detail include the following:

- *Preliminary Site-Wide Groundwater Study, Tyrone Mine Closure/Closeout (PGWS)* (DBS&A, 1997a)
- *Supplemental Groundwater Study, Tyrone Closure/Closeout (SGWS)* (DBS&A, 1997b).
- *Completion Report for DP-1341 Condition 82, Tyrone Mine Facility, Supplemental Groundwater Study* (DBS&A, 2007a)



- *Stage 1 Abatement Plan Proposal, Tyrone Mine Facility* (DBS&A, 2004)
- *Addendum to the Tyrone Mine Facility Stage 1 Abatement Plan Proposal* (DBS&A, 2006)
- *Tyrone Mine Facility Stage 1 Abatement Plan, Final Report* (DBS&A, 2011)

Beginning with the PGWS (DBS&A, 1997a), groundwater has been recognized to generally occur within one of three distinct but related hydrostratigraphic units at Tyrone: intrusive igneous rocks (Precambrian granite and Tertiary quartz monzonite), Tertiary/Quaternary Gila Conglomerate, and Quaternary alluvium, as described below.

- The primary intrusive igneous rocks at Tyrone are Precambrian granite and Tertiary quartz monzonite, which occur mainly in the Mine/Stockpile APP Study Area. Groundwater flow within these rocks is governed by secondary permeability (joints, fractures, and faults).
- The Tertiary/Quaternary Gila Conglomerate is an unconsolidated to semi-consolidated sedimentary deposit present in the Mangas Valley APP Study Area, in the Oak Grove Wash/Brick Kiln Gulch APP Study Area, and along the northeastern portion of the Mine/Stockpile APP Study Area. The contacts between the igneous rocks and the Gila Conglomerate are illustrated in Figure C-3.
- The Quaternary alluvium is also present within all three Tyrone Mine APP study areas and may contain perched water (e.g., Deadman Canyon and Oak Grove Wash) or regional groundwater (e.g., Mangas Valley).

Prior reports directly related to Tyrone groundwater flow model development include:

- *Tyrone Pit Lake Formation Modeling Report* (DBS&A, 1999a)
- *Tyrone Mine Pit Lake Formation Model Sensitivity Analysis and Verification Study* (DBS&A, 2002a)



- *Completion Report for DP-1341 Condition 83, Tyrone Mine Facility Groundwater Model* (DBS&A, 2007b)

The groundwater model documented in DBS&A's Condition 83 report (2007b) is the one that was updated as part of this Stage 2 APP submittal. Additional detail on the hydrogeology of Tyrone or the previous modeling efforts can be found in the above reports.

### **C.3 Conceptual Model of Groundwater Flow**

A conceptual model of groundwater flow is a representation or interpretation of how groundwater flow occurs within the region of interest and how flow is affected by various sources of recharge and discharge, as well as by physical properties of the aquifer such as hydraulic conductivity and faults. The overall conceptual model of groundwater flow at Tyrone is similar to that applied during the previous modeling studies. Although new information from additional monitor wells and aquifer tests has served to fill certain data gaps, and in some cases clarify groundwater flow regimes (e.g., perched water versus regional water), the basic conceptual model of groundwater flow and occurrence at Tyrone remains unchanged. An overview of the conceptual model of groundwater flow at Tyrone based on previous and current studies is provided below. DBS&A (1997c), the supplemental materials characterization study, provides a summary timeline for open-pit mining activities from 1968 through 1995.

The primary water-bearing units at the Tyrone Mine include the Precambrian Burro Mountain granite, the Tertiary quartz monzonite, the Gila Conglomerate, and the Quaternary alluvium. Maps provided in the SGWS show the distribution of these geologic units within the study area. The Quaternary alluvium occurs along surface drainages and lies above regional groundwater at most locations around Tyrone, with the exception of the Mangas Valley. The alluvium along most parts of the major axis of the Mangas Valley contains regional groundwater; these high-permeability sediments have a significant influence on groundwater flow in the area downgradient from the No. 3A leach stockpile. On Figure C-3, surface contacts are delineated for the intrusive igneous rocks (i.e., granite and quartz monzonite) and the Gila Conglomerate. Regional groundwater occurs within the igneous rocks throughout most of the Mine/Stockpile APP Study Area. The granite and quartz monzonite are lumped as a single hydrostratigraphic



unit in the conceptual hydrogeologic model because hydraulic properties for both rock types are governed by secondary porosity, such as fractures and fracture zones.

Plate 5-1 of the Stage 2 APP report shows regional aquifer water levels in the Mine/Stockpile APP Study Area for 2010. The interpreted contours of hydraulic head indicate a complex groundwater flow system in the vicinity of the Tyrone Mine. Groundwater beneath much of Tyrone flows to the Main or Gettysburg Pits, where it is extracted. Groundwater is also extracted at the Copper Mountain Pit. Groundwater not captured at one of the pits flows either to the northwest beneath the Mangas Valley within the Gila–San Francisco underground basin or to the southeast beneath Oak Grove Wash within the Mimbres underground basin.

Although mining has induced significant hydrologic changes in the past 30 to 50 years, a comparison of historical water level maps indicates that these primary characteristics of regional groundwater flow have been relatively consistent since about the mid-1990s. The PGWS (DBS&A, 1997a) presents maps of regional groundwater level elevations through time for the Mine/Stockpile APP Study Area. These maps indicate the existence of a cone of depression in the area of the Main Pit, most likely attributable to pumping from the Burro Chief Shaft, as early as 1982. A discernable cone of depression is evident around the Main and Gettysburg Pits by 1990.

Sources of recharge to the regional aquifer include groundwater inflow along upgradient boundaries, recharge from precipitation, downward seepage from perched water zones and drainages, and seepage from various mine facilities such as stockpiles and tailing ponds. Underflow into the study area comes primarily from the Big Burro Mountains to the southwest.

Areal recharge is likely greater within the disturbed region of the mine than it was under pre-mining conditions due to the removal of vegetation and the construction of leach and waste rock piles, which generally form permeable surfaces for infiltration and have berms along their top surfaces that contain storm water to prevent runoff. Beneath waste rock piles, impacted meteoric water that has infiltrated through the pile may infiltrate all the way to regional groundwater. Beneath leach stockpiles, some meteoric water and pregnant leach solution (PLS) may infiltrate to groundwater. Recharge rates applied in the groundwater model are





assumed to be representative of any fluids (precipitation, PLS, or a mixture of both) that infiltrate to the water table.

Discharge from the regional aquifer occurs as (1) extraction of groundwater from mine pits (due to the combined effects of pit dewatering systems and evaporation from open water surfaces), (2) pumping from water supply wells and remediation pumpback systems, (3) discharge to springs and seeps, and (4) groundwater outflow. Pumping systems that extract regional groundwater are currently operating in the Main, Gettysburg, and Copper Mountain Pits, at several locations around the No. 3A leach stockpile, and at the northern end of the reclaimed No. 1X tailing. The Fortuna No. 2 well, a supply well screened within the Gila Conglomerate, also extracts water from the regional aquifer. Groundwater in the study area not intercepted at mine pits or pumping wells flows downgradient into the Gila–San Francisco underground basin to the northwest or into the Mimbres underground basin to the southeast. There are no known discharges of regional groundwater to springs and seeps within the study area, other than those that occur within mine pits. Other springs and seeps that occur within the study area, such as at the entrance to the Deadman Canyon narrows and McCain Spring, are discharge points for shallow perched water.

A number of the faults illustrated in Plate 5-1 and Figure C-3 have a significant influence on groundwater flow. For example, water level discontinuities up to several hundred feet occur across portions of the Southern Star and Sprouse-Copeland Faults. These faults behave as barriers to horizontal groundwater flow or as zones of very low hydraulic conductivity, with the majority of groundwater flowing parallel to the trace of the fault. It is possible that faults may act as barriers to groundwater flow along part of their trace, but may be a less effective barrier to flow in other areas. In general, fault hydraulics are affected by numerous fracture properties that can vary markedly along the strike of the fault (CFCFF, 1996).

#### **C.4 Model Development and Calibration**

This section presents information on the development of the updated Tyrone groundwater flow model, including an overview of the simulation approach, the approach to and results of model calibration, and the results of previous model sensitivity analyses.



### **C.4.1 Overview of Simulation Approach**

The Tyrone groundwater flow model consists of three basic periods. The predevelopment or steady-state period is based on water level data and other information provided by Trauger (1972), as well as various mine records and reports on historical operations (e.g., DBS&A, 1997c). The steady-state model period is prior to open-pit mining that reached the water table, and is also prior to any known significant groundwater stresses in the vicinity of the mine area, such as significant groundwater pumping. The second simulation period is the historical transient simulation period, a 61-year period that runs from 1950 to 2010. This transient simulation period is subdivided into four separate periods in order to account for the deepening of the Main Pit through time into different model layers (discussed more completely in Section C.4.4.5). The final simulation period is the predictive simulation period, which runs from 2010 to 2060. Model runs are conducted using the output from the steady-state model as initial conditions for the historical transient model and output from the historical transient model as of 2010 as initial conditions for the predictive simulations. The updated model calibration was conducted for both the steady-state and historical transient simulation periods.

### **C.4.2 Model Code Selection**

DBS&A selected a variation of the USGS code MODFLOW (Harbaugh and McDonald, 1996) for simulation of groundwater flow at the Tyrone Mine. The U.S. Environmental Protection Agency (EPA) (U.S. EPA, 1995) summarizes the MODFLOW code as follows:

MODFLOW is a numerical model that uses a (block-centered) finite-difference solution to solve the governing equations for groundwater flow. It can be used to create two-dimensional areal or vertical models as well as quasi-three-dimensional or full three-dimensional flow, anisotropic and layered aquifer conditions. Layers can be simulated as confined, unconfined, or convertible between the two conditions. The model can also handle layers that pinch out. The model allows for analysis of external influences such as wells, areal recharge, drains, evapotranspiration, and interaction with surface-water bodies such as streams. This software has been recognized and accepted for use in many regulatory programs.

The breadth of capabilities and widespread acceptance of the MODFLOW code within the professional community make it a good tool for groundwater flow modeling at Tyrone.



Furthermore, MODFLOW has been used in conjunction with mine pit lake formation studies at other sites (e.g., Pavlik et al., 1995; GeoTrans, 1996).

The application of MODFLOW necessitates the assumption that at large scales, all rock units, including the fractured porphyry host-rock units, can be represented as an equivalent porous media (Gerhart, 1984). This assumption is considered to be valid as long as equivalent hydraulic parameters (hydraulic conductivity) are applied in the modeling (Berkowitz et al., 1988). However, groundwater flow along selected major fractures and faults can be represented numerically using assignment of no-flow, low-hydraulic conductivity, and high-hydraulic conductivity cells, depending on interpretations of hydrologic and geologic information. The inherent assumptions and approximations incorporated by MODFLOW through the mathematical equations used to represent groundwater flow are presented by Harbaugh and McDonald (1996).

One significant limitation of the MODFLOW code is that it cannot adequately account for dry cells. A dry cell occurs where the simulated water level falls below the bottom of the cell. When this situation occurs, the cell is changed to inactive status. This cell can “rewet” again in a subsequent iteration or time step. However, the drying/rewetting algorithm in MODFLOW often leads to oscillations and convergence failures (Painter et al., 2008). In order to correctly account for the resaturation of model cells during the simulations (as is required when the pit lakes form in predictive simulations), the MODFLOW-Surfact computer code (HydroGeoLogic, 1999), a variation of the MODFLOW code that allows for the resaturation of previously dry model cells, was applied. Another code, Groundwater Vistas version 6.11 (Environmental Simulations, 1998), was used for pre-processing and post-processing of model input and output. In addition, DBS&A used ancillary software, such as electronic spreadsheets and custom FORTRAN codes, to facilitate data manipulation, model construction, modification, and visualization of results.

### **C.4.3 Model Domain and Grid**

The model grid applied in the previous groundwater model was used for this effort as well (Figure C-4). The grid is oriented northwest-southeast in order to align the principal directions of the grid cells with the majority of predominant geological structural features, such as faults



and the presence of Gila Conglomerate. Grid horizontal spacing in the model ranges from 99 to 500 feet, with the smallest spacing prescribed in the vicinity of the Main and Gettysburg Pits to facilitate model convergence and mass balance. As in the previous model the current model consists of four layers in the vertical dimension, with the bottom of the model approximately 100 feet below the bottom of the Main Pit (Figure C-5).

#### ***C.4.4 Boundary Conditions***

The boundary conditions applied in the model are presented below.

##### ***C.4.4.1 Top Boundary***

The top model boundary is defined as the simulated location of the water table through time, which varies depending on location. In the model input files, the top of layer 1 is set to the approximate land surface elevation for a given model cell. In this way, simulated water levels above land surface (if any) could be identified during the model calibration process.

Areal recharge is applied to the water table in the model simulations (Section C.4.5.3). The total amount of applied areal recharge is 1,523 acre-feet per year (ac-ft/yr) under predevelopment (steady-state) conditions and 2,173 ac-ft/yr under mining conditions as of 2010.

##### ***C.4.4.2 Lateral Boundaries***

The lateral (side) model boundaries are a combination of prescribed groundwater flux and prescribed head (Figures C-6 through C-9). A prescribed groundwater flux of zero (no-flow condition) is applied along the Mangas Fault and portions of the northwestern and southern boundaries of the active model domain that approximately correspond to regional groundwater flow pathlines (Figures C-6 through C-9).

The southwestern model boundary, which corresponds to the lower elevations of the Big Burro Mountains, is a prescribed groundwater influx boundary. The specified flux at this boundary is held constant through time, representative of an assumed average groundwater inflow over the long term. This approach is reasonable because there are no uses of groundwater near the boundary that would significantly alter groundwater flow conditions. The amount of prescribed groundwater inflow applied to each model cell is proportional to the hydraulic conductivity of the



cell. Because the hydraulic conductivity assigned in the model generally decreases with depth (Section 4.5), the amount of prescribed inflow decreases with depth. For example, the prescribed inflow in the calibrated model for layer 1 is 237 ac-ft/yr, while the prescribed inflow for model layer 4 is 5.5 ac-ft/yr. The total simulated groundwater inflow into the Tyrone Mine area across the southwestern boundary is 493 ac-ft/yr, an amount that was determined through model calibration.

The downgradient model boundary to the northwest across the Mangas Valley is a prescribed hydraulic head boundary. The prescribed hydraulic head is adjusted through time according to water level fluctuations observed at Well 10, located adjacent to the boundary (Figure C-6), for which observed water level elevations are available from the late 1960s (Figure C-10). The consistent rise in observed water levels at Well 10 from 1980 through the early 1990s, followed by the notable decline through the current time, is attributed to the effects of groundwater recharge from active operation of the Mangas Valley tailing impoundments.

The downgradient model boundary to the southeast across Oak Grove Wash is also treated as a prescribed hydraulic head boundary. During the first 30-year period of the model (i.e., 1950 to 1980), the prescribed head value along this boundary was set to vary linearly from 5,300 feet above mean sea level (ft msl) at the southern end to 5,250 ft msl at the northern end, consistent with general historical information. The head value was assumed to decrease linearly through time in the remaining 30-year period (i.e., 1981 to 2010) as a result of pumping outside the model boundary, primarily from the Tyrone Mimbres Basin supply wells. In 2010, the head value along this boundary varied between 5,275 ft msl at the southern end to 5,175 ft msl at the northern end.

#### *C.4.4.3 Bottom Boundary*

The bottom model boundary is a prescribed groundwater flux of zero (no-flow). Available information is insufficient to determine required input values for potential alternate boundary conditions 100 feet or more below the bottom of the Main Pit.

#### *C.4.4.4 Internal Fault Boundaries*

A number of faults or fault zones are represented in the model as no-flow boundaries or as zones of reduced hydraulic conductivity. Faults internal to the model domain treated as no-flow



boundaries are illustrated in Figures C-6 through C-9; portions of faults treated as low-hydraulic conductivity zones are presented in Section C.4.5. The decision on how to represent the hydraulic effects of various faults was based on interpretation of regional groundwater elevation contour maps, well hydrograph data, and the results of model calibration.

One of the more significant updates from the previous model includes implementation of the northwest-southeast-trending Townsite Fault as an impermeable boundary from the vicinity of the Gettysburg Pit to the northeast corner of the Main Pit. A smaller, parallel fault near the Gettysburg Pit is also included in the model (e.g. Figure C-6). Implementation of these faults is based on more detailed hydrogeologic investigation, including the installation new monitor wells, conducted in the vicinity of the Gettysburg Pit to further evaluate the extent of groundwater and PLS capture.

#### *C.4.4.5 Open Pits*

Pits that intercept regional groundwater (Main, Gettysburg, and Copper Mountain Pits) were simulated using several types of boundary conditions. The simulation approach for each time period is outlined below. Note that the simulated values of groundwater inflow to the Main and Gettysburg Pits are significant model calibration targets.

*Historical Transient Simulation.* For the historical transient simulation period (1950 through 2010), the Gettysburg and Copper Mountain Pits, which occur only in model layer 1, were simulated using a drain boundary condition. In MODFLOW the drain boundary condition is one where a drain elevation, in this case the base of the respective pit (Figure C-6), is prescribed. A drain conductance was also prescribed and was treated as a model calibration parameter. The drain conductance is a function of the model grid size and local hydrogeologic conditions and cannot be measured directly in the field. During the simulations the model simulates groundwater inflow to the pits as the difference in the drain elevation and the hydraulic head elevation in adjacent model cells, multiplied by the prescribed conductance values. Groundwater can flow from the adjacent aquifer into drain cells, but groundwater flow from drain cells to the aquifer is not permitted (i.e., the pits can only act as a point of removal for groundwater). The drain condition was implemented at the approximate year that each pit intercepted regional groundwater (1988 for the Gettysburg Pit and 1998 for Copper Mountain Pit).



Unlike the Copper Mountain and Gettysburg Pits, the Main Pit extends into three model layers. In order to simulate the hydrologic effects and groundwater inflows to the Main Pit, a different simulation approach was applied. Specifically, the hydraulic head in the pit, assumed to be equivalent to the bottom elevation of the pit as the pit was excavated through time, was prescribed as a function of time. This approach is reasonable because the pit was pumped as it was excavated so that mining could continue.

To simulate the progression of deepening of the Main Pit through time and the resulting drawdown in the adjacent aquifer that occurred, the historical model calibration period was divided into four separate simulations. These four simulation periods correspond to the approximate time that the Main Pit reached a given model layer bottom. The Main Pit was represented by a zone of a high hydraulic conductivity of 1,000 feet per day (ft/d) (minimal resistance to water flow) to represent the absence of aquifer material. Surrounding the Main Pit, concentric zones of progressively lower hydraulic conductivity were used to avoid mass balance errors that could occur due to large contrasts in adjacent hydraulic conductivity values.

Simulation of the excavation of the Main Pit was conducted as follows:

- *Simulation 1 (1950–1980).* The Main Pit is not represented in the model during this time period because it had not been excavated deep enough to reach regional groundwater.
- *Simulation 2 (1981–1987).* The Main Pit is represented in model layer 1. The Main Pit in model layer 1 is simulated using a hydraulic conductivity of 1,000 ft/d.
- *Simulation 3 (1988–1989).* The Main Pit is represented in model layers 1 and 2. The Main Pit is simulated using hydraulic conductivities of 1,000 ft/d in model layer 1 and 500 ft/d in layer 2.
- *Simulation 4 (1990–2010).* The Main Pit is present in model layers 1 through 3. In each layer, the Main Pit is represented using a hydraulic conductivity of 1,000 ft/d.

*Predictive Simulations.* In the previous modeling report (DBS&A, 2007b), predictive simulation scenarios were presented where the pits were assumed to not be pumped and the water level in



the pit lakes was allowed to rise. In order to accomplish this, the model cells representative of the open portion of each of the pits were converted to active model cells with a very high hydraulic conductivity (1,000 ft/d), to represent very small resistance to flow within the pit lake. In addition, the storage coefficient was set to 1.0, representative of the lack of porous media where the rock has been excavated. This approach, in combination with the capability of the MODFLOW-Surfact code to simulate the rise of the water table into previously dry model cells, allows for the simulation of pit lake formation (Blandford et al., 2001). Predictive simulations where the pit lake water levels were allowed to rise were not conducted as part of the Stage 2 APP, however. As discussed in the report, DP-1341 closure requires that the pit sumps be pumped down as water accumulates, and pit lakes will not be allowed to form in the future at Tyrone.

#### *C.4.4.6 Underground Workings*

Underground workings associated with the Burro Chief Shaft and laterals were incorporated into the model through specification of high-hydraulic conductivity and high-storage coefficient model cells to assist with historical model calibration. The approximate locations of these features were estimated from historical drawings of the Burro Chief Shaft and adjacent workings, and their implementation into the model is evident in the figures that are discussed in Section C.4.5. Features associated with the Burro Chief Shaft and laterals occur beneath the water table and affect groundwater flow primarily in a limited area of model layer 2. They were included in the model to better account for early groundwater pumping that occurred from the Burro Chief Shaft. Although other underground workings may have had some influence on historical groundwater flow, they were not incorporated into the model due to a lack of data and because they appear to have been mined out with construction of the open pits.

### **C.4.5 Model Input Parameters**

Sections C.4.5.1 through C.4.5.4 present the final model input parameters determined through model calibration or as otherwise noted.

#### *C.4.5.1 Hydraulic Conductivity*

The horizontal hydraulic conductivity applied in each model layer is presented in Figures C-11 through C-14. In general, the most complex zonation of hydraulic conductivity occurs in model





layers 1 and 2 because the simulated water table occurs in these layers over much of the model domain (particularly layer 1) and most available information regarding water levels and aquifer properties is obtained from wells screened across or immediately below the water table. In addition, model layer 1 contains three general types of aquifer materials: igneous rock, Gila Conglomerate, and Quaternary alluvium overlying Gila Conglomerate along the Mangas Valley and its major tributaries (Figure C-3).

The calibrated value of hydraulic conductivity for the Gila Conglomerate in model layer 1 (Figure C-11) is 1.5 ft/d in the northwestern portion of the model domain. In this same area, the hydraulic conductivity applied to model layer 1 is 4 to 15 ft/d to account for the presence of saturated alluvium overlying Gila Conglomerate (i.e., the alluvium generally has higher hydraulic conductivity than the Gila Conglomerate, and both rock types are present within model layer 1). Northeast of the Main Pit, Gila Conglomerate hydraulic conductivity is set to 5 ft/d based on the results of an aquifer test conducted for well 286-2005-03 near the Tyrone main gate. This aquifer test indicated a hydraulic conductivity of 20 ft/d over the screened interval of the well, but the lower value of 5 ft/d for the entire model layer led to a better model calibration. This area also includes the Fortuna water supply wells (Figure C-6). Hydraulic conductivity of the Gila Conglomerate east and southeast of the Sprouse-Copeland Fault is 5 ft/d, which is similar to the magnitude of hydraulic conductivity determined from an aquifer test conducted for well 363-2005-04, adjacent to well MB-29 (DBS&A, 2007a).

Throughout much of the Mine/Stockpile Unit in model layer 1, the hydraulic conductivity of the quartz monzonite is 0.18 ft/d. West of the Main Pit and south of the Little Rock Mine area, the hydraulic conductivity of the quartz monzonite is 0.8 ft/d. The hydraulic conductivity of the granite west of the Main Pit is 0.06 ft/d in the Deadman Canyon and Little Rock Mine areas and 4 ft/d in the SX-EW Plant area, where the observed hydraulic gradient is markedly flatter (Plate 5-1). Figure C-11 also illustrates the high hydraulic conductivity value used to simulate the approximate regions excavated to form the Main and Gettysburg Pits and the zones of low hydraulic conductivity along fault traces to represent regions of reduced permeability. Relative to the previous model presented by DBS&A (2007b), some faults and low-permeability zones have been added southwest of the Gettysburg Pit along the south side of the mine to better replicate observed conditions (generally higher water levels) in this area, and the portion of the



Sprouse-Copeland Fault that trends north-northeast immediately east of the Nos. 1A and 1B leach stockpiles was included as a low-hydraulic conductivity (rather than a no-flow) feature.

The hydraulic conductivity in model layer 2 (Figure C-12) is similar to that in model layer 1, except that igneous rock, rather than Gila Conglomerate, occurs in the northwest portion of the model and extends farther northeast of the Main Pit. Moving vertically downward through the remaining two model layers (Figures C-13 and C-14), the assigned hydraulic conductivity is reduced based on a general conceptual model in which fracture porosity and connectivity are likely reduced with depth. The number of hydraulic conductivity zones also decreases with depth, reflecting the fact that observed data are limited (model layer 3) or nonexistent (model layer 4).

Vertical hydraulic conductivity is assumed to be equal to horizontal hydraulic conductivity for the igneous rocks in all model layers, reflecting the conceptual model of vertical groundwater flow along fractures as well as horizontal groundwater flow. For the Gila Conglomerate, vertical hydraulic conductivity was assumed to be one-tenth of the horizontal hydraulic conductivity.

#### *C.4.5.2 Storage Coefficient*

The storativity and specific yield applied in each model layer is presented in Figures C-15 through C-18. Consistent values of specific yield and storativity for each rock type (igneous or Gila Conglomerate) were applied throughout the model domain. The assigned specific yield and storativity values for Gila Conglomerate are 0.08 and 0.0001, respectively. The assigned specific yield and storativity values for the igneous rocks are generally 0.03 and 0.0001, respectively. A zone on the southern half of the mine was assigned a lower specific yield of 0.015, commensurate with the lower hydraulic conductivity of portions of this region (Figure C-15). The lower specific yield assigned to the igneous rocks (granite and quartz monzonite) relative to the Gila Conglomerate is indicative of the fact that the hydraulic properties of these rocks are controlled by fractures.

Figures C-15 and C-16 (illustrating storage properties in model layers 1 and 2, respectively) provide a good outline of where regional groundwater is assumed to occur in the model in Gila Conglomerate or in igneous rocks. Figures C-15 and C-16 also mark several model cells that contain underground workings associated with the Burro Chief Shaft; these model cells are



assigned higher storage coefficient values to approximate the presence of laterals throughout portions of these cells.

#### *C.4.5.3 Groundwater Recharge*

Groundwater recharge within the model domain was determined through model calibration and consideration of other studies and previous work for similar types of hydrogeologic settings. Assigned recharge within the groundwater model is divided into four general zones, as follows:

- Regions where the water table occurs in igneous bedrock and the ground surface has not been disturbed by mining
- Regions where the water table occurs in igneous bedrock and the ground surface has been disturbed by mining
- Regions where the water table occurs in Gila Conglomerate or Quaternary alluvium and the ground surface has not been disturbed by mining
- Regions where the water table occurs in Gila Conglomerate or Quaternary alluvium and the ground surface has been disturbed by mining

Figure C-19 illustrates the groundwater recharge applied in the calibrated groundwater flow model for predevelopment conditions. As illustrated in the figure, a recharge value of 0.5 inch per year (in/yr) was applied to igneous bedrock areas, whereas a higher value of 1.6 in/yr was applied to areas where the regional water table occurs in Gila Conglomerate. These average rates of recharge correspond to about 3 percent and 10 percent, respectively, of the average annual precipitation that occurs at Tyrone (approximately 16 in/yr).

Figure C-20 illustrates the groundwater recharge applied in the calibrated groundwater flow model for post-development (mining) conditions. As illustrated in the figure, base recharge values are the same as those applied for predevelopment conditions, but recharge within the disturbed footprint of the Mine/Stockpile Unit is increased to 1.81 in/yr, the value of infiltration for uncovered stockpiles determined by Golder (2011, copy provided in Appendix B of this Stage 2 APP). This general magnitude of recharge is confirmed by observed water level rises at some



monitor wells in the Mine/Stockpile Unit (e.g., well 2-5A), which generally indicate about 1.2 to 2 in/yr of recharge under operational conditions.

No recharge is applied within the lower portions of the Main and Gettysburg Pits, the assumption being that rainfall in these areas will primarily run off to the pit rather than infiltrate to regional groundwater. In addition, enhanced recharge believed to be representative of operational conditions is applied beneath the No. 1 tailing complex and the No. 3A leach stockpile. At the No. 3A leach stockpile, the enhanced recharge is assumed to be focused along the shallow alluvial channels beneath and immediately adjacent to the stockpile (Figure C-20). A summary of recharge applied in the groundwater model is provided in Table C-1.

Although not included in the final model, the conceptual model of enhanced recharge beneath drainages was also investigated during the prior model calibration process (DBS&A, 2007b). Enhanced recharge beneath portions of various drainage channels may occur in the vicinity of Tyrone, but the model simulation results were not sensitive to the input of greater recharge rates along active channel bottoms; therefore, this potential source of recharge was not simulated explicitly in the final model runs.

#### *C.4.5.4 Pumping Wells*

Pumping wells are prescribed in model cells that include a location of known groundwater withdrawals other than the open pits (Figures C-6 and C-7). Pumping at the mine has occurred in the past for water supply (Fortuna wells and Burro Chief Shaft) and for containment and abatement of impacted water (No. 3A leach stockpile and No. 1X tailing impoundment capture systems). All groundwater pumping (other than the Main Pit) occurs or occurred from model layer 1, except for water extracted from the Burro Chief Shaft, which corresponds to model layer 2.

Table C-2 lists prescribed pumping rates assigned through time in the model. Measurements or estimates of historical pumping were obtained from Tyrone Mine records, various DP quarterly or annual reports, and data reported by Hathaway (1986).



**Table C-1. Groundwater Recharge**

Recharge Zone	Groundwater Recharge (in/yr)											
	1950 - 1971	1972 - 1978	1979 - 1980	1981 - 1982	1983 - 1985	1986	1987 - 1992	1993	1994	1995 - 2003	2004	2005 - 2010
Gila Conglomerate	1.6	1.6	1.6	1.6	1.6	1.6	1.6	1.6	1.6	1.6	1.6	1.6
Igneous rock within disturbed area	0.5	0.5	0.5	1.81	1.81	1.81	1.81	1.81	1.81	1.81	1.81	1.81
Igneous rock outside disturbed area	0.5	0.5	0.5	0.5	0.5	0.5	0.5	0.5	0.5	0.5	0.5	0.5
No. 1 tailing impoundment	1.6	18	9	9	9	9	1.6	1.6	1.6	1.6	1.6	1.6
No. 1X tailing impoundment	1.6	1.6	1.6	36	36	36	36	36	18	18	18	1.6
No. 1A tailing impoundment	1.6	1.6	1.6	1.6	36	36	36	18	18	18	1.6	1.6
No. 3A stockpile	1.6	1.6	1.6	1.6	1.6	76	76	76	76	48	48	48

in/yr = Inch(es) per year



Table C-2. Historical Groundwater Pumping

Well or Capture System	Pumping Rate (ac-ft/yr)																																			
	1971	1972	1973	1974	1975	1976	1977	1978	1979	1980	1981	1982	1983	1984	1985	1986	1987	1988	1989	1990	1991	1992	1993	1994	1995	1996	1997	1998	1999	2000	2001	2002	2003	2004	2005 - 2010	
Burro Chief Shaft	338	363	235	192	210	227	232	282	515	728	295	232	64.6	470	668	614	560	506	693	108	77.2	27.9	64.6	0	0	0	0	0	0	0	0	0	0	0	0	0
Fortuna 1, 2	322	254	587	291	355	419	317	186	186	234	186	90.7	139	232	325	281	237	191	199	162	203	72.1	29.3	130	266	31.1	59.2	58.7	60	60	60	60	60	60	60	60
Well MF-7	0	0	0	0	0	0	0	0	0	286	357	87.8	223	355	177	0	0	0	0	0	0	0	0	0	0	0	0	0	0	0	0	0	0	0	0	0
No. 1X capture system	0	0	0	0	0	0	0	0	0	0	0	0	0	0	0	0	0	0	0	0	0	16	16	16	16	16	16	16	16	16	16	16	16	16	16	
<i>No. 3A stockpile</i>																																				
Canyon 4	0	0	0	0	0	0	0	0	0	0	0	0	0	0	0	0	0	0	0	0	0	0	0	0	0	0	0	0	2.67	1.05	2.72	2.07	4.04	0	0.058	
Canyon 6	0	0	0	0	0	0	0	0	0	0	0	0	0	0	0	0	0	0	0	0	0	0	0	0	0	13.8	13.2	32.5	52.9	45.4	31.7	33.3	19.8	10.0	5.66	
Canyon 7	0	0	0	0	0	0	0	0	0	0	0	0	0	0	0	0	0	0	0	0	0	0	0	0	0	22.8	17.9	15.2	34.0	19.9	29.3	26.6	21.0	10.8	3.12	
Canyon 8	0	0	0	0	0	0	0	0	0	0	0	0	0	0	0	0	0	0	0	0	0	0	0	0	0	21.1	54.1	37.4	69.2	53.0	57.5	38.0	34.6	22.4	4.85	
Canyon 9	0	0	0	0	0	0	0	0	0	0	0	0	0	0	0	0	0	0	0	0	0	0	0	0	0	0	0	0	0	6.47	6.87	4.85	4.85	4.85	4.85	
Canyon 10	0	0	0	0	0	0	0	0	0	0	0	0	0	0	0	0	0	0	0	0	0	0	0	0	0	12.9	12.9	10.2	24.3	16.1	17.9	22.7	13.18	8.52	16.2	
Canyon 11	0	0	0	0	0	0	0	0	0	0	0	0	0	0	0	0	0	0	0	0	0	0	0	0	0	0.0	7.2	3.7	6.0	5.3	27.2	58.2	53.4	38.8	16.2	
Trestle	0	0	0	0	0	0	0	0	0	0	0	0	0	0	0	0	0	0	0	0	0	0	0	0	0	51.7	49.0	52.2	62.1	49.0	48.7	38.0	13.5	12.6	1.83	
Flats	0	0	0	0	0	0	0	0	0	0	0	0	0	0	0	0	0	0	0	0	0	0	0	0	0	34.1	22.2	19.6	32.0	16.9	10.9	10.1	8.30	9.10	3.83	
L Line	0	0	0	0	0	0	0	0	0	0	0	0	0	0	0	0	0	0	0	0	0	0	0	0	0	46.2	54.9	38.3	88.3	54.4	35.9	20.2	20.4	19.0	3.01	

ac-ft/yr = Acre-feet per year



#### **C.4.6 Model Calibration**

Model calibration was conducted through the comparison of the following items:

- Simulated and observed hydraulic heads for the Tyrone Mine area as of 1950 (predevelopment conditions) and 2005
- Simulated and observed hydraulic heads through time (historical hydrographs) at selected wells
- Simulated and observed or estimated groundwater inflows to the Gettysburg and Main Pits

Model calibration was conducted using the standard iterative approach, where various model input parameters were adjusted within reasonable ranges until the simulation results adequately matched observed hydraulic head or (in the case of the pits) groundwater inflow calibration targets. Model calibration was achieved primarily through the adjustment of hydraulic conductivity, groundwater recharge, and the hydraulic characteristics of major faults. For transient model calibration runs, the steady-state model was updated so that appropriate initial conditions were available for input to the transient model.

##### *C.4.6.1 Steady-State Model Calibration*

A predevelopment model calibration was conducted for assumed hydrologic conditions as of 1950, which was approximately 38 years before excavation of the Main Pit intercepted regional groundwater in about 1988. Early water levels within the model domain obtained from Trauger (1972) were used to calibrate the model. Figure C-21 is a plot of the simulated steady-state water table, and Figure C-22 is a cross plot of simulated and observed hydraulic heads for this period. The reported measurement dates of observed data points used to develop Figure C-22 range from 1913 to 1970. The graph indicates a reasonable correspondence between observed and simulated water levels, with more significant scatter for water levels greater than about 5,650 ft msl. This is not surprising because these observed water levels occur in the more complex conditions of the fractured rock regional aquifer, as opposed to Gila Conglomerate or alluvium.



The simulated groundwater flow directions illustrated in Figure C-21 are similar to those provided by Trauger (1972), where groundwater flows northeast from the Big Burro Mountains toward the Tyrone Mine and then flows either to the southeast into the Mimbres Basin or the northwest into the Gila-San Francisco Basin. Trauger (1972) could not have known about the influence that some of the faults in the Tyrone Mine area have on groundwater flow, and therefore some of the complexities in the groundwater flow system caused by these faults are not depicted on his map of regional water levels. Note also that due to the presence of the Sprouse–Copeland and Southern Star Faults, both of which restrict horizontal groundwater flow, a significant pathway for water to exit the mine site is along the zone of relatively thick Gila Conglomerate that occurs adjacent to the Mangas Fault, which forms the northeastern border of the model domain.

The simulated mass balance for the calibrated steady-state model is presented in Table C-3. As indicated in the table, lateral groundwater inflow and groundwater recharge account for 24 and 76 percent of the total simulated inflow, respectively. Simulated outflow from the model domain to the Mimbres Basin and the Mangas Valley is 63 and 37 percent of the total outflow, respectively.

**Table C-3. Simulated Mass Balance for Steady-State (Predevelopment) Model**

Source	Simulated Inflow/Outflow (ac-ft/yr)	
	Inflow	Outflow
Inflow from Big Burro Mountains	493	—
Recharge	1,523	—
Outflow to Mangas Valley	—	1,274
Outflow to Mimbres Basin	—	742
Totals	2,016	2,016

ac-ft/yr = Acre-feet per year      --- = Not applicable

#### C.4.6.2 Transient Model Calibration

A transient model calibration was conducted for the period 1950 through 2010. Initial conditions for the transient calibration are the simulated hydraulic head values obtained from the predevelopment (steady-state) calibration. The simulated 2010 water table (Figure C-23) indicates the presence of a substantial cone of depression formed by dewatering of the Main





Pit, as well as a smaller cone of depression attributable to dewatering of the Gettysburg Pit. Groundwater that does not flow to the pits or other points of extraction (i.e., wells) flows either to the northwest down the Mangas Valley or to the southeast into the Mimbres Basin.

The plot of simulated versus observed hydraulic heads as of 2005 (Figure C-24) shows a reasonable correspondence between observed and simulated values at many locations, particularly given the complex groundwater flow system that exists at Tyrone, with steep hydraulic gradients and abrupt changes or discontinuities in hydraulic head occurring in some areas. The wells with measured water levels that show the greatest deviation from simulated water levels (200 feet or more) are labeled on Figure C-24. Some of the largest differences between simulated and observed water levels are:

- In general, simulated water levels are lower than observed values south and southeast of the Mine/Stockpile disturbed area (e.g., wells 2-11, 2-12, and 2-13).
- The simulated water level is high in the vicinity of the SX/EW Plant (e.g., well 166-2005-04).
- The simulated water level is high immediately north of the Main Pit, where the full extent of observed drawdown caused by dewatering at the Main Pit is not simulated by the model (e.g., wells P-6B and P-8A).

Simulated water levels were also compared to observed historical water levels at 70 wells, the locations of which are provided in Figure C-25. The observed and simulated hydraulic head at each of these wells are compared in Attachment C-1. Wells were selected for comparison based primarily on the length of their recorded water level history. In some instances, the water level measurements from subsequent replacement wells were appended to an earlier record to form the complete hydrograph used for model calibration (e.g., wells P-6 and P-8).

Figures C-26 and C-27 illustrate the simulated groundwater inflow to the Gettysburg and Main Pits, respectively. Simulated inflow to the Gettysburg Pit begins at about 132 gallons per minute (gpm) and steadily declines to about 63 gpm as of 2010. Groundwater inflow to the Gettysburg Pit cannot be determined from existing monitoring data, but the simulated values appear reasonable and within the expected range based on the general observations of Tyrone



operations personnel. Simulated inflow to the Main Pit increases to a high of about 3,000 gpm as of 1988 and declines to about 835 gpm as of 2010. DBS&A (2002b), using mass balance analysis, estimated groundwater inflow to the Main Pit to be about 1,390 gpm over the period 1991 through 2000 (excluding two anomalous years). Simulated groundwater inflow to the Main Pit over the same period is 1,148 gpm, about 17 percent lower than the values estimated by DBS&A (2002b).

Simulated inflow to the Copper Mountain Pit is zero as of 2010 because the simulated water level in the model is below the base of the pit. Observed groundwater inflow to this pit is not measured but it was believed to be relatively small prior to 2010 compared to that of the Gettysburg Pit and certainly the Main Pit.

Table C-4 presents the simulated mass balance for the calibrated historical transient model as of 2010. Compared to the steady-state model calibration, additional sources of water include enhanced recharge within the disturbed mining area (650 ac-ft/yr more than predevelopment conditions) and water released from storage due primarily to pit dewatering (1,162 ac-ft/yr). Simulated groundwater outflow occurs at open pits (1,449 ac-ft/yr), at extraction wells (136 ac-ft/yr), and (laterally) at the model boundaries (2,242 ac-ft/yr).

**Table C-4. Simulated 2010 Mass Balance for Historical Transient Model**

Source	Simulated Inflow/Outflow (ac-ft/yr)	
	Inflow	Outflow
Inflow from Big Burro Mountains	493	—
Recharge	2,173	—
Pumping Wells	—	136
Main Pit	—	1,347
Gettysburg Pit	—	102
Outflow to Mangas Valley	—	1,433
Outflow to Mimbres Basin	—	809
Storage	1,162	0.0
<b>Totals</b>	<b>3,828</b>	<b>3,827</b>

ac-ft/yr = Acre-feet per year      --- = Not applicable



### **C.4.7 Sensitivity Analysis**

An updated sensitivity analysis was not conducted for the revised model documented in this appendix. Based on experience with the previous model and the updating process for the current model, the sensitivity analyses presented in previous reports (e.g., DBS&A, 2007b) are probably good indicators of the most sensitive model input parameters. In general, the model simulation results are most sensitive to horizontal hydraulic conductivity and recharge, and the model is relatively insensitive to storage coefficient. Other observations from model calibration include that (1) the model is not very sensitive to changes in vertical hydraulic conductivity, and (2) the model is sensitive to assumptions regarding fault boundaries and no-flow zones (DBS&A, 2007b).

## **C.5 Predictive Simulation**

One predictive simulation was conducted using the updated groundwater flow model. The predictive simulation is representative of expected future groundwater conditions at Tyrone with implementation of closure measures as documented in the Settlement Agreement and Stipulated Final Order (Settlement Agreement) entered into by Tyrone and the NMED in December 2010. The predictive simulation is discussed in Section 5.1 of the Stage 2 APP report. In summary, the predictive simulation was conducted using the following assumptions:

- The predictive simulation was conducted for the period 2011 through 2060.
- The lateral boundary conditions (prescribed inflow and prescribed head) were held constant at 2010 values.
- Prescribed recharge was assumed to transition from 2010 values to closure values over a 20-year period. Covered top surfaces and side slopes of stockpiles were assigned a recharge rate to regional groundwater of 0.22 in/yr (Appendix B). Uncovered side slopes of stockpiles were assigned a recharge rate to regional groundwater of 1.81 in/yr (same as current).



- Pumping rates at existing extraction wells were held constant at 2010 values, with the exception of the No. 3A leach stockpile area where long-term extraction rates were assumed to be about one-half that of the reported 2010 rates. The locations of pumping were also adjusted to reflect more likely pumping locations during mine closure.
- The base of the Copper Mountain Pit was lowered 150 feet from 6000 ft msl to 5850 ft msl to approximately represent deepening of the pit that occurred during the latter half of 2010 and the first few months of 2011.
- The base of the Main Pit was lowered 100 feet from 5000 ft msl to 4900 ft msl.
- Dewatering at the pits was maintained using drain cells with elevations equivalent to the pit bottoms (Gettysburg and Copper Mountain) or by prescribing head at the bottom of the pit (Main Pit).

## **C.6 Summary and Conclusions**

The Tyrone groundwater flow model documented by DBS&A (2007b) was substantially updated and modified to include additional faults at Tyrone and additional observed data based on studies and observations that have occurred since submission of the prior model. The updated model is reasonably calibrated to existing data, such as observed water levels and estimated groundwater inflow to the Main and Gettysburg Pits, and is believed to be an improved tool for estimating future groundwater flow conditions for application in the Stage 2 APP and the determination of Alternative Abatement Standards as required by the Settlement Agreement.

## **References**

- Berkowitz, B., J. Bear, and C. Braester. 1988. Continuum models for contaminant transport in fractured porous formations. *Water Resources Research* 24(8):1225-1236.
- Blandford, T.N., M.J. Ronayne, and D. Earley, III. 2001. Simulation of lake formation at multiple mine pits in a block faulted porphyry copper deposit. In *Proceedings of MODFLOW 2001 and Other Modeling Odysseys, an International Ground Water Modeling Conference and*



*Workshops.* Sponsored by International Ground Water Modeling Center, Colorado School of Mines, Golden, Colorado. September 11-14, 2001.

Committee on Fracture Characterization and Fluid Flow (CFCFF). 1996. *Rock fractures and fluid flow: Contemporary understanding and applications.* National Academy Press.

Daniel B. Stephens & Associates, Inc. (DBS&A). 1997a. *Preliminary site-wide groundwater study, Tyrone Mine closure/closeout.* Prepared for Phelps Dodge Tyrone, Inc., Tyrone, New Mexico. May 31, 1997.

DBS&A. 1997b. *Supplemental groundwater study, Tyrone closure/closeout.* Prepared for Phelps Dodge Tyrone, Inc., Tyrone, New Mexico. November 14, 1997.

DBS&A. 1997c. *Supplemental materials characterization, Tyrone Mine closure/closeout.* Prepared for Phelps Dodge Tyrone, Inc., Tyrone, New Mexico. October 31, 1997.

DBS&A. 1999a. *Tyrone pit lake formation modeling report.* Prepared for Phelps Dodge Tyrone, Inc., Tyrone, New Mexico. January 22, 1999.

DBS&A. 1999b. *Addendum to the Tyrone pit lake formation modeling report: Predictive pit filling simulation results.* Prepared for Phelps Dodge Tyrone, Inc., Tyrone, New Mexico. June 18, 1999.

DBS&A. 2002a. *Tyrone Mine pit lake formation model sensitivity analysis and verification study.* Prepared for Phelps Dodge Tyrone, Inc., Tyrone, New Mexico. March 29, 2002.

DBS&A. 2002b. *Surface water runoff calculations for open pits and summary of historical pumping at the Tyrone Mine Main Pit.* Prepared for Phelps Dodge Tyrone, Inc., Tyrone, New Mexico. May 8, 2002.

DBS&A. 2004. *Stage 1 abatement plan proposal, Tyrone Mine facility.* Prepared for Phelps Dodge Tyrone, Inc., Tyrone, New Mexico. October 15, 2004.



- DBS&A. 2005. *Work plan for additional groundwater modeling analysis to supplement the existing Tyrone Mine pit lake formation model, DP-1341 Condition 83.* Prepared for Phelps Dodge Tyrone, Inc., Tyrone, New Mexico. July 25, 2005.
- DBS&A. 2006. *Addendum to the Tyrone Mine facility Stage 1 abatement plan proposal work plan for additional site characterization.* Prepared for Phelps Dodge Tyrone, Inc., Tyrone, New Mexico. December 6, 2006.
- DBS&A. 2007a. *Completion report for DP-1341 Condition 82, Tyrone Mine Facility, Supplemental groundwater study.* Prepared for Phelps Dodge Tyrone, Inc., Tyrone, New Mexico. August 2, 2007.
- DBS&A. 2007b. *Completion report for DP-1341 Condition 83, Tyrone Mine Facility, Groundwater model.* Prepared for Phelps Dodge Tyrone, Inc., Tyrone, New Mexico. November 15, 2007.
- DBS&A. 2011. *Tyrone Mine facility Stage 1 abatement plan final report.* Prepared for Freeport McMoRan Tyrone, Inc., Tyrone, New Mexico. June 30, 2011.
- Environmental Simulations, Inc. 1998. *Groundwater Vistas version 2.06.* Herndon, Virginia.
- GeoTrans, Inc. 1996. Numerical simulation of the effect on groundwater and surface water of the proposed zinc and copper mine near Crandon, Wisconsin (update to Appendix 4.2-3 of the environmental impact report, Foth and Van Dyke, 1995).
- Gerhart, J.M. 1984. A model of regional ground-water flow in secondary permeability terrane. *Groundwater* 22(2):168-175.
- Golder Associates (Golder). 2011. Technical memorandum from Lewis Munk and Todd Stein to Neil Blandford, DBS&A, regarding UNSAT-H simulations for the Stage 2 abatement plan proposal, groundwater modeling – Tyrone Mine. November 18, 2011



Hathaway, D.L. 1986. *Hydrogeologic evaluation of proposed transfer of water from the Gila River to Tyrone by the Phelps Dodge Corporation*. New Mexico State Engineer Office. September 1986.

Harbaugh, A.W. and M.G. McDonald. 1996. *User's documentation for MODFLOW-96, an update to the U.S. Geological Survey modular finite-difference ground-water flow model*. U.S. Geological Survey Open-File Report 96-485.

HydroGeoLogic, Inc. 1999. *Modflow-Surfact version 2.1, A comprehensive MODFLOW-based flow and transport simulator*.

Painter, S., H. Basagaoglu, and A. Liu. 2008. Robust representation of dry cells in single-layer MODFLOW models. *Groundwater* 46(6):873-881.

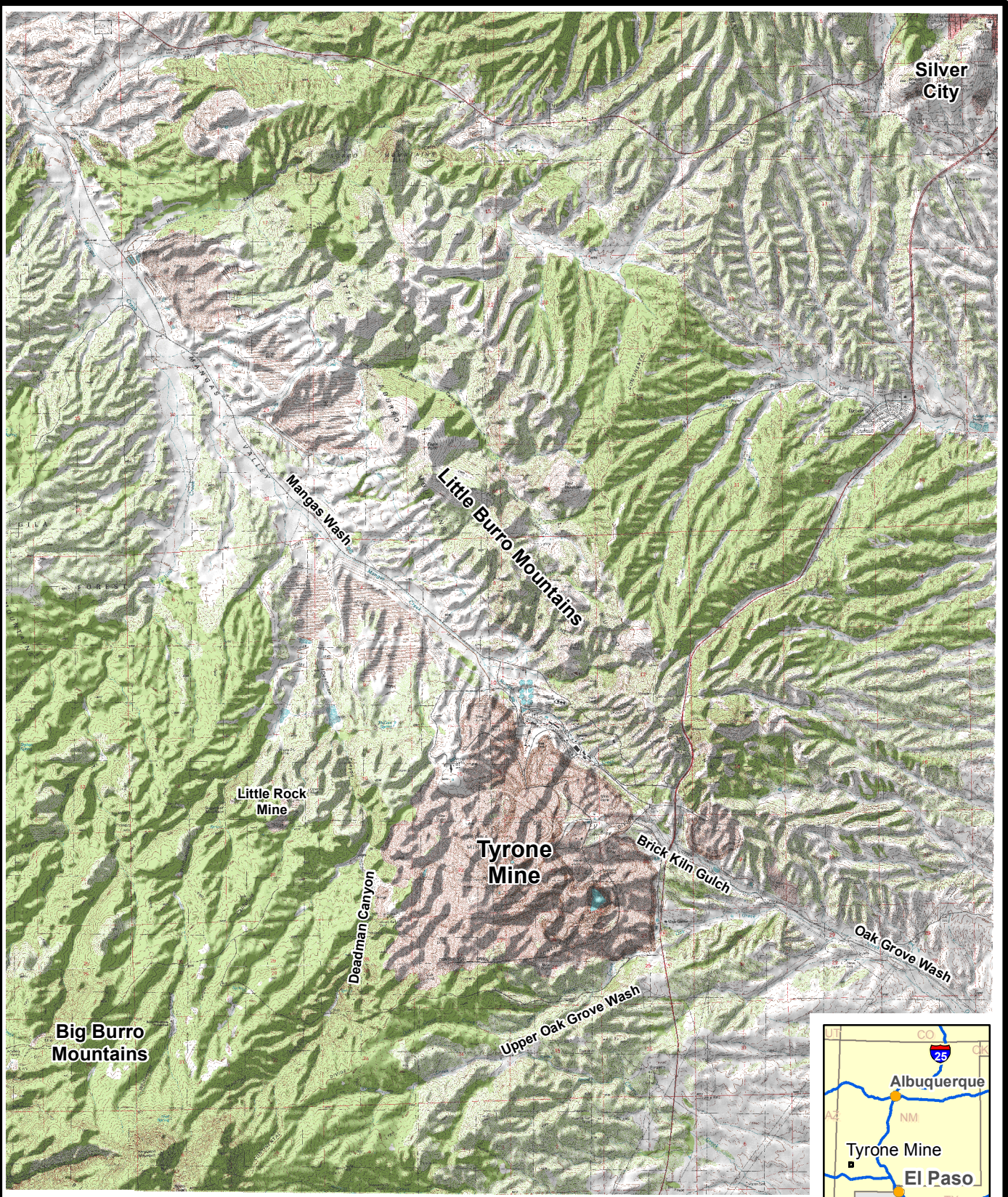
Pavlik, H.F., F.G. Baker, and X. Guo. 1995. Simulation of pit closure alternatives for an open pit mine. *Tailing and Mine Waste '95*. Balkema, Rotterdam.

Trauger, F.D. 1972. *Water resources and general geology of Grant County, New Mexico*. Prepared in cooperation with U.S. Geological Survey, New Mexico State Engineer Office, and Grant County Commission. Hydrologic Report 2, New Mexico State Bureau of Mines and Mineral Resources.

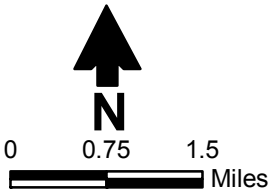
U.S. Environmental Protection Agency (EPA). 1995. *Mine site water balance report*. 66p.

## Figures





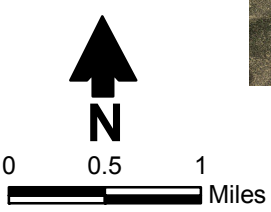
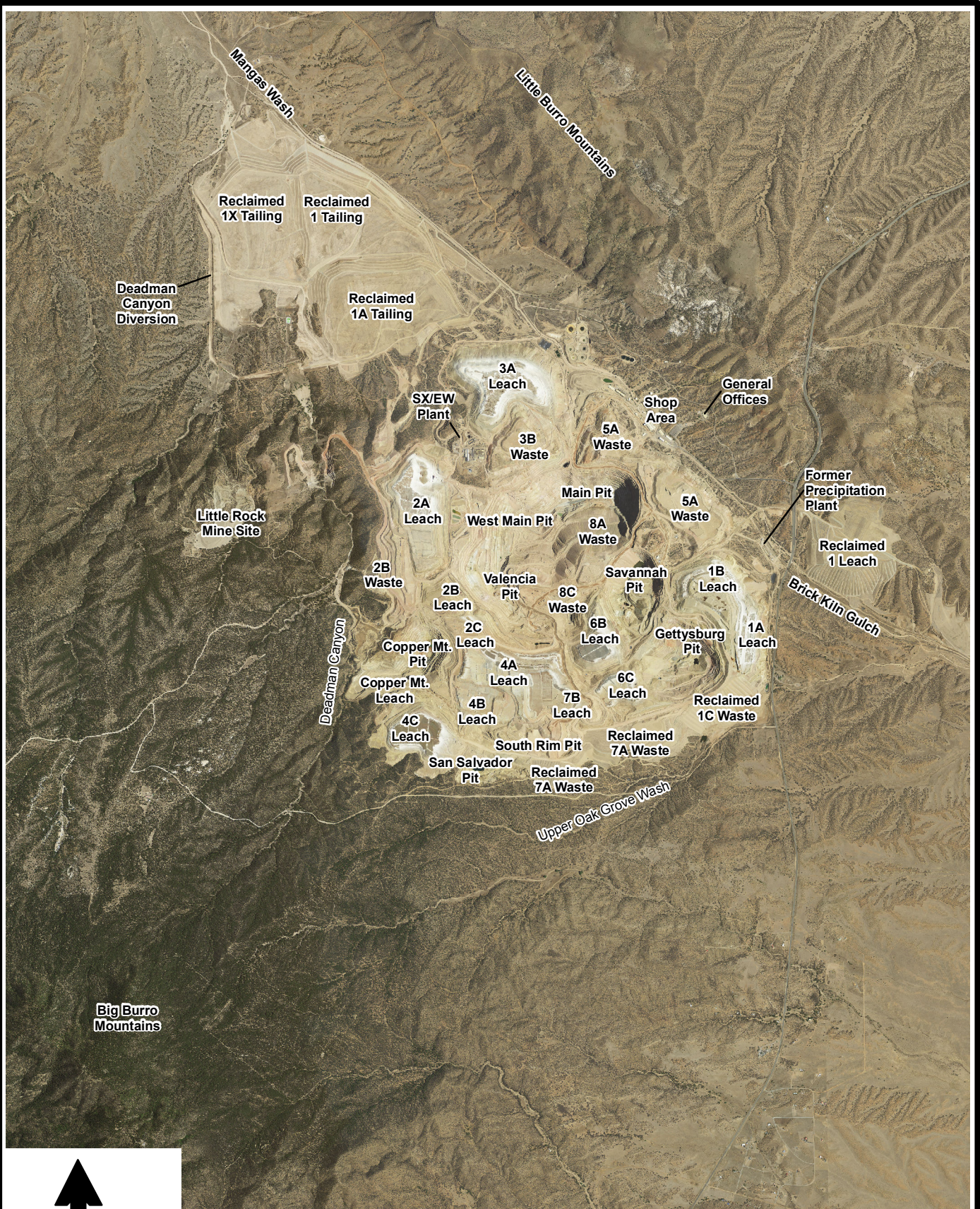
Source: USGS 7.5 minute topographic maps  
 Note: Hillshade reflects pre-mining topography.



S:\PROJECTS\MINE\_TYRONE\GIS\MXD\ES09.0176\MXD\SI\REPORT\_11-11\FIGC-01\_LOCATION\_MAP\MXD



S:\PROJECTS\MINE\_TYRONE\GIS\MXD\ES09.0176\MXD\REPORT\_11-11\FIGC-02\_MINE\_FACILITIES\_SIGNIFICANT\_GEOGRAPHIC\_FEATURES.MXD



Source: Aerial photograph from NAIP, 2011

**FREEM** **FREEMPORT-McMORAN**  
**COPPER & GOLD**

TYRONE STAGE 2 APP

### Mine Facilities and Significant Geographic Features

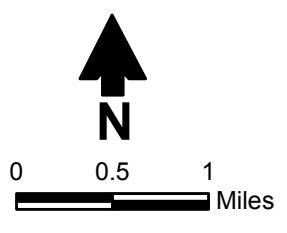
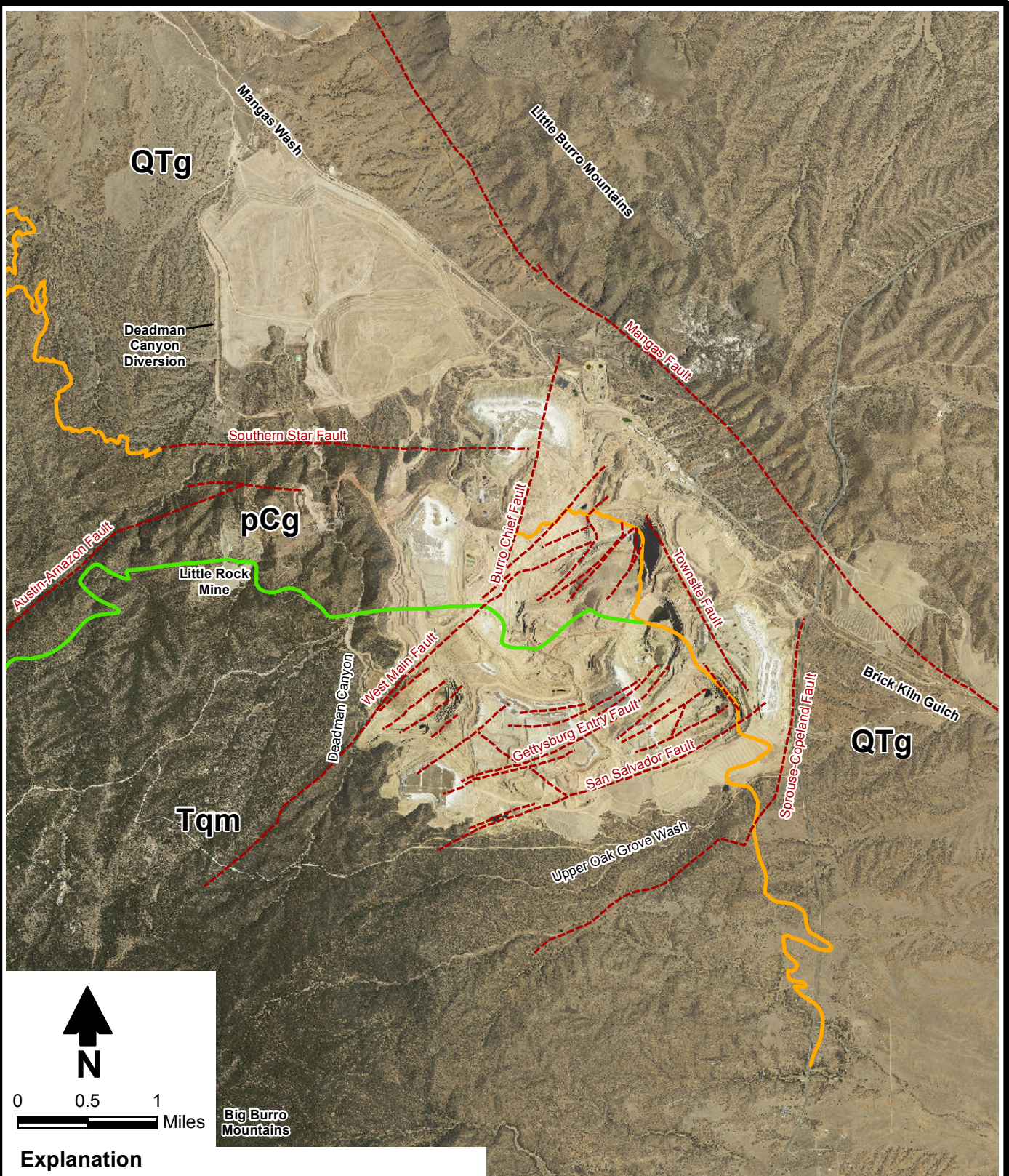


*Daniel B. Stephens & Associates, Inc.*  
01/16/2012 JN ES09.0176

Figure C-2



S:\PROJECTS\MINE\_TYRONE\GIS\MXD\ES09.0176\MXDS\STAGE\_2\_APP\_REPORT\_1-2012\FIGC-03\_APPROX\_SURFACE\_GEOLOGIC\_CONTACTS.MXD



Big Burro Mountains

**Explanation**

- Fault
- Geologic contact between pCg and Tqm
- Geologic contact between igneous rocks and QTg

pCg = Precambrian granite  
 Tqm = Tertiary quartz monzonite  
 QTg = Gila Conglomerate

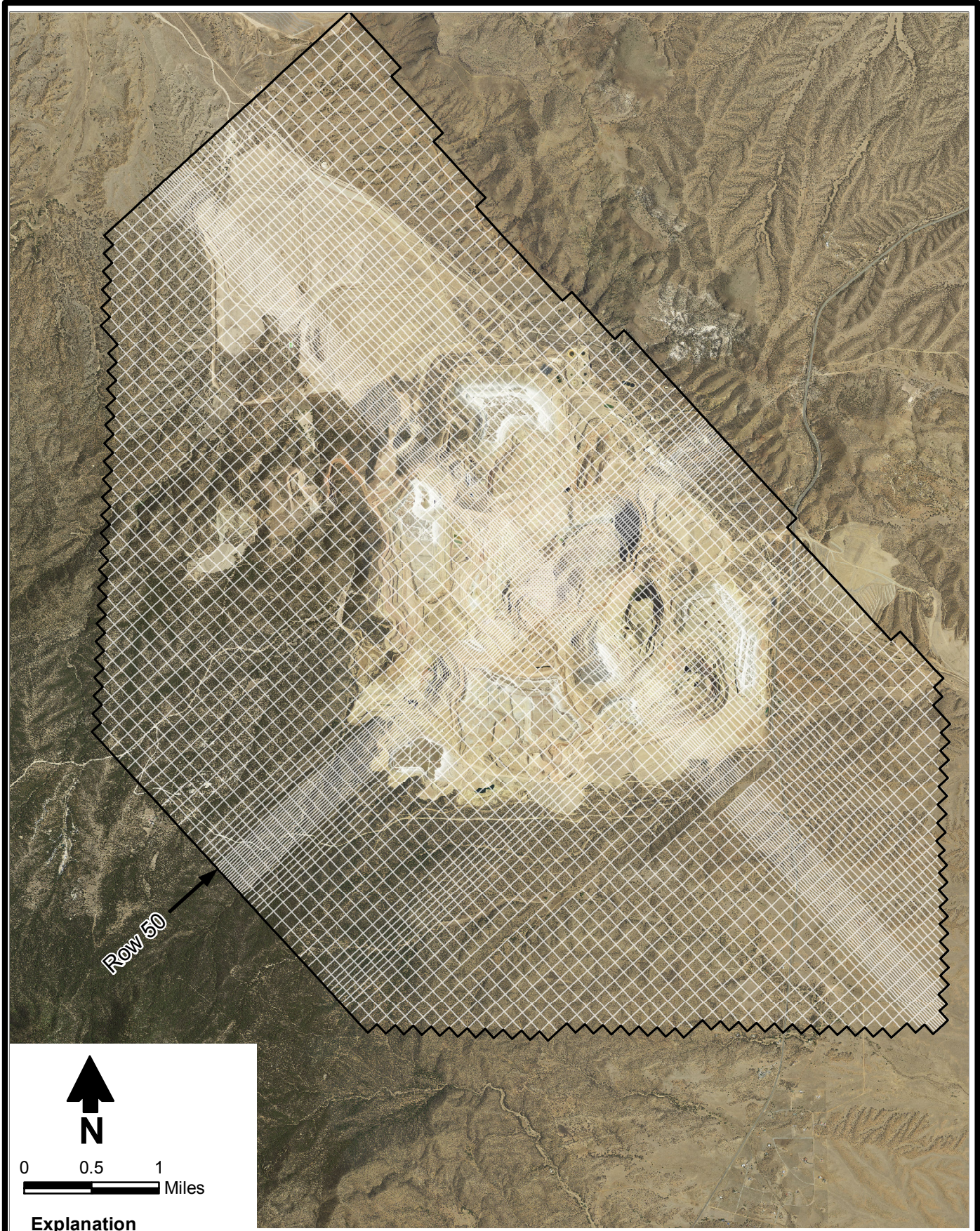
Source: Aerial photograph from NAIP, 2011

**FREEPORT-McMORAN**  
**COPPER & GOLD**  
 TYRONE STAGE 2 APP

**Approximate Surface Geologic Contacts  
 Between Major Rock Types at Tyrone**





S:\PROJECTS\MINE\_TYRONE\GIS\MXD\ES09.0176\MXD\SI\REPORT\_11-11\FIGC-04\_ACTIVE\_MODEL\_GRID.MXD



0 0.5 1  
Miles

**Explanation**

-  Active model boundary
-  Model grid cell

Source: Aerial photograph from NAIP, 2011



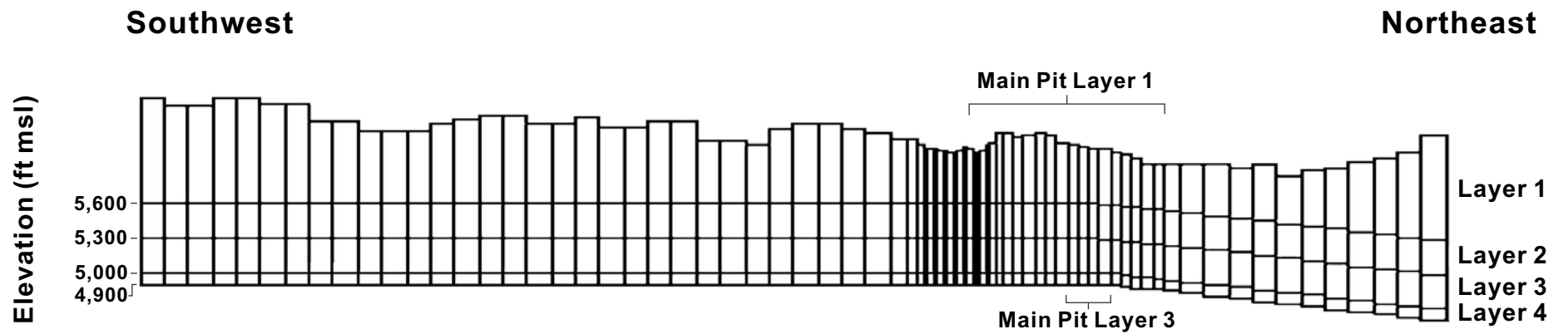
**TYRONE STAGE 2 APP  
Plan View of Active Model Grid**



**Daniel B. Stephens & Associates, Inc.**  
01/16/2012 JN ES09.0176

Figure C-4





Note: See Figure 5 for location of model row 50



TYRONE STAGE 2 APP

### Vertical Profile of Model Grid from Southwest to Northeast along Model Row 50 Through the Main Pit

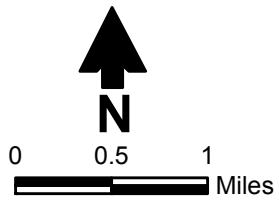
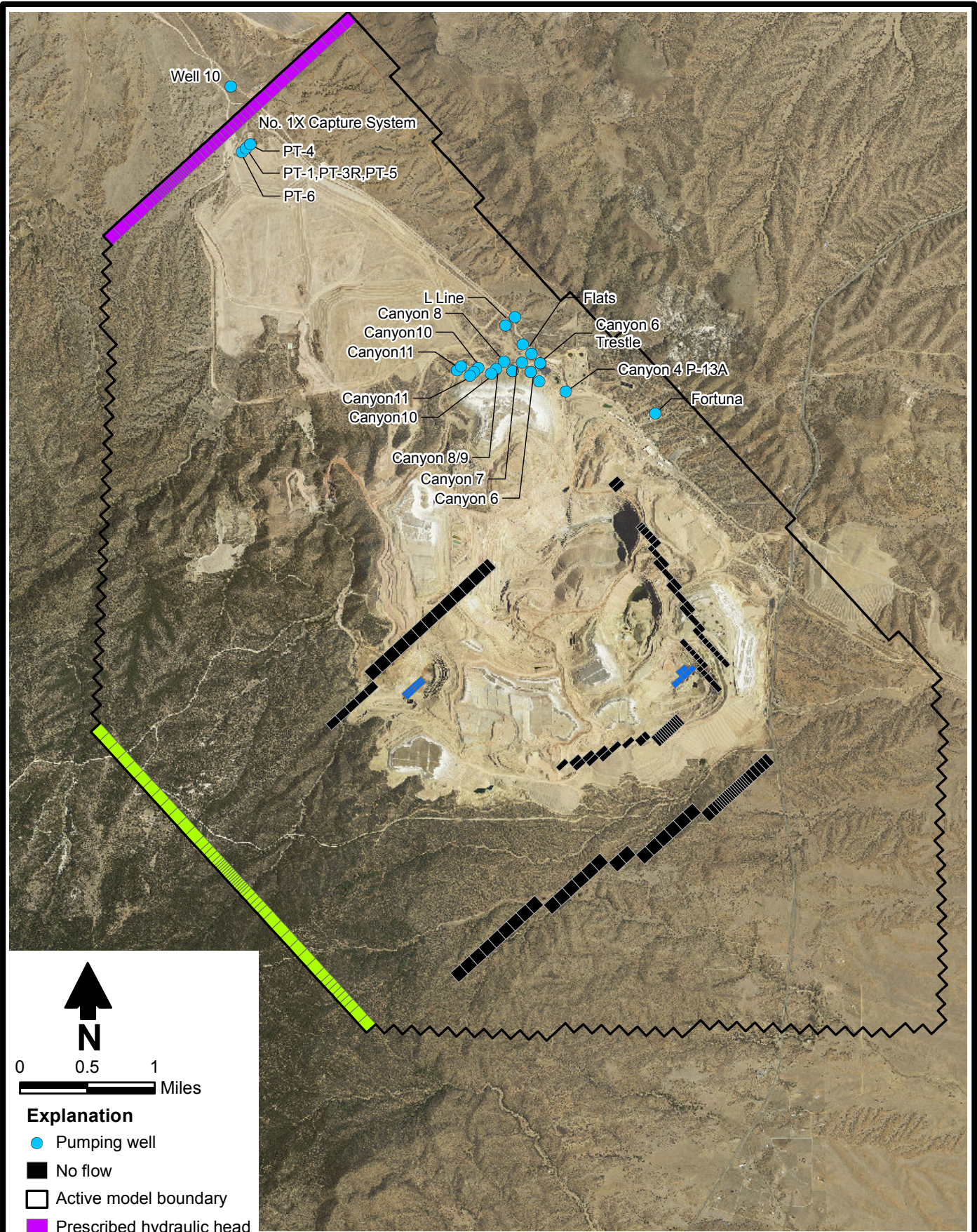
Figure C-5



Daniel B. Stephens & Associates, Inc.  
01/16/2012 JN ES09.0176



S:\PROJECTS\MINE\_TYRONE\GIS\MXD\SIES09.0176\MXD\S\REPORT\_11-11\FIGC-06\_BOUNDARY\_CONDITIONS\_LAYER1.MXD



**Explanation**

- Pumping well
- No flow
- Active model boundary
- Prescribed hydraulic head
- ➔ Drain cell (outflow)
- Prescribed inflow

Source: Aerial photograph from NAIP, 2011



TYRONE STAGE 2 APP

**Boundary Conditions in Model Layer 1**

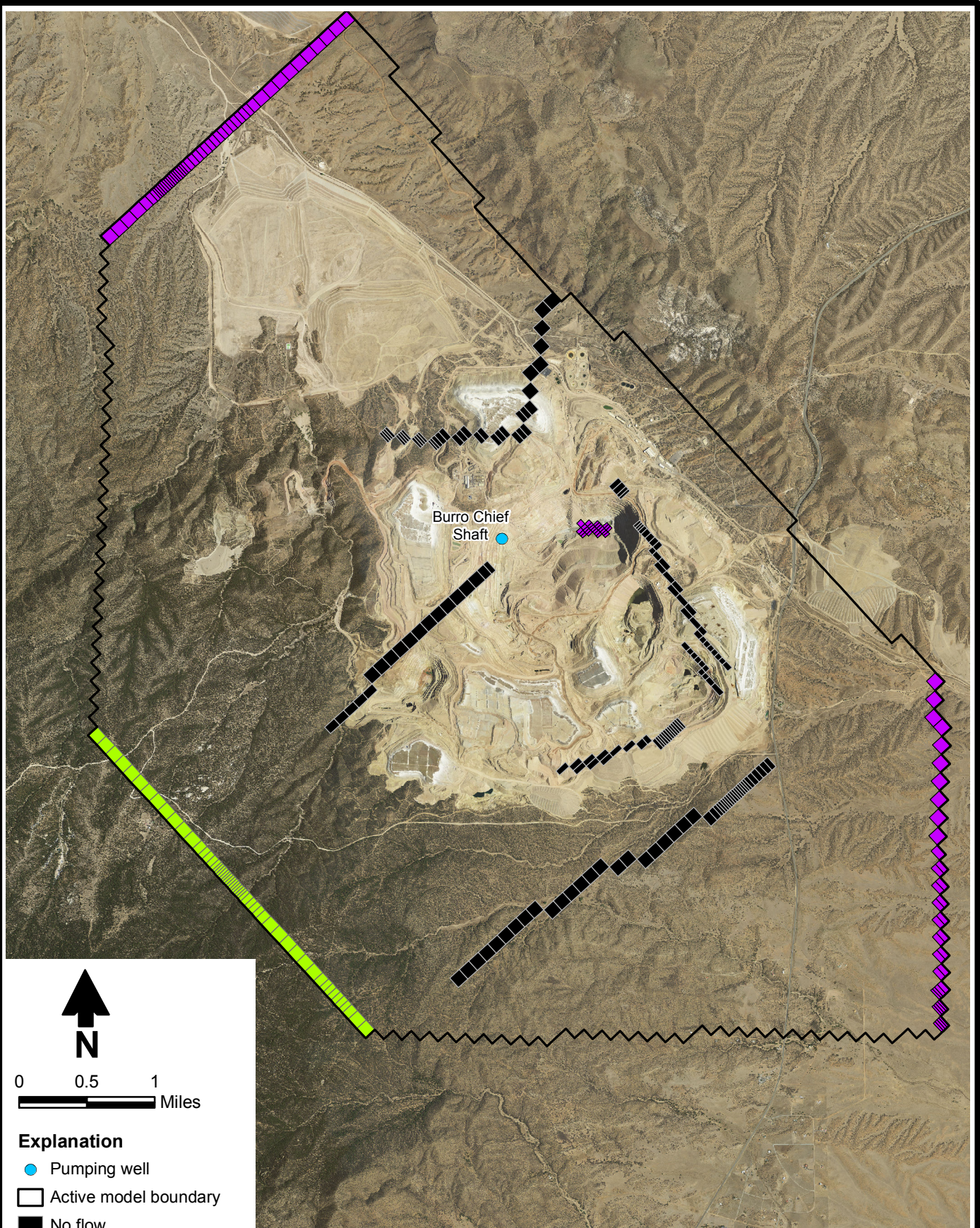


**Daniel B. Stephens & Associates, Inc.**  
 1/24/2012 JN ES09.0176

Figure C-6



S:\PROJECTS\MINE\_TYRONE\GIS\XDS\ES09.0176\MXD\REPORT\_11-11\FIG-C-07\_BOUNDARY\_CONDITIONS\_LAYER2.MXD



0 0.5 1  
Miles

**Explanation**

- Pumping well
- Active model boundary
- No flow
- Prescribed hydraulic head
- Prescribed inflow

Source: Aerial photograph from NAIP, 2011



TYRONE STAGE 2 APP  
**Boundary Conditions in Model Layer 2**

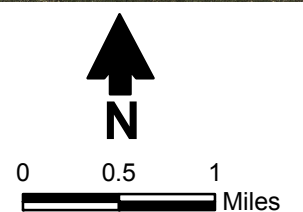
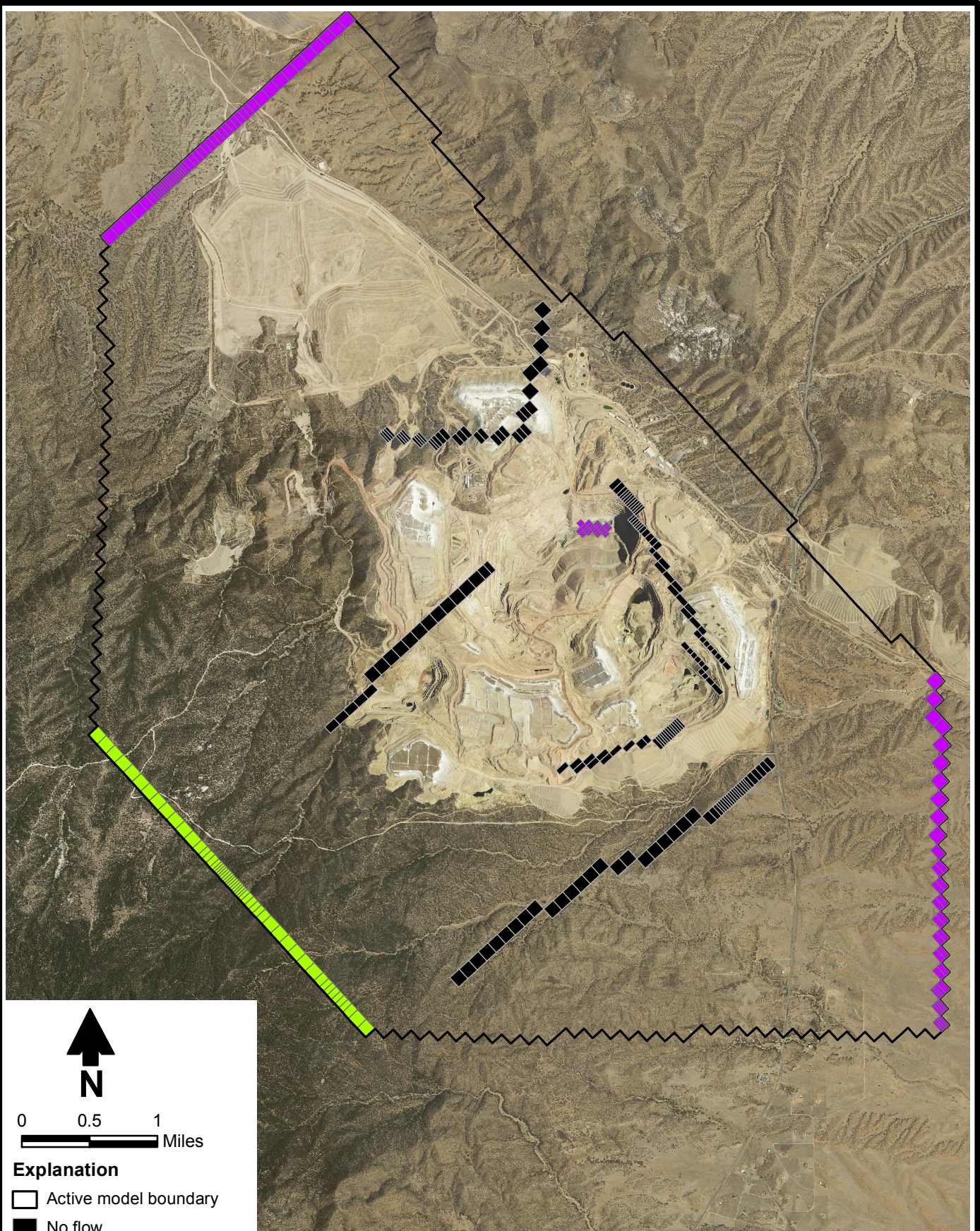






*Daniel B. Stephens & Associates, Inc.*  
01/16/2012 JN ES09.0176

Figure C-7



S:\PROJECTS\MINE\_TYRONE\GIS\MXD\ES09.0176\MXD\REPORT\_11-11\FIGC-08\_BOUNDARY\_CONDITIONS\_LAYER3.MXD



- Explanation**
-  Active model boundary
  -  No flow
  -  Prescribed hydraulic head
  -  Prescribed inflow

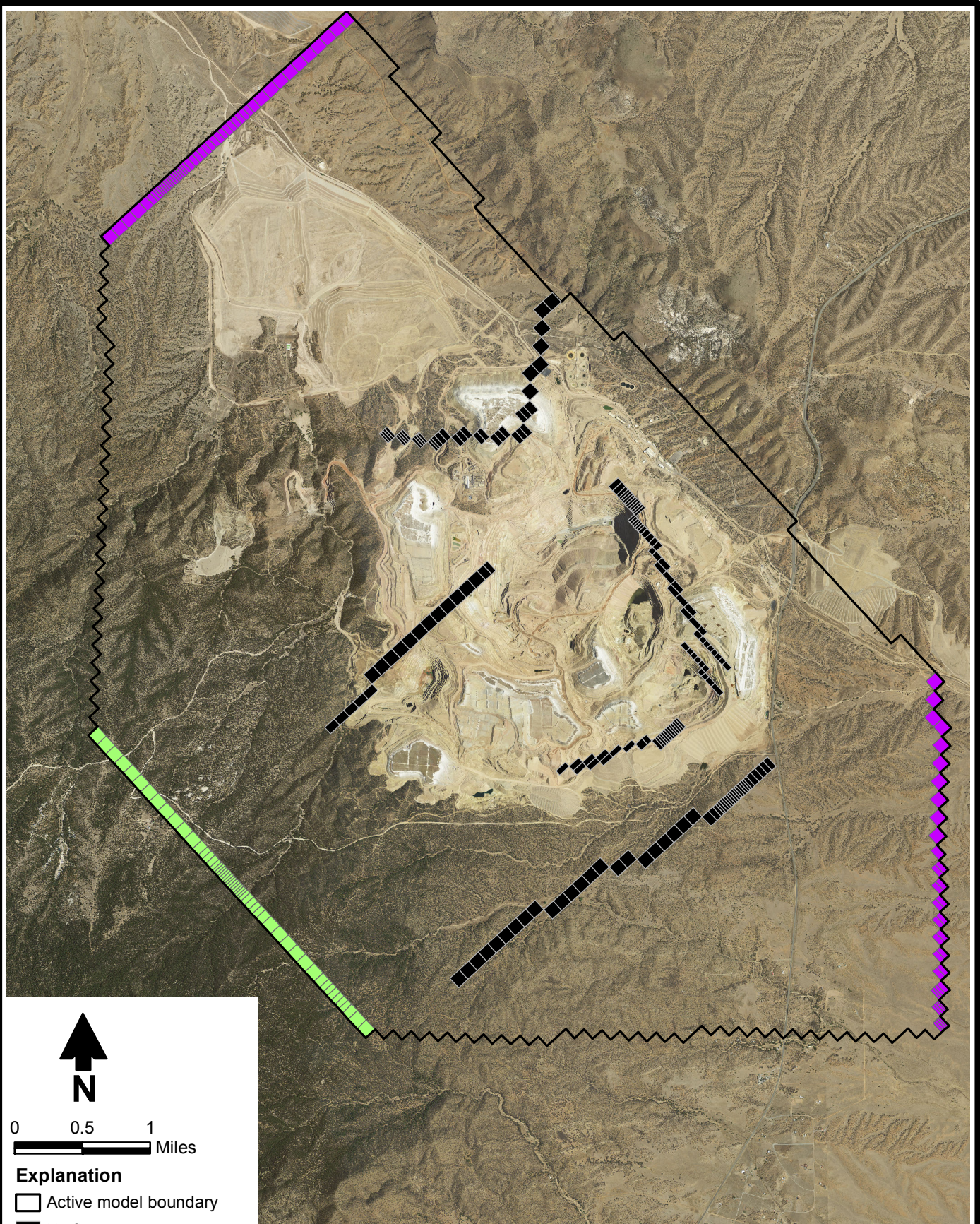
Source: Aerial photograph from NAIP, 2011



TYRONE STAGE 2 APP  
**Boundary Conditions in Model Layer 3**







S:\PROJECTS\MINE\_TYRONE\GIS\MXD\SIREPORT\_11-11\FIGC-09\_BOUNDARY\_CONDITIONS\_LAYER4.MXD



0 0.5 1  
Miles

**Explanation**

-  Active model boundary
-  No flow
-  Prescribed hydraulic head
-  Prescribed inflow

Source: Aerial photograph from NAIP, 2011



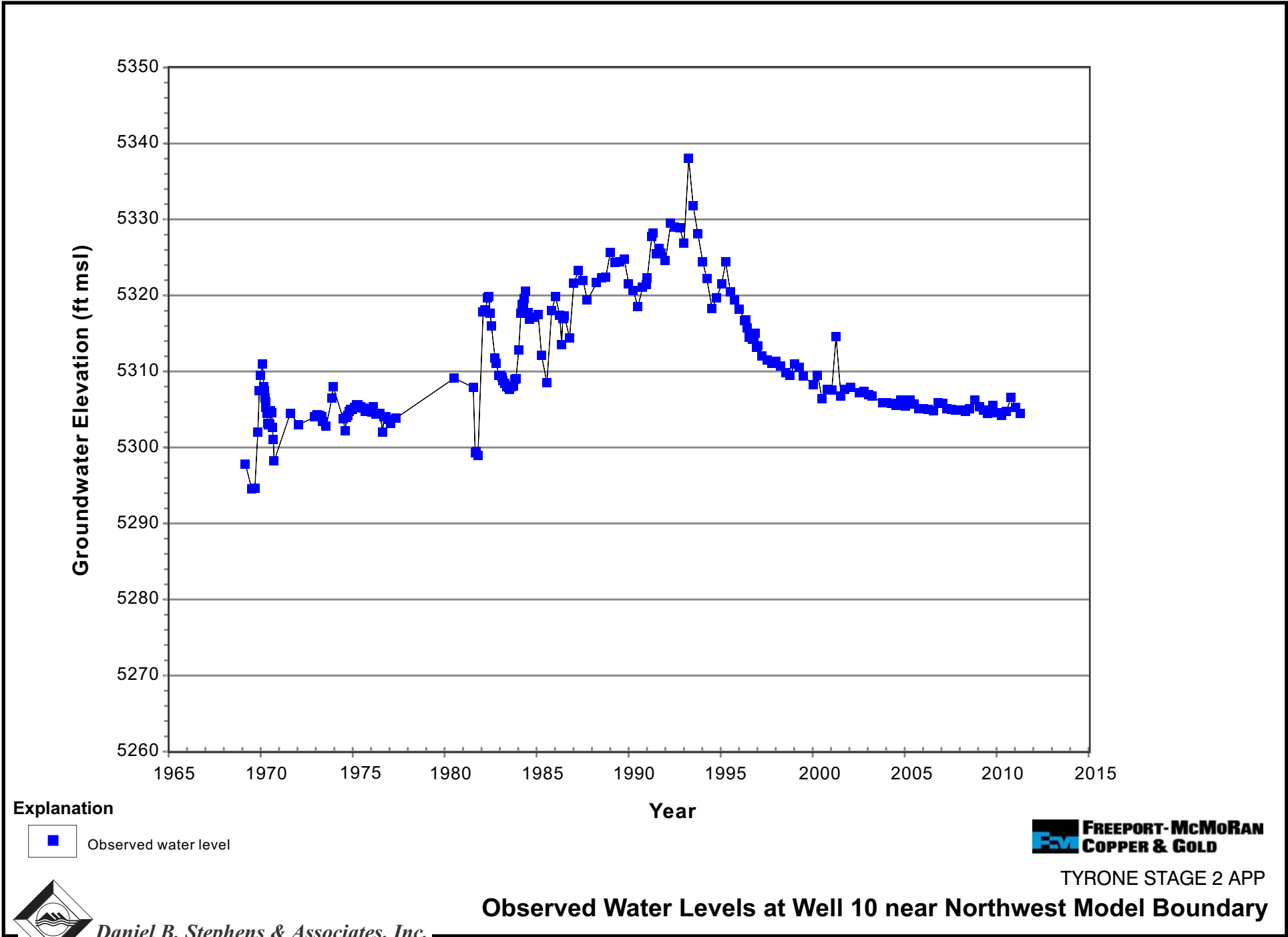
TYRONE STAGE 2 APP  
**Boundary Conditions in Model Layer 4**



**Daniel B. Stephens & Associates, Inc.**  
01/16/2012 JN ES09.0176

Figure C-9





Explanation

- Observed water level



TYRONE STAGE 2 APP

Observed Water Levels at Well 10 near Northwest Model Boundary

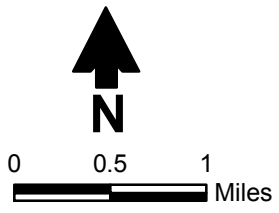
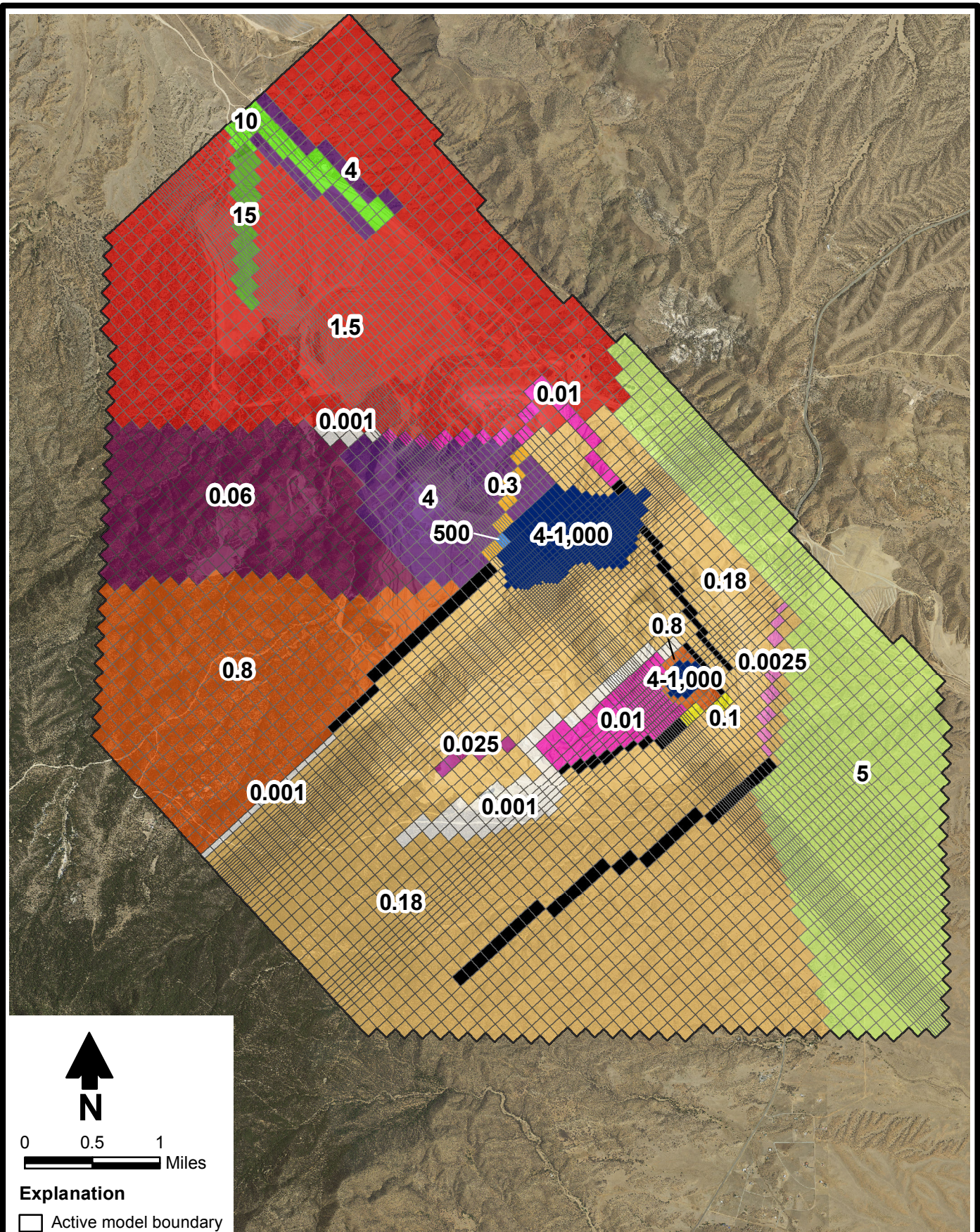
Figure C-10



Daniel B. Stephens & Associates, Inc.  
01/16/2012 JN ES09.0176



S:\PROJECTS\MINE\_TYRONE\GIS\XDS\ES09.0176\XDS\REPORT\_11-11\FIGC-11\_HYDRAULIC\_CONDUCTIVITY\_LAYER1.MXD



**Explanation**

- Active model boundary
- No-flow model cell

0.8 Hydraulic conductivity (ft/d)

Source: Aerial photograph from NAIP, 2011



TYRONE STAGE 2 APP

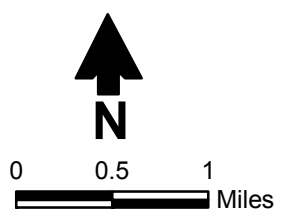
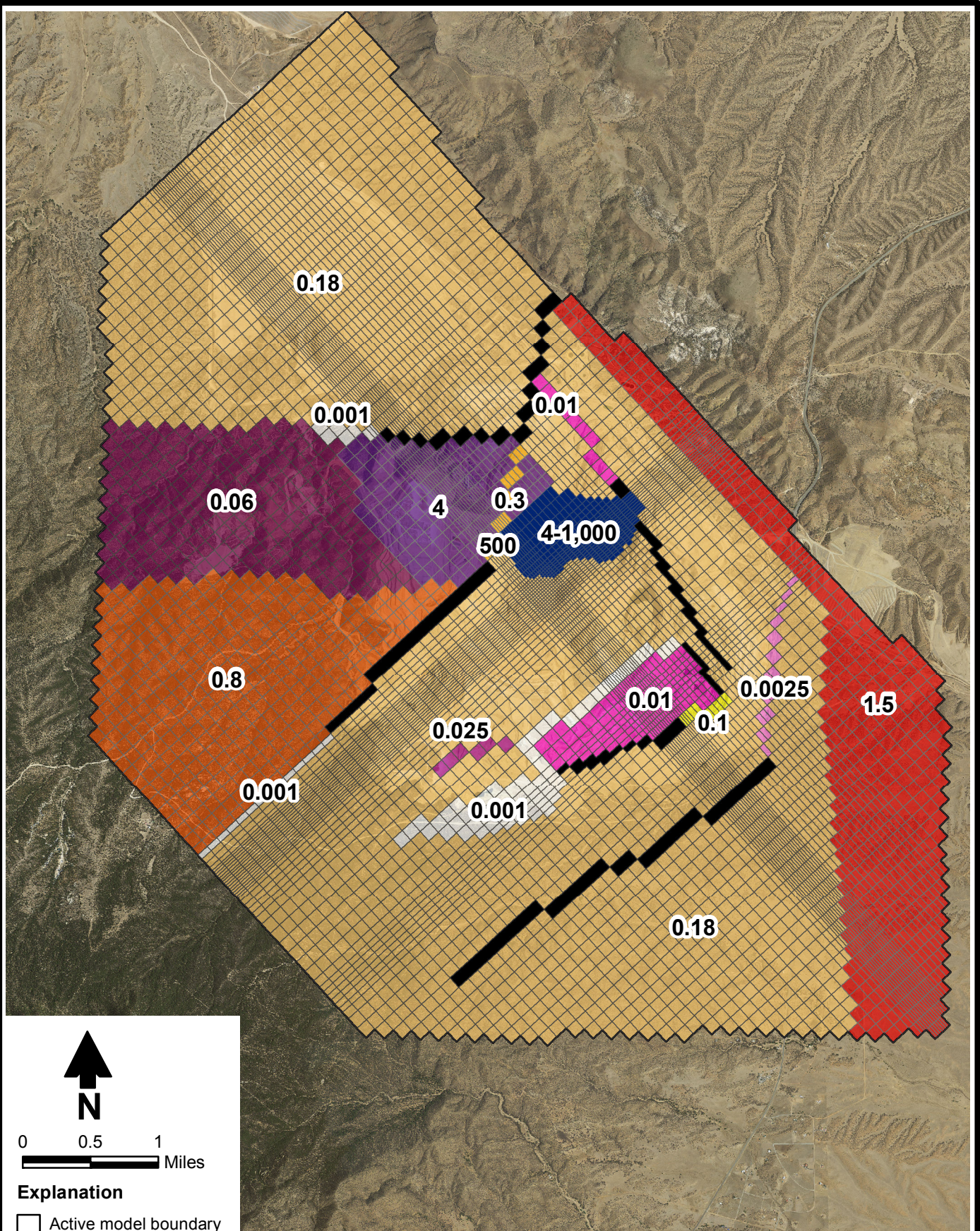
### Hydraulic Conductivity in Model Layer 1





Figure C-11



S:\PROJECTS\MINE\_TYRONE\GIS\MXD\ES09.0176\MXD\REPORT\_11-11\FIGC-12\_HYDRAULIC\_CONDUCTIVITY\_LAYER2.MXD



**Explanation**

-  Active model boundary
-  No-flow model cell
- 0.8** Hydraulic conductivity (ft/d)

Source: Aerial photograph from NAIP, 2011



TYRONE STAGE 2 APP

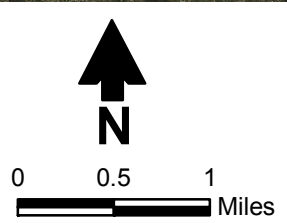
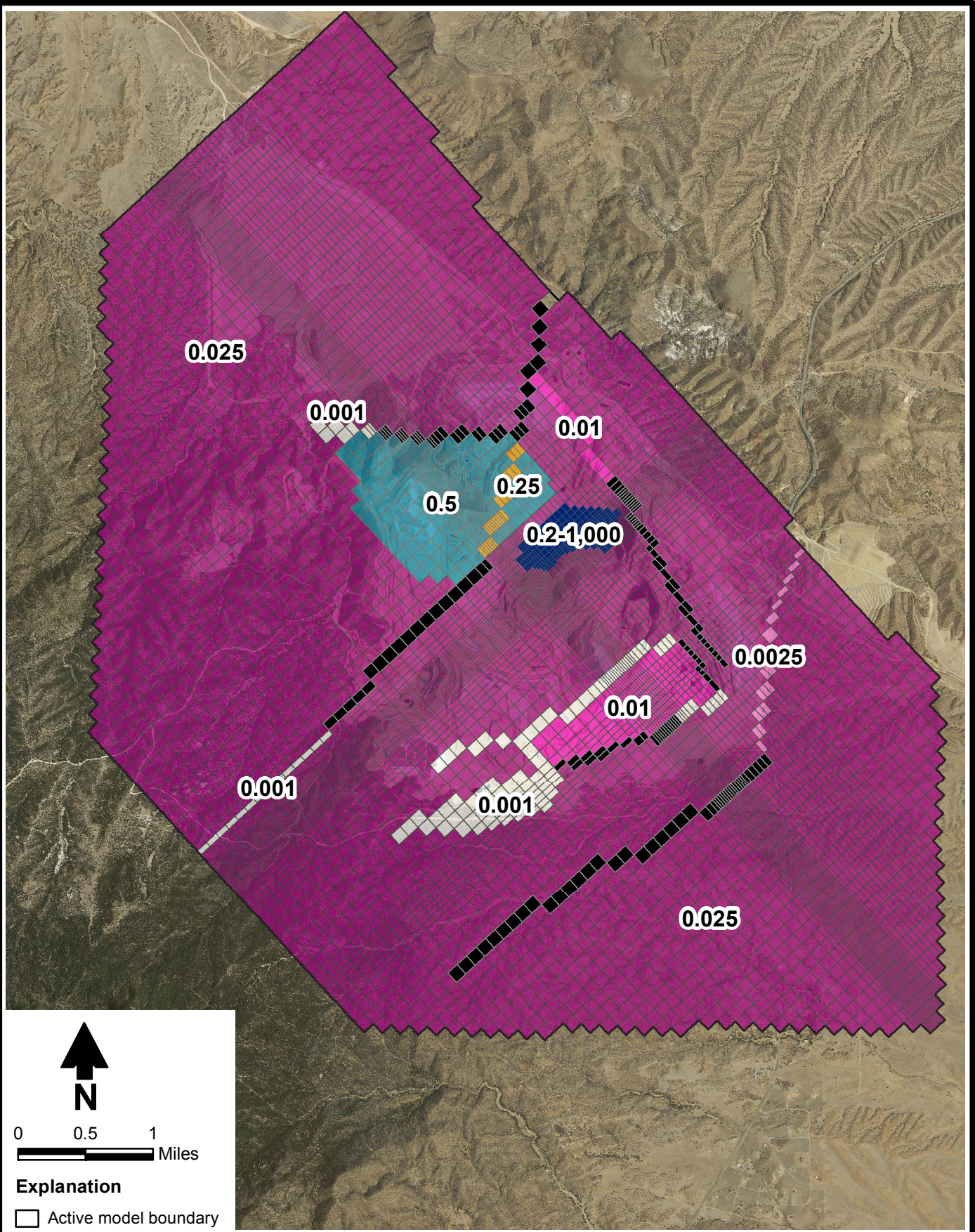
**Hydraulic Conductivity in Model Layer 2**



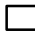

Figure C-12



S:\PROJECTS\MINE\_TYRONE\GIS\MXD\ES09.0176\MXD\REPORT\_11-11\FIG-C-13\_HYDRAULIC\_CONDUCTIVITY\_LAYER3.MXD



**Explanation**

-  Active model boundary
-  No-flow model cell
- 0.5** Hydraulic conductivity (ft/d)

Source: Aerial photograph from NAIP, 2011



TYRONE STAGE 2 APP

### Hydraulic Conductivity in Model Layer 3

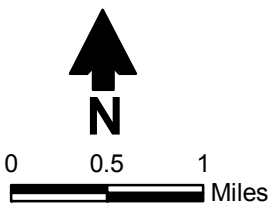
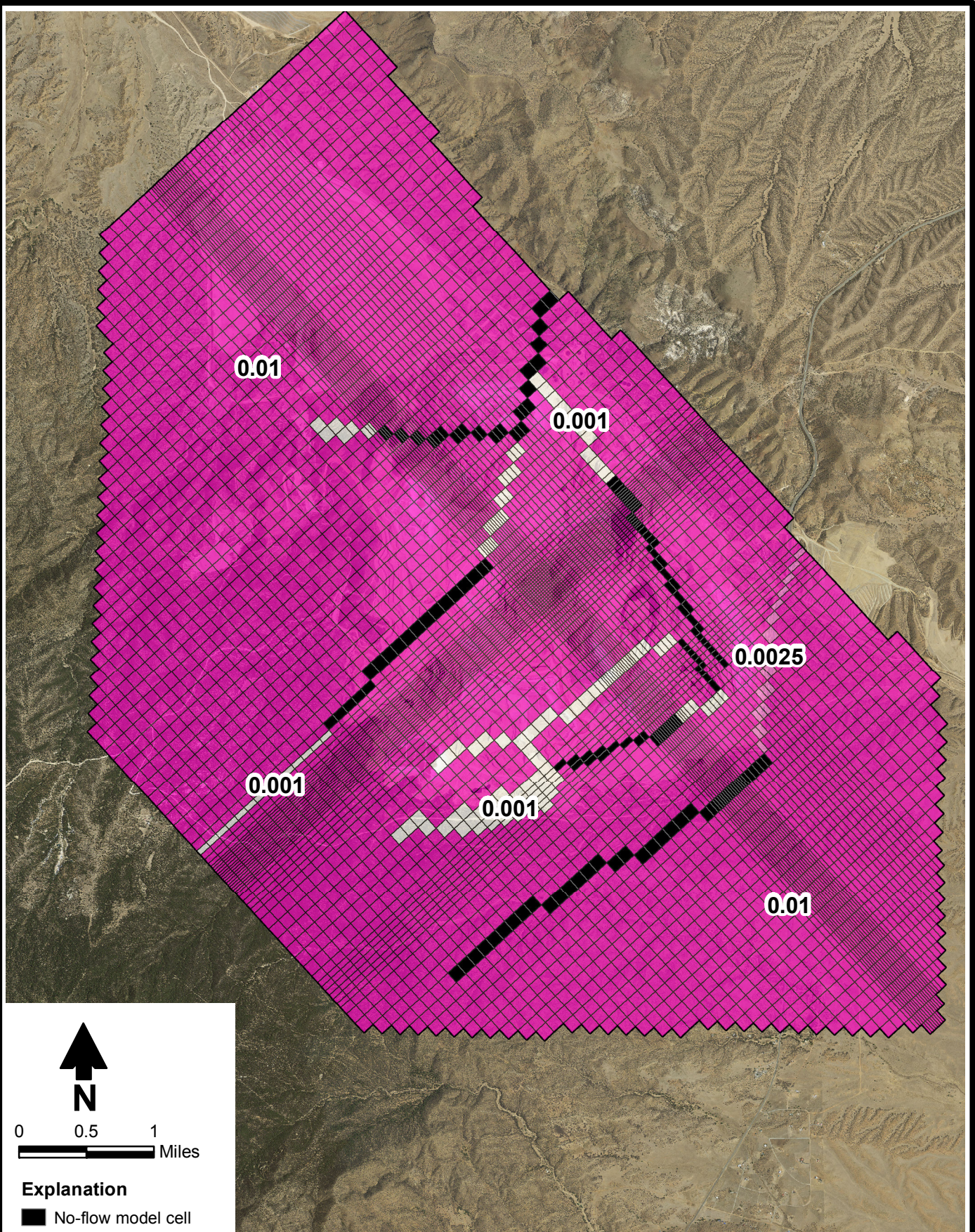


**Daniel B. Stephens & Associates, Inc.**  
 01/16/2012 JN ES09.0176



Figure C-13



S:\PROJECTS\MINE\_TYRONE\GIS\MXD\SIES09.0176\MXD\SIREPORT\_11-11\FIGC-14\_HYDRAULIC\_CONDUCTIVITY\_LAYER4.MXD



**Explanation**

-  No-flow model cell
-  Active model boundary
- 0.01** Hydraulic conductivity (ft/d)

Source: Aerial photograph from NAIP, 2011

**FREEPORT-McMoRAN**  
**COPPER & GOLD**

TYRONE STAGE 2 APP

### Hydraulic Conductivity in Model Layer 4



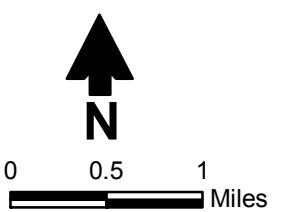
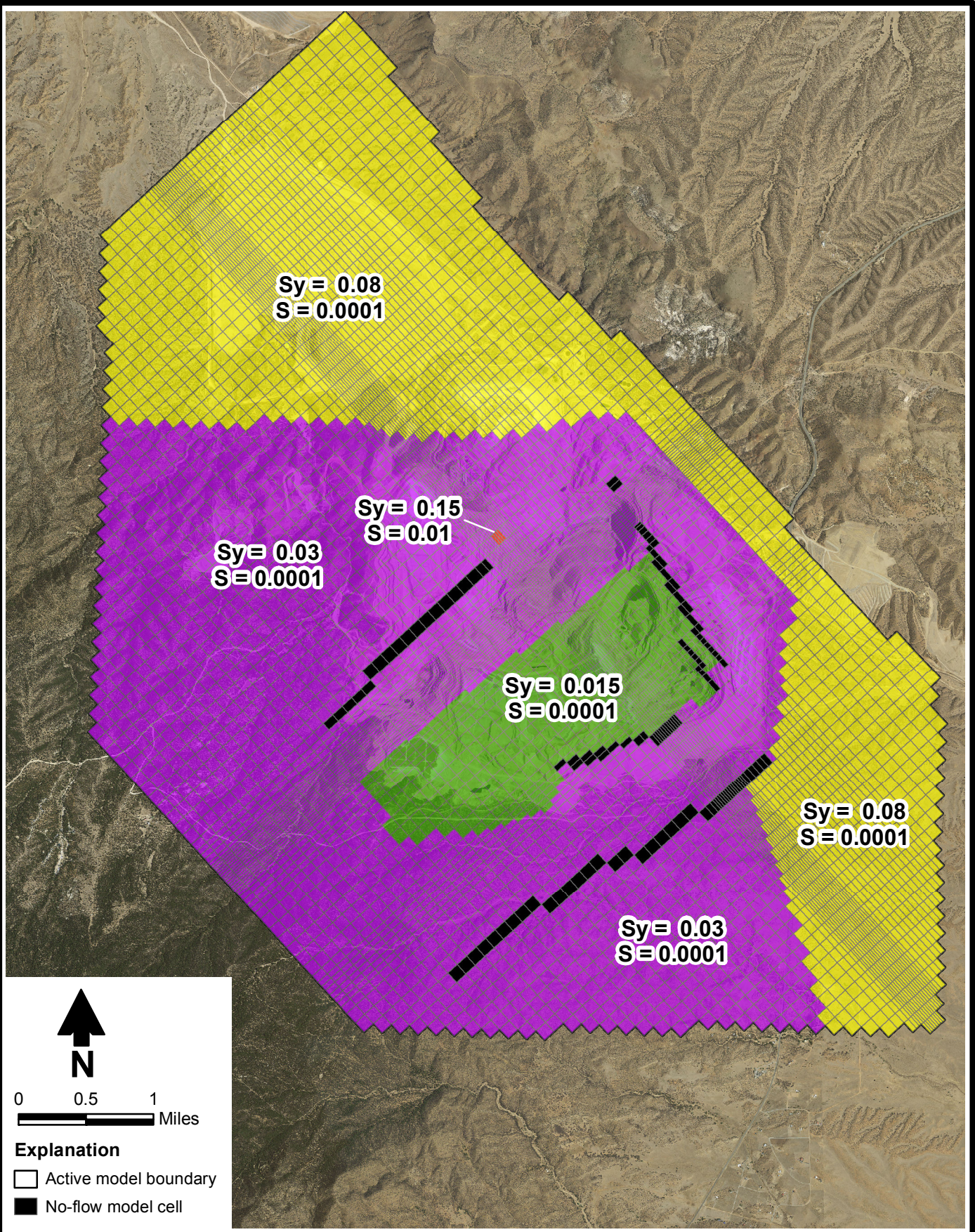
**Daniel B. Stephens & Associates, Inc.**  
01/16/2012

JN ES09.0176

Figure C-14



S:\PROJECTS\MINE\_TYRONE\GIS\MXD\ES09.0176\MXD\REPORT\_11-11\FIG-C-15\_STORAGE\_LAYER 1.MXD



**Explanation**

- Active model boundary
- No-flow model cell

**Notes:**  
 $S_y$  = Specific yield  
 S = Storativity

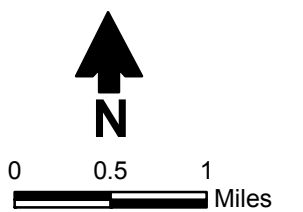
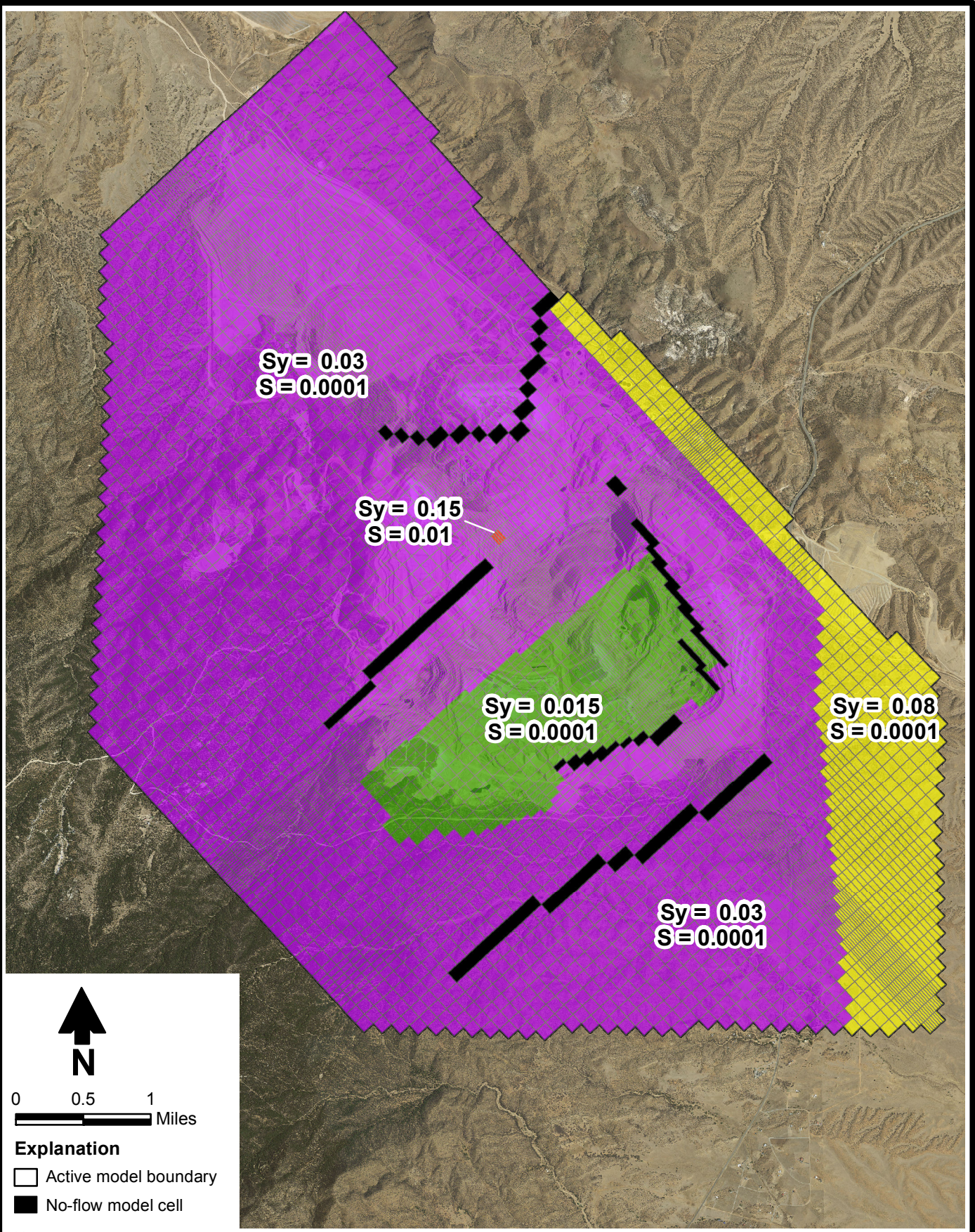
Source: Aerial photograph from NAIP, 2011

**F-M** **FREEPORT-McMoRAN**  
**COPPER & GOLD**

TYRONE STAGE 2 APP  
**Storage in Model Layer 1**



S:\PROJECTS\MINE\_TYRONE\GIS\MXD\ES09.0176\MXD\REPORT\_11-11\FIG-C-16\_STORAGE\_LAYER2.MXD



**Explanation**

□ Active model boundary

■ No-flow model cell

Notes:  
 $S_y$  = Specific yield  
 $S$  = Storativity

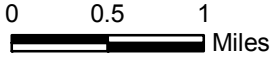
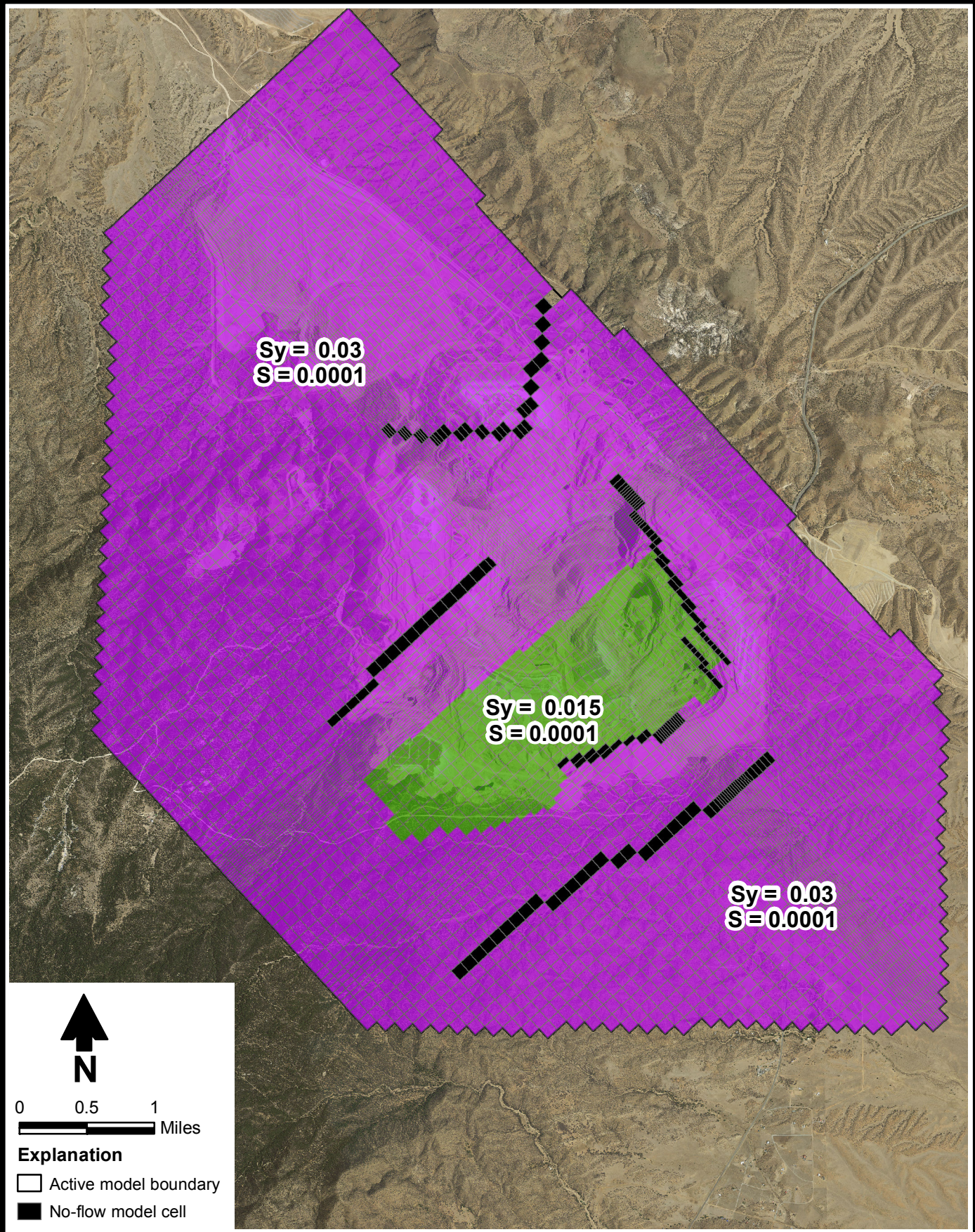
Source: Aerial photograph from NAIP, 2011



**TYRONE STAGE 2 APP  
Storage in Model Layer 2**



S:\PROJECTS\MINE\_TYRONE\GIS\MXD\S\REPORT\_11-11\FIG-C-17\_STORAGE\_LAYER3.MXD



- Explanation**
- Active model boundary
  - No-flow model cell

Notes:  
 $S_y$  = Specific yield  
 $S$  = Storativity

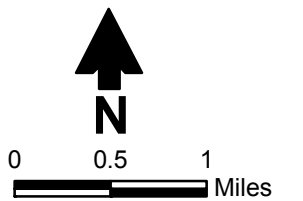
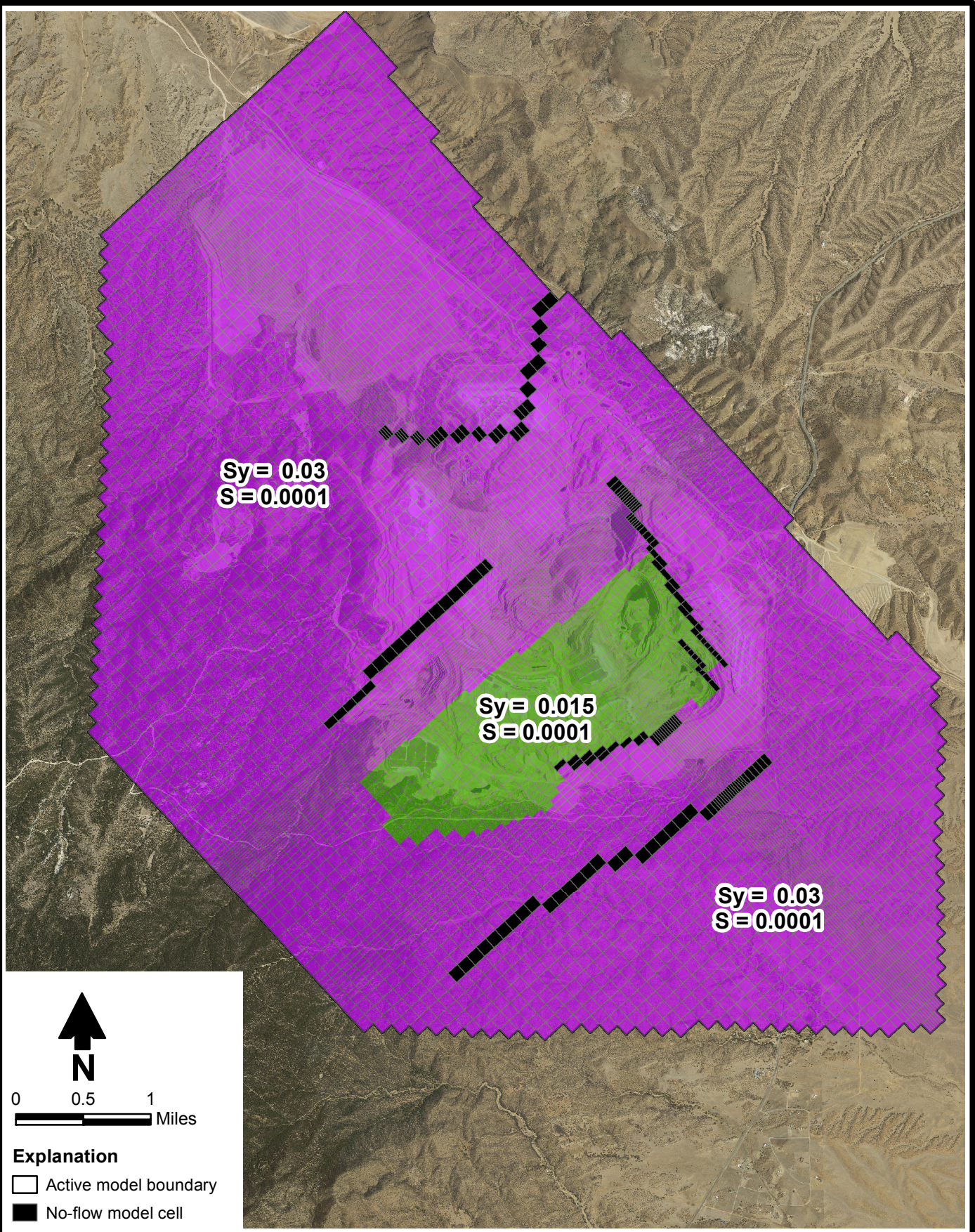
Source: Aerial photograph from NAIP, 2011



**TYRONE STAGE 2 APP  
 Storage in Model Layer 3**



S:\PROJECTS\MINE\_TYRONE\GIS\MXD\SI\ES09.0176\MXD\SI\REPORT\_11-11\FIGC-18\_STORAGE\_LAYER4.MXD



**Explanation**

- Active model boundary
- No-flow model cell

Notes:  
 Sy = Specific yield  
 S = Storativity

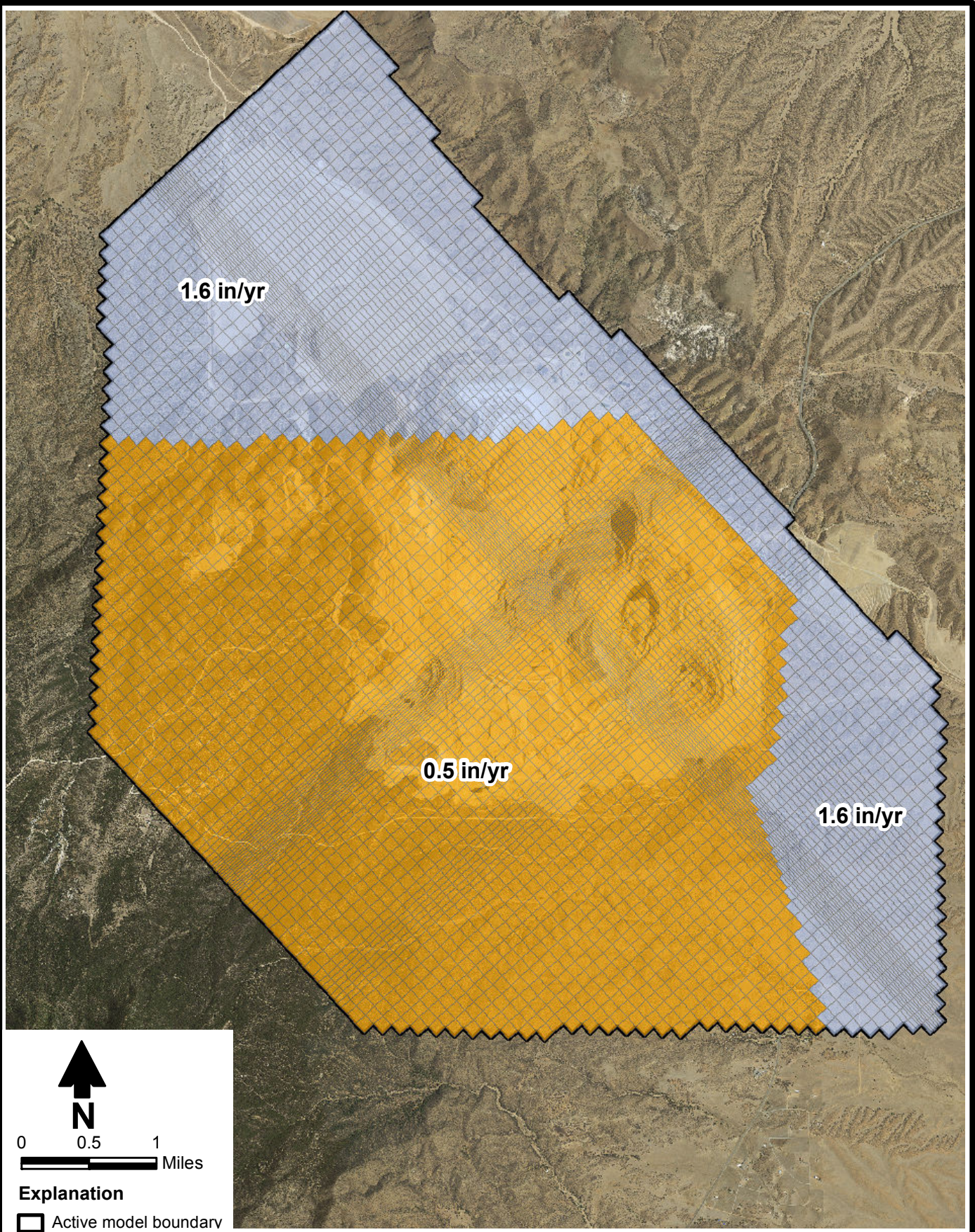
Source: Aerial photograph from NAIP, 2011


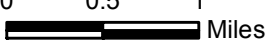





**TYRONE STAGE 2 APP  
 Storage in Model Layer 4**



S:\PROJECTS\MINE\_TYRONE\GIS\MXD\ES09.0176\MXD\SI\REPORT\_11-11\FIGC-19\_RECHARGE\_STEADY\_STATE.MXD



  
 0    0.5    1  
 Miles  
**Explanation**  
 Active model boundary  
 Igneous rock  
 Gila Conglomerate

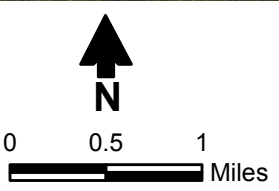
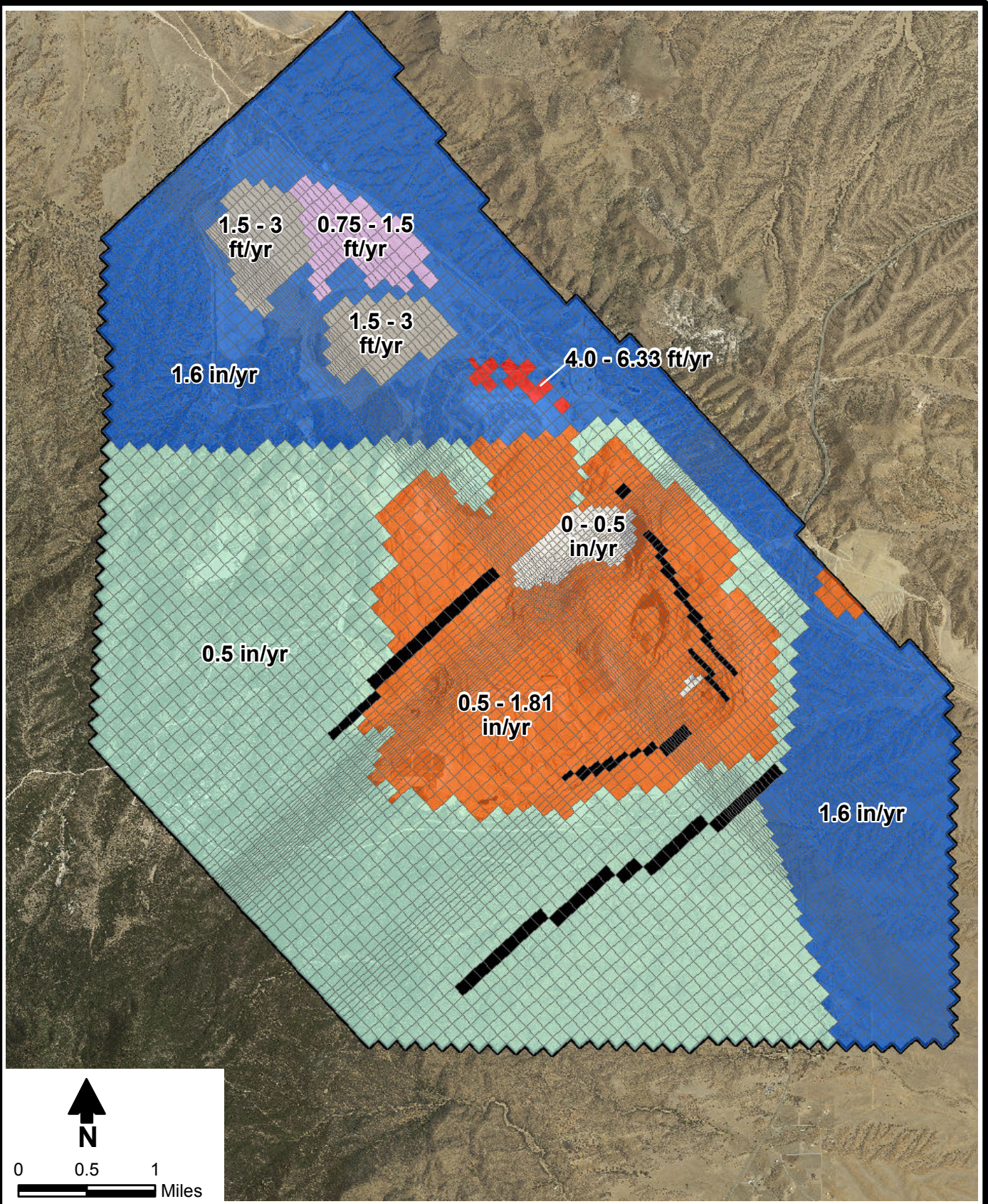
Source: Aerial photograph from NAIP, 2011





TYRONE STAGE 2 APP  
**Simulated Steady-State Recharge**



S:\PROJECTS\MINE\_TYRONE\GIS\IMXDS\ES09.0176\IMXDS\STAGE\_2\_APP\_REPORT\_1-2012\FIGC-20\_SIMULATED\_POST-DEV\_GW\_RECHARGE.MXD



Source: Aerial photograph from NAIP, 2011

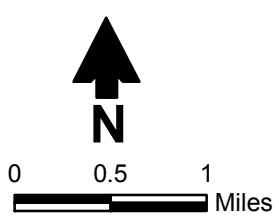
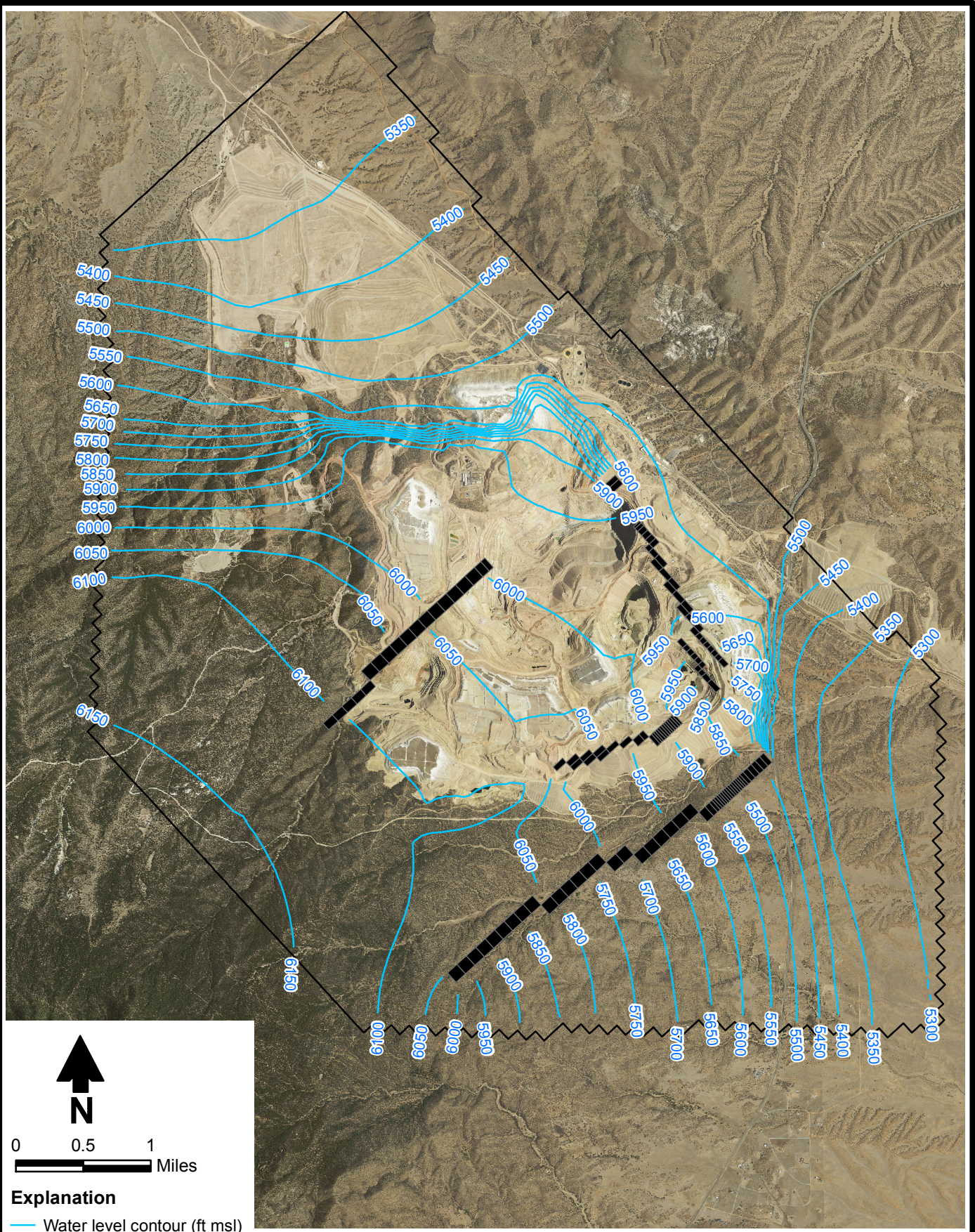
- Explanation**
-  Active model boundary
  -  No-flow model cell



TYRONE STAGE 2 APP  
**Simulated Post-Development  
 Groundwater Recharge**



S:\PROJECTS\MINE\_TYRONE\GIS\MXD\ES09.0176\MXD\REPORT\_11-11\FIGC-21\_WATER\_LEVEL\_CONTOUR\_STEADY\_STATE.MXD



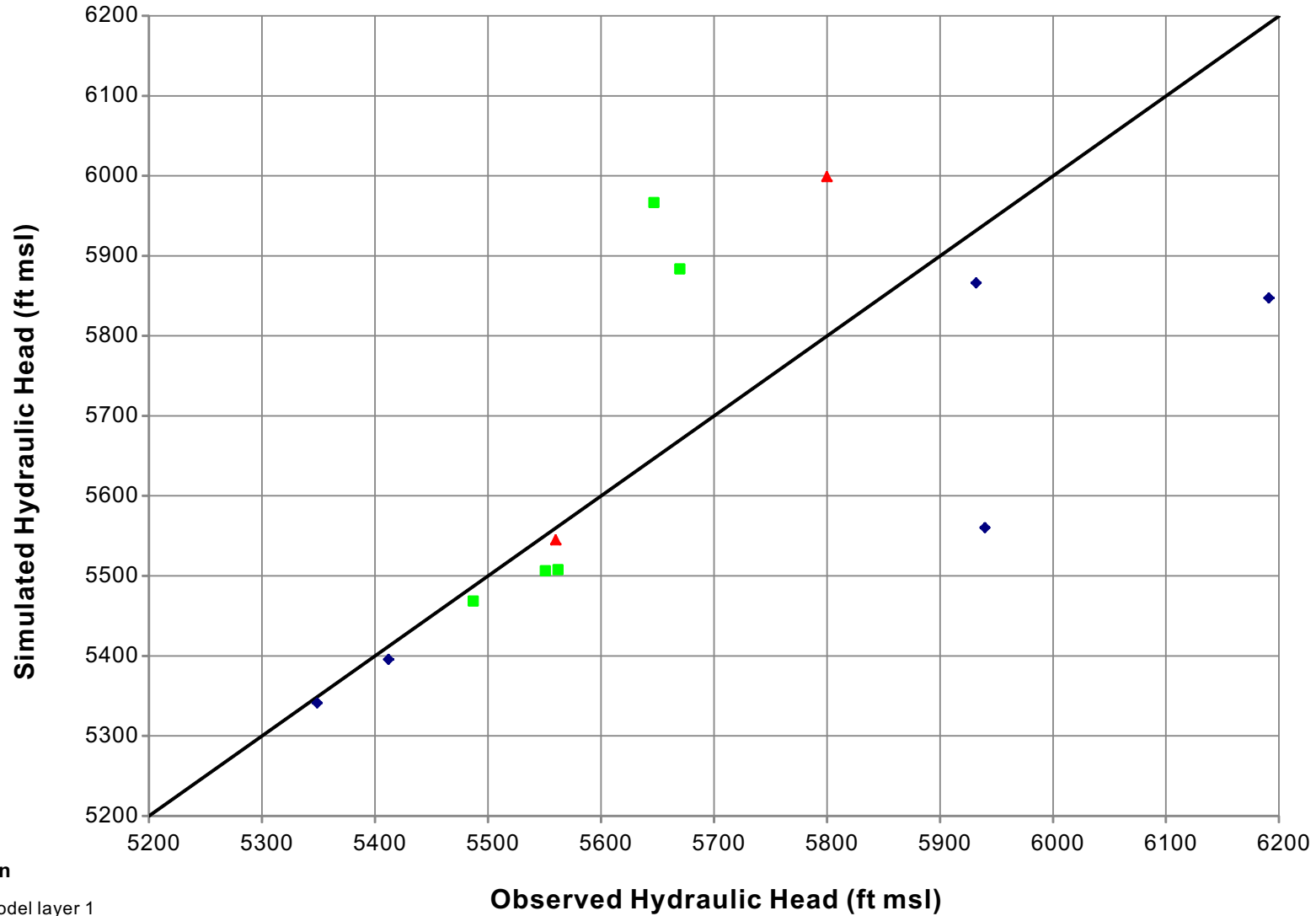
- Explanation**
- Water level contour (ft msl)
  - Active model boundary
  - No-flow model cell

Source: Aerial photograph from NAIP, 2011






**TYRONE STAGE 2 APP  
Simulated Steady-State Water Table**





**Explanation**

-  Model layer 1
-  Model layer 2
-  Model layer 3



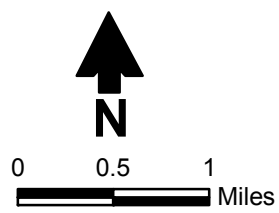
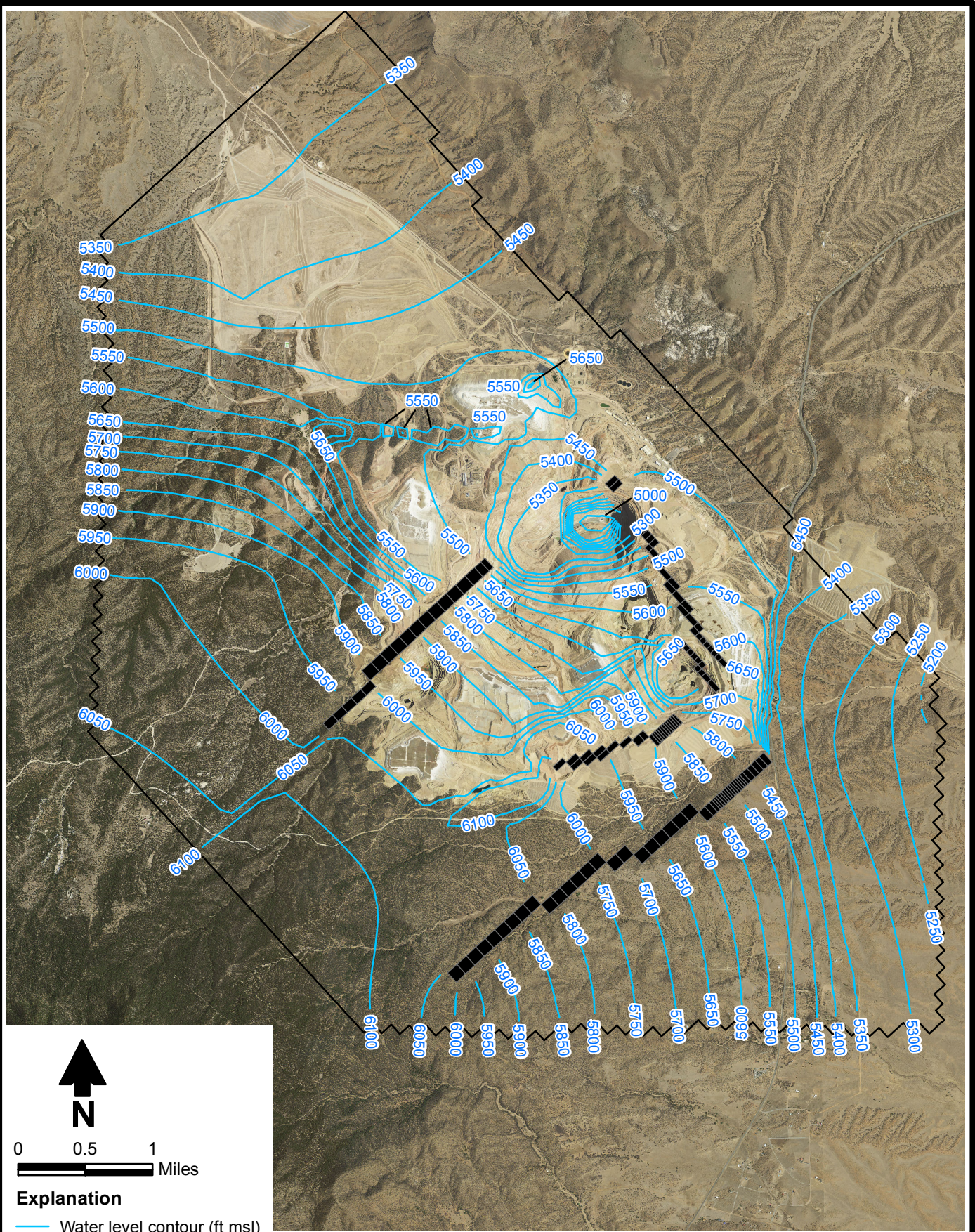
TYRONE STAGE 2 APP

**Simulated vs. Observed Hydraulic Heads for Steady-State Model**





S:\PROJECTS\MINE\_TYRONE\GIS\MXD\REPORT\_11-11\FIG-C-23\_WATER\_LEVEL\_CONTOUR\_2010.MXD



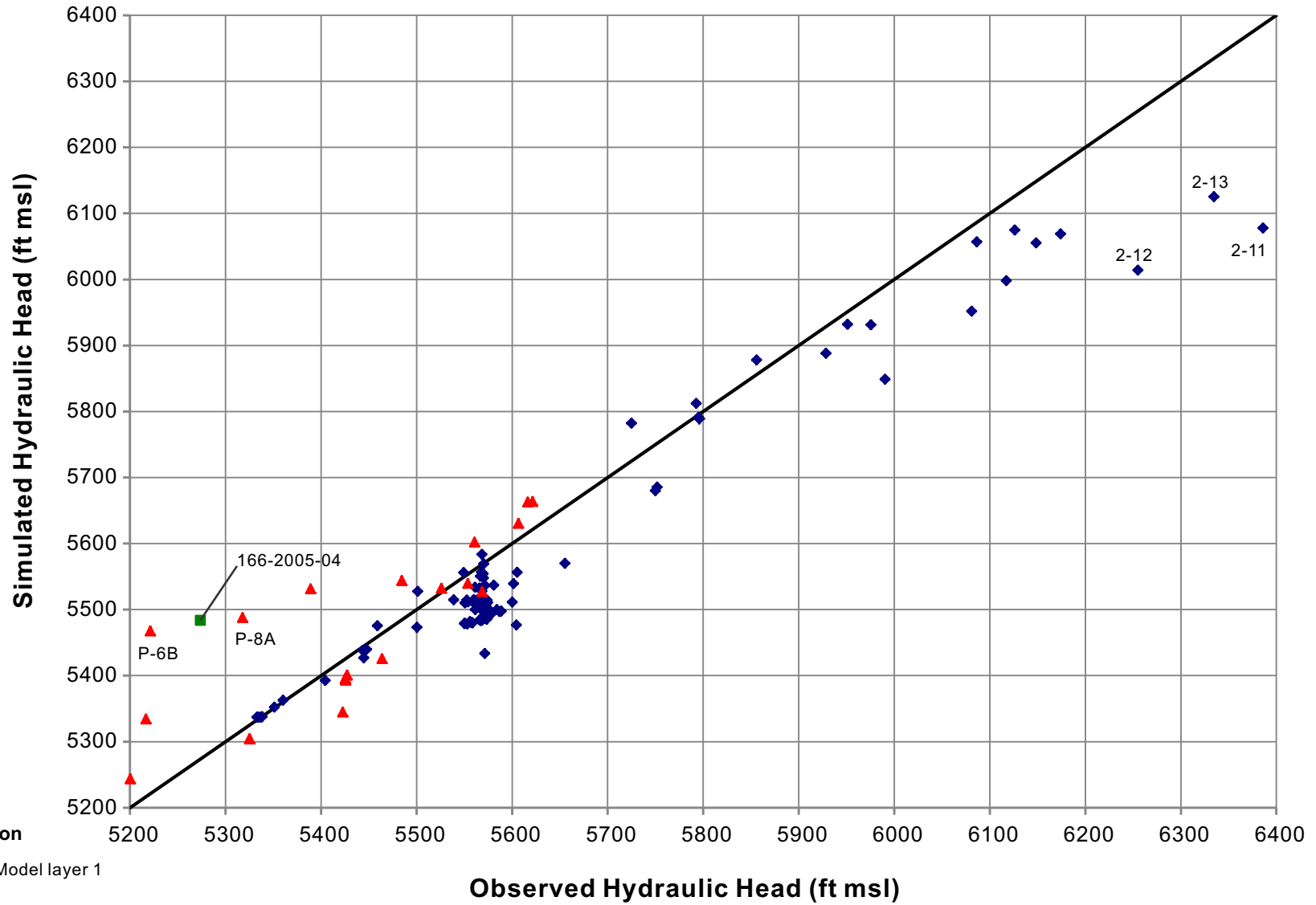
- Explanation**
- Water level contour (ft msl)
  - Active model boundary
  - No-flow model cell

Source: Aerial photograph from NAIP, 2011






TYRONE STAGE 2 APP  
**Simulated 2010 Water Table**





**Explanation**

-  Model layer 1
-  Model layer 2
-  Model layer 3



TYRONE STAGE 2 APP

**Simulated vs. Observed 2005 Hydraulic Heads**









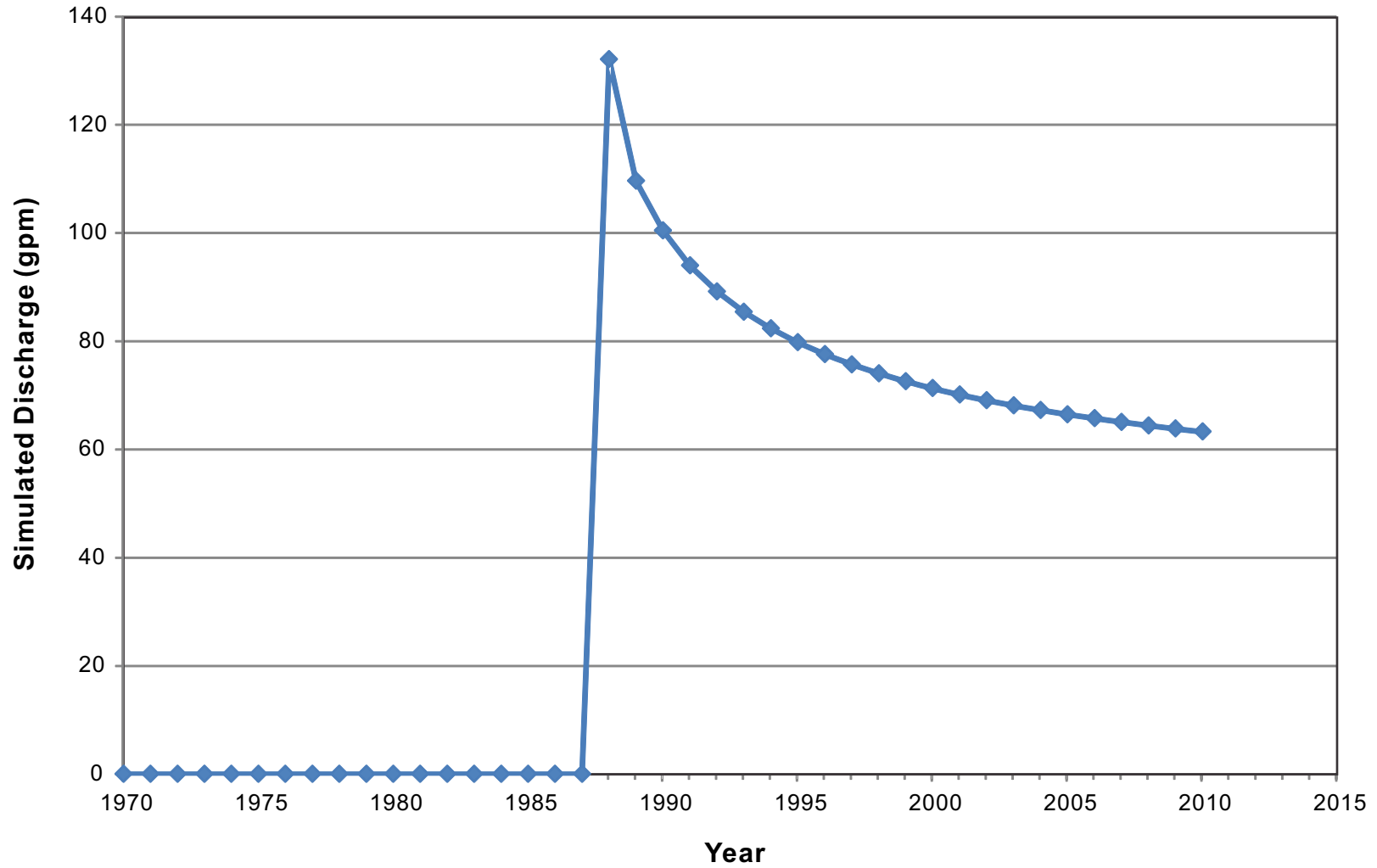
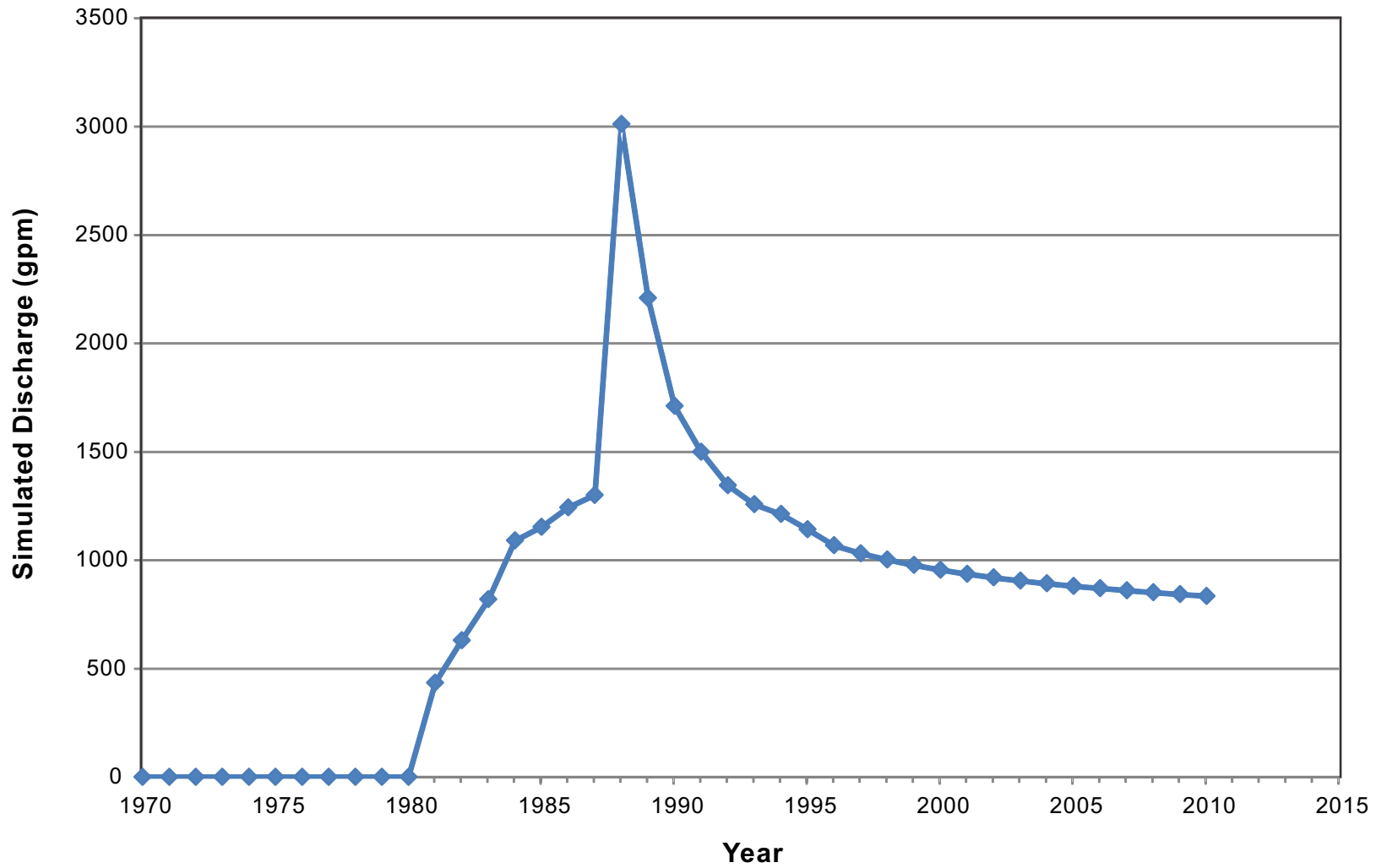


Figure C-26





TYRONE STAGE 2 APP

### Simulated Historical Groundwater Discharge to the Main Pit

Figure C-27



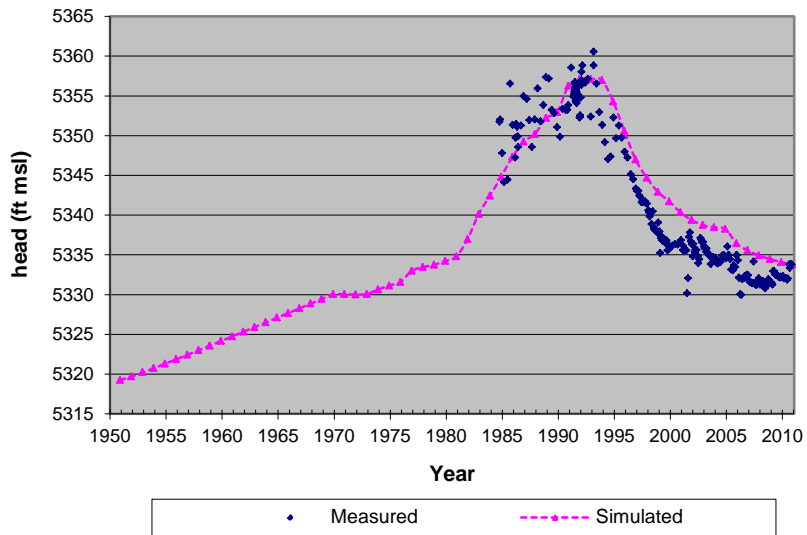
Daniel B. Stephens & Associates, Inc.  
01/16/2012 JN ES09.0176

**Attachment C-1**

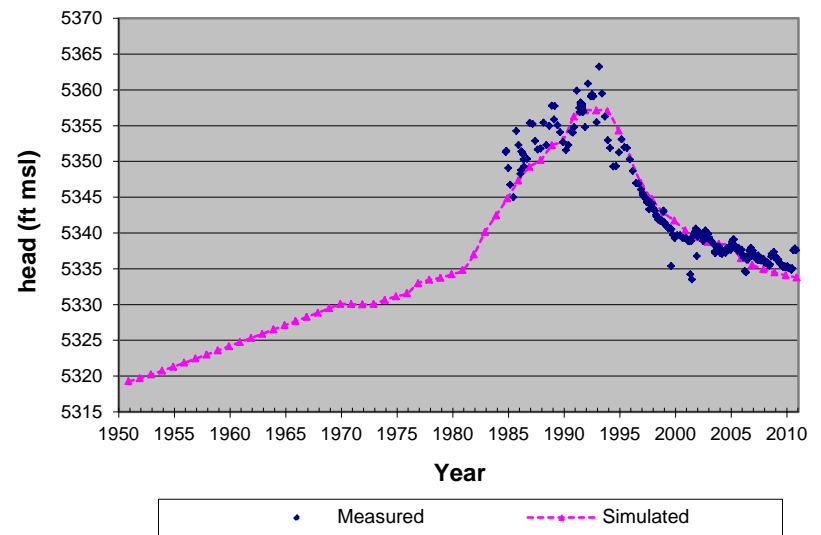
**Simulated and Observed  
Historical Water Levels**



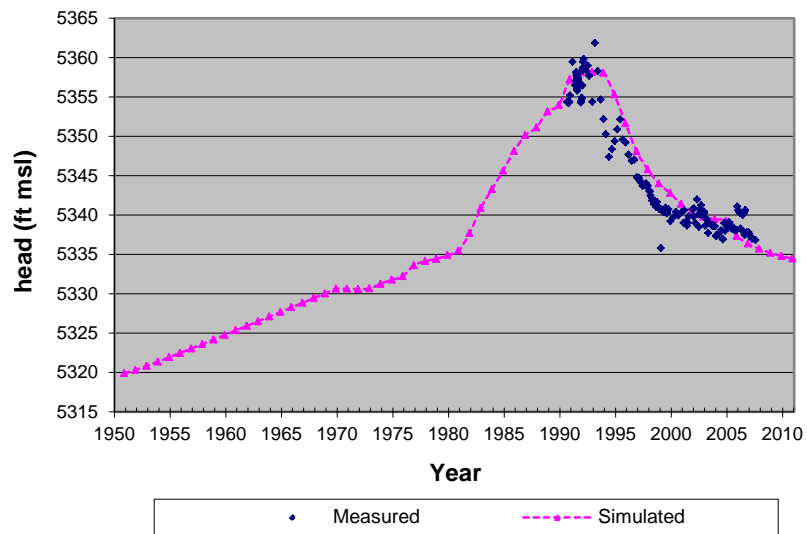
**Well 18**



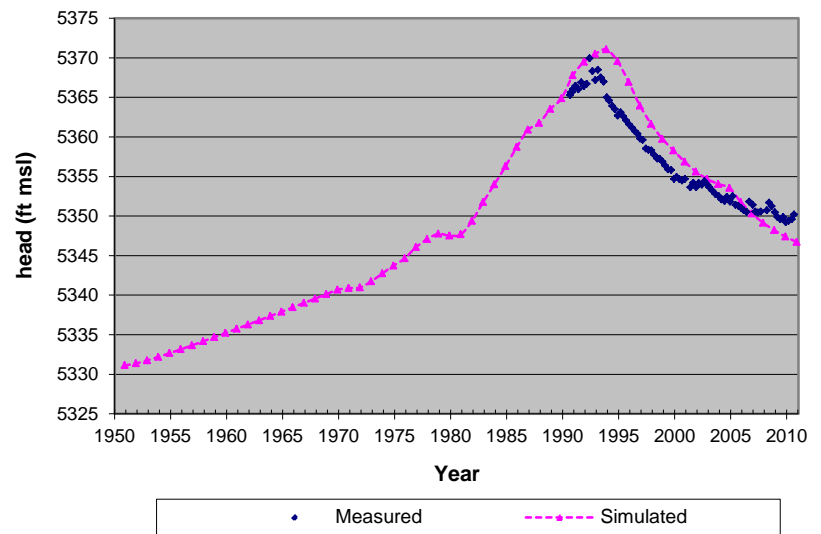
**Well 20**



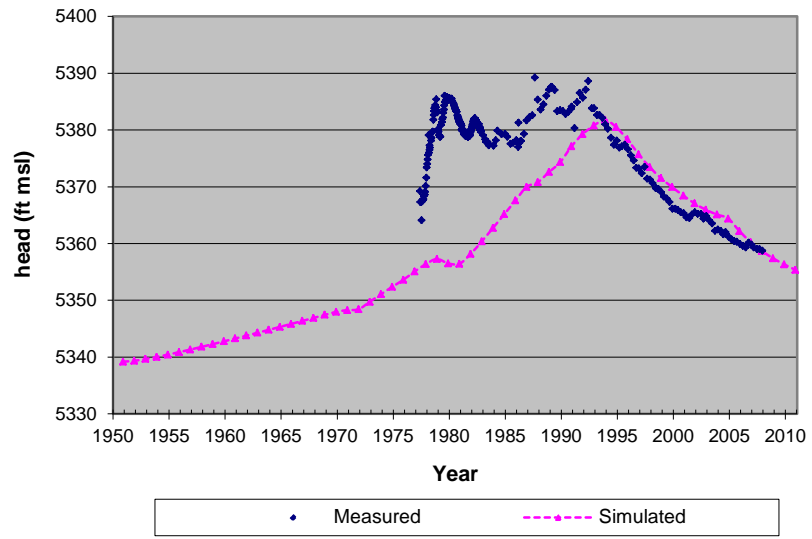
**Well PZ-1**



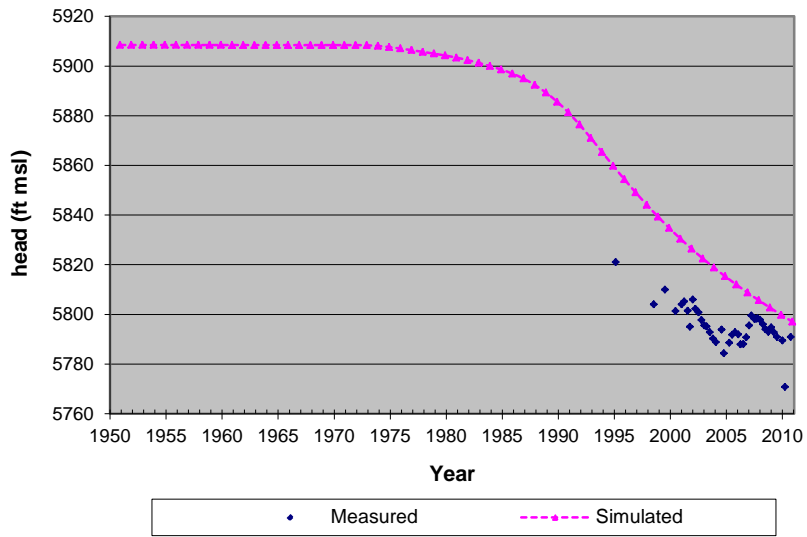
**Well 45**



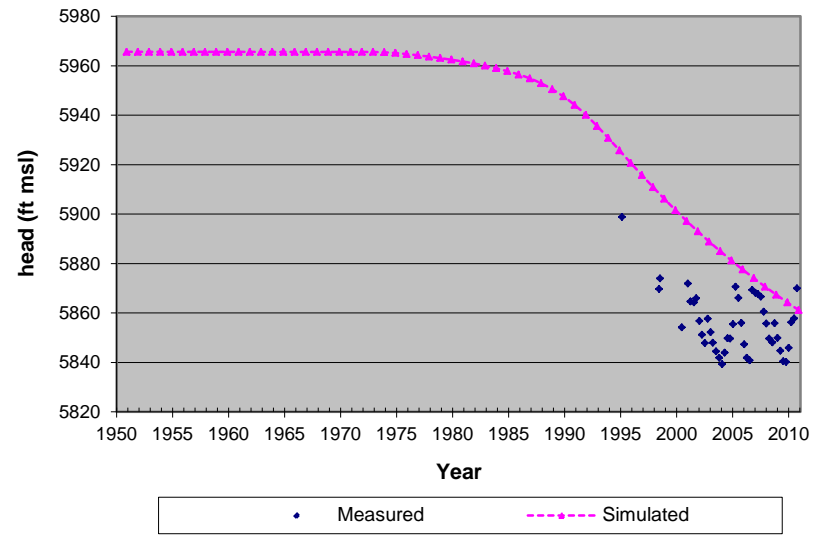
Well P1-2



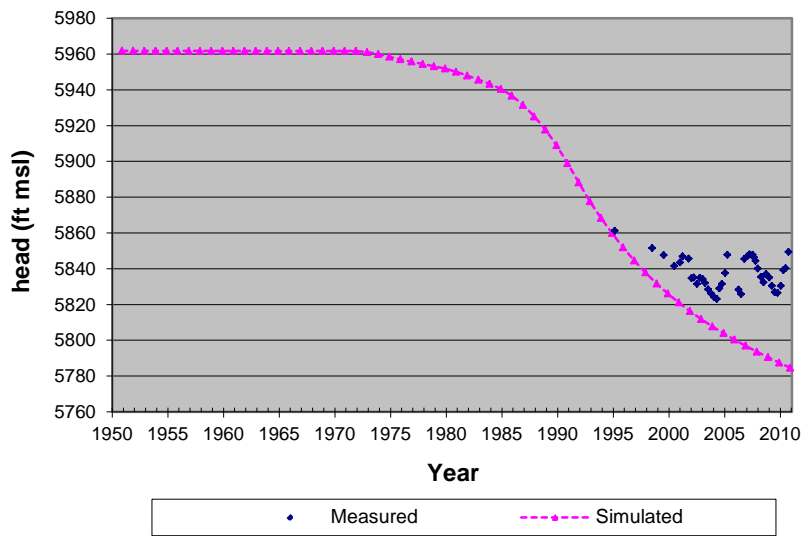
**Well LRW-1**



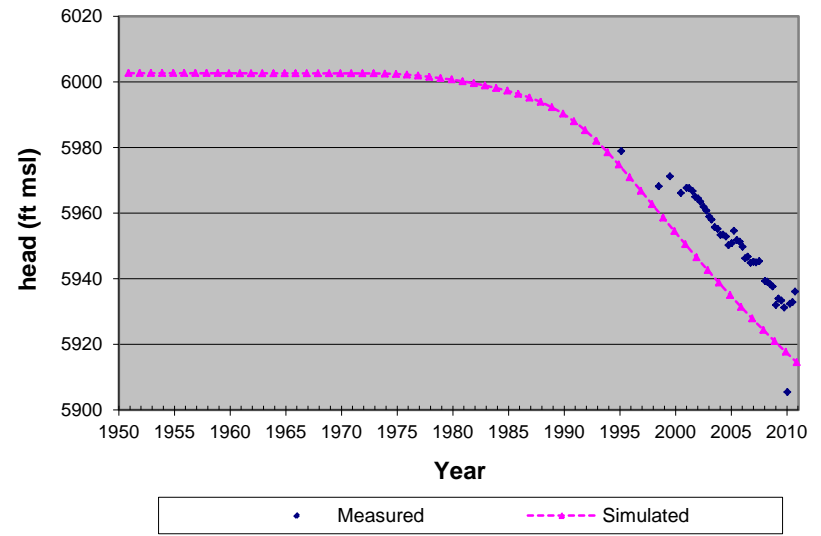
**Well LRW-3**



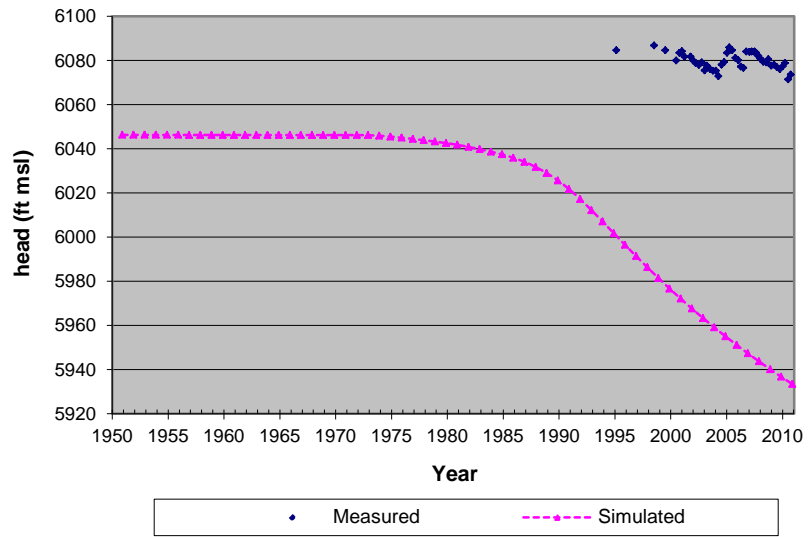
**Well LRW-7**



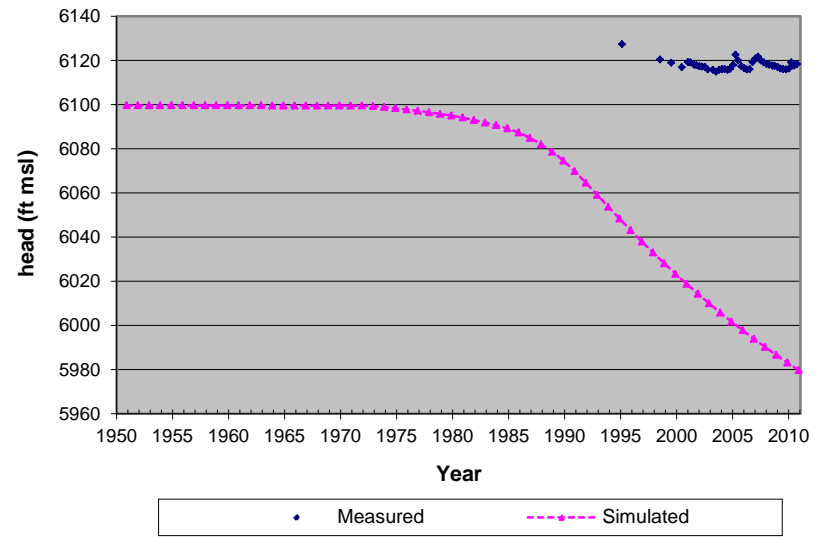
**Well LRW-2**



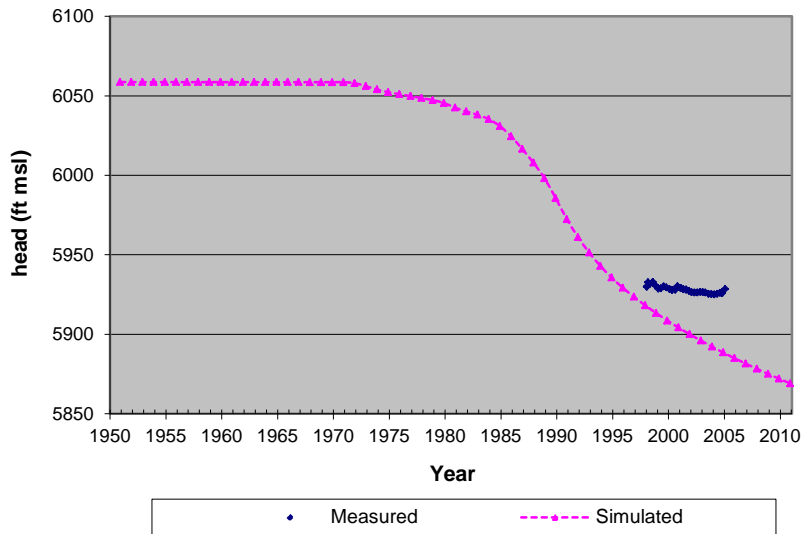
**Well LRW-4**



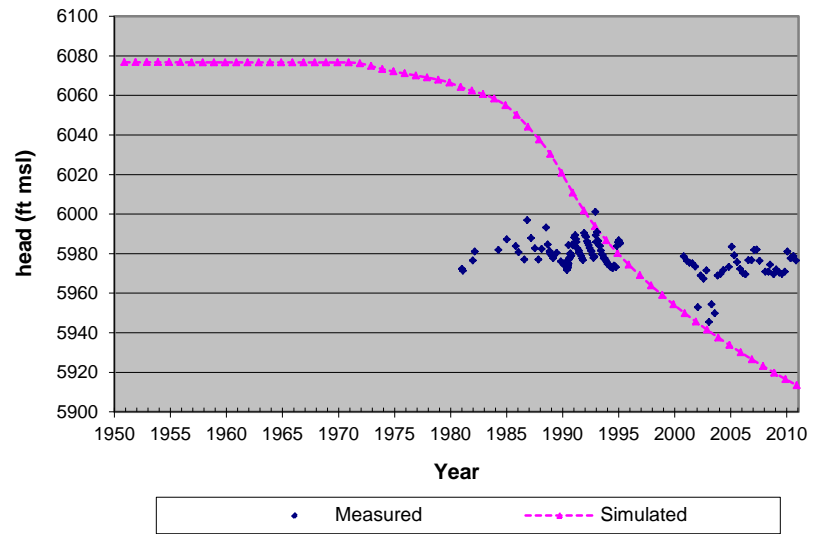
**Well LRW-5**



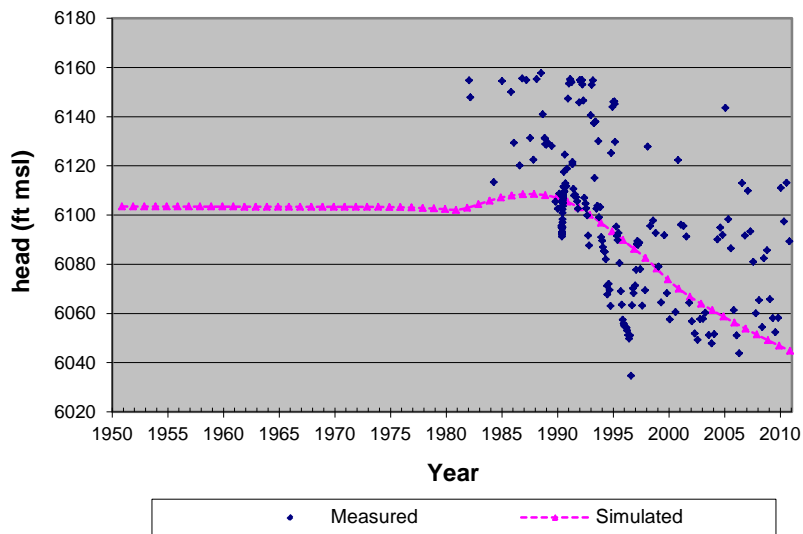
**Well TWS-41**



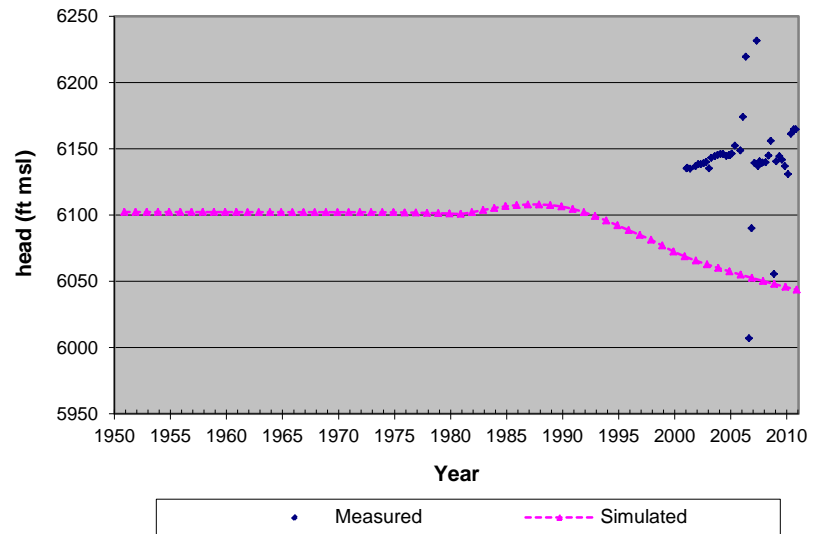
**Well TWS-9**



**Well TWS-8**

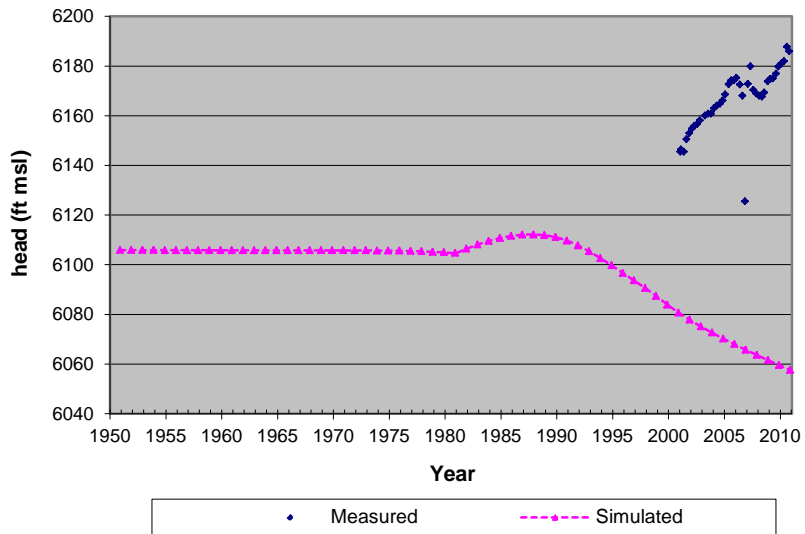


**Well 2-16**

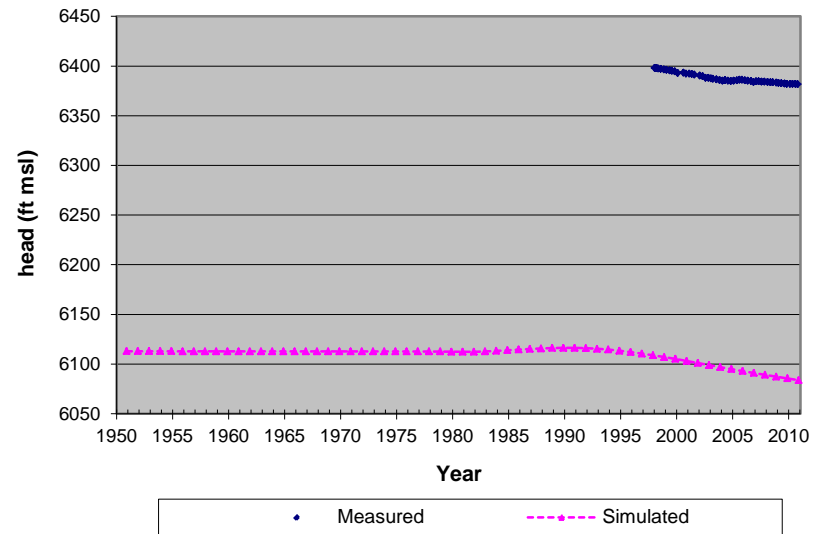




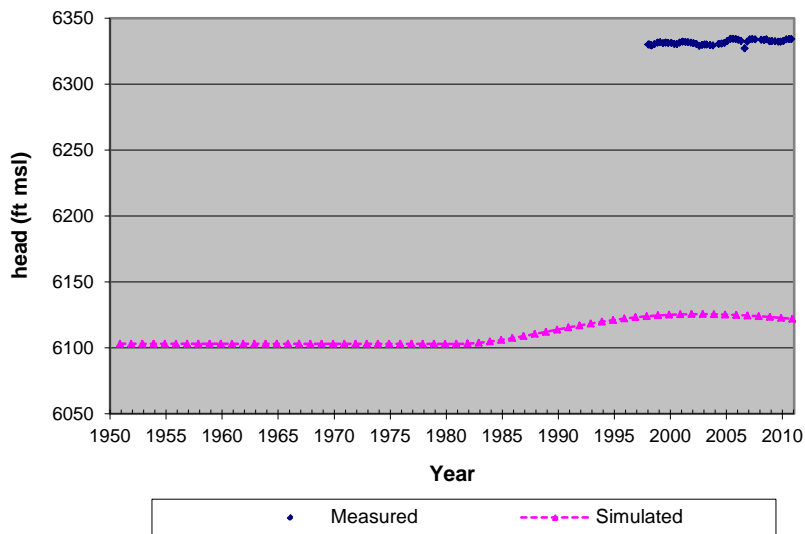
**Well 2-15**



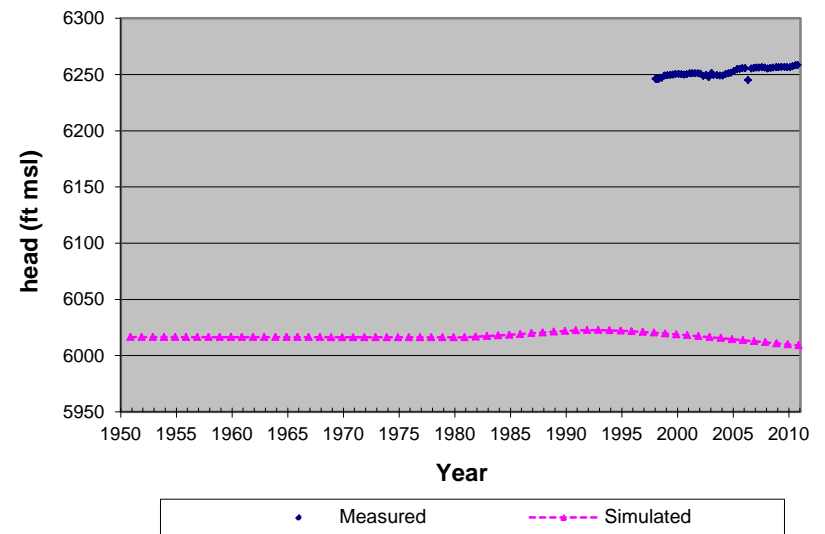
**Well 2-11**



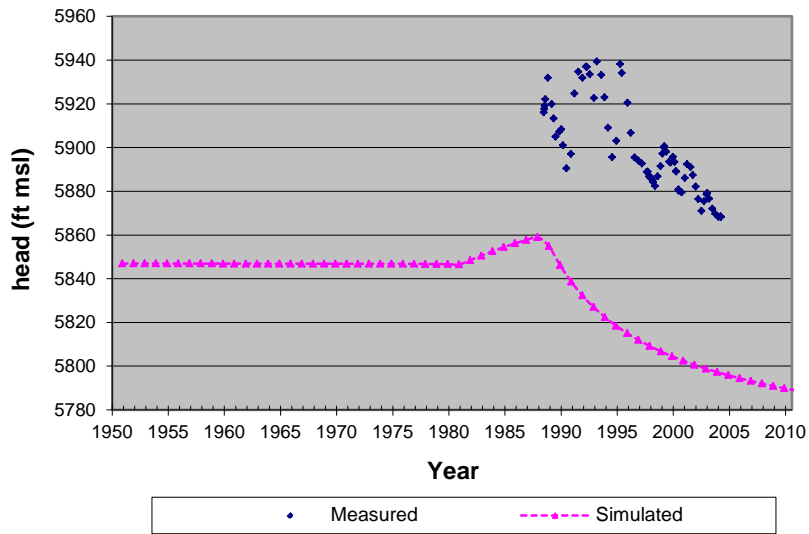
**Well 2-13**



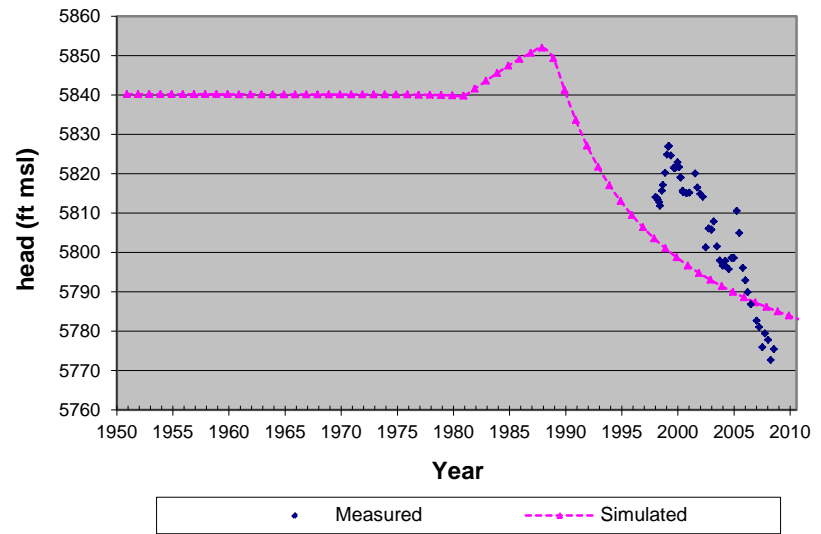
**Well 2-12**



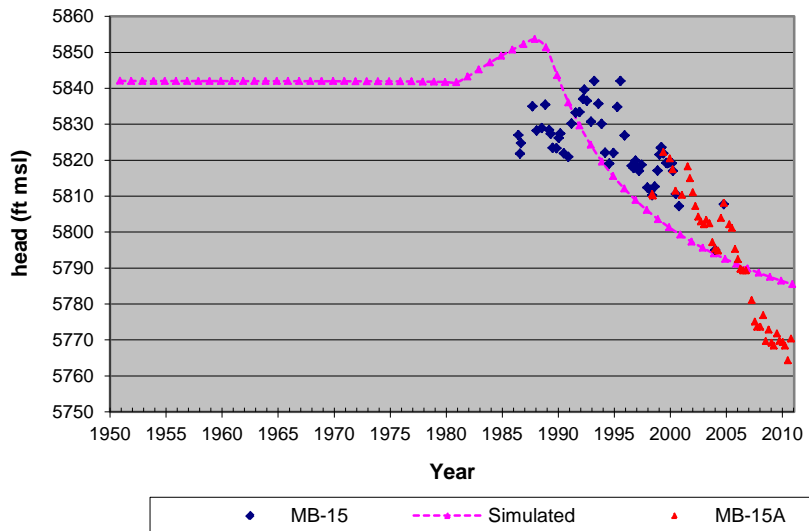
**Well MB-18D**



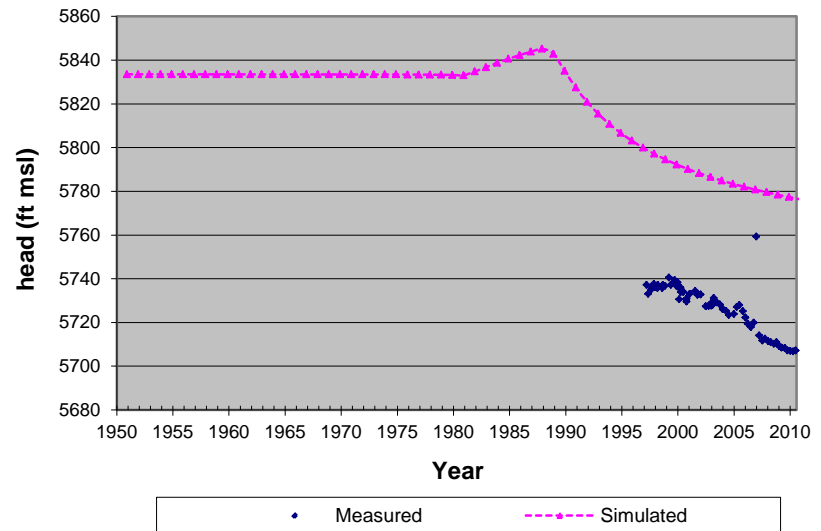
**Well MB-37**



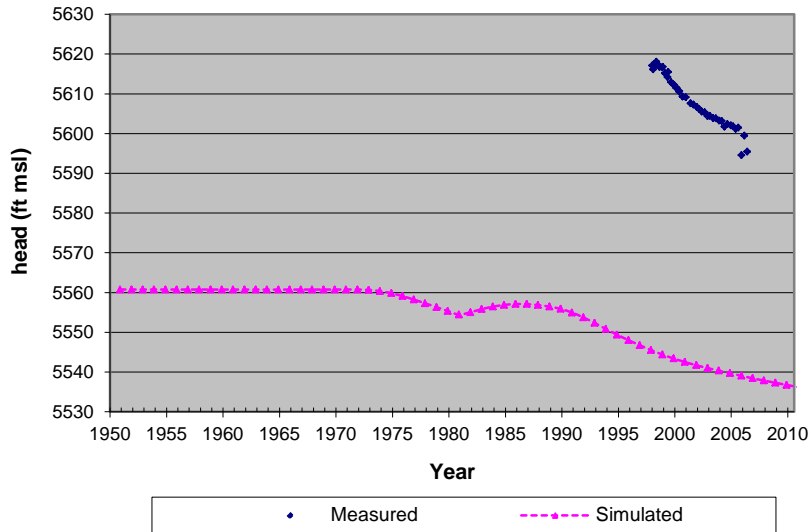
**Well MB-15**



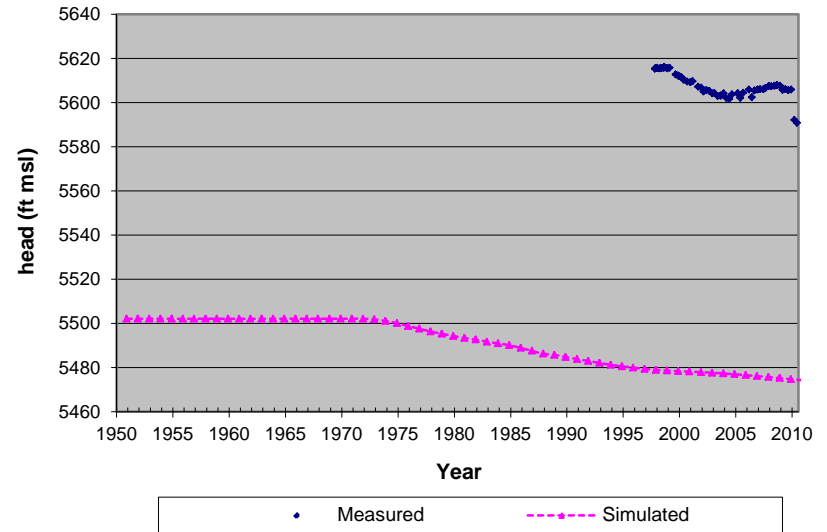
**Well MB-32**



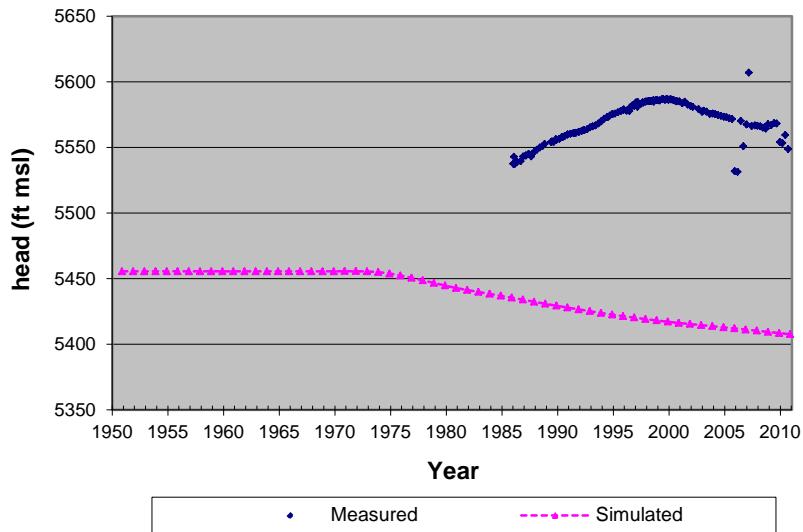
**Well MB-36**



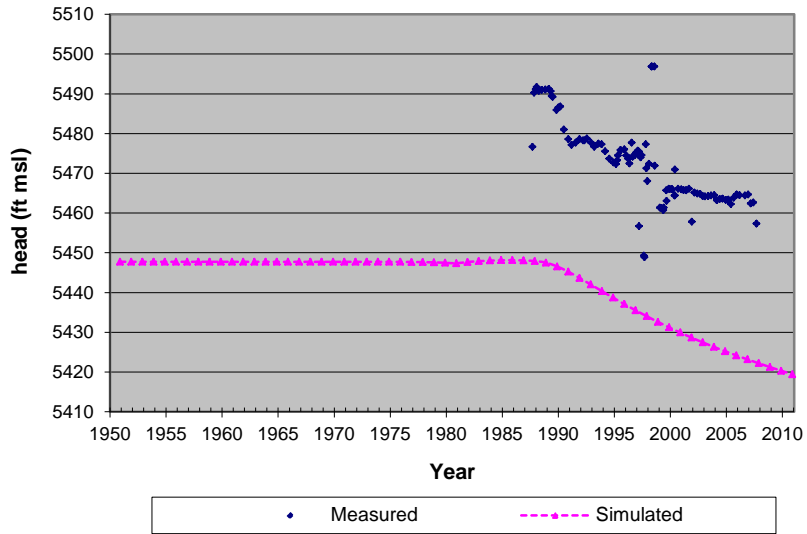
**Well MB-35**



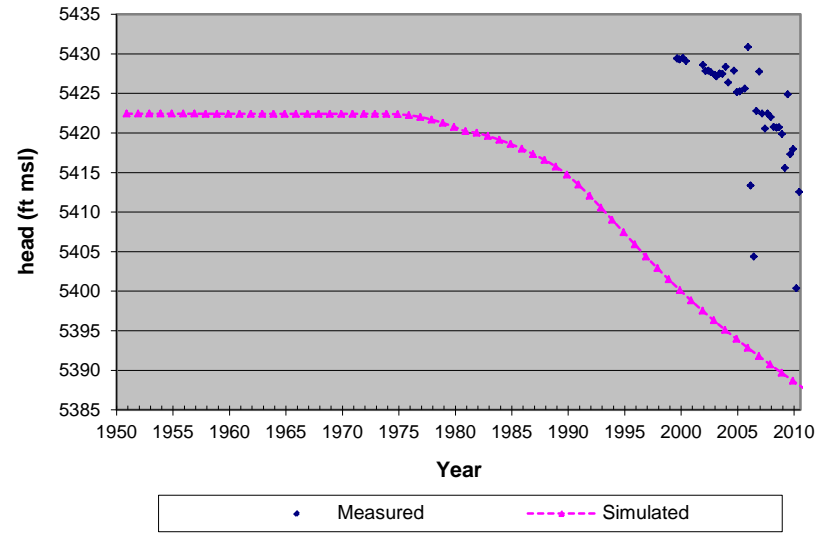
**Well MB-12**



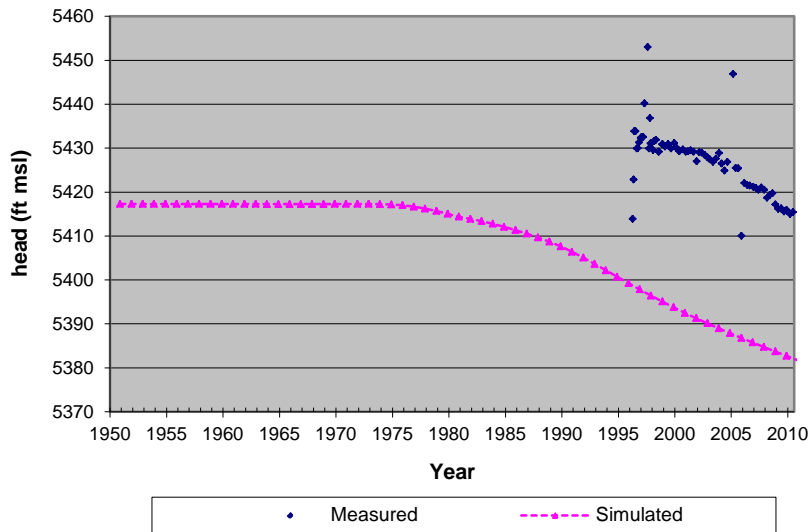
**Well MB-17 (Layer 2)**



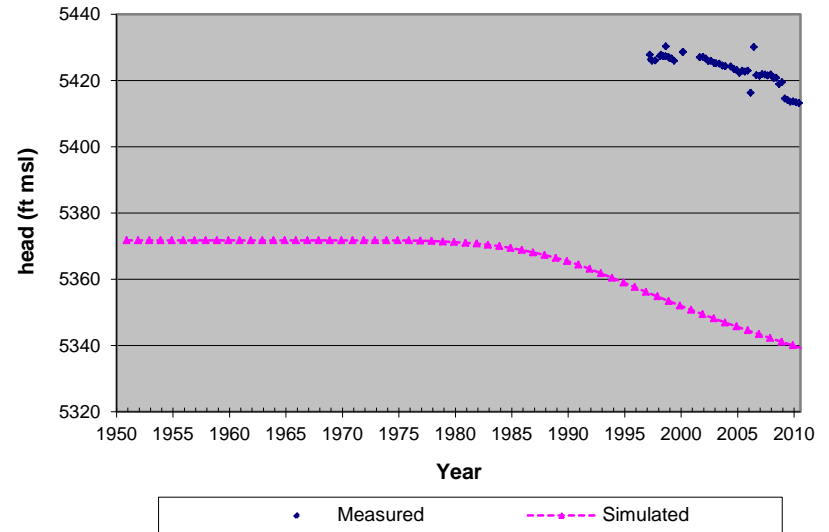
**Well MB-41 (Layer 2)**



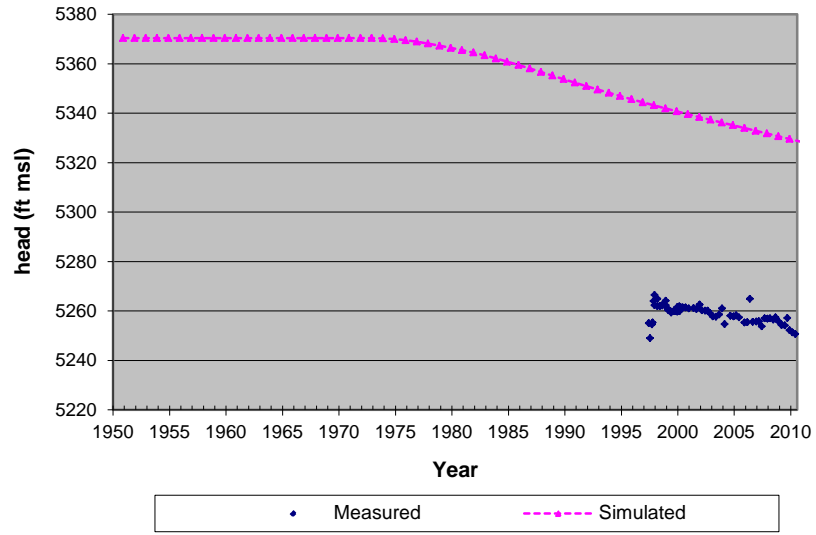
**Well MB-27 (layer 2)**



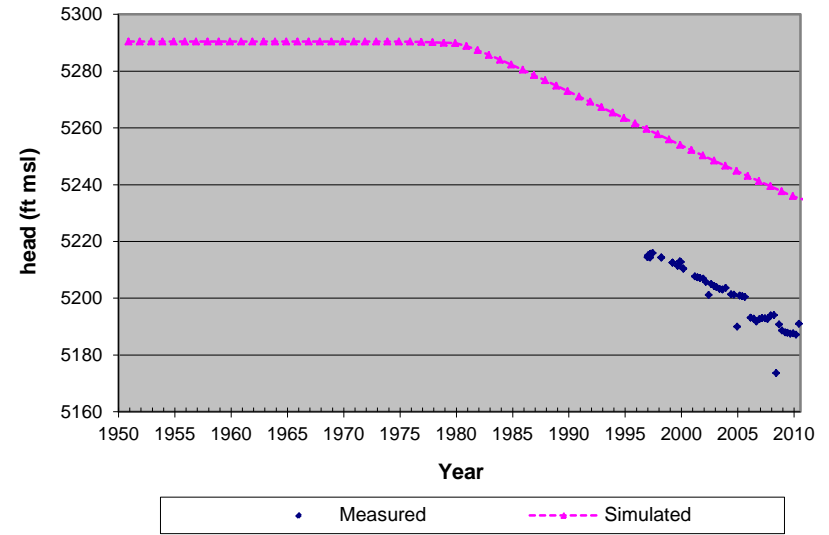
**Well MB-31 (Layer 2)**



**Well MB-33 (Layer 2)**

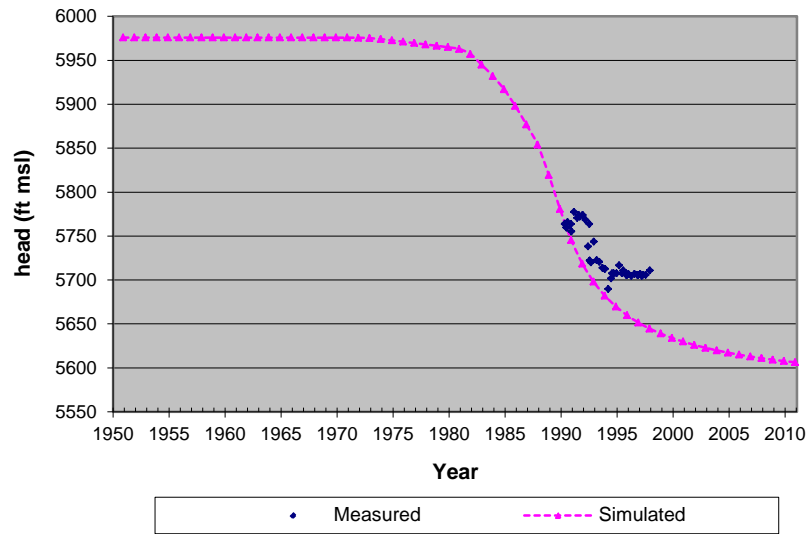


**Well MB-28 (Layer 2)**

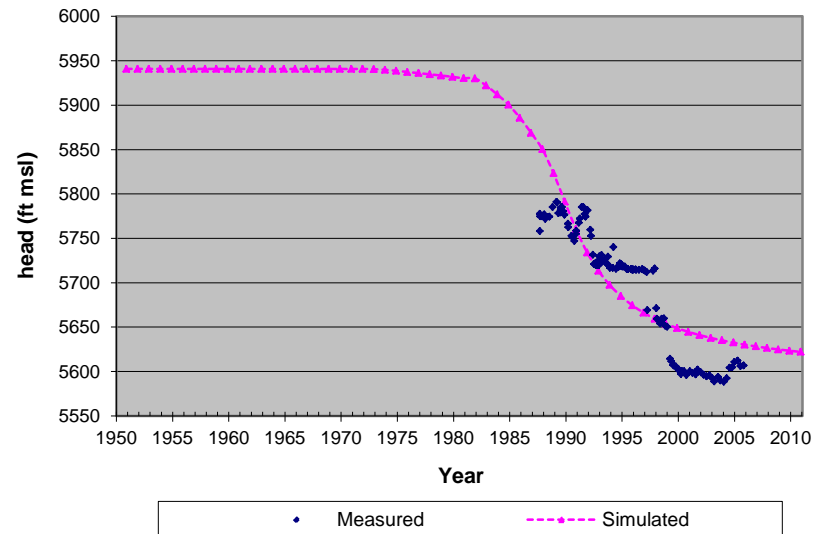




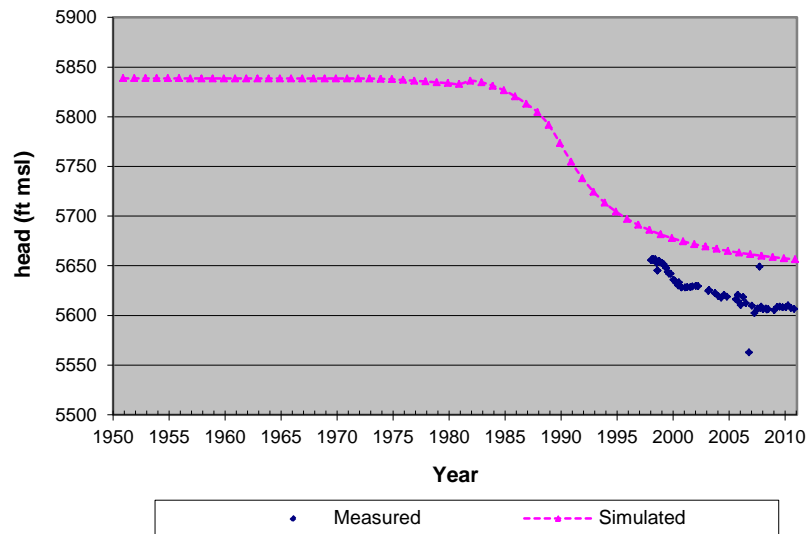
### Well EM-1



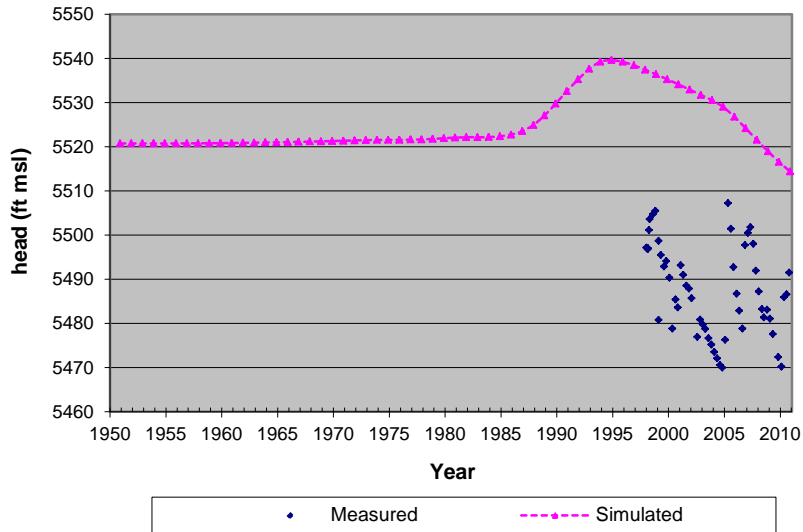
### Well GLD-3 (Layer 2)



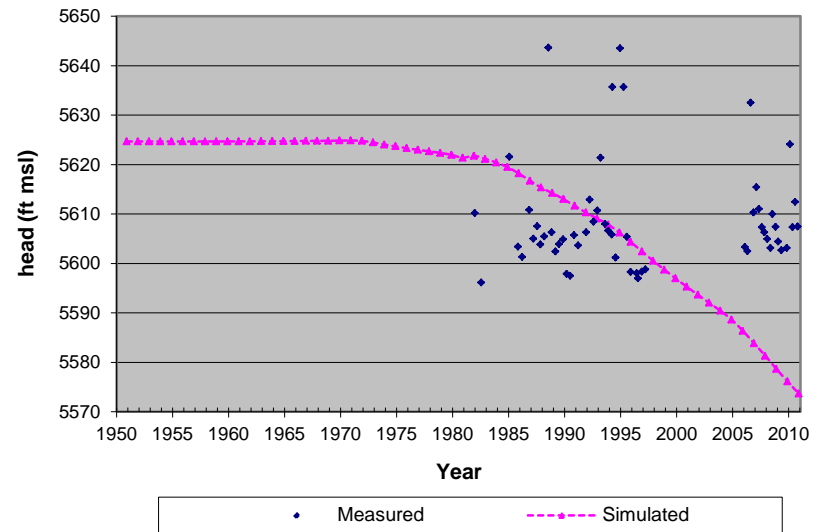
### Well GLD-7A (Layer 2)



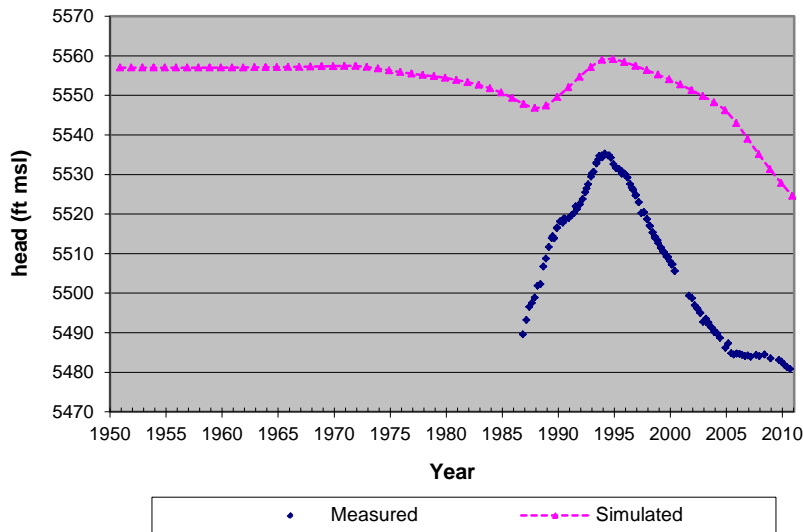
**Well TWS-42**



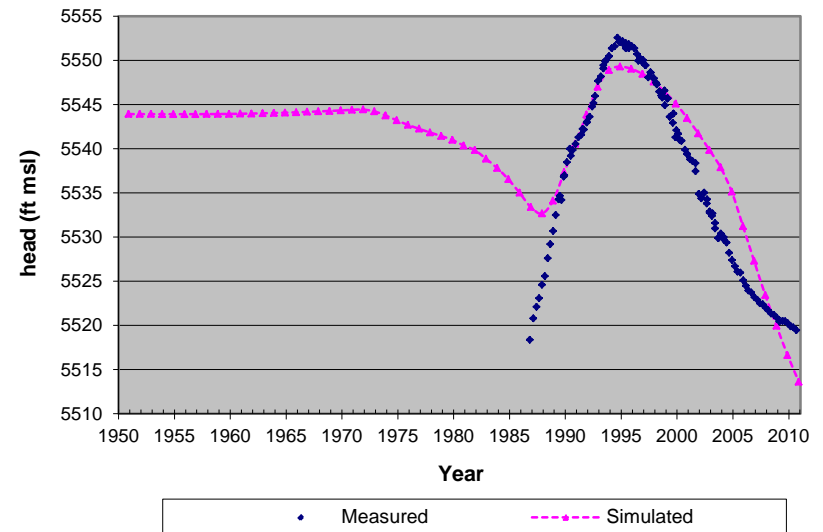
**Well TWS-19 (Layer 2)**



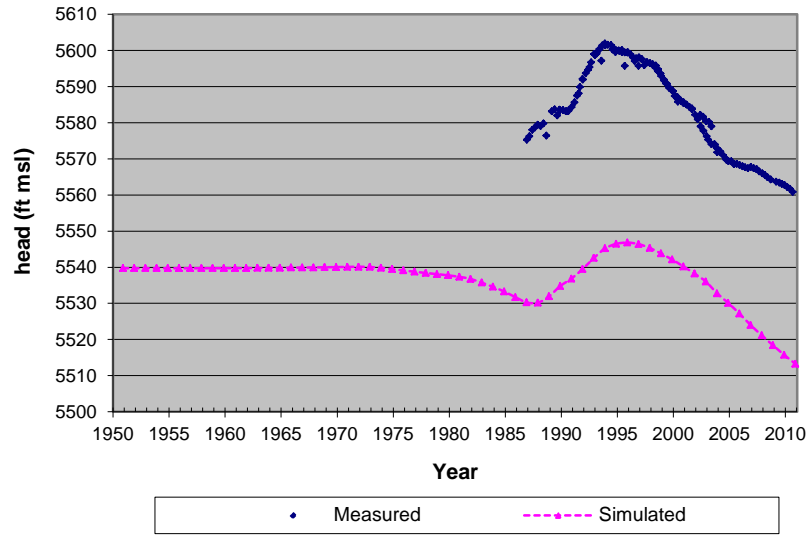
**Well 26 (Layer 2)**



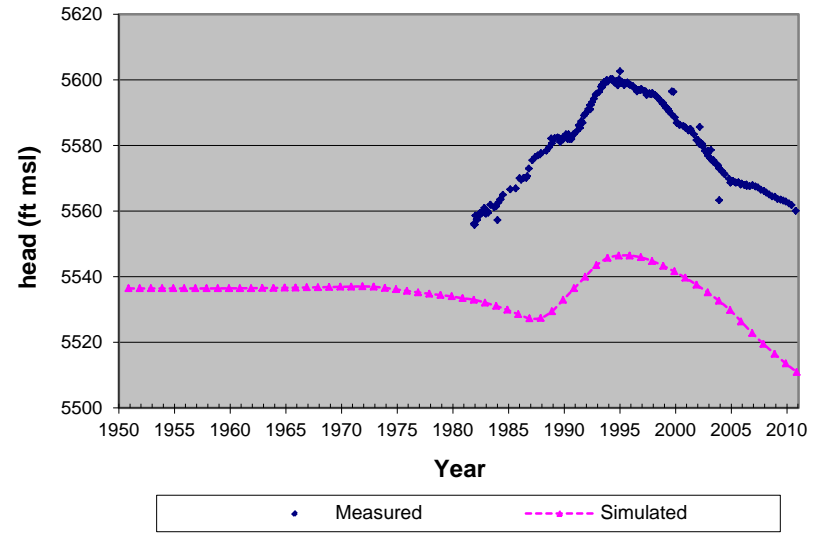
**Well 27 (Layer 2)**



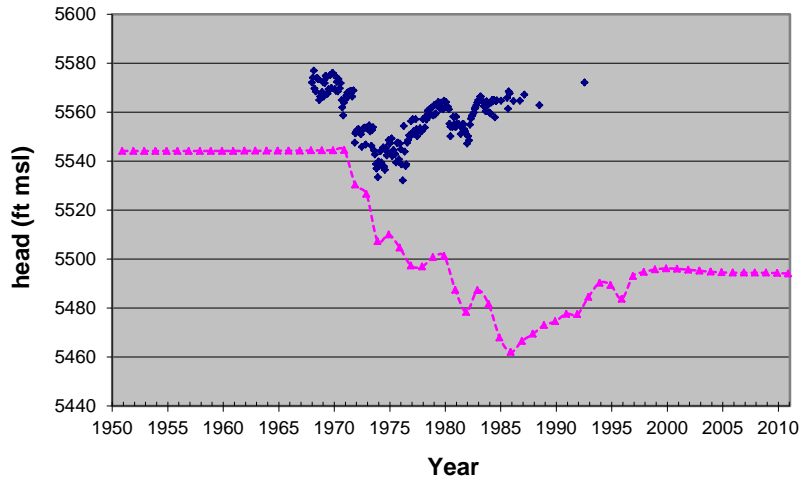
**Well 29**



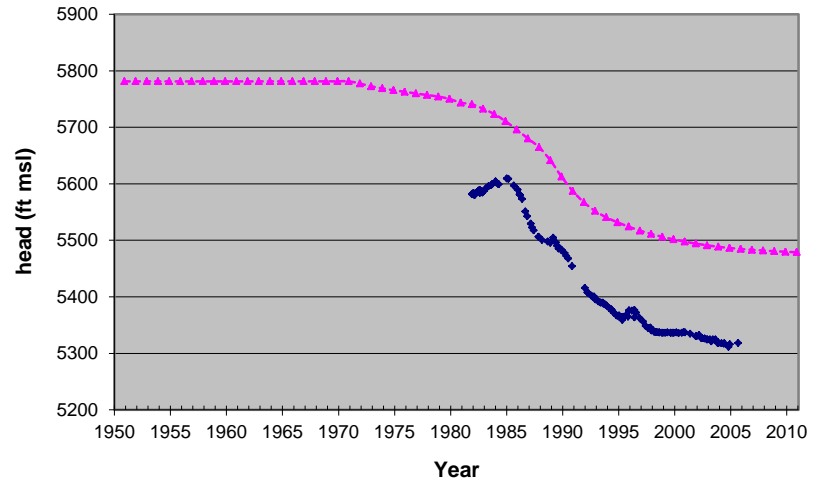
**Well P-3 (Layer 2)**



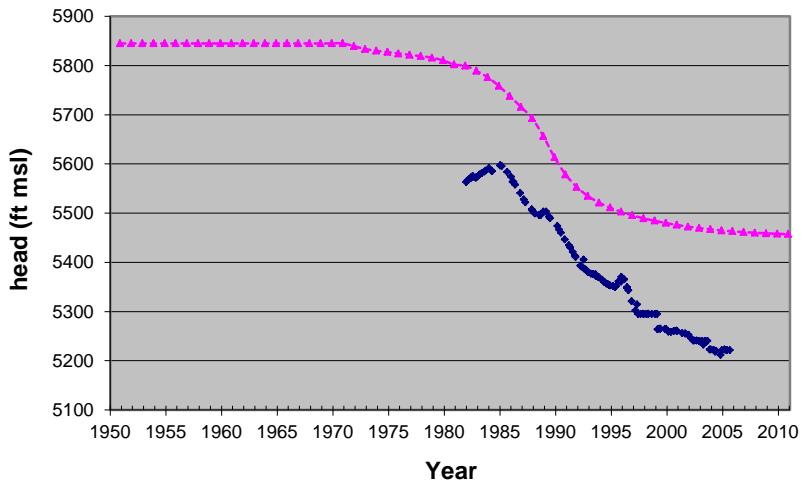
**Well 1 (Layer 2)**



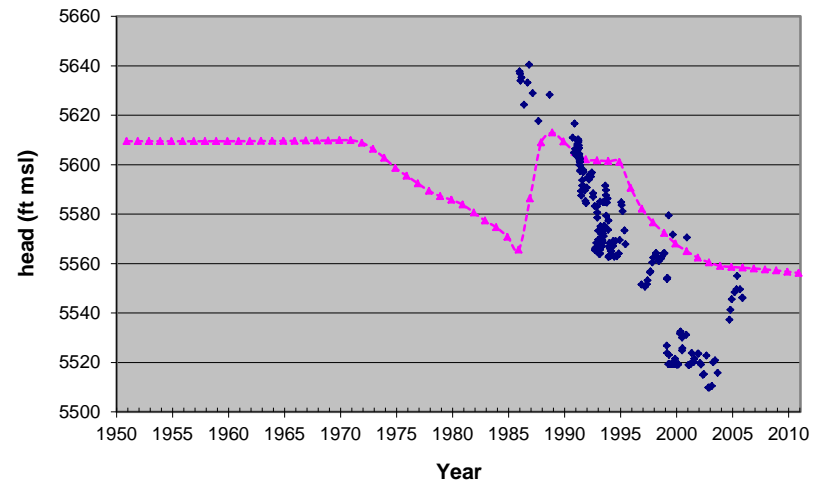
**Well P-8 (Layer 2)**



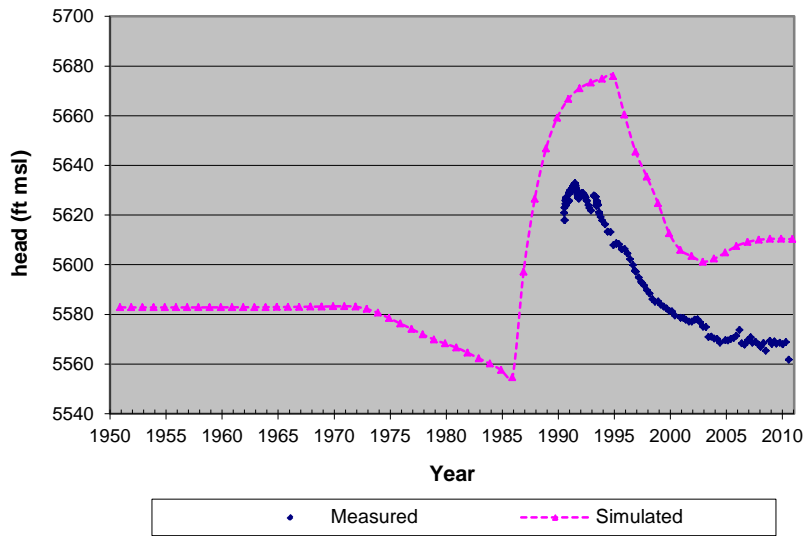
**Well P-6 (Layer 2)**



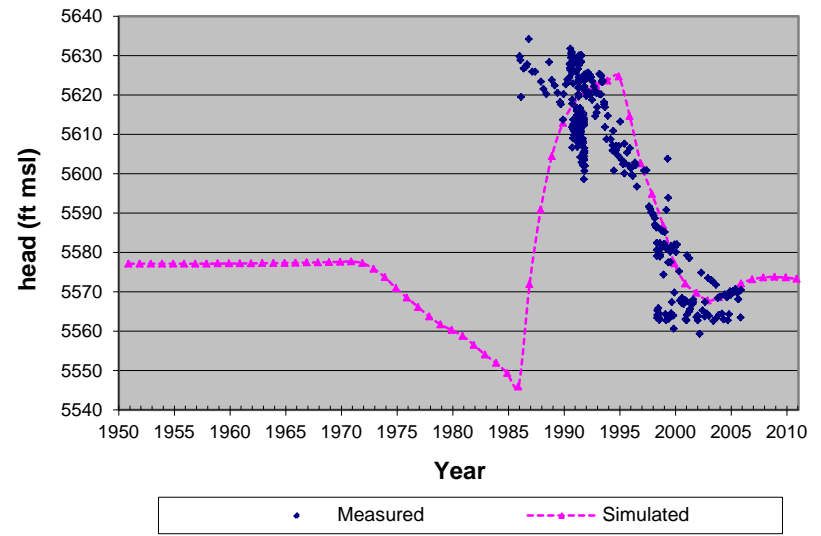
**Well P-13**



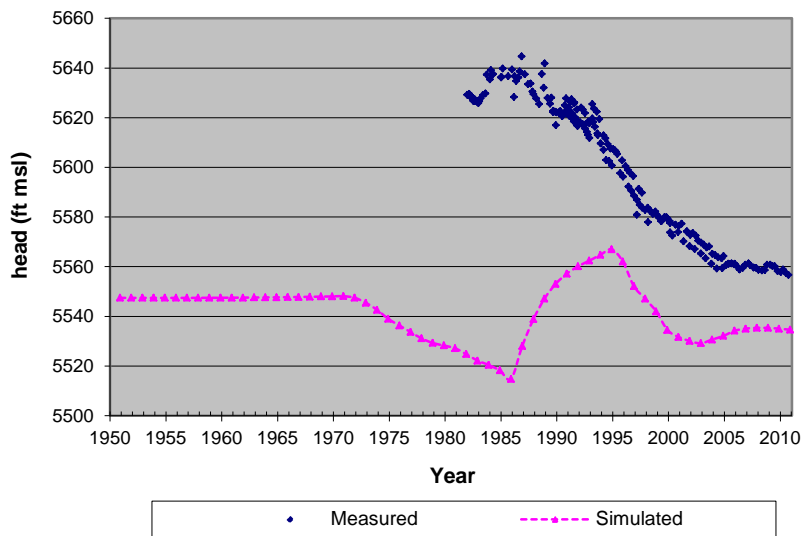
**Well P-16**



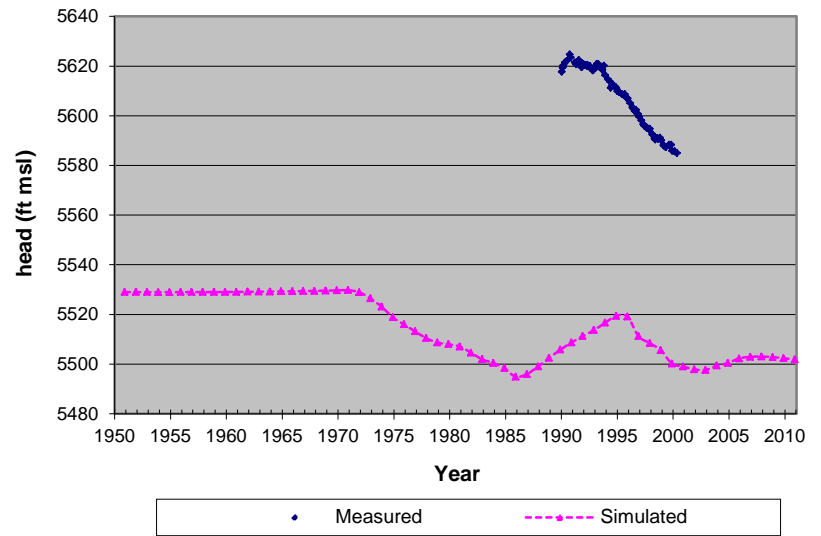
**Well P-12**



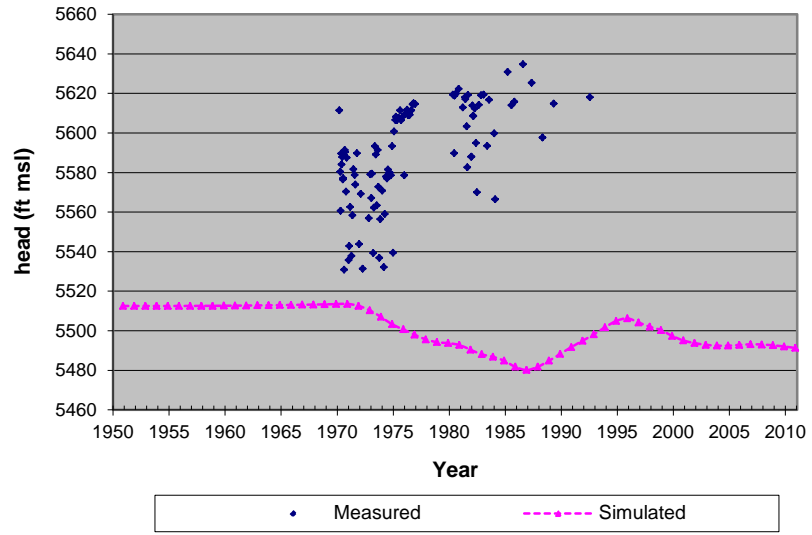
**Well P-10A**



**Well P-14**

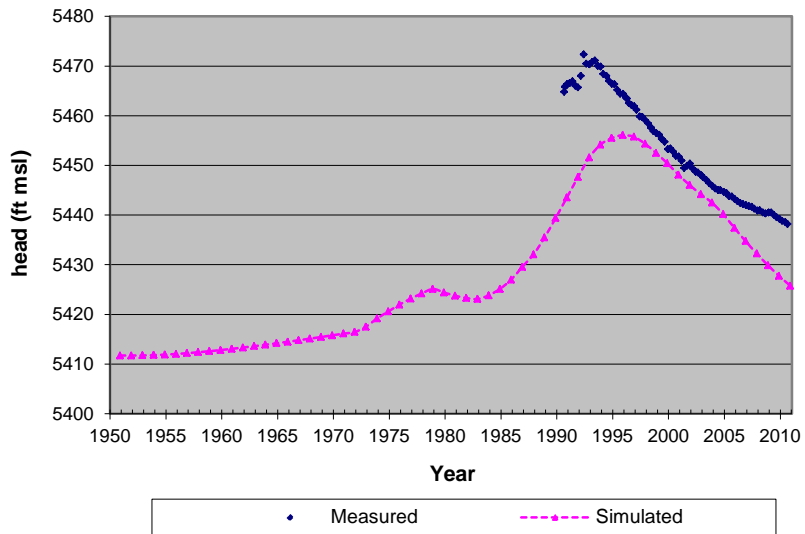


### Well 4

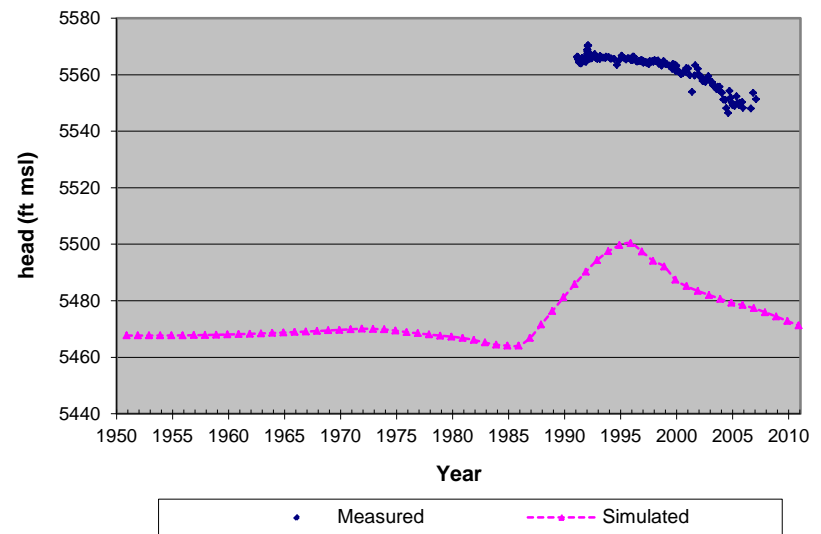




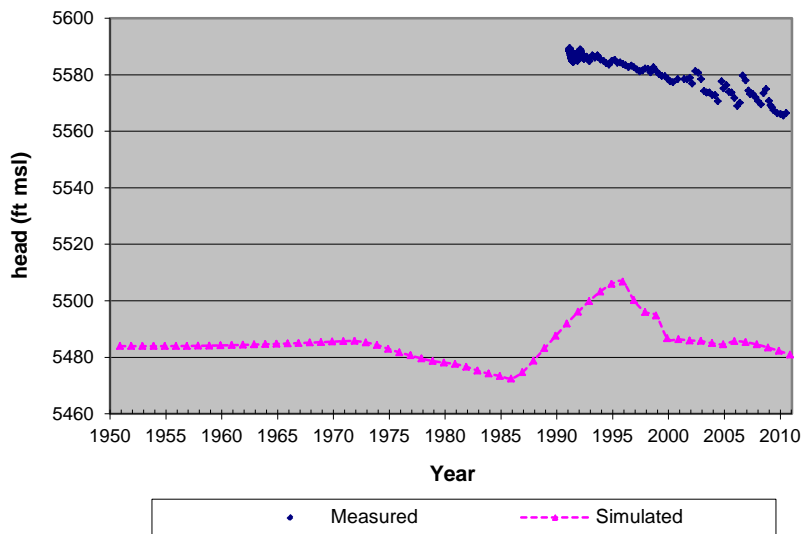
**Well 46**



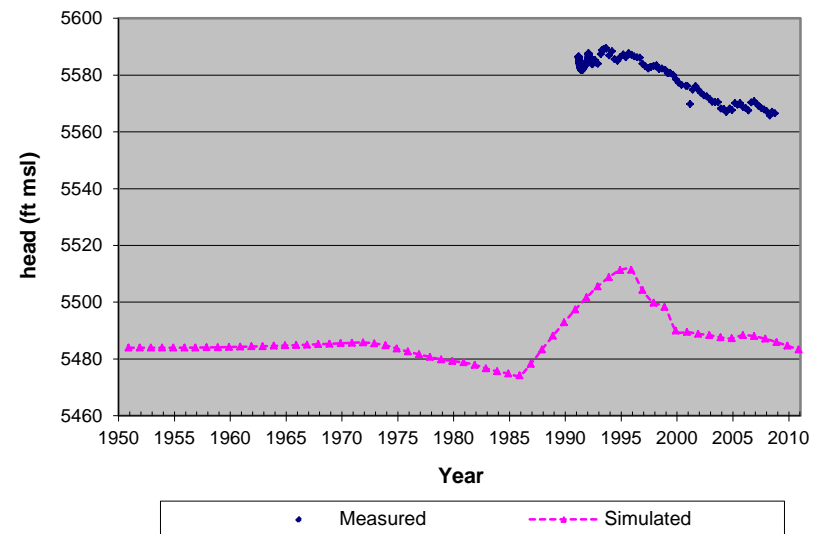
**Well P-68**



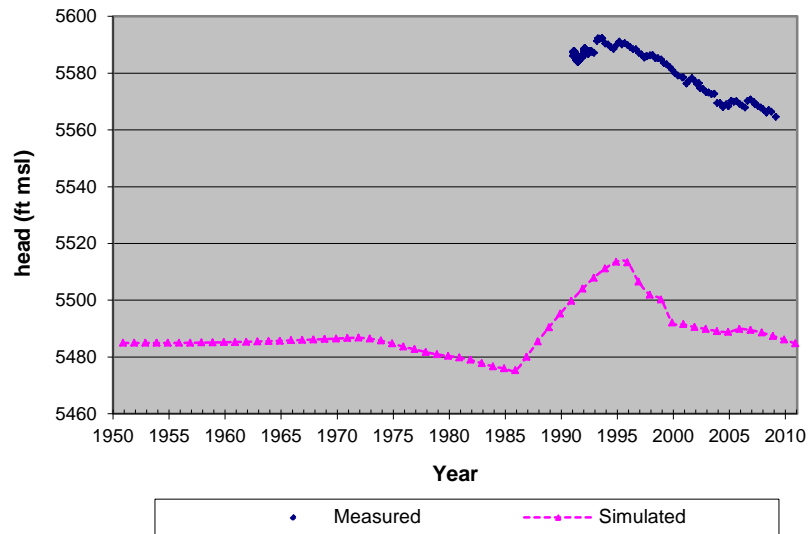
**Well P-58**



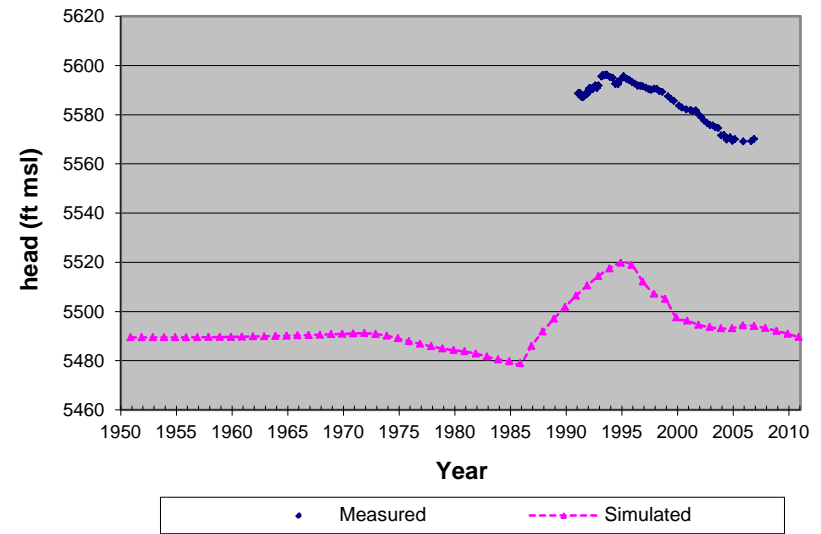
**Well P-74**



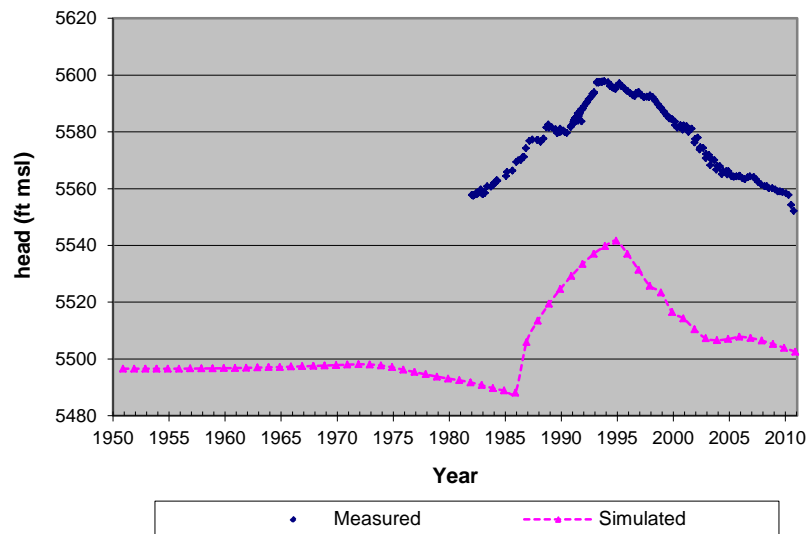
**Well P-45**



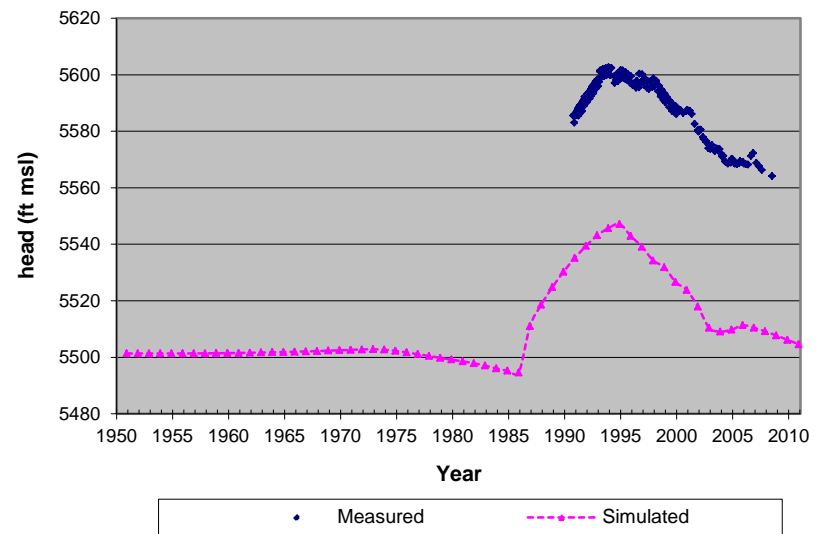
**Well C10-42**



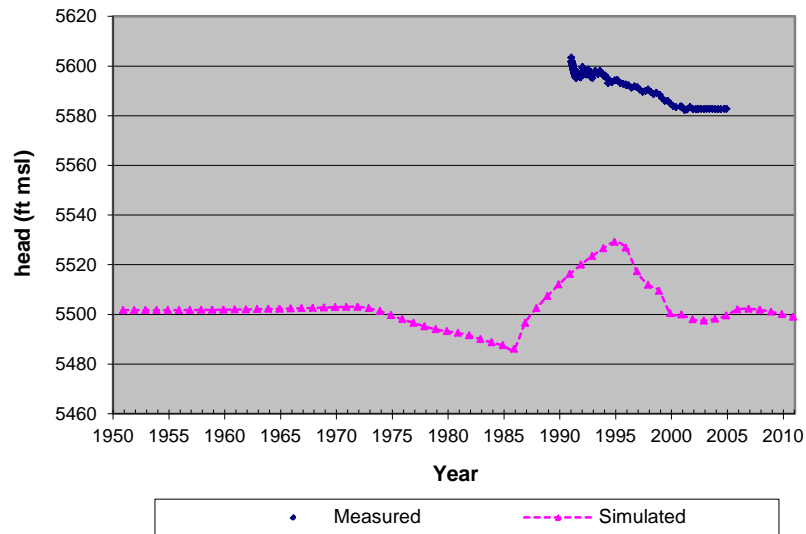
**Well P-5**



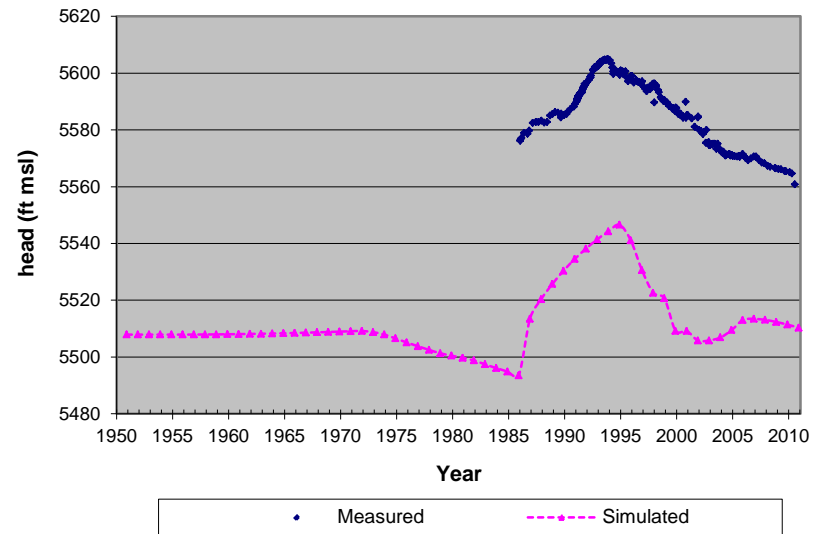
**Well C11-1**



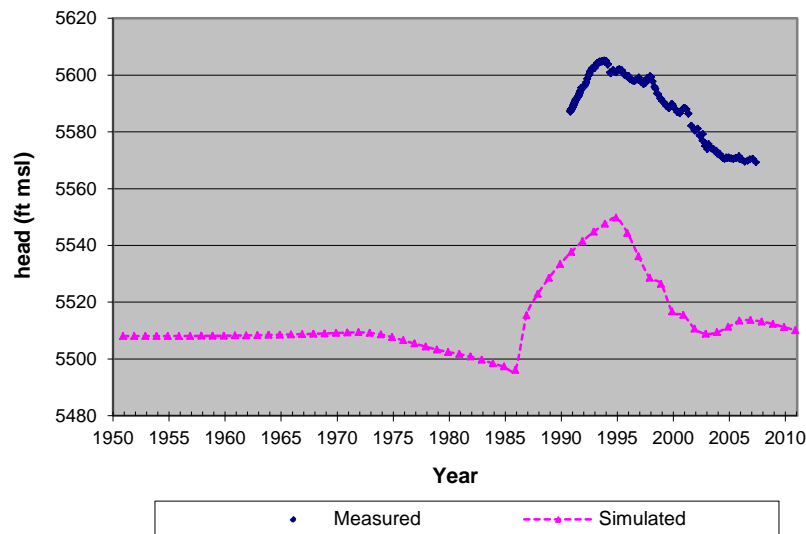
**Well P-36**



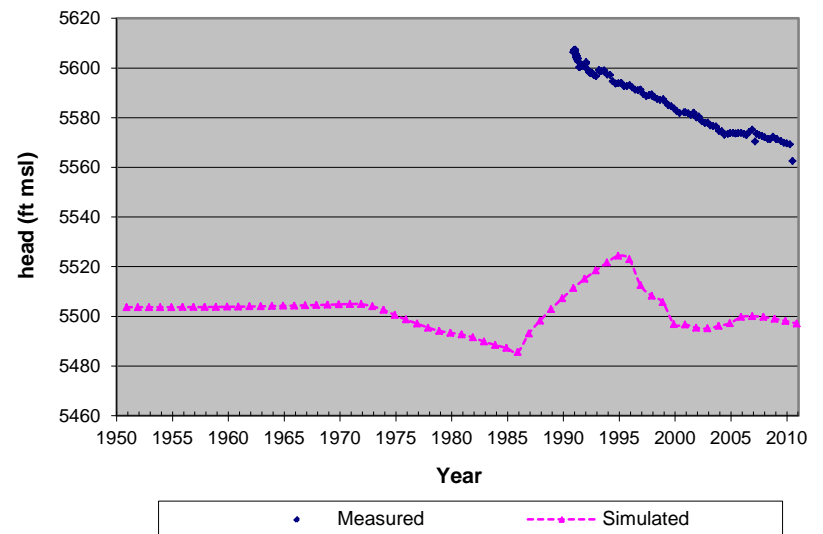
**Well P-11**



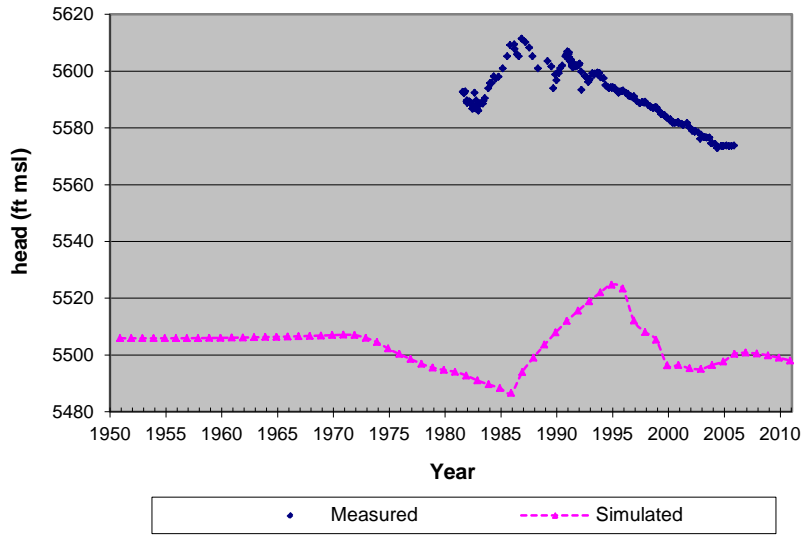
**Well C9-5**



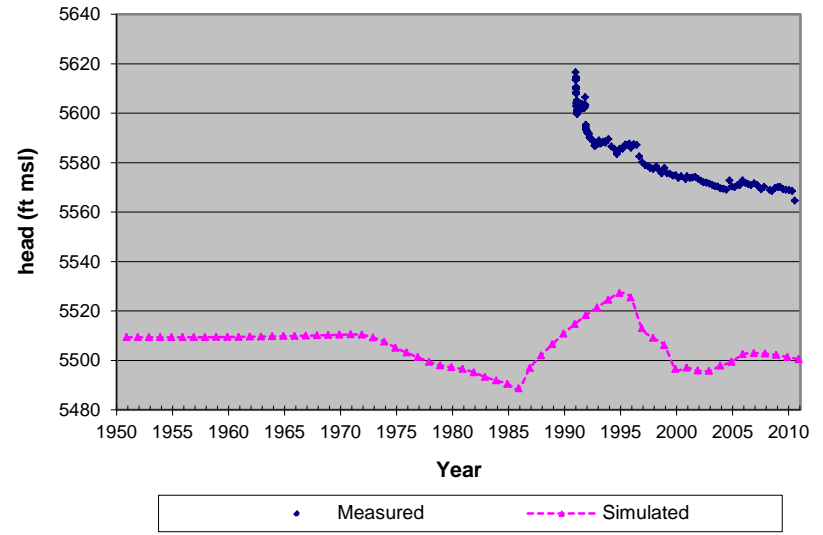
**Well O-3R**



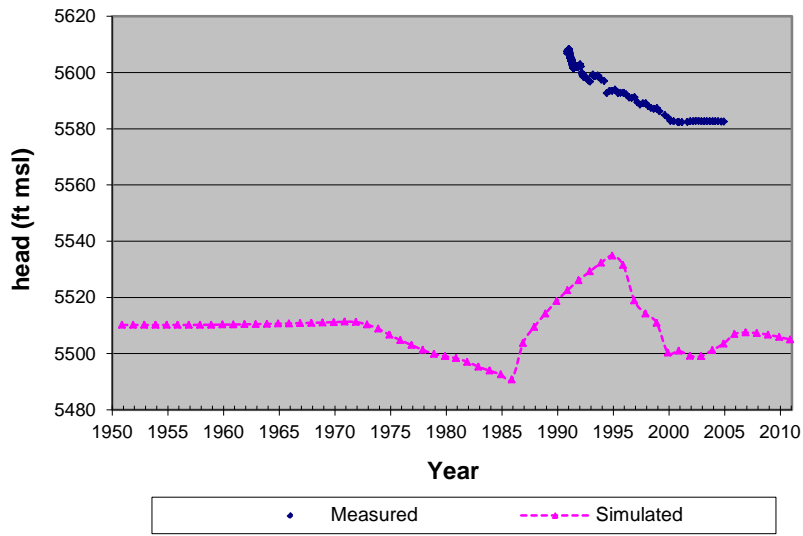
**Well 6-2**



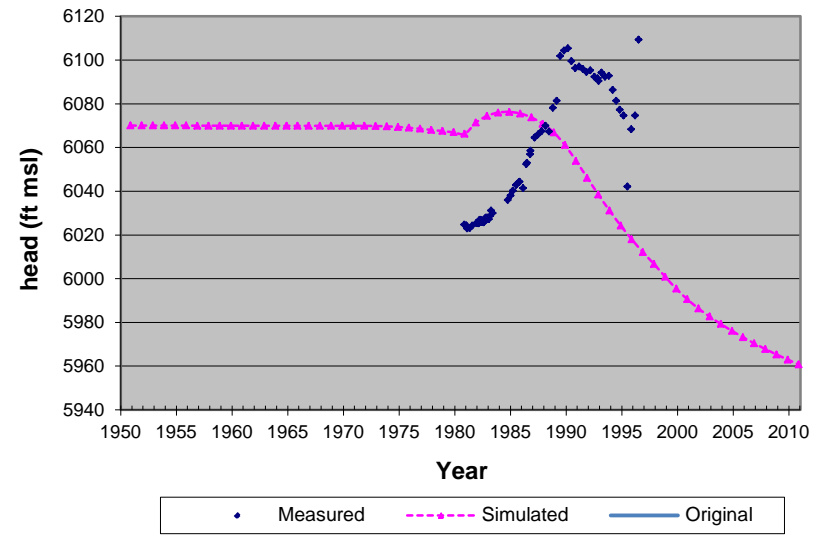
**Well P-34**



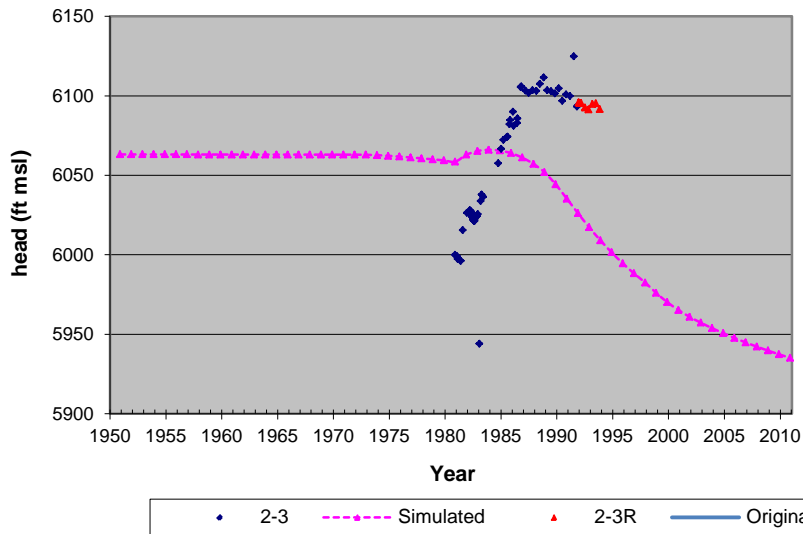
**Well P-28**



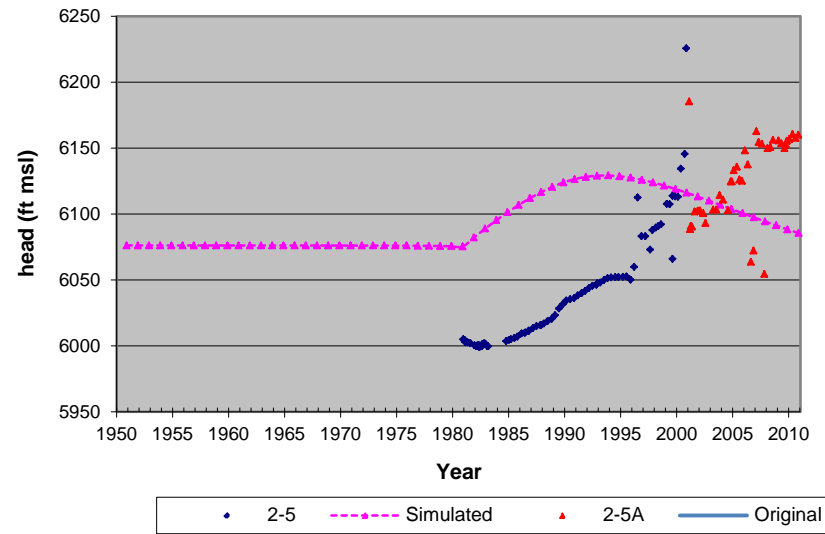
**Well 2-2**



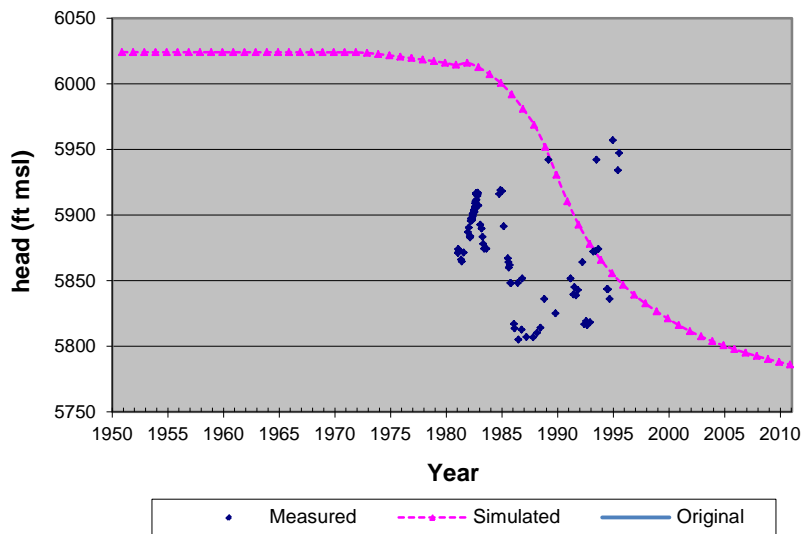
**Well 2-3 & 2-3R**



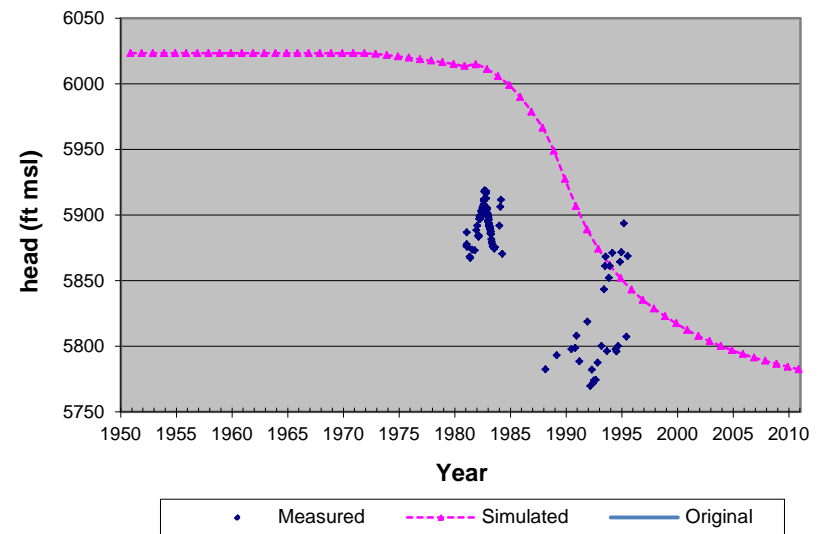
**Well 2-5 & 2-5A**



**Well 2-6**



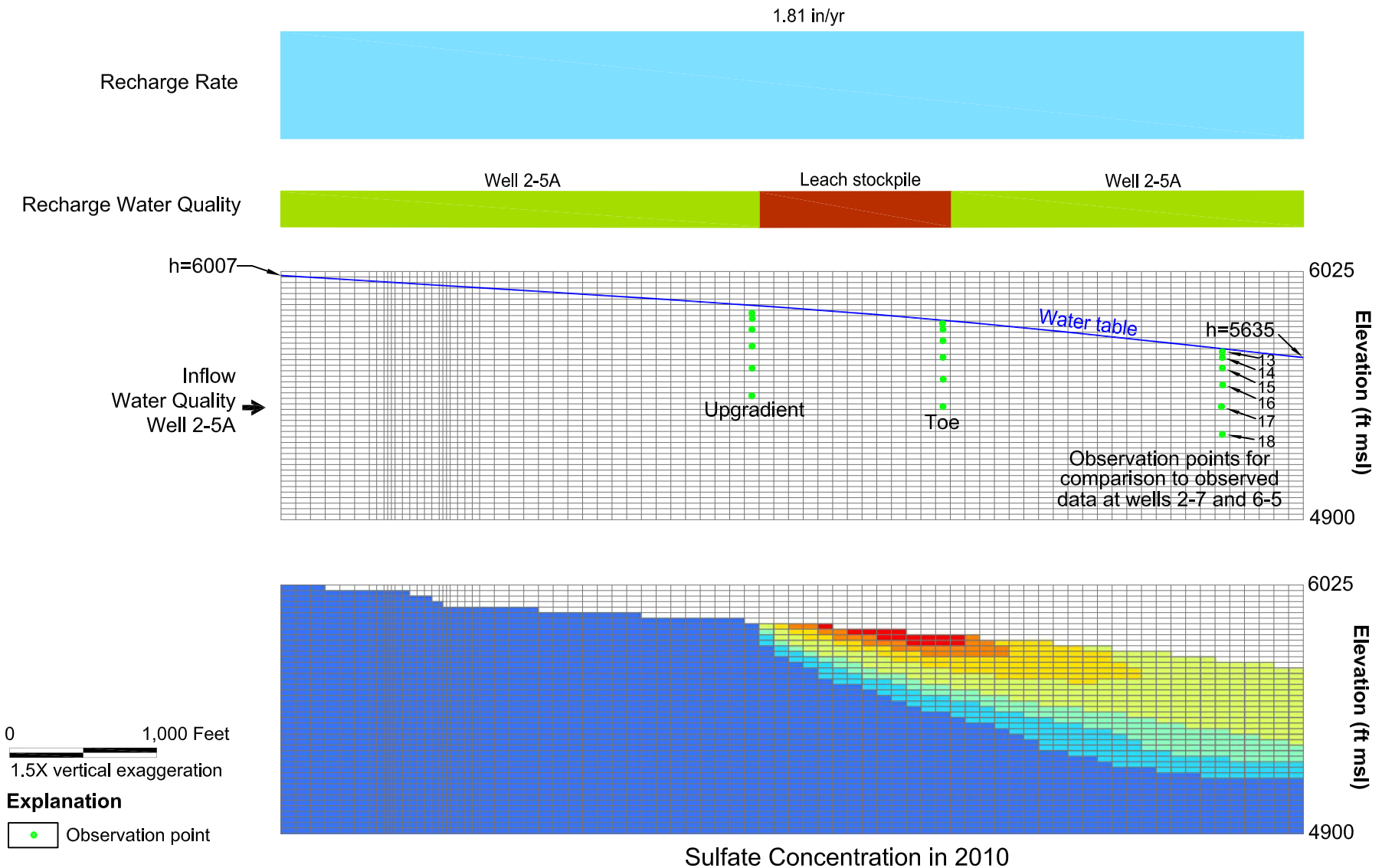
**Well 6-4**



## **Appendix D**

### **PHT3D Chemical Time Series**





**Explanation**

● Observation point

**Note:** h = Hydraulic head (ft msl)

Sulfate concentration (mg/L)

- |               |                 |                 |
|---------------|-----------------|-----------------|
| □ Dry         | □ 3,001-5,000   | □ 15,001-20,000 |
| □ 1-1,500     | □ 5,001-10,000  | □ 20,001-27,500 |
| □ 1,501-3,000 | □ 10,001-15,000 |                 |

Sulfate Concentration in 2010



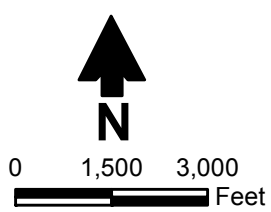
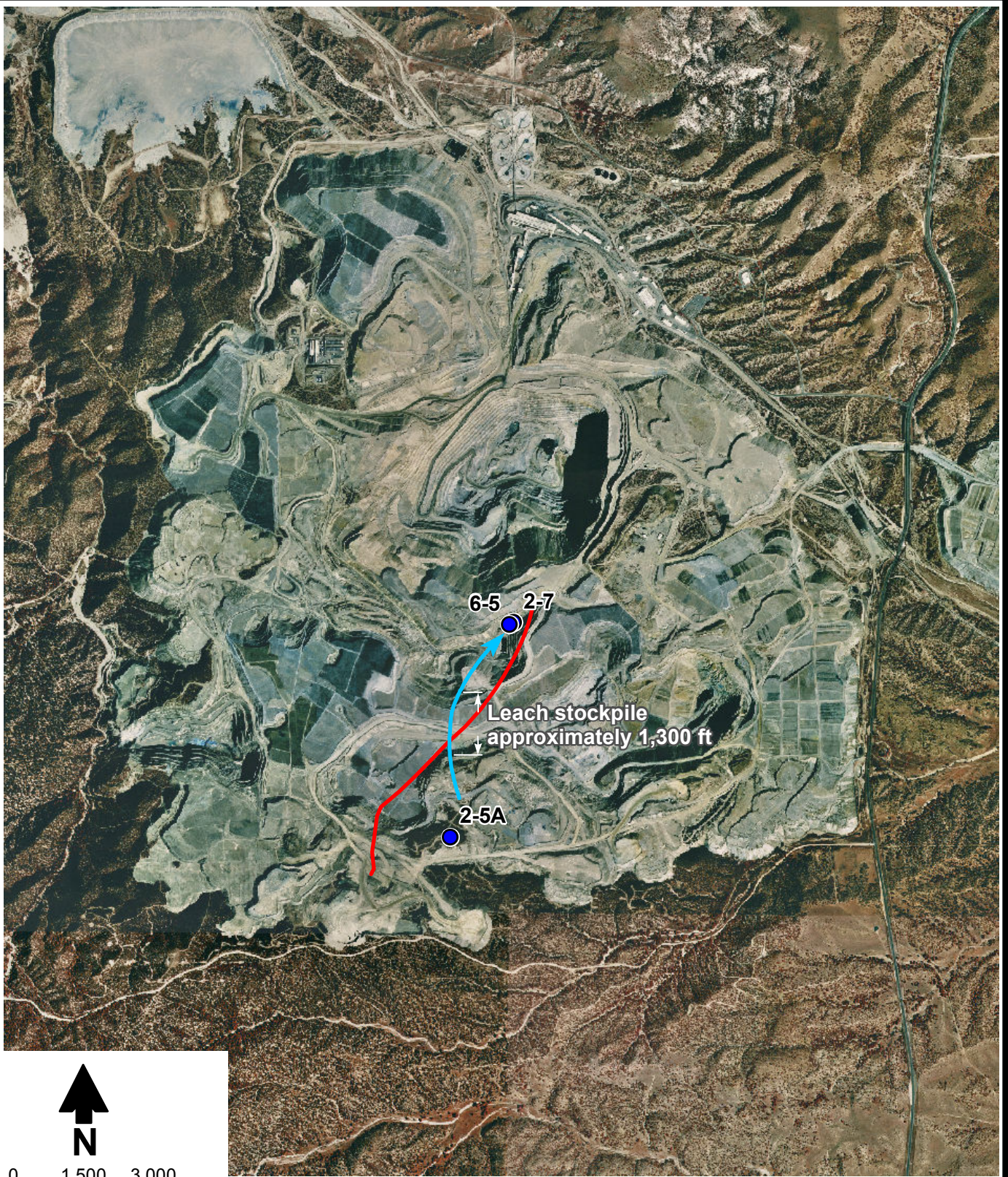
TYRONE STAGE 2 APP

**Current Condition Cross Section Model Description and Simulated 2010 Sulfate Concentrations**





S:\PROJECTS\MINE\_TYRONE\GIS\MXD\ES09.0176\MXD\STAGE\_2\_APP\_REPORT\_1-2012\FIGD-02\_COMPARISON\_SIMULATED\_VS\_OBSERVED\_GW\_FLOW\_PATHS.MXD



Source: Aerial photograph, USGS, 9/27/1996

**Explanation**

- Monitor well
- Approximate historical groundwater flow path based on observed water levels
- Current condition cross section model

**FREEM** **FREEMPORT-McMoRAN**  
**COPPER & GOLD**  
TYRONE STAGE 2 APP

**Comparison of Simulated and Observed Groundwater Flow Paths**

 **Daniel B. Stephens & Associates, Inc.**  
2/29/2012 JN ES09.0176

Figure D-2





**Table D-1. Constituent Input Concentrations for Current Condition Cross-Section Simulation**

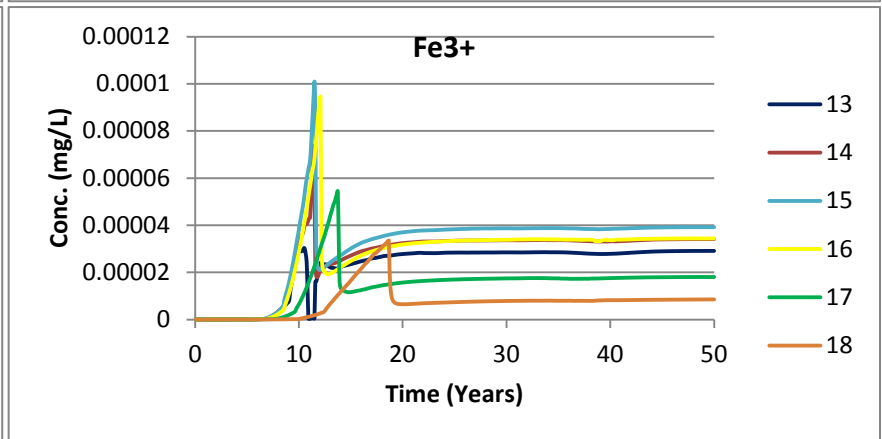
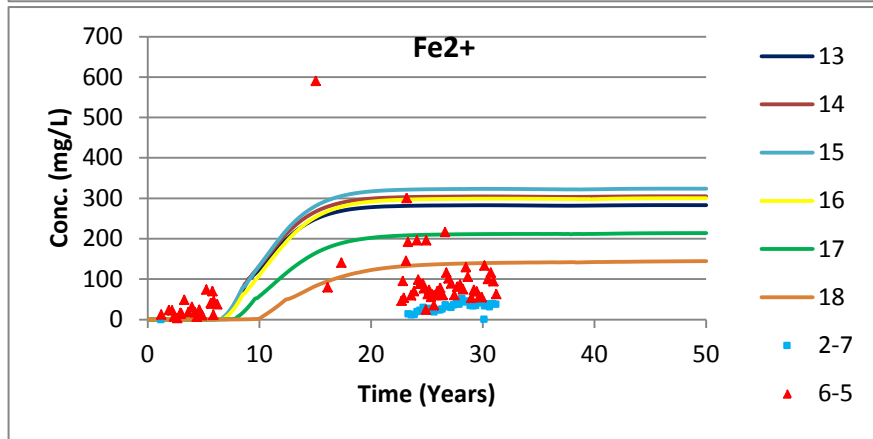
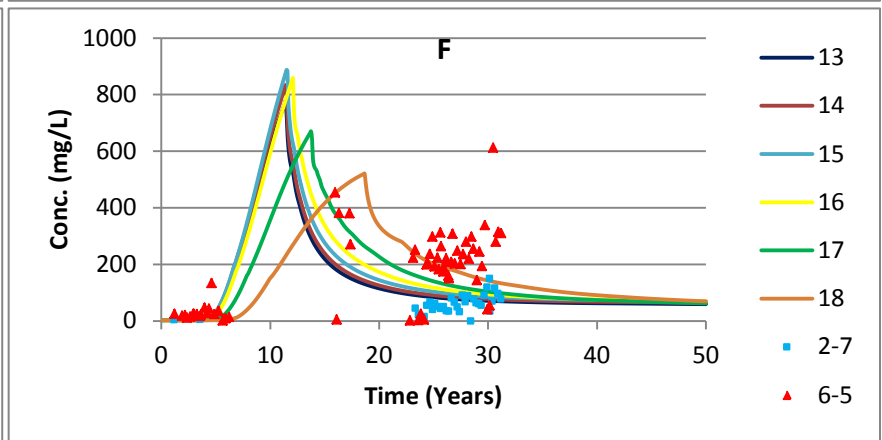
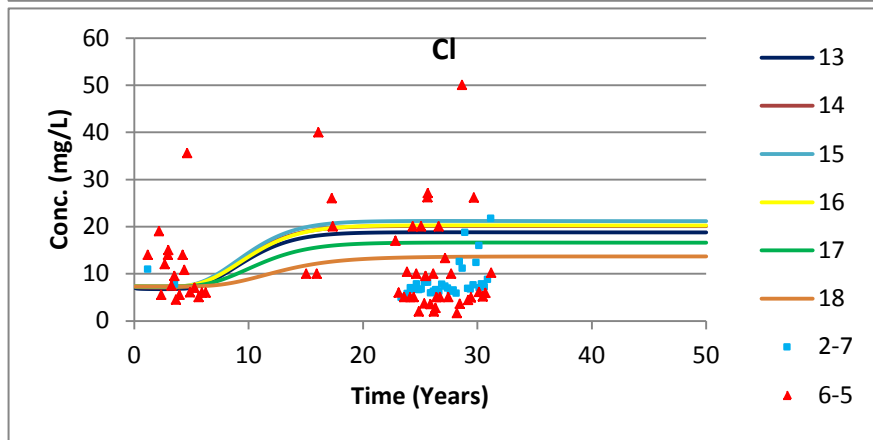
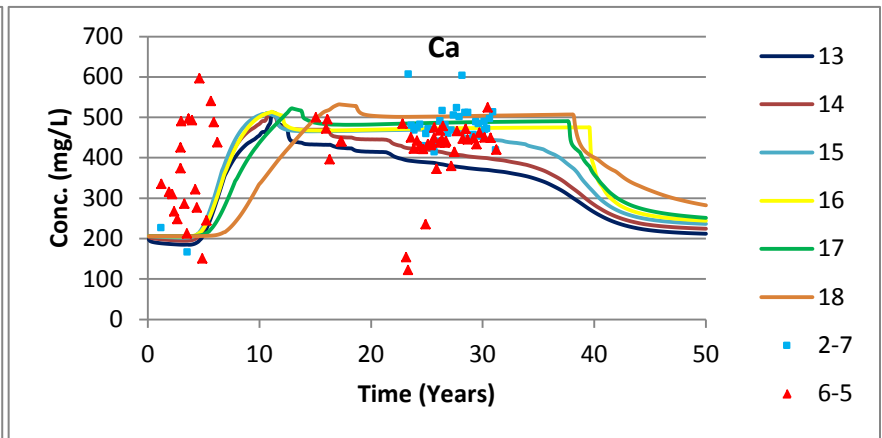
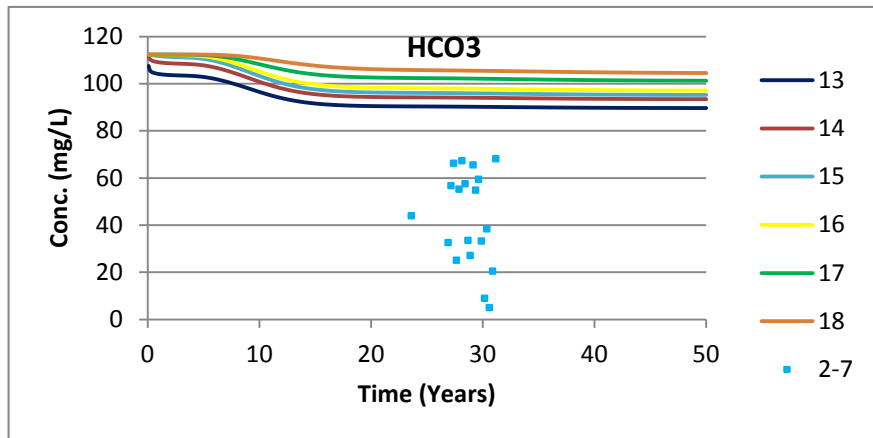
Constituent	Concentration (mg/L <sup>a</sup> )	
	Leach Stockpile Seepage	Cross Section
<i>Sampling Point</i>	<i>Average of LD2P and 2A-PLS Collections</i>	<i>Well 2-5A</i>
<i>Sampling Date</i>	<i>2001-2009</i>	<i>2001-2009</i>
Aluminum (Al)	5,939.10	0.07
Arsenic (As)	0.68	0.02
Bicarbonate (HCO <sub>3</sub> )	1.22	112.37
Cadmium (Cd)	16.45	0.00
Calcium (Ca)	499.14	168.24
Chloride (Cl)	114.61	7.32
Chromium (Cr)	0.90	0.01
Cobalt (Co)	25.73	0.02
Copper (Cu)	697.54	0.02
Fluoride (F)	463.68	1.64
Iron (ferrous) (Fe <sup>2+</sup> )	2,371.28	3.52
Iron (ferric) (Fe <sup>3+</sup> )	124.80	0.19
Lead (Pb)	0.29	0.02
Magnesium (Mg)	2,812.38	45.41
Manganese (Mn)	1,650.00	2.17
Nickel (Ni)	6.86	0.01
Oxygen (O(0))	0.00	2.00
Potassium (K)	15.61	3.78
Silica (Si)	100.00	1.00
Sodium (Na)	23.73	47.68
Sulfate (SO <sub>4</sub> )		
After charge balance adjustment	56,351.00	629.43
Before charge balance adjustment	56,716.00	551.62
pH (s.u.)	2.01	6.47
pe (s.u.)	8.00	4.00
Zinc (Zn)	1,962.04	0.44

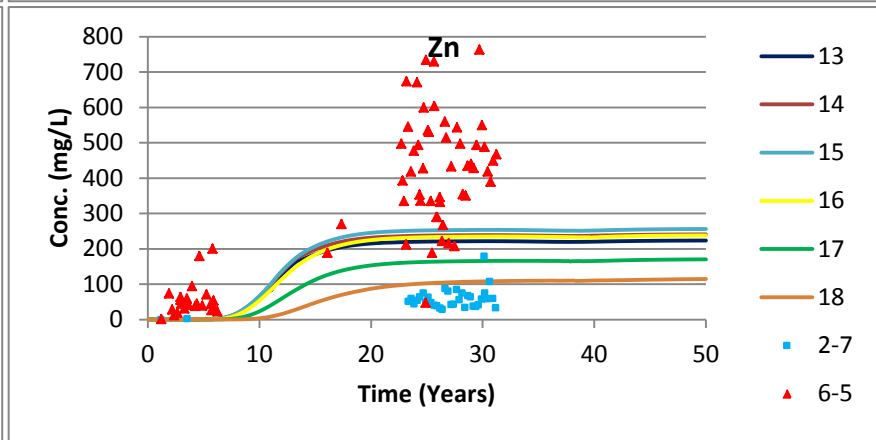
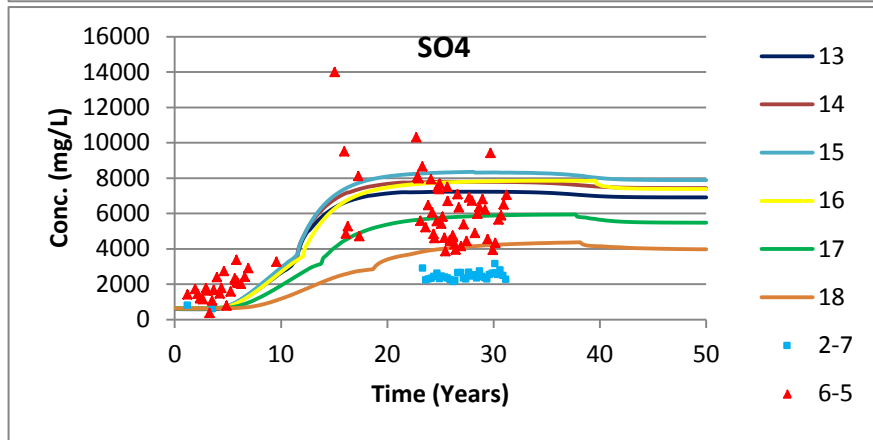
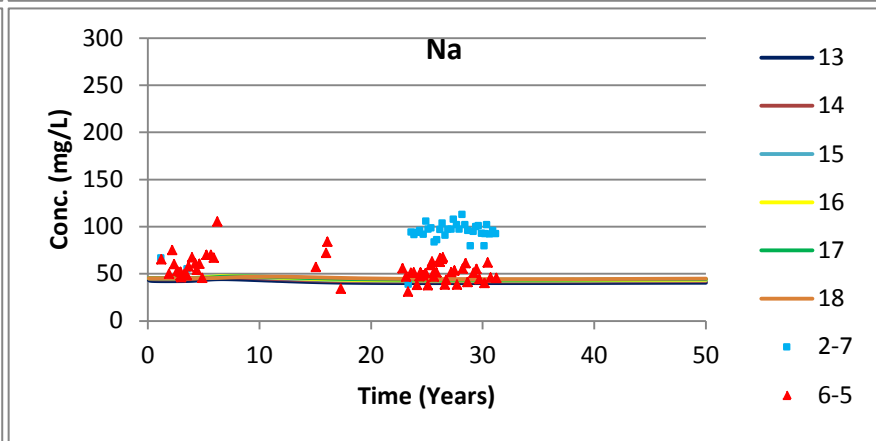
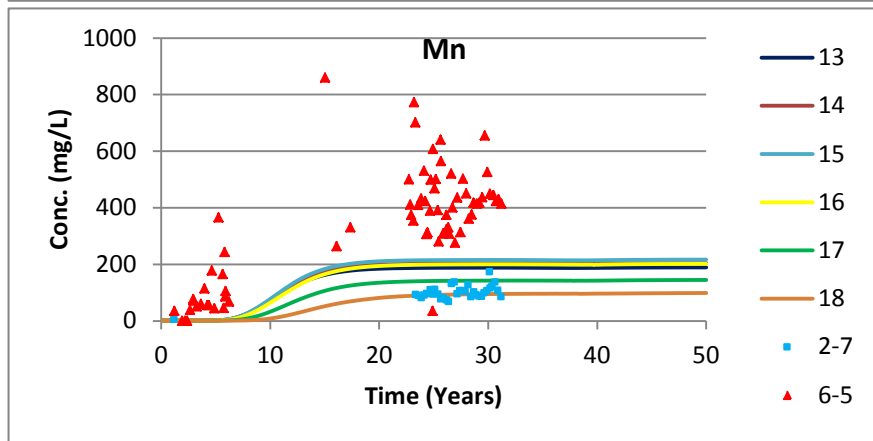
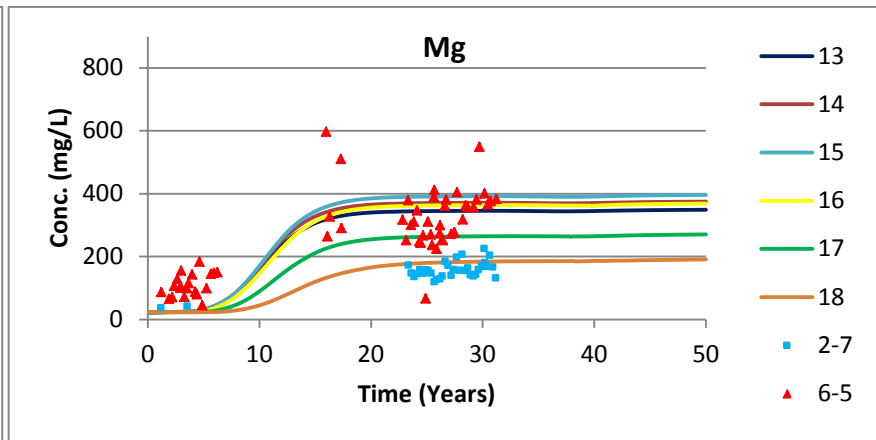
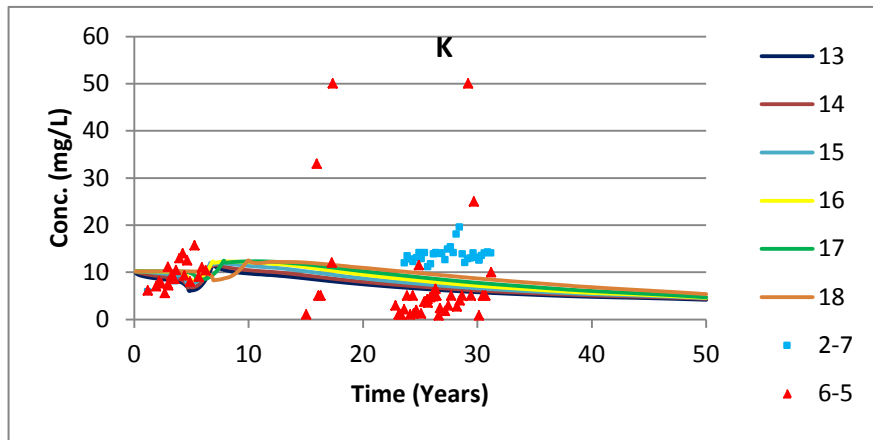
<sup>a</sup> Unless otherwise noted

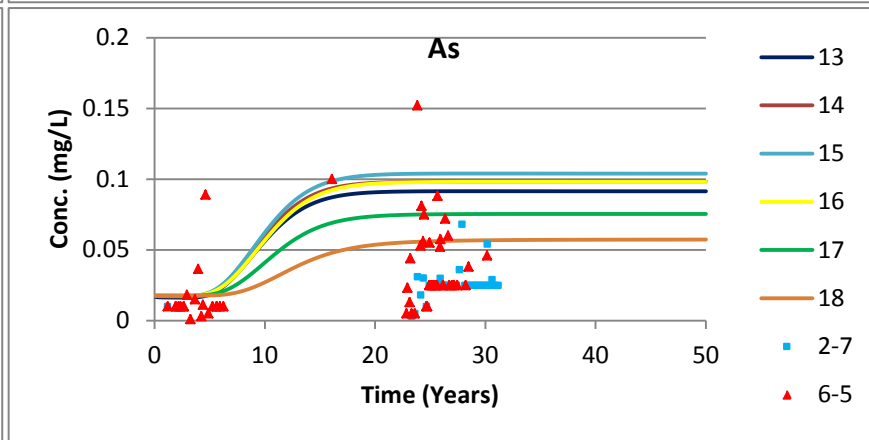
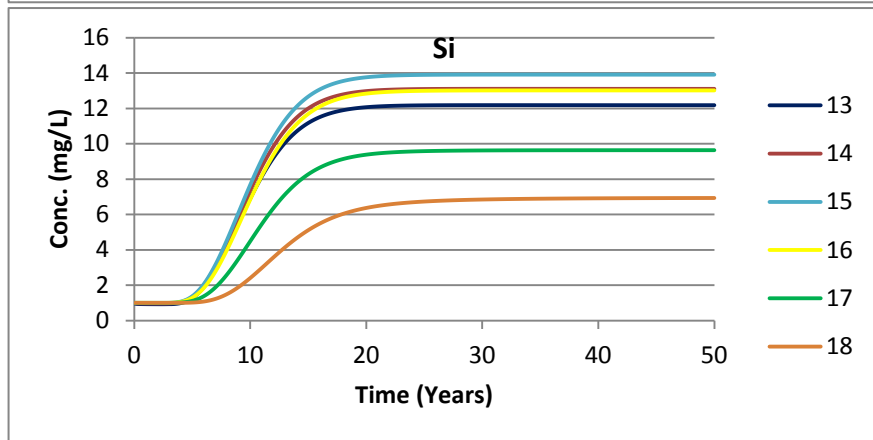
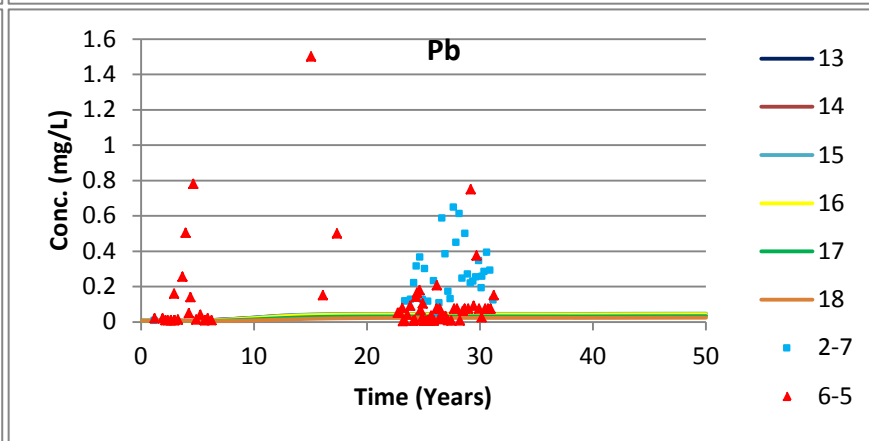
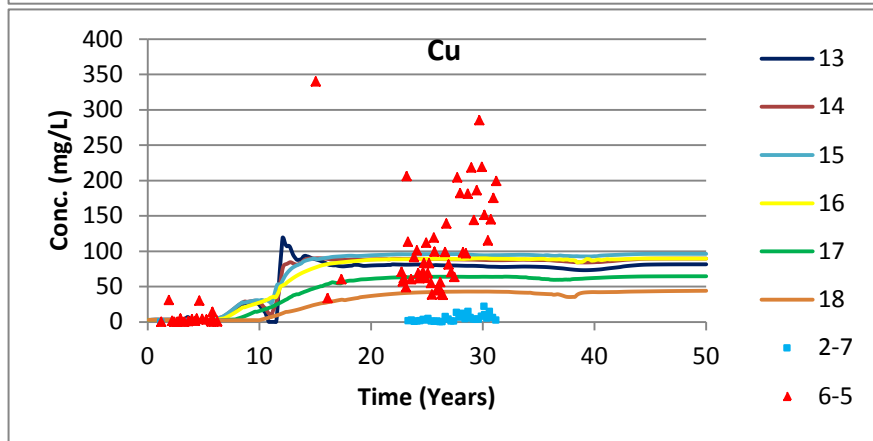
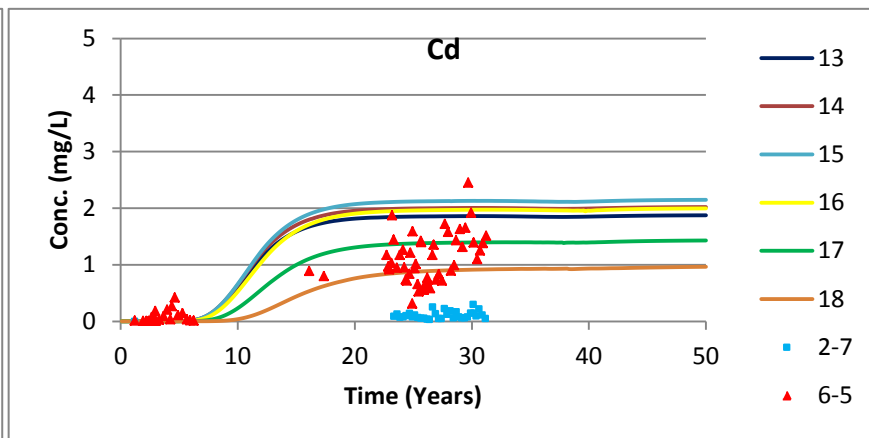
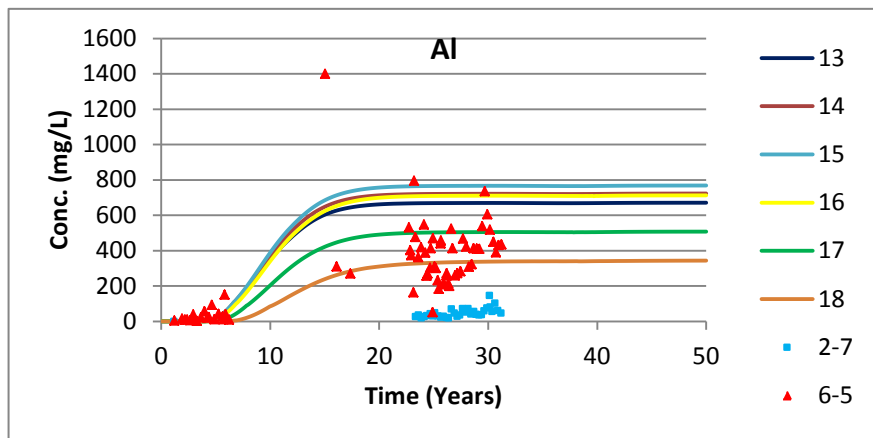
mg/L = Milligrams per liter

s.u. = Standard units

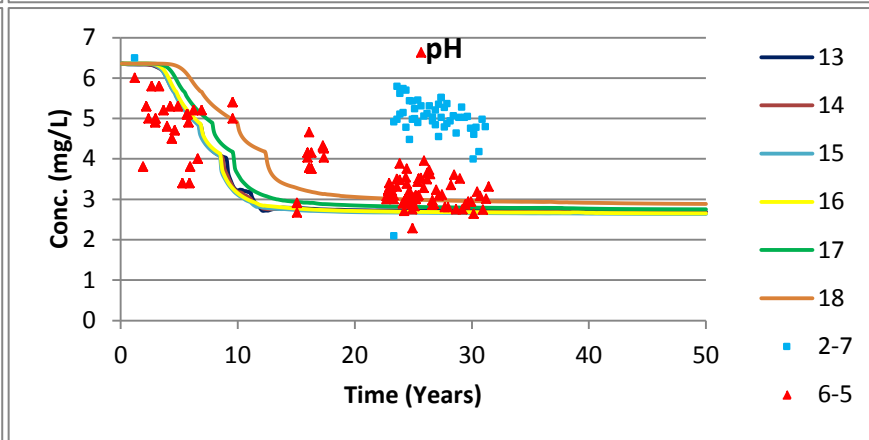
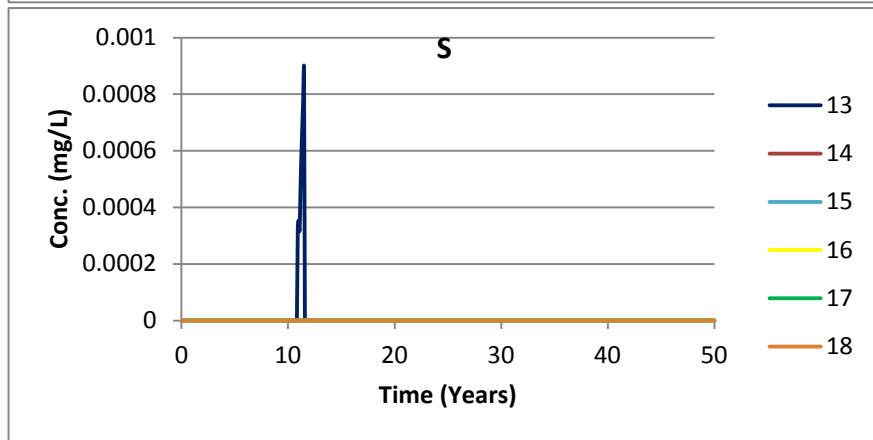
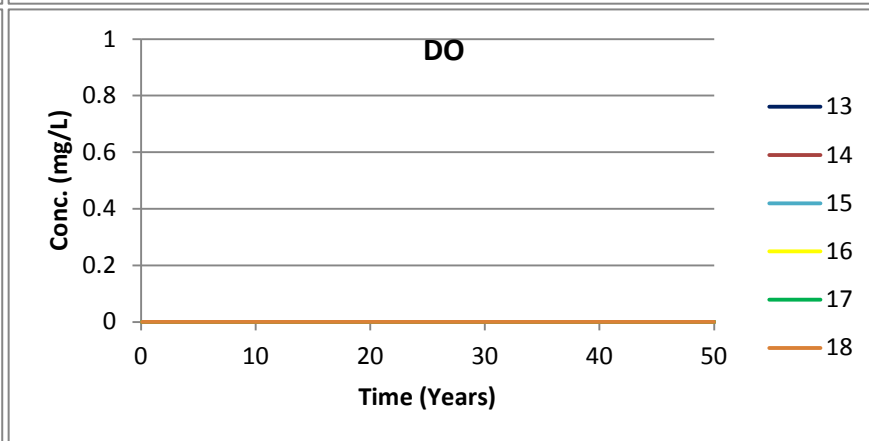
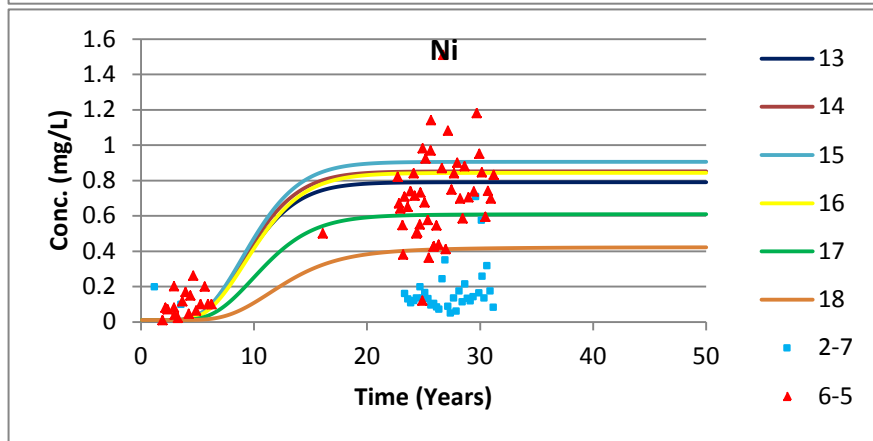
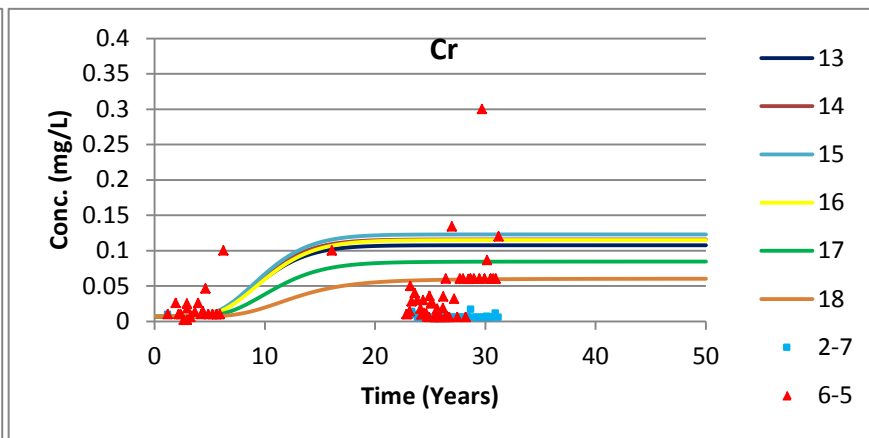
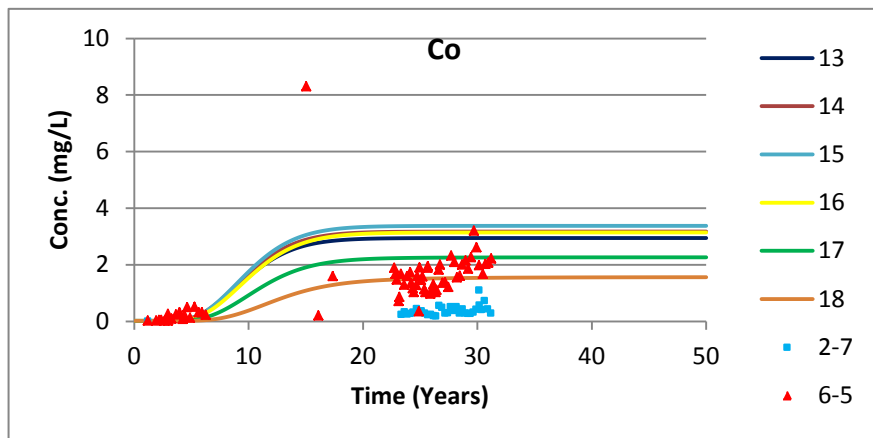
pe = Oxidation-reduction potential

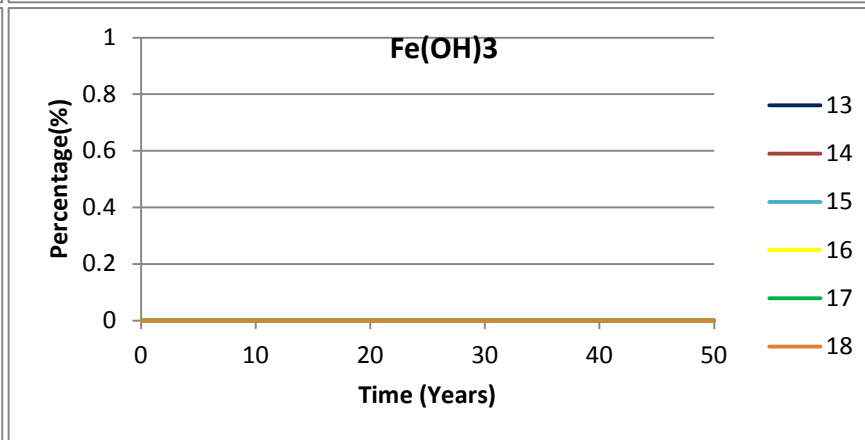
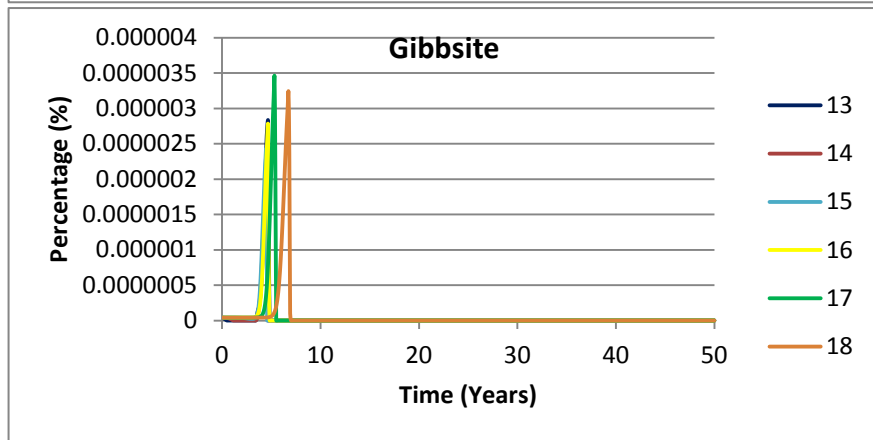
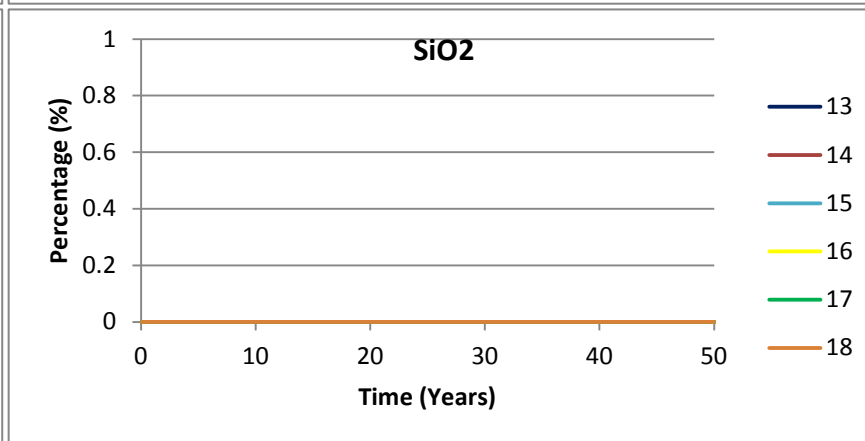
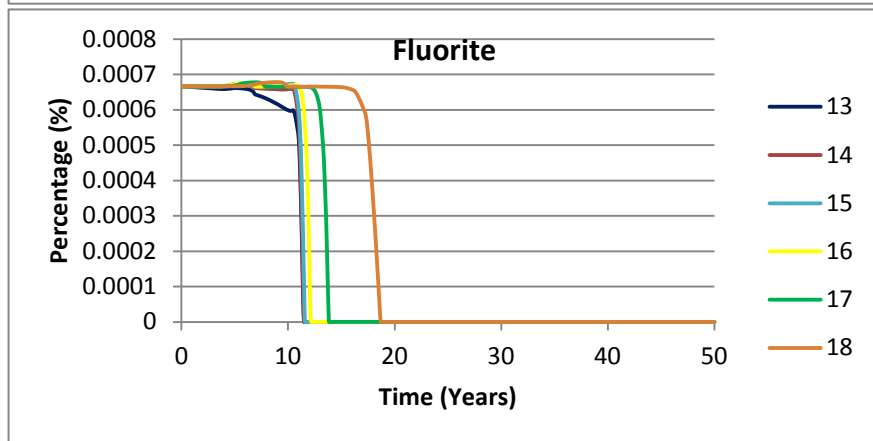
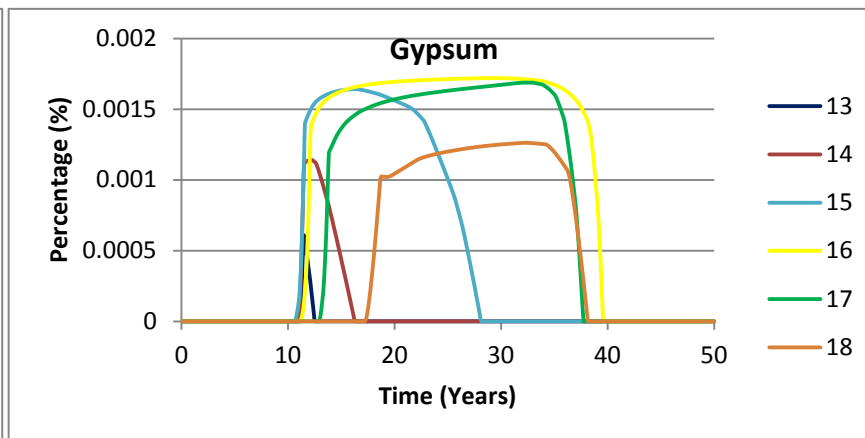
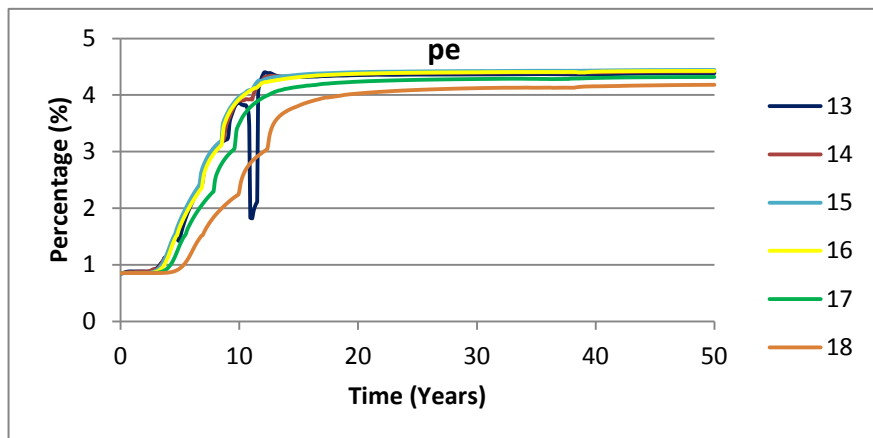


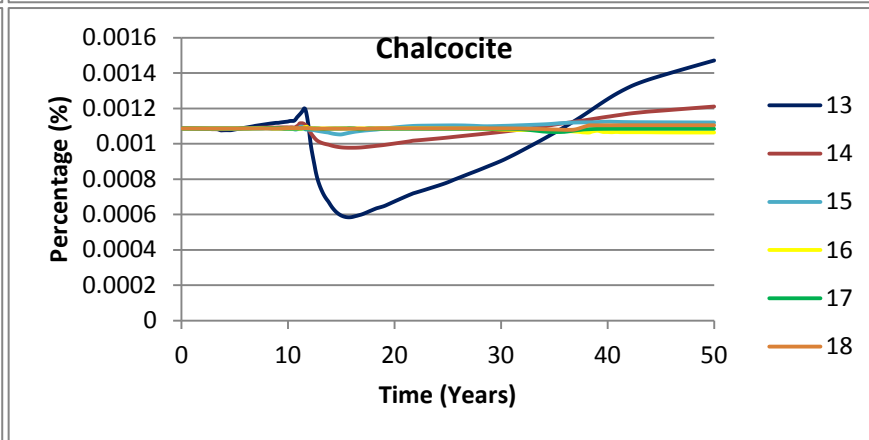
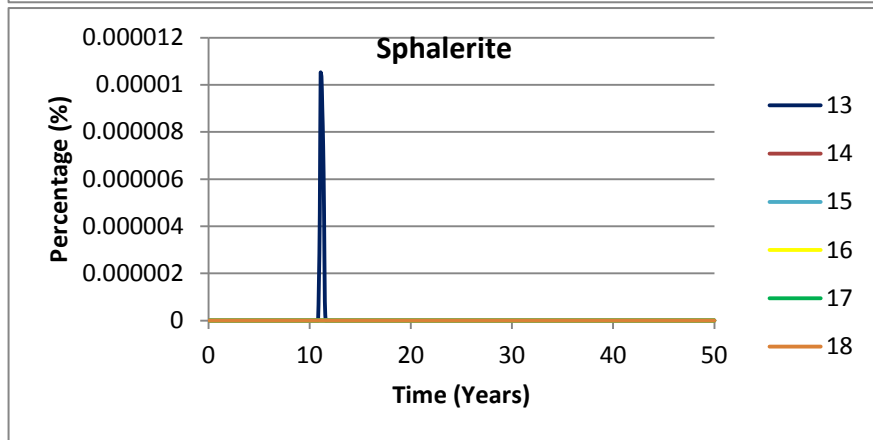
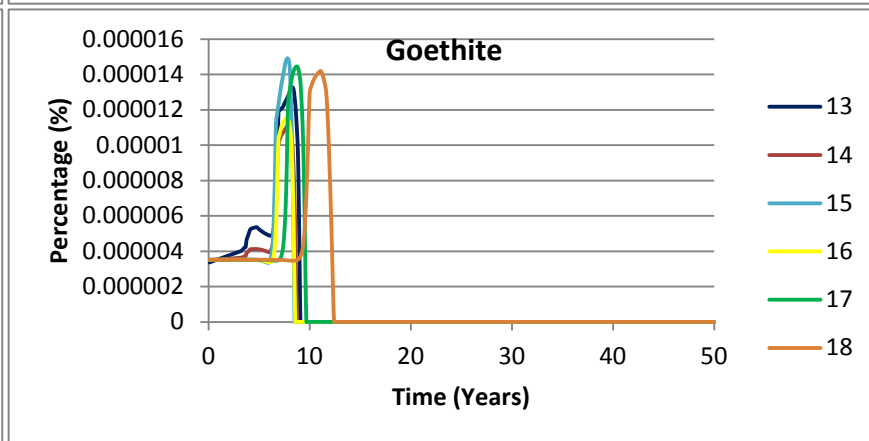
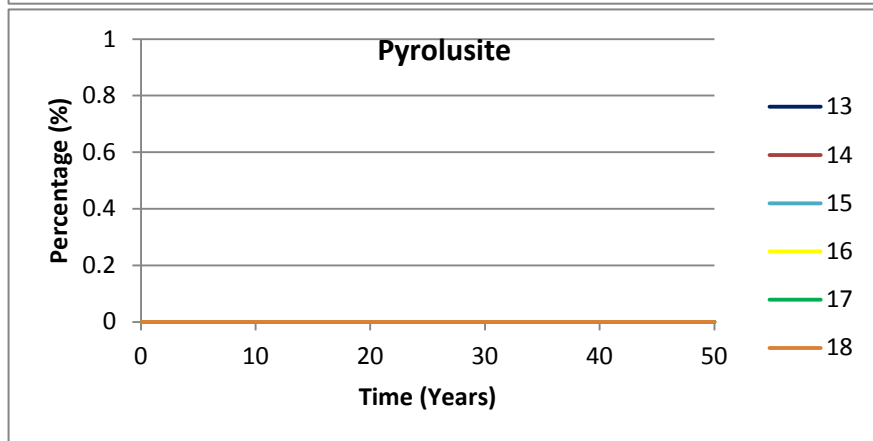
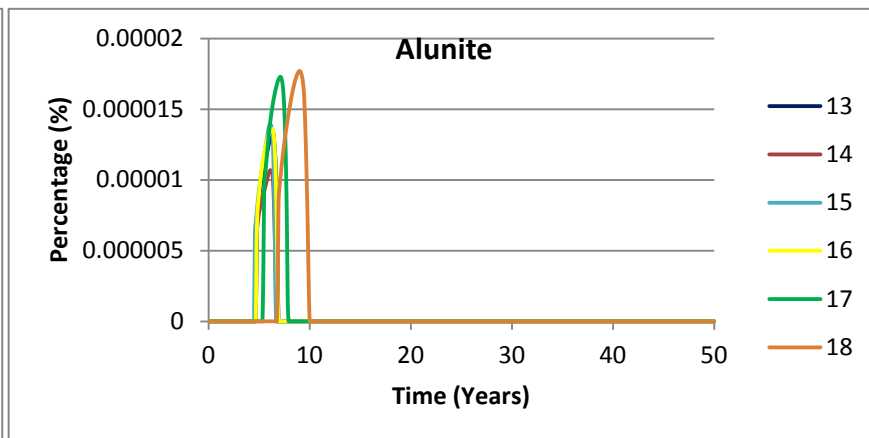
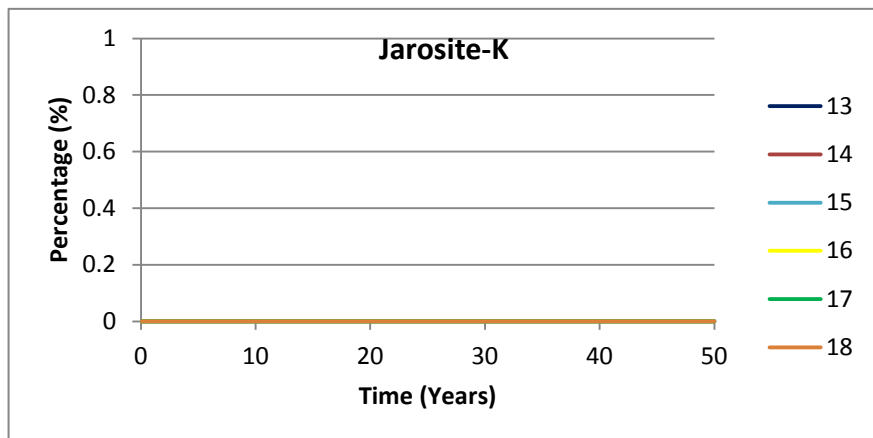


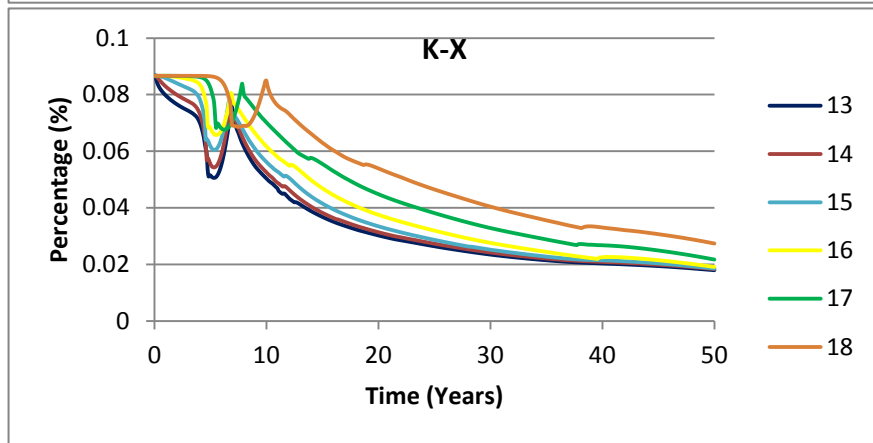
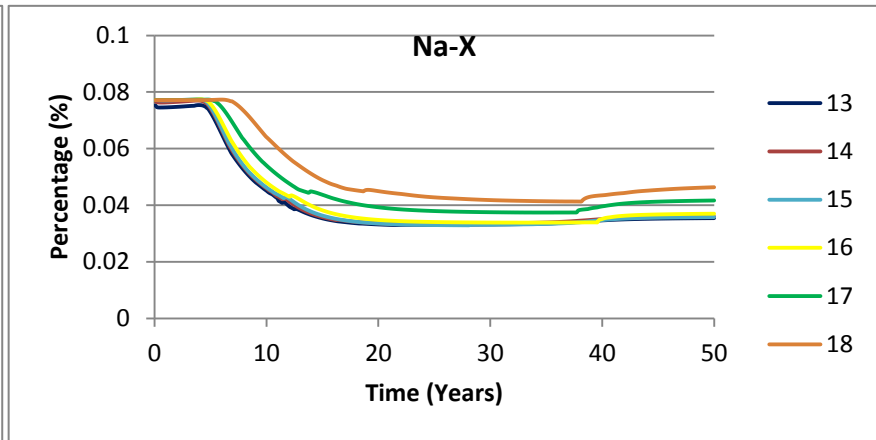
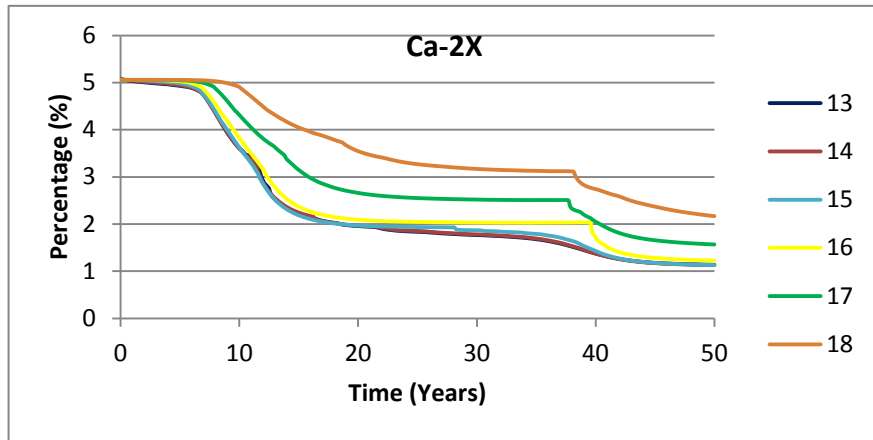












## **Appendix E**

### **Predicted Surface Water Inflow to the Main and Gettysburg Pits**



REPORT

# PIT RUNOFF SIMULATIONS FOR THE STAGE 2 ABATEMENT PLAN PROPOSAL

TYRONE MINE

**Submitted To:** Daniel B Stephens & Associates, Inc.  
6020 Academy NE, Suite 100  
Albuquerque, NM 87002

**Submitted By:** Golder Associates Inc.  
18300 NE Union Hill Road, Suite 200  
Redmond, WA 98052 USA

**Distribution:** Neil Blandford

February 23, 2012

Project No. 113-80040

**A world of  
capabilities  
delivered locally**





---

## EXECUTIVE SUMMARY

Freeport-McMoRan Tyrone Inc. (Tyrone) and the New Mexico Environment Department (NMED) entered into a Settlement Agreement and Stipulated Final Order (Settlement Agreement) in December 2010. The Settlement Agreement was entered into in response to the Decision and Order on Remand issued by the New Mexico Water Quality Control Commission (NMWQCC) on February 4, 2009 and Tyrone's appeal thereof.

In June 2011, Tyrone submitted the proposed modeling approach for the prediction of groundwater quality after implementation of closure measures. The modeling and analysis will be submitted with the Tyrone Stage 2 Abatement Plan as required by Item 31 of the Settlement Agreement. The simulation results from this effort will be used to assist with the determination of alternative abatement standards (AAS) for groundwater at Tyrone. Surface runoff from the pit walls and adjacent stockpile surfaces surrounding the Main and Gettysburg Pits are required as a component in the Stage 2 Abatement Plan Proposal groundwater modeling.

A series of Monte Carlo simulations were run to estimate the volume and water quality associated with runoff into the Main and Gettysburg Pits during the post-closure period. The water is assumed to report to sump areas where it will be treated. The water quality of the runoff within the pit area will vary due to differences in the mineralogy of the stockpile and open pit surfaces. The flows will also be variable due to differences in the surface conditions. The contribution from the pit wall runoff is greatest during the summer monsoon season. As a result, the rate and quality of the runoff that will have to be treated will vary over the course of the year and between years due to variability in climate conditions. In order to evaluate the scope of the variability, two sets of simulations were run. A 50-year simulation period evaluated the long-term average flow and water quality conditions. A second set of simulations with a one-year duration evaluated the variability of these conditions on an annual and monthly basis.

Regional climate data was used for the runoff calculations. The record contains climate data over a sufficiently long period to be representative of the climate range and variability at the mine site. The daily precipitation data were combined with the catchment surface areas to estimate the runoff rate for each of the open pits. A total of 1,000 Monte Carlo realizations were run for each of the two pits over the 50-year simulation period. The average (mean) runoff for the Main Pit is approximately 60 gallons per minute (gpm) and 6 gpm for the Gettysburg Pit over the 50-year simulation period. The mass loading was estimated by combining the flows with constituent concentrations representative of the different exposed mineralogies around the pits. The average sulfate concentration is 2,380 milligrams per liter (mg/l) in the Main Pit compared to 6,070 mg/l in the Gettysburg Pit due to the relatively small stockpile areas that contribute runoff in the Gettysburg Pit (and thus the greater contribution of higher-concentration runoff from the pit walls).

A total of 10,000 realizations were run for the one-year simulations. There is a broad range in the distribution of results due to variability in the annual precipitation within the regional climate record. The mean and median values are similar to the average 50-year simulation results although the range for one-year minimum and maximum results is much greater, as would be expected given the variability in the annual precipitation over the climate record used. The maximum (95<sup>th</sup> percentile) runoff rate into the Main Pit over a one-year period is around 132 gpm.

The average constituent concentrations in the cumulative runoff to the Main Pit from the one-year simulations increase are from 10% to 30% lower than the average concentrations from the 50-year simulations. The 50-year simulations are more likely to include one or more of the climate years with large storm events that result in high runoff volumes (and greater mass loading) from the pit walls.

## Table of Contents

EXECUTIVE SUMMARY .....	ES-1
1.0 PIT RUNOFF CALCULATIONS .....	1
1.1 Methodology .....	1
2.0 SIMULATION RESULTS .....	4
2.1 50-Year Simulation .....	4
2.2 One-Year Simulation .....	4
3.0 CLOSING .....	6
4.0 REFERENCES .....	7

## List of Tables

Table 1	Plan Area, Rock Type, Closure Condition and CN Assumed in Runoff Calculations
Table 2	Water Quality of Pit Runoff by Zone and Consolidated Flow
Table 3	Water Quality Assumed for Leach and Waste Rock Stockpile Runoff
Table 4	50-Year Simulation Results – Runoff within Main Pit (Gallons)
Table 5	Average Constituent Concentration in the Cumulative Runoff in the Main Pit at the End of the 50-Year Simulation Period
Table 6	50-Year Simulation Results – Runoff within Gettysburg Pit (Gallons)
Table 7	Average Constituent Concentration in the Cumulative Runoff in the Gettysburg Pit at the end of One-Year Simulation Period
Table 8	One-Year Simulation Results – Annual Runoff within Main Pit (Gallons)
Table 9	One-Year Simulation Results – Annual Runoff within Main Pit by Month (Gallons)
Table 10	Average Constituent Concentration in Main Pit at the End of One-Year Simulation Period
Table 11	One-Year Simulation Results – Annual Runoff within Gettysburg Pit (Gallons)
Table 12	Average Constituent Concentration in Gettysburg Pit at the End of One-Year Simulation Period

## List of Figures

Figure 1	Plan View of Main and Gettysburg Pits and Adjacent Stockpiles
Figure 2	Time History Chart of Mean Runoff Water Quality in Main Pit (One-Year Simulation Model)

---

## 1.0 PIT RUNOFF CALCULATIONS

A series of Monte Carlo simulations were run to estimate the volume and water quality associated with runoff into the Main and Gettysburg Pits during the post-closure period. Sources of runoff include the pit walls and bottom as well as adjacent stockpile surfaces upon which the surface runoff reports to the pits. The water is assumed to report to sump areas where it will be pumped to a water treatment plant and treated to meet section 3103 standards. The water quality of the runoff will vary due to differences in the mineralogy of the stockpile and open pit surfaces. The flows will also be variable due to differences in the surface conditions. These results show the difference in the contribution from the pit wall runoff being more important during the summer monsoon season. As a result, the rate and quality of the runoff that will have to be treated will vary over the course of the year and between years due to variability in climate conditions. In order to evaluate the scope of the variability, two sets of simulations were run. A 50-year simulation period was run to evaluate the long-term average flow and water quality conditions. The second set of simulations had a one-year duration to evaluate the variability of these conditions on an annual and monthly basis.

### 1.1 Methodology

The Soil Conservation Service Curve Number (SCS-CN) method (USDA-SCS 1986) was used to calculate runoff. The SCS-CN model is a commonly used method for estimating the portion of precipitation that becomes runoff during a storm event. Precipitation excess (runoff) is assumed to be a function of cumulative precipitation, soil cover, land use, and antecedent moisture conditions. The precipitation excess, and hence the runoff, is assumed to be zero until the accumulated rainfall exceeds some initial abstraction value. The SCS-CN method uses curve numbers to represent different types of soil and cover characteristics in a watershed. The curve number determines what portion of precipitation is intercepted. The larger the curve number, the greater the fraction of precipitation that reports as runoff. The SCS-CN method was used to estimate the runoff in the DP-1341 Condition 89 Feasibility Study (Golder Associates 2007a).

The SCS-CN equation for estimating runoff is:

$$Q = (P - I_a)^2 / (P - I_a) + S \quad [\text{Eq. 1}]$$

Where Q is the depth of direct runoff (inches), P is the total precipitation (inches),  $I_a$  represents interception (inches), surface storage, and infiltration that occurred before runoff begins. S is the potential maximum retention at the start of the storm (inches) and is a function of the curve number (CN):

$$S = (1000 - 10 \text{ CN}) / \text{CN} \quad [\text{Eq. 2}]$$

Field data were used to develop a relationship between  $I_a$  and S.

$$I_a = 0.2 S \quad [\text{Eq. 3}]$$



Figure 1 contains a plan view of the boundaries of the Main and Gettysburg Pits and the portions of the adjacent stockpile areas that are within the catchment area of the pits. The arrows indicate direction of runoff. Table 1 contains the surface area and CN for each of the subareas. The CN for stockpiles is based on field measurements at the Chino Mine following several large storm events (Golder Associates 2007b). The CN assigned to the pit wall is based on professional judgment since there are no direct measurements of runoff available to develop an estimate. The type and cover status in the table are related to the water quality of the runoff discussed below.

The precipitation (P) in equation [1] is based on regional climate data from the Ft. Bayard weather station (Western Regional Climate Center, 2001, Station Number 289265, Fort Bayard) located approximately 15 miles from the Tyrone Mine. The record contains measured daily precipitation and other climate data. The data record is sufficiently long to be representative of the climate range and variability at the mine site. The daily precipitation data are combined with the associated CN to estimate the runoff depth (Q) and multiplied by the surface area to estimate the runoff rate for each of the components. The climate data used in the simulations is from the period 1897 to 2006 to be consistent with the record used for the Condition 89 Feasibility Study (Golder Associates 2007a) and are based on a one-day time step (i.e., daily precipitation).

Simulations were run over two durations. Simulations (50-year) were run to examine the long-term conditions. A second set of simulations was run with a one-year duration to investigate the short-term variability in the runoff due to climate variability.

For the 50-year simulations, the climate record is treated as a continuous “loop” in which the starting year in the climate record is sampled randomly (always beginning on January 1<sup>st</sup>). The record follows the same sequence in the Ft. Bayard climate record until year 2006 is reached when the sequence returns to the 1897 data. This approach preserves the integrity of the 110 year data record while allowing the climate conditions to vary between simulations. In the one-year simulations, the model randomly selects a one-year period from the 110 year data record for each simulation.

The water quality associated with the runoff varies. There are three categories of water quality assumed in the analysis:

- Pit wall runoff
- Runoff from uncovered stockpile areas
- Runoff from covered stockpile area

The water quality of the runoff within the Main Pit boundary is based on wall washing station results from field experiments conducted by SARB (2000). The water quality from the experiments was observed to vary within the pit and could be broadly divided into three mineralized zones within the pit boundaries,

oxide, sulfide, and chalcantite. The average pit wall runoff compositions from the wall washing tests are shown in Table 2. In addition to the three mineralized zones, there is a portion of the pit wall that exposes Gila Conglomerate. This area is assumed to have a similar runoff quality to the oxide zone. The area of the three zones is approximately 50% oxide, 30% sulfide and 20% chalcantite. The water quality of the pit runoff is calculated by flow weighting the contributions from the three zones. The runoff from the Gettysburg Pit surfaces is assumed to be of the same quality as the flow-weighted average runoff in the Main Pit (see Table 2).

The water quality of the runoff from the stockpiles is based on the results of Meteoric Water Mobility Procedure (MWMP) tests. The MWMP tests were conducted as part of the Supplemental Materials Characterization Study for DP-1341, Condition 80 (EnviroGroup 2005). Separate runoff quality estimates were developed for the Leach Ore Stockpiles and Waste Rock Piles using the associated MWMP results (Golder Associates 2007a, Appendix D). Representative MWMP results for the Leach Ore Stockpile and Waste Rock Pile were selected based upon a comparison with the average results for each data set. The selected runoff qualities for the Leach Ore Stockpiles and Waste Rock Piles are listed in Table 3. All of the leach stockpile surfaces that report to the Main and Gettysburg Pits are assumed to be covered in the simulations. Hence, only the waste rock water quality data were incorporated in the simulations.

There are no water quality data available for the runoff from covered stockpile areas. For the purpose of this analysis, the constituent concentrations are assumed to be 10% of the concentrations for the waste rock stockpile runoff. The runoff from these areas is assumed to be routed along water conveyance structures to minimize contact with the exposed rock within the open pit to minimize the dissolution of minerals.

This analysis focuses solely on flow and water quality associated with runoff. Direct precipitation, evaporation, groundwater inflow, and other processes occurring within the pit lake or sumps were not considered.



---

## 2.0 SIMULATION RESULTS

The results from the Main and Gettysburg Pits runoff simulations are summarized below. The results for the 50-year simulations are presented in Section 2.1 followed by the one-year simulation results in Section 2.2.

### 2.1 50-Year Simulation

Table 4 contains the mean, median, minimum and maximum runoff volumes in the Main Pit over a 50-year simulation period. The minimum and maximum values correspond with the 0.05 and 0.95 percentile values. A total of 1,000 realizations were run. The range between the high and low values is relatively small which suggests that a 50-year climate period is fairly representative of the long-term climate variability at the site. The average (mean) annual runoff volume is approximately 31.1 million gallons or around 60 gallons per minute (gpm). The maximum rate is 35.0 million gallons or 67 gpm.

The flows and constituent concentrations were used to calculate the mass loading associated with the runoff. The cumulative mass over the 50-year period was divided by the total runoff to calculate the long-term average water quality in the runoff to the pit. The average constituent concentrations in the Main Pit cumulative runoff at the end of the 50-year simulation period are shown in Table 5. The relatively high constituent concentrations in the pit wall runoff are diluted by the relatively low concentration in the runoff from the stockpiles. For example, the 50-year average sulfate concentration is 2,405 milligrams per liter (mg/l) compared to a concentration of almost 12,000 mg/l in the runoff contribution from the pit walls.

Table 6 contains the results from the runoff simulations for the Gettysburg Pit. The inputs to the model are identical except for the pit and stockpile areas. The long-term average annual rate is about 8 gpm. The average constituent concentrations in the cumulative runoff at the end of the 50-year simulation period for the Gettysburg Pit are shown in Table 7. The mean sulfate concentration is 6,131 mg/l, higher than in the Main Pit due to the relatively small stockpile areas that contribute lower-concentration runoff.

### 2.2 One-Year Simulation

Table 8 contains the mean, median, minimum and maximum runoff volumes within the Main Pit for a one-year simulation period. The minimum and maximum values correspond with the 0.05 and 0.95 percentile values. A total of 10,000 realizations were run. There is a broad range in the distribution of results due to variability in the annual precipitation within the Ft. Bayard climate record. The majority of the runoff is from the stockpiles surrounding the pit. Runoff within the pit accounts for approximately 20% of the total volume. While the two areas are similar (the area represented by the stockpiles is 75 acres larger than the pit), the higher CN for the stockpile runoff results in a significantly higher runoff volume.



The mean and median values from the one-year simulations are similar to the 50-year simulation results when converted to an annual basis. The range for one-year minimum and maximum results is much greater for the one-year simulations as would be expected given the variability in the annual precipitation over the 110-year climate record. The maximum rate over a one-year period is around 133 gpm.

Table 9 contains the mean, median and maximum runoff volumes in the Main Pit on a monthly basis. The percentage of simulations where there was no runoff is also shown. The distribution of monthly runoff results is positively skewed as indicated by the large percentile of months with no runoff. These results are due to the relatively low precipitation depths during the non-monsoon months when the rainfall typically does not exceed the initial abstraction ( $I_a$ ) depth (Equation 3). The greatest maximum (0.95 percentile) monthly average rate (758 gpm) occurs in August.

A time-history chart of the average constituent concentrations in the cumulative runoff to the Main Pit from the one-year simulations is shown in Figure 2. The concentrations are lower during the first half of the year when there is little runoff from the pit walls. The concentrations increase in the summer when monsoon runoff from the pit walls produces significantly higher levels of dissolved minerals. The average constituent concentrations in the cumulative runoff at the end of one-year simulation period are shown in Table 10. The average concentrations from the one-year simulations are from 10% to 30% lower than the average concentrations from the 50-year simulations (e.g., 1,932 mg/l versus 2,405 mg/l  $SO_4$  in the Main Pit). The 50-year simulations are more likely to include one or more of the climate years with large storm events that result in high runoff volumes (and greater mass loading) from the pit walls.

Table 11 contains the mean, median, minimum and maximum runoff volumes within the Gettysburg Pit for a one-year simulation period. All inputs other than the capture area are identical to those in the Main Pit one-year simulations. The long-term average annual rate is about 7 gpm slightly less than the 50-year average. The average annual constituent concentrations in the cumulative runoff are shown in Table 12. The sulfate concentration is 5,022 mg/l, more than twice the average concentration in the Main Pit due to the relatively small stockpile areas that contribute runoff in Gettysburg (and thus the greater contribution of higher-concentration runoff from the pit walls).

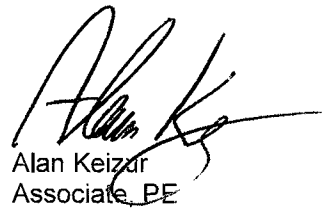
### 3.0 CLOSING

The Monte Carlo simulation estimates of the volume and water quality associated with runoff into the Main and Gettysburg Pits during the post-closure period are based on currently available information. Sources of runoff include the pit walls and bottom as well as adjacent stockpile surfaces upon which the surface runoff reports to the pits. The runoff rates will vary seasonally with the majority of the runoff occurring during the summer monsoon season. The water quality of the runoff will vary within the pit areas due to differences in the mineralogy of the stockpile and open pit surfaces. The flows will also be variable due to differences in the surface conditions. Any changes to pit geometry or assumptions concerning the stockpile dimensions or surface mineralogy may result in changes to projected flow and water quality projections.

#### GOLDER ASSOCIATES INC.



Charles Voss  
Principal



Alan Keizer  
Associate, PE

CV/AK/km



#### 4.0 REFERENCES

- EnviroGroup Limited. 2005. Supplemental Materials Characterization of the Leached Ore Stockpiles and Waste Rock Stockpiles, Final Report for DP 1341, Condition 80, Tyrone Mine. Prepared for Phelps Dodge Tyrone Inc. December 29
- Golder Associates Inc. 2007a. DP-1341 Condition 89 Feasibility Study, Phelps Dodge Tyrone, Inc. November 12
- Golder Associates Inc. 2007b. Technical Memorandum, RE UNSAT-H Simulations for DSM Feasibility Study – Tyrone Mine., May 30
- USDA-SCS (U.S. Department of Agriculture-Soil Conservation Service) 1986. Urban Hydrology for Small Watersheds, Technical Release No. 55, U.S. Government Printing Office, Washington, DC
- SARB. 2000. Pit Lake Water Quality Modeling, Tyrone Mine. Prepared for Phelps Dodge Tyrone Inc., February 29.

## TABLES

**Table 1 Plan Area, Rock Type, Closure Condition and CN Assumed in Runoff Calculations**

Component	Area (acres)	Type	Covered/Uncovered	CN
Main Pit	337	Oxide zone	Uncovered	75
Main Pit	202	Sulfide zone	Uncovered	75
Main Pit	135	Chalcanthite zone	Uncovered	75
3B	60	Waste rock	Uncovered	85
2A (top)	41	Leach rock	Covered	85
2A (slopes)	99	Leach	Uncovered	85
4A/2B/2C/7B	177	Leach rock	Uncovered	85
8A	133	Waste	Uncovered	85
8C	88	Waste rock	Covered	85
6B (top only)	34	Leach	Covered	85
6B West	9	Leach	Uncovered	85
Lube Area	76	Waste	Covered	85
5A	31	Waste	Uncovered	85
Gettysburg Pit	223	Oxide/Sulfide/Chalc.	Uncovered	75
6C	12	Leach	Uncovered	85
1A/1B	46	Leach	Uncovered	85



**Table 2: Water Quality of Pit Runoff by Zone and Consolidated Flow**

Constituent	Oxide Zone (mg/l)	Sulfide Zone (mg/l)	Chalcanthite Zone (mg/l)	Flow Weighted (mg/l)
Al	85.7	593	170	254.75
B	0.14	0.17	0	0.121
Ca	119.5	38.6	460	163.33
Cd	0.26	0.31	1.2	0.463
Cl	8	205	439	151.3
Co	0.89	1.6	6.6	2.245
Cr	0	0.12	0	0.036
Cu	93	444	28,750	5929.7
F	34.4	6.76	37.2	26.668
Fe	23.2	1,371	45	431.9
K	35.5	0	5	18.75
Mg	98	37.3	207	101.59
Mo	0	0.04	0	0.012
Mn	26.6	8.4	57.1	27.24
Na	49.3	3.4	5.7	26.81
Pb	0	0.2	0	0.06
SO4	1,441	6,880	45,650	11915
Zn	41.6	99	116	73.7

**Table 3: Water Quality Assumed for Leach and Waste Rock Stockpile Runoff**

<b>Water Quality Constituent</b>	<b>Waste Rock Stockpiles (mg/l)</b>	<b>Leach Stockpiles (mg/l)</b>	<b>Covered Stockpiles (mg/l)</b>
Al	1.63	24	0.163
B	0.0052	0.01	0.00052
Ca	22.9	19.1	2.29
Cd	0.0164	0.164	0.00164
Cl	0.242	0.5	0.0242
Co	0.0775	0.301	0.00775
Cr	0.0003	0.0015	0.00003
Cu	10.2	31	1.02
F	0.737	5.13	0.0737
Fe	0.0134	0.587	0.00134
K	1.49	1.13	0.149
Mg	9.42	17.9	0.942
Mo	0.00113	0.0053	0.000113
Mn	2.99	13.2	0.299
Na	2.77	0.37	0.277
Pb	0.00168	0.0078	0.000168
SO <sub>4</sub>	137	364	13.7
Zn	1.69	15.1	0.169

**Table 4: 50-Year Simulation Results –Runoff within Main Pit (Gallons)**

Mean	Median	Min. (0.05 percentile)	Max. (0.95 percentile)
1,555,000,000	1, 571,000,000	1,383,000,000	1,751,000,000

**Table 5: Average Constituent Concentration in the Cumulative Runoff in the Main Pit at the End of the 50-Year Simulation Period**

Constituent	Concentration (mg/l)
Al	143.2
B	0.03
Ca	45.0
Cd	0.10
Cl	29.7
Co	0.48
Cr	0.01
Cu	1164
F	5.63
Fe	84.3
K	4.52
Mg	25.2
Mo	0.003
Mn	7.03
Na	6.82
Pb	0.01
SO4	2405
Zn	15.36

**Table 6: 50-Year Simulation Results – Runoff within Gettysburg Pit (Gallons)**

Mean	Median	Min. (0.05 percentile)	Max. (0.95 percentile)
198,000,000	200,000,000	173,000,000	225,000,000

**Table 7: Average Constituent Concentration in the Cumulative Runoff in the Gettysburg Pit at the End of 50-Year Simulation Period**

Constituent	Concentration (mg/l)
Al	209.7
B	0.06
Ca	94.4
Cd	0.24
Cl	77.1
Co	1.18
Cr	0.02
Cu	3023
F	13.9
Fe	219.8
K	10.28
Mg	56.3
Mo	0.01
Mn	15.3
Na	15.0
Pb	0.03
SO4	6131
Zn	38.3

**Table 8: One-Year Simulation Results – Annual Runoff within Main Pit (Gallons)**

Mean	Median	Min. (0.05 percentile)	Max (0.95 percentile)
31,108,000	27,909,000	4,878,000	70,035,000

**Table 9: One-Year Simulation Results – Annual Runoff within Main Pit by Month (Gallons)**

Month	Mean	Median	Perc. w/ No Runoff	Max. (0.95 perc.)
January	919,000	0	0.60	3,868,000
February	828,000	0	0.51	4,483,000
March	430,000	0	0.66	1,594,000
April	270,000	0	0.76	1,483,000
May	688,000	0	0.75	5,007,000
June	2,302,000	65,000	0.44	10,947,000
July	6,617,000	2,552,000	0.08	22,609,000
August	7,863,000	4,338,000	0.08	33,842,000
September	5,148,000	870,000	0.20	28,150,000
October	3,568,000	103,000	0.43	23,120,000
November	1,461,000	0	0.59	10,712,000
December	1,017,000	0	0.54	6,616,000

**Table 10: Average Constituent Concentration in Main Pit at the End of One-Year Simulation Period**

Constituent	Concentration (mg/l)
Al	137.6
B	0.022
Ca	39.1
Cd	0.082
Cl	23.6
Co	0.396
Cr	0.006
Cu	927
F	4.58
Fe	67.1
K	3.81
Mg	21.4
Mo	0.003
Mn	6.03
Na	5.83
Pb	0.010
SO4	1932
Zn	12.5

**Table 11: One-Year Simulation Results – Annual Runoff within Gettysburg Pit (Gallons)**

Mean	Median	Low (0.05 percentile)	High (0.95 percentile)
3,950,000	3,313,000	436,000	10,474,000

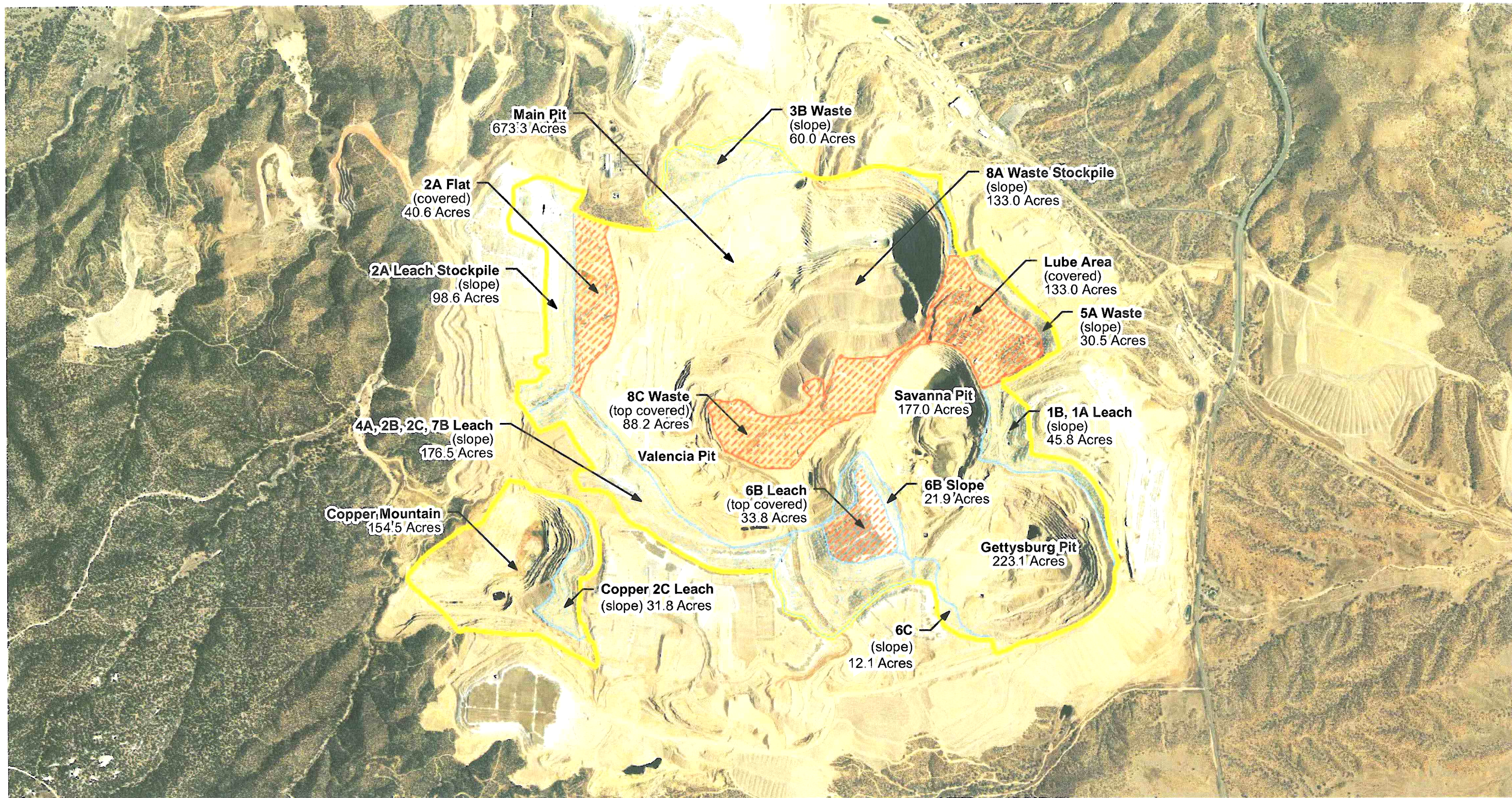
**Table 12: Average Constituent Concentration in Gettysburg Pit at the End of One-Year Simulation Period**

Constituent	Concentration (mg/l)
Al	201.1
B	0.053
Ca	81.1
Cd	0.202
Cl	62.9
Co	0.976
Cr	0.0150
Cu	2465
F	11.5
Fe	179.1
K	8.65
Mg	47.6
Mo	0.006
Mn	13.0
Na	12.7
Pb	0.0259
SO4	5022
Zn	31.6



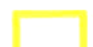


## FIGURES





Source: Aerial photograph from NAIP, 2011  
 Daniel B. Stephens & Associates, Inc., 2/22/2012

**EXPLANATION**

-  Open Pit Surface Drainage Area
-  Flat Reclaimed Areas (Store and Release Cover)
-  Interior Slope Areas (No Cover)

Notes: 1. Inside the open pit surface drainage areas, surface runoff will be to one of the pits.  
 2. Outside the open pit surface drainage areas, all stockpiles will be covered.

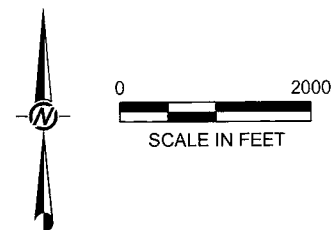
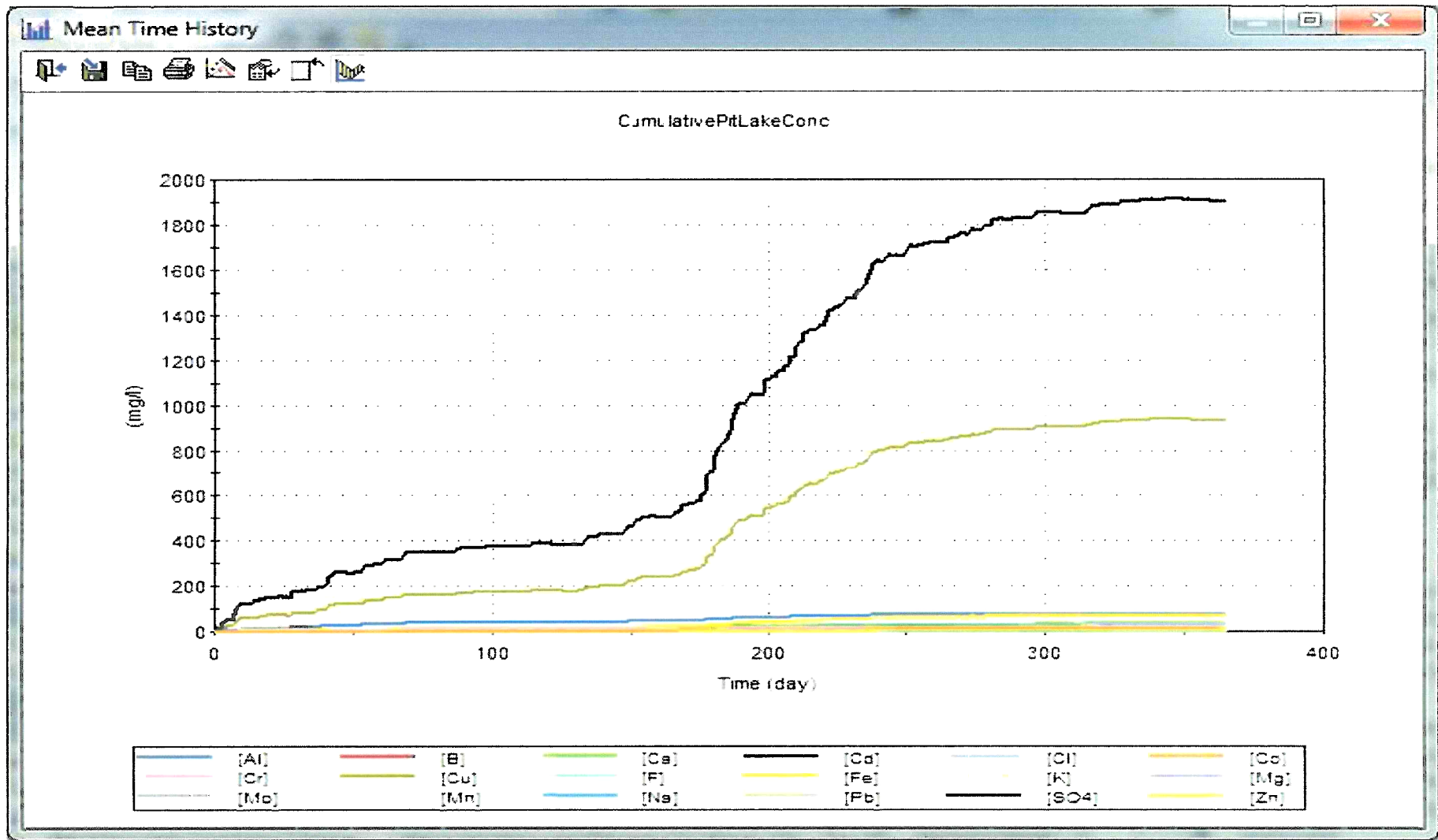


FIGURE 1  
**OVERVIEW OF RECLAMATION  
 AND COVER REQUIREMENTS**  
 G&K/TYRONE CCP UPDATE 2011/NM





**FIGURE 2**  
**TIME HISTORY CHART OF MEAN RUNOFF WATER QUALITY IN MAIN PIT (ONE-YEAR SIMULATION MODEL)**

G&K/Tyrone CCP Update 2011/NM

At Golder Associates we strive to be the most respected global group of companies specializing in ground engineering and environmental services. Employee owned since our formation in 1960, we have created a unique culture with pride in ownership, resulting in long-term organizational stability. Golder professionals take the time to build an understanding of client needs and of the specific environments in which they operate. We continue to expand our technical capabilities and have experienced steady growth with employees now operating from offices located throughout Africa, Asia, Australasia, Europe, North America and South America.

Africa	+ 27 11 254 4800
Asia	+ 852 2562 3658
Australasia	+ 61 3 8862 3500
Europe	+ 356 21 42 30 20
North America	+ 1 800 275 3281
South America	+ 55 21 3095 9500

[solutions@golder.com](mailto:solutions@golder.com)  
[www.golder.com](http://www.golder.com)

**Golder Associates Inc.**  
**18300 NE Union Hill Road, Suite 200**  
**Redmond, WA 98052 USA**  
**Tel: (425) 883-0777**  
**Fax: (425) 882-5498**

